



TECHNISCHE  
UNIVERSITÄT  
WIEN  
Vienna | Austria

## DISSERTATION

# Thermoplastic Polyurethane Elastomers with hetero-atom containing degradation motifs

ausgeführt zum Zwecke der Erlangung  
des akademischen Grades eines Doktors der technischen Wissenschaften

unter der Leitung von  
**Univ. Prof. Dipl.-Ing. Dr. techn. Robert Liska**  
und  
**Ass. Prof. Dipl.-Ing. Dr. techn. Stefan Baudis**

E163  
Institut für Angewandte Synthesechemie



eingereicht an der Technischen Universität Wien  
Fakultät für Technische Chemie

von  
**Dipl.-Ing. Philip Schwarzl**  
01355606

Wien, 23.05.2024



# DANKSAGUNG

---

Zuallererst möchte ich mich bei dir, **Prof. Robert Liska** bedanken. Durch dich bekam ich die Möglichkeit von Linz nach Wien zu kommen und meine Dissertation in dieser tollen Arbeitsgruppe machen zu dürfen. Weiters haben dein fachkundiges Wissen und deine Ratschläge es mir immer wieder ermöglicht einen neuen Blickwinkel auf meine Arbeit zu bekommen und somit auch in schwierigeren Phasen neue Lösungsansätze zu erlangen.

Ein besonderer Dank gilt auch meinem Betreuer **Dr. Stefan Baudis**. Durch dein einschlägiges TPU-Wissen konntest du mir bei vielen Aufgabenstellungen sofortige Hilfestellung leisten. Außerdem stand deine Bürotür für Fragen aller Art immer für mich offen.

Danke auch an **Dr. Patrick Knaack**, **Dr. Davide Ret** und **Walter Dazinger**, die für technische Probleme aller Art zu Hilfe eilen konnten und besonders bei diversen Messungen für Studentenpraktika oder für Auftragsmessungen immer unterstützend mitgewirkt haben.

In diesem Zusammenhang möchte ich mich auch bei **Dr. Katharina Ehrmann**, **Stefan Helfert** und **Markus Fitzka** für die praktische Wissensübermittlung und Messunterstützung bei unserer THF-GPC bedanken. Ein ausdrücklicher Dank gilt dir **Kathi**, die mich zusätzlich auch zu Beginn meiner Arbeit tatkräftig mit vielen Tipps und Tricks zum Thema TPUs versorgt hat und dir **Markus**. Gemeinsam konnten wir auch die kniffligsten GPC-Probleme bei Messungen oder Wartungen lösen.

Vielen Dank auch an **Dr. Thomas Koch** und **Stefan Zellhofer** für die Hilfe bei diversen Materialtests wie Zugversuchen oder DMTA Messungen.

Weiters möchte ich mich bei **Jürgen Greiner** und **Dagmar Reinisch** bedanken, die im Hintergrund für einen reibungslosen Ablauf in dieser Arbeitsgruppe sorgen und bei organisatorischen Dingen oder für Bestellungen immer vor Ort waren.

Außerdem gilt natürlich ein ganz großer Dank der gesamten FBMC-Arbeitsgruppe, welche die letzten Jahre an der TU Wien unvergesslich machten. Unter allen Arbeitskolleginnen und Kollegen möchte ich jedoch ein paar besonders hervorzuheben:

Zum ersten meine Univ.-Ass.-Kollegen **Raffael Wolff**, **Roland Taschner**, **Yazgan Mete**, **Sarah Keck** und **Antonella Fantoni** ohne die die vielen Betreuungsstunden in den Praktika mit Sicherheit nur halb so lustig gewesen wären und dann meiner H35-Gang bestehend aus **Florian Mayer**, **Markus Fitzka** und **Larissa Ruppitsch** die auch an schwierigen Labortagen immer ein offenes Ohr und motivierende Worte zur Hand hatten und für Fragen aller Art zur Verfügung standen. Besonders die abseits der Arbeit eingeführte H35-Restaurantwoche war immer ein Highlight und bleibt hoffentlich auch in Zukunft so erhalten.

Ein ausdrücklicher Dank gilt hierbei meinem Bench-Buddy **Flo**. Die warst immer eine riesige Unterstützung für mich speziell bei Rückschlägen und hast vor allem im Finish immer wieder motivierende Worte für mich parat gehabt

Ein besonders herzlicher Dank gilt natürlich auch meiner gesamten Familie vor allem meinen **Eltern, Großeltern** und meinem **Bruder**. Ihr habt mir diese Ausbildung ermöglicht und habt mich von Anfang an immer unterstützt.

Zuletzt möchte ich noch dir danken, **Katharina**. Du hast mich in allen Entscheidungen bis hierher immer unterstützt und mich nach einem Tag mit Rückschlägen immer wieder aufbauen und die nötige Geduld mit mir aufbringen können. Ich hoffe ich konnte dir diese Unterstützung ebenfalls in den letzten Jahren geben und freue mich schon auf (hoffentlich sehr viele) wunderschöne gemeinsame Jahre mit dir!

**DANKE!**

# ABSTRACT

---

Cardiovascular diseases, which include all diseases of the heart and blood vessels, are still the most common cause of death today. A common method of treating vascular diseases is bypass-surgery, in which a blocked or narrowed vessel is bridged with the help of a body's own (autologous) or artificial (alloplastic) vascular prosthesis. The production of artificial implants with small diameters poses a particular challenge, as long-term use often leads to vascular occlusion due to circulatory disorders. As a result, there are few suitable materials for this application. One way around this problem is to use *in situ* tissue engineering. This involves the use of a degradable tubular vascular prosthesis that supports the formation of the body's own tissue and thus enables the formation of new vessels on this artificial structure.

Thermoplastic polyurethanes (TPUs) have proven to be promising materials for this application. Their segmented structure into soft-blocks (macrodiol) and hard-blocks (diisocyanate and chain extender) allows the combination of two opposing properties. These are good mechanical properties such as flexibility and strength to withstand blood pressure, and degradability to allow degradation of the exogenous material. The non-crosslinked, linear polymer structure also enables good processability.

However, currently available TPUs either have high mechanical properties combined with a moderate degradation rate or the opposite is the case. In addition, TPUs with carboxylic ester-based chain extenders (CE) in particular tend to form inflammatory degradation products, such as the CE bis(hydroxyethyl) terephthalate (BHET).

In order to achieve an increased degradation rate with simultaneously very good mechanical properties, thermoplastic polyurethanes (TPUs), polythiourethanes (TPTUs) and polyurea urethanes (TPUUs) based on degradable chain extenders were synthesized as part of this research work and investigated with respect to their mechanical and thermal properties as well as their degradability. The formation of hydrogen bonds and steric hindrance between the hard-blocks was investigated in more detail using ATR-FTIR spectroscopy.

The soft-block was polytetrahydrofuran (pTHF) and the hard-block was the aliphatic hexamethylene diisocyanate (HMDI) combined with various chain extenders to make the resulting properties dependent only on the choice of CE. The focus was on hydrolytically degradable heteroatom-containing diols, diamines and dithiols as chain extenders. Specifically, phosphate-, silicic acid- and boronic acid-esters were used. In addition, a disulfide-containing CE was used to enable reductive polymer degradation. A furan-based substitute for BHET was also synthesized, which can be produced from renewable feedstocks.

The new materials were compared with already known TPUs containing bis(hydroxyethyl)terephthalate (BHET) as a chain extender and the commercially available Pellethane® 2363-80A. In addition, TPUs with two different chain extenders based on BHET and a second diol, diamine and dithiol were synthesized to investigate the influence of the CE combinations on the final properties of the material and to allow fine-tuning of the degradation rate.

# KURZFASSUNG

---

Kardiovaskuläre Erkrankungen, zu denen alle Erkrankungen des Herzens und der Blutgefäße gehören, sind auch heute noch die häufigste Todesursache. Eine häufige Methode zur Behandlung von Gefäßerkrankungen ist die Bypass-Operation, bei der ein verschlossenes oder verengtes Gefäß mit Hilfe einer körpereigenen (autologen) oder künstlichen (alloplastischen) Gefäßprothese überbrückt wird. Insbesondere die Herstellung von künstlichen Implantaten mit kleinen Durchmessern stellt eine große Herausforderung dar, da es hier bei Langzeitanwendung häufig zu Gefäßverschlüssen aufgrund von Durchblutungsstörungen kommt. Daher gibt es für diese Anwendung nur wenige geeignete Materialien. Eine Möglichkeit, dieses Problem zu umgehen, ist der Einsatz von *In Situ* Tissue Engineering. Dabei wird eine abbaubare röhrenförmige Gefäßprothese eingesetzt, die die Neubildung von körpereigenem Gewebe unterstützt und so die Gefäßneubildung an dieser künstlichen Struktur ermöglicht.

Thermoplastische Polyurethane (TPUs) haben sich für diese Anwendung als vielversprechende Materialien erwiesen. Ihre segmentierte Struktur in Weich-Blöcke (Makrodiol) und Hart-Blöcke (Diisocyanat und Kettenverlängerer) ermöglicht die Kombination zweier gegensätzlicher Eigenschaften. Dies sind gute mechanische Eigenschaften wie Flexibilität und Festigkeit, um dem Blutdruck zu widerstehen, und Abbaubarkeit, um die Rückbildung des körperfremden Materials zu ermöglichen. Die unvernetzte, lineare Polymerstruktur ermöglicht weiterhin eine gute Verarbeitbarkeit.

Dennoch weisen die derzeit verfügbaren TPUs entweder hohe mechanische Eigenschaften in Kombination mit einer moderaten Abbaurrate auf oder das Gegenteil ist der Fall. Darüber hinaus neigen insbesondere TPUs mit Carboxyl Ester-basierten Kettenverlängerern (CE) zur Bildung von entzündungsfördernden Abbauprodukten, wie zum Beispiel dem CE Bis(hydroxyethyl)terephthalat (BHET).

Um eine erhöhte Abbaurrate bei gleichzeitig sehr guten mechanischen Eigenschaften zu erreichen, wurden im Rahmen dieser Forschungsarbeit thermoplastische Polyurethane (TPUs), Polythiourethane (TPTUs) und Polyharnstoffurethane (TPUUs) auf Basis abbaubarer Kettenverlängerer synthetisiert und hinsichtlich ihrer mechanischen und thermischen Eigenschaften sowie ihrer Abbaubarkeit untersucht. Die Ausbildung von Wasserstoffbrückenbindungen und die sterische Hinderung zwischen den Hart-Blöcken wurde mittels ATR-FTIR-Spektroskopie näher untersucht.

Als Weich-Block wurde Polytetrahydrofuran (pTHF) und als Hart-Block das aliphatische Hexamethylendiisocyanat (HMDI) mit verschiedenen Kettenverlängerern kombiniert, um die resultierenden Eigenschaften nur von der Wahl des CEs abhängig zu machen.

Der Schwerpunkt lag dabei auf hydrolytisch abbaubaren heteroatomhaltigen Diolen, Diaminen und Dithiolen als Kettenverlängerer. Im Einzelnen wurden Phosphat-, Kieselsäure- und Boronsäure-Ester eingesetzt. Zusätzlich wurde ein Disulfid-haltiger CE eingesetzt, welcher einen reduktiven Polymerabbau ermöglicht. Außerdem wurde ein Furan-basierter Ersatz für BHET synthetisiert, der aus erneuerbaren Basischemikalien hergestellt werden kann. Die neuen Materialien wurden mit bereits bekannten TPUs, die Bis(hydroxyethyl)terephthalat (BHET) als Kettenverlängerer enthalten, und dem kommerziell erhältlichen Pellethane® 2363-80A verglichen. Darüber hinaus wurden TPUs mit zwei verschiedenen Kettenverlängerern auf Basis von BHET und einem zweiten Diol, Diamin und Dithiol synthetisiert, um den Einfluss der CE-Kombinationen auf die finalen Eigenschaften des Materials zu untersuchen und eine Feinabstimmung der Abbauraten zu ermöglichen.



# TABLE OF CONTENTS

---

<b>INTRODUCTION</b>	<b>1</b>	
<b>1. The cardiovascular system</b>	<b>1</b>	
<b>2. Diseases of the cardiovascular system</b>	<b>3</b>	
<b>3. Therapies</b>	<b>4</b>	
3.1. Conventional therapies	4	
3.2. Protein, gene and cell therapies	6	
<b>4. Tissue engineering</b>	<b>8</b>	
4.1. Vascular tissue engineering	9	
4.2. Materials for scaffold based vascular tissue engineering	12	
4.2.1. Bio-based materials for vascular tissue engineered scaffolds	12	
4.2.2. Synthetic materials for vascular tissue engineered scaffolds	14	
<b>5. Thermoplastic poly(urethane/urea/thiourethane) elastomers</b>	<b>17</b>	
<b>OBJECTIVE</b>	<b>22</b>	
<b>STATE OF THE ART</b>	<b>24</b>	
<b>1. Degradation motifs of TPUs</b>	<b>25</b>	
1.1. Hard-block degradation	25	
1.2. Soft-block degradation	29	
<b>2. Further concepts for degradable biomaterials</b>	<b>31</b>	
<b>GENERAL PART - RESULTS AND DISCUSSION (Gen.)</b>	<b>38</b>	
<b>SUMMARY AND CONCLUSION</b>	<b>127</b>	
<b>EXPERIMENTAL PART (Exp.)</b>	<b>135</b>	
	<b>Gen.</b>	<b>Exp.</b>
<b>1. Reference polymers</b>	<b>38</b>	<b>135</b>
1.1. General polymer procedure / Synthesis of TPU-BHET	39	135
1.2. Synthesis of the CE bis(hydroxypropyl)carbonate (BHPC)	44	139
1.3. Synthesis of TPU-BHPC	45	140
1.4. General characterization of reference materials	46	141
1.5. Mechanical and thermal properties of references	50	
1.6. Degradation behavior of reference polymers	52	

	<b>Gen.</b>	<b>Exp.</b>
<b>2. Further carboxylic ester-based CE</b>	<b>54</b>	<b>142</b>
2.1. Synthesis of BHEF	54	142
2.2. Synthesis of TPU-BHEF	55	143
2.3. General characterization	56	
2.4. Mechanical and thermal properties	59	
2.5. Degradation behavior	61	
<b>3. Inorganic ester-based CEs</b>	<b>63</b>	<b>145</b>
<b>3.1. Synthesis and purification of CEs</b>	<b>63</b>	<b>145</b>
3.1.1. Phosphate ester-based CE	63	145
3.1.2. Silicic acid ester-based CE	70	147
3.1.3. Boronic acid ester-based CE	74	148
<b>3.2. TPUs, TPUUs and TPTUs with one CE</b>	<b>75</b>	<b>149</b>
3.2.1. Synthesis of TPUs, TPUUs and TPTUs with one CE	76	149
3.2.2. General characterization of polymers with one CE	77	
3.2.3. Mechanical and thermal properties of polymers with one CE	81	
3.2.4. Degradation behavior of polymers with one CE	84	
3.2.5. Model compounds of boronic acid esters	92	154
<b>3.3. TPUs with two different CEs</b>	<b>99</b>	<b>156</b>
3.3.1. Synthesis of TPUs with two different CEs	100	156
3.3.2. General characterization of polymers with two different CEs	102	
3.3.3. Mechanical and thermal properties of polymers with two different CEs	107	
3.3.4. Degradation behavior of polymers with two different CEs	110	
<b>4. Influence of disulfides in the CE</b>	<b>115</b>	<b>165</b>
4.1. Synthesis of TPU-HEDS	116	165
4.2. Synthesis of TPU-BHET-HEDS	117	167
4.3. General characterization	118	
4.4. Mechanical and thermal properties	121	
4.5. Degradation behavior	123	

<b>APPENDIX</b>	<b>170</b>
1. NMR spectra	170
2. ATR-FTIR spectra	188
3. DMTA spectra	193
4. Tensile testing	201
<b>MATERIALS AND METHODS</b>	<b>202</b>
<b>ABBREVIATIONS</b>	<b>206</b>
<b>REFERENCES</b>	<b>208</b>



# INTRODUCTION

## 1. The cardiovascular system

The cardiovascular system consists of the human heart, arteries, veins and other blood vessels. In general, about 4-6 liters of blood are flowing through this system. This is approximately 7-8 % of the body weight. In about one minute, the whole volume is circulating through the whole human body. A healthy human heartbeat is 50-60 per minute. The blood in the cardiovascular system is always kept in a continuous flow from the left heart to the right heart passing the aorta, arteries, arterioles, capillaries, venules, veins and the vena cava. This is also called the systemic circulation. Beside this, there is also the pulmonary circulation where the human blood gets rid of carbon dioxide and is saturated with oxygen. Thereby, deoxygenated blood is transported via the pulmonary artery from the right heart to the lungs (gaseous exchange) and back to the left heart via the pulmonary vein (Figure 1). Then the systemic circulation starts again. Because the human heart is not strong enough to pump the blood through the whole body, especially via the very thin capillaries, myogenic and neurogenic processes also control the blood flow through the vessels. Therefore, some blood vessels have smooth muscles in their walls for continuous contraction and relaxation. The autonomous nervous system controls neurogenic processes.<sup>1</sup>

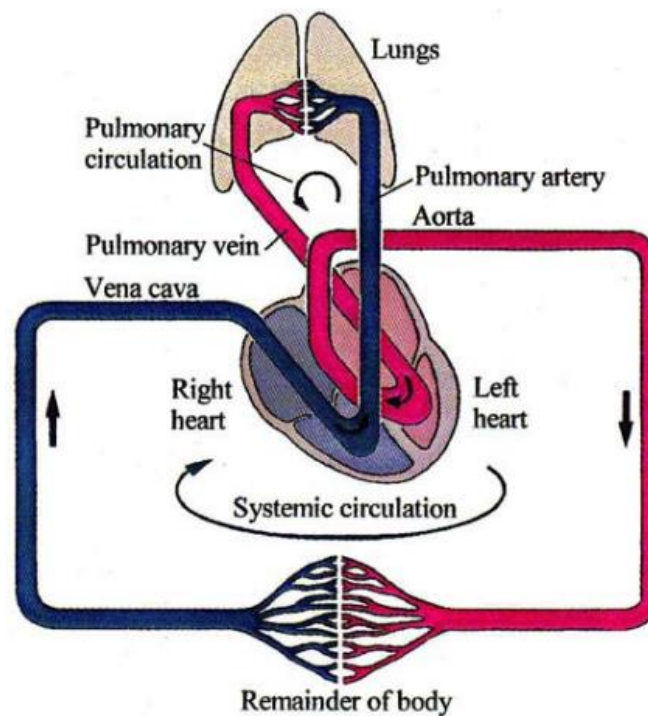


Figure 1: Circulation of blood through the human body beginning from the left heart via the blood vessels to the right heart (systemic circulation) and the pulmonary circulation beginning in the right heart via pulmonary artery, lung, pulmonary vein and the right heart.<sup>1</sup>

In general, the human blood vessel consists of three concentric tunics: tunica intima, tunica media and tunica externa (Figure 2). The tunica intima, which is found next to the lumen, consist mainly of endothelial cells.<sup>1</sup> The layer must be extremely smooth to support blood flow and to avoid blood stream turbulences. Otherwise the risk of formation of thrombi would be higher. Furthermore, it acts as a barrier between the plasma and the vessel and segregate chemical mediators. These mediators control the circulation of the blood cells, the vasomotor tone and the growth of the blood vessels.<sup>2</sup> The tunica media consists of smooth vascular muscle cells. The main function of these muscles is the regulation of the blood flow and sets the vascular tone.<sup>3</sup> The tunica externa or tunica adventitia is a fibrous network of fibroblasts, which is nerved by smooth vessels and nerves to supply the blood vessel.<sup>2</sup>

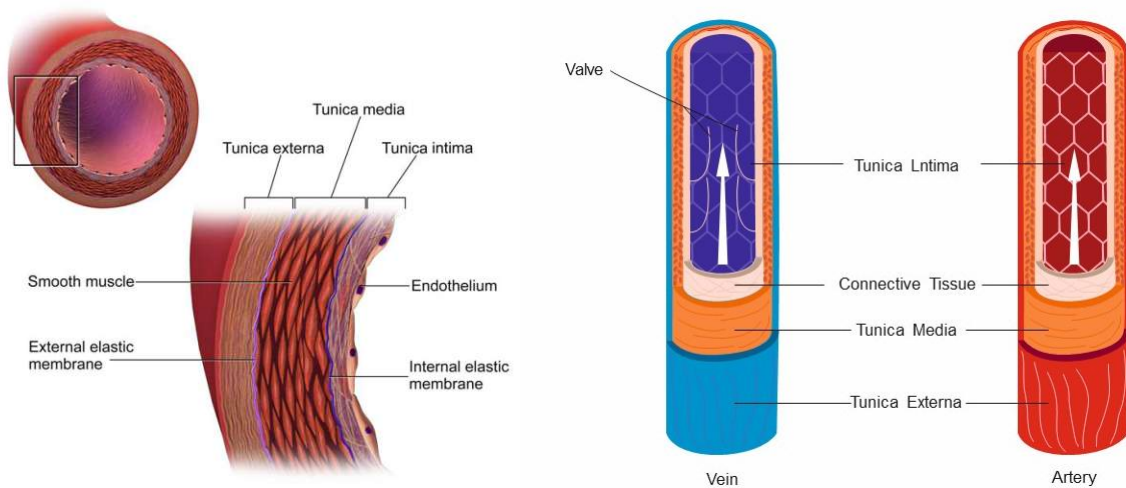


Figure 2: Structure of blood vessel <sup>4</sup> (left), graphical description of vein and artery <sup>5</sup> (right).

Furthermore, there are also different types of blood vessels, which have a slightly adopted structure. Arteries always takes blood away from the heart and therefore transport oxygen-rich blood in the systemic circulation and oxygen-poor blood in the pulmonary circulation. Veins, however, always carry blood towards the heart. In addition to the venules and capillaries, veins are part of the low-pressure system of the bloodstream.<sup>6</sup> The blood pressure generated by the heart is not sufficient to transport the blood through the entire body. Therefore, veins often run parallel to arteries in order to use their expansion for their own blood transport. The veins are also supported by the skeletal muscles. Since the blood pressure is still very low, there are so-called back-pressure valves to prevent the blood from flowing back (Figure 2). In general, the arterial walls are stronger than those of veins because they have to compensate the higher blood pressure.<sup>7</sup>

## 2. Diseases of the cardiovascular system

All diseases of the heart and blood vessels are summarized under cardiovascular diseases, which still continue to be among the leading causes of death. In 2017, 31.8 % of deaths worldwide were caused by cardiovascular diseases (Figure 3).<sup>8</sup> In addition to risk factors that cannot be influenced, such as age, gender and genetic predisposition, risk factors that can be influenced include high blood pressure, unhealthy diet, overweight, lack of exercise, hypercholesterolemia, smoking, alcohol consumption and air pollution. The blood vessels can be affected by various diseases. They include, for example, malformations, injuries, inflammation, functional disorders or occlusive diseases. Examples for such diseases are coronary heart disease, infarcts, arterial occlusive diseases or diseases of the veins. Infarctions generally arise from an occluded vessel in an organ, which leads to an insufficient blood supply (e.g. heart, lung, brain infarction). Occlusion of the coronary arteries leads to a heart attack, which is cured via a bypass operation. Such occlusions are often a result of thrombosis. Thrombi generally have their origin in veins because of lower blood flow velocity, which are caused by coagulation disorders. In arterial occlusive diseases, inflammation or deposits cause the slow closure of blood vessels. One of the most important diseases is atherosclerosis. Factors could be a malfunction of the vascular endothelium, cholesterol deposits or chronic inflammations of the blood vessel. Beside atherosclerosis, an aneurysm is a pathological bagging of a blood vessel. Usually this affects an artery. The cross section of the artery is widened at the affected area.<sup>8</sup>

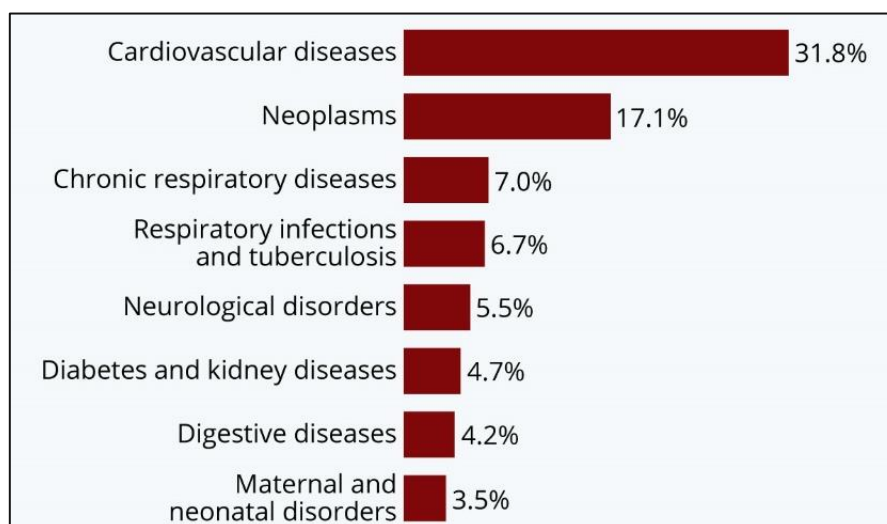


Figure 3: Top Global Causes of Death in 2017. Nearly one-third caused by cardiovascular diseases.<sup>8</sup>

### 3. Therapies

Conventional treatment for vascular diseases generally includes surgery-based therapies such as vasodilation (angioplasty), stent implantation, or bypassing. In addition, anti-thrombotic drugs are usually administered. Conventional surgery-based therapies are increasingly supported by biopharmaceutical-based therapies, such as cell, gene or protein therapies.<sup>9</sup> In the following, the most important conventional medical treatment options as well as other therapies are discussed.

#### 3.1. Conventional therapies

*Angioplasty* is a treatment to widen small diameter blood vessel stenosis caused by arteriosclerosis. Angioplasty is rarely performed via direct vascular access, but mostly not surgically as percutaneous transluminal angioplasty (PTA) via balloon dilatation. For this purpose, after a small puncture through the skin (percutaneous) under X-ray control, a balloon catheter is moved until location of stenosis with the help of a guide wire inside a blood vessel (transluminal). The balloon is expanded until the stenosis is widened enough and the inner wall of the vessel is smoothed (Figure 4 left). Complications such as secondary bleeding, injured vascular walls or blood clots (thrombus) can occur. Angioplasty is carried out both in the area of the pelvic and leg arteries and in the area of the renal and intestinal arteries.<sup>9, 10</sup>

The dilation of the coronary arteries in heart disease via a balloon catheter is called percutaneous transluminal coronary angioplasty (PTCA). Access is also via a leg artery. The PTCA is carried for short stenosis of one or two coronary arteries.<sup>9, 10</sup> In combination with the implantation of a coronary stent, it is a very effective method to treat acute heart attacks. However, anti-thrombotic drugs must still be taken.<sup>11</sup>

*Stents or coronary stents* are tube-like vascular implants. They are used for short-distance arteriosclerotic vasoconstrictions, for example coronary arteries that have been dilated via an angioplasty. The stent is inserted into the coronary artery using an applicator and is pushed forward until the former stenosis. The scissor-lattice-like coronary stent unfolds in the blood-vessel, supports it from the inside and is intended to prevent it from restenosis (Figure 4 right). Nevertheless, there is a risk of restenosis or re-occlusion.<sup>9, 12</sup> For this reason, coronary stents with a special drug coating (drug eluting stents, DES) are now used. Furthermore, patients also receive anticoagulant medication after the procedure.<sup>13</sup>



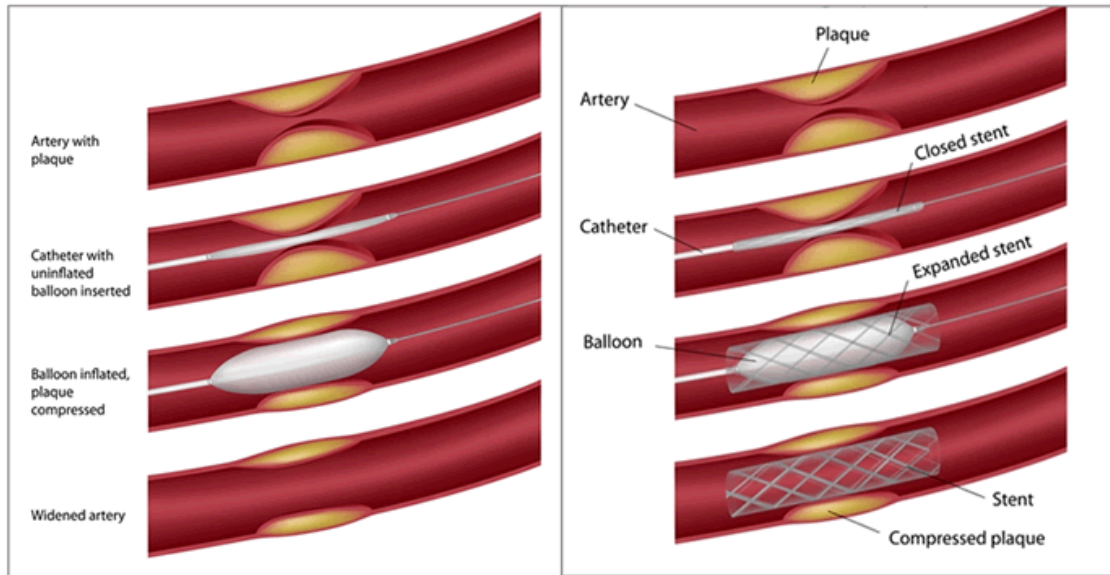


Figure 4: Balloon angioplasty (left) and stenting (right).<sup>14</sup>

*Bypass-grafting* is a surgically created deviation circuit in the vascular system for bridging vascular occlusions or constrictions. For the vascular prosthesis body's own (autologous) or artificial (alloplastic) material is used. In both cases, the affected vascular vessel is not removed. A distinction is made between anatomical bypass (natural course of vessels) or extra-anatomical bypass (non-natural course of vessels).<sup>9, 10</sup>

There are two ways to bypass the coronary arteries. The aorto-coronary vein bypass requires the removal of a piece of a superficial leg vein. This is inserted between the part of the aorta close to the heart and the coronary vessels beyond the stenosis (Figure 5). An artery bypass (mammary bypass) is less often used, e.g. if the leg veins are not suitable for bypass due to varicose veins. However, the use of the leg vein shows an increased risk of restenosis.<sup>15</sup> Both operations require the use of a heart-lung machine.<sup>10</sup>

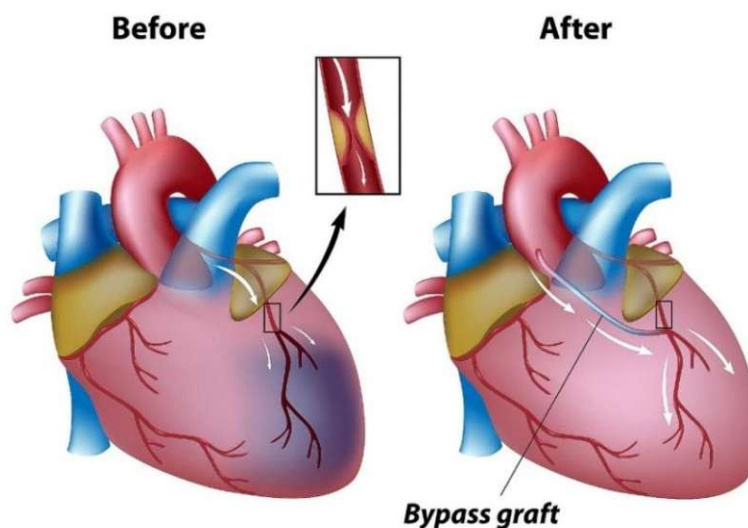


Figure 5: Illustration of a coronary artery bypass graft surgery.<sup>16</sup>

*Anti-thrombotic therapy* is one of the most important first-line treatment options for patients with angina pectoris or a prospective heart attack. Anti-thrombotic agents can prevent a blood vessel from being completely closed because they suppress the formation of thrombin. After angioplasty or the insertion of a stent, anti-thrombotic medication must often be taken to lower the risk of restenosis.<sup>9, 17</sup>

Suitable drugs include, unfractionated heparin (UFH), low molecular weight heparin (LMWH) in combination with acetyl salicylic acid<sup>9, 18</sup>, factor Xa inhibitors (fondaparinux) or direct thrombin inhibitors (DTI).<sup>19</sup>

Heparins are body's own polysaccharides, which have an inhibiting effect on hemostasis. In comparison, factor Xa inhibitors show a lower risk of subsequent bleeding but cannot be used during angioplasty.<sup>19</sup> DTIs suppress the formation of fibrin from fibrinogen and thus reduce blood coagulation.<sup>9</sup>

### **3.2. Protein, gene and cell therapies**

*Proteins* act as effective hormones, antibodies and enzymes with the ability to catalyze biochemical reactions. They play an essential role in structural and mechanical functions, including cell cycle regulation, signal transduction, immune responses and energy supply. Dysfunctions in certain proteins are closely linked to many human diseases. Therapeutic proteins are used to treat diseases characterized by the absence or defect of certain proteins or the inhibition of certain biological processes. Recombinant DNA technology enables the cost-effective production of important human proteins in mammalian cells, bacteria or yeast.<sup>9</sup> Treatment methods involving the application of cell-penetrating peptides (CPPs) or protein transduction domains (PTDs) as effective carriers for proteins, genes and particles that enable the penetration of water-soluble proteins into cells.<sup>9, 20, 21</sup>

In the field of vascular disease treatment, a protein-based angio-therapy strategy involving the dual supply of angiogenic and arteriogenic factors shows remarkable improvements in myocardial collateral growth, blood flow and cardiac function in animal models of ischemic hearts.<sup>9, 22</sup>

Angiogenesis, the sprouting or splitting of blood vessels, and arteriogenesis, the formation of arteries and smaller arterioles with a complete vessel wall through the formation of new smooth muscle cells, are key processes. In angiogenesis-mediated treatment of ischemic heart disease, growth factors such as vascular endothelial growth factors (VEGF), fibroblast growth factors (FGF) and hepatocyte growth factors (HGF) are used to promote neovascularization (Formation of new blood vessels).<sup>9, 23, 24</sup>

An alternative approach is the use of heat shock proteins (HSPs), which can protect proteins from aggregation. HSPs, like molecular chaperones, can fold or refold damaged proteins and

facilitate the degradation of severely damaged proteins. Aging and hyperlipidemia have been observed to decrease the expression of cardioprotective HSPs in response to stress conditions, leading to impaired cardiac function under ischemic conditions (reduced blood circulation). HSPs play a central role in protection against various stress factors such as ischemia, high temperature and oxidative stress in all human cell types.<sup>9, 25-27</sup>

*Gene therapy* is a medical approach that involves introducing, altering, or removing genetic material from patient cells to treat or prevent disease. The goal is to correct or replace faulty genes, regulate gene expression, or introduce new genes to address the underlying genetic problems.<sup>28</sup>

There are several technical options for introducing genes into the patient's target cells. One is the introduction of therapeutic genes using viral vectors such as lentiviruses or adeno-associated viruses (AAV).<sup>29</sup> In addition, non-viral vectors such as plasmids can also be used.<sup>9</sup> According to Ginn et al., cardiovascular diseases are the fourth most common application of gene therapy after cancer treatment, monogenetic diseases, and infectious diseases. Cardiovascular gene therapy offers new treatment options, particularly in therapeutic angiogenesis and in cases where there is a risk of restenosis after angioplasty. Gene therapy can also be used in risk factor management. This includes prevention of bypass graft failure and prevention of myocardial diseases.<sup>29</sup>

However, the main focus of cardiovascular gene therapy has been on therapeutic angiogenesis to improve blood flow to ischemic tissue. In addition, two major types of ischemic disease have often been studied, such as myocardial ischemia due to coronary artery disease and lower limb ischemia due to peripheral artery disease. Fibroblast growth factors and vascular endothelial growth factors have been widely used for treatment.<sup>29</sup>

*Cell therapy* is the transplantation of animal or human cells to repair or replace damaged cells or tissues.<sup>9</sup> This therapy has been shown to promote the formation of new blood vessels (vascularization). Cell transplantation may be used as an alternative therapeutic measure to promote regeneration in ischemic heart disease and heart failure. Various cell types such as embryonic stem cells, skeletal myoblasts, bone marrow-derived cells, adipose-derived cardiac progenitor cells, and umbilical cord cells can be used.<sup>9, 30</sup>

Cells from bone marrow have the ability to differentiate, migrate and reproduce into various cell types. These include endothelial progenitor cells (EPCs), mesenchymal stem cells (MSCs), hematopoietic stem cells (HSCs) and multipotent adult progenitor cells (MAPCs).<sup>9</sup>

Numerous studies in animal models as well as in humans have shown that stem cells have therapeutic potential in acute myocardial infarction and chronic heart failure in advanced stages of the disease.<sup>31-33</sup>

## 4. Tissue engineering

For many diseases it is necessary to replace parts of organs or the whole organ by transplantation. The increasing need of organs for transplants is already leading to a bottleneck. In addition, transplantation sometimes leads to rejection reactions of the body, which means that a considerable number of patients cannot get a suitable donor organ. Therefore, tissue engineering or regenerative medicine is an alternative to transplantation. Using cell engineering, bioengineering and materials science substitutes are created for transplants. These are intended to restore the function of the damaged organ.<sup>34</sup>

Tissue engineering (TE) is basically divided into two categories: The use of matrices with or without cells. Matrices without cells serve the body as a kind of supporting material to regenerate the body's own cells. It is therefore necessary that these materials are biocompatible so that they are not rejected by the body. In some areas of application, it is even necessary that these materials are biodegradable in order to avoid the long-term use of a foreign material. These materials are displaced and degraded by the formation of the extracellular matrix (ECM). Furthermore, cells can be injected to accelerate the regeneration of natural tissue, e.g. using hydrogels as a carrier or directly.<sup>35-37</sup>

Basically, tissue engineering consists of four building blocks: Scaffold (framework for the incorporation of cells), cells (stem cells or already differentiated cells), growth-factors (certain proteins for cell growth) and an organism (*in vivo*-seeding) or a culture medium (*in vitro*-seeding). Usually, *in vivo*-seeding is preferred, wherein the biocompatible scaffold is implanted in the patient and cells start to grow directly in the body. Nevertheless, *in vivo*-seeding is not always possible.

*In vitro*-seeding (Figure 6) on the other hand includes, cell biopsy from the patient himself (autologous), from a donor (allogenic) or from animals (heterologous), isolation, cultivation and proliferation. The cells are then reared in a nutrient solution using growth factors (mechanical and chemical stimuli) and the appropriate scaffold. Finally, the grown tissue is transplanted into the patient.<sup>38</sup>

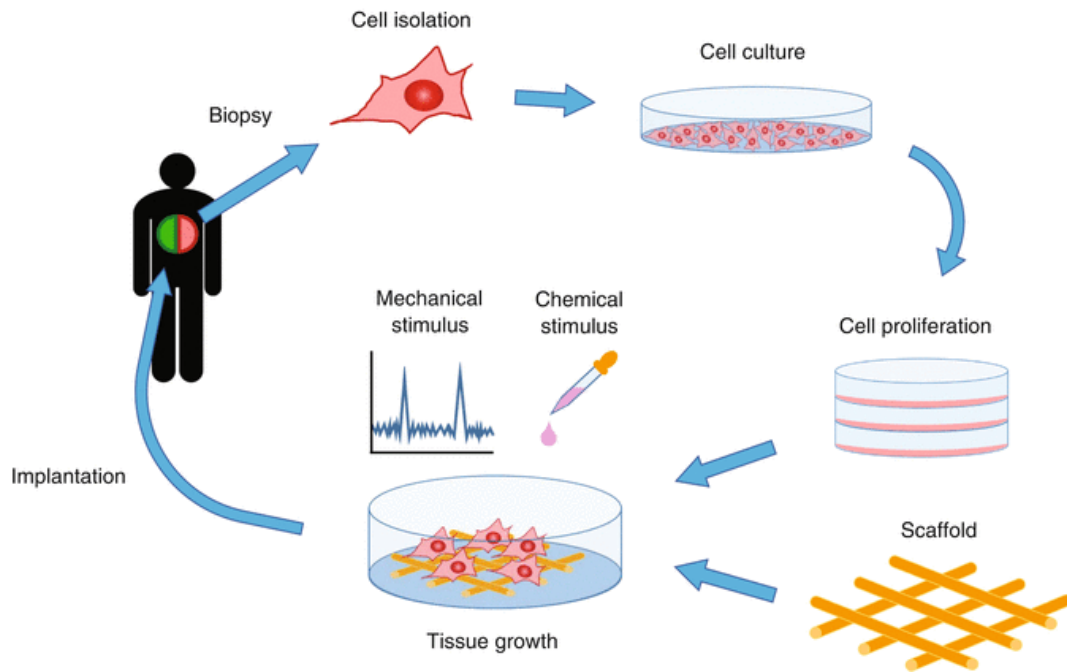


Figure 6: Cycle of tissue engineering via in vitro seeding.<sup>38</sup>

#### 4.1. Vascular tissue engineering

As already described in chapter 2. Diseases of the cardiovascular system, vascular diseases such as atherosclerosis are among the most common serious diseases worldwide. A particularly serious illness is the narrowing or shooting of coronary arteries, which can lead to a heart attack. This is usually treated by means of coronary artery bypass graft surgery (CABG). Blood vessels, usually the mammary artery or the saphenous vein, are removed from the patient and used as a bypass.<sup>39</sup>

Although lots of people need such a bypass surgery one or more times in their lives, the use of the body's own blood vessels is not always possible due to previous illnesses. That is why it is becoming increasingly necessary to resort to alternatives. Possible solutions for this are the synthesis of small-diameter blood vessel substitutes, which is also known under the term vascular tissue engineering.<sup>40, 41</sup>

In general, there are three different strategies to prepare blood vessel replacement materials via vascular tissue engineering (VTE):

- (1) *In vivo* or *in situ* regeneration: In this connection, an artificial, inert, non-biodegradable material is used as a vessel replacement material. By using cells and the body as a bioreactor, natural tissue is formed covering this material. The artificial material is, so to speak, enclosed by newly formed tissue.<sup>39</sup> Campbell *et al.* uses for example Silastic inert tubes and autologous myofibroblasts to build up a new vessel wall covering the artificial tube.<sup>42</sup>

- (2) *In vitro* self-assembly and growth of cells: A natural blood vessel is grown using suitable cells *in vitro* on a suitable nutrient medium. After formation of natural tissue, the blood vessel is available for transplantation.<sup>39, 43</sup> Auger *et. al* used for example a cohesive plastic film to enable smooth human muscle cells the formation of human tissue in a defined order. Furthermore, they used ascorbic acid to stimulate cell growth.<sup>44</sup>
- (3) *In vitro* or *in vivo* scaffold based material: An artificial, preferably biodegradable scaffold is created, whereby it is easier to achieve precisely defined properties and shapes compared to both previous described methods. The scaffold should help vascular cells (e.g. endothelial cells) to build a natural vessel according to the given shape and structure. Both, *in vitro* or *in vivo* reproduction is possible. For the *in vitro* method, the scaffold is placed in a bioreactor with suitable cells and the vessel is implanted after natural tissue has formed. Compared to that, via *in vivo* method, the scaffold is implanted directly, and the tissue is reproduced by the body itself. Due to faster and easier execution the *in vivo* method is preferred, although the materials requirements are higher.<sup>39, 45</sup>

Nonetheless, very high demands are placed on the materials used in all above mentioned methods. Due to the constantly changing blood pressure, in combination with the biological environment, the following properties must be given:

- (1) The material must be porous in order to facilitate the integration of the cells. In addition, it must be possible to regenerate natural tissue, whereby nutrients must be transported through the walls of the scaffold and waste products must be removed.
- (2) Ideally, the scaffold should be biodegradable in order to avoid permanent foreign material remaining in the body. Moreover, the degradability must be adjusted that enough new tissue can reproduce before the scaffold is completely degraded (Figure 8).<sup>39</sup>
- (3) The correct surface quality is necessary in order to enable cell attachment and reproduction. If the material is not biocompatible, it can lead to immune reactions and consequently to the formation of thrombi.<sup>46</sup>
- (4) The mechanical properties must correspond as closely as possible to those of the natural blood vessel. Differences in the elastic modulus at the junction between the vascular prosthesis and the natural vessel can lead to flow disorders, narrowing (Stenosis) or enlargement and even to a disruption.<sup>47, 48</sup>
- (5) Finally, the material must have a sufficiently small diameter and a suitable shape.<sup>49</sup>

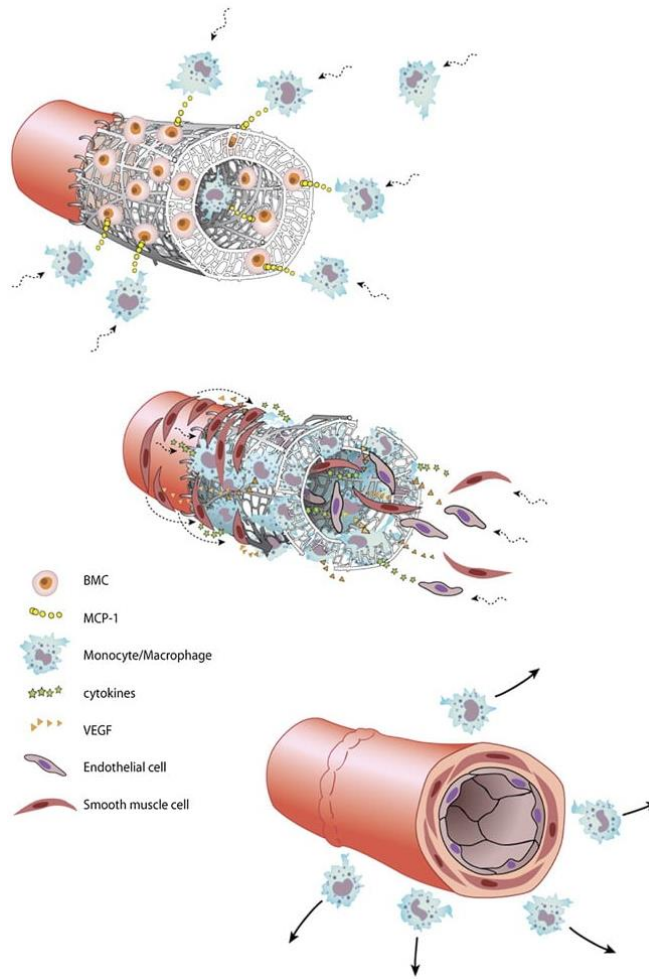


Figure 7: Proposed transformation of a vascular graft into natural tissue.<sup>50</sup>

Figure 8 shows the ideal mechanical behavior of the degrading scaffold and the reconstructed tissue over the implantation time. The mechanical properties of the combined construct (blue line) are thus composed of the weakening mechanical properties of the degrading scaffold (green line) and the newly formed ECM cell-matrix (red line) together. Ideally, the mechanical properties of the entire construct should remain constant from implantation to complete regeneration of the natural tissue.<sup>39</sup>

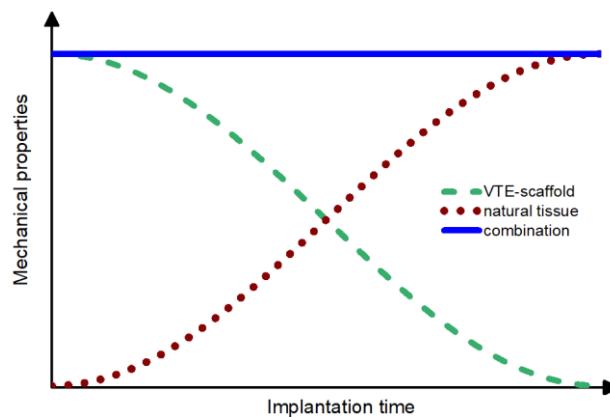


Figure 8: Schematic drawing of the mechanical properties as a function of the implantation time for VTE-scaffolds.

## 4.2. Materials for scaffold based vascular tissue engineering

In the following section outlines various macromolecules, which are well suited as materials for scaffold based vascular prostheses. Basically, there is the possibility to use natural or synthetic macromolecules, however, the following properties must be considered for material choosing:

- (1) mechanical properties (elasticity, tensile strength...)
- (2) physiological properties (biocompatibility, biodegradability)

Because these properties influence each other negatively, a trade-off between mechanical and physiological properties must be found often. This means if the mechanical properties of a macromolecule are improved, the physiological properties usually decline and vice versa. The most obvious choice of material for a scaffold would be the use of natural macromolecules. These show very good physiological properties but have generally poor mechanical properties compared to synthetic macromolecules. Therefore, it is often necessary to improve the mechanical properties with synthetic additives.<sup>39</sup>

### 4.2.1. Bio-based materials for vascular tissue engineered scaffolds

The following describes collagen, elastin, fibrin, chitosan and hyaluronic acid as natural macromolecular materials, which are used for vascular tissue engineered scaffolds. Chemical structures of these are shown in Figure 9.

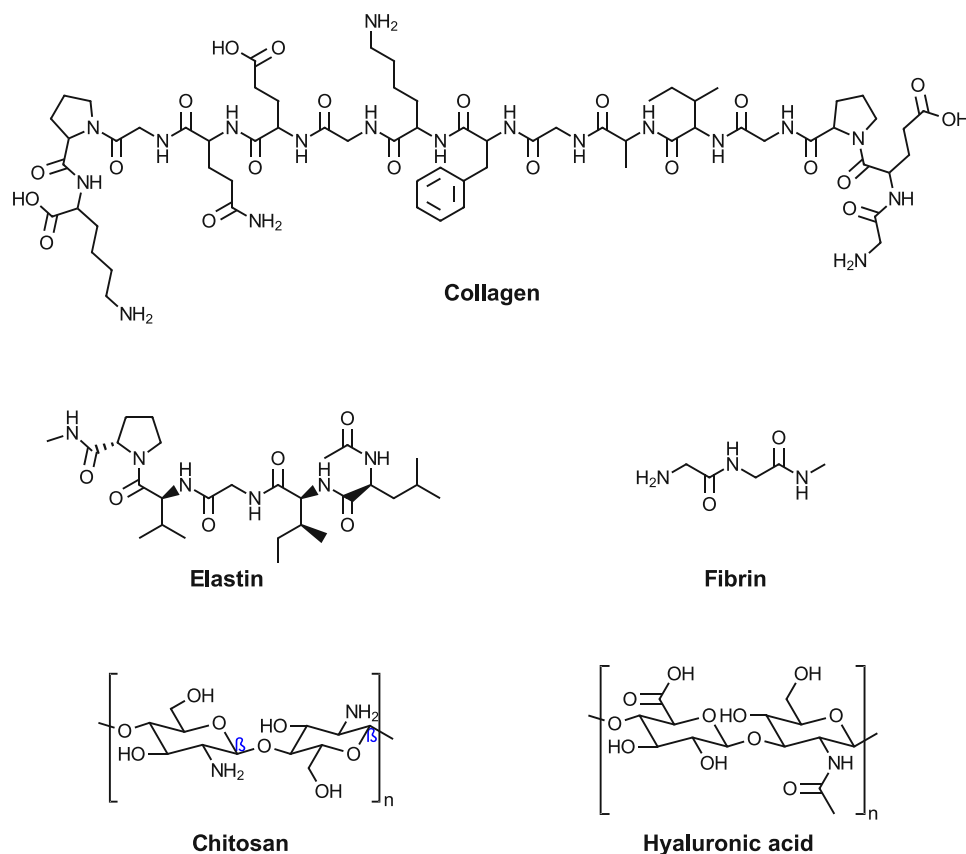


Figure 9: Chemical structures of collagen, elastin, fibrin, chitosan and hyaluronic acid.



*Collagen* can be extracted from the extracellular matrix in large amounts, where it occurs as the main component.<sup>51</sup> However, the first scaffolds made of collagen gel showed very poor mechanical properties and ripped even at very low pressures (~ 10 mmHg).<sup>52</sup> It was later shown that the mechanical properties could be improved by using Dacron mesh (polyethylene terephthalate by DuPont®).

The material was not ripped until a pressure of 180 mmHg was exceeded. Promising elastic properties are also achieved through the copolymerization of collagen and elastin and subsequent crosslinking using glycosaminoglycans.<sup>53, 54</sup> Nevertheless, the best mechanical properties could be achieved by covalent crosslinking of collagen fibers and glutaraldehyde. However, glutaraldehyde is not biocompatible and, due to its toxicity, leads to cell death in certain amounts.<sup>55</sup>

*Elastin* is mainly present in the arterial walls. It ensures that the vessels are elastic and makes it possible to endure the stress caused by blood pressure.<sup>56</sup> As already mentioned above, elastin shows good mechanical properties in combination with collagen and additives for crosslinking in the correct ratio. Leach *et al.* described an elastin-based scaffold that was crosslinked with ethylene glycol glycidyl ether (EDGE). However, this material was more rigid than elastin alone.<sup>57</sup> The combination of elastin with degradable synthetic polymers show more promising results.<sup>48, 58</sup>

*Fibrin* is an insoluble protein that its main task is to regulate blood coagulation. A major advantage of fibrin is the preparation out of patient's blood. As a result, there is no immune response.<sup>59, 60</sup> Ye *et al.* produced a three-dimensional scaffold made of fibrin gel for vascular tissue engineering. Uniform cell growth and collagen formation were shown on the scaffold.<sup>59</sup> However, due to degradation in the nutrient medium, the mechanical properties already decline to such an extent that implantation was no longer possible.<sup>60</sup> Cummings *et al.* were able to improve the mechanical properties by combining fibrin with collagen. Fibrin provides the elastic behavior; collagen provides the necessary stiffness.<sup>61</sup>

*Chitosan* is derived from chitin and is therefore available in very large quantities (e.g. crustaceans). For tissue engineering applications, it has many advantages such as low-cost availability, anti-microbial activities, biocompatibility and biodegradability.<sup>62, 63</sup> However, scaffolds that consist only of chitosan show inferior mechanical properties than natural blood vessels and are therefore only suitable in combination with other macromolecules. In combination with poly(ethylene glycol)<sup>64</sup>, gelatin<sup>62, 65</sup> or poly(caprolactone)<sup>66</sup> the mechanical properties can be improved. Sarasam *et al.* showed that a 1:1 mixture of chitosan and poly(caprolactone) had twice the tensile strength as chitosan alone.<sup>66</sup>

*Hyaluronic acid* (HA) belongs to the non-sulfated glycosaminoglycans (GAGs). In the human body it occurs in arteries, veins, connective tissue, articular cartilage, human serum and in the umbilical cord.<sup>67, 68</sup> HA can be obtained *in vitro* by fermentation of streptococci or from the chlorella-virus.<sup>69</sup>

In sufficient purity, synthetic HA is both biocompatible and biodegradable.<sup>70</sup> HA is used in medicine to repair articular cartilage damage.<sup>71-73</sup> In contrast, degradation fragments are used in cosmetics, since these can be more easily absorbed by the skin<sup>74</sup>. Biomaterials from HA generally have much poorer mechanical properties than natural blood vessels and have not been tested *in vivo* to date. Since HA is only present in small amounts in arteries and veins compared to the biomaterials already described, the focus of research for vascular tissue engineered scaffolds is more on these or on the synthetic macromolecules described below.<sup>39</sup>

#### 4.2.2. Synthetic materials for vascular tissue engineered scaffolds

Due to the relatively poor mechanical properties and the time-consuming production, natural materials cannot currently be used as the sole component for scaffolds in vascular tissue engineering. Therefore, synthetic materials are also used as single component or as mixture with natural macromolecules.<sup>39</sup> Nevertheless, synthetic macromolecules also have disadvantages. It is known, for example, that degradation products from these can lead to inflammatory reactions.<sup>75</sup> Furthermore, it has not yet been clarified whether these degradation products can accumulate in the body or can be transported further via the lymphatic system and thus lead to consequential damage at other regions in human body.<sup>76</sup> The following macromolecules or polymers were most closely within the scope of the VTE: poly(glycolic acid) (PGA), poly(lactic acid) (PLA), poly(L-lactic acid) (PLLA), poly( $\epsilon$ -caprolactone) (PCL), polyhydroxyalkanoates (PHAs), polydioxane (PDO) and polyurethanes (PUs). Chemical structures are shown in Figure 10.

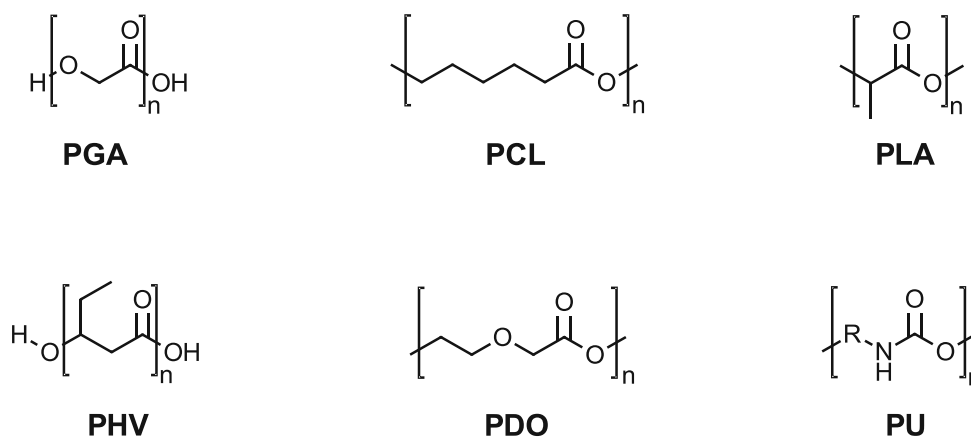


Figure 10: Chemical structures of poly(glycolic acid) (PGA), poly( $\epsilon$ -caprolactone) (PCL), poly(lactic acid) (PLA), poly-3-hydroxyvalerate (PHV) as an polyhydroxyalkanoate (PHA), polydioxane (PDO) and polyurethane (PU).

*Poly(glycolic acid) (PGA)* is synthesized via ring-opening polymerization of glycolide.<sup>77-79</sup> The degradation products are glycolic acid, which is metabolized by the body, and carbon dioxide. It degrades in the human body within 1 – 6 months, depending on the physiological environment.<sup>39</sup> Due to the high rate of degradation, it is only suitable for vascular tissue engineering in combination with slower degrading macromolecules. Iwasaki *et al.* showed that e.g. poly( $\epsilon$ -caprolactone) and poly(lactic acid) are suitable for such application.<sup>80, 81</sup>

*Poly(lactic acid) (PLA)* is more hydrophobic compared to PGA, due to additional methyl groups and therefore degrades much slower. It is a thermoplastic polyester and is synthesized via ring-opening polymerization of lactic acid.<sup>39</sup> Due to the chirality of lactic acid, a distinction is made between *D*-PLA and *L*-PLA. The enantiomerically pure *L*-PLA is semi-crystalline and has a high mechanical strength.

The racemic mixture, on the other hand, is amorphous and degrades much faster.<sup>76</sup> Chu *et al.* showed that EC growth is poor on PLA scaffolds. To improve EC growth, the surface can be modified with fibronectin for example.<sup>82</sup>

However, the degradation mechanism is still a problem for the usage of PGA and PLA. The initial degradation rate is very low, but as soon as the material has started to degrade and water has been interspersed, the degradation proceeds very fast. In contrast to the re-growth of the natural vessel, the degradation is not a nearly linear process.<sup>83</sup>

*Poly( $\epsilon$ -caprolactone) (PCL)* is an aliphatic polyester and, due to its high hydrophobicity, degrades much slower than PGA or PLA. The degradation takes place by means of hydrolysis and  $\epsilon$ -hydroxycaproic acid is released. The degradation products are immediately removed by macrophages or giant cells.<sup>39</sup> PCL is biocompatible and shows better mechanical properties than PLA and PGA. The degradation rate can be increased via copolymerization with faster degradable polymers.<sup>80</sup>

*Polyhydroxyalkanoates (PHAs)* or polyhydroxy fatty acids are naturally occurring, linear biopolyesters. They are formed by bacteria as reserve material of carbon and energy. PHAs are biodegradable and can be produced synthetically. The most important representatives of polyhydroxyalkanoates are poly(3-hydroxybutyrate), poly(3-hydroxyvalerate), poly(4-hydroxybutyrate), poly(3-hydroxyhexanoate) and poly(3-hydroxyoctanoate).<sup>84</sup> However, it has been shown that inflammation can result in prolonged use in the body and is therefore only partially biocompatible.<sup>85</sup> Nevertheless, PHAs enable cell proliferation and can be used as scaffolds for applications in tissue engineering.<sup>39</sup> Shum-Tim *et al.* implanted an aorta scaffold of PHAs and PGA in a lamb. The replaced vessel showed good mechanical properties even 5 months after

the operation. In order to accelerate cell growth, the scaffold was treated with ovine carotid artery cells.<sup>86</sup>

*Polydioxane (PDO)* is a poly(ether-ester), which consists of an ethylene glycol- and a glycolic acid- unit. It is synthesized via ring-opening polymerization of *p*-dioxanone. PDO is biodegradable and was used as the first absorbable surgical suture material.<sup>87</sup> However, the degradation rate is lower than that of PGA and PLA.

Greisler *et al.* showed that a PDO-based scaffold developed an endothelial layer after only 2 weeks as a rabbit aorta replacement material.<sup>88</sup> By mixing PDO with elastin, the elastic behavior can be improved and mechanical properties similar to those of a natural blood vessel can be achieved.<sup>87, 89</sup>

### *Polyurethanes (PUs)*

Polyurethanes (PUs) are a widely used class of polymers developed by Dr. Otto Bayer and partners.<sup>90</sup> They are characterized by a urethane linkage and are synthesized by the addition reaction of an alcohol and an isocyanate with at least 2 functional groups for both.<sup>91</sup>

In addition, PUs have easily tunable properties due to the wide range of possible starting materials of polyols and diisocyanates.<sup>91</sup> The fields of biomedicine and tissue engineering are emerging applications due to the chemical stability, high surface area and flexibility of PUs. They are used as synthetic scaffolds for cell cultures or vascular grafts, such as synthetic veins or components of a pacemaker.<sup>92, 93</sup>

## 5. Thermoplastic poly(urethane/urea/thiourethane) elastomers

Thermoplastic polyurethane (TPU), polyurea urethane (TPUU) and polythiourethane (TPTU) elastomers are in general block-copolymers based on difunctional diols, diamines or dithiols and diisocyanates. Figure 11 shows the structural differences between urethanes, ureas and thiourethanes.

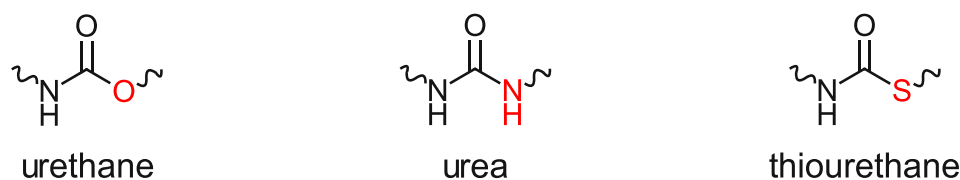


Figure 11: Chemical structures of urethanes (TPUs), ureas (TPUUs) and thiourethanes (TPTUs).

The synthesis is a polyaddition reaction and the degree of polymerization is based on the law of Carothers. Therefore, it is inevitable to use chemicals of high purity and to have exact stoichiometry to obtain a high degree of polymerization and therefore high molecular weights.<sup>94</sup> In contrast to chain growth polymerization, in which monomers are added to a growing polymer chain, in polyaddition two or more reactive monomers, often with different functional groups, are reacted to form a polymer with a more complex structure.<sup>94</sup>

Polyaddition reactions usually combine two or more types of monomers, such as diols and diisocyanates. The reaction proceeds by the formation of covalent bonds between the monomers. Mathematically, the relationship between the degree of polymerization ( $X_n$ ) and the conversion of monomer to polymer ( $p$ ) in a step-growth polymerization can be described by the Carothers equation (Eqn.1).<sup>95</sup> The equation assumes that the polymerization reaction follows a step-growth mechanism, in which two monomers combine to form a dimer, and the dimers then combine to form higher oligomers and finally a polymer.

The Carothers equation is useful for predicting the degree of polymerization and the molecular weight of the resulting polymer as a function of reaction conditions.<sup>96</sup> It can also be used to optimize the reaction conditions to achieve a desired degree of polymerization or molecular weight.

For the factor  $r$ , which describes the stoichiometric ratio of the functional groups of the monomers, the purity of the substances in particular has a major impact. Theoretically, an infinite degree of polymerization could be achieved, but already a deviation of 1% ( $r=0.99$ ) would lead to a maximum degree of polymerization of 199 (Table 1). In Figure 12 the degree of polymerization is plotted against a conversion ( $p$ ) between 0.8 and 1.00 at  $r=1$ , 0.99, 0.975 and 0.95. It can be observed that a deviation of 5% ( $r=0.95$ ) leads to a maximum degree of polymerization of 39 and thus less high molecular weights can be obtained (Table 1).

$$\bar{X}_n = \frac{1+r}{1+r-2rp}$$

Eqn.1

$\bar{X}_n$  degree of polymerization  
 r stoichiometric ratio of functional groups of the monomers,  $r \leq 1$   
 p conversion of monomers

Table 1: Maximum degree of polymerization  $X_n$  at different  $r$  values for a conversion of 1 (100%).

p	$X_{n, \max} (r=1)$	$X_{n, \max} (r=0.99)$	$X_{n, \max} (r=0.975)$	$X_{n, \max} (r=0.95)$
1.00	$\infty$	199	79	39

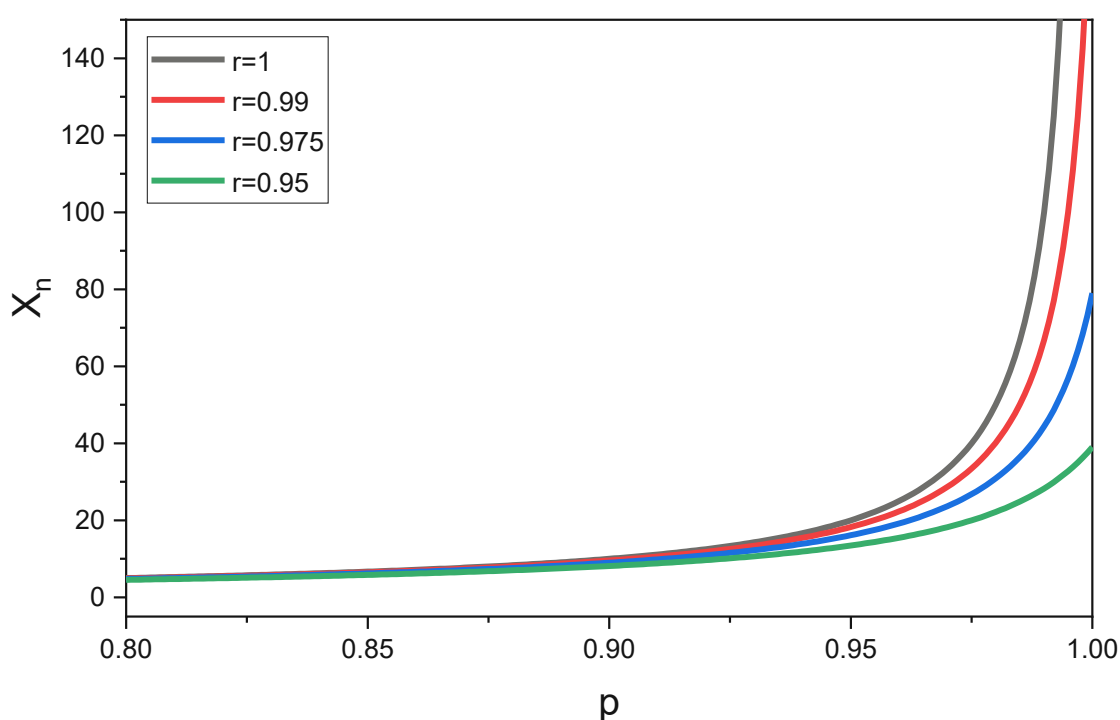
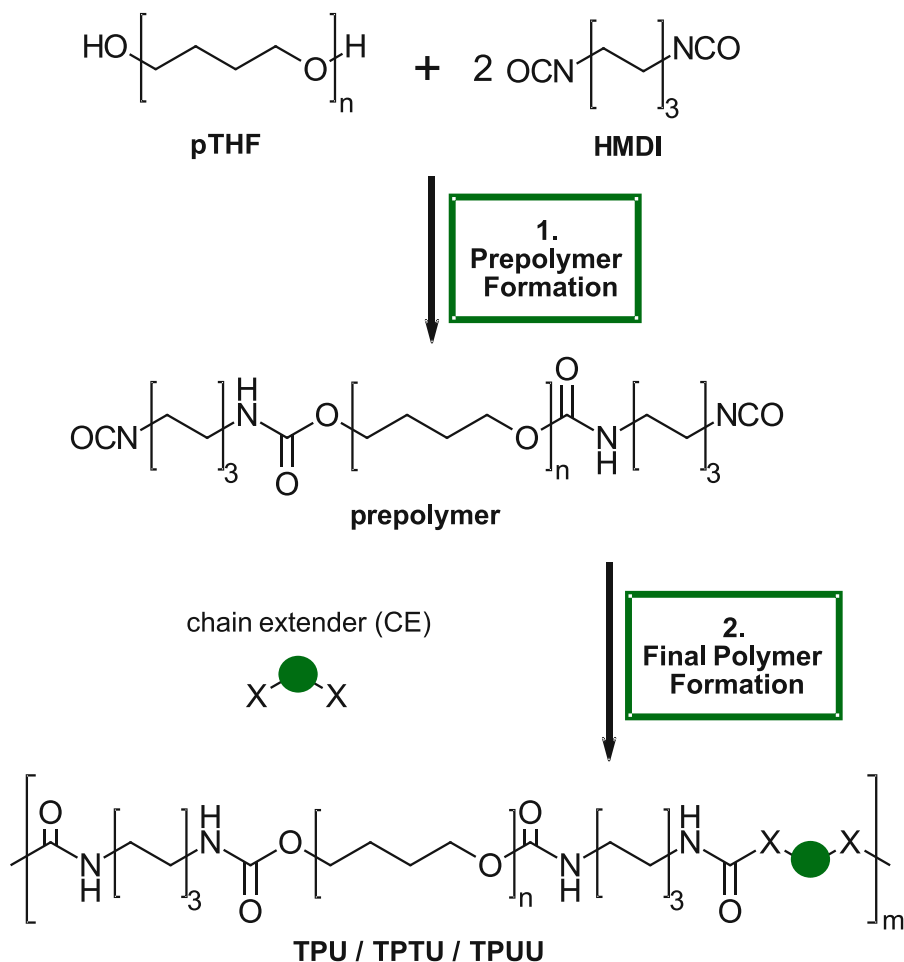


Figure 12: Degree of polymerization  $X_n$ , as a function of conversion  $p$  and  $r$  in a linear step growth reaction.

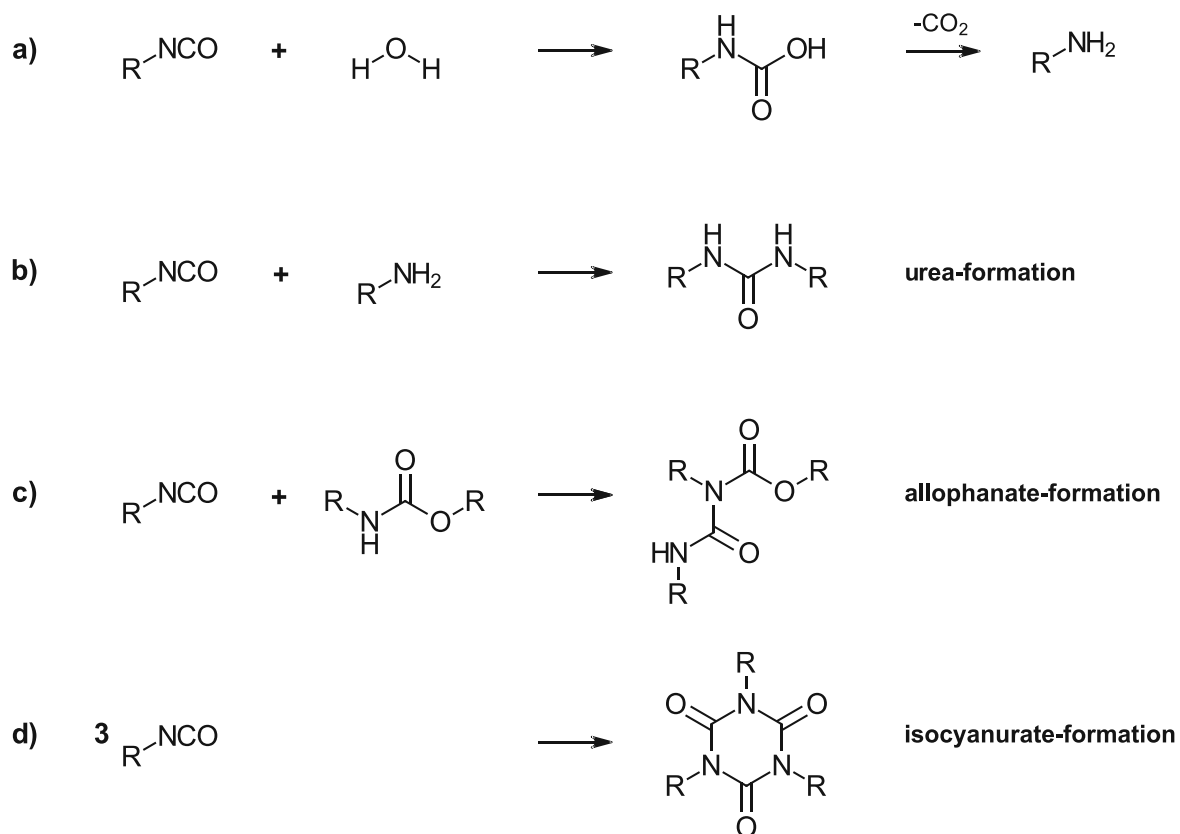
In general, there are two different methods of TPU preparation. The easier way is to use a macrodiol and a diisocyanate to obtain the final polymer via a single step reaction. The more complex way is to use two step prepolymer synthesis by the reaction of macrodiols and diisocyanates resulting in an isocyanate terminated prepolymer (macro-diisocyanate). The final polymer is prepared via the addition of a difunctional chain extender (CE, Scheme 1), which leads to a more homogeneous distribution of the components in the TPU backbone.<sup>97-99</sup> By using a diol as CE, TPUs are obtained. If using diamines or dithiols as CE molecules, TPUUs or TPTUs can be synthesized. To enhance the reactivity of the components, catalysts such as organo-tin compounds or tertiary amines in combination with elevated temperatures are used.<sup>91</sup>



Scheme 1: Two step TPU/TPUU/TPTU synthesis method with chain extenders (e.g. diols, diamines, dithiols),  $X=\text{OH}$ ,  $\text{NH}_2$  or  $\text{SH}$ . Polytetrahydrofuran (pTHF) and hexamethylenediisocyanate (HMDI) are used as examples for macrodiol and diisocyanate component.

To ensure a thorough conversion and to achieve a high molecular weight in TPU synthesis, it is critical to ensure the purity of all reactants. Reduction in the degree of polymerization can be caused not only by impurities but also by side reactions. Excessive moisture in solvents and monomers is a common challenge in TPU synthesis. Isocyanates react rapidly with water to form unstable carbamic acid, which reacts further to form amines with the elimination of carbon dioxide (Scheme 2a). Amines have the ability to further react with isocyanates to form urea compounds (Scheme 2b). While this side reaction is intentionally used in the production of polyurethane foams to utilize  $\text{CO}_2$  as a blowing agent,<sup>100</sup> it creates a stoichiometric imbalance in the production of linear polyurethanes (TPUs). This imbalance occurs between the macrodiol, diisocyanate and chain extender because fewer isocyanate groups are available to react with the chain extender in the second polymerization step.

Other side reactions can occur, such as the addition of an isocyanate group to a urethane group (allophanates-formation, Scheme 2c) or the trimerization of isocyanate groups (isocyanurate-formation, Scheme 2d).



Scheme 2: Possible side reactions of isocyanates during TPU synthesis: Hydrolysis of isocyanates to unstable carbamic acid, followed by decarboxylation to form amines (a), urea formation with amines (b), allophanates formation with urethanes (c) and isocyanurate formation via trimerization (d).

The merging of thermoplastic and elastic properties of thermoplastic poly(urethane/urea/thiourethane) elastomers are obtained via a segmented structure. The thermoplastic properties are achieved by the linear, non-covalently cross-linked structure of the polymer. This is obtained by using only difunctional monomers. Furthermore, the final polymer remains meltable and soluble, which makes it suitable for the electrospinning process. The elastomeric properties, on the other hand, are achieved by the combination of physical crosslinking through hydrogen bonding and the use of flexible difunctional polymers.<sup>101</sup>

Specifically, this is accomplished by forming soft and hard-blocks. The soft-block usually consists of a macrodiol as elastic and amorphous part. The partial crystalline hard-block on the other hand is formed via diisocyanates and the chain extender, a low molecular weight diol, diamine or dithiol. Due to intramolecular hydrogen bond formation between urethane, urea or thiourethane groups physical crosslinking can be obtained.<sup>102</sup>

Besides that, depending on the selected chain extender, further hydrogen bonds can be formed. Due to the modular structure of TPUs, the mechanical properties are highly tunable. Elasticity can be increased by using a higher molecular weight macrodiol for instance and the rigidity can be enhanced by selecting more rigid diisocyanates and CE structures and increasing the ratio of urethane, urea or thiourethane content.<sup>99</sup>



TPUs generally, show glass transition temperatures ( $T_g$ ) far below 0 °C, and therefore no glassy behavior is present at body temperature (application temperature, 37 °C) which makes them suitable as vascular grafts.<sup>103, 104</sup> If materials with a  $T_g$  above body temperature were used, the material would not behave elastically like blood vessels.

Figure 13 demonstrates the aggregation of hard-blocks, resulting in a wide-meshed crosslinked polymer with thermoplastic and elastomeric properties.

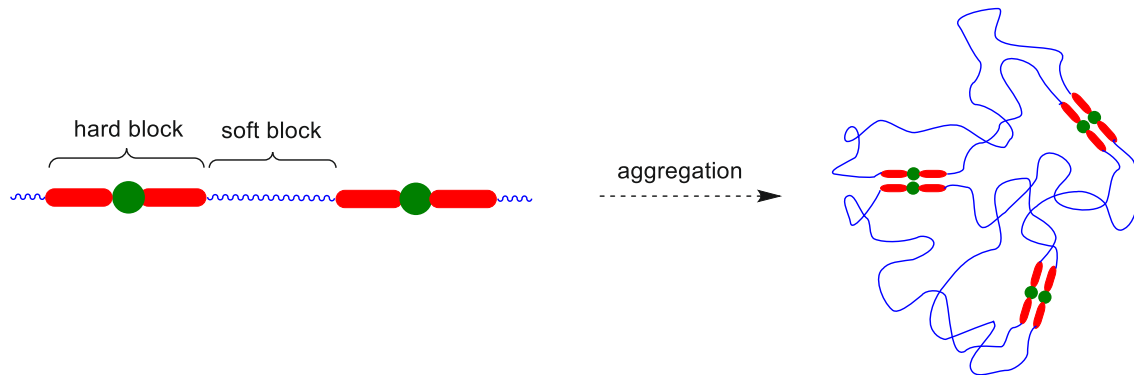


Figure 13: Thermoplastic and elastic properties of TPUs via hard and soft-blocks.

By incorporating degradable motifs into the polymer backbone, it is possible to produce degradable TPUs, TPUUs or TPTUs. In addition to good mechanical properties, the degradability of the polymer is of high interest for vascular tissue engineering.<sup>105, 106</sup> Therefore, cleavable bonds can be induced on the one hand into the hard-block (e.g. cleavable chain extender), or on the other hand into the soft-block (e.g. modified cleavable macrodiols) as shown in Figure 14.<sup>107</sup> Degradation concepts of TPUs, TPUUs and TPTUs is discussed in detail in the State of the Art section of this thesis.

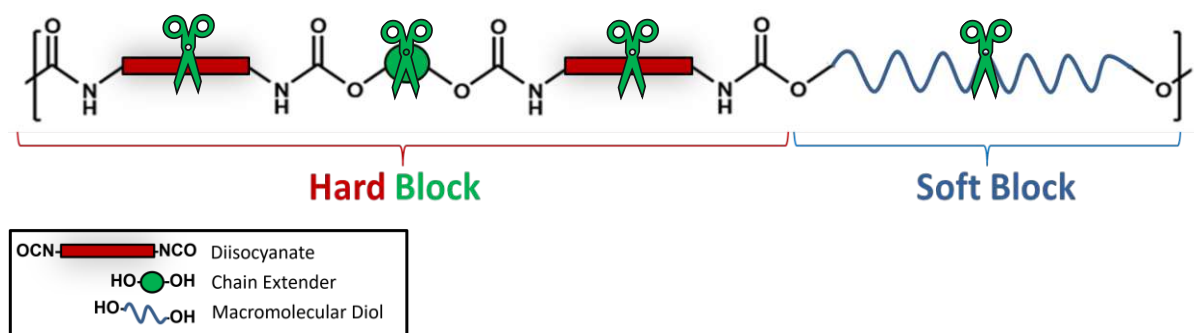


Figure 14: Degradation of TPUs can occur at cleavable groups within the diisocyanate or chain extender (hard-block degradation) or within the macromolecular diol (soft-block degradation).

## OBJECTIVE

---

Numerous studies have shown that thermoplastic polyurethane elastomers (TPUs) can serve as suitable materials for biodegradable vascular implants. These TPUs are divided into soft-block and hard-block degradable TPUs based on their structural composition. However, the focus of research is mainly on soft-block degradable materials, while hard-block degradable polymers are mainly based on the concept of chain extenders with hydrolysable carboxylic esters. These materials must fulfill certain stringent requirements for application as vascular implants:

- They must degrade at a rate that allows new tissue formation.
- Their mechanical properties should be as close as possible to those of natural blood vessels.
- They must be biocompatible and not produce toxic degradation products.

Therefore, the aim of this work is to meet these requirements and to achieve better properties than those that have been developed so far with carboxylic ester-based chain extenders used in hard-blocks. Throughout this research, it should be shown, how the use of new carboxylic esters or the introduction of chain extenders with heteroatom-based degradation motifs could be a possible solution. This includes phosphate esters, silicic acid esters, and boronic acid esters, which, according to the literature, have promising properties that could increase the degradation rate while maintaining sufficiently good mechanical properties:

*Phosphate ester*-based polymers are of increasing interest for applications as biocompatible and biodegradable materials for drug delivery systems or tissue engineering. They show a strong tendency to hydrolytic degradation and can also be degraded by enzymes in a biological environment.

Bifunctional *silicic acid esters* already serve as linkers in polymeric structures and can be degraded under certain conditions by changing their substituents on the silicon atom. This enables increased hydrolytic degradation. For example, methyl groups degrade faster than the bulkier and sterically demanding isopropyl groups.

Due to their structure, *boronic acid esters* can form dynamic B-O bonds, which could enable an improved degradation rate with good mechanical properties at the same time.

In addition to thermoplastic polyurethanes (TPUs) and polyurea urethanes (TPUUs), *thermoplastic polythiourethanes (TPTUs)* are also being investigated to determine whether they can contribute to an improvement in mechanical properties. In contrast to polyurethanes, they should have more ordered domains and higher flexibility due to their sulfur atom.

Apart from these concepts, which are mainly based on the hydrolytic degradation of esters, it would be interesting to investigate other degradation methods such as reductively degradable chain extenders, especially *disulfides*. The chemical structures of the different degradation motifs are presented in Figure 15.

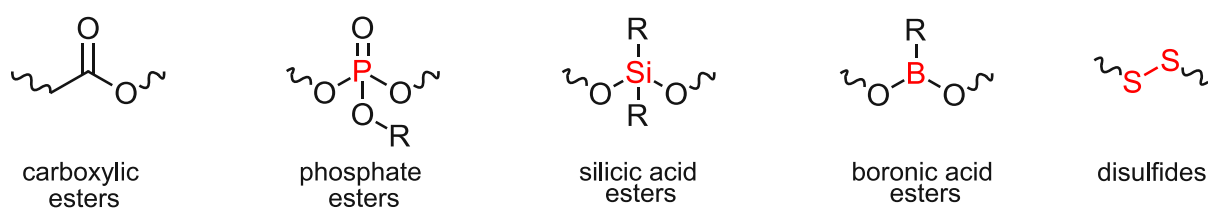


Figure 15: Structural differences between carboxylic esters and heteroatom containing degradable moieties.

# STATE OF THE ART

---

Thermoplastic polyurethanes (TPUs) have emerged as versatile biomaterials and are widely used in biomedicine due to their unique combination of properties. The journey of TPUs as biomaterials began in the mid-20th century, marking an important chapter in the development of flexible and biocompatible materials for medical applications.

The beginnings of polyurethanes date back to the 1930s, when Otto Bayer and his team first synthesized these polymers.<sup>108, 109</sup> However, it was not until the 1950s that researchers realized the potential of polyurethanes as biomaterials, driven by the need for more conformable and biocompatible materials in the medical field.<sup>110</sup> The transition from rigid PUs to thermoplastic polyurethanes (TPUs) expanded their potential applications, particularly in the biomedical field.

In modern medical applications, biodegradable thermoplastic polyurethanes (TPUs) have been of great benefit, particularly in the development of vascular grafts.<sup>111, 112</sup> One example in this area is the Vectra<sup>®</sup> graft, a poly(ether urethane)-urea vascular graft manufactured by Thoratec Corp. in the United States and approved by the U.S. Food and Drug Administration (FDA) in 2000.<sup>111</sup> In the context of developing an optimal small-diameter vascular graft (with an inner diameter of less than 6 mm), anti-thrombosis properties, inhibition of intimal hyperplasia, and facilitation of rapid and adequate endothelialization within the graft lumen are the main expectations.

Various strategies have been employed to address the challenges associated with reducing thrombogenicity and improving intimal hyperplasia inhibition in small-diameter vascular grafts made from biodegradable polyurethanes (PUs). These approaches include surface and compositional modifications with non-thrombogenic components,<sup>113-115</sup> promotion of endothelialization,<sup>116, 117</sup> release of nitric oxide<sup>118, 119</sup> and drug delivery mechanisms.<sup>120, 121</sup>

In an effort to enhance the bioactivity of PU scaffolds, the integration of natural materials such as collagen, elastin, elastin-like peptides (ELP), laminin, fibrin, and decellularized extracellular matrix (ECM) has been explored.<sup>122</sup> The resulting synthetic/natural composites show potential for cardiovascular repair and regeneration.<sup>123-128</sup> This strategic combination aims to exploit the synergistic benefits of the synthetic and natural components and improve the overall efficacy of the biomaterial in the context of cardiovascular applications.

# 1. Degradation motifs of TPUs

In general, degradable TPUs can be divided into two different concepts. One type is hard-block degradation, which is obtained through cleavable groups within the chain extender or diisocyanate. The more prominent concept in the literature is soft-block degradable TPUs, which are obtained by incorporating a cleavable group within the macrodiol. Combinations of both concepts are rarely discussed in the literature.

## 1.1. Hard-block degradation

By applying the concept of hard-block degradation, a degradable macrodiol in the soft-block can be omitted. Since the hydrolytically degradable groups in the macrodiol are mostly polar groups, a more apolar macrodiol can be used. This ultimately leads to better phase separation and therefore better mechanical properties.<sup>129</sup> An example of this is the use of polyethers such as polytetrahydrofuran instead of polyesters.

In principle, the concept of hard-block degradation is based on degradable diisocyanates or chain extenders. However, no directly degradable diisocyanates are known for TPUs as vascular grafts. There is also little information in the literature for other applications. One example is the use of glycolide ethylene glycol glycolide diisocyanate by Bezwada, LLC.<sup>130</sup>

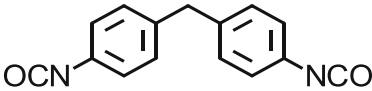
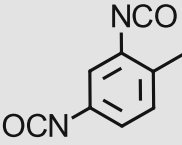
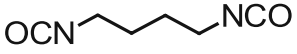
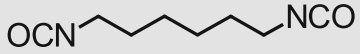
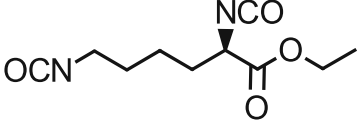
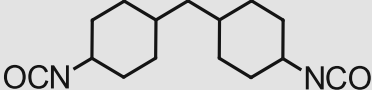
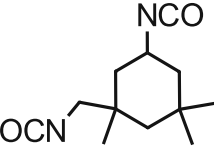
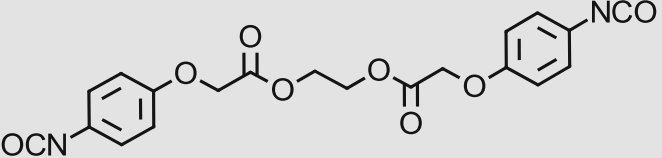
However, the choice of diisocyanate component can still influence degradability. The use of aliphatic structures can reduce the crystallinity of the hard-block and thus increase the degradation rate of the entire polymer structure.<sup>130</sup>

In the initial synthesis of biodegradable thermoplastic polyurethanes (TPU), aromatic diisocyanates, including 4,4'-methylene diphenyl diisocyanate (MDI) and toluene-2,4-diisocyanate (TDI), in combination with biodegradable soft-blocks.<sup>131, 132</sup> However, due to the potential toxicity and carcinogenicity of the degradation products (aromatic diamines), the use of these diisocyanates in the synthesis of biodegradable polyurethanes are limited.<sup>133, 134</sup> As a result, the development of biodegradable TPUs shifted to the use of aliphatic diisocyanates such as 1,4-butane diisocyanate (BDI), 1,6-hexamethylene diisocyanate (HMDI), and lysine-based diisocyanate (LDI), as well as cycloaliphatic diisocyanates such as isophorone diisocyanate (IPDI) and 4,4'-diisocyanato dicyclohexylmethane (H<sub>12</sub>MDI).<sup>122</sup> Among these BDI, HMDI and LDI are the most commonly used linear aliphatic diisocyanates, mainly because of the nontoxicity of their degradation products (diamines and lysine).<sup>135-140</sup>

Research results indicate that the use of more symmetrical diisocyanates results in higher strength and elasticity of the final polymers due to the formation of well-ordered hard segments.<sup>103, 141, 142</sup> Conversely, the use of cycloaliphatic diisocyanates such as IPDI and H<sub>12</sub>MDI limits the flexibility of the polymer chains, resulting in stiffer TPUs compared to TPUs based on linear aliphatic diisocyanates.<sup>143, 144</sup>

Furthermore, the incorporation of LDI can accelerate hydrolytic degradation because it affects the aggregation and hydrophilicity of the hard segments, which is due to the presence of a hydrolysable ester bonds in the side group.<sup>138, 145-147</sup> Table 2 shows a selection of commonly used diisocyanates for hard-blocks of TPUs and a degradable diisocyanate developed by Bezwada, LLC.

Table 2: Selection of used diisocyanates in literature for thermoplastic polyurethanes.

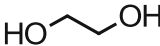
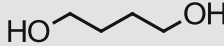
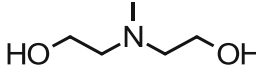
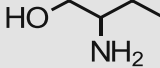
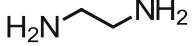
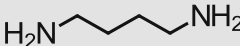
Diisocyanate	Chemical structure	References
4,4'-Methylene diphenyl diisocyanate (MDI)		132
Toluene-2,4-diisocyanate (TDI)		131
1,4-Butane diisocyanate (BDI)		136, 141, 148-151
1,6-Hexamethylene diisocyanate (HMDI)		103, 133, 140, 141, 152-155
Lysine-based diisocyanate (LDI)		138, 145-147, 156-158
4,4'-Diisocyanato dicyclohexylmethane (H <sub>12</sub> MDI)		103, 143, 159, 160
Isophorone diisocyanate (IPDI)		103, 144, 154, 161, 162
Glycolide ethylene glycol glycolide diisocyanate (Bezwada, LLC)		130

In addition to incorporating degradable groups into the diisocyanate component, it is also possible to incorporate degradable functionalities into the chain extender. The following also shows that the chain extender component is much more suitable for incorporating cleavable groups compared to diisocyanates.

Chain extenders play a crucial role in shaping the properties of biodegradable thermoplastic polyurethanes (TPUs), acting as molecular bridges between macrodiols and diisocyanates to form the final polymer chains. The choice of chain extender significantly influences the

mechanical properties and degradation behavior of the resulting polymers.<sup>122</sup> Various low molecular weight diols or diamines are used as chain extenders, including 1,4-butanediol (BDO), ethylene glycol (EG), ethylenediamine (EDA), 1,4-butanediamine (BDA) and propylene glycol.<sup>141, 163-167</sup> Both BDO and BDA have gained popularity as chain extenders because they effectively promote the formation of highly ordered hard segments within the TPU backbone, a key factor in improving the overall strength of the material.<sup>168</sup> The molecular structure of the chain extenders, particularly their symmetry, plays a crucial role in favoring the ordered arrangement of the chain extenders.<sup>130</sup> Table 3 shows the most common used non-cleavable chain extenders for thermoplastic polyurethanes.

Table 3: Selection of non-cleavable chain extenders in literature for thermoplastic polyurethanes.

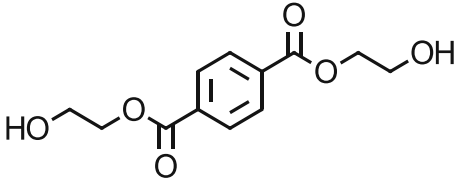
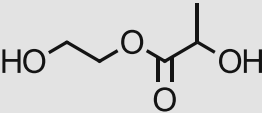
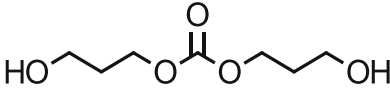
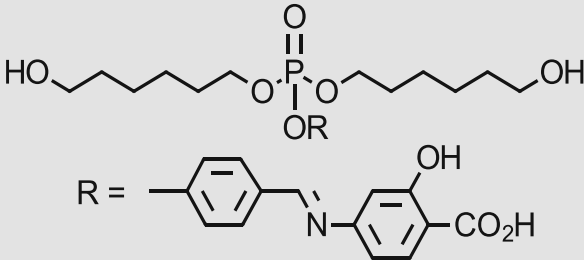
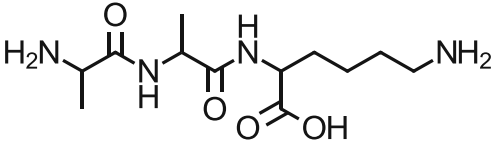
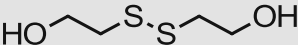
Non-cleavable chain extenders	Chemical structure	References
Ethyleneglycol (EG)		155, 159, 160
1,4-Butanediol (BDO)		132, 148, 169-171
2,2-(Methylimino)diethanol (MDEA)		132, 172
2-Amino-1-butanol (AB)		154
Ethylenediamine (EDA)		125, 162, 173
1,4-Butanediamine (BDA)		136, 149, 151, 174

In addition, the incorporation of hydrolysable bonds into certain chain extenders, such as ester and phosphate ester functions or peptides, can accelerate the breakdown of hard segments within the TPU.<sup>130</sup> For example, incorporation of a degradable ester chain extender based on lactic acid and ethylene glycol was shown to accelerate the hydrolytic degradation of TPUs *in vitro*.<sup>175</sup>

In particular, peptide-based chain extenders have been explored to promote enzyme-mediated degradation and improve biocompatibility in TPUs, providing a new way to tailor the properties of these biomaterials.<sup>130</sup> The use of amino acids as precursors for chain extenders introduces degradable ester bonds and represents an innovative approach to improving mechanical properties while introducing controlled degradation mechanisms.<sup>176-178</sup>

Furthermore, it must be emphasized that the wide variety of chain extension monomers allows the integration of desired functional groups, making them easier to modify than other segments of the polymer chain. The reactive end groups of these monomers, such as alcohols, amines or thiols, form bonds with isocyanate groups, creating urethane, urea and thiourethane bonds, respectively. The simplicity of further diols and diamines such as 1,4-butanedi-amine (BDA)<sup>136, 149</sup>, 2-amino-1-butanol (AB)<sup>154</sup> and 2,2-methyliminodiethanol (MDEA)<sup>132, 172</sup> makes them common non-cleavable chain extenders. For the degradability of hard-blocks, chain extenders with cleavable ester groups such as bis(2-hydroxyethyl)terephthalate (BHET)<sup>103, 129, 133, 179</sup> and Ethylene glycol-lactic acid ester diol (EGLA)<sup>133, 175</sup> have been reported. In addition, cleavable chain extenders based on phosphate esters/organophosphates (OPEs)<sup>180, 181</sup>, disulfide bonds<sup>182, 183</sup> or carbonate functions such as bis(hydroxypropyl)carbonate (BHPC)<sup>152, 183, 184</sup> have been reported. Table 4 shows a selection of cleavable chain extenders for thermoplastic polyurethane elastomers.

Table 4: Selection of cleavable/degradable chain extenders in literature for thermoplastic polyurethanes.

Cleavable chain extenders	Chemical structure	References
Bis(2-hydroxyethyl) terephthalate (BHET)		103, 129, 133, 152, 179
Ethylene glycol-lactic acid ester diol (EGLA)		133, 175
Bis(hydroxypropyl)carbonate (BHPC)		129, 152, 183, 184
Phosphate esters / Organophosphates (OPEs)		181
Alanine-Alanine-Lysine (AAK)		185
2-Hydroxyethyl disulfide (HEDS)		140, 182, 183



## 1.2. Soft-block degradation

Another way to incorporate degradation into thermoplastic polyurethanes is via biodegradable macrodiols. The most commonly used macrodiols are based on ester, ether or carbonate moieties.

Among these, polyester diols are the most commonly used for soft-block degradable TPUs as they are unstable to hydrolytic and enzymatic degradation.<sup>186, 187</sup> The semi-crystalline poly(caprolactone) diol (pCL) has been extensively studied in the synthesis of biodegradable TPUs due to its good biocompatibility and low  $T_g$  (-60 °C), which can lead to high flexibility of TPUs.<sup>188, 189</sup> The partial crystallinity is due to the polarity of the ester groups, which usually results in poorer mechanical properties.<sup>130, 190</sup> In addition, esters are hydrolytically degraded to acidic degradation products, which can lead to inflammation of the surrounding tissue.<sup>191, 192</sup> In addition, they tend to have degradation rates that are difficult to predict due to autocatalytic reactions.<sup>193, 194</sup>

By using poly(carbonate)diols instead of polyesters, the side effect of inflammation can be reduced or eliminated, as CO<sub>2</sub> and alcohols are formed during degradation. In addition, the degradation rate of the graft can be reduced compared to ester-based TPUs, and the degradation rate is more controllable since no autocatalytic reactions occur.<sup>135, 174, 193, 195</sup> Degradable polycarbonates reported in the literature include poly(trimethyl carbonate) (pTMC)<sup>196-198</sup> and poly(1,6-hexamethylene carbonate) (pHMC).<sup>169, 171, 174</sup> These can also be used in combination with pCL as a copolymer to better control the degradation rate.<sup>174</sup>

Ether-based polyurethanes, on the other hand, are resistant to hydrolysis and show good flexibility at low temperatures.<sup>187</sup> However, they are not resistant to oxidation because oxygen breaks the ether bond. This makes the polymer less flexible and brittle.<sup>199</sup>

Copolymers of hydrophilic polyether diols such as polyethylene glycol (PEG), polypropylene oxide (PPO) or polytetrahydrofuran (pTHF) in combination with polyesters can be used to produce soft-block degradable TPUs.

Polyethers may also be used in combination with polycarbonates. Wang *et al.* describe a copolymer based on pTMC, PEG and PPO.<sup>200</sup>

Using a polyether-based copolymer with polyesters or polycarbonates can increase the degradation rate by increasing the hydrophilicity of the polymer.<sup>122, 151, 201</sup> However, copolymerization with polyethers reduces the enzymatic degradability.<sup>201, 202</sup>

In addition to the choice of functional groups in the macrodiol, the molecular weight of the soft-block also has a decisive effect on the final degradation rate and the mechanical properties, which can therefore be fine-tuned.<sup>201, 203, 204</sup> Table 5 shows a selection of polyester-, polycarbonate- and polyether-diols for thermoplastic polyurethane elastomers.

Table 5: Selection of macrodiols in literature for thermoplastic polyurethanes.

Macrodiols	Chemical structure	References
Poly(caprolactone) (pCL)		132, 136, 140, 141, 159, 160, 171, 205
Poly(D,L-lactide) (PDLLA)		125, 173
Poly(trimethyl carbonate) (pTMC)		135, 196-198
Poly(1,6-hexa- methylene carbonate) (pHMC)		169, 171, 174
Polyethylene glycol (PEG)		200
Polytetrahydrofuran (pTHF)		103, 133, 152, 171, 205, 206

## 2. Further concepts for degradable biomaterials

Degradable polymers play a central role in biomaterials, such as temporary implants, degradable sutures and drug delivery systems. Their ability to degrade in a variety of environments and over time without toxic by-products eliminates the need for additional surgery to remove non-degradable implants.<sup>207-209</sup> This helps to reduce recovery time and healthcare costs. Customization of polymer properties enables controlled degradation rates, supporting long-term tissue regeneration and sustained drug delivery.<sup>207</sup>

The biocompatibility requirements of degradable materials exceed those of their non-degradable counterparts, as potential toxic impurities and the toxicity of degradation products must also be considered. The successful use of limited non-toxic monomeric starting materials has contributed to the development of degradable biomaterials.<sup>207, 210</sup>

However, before discussing biodegradable materials in detail, some general terms need to be clarified. Degradation involves the cleavage of bonds leading to structural changes and can occur by hydrolysis, enzymatic activity or exposure to light.<sup>207, 211, 212</sup> The resulting reduction in the molecular weight of the polymer results in a loss of mechanical stability. Hydrolytic or enzymatic degradation is prevalent in therapeutically relevant *in vivo* environments, with the term "biodegradation" reserved specifically for scenarios involving biological entities. The local biological environment, which includes temperature, pH, enzyme concentration, and cell activity, influences the rate of polymer degradation.<sup>207</sup>

Erosion, defined as mass loss that affects the physical size or shape of a component, is critical to the evolution of polymers. There are two different ways of erosion within a polymer.<sup>213</sup> Mass erosion involves mass loss throughout the material, while surface erosion is limited to the surface of the material.<sup>214, 215</sup> Surface erosion is advantageous in drug delivery because it ensures drug release independent of diffusion and allows for easy modification by adjusting the device geometry.<sup>216, 217</sup> Notably, both degradation and erosion processes can occur in the absence of water.<sup>207</sup>

A careful approach to the design, chemistry and function of polymers enables the synthesis of degradable biomaterials with precise and relevant degradation times, leading to the production of non-toxic and functional degradation products, e.g. for drug delivery.<sup>207, 218</sup> Although current investigations are mainly focused on synthetic polymers, especially polyesters, alternative structures such as polyanhydrides or polycarbonates may challenge their dominance in the future.<sup>210</sup> Besides these polymer groups, further carboxylic esters and heteroatom-based polymer classes or functional groups also show interesting properties suitable for biomaterials, such as polyphosphazenes, polyphosphonates, polyphosphoesters, or silicic acid esters, boronate esters, disulfides, respectively.<sup>210, 219-226</sup>

## Carboxylic esters derived from furan

Increasing interest in the synthesis of novel degradable chemicals and materials from renewable resources has inspired the search for new monomers in polymer research.<sup>227-229</sup> This paradigm shift is driven by the urgent need for alternatives to counter the foreseeable depletion of fossil resources and the environmental impact associated with fossil CO<sub>2</sub> emission reduction.<sup>227</sup> While significant efforts are often directed towards novel energy sources, there is an increasing focus on the production of chemical feedstocks from renewable resources, occupying both academic and industrial research.<sup>227, 230</sup>

In this environment, two important non-petroleum monomer precursors derived from polysaccharides or sugars with pentose and hexose units are furfural (Figure 16a) and 5-(hydroxymethyl)furfural (HMF, Figure 16b).<sup>227, 230, 231</sup> These furfural derivatives can be polymerized to yield materials comparable to those derived from fossil monomers, thus providing a sustainable alternative.<sup>227, 231</sup> Although furfural has been an industrial raw material for nearly a century, the production of HMF has been difficult, but recent research shows significant progress.<sup>227, 231</sup> HMF serves as a precursor for important furan monomers, such as furan-2,5-dicarboxylic acid (FDCA, Figure 16c), which have a structural similarity to their aromatic counterparts, making them suitable for the synthesis of polymers, especially polyesters and polyamides.<sup>227</sup> This advance in polymer science embodies a sustainable approach to high-performance materials that contributes to a smaller environmental footprint and is consistent with the goal of a greener future.

Furan-2,5-dicarboxylic acid (FDCA) has the potential to replace terephthalic acid in polyester synthesis.<sup>230, 232, 233</sup> This carbohydrate-derived compound contributes to sustainable and environmentally friendly polymer production.<sup>188</sup> In recognition of its importance, the U.S. Department of Energy has designated FDCA as a priority chemical for promoting a "green" chemical industry.<sup>230</sup>



Figure 16: Chemical structures of renewable furan-based precursors and monomers: Furfural (a), 5-(hydroxymethyl)furfural (HMF, b) and furan-2,5-dicarboxylic acid (FDCA, c).

Polymerization of the dimethyl ester of FDCA with ethylene glycol results in polyethylene-2,5-furandicarboxylate (PEF), a renewable polymer with superior properties compared to polyethylene terephthalate (PET). PEF exhibits improved barrier properties, higher tensile strength, and better recyclability, making it a promising next-generation polyester.<sup>228, 234</sup>

Due to the promising results of PEF compared to conventional PET, an FDCA-based chain extender could also be suitable for the production of TPUs and thus serve as an effective sustainable substitute for conventional aromatic ester-based chain extenders such as bis(hydroxyethylene)terephthalate (BHET).<sup>103, 133</sup>

Besides ester-based chain extenders for degradable thermoplastic polyurethane elastomers, introducing heteroatom-based functional groups, such as phosphate esters, silicic acid esters, boronic acid esters and disulfides into the CE may also show interesting properties as reported in literature.<sup>181, 210, 219-226, 235, 236</sup>

### Phosphate esters

Poly(phosphoesters), PPEs are a widespread class of polymers in nature e.g. as structural part of deoxy- and ribonucleic acid (DNA & RNA). In industry they are used as flame-retardant materials. Besides that, poly(phosphoester)s are getting more interesting as biocompatible and biodegradable polymers for applications such as drug delivery systems or in tissue engineering.<sup>237</sup> The chemical structure of PPEs is shown in Figure 17a.

Unlike polyesters derived from carboxylic acid esters, the phosphorus atom can form three stable bonds in addition to the P=O double bond. This unique ability makes phosphate esters, and PPEs, a versatile tool for modifying the backbone and side chains of synthetic polymers and offers a clear advantage over carboxylic acid esters.<sup>237</sup>

Phosphoester-based polymers have a pronounced tendency to hydrolytic degradation. Furthermore, the phosphoester bond can also be cleaved by enzymes in biological environment, e.g. cleavage by alkaline phosphatase (ALP).<sup>180, 238-240</sup> Therefore, polyphosphoesters are promising candidates for incorporation into regenerative scaffolds, such as those reported by Watson *et al.*<sup>235</sup>

Becker *et al.* reported PPEs synthesized via acyclic diene metathesis polymerization. As side chains located on the phosphorus atom catechol and ethyl groups were chosen to prepare hydrogels for drug delivery or tissue engineering.<sup>236</sup>

Electrospun poly(thioether-phosphoesters) are described by Polloni *et al.* by combining polyesters and phosphate esters with phenolic side groups.<sup>241</sup>

Dahiyat *et al.* introduced phosphate esters into the backbone of degradable polyurethane elastomers to synthesize drug-carrying polymers. As side chain *p*-aminosalicylic acid was used with the spacer molecule *p*-hydroxybenzaldehyde between the phosphorus atom and the active substance to be released (Figure 17b).<sup>181</sup>

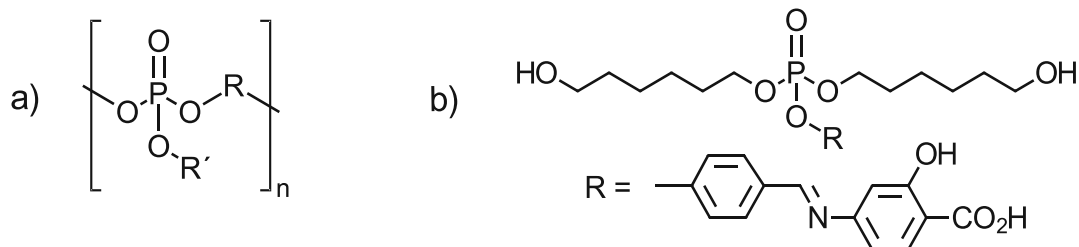


Figure 17: Chemical structures of poly(phosphoesters) in general (a) and a phosphate ester based chain extender with *p*-aminosalicylic acid side chains for drug-carrying polyurethane elastomers by Dahiyat *et al.* (b)<sup>181</sup>

### Silicic acid esters

Apart from phosphate esters, there has recently been increased interest in using silicic acid esters or silyl ethers to synthesize biodegradable and biocompatible materials.<sup>219-221, 242</sup> Silicic acid esters, characterized by the Si-O-C linkage, are widely used as protecting groups in organic chemistry, especially for alcohols.<sup>243-245</sup> Bifunctional silicic acid esters, exemplified by the general linkage O-Si(R)<sub>2</sub>-O, where R could represent any carbon chain, can serve as linkers in polymeric structures (Figure 18).<sup>219</sup>

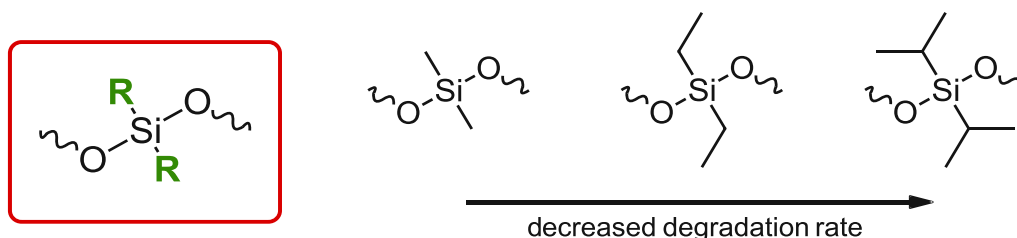


Figure 18: General chemical structure of bifunctional silicic acid esters. R could represent any carbon chain, which determines the degradation rate of the labile Si-O bond.

In addition, the degradation of silicic acid esters results in the formation of non-toxic and non-inflammatory by-products that distinguish them from ester-based molecules. Degradation of esters results in the formation of carboxylic acids, which can induce inflammation in surrounding tissues.<sup>246</sup> However, silicic acid esters exhibit accelerated degradation under acidic conditions, as the rate of degradation decreasing with increased pH value.<sup>219</sup> The degradation of these silicic acid esters can be tailored by modifying their silicic acid ester chemistry, as demonstrated by Parrott *et al.* For example, methyl groups exhibit faster degradation compared to the bulkier, sterically demanding isopropyl groups (Figure 18).<sup>219</sup> Bunton *et al.* prepared degradable crosslinked networks using base-catalyzed addition reactions involving silicic acid ester-containing acrylates and thiols. Controlled release of the drug surrogate, disodium fluorescein, was demonstrated within these networks, highlighting the potential for tailored drug release by manipulating the substituents attached to the Si atom.<sup>247</sup>

In literature degradable silicic acid esters are mainly used for polymer networks.<sup>219, 247</sup> Nevertheless, there are also research groups that deal with linear hydrolytically labile polymers.<sup>221</sup>

Shieh *et al.* introduced a category of cyclic olefins containing bifunctional silicic acid esters. These cyclic olefins exhibit efficient copolymerization with norbornene-based monomers, resulting in copolymers that undergo backbone degradation in mildly acidic aqueous environments. The degradation rates of these copolymers can be adjusted across several orders of magnitude depending on the specific silicic acid esters substituents.<sup>221</sup>

Since the backbone degradation rate of silicic acid esters tends to be lower under neutral conditions compared to acidic pH, the preparation of a CE based on dimethyl esters, in which the steric hindrance around the silicon atom is minimized, looks promising. Furthermore, the higher flexibility of the Si-O bond compared to the C-O bond of esters should lead to novel mechanical properties of the final polymers.<sup>248</sup>

### Boronic acid esters

Another interesting degradable molecule class are boronic acid esters. Boronic acids are mild organic Lewis acids with a trivalent boron atom, substituted with one alkyl and two hydroxyl residues.<sup>249-251</sup> Replacing the hydroxy groups with alkoxy or aryloxy groups is easy due to the lack of hydrogen donor capability, resulting in the formation of boronic acid esters (also called boronate esters or boronic esters)<sup>251-253</sup> (Figure 19a). Furthermore, boronic acids are able to form dynamic covalent bonds with diols.<sup>249, 254, 255</sup>

The stability of the B-O bond, and therefore the equilibrium of the dynamic bond, is dependent on different factors such as the pH value of the solution, steric hindrance of the B-O bond and the acidity of the selected diol and boronic acid. Therefore, the equilibrium of the reaction can be shifted by changing these factors to the boronate ester or to the boronic acid favorable form<sup>256-259</sup>. In general polymers containing boronic acids and the derived esters are used for hydrogels, nanomaterials, molecular sensing and cell capture or culture.<sup>253</sup>

Boronic acid esters have been used for self-healing hydrogels. This innovative approach has potential applications in drug delivery and tissue engineering.<sup>260, 261</sup> Shi *et al.* demonstrated the preparation of hydrogels by incorporating boronic acid-modified hyaluronic acid and PVA. These hydrogels show suitability for drug delivery and encapsulation and protection of neural progenitor cells while avoiding toxic effects.<sup>260</sup>

Cash *et al.* carried out the synthesis of crosslinked boronic ester networks by radical-initiated thiol-ene polymerization using 4-((allyloxy)methyl)-2-(4-vinylphenyl)-1,3,2-dioxaborolane (VPBE, Figure 19b), demonstrating inherent self-healing properties under ambient conditions.<sup>254</sup>

In our research group photopolymerized crosslinked networks via thiol-ene reaction based on the allyl ether 1,4-bis(4-vinyl-1,3,2-dioxaborolan-2-yl)-benzene (VDB, Figure 19c) were prepared via SLA printing, resulting in porous and degradable materials suitable for bone regeneration by Sinaweil *et al.*<sup>223</sup>

Chen *et al.* developed a method for preparing crosslinked rubber with self-healing, formability, and re-processability. Using thermally initiated thiol-ene polymerization of butadiene rubber and the boronic ester-containing crosslinker 2,2'-(1,4-phenylene)-bis[4-mercaptan-1,3,2-dioxaborolane] (BDB, Figure 19d), they synthesized a diene rubber network with permanent crosslinks. The dynamic exchange of boronic ester bonds in these covalently crosslinked rubber networks allows for rearrangement, enabling processes such as healing, reshaping, and recycling.<sup>222</sup> Beside that BDB was also used to prepare liquid crystalline polymer network with exchangeable boronic ester bonds by Saed *et al.*<sup>259</sup>

To the best of our knowledge, no boronic acid ester-based chain extender has been used in thermoplastic polyurethanes, so the concept was transferred from crosslinked polymers to linear poly(thio)urethanes.

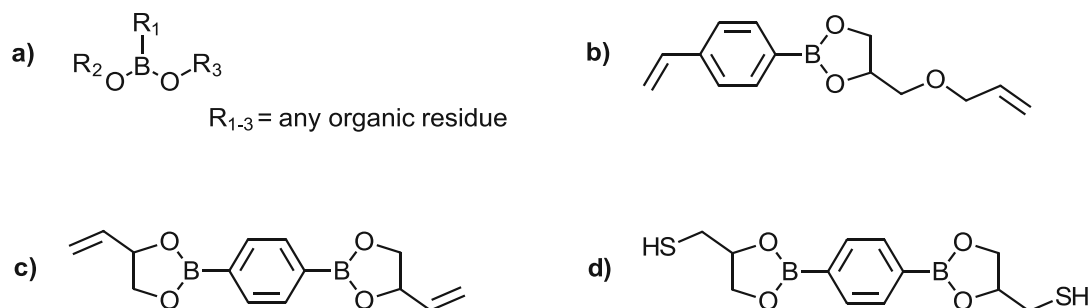


Figure 19: Chemical structures of boronic acid esters (a), 4-((allyloxy)methyl)-2-(4-vinylphenyl)-1,3,2-dioxaborolane (VPBE, b), 1,4-bis(4-vinyl-1,3,2-dioxaborolan-2-yl)-benzene (VDB, c) and 2,2'-(1,4-phenylene)-bis[4-mercaptan-1,3,2-dioxaborolane] (BDB, d).

## Disulfides

In addition to hydrolytically degradable polymer concepts such as esters, silicic acid esters, phosphates and boronic acid esters, a new concept of reduction-responsive biodegradable polymers has emerged in recent years. They represent a compelling route for the development of advanced biomedical materials that enable advanced delivery systems for both biotherapeutics and small molecule drugs. These materials are characterized by the presence of disulfide bonds in the backbone, side chain or as crosslinker.<sup>262</sup> While these disulfide bonds are stable in the bloodstream and extracellular environment, they can be rapidly cleaved in a reductive environment by thiol-disulfide exchange reactions that occur within minutes to hours.<sup>226, 263</sup> This rapid chemical degradation distinguishes them from hydrolytically degradable polymers such as aliphatic polyesters and polycarbonates, which degrade gradually over days, weeks, or months.<sup>264, 265</sup>



Thiol-disulfide exchange reactions, known for their rapid and reversible nature, play a central role in maintaining the biological functions of living cells, including the stabilization of protein structures, enzymatic activity, and redox cycling.<sup>266, 267</sup>

The low molecular weight biological thiol, glutathione (GSH, Figure 20a), together with glutathione disulfide (GSSG) as redox couple, plays a crucial role in maintaining the redox potential in animal cells.<sup>268</sup> In body fluids, extracellular matrices and on cell surfaces, proteins rich in stabilizing disulfides contribute to a relatively high redox potential due to a low GSH concentration. This could be also relevant for vascular implants, where human blood enzymes such as protein disulfide isomerases, thioredoxins, and glutaredoxin-1 can cleave disulfide bonds.<sup>269-272</sup> To mimic an enzymatic/redox active environment, dithiothreitol (DTT, Figure 20b) and tris(2-carboxyethyl)phosphine (TCEP, Figure 20c) can be added in addition to GSH. DTT, a well-established reagent for reducing disulfides in proteins<sup>273, 274</sup>, and TCEP, a bulkier alternative that slowly reduces cysteines in folded proteins<sup>275, 276</sup>, are used for this purpose.

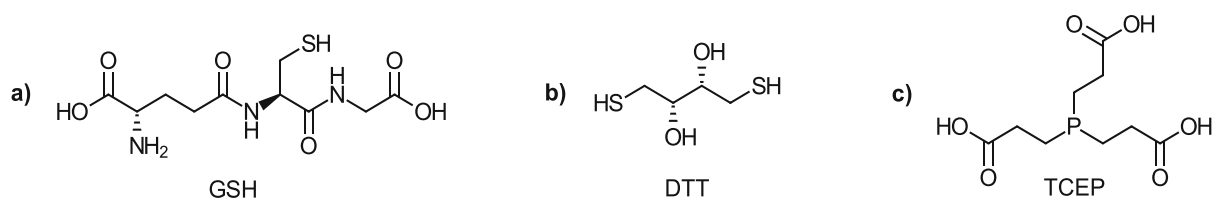


Figure 20: Chemical structures of selected thiols to reduce disulfide bonds under physiological conditions: Glutathione (GSH, a), dithiothreitol (DTT, b) and tris(2-carboxyethyl)phosphine (TCEP, c).

In addition, the presence of redox-active chain extenders with disulfide-cleavable bonds has been documented in the literature. Reductively cleavable chain extenders such as 2-hydroxyethyl disulfide (HEDS)<sup>182, 277</sup>, 11,11'-dithiodiundecanol (DTU)<sup>278</sup> or dimerized L-cysteine esters<sup>279, 280</sup> has been used to significantly accelerate degradation when exposed to glutathione under physiological conditions (Figure 21). While the mechanical properties of the reported thermoplastic polyurethanes were not investigated, also subsequent studies based on these structures did not mention the mechanical properties of the polymers.<sup>225, 281, 282</sup> Zhang *et al.* performed the only study that reported mechanical TPU performance focused on the deactivation of disulfide reversibility without addressing degradability in the presence of a reductive environment.<sup>277</sup>

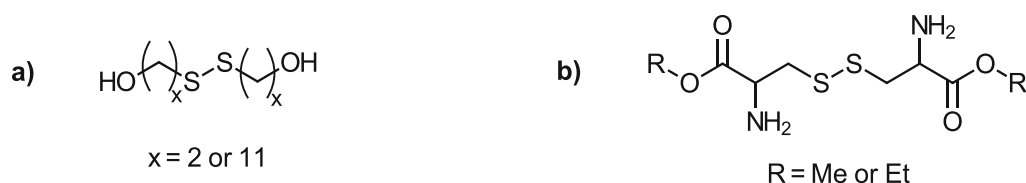


Figure 21: Chemical structures of disulfide based CEs used in literature: 2-hydroxyethyl disulfide (HEDS, x=2, a)<sup>182</sup>, 11,11'-dithiodiundecanol (DTU, x=11, a)<sup>278</sup> or dimerized L-cysteine methyl/ethyl esters (b)<sup>279, 280</sup>.

# GENERAL PART - RESULTS AND DISCUSSION

## 1. Reference polymers

In this chapter, reference polymers and benchmark materials are described. TPU-BHET was selected as internal reference polymer, because it was the first TPU in this research group with a degradable or cleavable chain extender. It was first prepared by Stefan Baudis in his dissertation.<sup>133, 283</sup>

The commercially available Pellethane®-2363-80A (Pellethane, Pell) was taken as template for the design of TPU-BHET. It consists of polytetrahydrofuran (pTHF), the aromatic 4,4'-methylene diphenyl diisocyanate (MDI) and the aliphatic chain extender 1,4-butanediol (BDO) in an unknown ratio.

In Figure 22 the difference of chemical composition between Pellethane and TPU-BHET is shown. For TPU-BHET, the aromatic MDI is replaced by the less toxic aliphatic hexamethylene diisocyanate (HMDI). Furthermore, the aliphatic BDO is replaced by the degradable bis(hydroxyethylene)terephthalate (BHET). It consists of a degradable ester group and replaces the aromatic structure of MDI, which improves the mechanical properties. Another major advantage of BHET is its commercial availability and easy purification by recrystallization from water.<sup>133</sup>

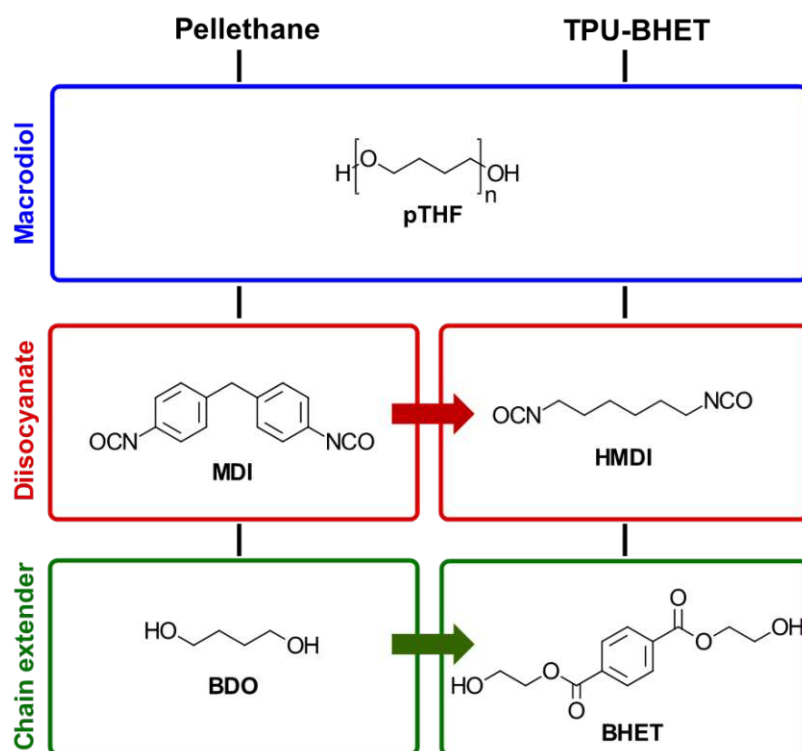
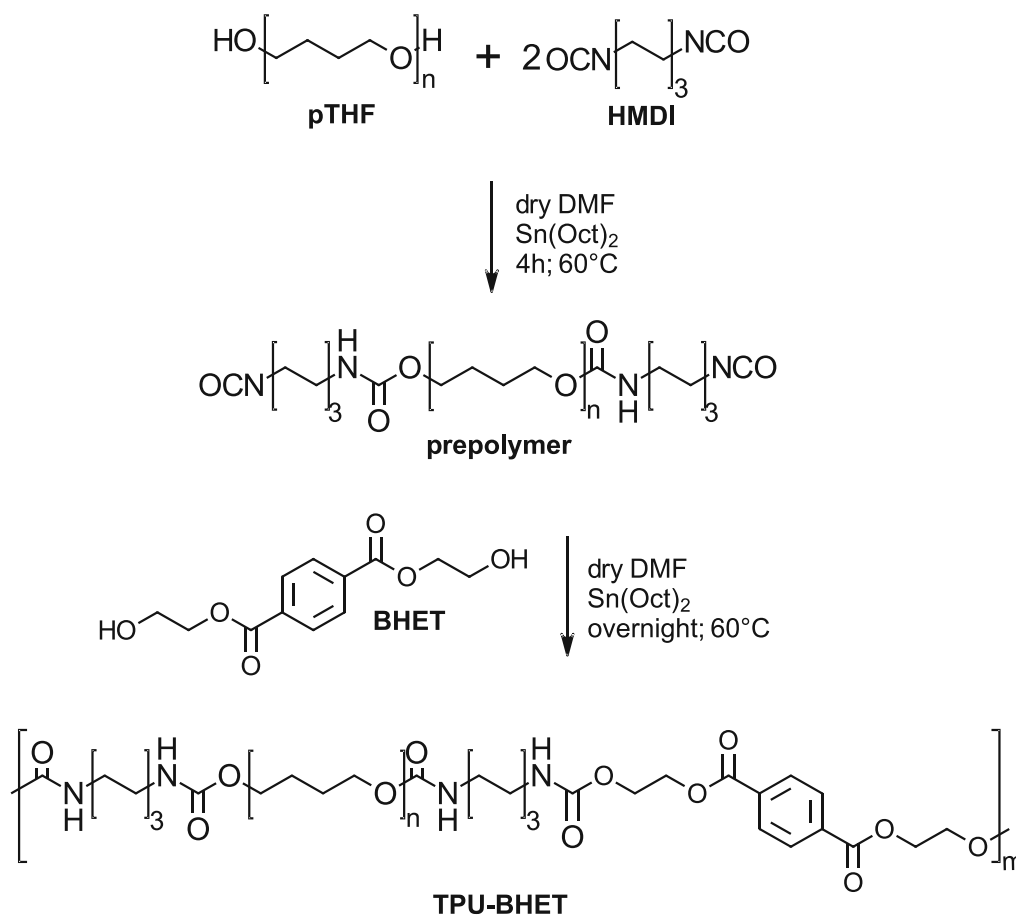


Figure 22: Composition of reference TPUs. The commercially available Pellethane consists of polytetrahydrofuran (pTHF), 4,4'-methylene diphenyl diisocyanate (MDI) and 1,4-butanediol (BDO) as chain extender. In contrast to that TPU-BHET uses aliphatic hexamethylene diisocyanate (HMDI) as diisocyanate and bis(hydroxyethylene)terephthalate (BHET) as degradable chain extender.

## 1.1. General polymer procedure / Synthesis of TPU-BHET

TPU-BHET synthesis was performed via the two-step method. In the first step, the prepolymer is formed via the addition of two equivalents of HMDI to one equivalent of pTHF. The prepolymer could therefore be also described as macro-diisocyanate. In the second step, the addition of the chain extender (BHET) leads to the formation of the final polymer (Scheme 3). Since the best mechanical properties for TPU-BHET were obtained with a ratio of 1/2/1 for pTHF/HMDI/BHET in previous studies by Baudis *et al.*,<sup>133</sup> this ratio was set as standard ratio for all synthesized polymers with one chain extender during this work. In addition, the materials can be better compared with each other with regard to the choice of chain extender if the same ratio is selected in each case.

In order to obtain polymers with a high molecular weight and thus good mechanical properties, side reactions must be avoided and the use of dry and clean reactants and solvents must be ensured. To avoid stoichiometric imbalance, it is also necessary to determine the exact molecular weight of the macrodiol pTHF and the isocyanate content of the diisocyanate HMDI before starting the actual synthesis. Because of the importance of the points just described, they are discussed in detail below.



Scheme 3: Synthesis of TPU-BHET via two-step polymerization. 1<sup>st</sup> step: prepolymer formation from polytetrahydrofuran (pTHF) and hexamethylene diisocyanate (HMDI), 2<sup>nd</sup> step: polyaddition reaction with the chain extender bis(hydroxyethyl)terephthalate (BHET).

## Water content of reactants and solvents

The purity of all reactants is critical in a polyaddition reaction such as the formation of polyurethanes. But not only impurities could lead to a decrease in the degree of polymerization, also side reactions.

A common problem in TPU synthesis, is excessive moisture in solvents and monomers. Therefore, all reactants such as polytetrahydrofuran (pTHF) and chain extenders (CE) were dried (< 0.1 mbar) and were further dried partially at elevated temperatures prior to use. In the production of linear polyurethanes (TPUs), however, side reactions with water leads to a stoichiometric imbalance between pTHF, HMDI and CE, as fewer isocyanate groups are available to react with the CE in the second polymerization step.

## Hydroxy value of polytetrahydrofuran (pTHF)

The exact molecular weight of the used macrodiol polytetrahydrofuran (pTHF,  $\overline{M}_n=1000 \text{ g mol}^{-1}$ ) was determined via hydroxy-value titration according to DIN 53240-1. The hydroxy-value (OHZ) is defined as the amount of KOH (mg), which is necessary to neutralize the acetic acid during acetylation of a defined amount of sample.

The hydroxy-value (OHZ) and the number-average molar-mass ( $\overline{M}_n$ ) was determined in triplicates via Eqn.2. The calculated  $\overline{M}_n$  of the investigated pTHF-batch was  $984 \pm 10.6 \text{ g mol}^{-1}$ , which fits quite well to the value from the data sheet ( $\overline{M}_n=983 \text{ g mol}^{-1}$ ) provided by Sigma-Aldrich.

$$OHZ = \frac{(V_1 - V_2) \cdot c \cdot 56.1}{m} \quad \overline{M}_n = 1000 * \frac{2 \cdot 56.106}{OHZ} \quad \text{Eqn.2}$$

$V_1$  consumption, in mL, of hydrochloric acid for blind value

$V_2$  consumption, in mL, of hydrochloric acid for sample

$c$  actual concentration, in  $\text{m L}^{-1}$ , of hydrochloric acid

$m$  initial sample weight, in g

$\overline{M}_n$  number-average molar-mass in  $\text{g mol}^{-1}$

56.106 molar mass KOH, in  $\text{g mol}^{-1}$

2 number of OH-groups per molecule

OHZ hydroxy-value, in  $\text{mg KOH g}^{-1}$

Table 6: OHZ and resulting  $\overline{M}_n$  via hydroxy-value titration according to DIN 53240-1.

macrodiol	OHZ / $\text{mg KOH g}^{-1}$	$\overline{M}_n$ / $\text{g mol}^{-1}$
Titration 1	114.48	980.2
Titration 2	112.66	996.0
Titration 3	114.99	975.9
<b>pTHF average</b>	<b>114.04</b>	<b><math>984.0 \pm 10.6</math></b>

## Isocyanate-content of hexamethylene diisocyanate (HMDI)

The isocyanate content (wt% NCO) of crude hexamethylene diisocyanate (HMDI) and distilled HMDI was determined according to DIN EN ISO 11909, which describes the weight percent of isocyanate (NCO) moieties in a given sample. Via the addition of a butylamine-solution (2 M), the isocyanates are converted into urea groups. The amount of residual dibutyl amine is determined via titration with hydrochloric acid (0.5 M) (Scheme 4).

The theoretical NCO-content (NCO th.) of HMDI was calculated as 49.96 wt% by Eqn.3.



Scheme 4: General reaction of urea formation due to excess of dibutylamine.

$$\text{NCO th. (wt\%)} = \frac{2 \cdot M_{\text{NCO}}}{M_{\text{HMDI}}} \quad \text{NCO (wt\%)} = \frac{(V_1 - V_2) \cdot c}{m} \cdot 4.2 \quad \text{Eqn.3}$$

$M_{\text{NCO}}$  molecular weight NCO group, 42.02 g mol<sup>-1</sup>

$M_{\text{HMDI}}$  molecular weight hexamethylene diisocyanate, 168.2 g mol<sup>-1</sup>

$V_1$  consumption, in milliliters, of hydrochloric acid during the titration of dibutyl amine solution

$V_2$  consumption, in milliliters, of hydrochloric acid during the determination

$c$  actual concentration, in moles per liter, of hydrochloric acid

$m$  initial sample weight, in grams

The NCO-content of HMDI could be increased by distillation from 47.32 to 49.27 wt % (Table 2). By calculating the ratio of the NCO-content resulting from titration and the theoretical NCO-content, which was determined via Eqn.2, the NCO-activity could be calculated. Therefore, via distillation of HMDI, the NCO-activity could be increased from 94.7 until 98.6 %. As a result, HMDI was always freshly distilled one or two days before TPU synthesis and was stored under argon in the refrigerator.

Table 7: Comparison of NCO-activity before and after distillation of HMDI.

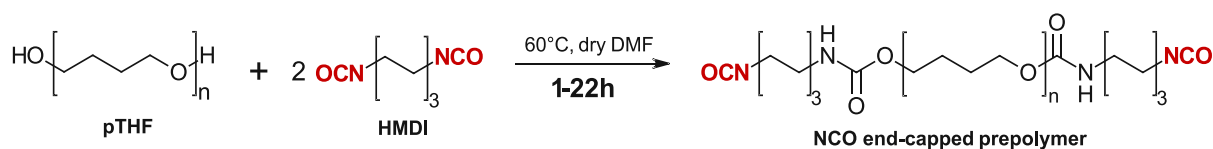
HMDI	NCO-content / wt%	NCO-activity / %*
HMDI crude	47.32	94.7
HMDI after distillation	49.27	98.6
HMDI theoretical	49.96	100.0

\*NCO-activity: ratio of NCO-content and theoretical NCO-content.

## Isocyanate-content of prepolymer

The isocyanate-content (wt% NCO) of the prepolymer (OCN-pTHF-NCO) was determined as described before, according to DIN EN ISO 11909. Via the addition of a butylamine-solution (0.5 M), the isocyanate moieties of not converted HMDI and already formed HMDI end-capped prepolymer (Scheme 5) are converted into urea groups. The amount of residual dibutylamine is determined via titration with hydrochloric acid (0.5 M) (Scheme 4).

The theoretical NCO-content (NCO th.) of the reaction mixture (HMDI and pTHF) was calculated as 12.58 and of the prepolymer after full conversion as 6.29 by Eqn.3. The actual NCO-content during prepolymer formation was determined after 1, 2, 3, 4, 5, 6, 7, 21 and 22 h reaction time via Eqn.4.



Scheme 5: Synthesis of prepolymer for isocyanate content determination.

$$\text{NCO th. (wt\%)} = \frac{M_{\text{NCO}}}{M_{\text{HMDI}} + M_{\text{pTHF}}} \quad \text{Eqn.4}$$

$M_{\text{NCO}}$  molecular weight NCO group, 42.02 g mol<sup>-1</sup>

$M_{\text{HMDI}}$  molecular weight hexamethylene diisocyanate, 168.2 g mol<sup>-1</sup>

$M_{\text{pTHF}}$  molecular weight polytetrahydrofuran, 1000 g mol<sup>-1</sup>

Figure 23 shows the optimum reaction time for the prepolymer synthesis of HMDI and pTHF. The first value at  $t_0$  is the theoretical maximum NCO-content of HMDI and pTHF before any reaction. The reference line at 6.29 is the theoretical value of the prepolymer (HMDI-pTHF-HMDI) and therefore the optimal NCO-content at the end of the reaction. After 3 h nearly the optimal value is reached. The NCO-content is nearly constant between 3 and 5 h before it starts to decrease further below 6.29. This means the optimal reaction time for the prepolymer synthesis is between 3 and 5 h. The further decreasing NCO-content until 22 h could be explained by the formation of allophanates or isocyanurates (Scheme 6) because therefore the total reactive NCO moieties are lower compared to the prepolymer itself.

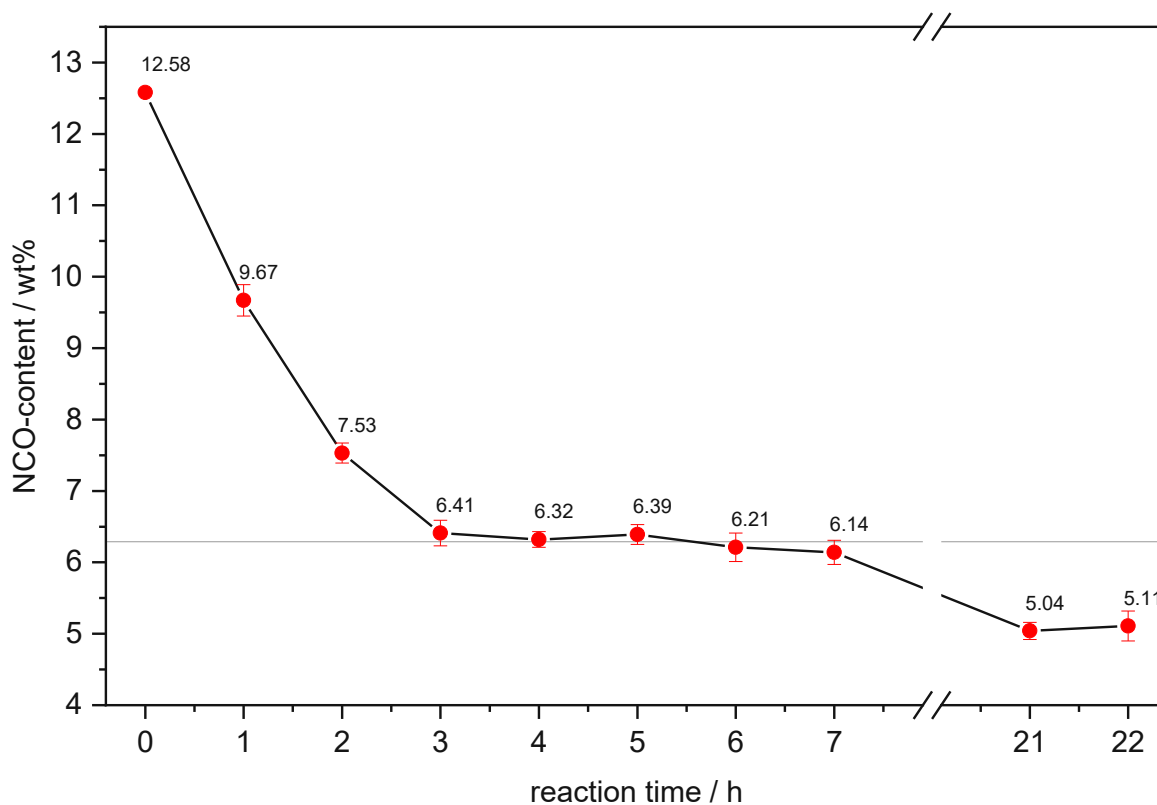
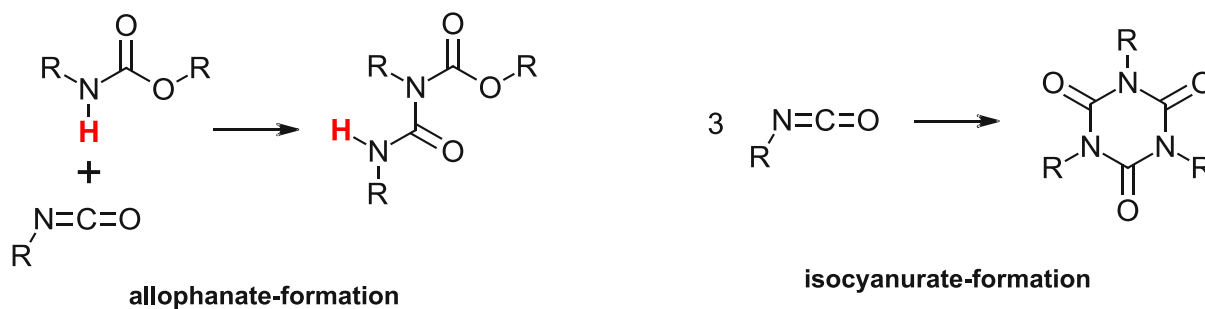


Figure 23: Development of NCO-content (wt%) during prepolymer formation.



Scheme 6: Possible side reactions of isocyanates by increased reaction time of prepolymer formation.

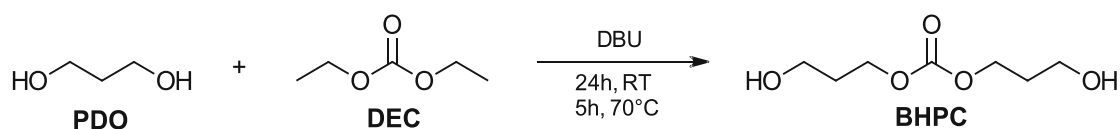
As a result, in contrast to the original synthesis procedure by Baudis *et al.*,<sup>133</sup> the prepolymer formation was prolonged from 2 h to 4 h and the reaction temperature was decreased from 90 °C to 60 °C because isocyanate content determination during prepolymer formation showed an optimum reaction time between 3 - 5 h at 60 °C. The 2<sup>nd</sup> step of the synthesis was also performed at 60 °C overnight.

## 1.2. Synthesis of the CE bis(hydroxypropyl)carbonate (BHPC)

As mentioned above bis(hydroxyethylene)terephthalate (BHET) is an ester-based degradable chain extender. During the ester hydrolysis acidic degradation products such as carboxylic acids are formed, which have a negative effect on healing of human tissue.<sup>246</sup>

Therefore, a new degradable chain extender was developed in this group by Paul Potzmann during his master thesis,<sup>183</sup> which was inspired by the well-known biomaterial poly(trimethylene carbonate) (pTMC).<sup>284, 285</sup> In contrast to the original procedure 1,8-diazabicyclo[5.4.0]undec-7-ene (DBU) was used as catalyst instead of titanium isopropoxide, because titanium complexes require dry reaction conditions.<sup>286</sup> Furthermore, Lohmeijer *et al.*<sup>287</sup> reported the ring-opening polymerization of cyclic esters were it was shown that DBU is more efficient as catalyst than 1,5,7-triazabicyclo[4.4.0]dec-5-ene (TBD). Furthermore, as a conclusion from this study it is possible to synthesize BHPC by using DBU as catalyst without the removal of ethanol via distillation.

The reaction was carried out at room temperature for 24 h. Afterwards the temperature was increased to 70 °C for additional 5 h while the by-product ethanol was continuously distilled off under reduced pressure (400 mbar). The reaction scheme is shown in Scheme 7.



Scheme 7: Synthesis of bis(hydroxypropyl)carbonate (BHPC) via diethyl carbonate (DEC).

During the removal of ethanol, a change from a suspension to a clear solution was observed. Finally, the raw product was purified via column chromatography with ethyl acetate, resulting in a clear liquid, which was characterized via <sup>1</sup>H-NMR spectroscopy (Appendix 2).

Since the synthesis method with ethanol removal has about twice the yield compared to the other method, it was still preferred in this work. This could be explained by the formation of cyclic carbonates by propanediol (PDO) and diethyl carbonate (DEC), which are still easy separable by column chromatography but lead to a decrease in the final yield (28.9 %).



### 1.3. Synthesis of TPU-BHPC

Beside TPU-BHET and purchased Pellethane, the reference polymer TPU-BHPC was prepared with the above described non-acidic degradable chain extender BHPC.

In contrast to the already described BHPC based TPU in this group, which contains poly(hexamethylene carbonate) (pHMC,  $\overline{M}_n = 860 \text{ g mol}^{-1}$ ) as macrodiol,<sup>152</sup> TPU-BHPC for this work was synthesized with polytetrahydrofuran (pTHF,  $\overline{M}_n = 1000 \text{ g mol}^{-1}$ ) as macrodiol instead (Figure 24).

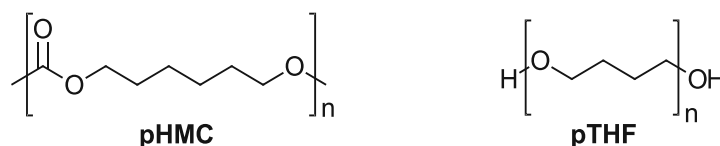
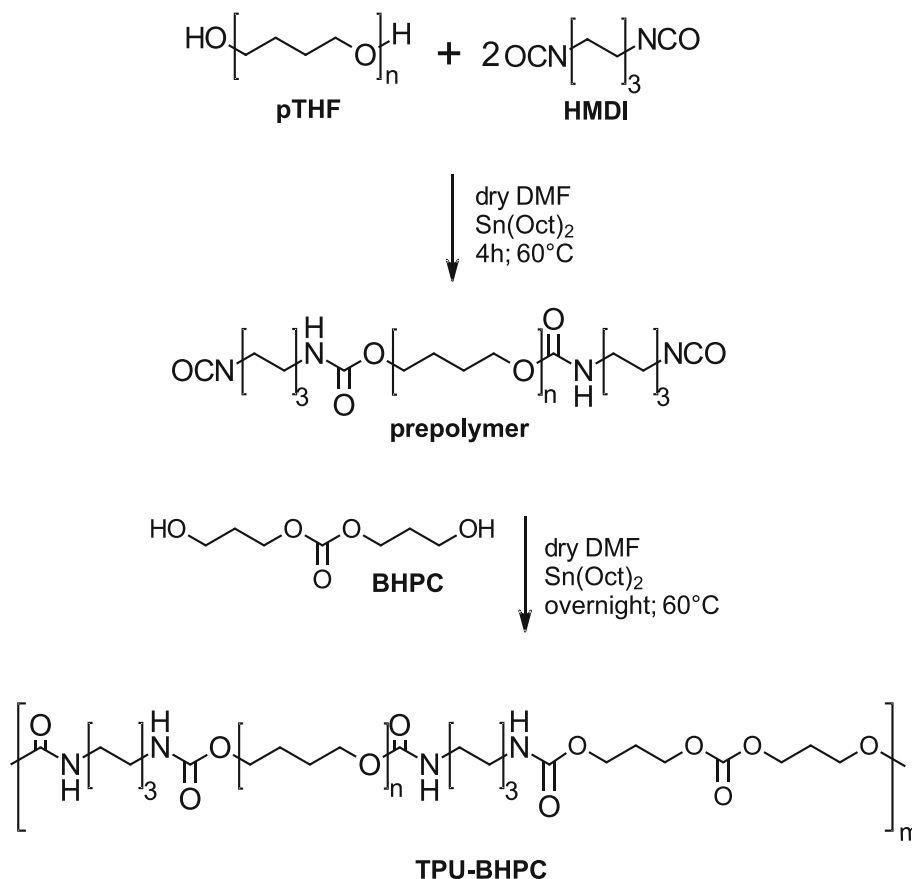


Figure 24: Chemical structures of poly(hexamethylene carbonate) (pHMC) and polytetrahydrofuran (pTHF).

Since pTHF was used as macrodiol in all other polymers during this work, the influence of different macrodiols could be excluded thereby, especially with regard to the mechanical properties. The synthesis of TPU-BHPC was carried out analogously to the synthesis of TPU-BHET with a ratio of 1/2/1 for pTHF/HMDI/BHPC (Scheme 8).



Scheme 8: Synthesis of TPU-BHPC via two-step polymerization. 1<sup>st</sup> step: prepolymer formation from polytetrahydrofuran (pTHF) and hexamethylene diisocyanate (HMDI), 2<sup>nd</sup> step: polyaddition reaction with the chain extender bis(hydroxypropylene)carbonate (BHPC).

## 1.4. General characterization of reference materials

As benchmark material the commercially available thermoplastic polyurethane Pellethane<sup>®</sup> 2363-80A (Pellethane, Pell) was selected because of its easy availability. Pellethane is a non-degradable TPU with very good mechanical properties and already used as small-diameter vascular graft.<sup>288, 289</sup> It consists of polytetrahydrofuran (pTHF), 4,4'-methylene diphenyl diisocyanate (MDI) and 1,4-butanediol (BDO) in a unknown ratio.<sup>290</sup>

Furthermore, the in our working group established TPU-BHET and TPU-BHPC were used as reference polymers.<sup>133, 183, 283</sup> All reference polymers consist of polytetrahydrofuran (pTHF) as soft-block and hexamethylene diisocyanate (HMDI) to enable comparability of the materials depending on the chain extender. The chemical structures of the components of Pellethane, TPU-BHET and TPU-BHPC are shown in Figure 25.

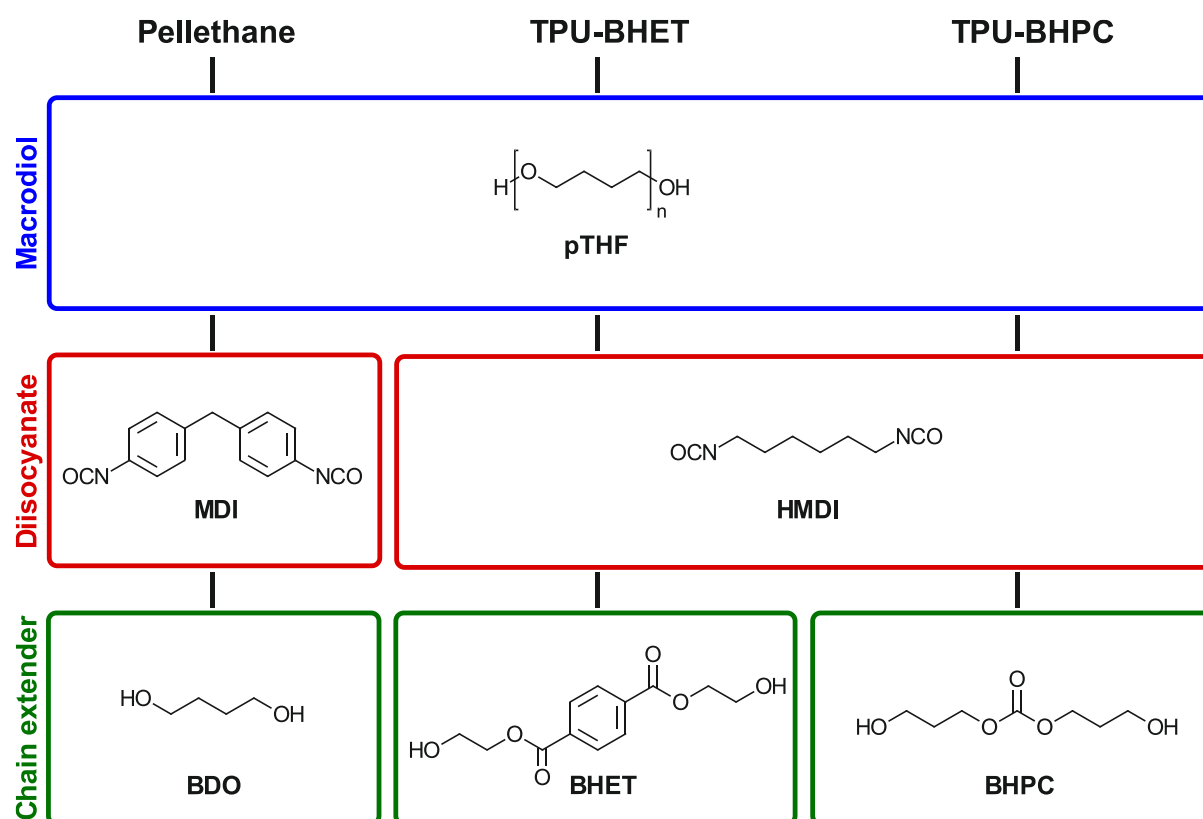


Figure 25: Composition of reference TPUs. The commercially available Pellethane consists of polytetrahydrofurane (pTHF), 4,4'-methylene diphenyl diisocyanate (MDI) and 1,4-butanediol (BDO) as chain extender. In contrast to that TPU-BHET and TPU-BHPC uses hexamethylene diisocyanate (HMDI) as diisocyanate and bis(hydroxyethylene)terephthalate (BHET) or bis(hydroxypropyl)carbonate (BHPC) as chain extender.

## NMR and ATR-FTIR spectroscopy

By means of  $^1\text{H-NMR}$  spectroscopy, the component ratios between macrodiol, diisocyanate and chain extender could be verified. In more detail, the ratio between diisocyanate (HMDI) and the chain extenders (BHET or BHPC) could be determined via the integrals of the  $\text{CH}_2$  peak of HMDI and the aromatic signal of BHET ( $\text{CH}^{\text{Ar}}$ ) or the  $\text{CH}_2\text{-O}$  peak of BHPC, respectively.

Furthermore, by comparing the  $\text{CH}_2$  Signal of pTHF and a chain extender signal the hard-block content could be determined in  $^1\text{H-NMR}$  accuracy, which is described later in more detail. The  $^1\text{H-NMR}$  spectra of all discussed polymers were measured in  $\text{DMSO-}d_6$  and are attached in the appendix (1. NMR spectra). ATR-FTIR spectra are also attached to the appendix section (2. ATR-FTIR spectra).

A very simple but effective method to investigate the formation of hydrogen bonding in segmented polyurethanes is Fourier Transform Infrared Spectroscopy (FTIR).<sup>97, 291</sup> Especially, the amine region ( $\text{N-H}$ ,  $3500\text{-}3100\text{ cm}^{-1}$ ) and the carbonyl region ( $\text{C=O}$ ,  $1850\text{-}1600\text{ cm}^{-1}$ ) gives information about ordered and disordered hydrogen bonds of urethanes and therefore also about the microphase separation of TPUs.<sup>291-294</sup> The amine and carbonyl region of Pellethane, TPU-BHET and TPU-BHPC are shown in Figure 26.

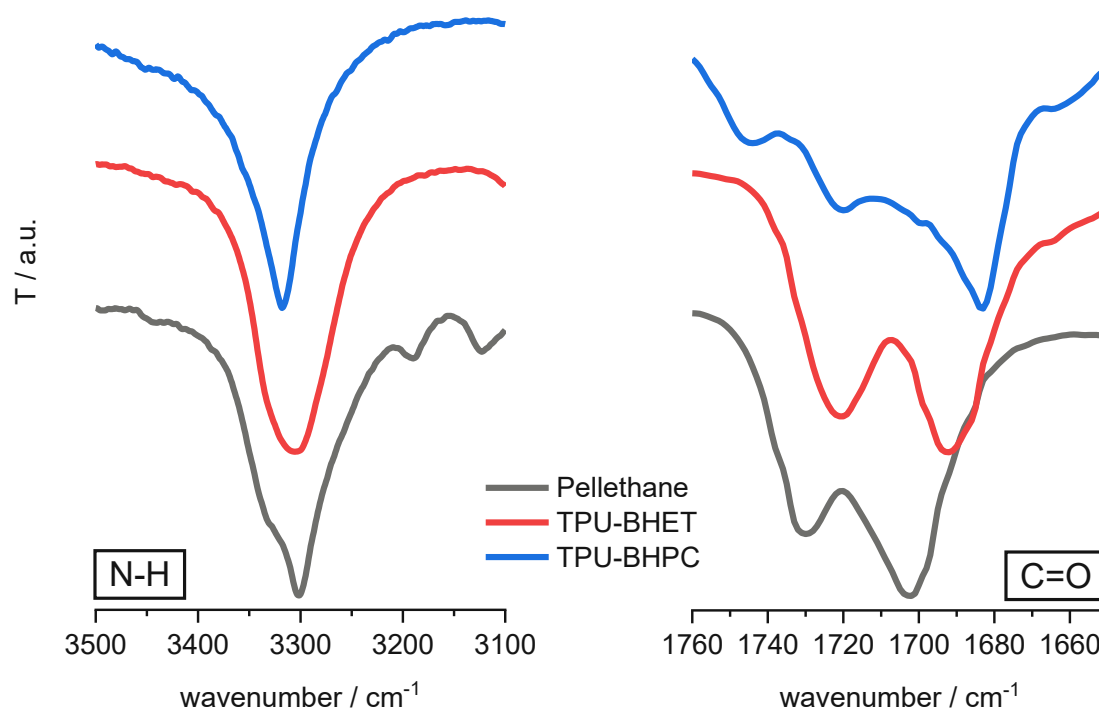


Figure 26: ATR-FTIR spectra of reference polymers Pellethane, TPU-BHET and TPU-BHPC. Two FTIR regions are shown. The amine region ( $3500\text{-}3100\text{ cm}^{-1}$ ) and the carbonyl region ( $1760\text{-}1650\text{ cm}^{-1}$ ), which are both characteristic for the hydrogen bond interactions and therefore for hard-block formation of TPUs.

The amine region shows a shift to higher wavenumbers from Pellethane to TPU-BHPC. Therefore, it can be assumed that TPU-BHPC forms less strong hydrogen bond interactions compared to Pellethane. TPU-BHET shows an amine band between the two other TPUs. Furthermore, a peak broadening can be observed for TPU-BHET and Pellethane compared to TPU-BHPC, which shows us a higher steric hindrance of these polymers. These results from the steric more demanding chain extender BHET (TPU-BHET) and the diisocyanate MDI (Pellethane), which both contain stiff aromatic moieties. Free amines, which would show an absorption band at  $\sim 3450\text{ cm}^{-1}$  could not be observed in any spectra. The carbonyl region, which is shown between  $1760\text{-}1650\text{ cm}^{-1}$ . Each of the investigated polymers show larger signals for the hydrogen bonded carbonyl band ( $1700\text{-}1680\text{ cm}^{-1}$ ), compared to the free C=O band at  $1730\text{-}1720\text{ cm}^{-1}$ , which indicates strong hydrogen bonding interactions for all polymers. Nevertheless, TPU-BHET shows a more intense signal at  $1720\text{ cm}^{-1}$ , which can result from an overlay of free C=O and the ester band of the chain extender bis(hydroxyethylene) terephthalate (BHET). In contrast to the other polymers FTIR spectrum of TPU-BHPC shows also a third signal in the carbonyl region at  $\sim 1750\text{ cm}^{-1}$ , which stems from the carbonate moiety in bis(hydroxypropyl)carbonate (BHPC).<sup>295</sup>

### Hard-block content and molecular weight

The mechanical properties of polyurethanes are determined by the chemical structure and therefore by the choice of macrodiol (MD), diisocyanate (DI) and chain extender (CE). Because thermoplastic polyurethanes are linear macromolecules, the final mechanical properties are furthermore influenced by the flexibility of the macrodiol (soft-block) and the capability to form physical crosslinking between different polymer chains. In our case, the physical crosslinking, is formed by the interaction between the hard-blocks of the different linear polymer chains via hydrogen bonding and therefore the ordered domains are determined by the hard-block content. The soft-block on the other hand determines the amorphous phase of the polymer.<sup>296</sup>

The hard-blocks of the polyurethanes in this work are always consisting of the selected chain extender and hexamethylene diisocyanate (HMDI).

Therefore, it is important to know the hard-block content of the final polymer. The theoretical hard-block content, is given as wt% of hexamethylene diisocyanates (HMDI) and the chain extender (CE) compared to the total weight of the polymer (Eqn.5) for a given ratio of 1:2:1 (MD:DI:CE). The calculated hard-block content can be determined via  $^1\text{H-NMR}$  spectra of the final polymers (Appendix, 1. NMR spectra), by furthermore comparing the integrals of  $\text{CH}_2$  (polytetrahydrofuran) and the integral of representative protons of the chain extender molecule.

$$\frac{M(CE) + 2 * M(DI)}{M(CE) + 2 * M(DI) + M(MD) * f(NMR)} = \%HB_{th/cal} \quad \text{Eqn.5}$$

M	molar mass of CE, DI and MD, g mol <sup>-1</sup>
CE	chain extender
DI	diisocyanate (HMDI)
MD	macrodiol (pTHF)
f(NMR)	<sup>1</sup> H-NMR factor (ratio between pTHF and CE, <b>for %HB<sub>th</sub>=1</b> )
%HB	Hard-block content, in wt%

Due to a constant used ratio of 1:2:1 (pTHF:HMDI:CE) and a comparable molecular weight of the chain extender (CE) the theoretical hard-block content for the reference polymers TPU-BHET and TPU-BHPC is in a narrow range between 34.0 to 37.1 wt% (Table 8). Nevertheless, the hard-block content calculated via <sup>1</sup>H-NMR spectroscopy (Appendix, 1. NMR spectra) is lower compared to the theoretical values and in a range between 31.3 and 33.5 wt%. A reason for that could be a reaction of the prepolymer (OCN-pTHF-NCO) with traces of water, which leads to the formation of amines instead of isocyanates. These are unable to react with the chain extender molecule. As a result, less chain extender can be incorporated in the second synthesis step, leading to a reduction in hard-block content compared to full conversion. For the benchmark material Pellethane, the hard-block content could not be calculated due to an unknown ratio of macrodiol, diisocyanate and chain extender. In addition to the hard-block content, the number-average molar mass  $\overline{M}_n$ , of the polymer also provides an initial insight into the mechanical properties to be expected.<sup>297</sup>

With increasing molecular weight, the following material properties also increase (e.g. tensile strength, melting point, elongation at break, and glass transition temperature  $T_g$ ). However, this comparison can only be made for structurally similar polymers.<sup>297</sup> In addition, also the polydispersity index (PDI) is an important material factor, which is obtained from GPC measurements. It is defined as the ratio of the mass-average molar mass  $\overline{M}_w$  and the number-average molar mass  $\overline{M}_n$  and describes the molecular weight distribution of the polymer.<sup>298-300</sup> Table 8 shows the number-average molar mass  $\overline{M}_n$  and the PDI of TPU-BHET, TPU-BHPC and the benchmark material Pellethane obtained from GPC measurements via triple-detection calibration method. Pellethane shows the highest  $\overline{M}_n$  followed by TPU-BHET and TPU-BHPC. The PDI of 1.7 to 2.1 are quite narrow for polymers, which were synthesized via polyaddition reaction. Therefore, TPU-BHPC shows a bit of a more uniform molecular weight distribution compared to Pellethane and TPU-BHET, respectively.

Table 8: Overview of reference polymers TPU-BHET, TPU-BHPC and commercially available Pellethane in terms of number-average molar mass  $\overline{M}_n$ , polydispersity (PDI) and hard-block content (theoretical and calculated).

polymer	$\overline{M}_n$ / kDa <sup>a</sup>	PDI <sup>b</sup>	HB <sub>th</sub> / wt% <sup>c</sup>	HB <sub>cal</sub> / wt% <sup>d</sup>
TPU-BHET	23.3	2.1	37.1	33.5
TPU-BHPC	17.3	1.7	34.0	31.3
Pellethane <sup>®</sup>	56.3	1.9	-	-

<sup>a</sup> Number-average molar mass. <sup>b</sup> polydispersity. <sup>c</sup> theoretical hard-block content (HB<sub>th</sub>).

<sup>d</sup> calculated hard-block content from <sup>1</sup>H-NMR (HB<sub>cal</sub>).

## 1.5. Mechanical and thermal properties of references

To evaluate the suitability of a TPU for use as a vascular graft, mechanical properties such as elongation at break, ultimate tensile strength, and elastic modulus can be determined. The mechanical properties of the final graft should be as close as possible to those of the natural tissue, since, for example, a mismatch between the elastic modulus of the implant and the natural tissue is one of the major causes of graft failure.<sup>152, 301</sup>

The mechanical properties were determined via tensile testing of solution cast polymer films (ISO 527, Type 5B, bone-shaped). The sample thickness was between 20 and 40  $\mu\text{m}$ . Detailed description of solution casting and tensile testing is shown in the section Materials and Methods.

The glass transition temperature  $T_g$  was determined via Dynamic Mechanical Thermal Analysis (DMTA) by the maximum of the loss modulus curve (Appendix, 3. DMTA spectra) to evaluate the suitability of the material at body temperature, as a  $T_g$  higher than 37 °C would mean a brittle and “glassy” behavior of the TPU at application temperature as vascular graft.

In Table 9 the reference polymers are compared in terms of  $\overline{M}_n$ , calculated hard-block content, mechanical properties and glass transition temperature. For a better overview, the mechanical properties are furthermore shown graphically in Figure 27. At first view, it can be observed that with increasing molecular weight  $\overline{M}_n$ , the elongation at break and the ultimate tensile strength also increase and the elastic modulus decreases. However, this can also be attributed to the structure of the chain extenders or diisocyanates. As in previous studies, it could be shown that the ultimate tensile strength can be increased with aromatic structures.<sup>133, 152</sup> Especially Pellethane, which uses MDI as diisocyanate, shows outstanding mechanical properties.

Table 9: Comparison of number-average molar mass  $\overline{M}_n$ , calculated hard-block content, mechanical properties and glass transition temperature of reference polymers TPU-BHET and TPU-BHPC with the reference Pellethane.

polymer (CE)	$\overline{M}_n$ / kDa <sup>a</sup>	HB <sub>cal</sub> / wt% <sup>b</sup>	$\epsilon_b$ / % <sup>c</sup>	TS / MPa <sup>d</sup>	E / MPa <sup>e</sup>	$T_g$ / °C <sup>f</sup>
BHET	23.3	33.5	1315 $\pm$ 54	14.1 $\pm$ 0.7	31.0 $\pm$ 1.4	-71
BHPC	17.3	31.3	878 $\pm$ 75	12.8 $\pm$ 0.9	22.5 $\pm$ 0.3	-57
Pellethane <sup>®</sup>	56.3	-	1651 $\pm$ 115	25.2 $\pm$ 1.2	14.2 $\pm$ 0.3	-52

<sup>a</sup> Number-average molar mass. <sup>b</sup> calculated hard-block content from <sup>1</sup>H-NMR (HB<sub>cal</sub>). <sup>c</sup> Elongation at break  $\epsilon_b$ .

<sup>d</sup> tensile strength TS. <sup>e</sup> elastic modulus E. <sup>f</sup> Glass transition temperature  $T_g$  obtained from the maxima of loss modulus curves.

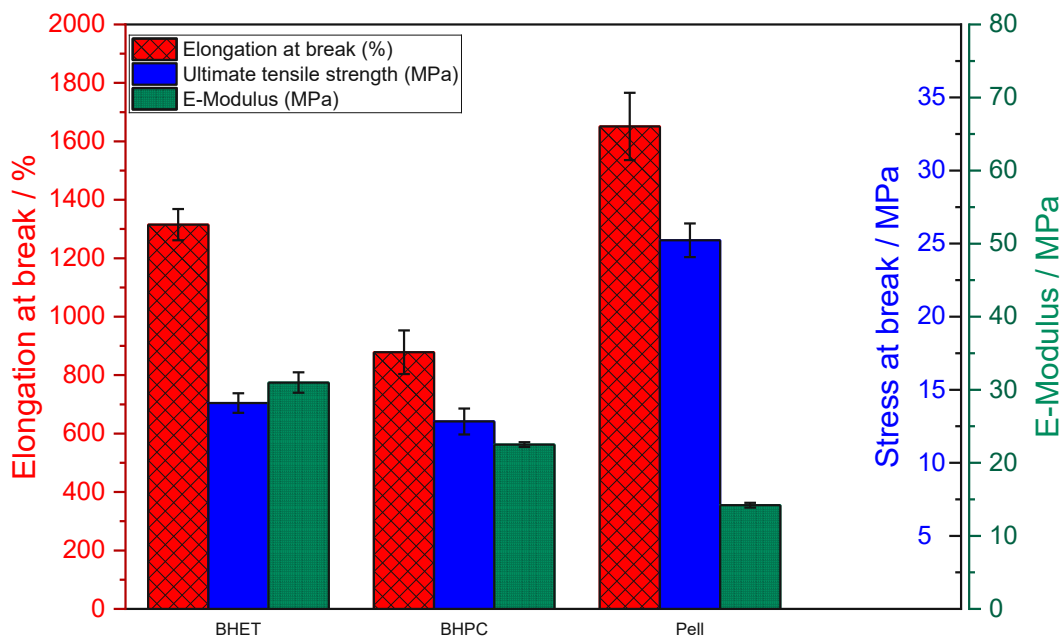


Figure 27: Elongation at break, ultimate tensile strength and elastic modulus of TPU-BHET and TPU-BHPC in comparison with commercially available Pellethane.

Particularly the combination of high elongation at break, high ultimate tensile strength and low elastic modulus of the final graft should be emphasized as these mechanical properties fits quite well to the natural tissue of blood vessels. This is also a main reason why Pellethane is a suitable material for vascular grafts, since there is no mismatch between the E-modulus of the implant and the natural blood vessel.<sup>152, 301</sup>

TPU-BHPC shows the lowest elongation at break and ultimate tensile strength, which can be explained by the non-aromatic chain extender compared to TPU-BHET. Representative Stress-Strain curves of Pellethane, TPU-BHET and TPU-BHPC are shown in the Appendix section 4. Tensile testing.

Furthermore, the strength of the hydrogen bond interactions, which was shown before by IR spectroscopy (Figure 26) matches with the observations of the respective mechanical properties: Pellethane shows the highest hydrogen bond interactions, TPU-BHPC the lowest. The glass transition temperature  $T_g$  determined via DMTA (Table 9) are for all reference polymers below 0 °C. That shows that they are all flexible at body temperature and therefore they are all suitable for vascular tissue engineering from this point of view.<sup>129</sup> TPU-BHET shows the lowest  $T_g$  (-71 °C), followed by TPU-BHPC (-57 °C) and Pellethane (-52 °C), which fits to the already obtained results from previous studies.<sup>103, 152</sup>

## 1.6. Degradation behavior of reference polymers

Degradation behavior of TPU-BHET and Pellethane was investigated in terms of mass loss and molecular weight reduction. Therefore, circular specimens were punched out of solution cast polymer films with a diameter of 1 cm, and a mass between 20 and 30 mg. They were stored for 70 days in PBS buffer solution (pH=7.4, 4x) with a fourfold salt concentration to avoid an exceedance of the buffer capacity. Furthermore, degradation studies were performed at body temperature (37 °C) and at elevated temperatures (90 °C) to accelerate possible degradation.

In Figure 28 the mass erosion of the reference polymers TPU-BHET and Pellethane are compared at 37 °C and 90 °C over a time period of 70 days. As previous studies showed, Pellethane is not degrading at body temperature and shows only a very small mass reduction at 90 °C.<sup>103, 152</sup> TPU-BHET as a hard segment degrading polymer shows mass loss at both temperatures as expected. However, it must be emphasized that the degradation rate is higher in the first few days and decreases as the degradation time increases.

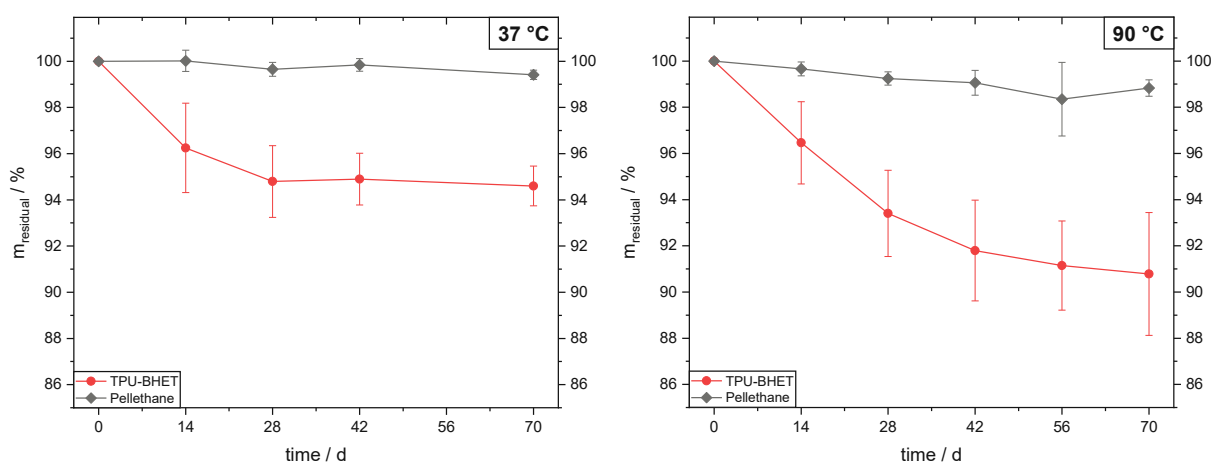


Figure 28: Residual mass  $m_{\text{residual}}$  in % of TPU-BHET and commercially available Pellethane in PBS buffer solution (4x) at 37 °C (left) and at 90 °C (right).

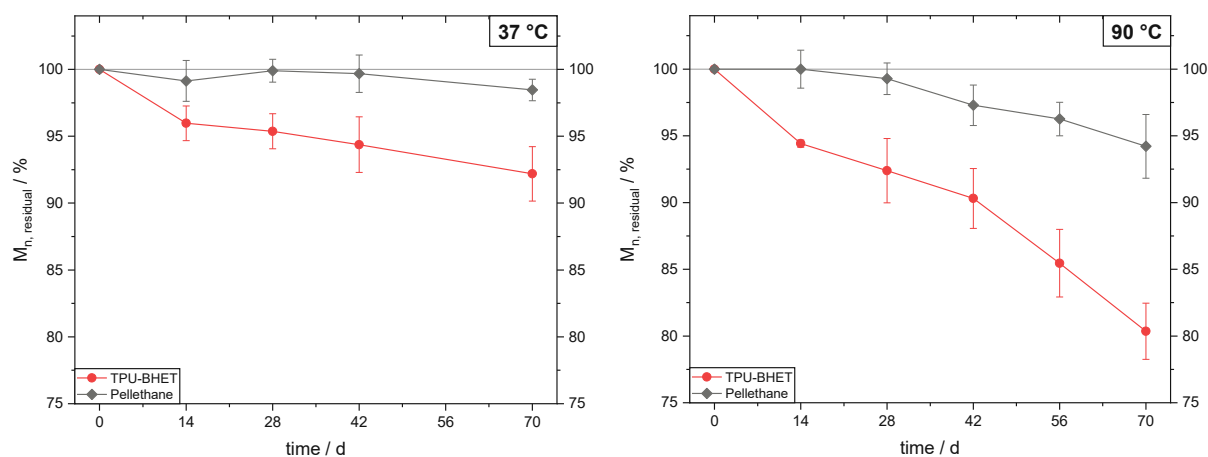


Figure 29: Development of number-average molar mass  $\overline{M}_n$ , residual in % of original  $\overline{M}_n$ , before degradation over a time period of 70 d of TPU-BHET and Pell as reference in PBS buffer solution (4x) at 37 °C (left) and 90 °C (right).



In Figure 29 the change of the number-average molar mass  $\overline{M}_n$  is plotted against the degradation time at 37 °C and 90 °C. Pellethane shows nearly no  $\overline{M}_n$  change at body temperature, but a surprisingly significant decrease at 90 °C. TPU-BHET shows a more constant decrease of  $\overline{M}_n$  compared to the mass erosion.

Comparing the mass erosion and the molecular weight change, information about the degradation mechanism can be concluded. A possible distinction is made between surface and bulk erosion.<sup>213</sup> For surface erosion, a more or less linear mass loss is generally observed. The molecular weight should not change, as only the surface starts to degrade. A bulk eroding material is characterized by a  $\overline{M}_n$  decrease and a mass erosion. In addition, mass erosion often begins with a certain time delay, as the degradation medium needs time to penetrate the material at bulk eroding materials. TPU-BHET shows a simultaneous reduction in mass and molecular weight and could therefore be classified as a bulk erosion material. As Pellethane, shows only a small reduction of  $\overline{M}_n$  at 90°C. Both polymers, TPU-BHET and Pellethane are used as reference TPUs for all following degradation studies. TPU-BHPC was not selected as reference polymer to evaluate the degradation behavior, as BHPC is not a carboxylic acid ester-based CE as the CEs discussed in the next two chapters, because it is derived from carbonic acid.

The reference polymer TPU-BHET was successfully prepared as in previous studies by Baudis *et al.*,<sup>133</sup> but the reaction conditions of the prepolymer synthesis step were changed based on more detailed investigations using NCO end group titration. The second reference polymer, TPU-BHPC, was modified compared to the work of Paul Potzmann<sup>183</sup> by using the macrodiol polytetrahydrofuran (pTHF) instead of poly(hexamethylene carbonate) (pHMC). This allows a better comparability of the chain extender molecules due to the same structure of the prepolymer (pTHF+HMDI). Both reference polymers show good mechanical properties. However, the incorporation of a degradable chain extender in both polymers leads to a downgrading of all three measured parameters compared to the benchmark material Pellethane. Specifically, there is a decrease in elongation at break, a decrease in ultimate tensile strength and an increase in stiffness. Degradation studies at 37°C and 90°C in PBS buffer solution (pH=7.4) showed the positive influence of the chain extender BHET on an increased degradation rate compared to Pellethane.

## 2. Further carboxylic ester-based CE

Furan-2,5-dicarboxylic acid (FDCA), is a remarkable renewable building block that has the potential to replace terephthalic acid in the synthesis of polyesters and various existing polymers with aromatic structural components.<sup>230, 233</sup> This unique compound can be derived from certain carbohydrates, making it a sustainable and environmentally friendly resource.<sup>233</sup> Recognizing its importance, the U.S. Department of Energy has identified FDCA as one of 12 priority chemicals to spur the development of a "green" chemical industry and enable a greener future.<sup>230</sup>

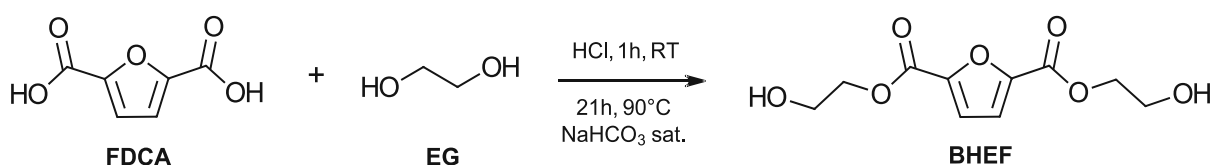
When the dimethyl ester of FDCA is polymerized with ethylene glycol, polyethylene 2,5-furandicarboxylate, commonly known as PEF, is formed. PEF has a remarkable set of physical, mechanical, and thermal properties compared to those of polyethylene terephthalate (PET).<sup>228, 234</sup> This promising development in polymer science paves the way for sustainable, high-performance materials with a smaller environmental footprint.

For this reason, the chain extender bis(2-hydroxyethyl)furan-2-5-dicarboxylate (BHEF) produced from FDCA (Scheme 9) is expected to perform similar in TPU-BHEF to the previously well-studied chain extender (CE) bis(hydroxyethylene)terephthalate (BHET) in TPU-BHET.<sup>103,</sup>

133

### 2.1. Synthesis of BHEF

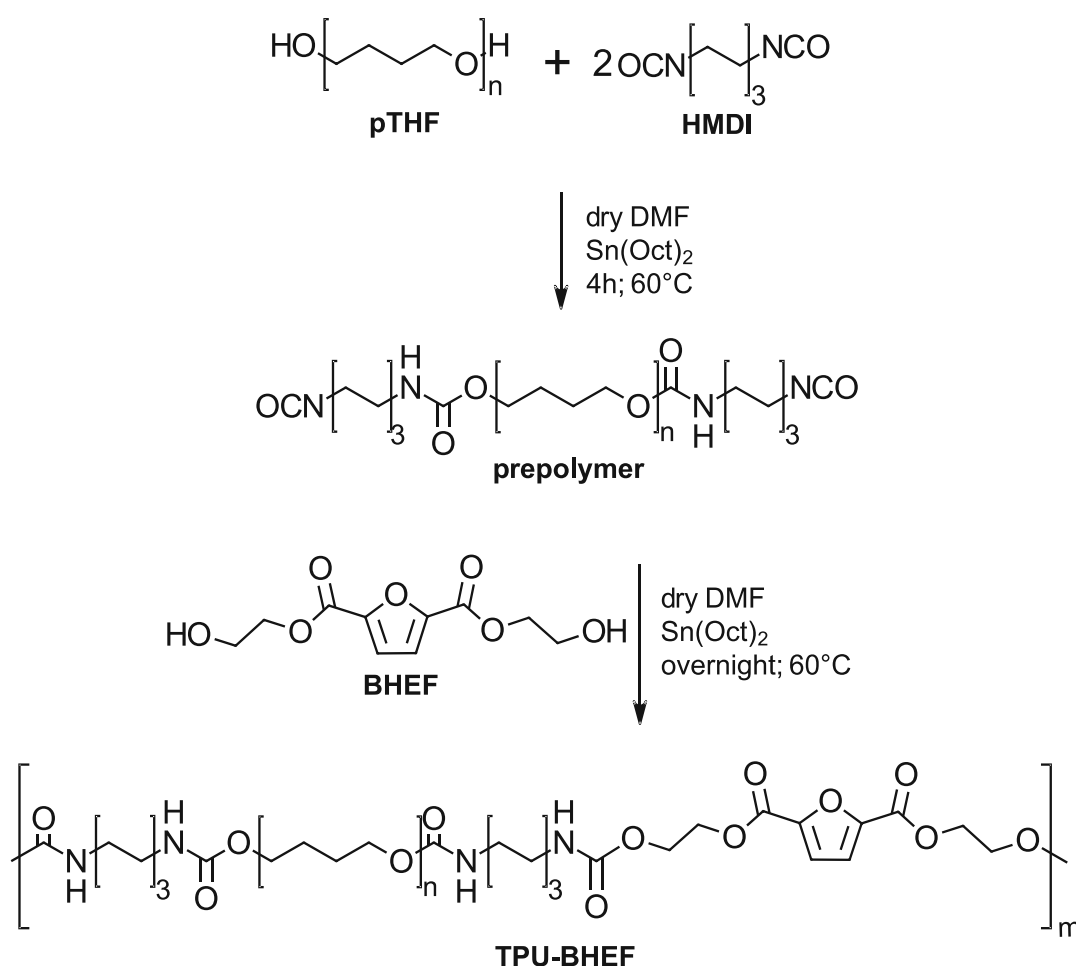
Bis(2-hydroxyethyl)furan-2-5-dicarboxylate (BHEF) was synthesized according to literature with some adjustments (Scheme 9).<sup>227, 228</sup> Additionally to the procedure described by Gomes *et al.*,<sup>227</sup> crude BHEF was purified via column chromatography with acetone to ensure a clean CE molecule, which is inevitable for a polyaddition reaction. <sup>1</sup>H-NMR and <sup>13</sup>C-APT-NMR spectra (Appendix, 1. NMR spectra) and the narrow melting range between 86.1 – 87.4 °C confirmed the product purity. For the synthesis itself FDCA (1 eq.), a large excess of ethylene glycol (EG, 20 eq.) and concentrated hydrochloric acid (HCl, 2.5 eq.) enables an esterification. The large excess of EG shifts the reaction equilibrium to the product side and prevents acidic hydrolysis of the ester. After neutralizing with saturated sodium bicarbonate solution (NaHCO<sub>3</sub>), the excess of EG was removed at 50 °C (< 0.1 mbar). The crude product was dissolved in acetone and filtered to remove NaHCO<sub>3</sub> and was dried again under vacuum resulting in a light-yellow powder. The final purification was done by column chromatography in acetone, resulting in a white powder with a yield of 55.6 %.



Scheme 9: Synthesis of bis(2-hydroxyethyl)furan-2-5-dicarboxylate (BHEF).

## 2.2. Synthesis of TPU-BHEF

Additionally, to the ester-degradable TPU-BHET, the structural very similar BHEF was used as chain extender for TPU-BHEF. According to literature, furan-2,5-dicarboxylic acid-based PEF shows very good physical, mechanical, and thermal properties compared to those of terephthalic acid-based PET.<sup>228, 234</sup> The synthesis of TPU-BHEF (Scheme 10) was performed according to already described synthesis of TPU-BHET (1.1. General polymer procedure / Synthesis of TPU-BHET) but only at about one-third the batch size because there was not enough BHEF available for a standard approach due to the low yield mentioned above. For purification TPU-BHEF was precipitated in diethyl ether resulting in a white powder with a yield of 74.7 %. The low yield could be explained by the very fine precipitate, which was more difficult to decant compared e.g. to TPU-BHET.



Scheme 10: Synthesis of TPU-BHEF via two-step polymerization. 1st step: prepolymer formation from polytetrahydrofuran (pTHF) and hexamethylene diisocyanate (HMDI), 2nd step: polyaddition reaction with the chain extender bis(2-hydroxyethyl)furan-2,5-dicarboxylate (BHEF).

## 2.3. General characterization

To verify the proportions of TPU components (pTHF, HMDI and BHEF), and to determine the hard-block content,  $^1\text{H-NMR}$  spectroscopy was conducted in  $\text{DMSO-}d_6$ . For an initial understanding of the macromolecular characteristics of the polymers, molecular weights were determined using gel permeation chromatography (GPC). Additionally, ATR-IR spectroscopy was used to estimate the strength of the physical cross-linking between linear TPUs.

BHEF, the furan analog of BHET, can provide an alternative to fossil feedstocks that is entirely derived from biological sources. In addition, FDCA-based polymers exhibit similar mechanical, thermal, and physical properties to those derived from terephthalic acid.<sup>228, 234</sup>

Burgess *et al.*<sup>234</sup> also demonstrated that BHEF is stiffer than BHET due to the active mechanism of phenyl ring inversion in BHET, while furan ring inversion is strongly suppressed in BHEF. The structural differences between BHET and BHEF, as the chemical structures of macrodiol pTHF and diisocyanate HMDI for TPU-BHEF and reference polymer TPU-BHET are shown in Figure 30.

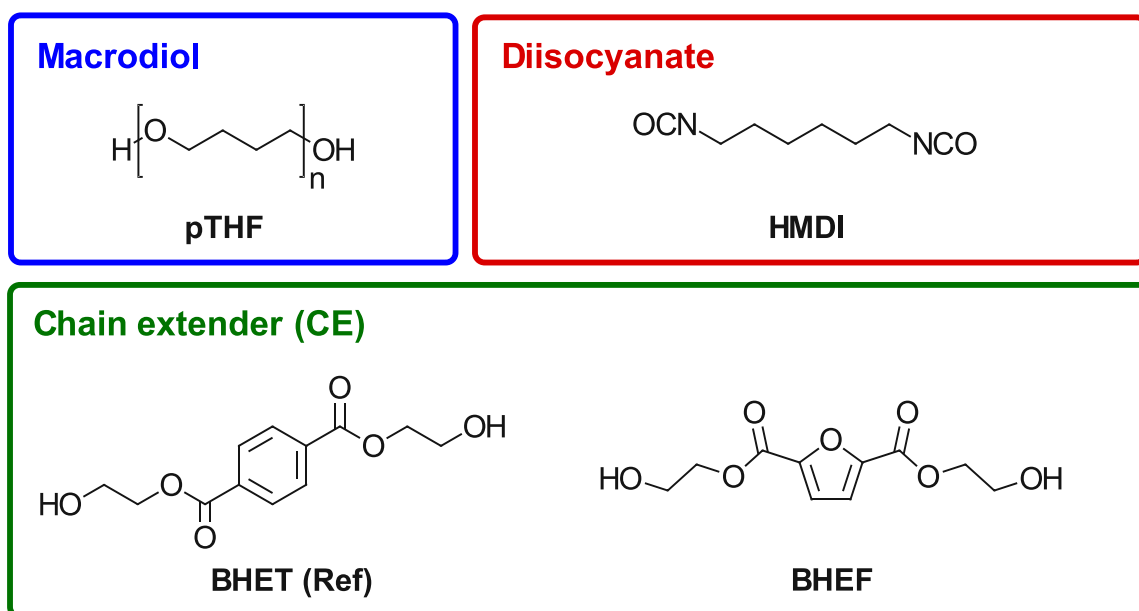


Figure 30: Structures of components for TPU synthesis: pTHF (polytetrahydrofuran) as macrodiol, HMDI (hexamethylenediisocyanate) and BHET (bis(2-hydroxyethyl)terephthalate, reference) or BHEF (bis(2-hydroxyethyl)furan-2-5-dicarboxylate) as chain extenders.

## NMR and ATR-IR spectroscopy

$^1\text{H-NMR}$  spectroscopy was used to determine the ratio between pTHF, HMDI and BHEF and to calculate the hard-block content by comparing the integrals of  $\text{CH}_2$  (pTHF) and the aromatic CH (BHEF). All spectra are shown in the appendix (1. NMR spectra).

The nature of hydrogen-bonding interaction between hard-blocks in TPU-BHEF was analyzed via FTIR spectroscopy<sup>97, 291</sup> and furthermore compared to the reference polymers TPU-BHET, TPU-BHPC and Pellethane (Figure 31). Focusing on amine (N-H,  $3500\text{-}3100\text{ cm}^{-1}$ ) and carbonyl (C=O,  $1760\text{-}1650\text{ cm}^{-1}$ ) regions, this study provides detailed information about ordered and disordered hydrogen bonding in thermoplastic polyurethane.<sup>291-294</sup>

The amine region in Figure 31 (left) shows a similar shift of TPU-BHEF and TPU-BHPC, indicating a similar strength of hydrogen bond interactions. Compared to TPU-BHET and Pellethane the interactions are still weaker because of a shift to higher wavenumbers. By comparing the structure of BHET and BHEF, Burgess *et al.*<sup>234</sup> described a rotation of the carbonyl moieties next to the aromatic ring for BHET and a stiffer furan structure for BHEF like structures resulting from nonlinear axis of ring-rotation and ring polarity. The less flexible structure of BHEF may result in less hydrogen bonding between the hard-blocks.

In the carbonyl region (Figure 31 right) a small absorption band at  $\sim 1740\text{ cm}^{-1}$  is observed for TPU-BHEF showing us free carbonyls without hydrogen bonds.<sup>97</sup> Disordered H-bonds are located at  $\sim 1720\text{ cm}^{-1}$  and ordered H-bonds are located at  $1680\text{-}1690\text{ cm}^{-1}$ . The absorption band for the ordered hydrogen bonds is a bit more pronounced compared to the disordered ones, which is also observed for TPU-BHET. This leads to the assumption that there is a higher content of ordered compared to disordered hydrogen bonds for both ester-based TPUs.<sup>97</sup>

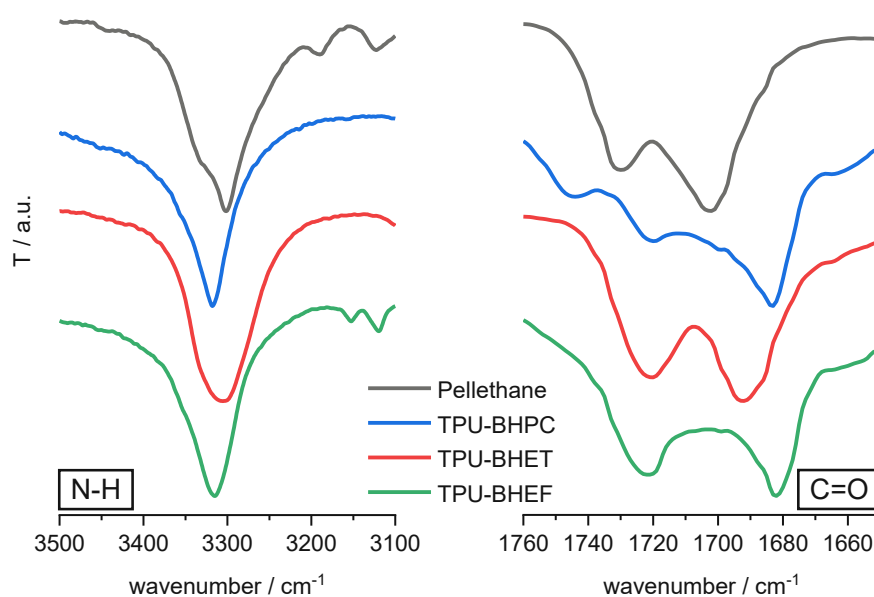


Figure 31: ATR-FTIR spectra of TPU-BHEF and reference polymers Pellethane, TPU-BHPC and TPU-BHET. The amine region ( $3500\text{-}3100\text{ cm}^{-1}$ ) and the carbonyl region ( $1760\text{-}1650\text{ cm}^{-1}$ ) are shown, which are both characteristic for the hydrogen bond interactions and therefore for hard-block formation of TPUs.

## Molecular weight and hard-block content

Since the same ratios of pTHF/HMDI/CE (1/2/1) were used for TPU-BHEF as for the reference polymers, the hard-block contents are also very similar. TPU-BHEF has a slightly lower theoretical hard-block content ( $HB_{th}$ ) but a slightly higher calculated hard-block content ( $HB_{cal}$ ) than TPU-BHET (Table 10).

$HB_{cal}$  was calculated by  $^1H$ -NMR spectroscopy (see 1.4. General characterization, spectra are shown in the appendix, 1. NMR spectra). One reason for lower  $HB_{cal}$  compared to  $HB_{th}$  may be the formation of amines in presence of residual water traces. Since there are fewer isocyanate groups of the prepolymer available to react with the CE, BHEF is not fully incorporated and therefore the hard-block content ( $HB_{cal}$ ) is minimally reduced. For Pellethane, the hard-block content could not be calculated due to an unknown ratio of macrodiol, diisocyanate and chain extender.

Furthermore, Table 10 shows the number-average molar mass  $\overline{M}_n$  and the polydispersity (PDI) determined by GPC. The  $\overline{M}_n$  is slightly higher than for TPU-BHPC and lower than for TPU-BHET. The polydispersity is 1.7, indicating a very low molar mass distribution for polyadducts, which should result in very uniform properties. Due to the similar  $\overline{M}_n$  and PDI values, comparable mechanical properties between TPU-BHEF and TPU-BHPC can be expected from this side.<sup>297</sup>

Table 10: Overview of synthesized polymers and commercially available Pellethane in terms of number-average molar mass  $\overline{M}_n$ , polydispersity (PDI) and hard-block content (theoretical and calculated).

polymer	$\overline{M}_n$ / kDa <sup>a</sup>	PDI <sup>b</sup>	$HB_{th}$ / wt% <sup>c</sup>	$HB_{cal}$ / wt% <sup>d</sup>
TPU-BHET	23.3	2.1	37.1	33.5
TPU-BHEF	17.8	1.7	36.7	33.9
Pellethane	56.3	1.9	-	-
TPU-BHPC	17.3	1.7	34.0	31.3

<sup>a</sup> Number-average molar mass. <sup>b</sup> polydispersity. <sup>c</sup> theoretical hard-block content ( $HB_{th}$ ). <sup>d</sup> calculated hard-block content from  $^1H$ -NMR ( $HB_{cal}$ ).

## 2.4. Mechanical and thermal properties

For the evaluation of a thermoplastic polyurethane`s suitability as a vascular graft, it is essential to determine its mechanical properties, including elongation at break, ultimate tensile strength and elastic modulus. The aim is to match these mechanical properties as closely as possible to those of natural tissue to ensure optimal compatibility and performance in vascular graft application.

Tensile testing was performed by solution cast polymer films according to ISO 527 (Typ 5B, bone-shaped) with a film thickness between 20 and 40  $\mu\text{m}$ . For a complete description of the solution casting and tensile testing procedures, please refer to the Materials and Methods section. Thermal properties in terms of glass transition temperature ( $T_g$ ) were determined by DMTA (Appendix, 3. DMTA spectra), to ensure a still rubbery state at body temperature.

As above mentioned the number-average molar mass  $\overline{M}_n$  of TPU-BHEF is in the range of TPU-BHPC and a little bit lower than TPU-BHET. Mechanical properties are presented in Table 11 and in a graphical form in Figure 32.

Although comparisons of PEF and PET reported in the literature suggest very similar mechanical properties,<sup>228, 234</sup> worse values were measured for TPU-BHEF than for TPU-BHET for both elongation at break and ultimate tensile strength. Similar values were obtained for elastic modulus (Table 11, Figure 32). Furthermore, TPU-BHEF was expected to have stiffer mechanics according to Burgess *et al.*<sup>234</sup> who showed that the furan-rings in BHEF are stiffer compared to the aromatic ring in BHET, allowing less rotation of the carbonyl substituents. An explanation for the poorer mechanical properties of TPU-BHEF can therefore only be found in the lower number-average molar mass  $\overline{M}_n$ , since the hard-block content  $\text{HB}_{\text{cal}}$  also showed comparable values. The molar mass is about 25 % lower (Table 16).

Table 11: Comparison of number-average molar mass  $\overline{M}_n$ , calculated hard-block content, mechanical properties and glass transition temperature of TPU-BHEF with reference polymers.

polymer (CE)	$\overline{M}_n$ / kDa <sup>a</sup>	$\text{HB}_{\text{cal}}$ / wt% <sup>b</sup>	$\epsilon_b$ / % <sup>c</sup>	TS / MPa <sup>d</sup>	E / MPa <sup>e</sup>	$T_g$ / °C <sup>f</sup>
BHET	23.3	33.5	1315 $\pm$ 54	14.1 $\pm$ 0.7	31.0 $\pm$ 1.4	-71
BHEF	17.8	33.9	841 $\pm$ 69	9.6 $\pm$ 0.8	30.9 $\pm$ 2.6	-62
Pellethane	56.3	-	1651 $\pm$ 115	25.2 $\pm$ 1.2	14.2 $\pm$ 0.3	-52
BHPC	17.3	31.3	878 $\pm$ 75	12.8 $\pm$ 0.9	22.5 $\pm$ 0.3	-57

<sup>a</sup> Number-average molar mass. <sup>b</sup> calculated hard-block content from <sup>1</sup>H-NMR ( $\text{HB}_{\text{cal}}$ ). <sup>c</sup> Elongation at break  $\epsilon_b$ .

<sup>d</sup> tensile strength TS. <sup>e</sup> elastic modulus E. <sup>f</sup> Glass transition temperature  $T_g$  obtained from the maxima of loss modulus curves.

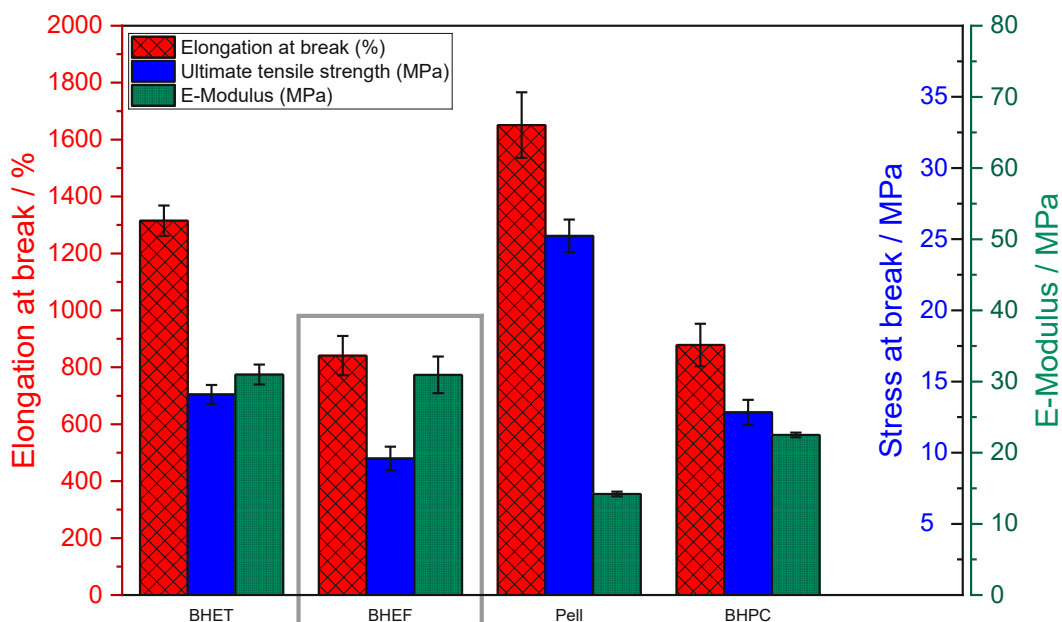


Figure 32: Elongation at break, ultimate tensile strength and elastic modulus of TPU-BHET, TPU-BHEF and TPU-BHPC in comparison with commercially available Pellethane.

Compared to TPU-BHPC, TPU-BHEF shows a similar molecular weight and elongation at break. However, due to the aromatic structure of BHEF, this material is stiffer (higher elastic modulus) than TPU-BHPC. Unfortunately, the desired combination of high elongation at break and low elastic modulus as for Pellethane was not achieved. TPU-BHEF performed worse than Pellethane for both values. Nevertheless, a TPU with good mechanical properties could be produced with the bio-based chain extender BHEF.

DMTA measurements showed a glass transition temperature of  $-62\text{ }^{\circ}\text{C}$ , which is significantly lower than the application temperature of  $37\text{ }^{\circ}\text{C}$  and could therefore be used as a vascular implant from this point of view. The  $T_g$  is intermediate between the reference polymers TPU-BHET, TPU-BHPC and the commercially available Pellethane (Table 11).



## 2.5. Degradation behavior

The degradation behavior of TPU-BHEF was investigated by circular samples, which were punched out of solution cast polymer films. The samples were stored in PBS buffer solution (pH=7.4) at 37 °C and 90 °C for maximum 70 d. More detailed description of preparing polymer films and performing degradation studies are shown in the Materials and Methods section.

Due to the similar chemical structure of BHEF and BHET, TPU-BHEF is expected to have a similar degradation rate as the reference polymer TPU-BHET. Both chain extenders show two hydrolytically degradable ester functionalities. By mass erosion experiments (Figure 33) it demonstrated that at 37 °C TPU-BHEF degrades much slower at the beginning and then undergoes a very strong degradation between 28 and 42 days. In comparison, TPU-BHET shows the highest mass degradation in the first 14 days, followed by a very low further degradation rate. At 90 °C, both show almost the same degradation curve within the first 56 days, but TPU-BHEF degrades slightly more in the last 14 days. After 70 days, the total mass loss at 90 °C is about 13 % (TPU-BHET about 9 %).

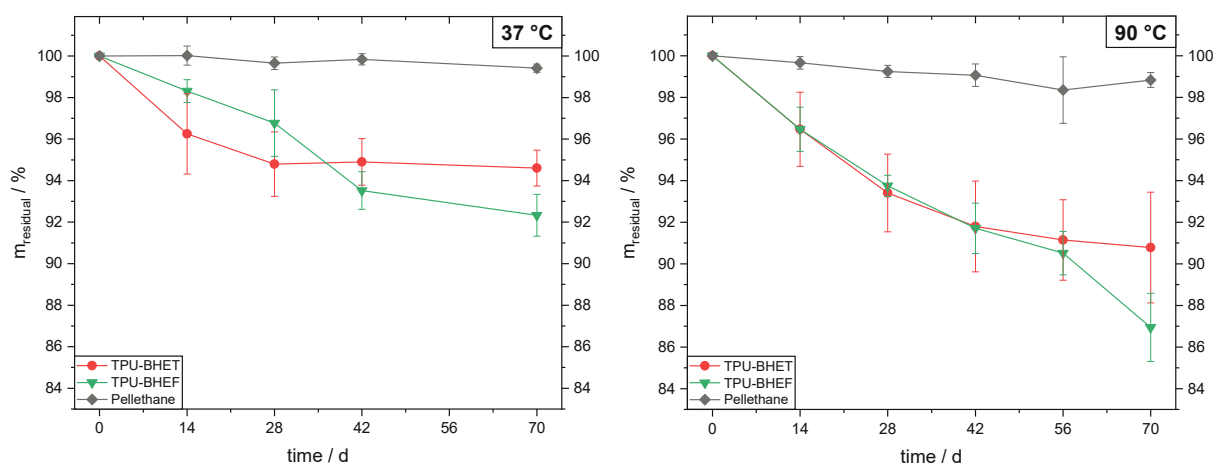


Figure 33: Residual mass  $m_{\text{residual}}$  in % of TPU-BHET, TPU-BHEF and commercially available Pellethane in PBS buffer solution (4x) at 37 °C (left) and at 90 °C (right).

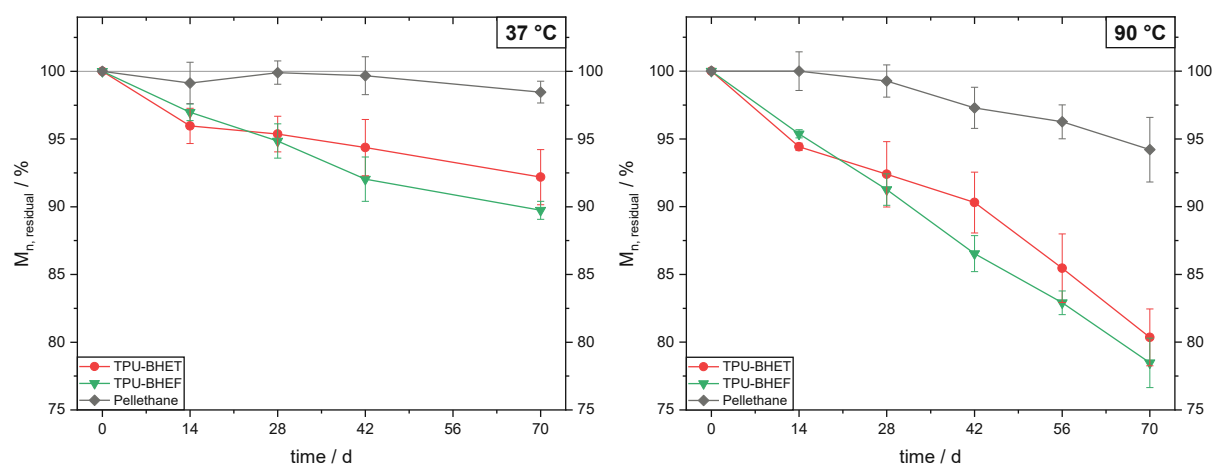


Figure 34: Development of number-average molar mass  $\overline{M}_n$ , residual in % of original  $\overline{M}_n$ , over a time period of 70 d of TPU-BHET, TPU-BHEF and Pell as reference in PBS buffer solution (4x) at 37 °C (left) and 90 °C (right).

By comparing the mass loss (Figure 33) and the molar mass reduction (Figure 34) it is possible to distinguish between surface and bulk erosion.<sup>213</sup>

A constant molecular weight reduction is observed at both 37 °C and 90 °C. However, in percentage terms, it is higher compared to mass loss. At both degradation temperatures, the  $\overline{M}_n$  decrease is higher than for the reference polymer TPU-BHET. Since, at 37 °C and 90 °C a mass loss and a molar mass reduction can be observed, bulk erosion is the dominant degradation process. To sum up, TPU-BHEF is degrading a bit faster in terms of mass erosion and molecular weight decrease at both degradation temperatures.

It was shown that the chain extender bis(2-hydroxyethyl)furan-2-5-dicarboxylate (BHEF) could be prepared in sufficient purity to be used in the polyaddition reaction for the synthesis of TPUs. The resulting TPU-BHEF showed good mechanical properties. However, there was no improvement over the reference materials TPU-BHET and TPU-BHPC. The elongation at break is in the range of the carbonate based TPU-BHPC and the elastic modulus is comparable to the ester based TPU-BHET. The ultimate tensile strength is lower than for both reference materials. The benchmark material Pellethane shows better values for all three parameters. In terms of degradability, a slight improvement was achieved in both mass erosion and molecular weight degradation compared to TPU-BHET. However, this is only in the range of 3-4% at 37 °C and 90 °C.

As a consequence, a different concept of chain extenders is introduced, which hopefully will significantly increase and improve the degradability compared to the reference polymers and TPU-BHEF. The new concept includes degradation motifs based on inorganic esters instead of esters derived from carboxylic acids or carbonic acid.

### 3. Inorganic ester-based CEs

As shown in the previous chapter, the carboxylic ester-based chain extender bis(2-hydroxyethyl)furan-2-5-dicarboxylate (BHEF) could achieve good mechanical properties, but these could not be improved over the reference materials and the hydrolytic degradation rate was only minimally improved.

For this reason, the concept of carboxylic acid ester-based chain extenders is changed to inorganic ester-based chain extenders. These include phosphate esters,<sup>181, 235, 236</sup> silicic acid esters<sup>219-221</sup> and boronic acid esters,<sup>222, 223</sup> which, according to the literature, have very interesting properties and could therefore increase the degradation rate while maintaining sufficiently good mechanical properties.

#### 3.1. Synthesis and purification of CEs

In the following chapter the synthesis, synthesis attempts of phosphate-, silicic acid- and boronic acid ester-based chain extenders and purification of commercially available chain extenders (CEs) are described.

##### 3.1.1. Phosphate ester-based CE

Poly(phosphates) and poly(phosphoesters) are abundant in nature and serve as essential components in molecules such as DNA and RNA (Figure 35). In addition to their natural role, poly(phosphoesters) are gaining attention as biocompatible and biodegradable polymers with potential applications in drug delivery systems and tissue engineering.<sup>237</sup>

These polymers exhibit a strong propensity for hydrolytic degradation, and their phosphate ester bonds can be cleaved enzymatically in biological environments, such as by alkaline phosphatase (ALP).<sup>180, 238-240</sup> These properties make poly(phosphates) promising for use in the construction of regenerative scaffolds, as demonstrated in studies by Watson et al.<sup>235</sup>

Based on the design of the poly(phosphates), bis(4-hydroxybutyl) ethyl phosphate (BHBEP) was synthesized as a chain extender for hard-block degradable TPUs (Figure 35).

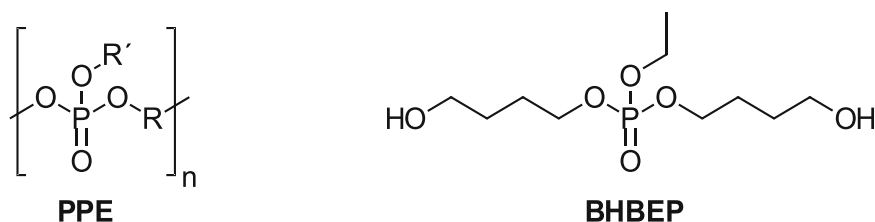
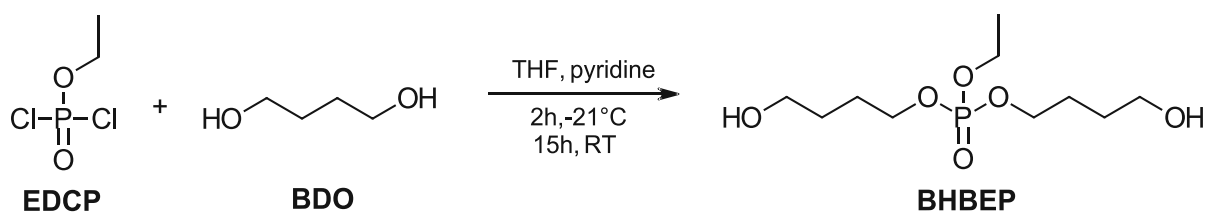


Figure 35: Chemical structures of poly(phosphates) a subclass of poly(phosphoester)s (PPEs) and bis(4-hydroxybutyl) ethyl phosphate (BHBEP).

The synthesis of bis(4-hydroxybutyl) ethyl phosphate (BHBEP) was performed according to literature with some adjustments.<sup>302</sup> The reaction scheme is shown in Scheme 11. The whole reaction was carried out with dry chemicals. A mixture of 1,4-butanediol (BDO, 2.5 eq.) and pyridine (2.5 eq.) in THF and another mixture of ethyl dichlorophosphate (EDCP, 1 eq.) in THF were added dropwise to cooled THF (-21 °C) with approximately the same speed over a period of about 30 min to avoid a polymerization reaction. On the next day a white precipitate was observed resulting from pyridinium hydrochloride. The solution was again cooled to -35 °C to precipitate as much pyridinium hydrochloride as possible before it was removed by filtration. After removing all solvents and excess of BDO under vacuum (< 0.1 mbar), a slightly yellow liquid was received with a good yield of 92.9 %. The successful synthesis of BHBEP was confirmed by <sup>1</sup>H-NMR and <sup>13</sup>C-NMR spectroscopy (Appendix, 1. NMR spectra). In addition, reaction approaches were also tried in which EDCP (1.0 eq.) was added to an excess of BDO (2.5 eq.). However, this resulted in both a lower yield and more impurities, so the approach described above was used.



Scheme 11: Synthesis of bis(4-hydroxybutyl) ethyl phosphate (BHBEP).

Furthermore, HPLC in H<sub>2</sub>O/MeCN (70/30) was measured to further confirm the purity (Figure 36). The main peak at 3.47 min results from BHBEP, but there is furthermore another peak at ~2.2 min which could not be identified because HPLC measurements of reactants show different retention time. Therefore, further attempts were made to purify BHBEP by column chromatography.

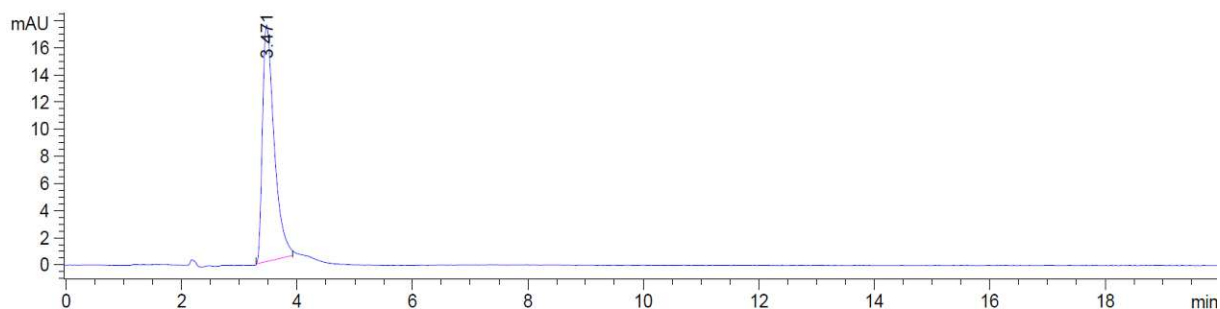


Figure 36: HPLC spectra of BHBEP after filtration.

## Purification attempt of BHBEF via column chromatography

Because an unknown impurity was detected in the HPLC spectrum (Figure 36), an attempt was made to purify BHBEF by column chromatography using ethyl acetate as the mobile phase. After separation three different fractions were identified via thin-layer chromatography (TLC). The amount of each fraction and the related  $R_f$ -values are shown in Table 12.  $^1\text{H-NMR}$  spectra of each fraction in  $\text{CDCl}_3$  are shown in Figure 37 - Figure 39.  $^1\text{H-NMR}$  spectra of fraction 1 and 3 could not assigned to a certain compound. The  $^1\text{H-NMR}$  spectra of fraction 2 (Figure 38) shows broader peaks with fitting integrals to a polymerization product between BDO and EDCP. Because,  $^1\text{H-NMR}$  and  $^{13}\text{C-NMR}$  spectra before column chromatography fits quite well to the expected shifts and integrals from BHBEF (Figure 40 and Figure 41), it could be assumed that the product was decomposed during the separation on the column and oligomerized/polymerized products were formed.

Table 12: Amount and  $R_f$ -values of all collected fractions after column chromatography, crude yield was 1329 mg.

collected fraction	m / mg	m / %	$R_f$	$^1\text{H-NMR}$ spectra
fraction 1	96.3	7.2	0.50	Figure 37
fraction 2	397.5	29.9	0.32	Figure 38
fraction 3	556.1	41.9	0.25	Figure 39
SUM	1049.9	79.0	-	-

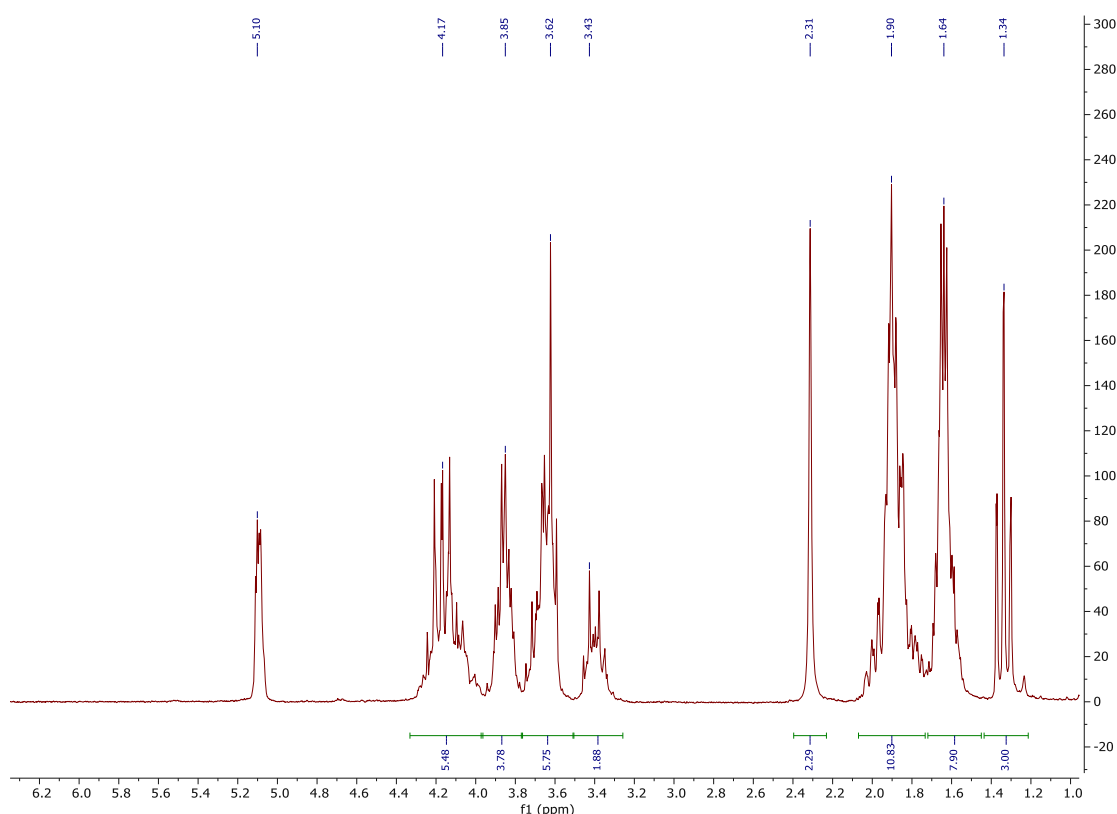


Figure 37:  $^1\text{H-NMR}$  spectra of Fraction 1 ( $R_f=0.50$ ) in  $\text{CDCl}_3$ .

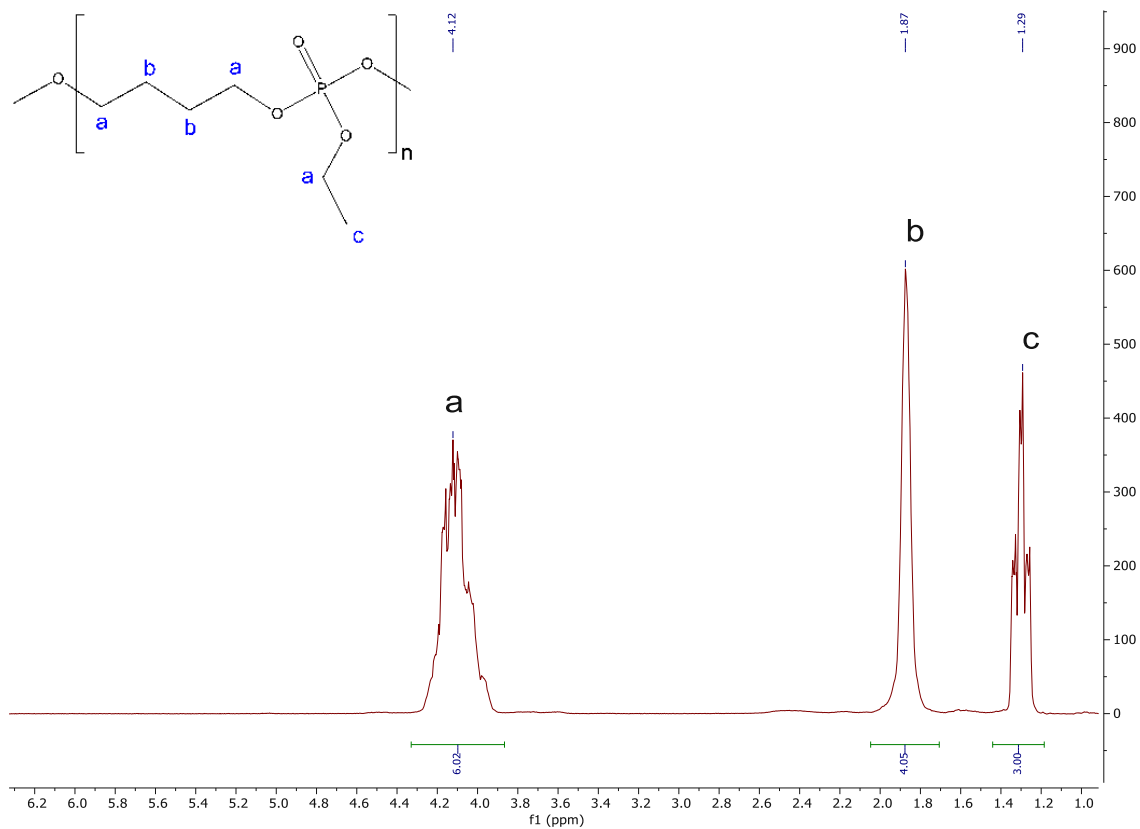


Figure 38:  $^1\text{H-NMR}$  spectra of Fraction 2 ( $R_f \sim 0.32$ ) in  $\text{CDCl}_3$ .

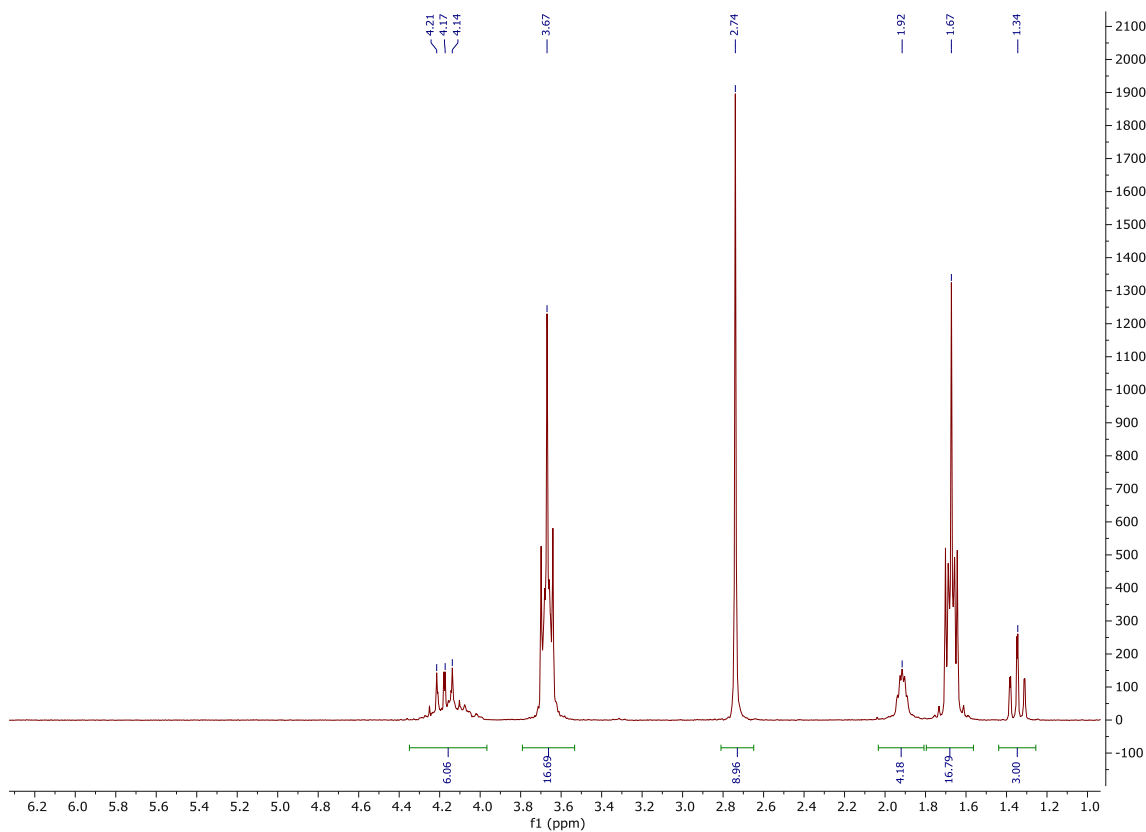


Figure 39:  $^1\text{H-NMR}$  spectra of Fraction 3 ( $R_f \sim 0.25$ ) in  $\text{CDCl}_3$ .

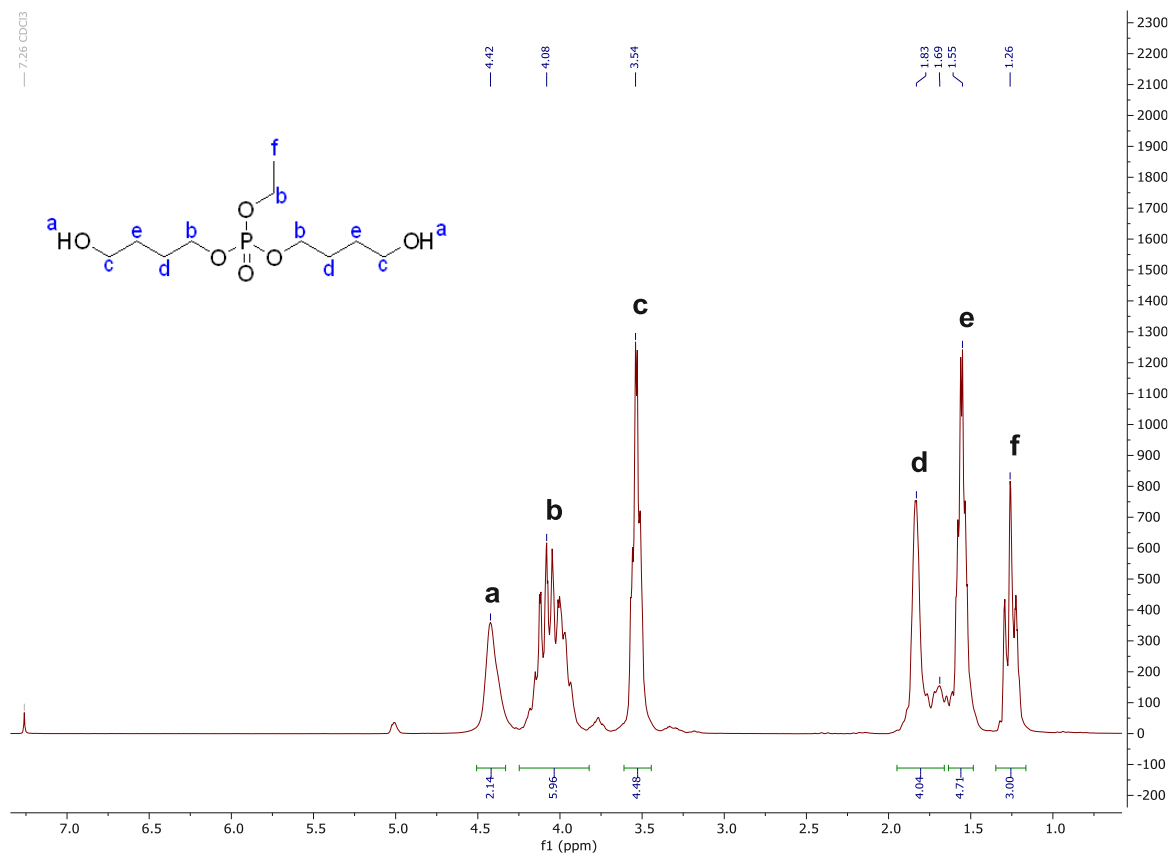


Figure 40: <sup>1</sup>H-NMR spectrum of bis(4-hydroxybutyl) ethyl phosphate (BHBEP) in CDCl<sub>3</sub>.

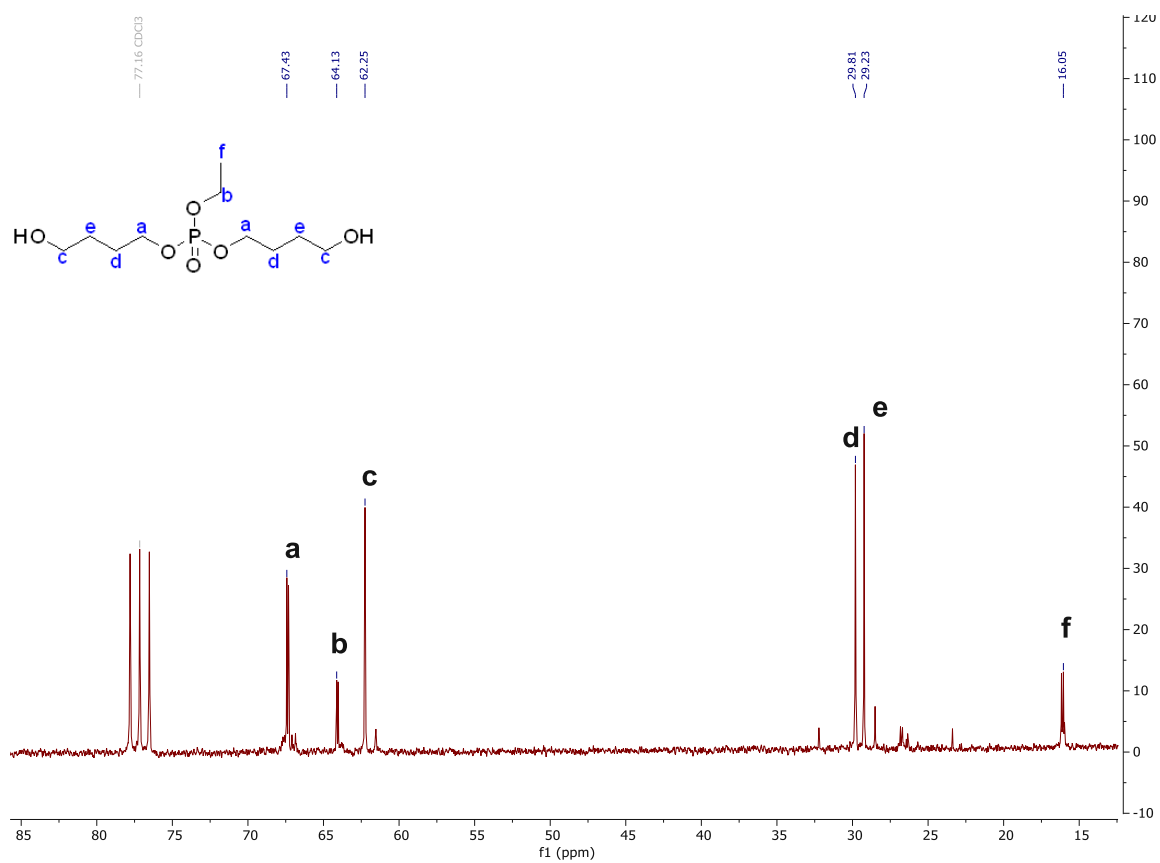


Figure 41: <sup>13</sup>C-NMR spectrum of bis(4-hydroxybutyl) ethyl phosphate (BHBEP) in CDCl<sub>3</sub>.

## Hydroxy number of BHBEP via $^{31}\text{P}$ -NMR spectroscopy

Beside  $^1\text{H}$ -NMR and  $^{13}\text{C}$ -NMR spectra,  $^{31}\text{P}$ -NMR spectra were used to identify the phosphate-based chain extender bis(4-hydroxybutyl) ethyl phosphate (BHBEP, Figure 42). Especially, the determination of the hydroxy number via  $^{31}\text{P}$ -NMR spectroscopy has to be mentioned in this way.

Therefore, the hydroxy-group content was determined according to literature,<sup>262, 303</sup> but using a different internal standard (cyclohexanol). As described in Figure 43, BHBEP and the internal standard is reacting with 2-chloro-4,4,5,5-tetramethyl-1,3,2-dioxaphospholane (TMDP), forming  $^{31}\text{P}$ -NMR active species, which show a different chemical shift (TMPD-sample and TMPD-CycO). Furthermore, chromium(III) acetylacetonate ( $\text{Cr}(\text{acac})_3$ ) is added to the internal standard solution as relaxation agent to reduce the relaxation time.<sup>304, 305</sup> Dry pyridine acts as acid scavenger for hydrogen chloride. Figure 44 shows  $^{31}\text{P}$ -NMR spectra of the chain extender bis(4-hydroxybutyl) ethyl phosphate (BHBEP). At  $\sim 175$  ppm residual TMDP can be detected. The internal reference peak is shown at  $\sim 145$  ppm which is set in relation to the sample peak at  $\sim 147$  ppm. Although, only dry substances and solvents were used, some residual water is reacting instantly with TMDP which is detected at about 132 ppm. By Eqn.6, the molar number of OH-groups per each mol of sample can be calculated (eq. for a diol, the molar number of OH-groups per each mol diol should be 2). Table 13 shows the amounts of reagents, which were used and the resulting number of hydroxy groups per each molecule of the chain extender bis(4-hydroxybutyl) ethyl phosphate (BHBEP).

As a result, 2.04 mol of OH groups per each mol of BHBEP were determined via the  $^{31}\text{P}$ -NMR method, which shows only a deviation of 2% compared to the ideal value of 2.00 mol and is therefore suitable for TPU synthesis.

$$n(\text{OH/sample}) = \frac{\text{Int}(\text{TMDP} - \text{sample}) * n(\text{CycOH})}{\text{Int}(\text{TMDP} - \text{CycO}) * n(\text{sample})} \quad \text{Eqn.6}$$

$n(\text{OH/sample})$	number of OH-groups in mol per each mol sample
$\text{Int}(\text{TMDP-sample})$	Integral of TMDP-sample peak in $^{31}\text{P}$ -NMR spectrum
$\text{Int}(\text{TMDP-CycO})$	Integral of TMDP-Cyclohexanol peak in $^{31}\text{P}$ -NMR spectrum
$n(\text{CycOH})$	amount of cyclohexanol in mol
$n(\text{sample})$	amount of BHBEP in mol

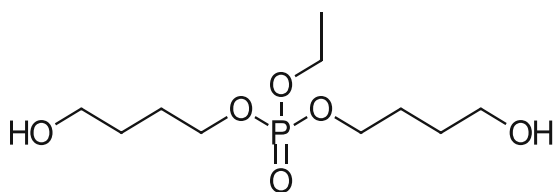


Figure 42: Chemical structure of bis(4-hydroxybutyl) ethyl phosphate (BHBEP).



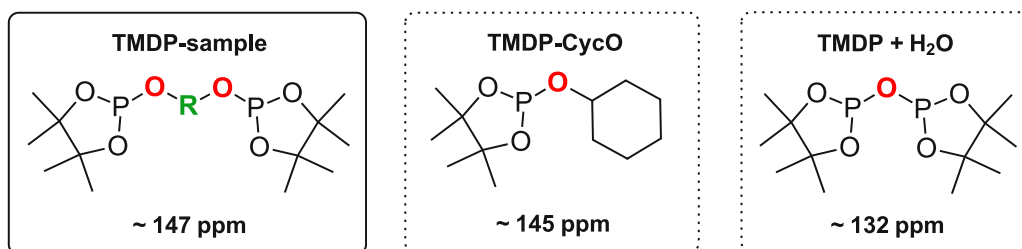
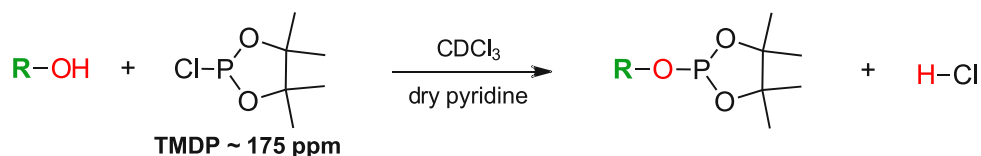


Figure 43: Reaction of hydroxyl groups of the chain extender and cyclohexanol with the phosphorus reagent TMDP.

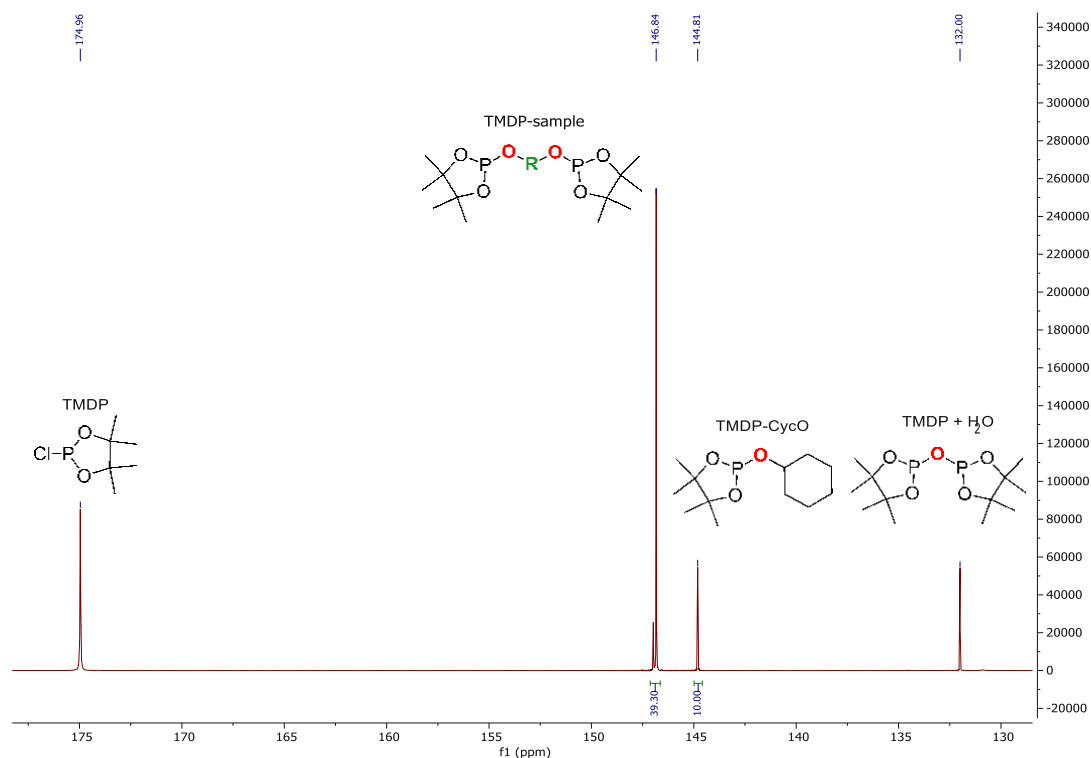


Figure 44: <sup>31</sup>P-NMR spectrum of hydroxy content determination of bis(4-hydroxybutyl) ethyl phosphate (BHBEP).

Table 13: Amount of chain extender (BHBEP), internal standard (cyclohexanol), phosphorus reagent (TMDP), relaxation agent (Cr(acac)<sub>3</sub>) and the resulting hydroxy content.

	n / mmol	equivalents	Integral <sup>31</sup> P-NMR	chemical shift / ppm <sup>1</sup>
BHBEP	78.07	1.00	39.30	146.84
cyclohexanol	40.58	0.52	10.00	144.81
TMDP	629.28	8.06	-	174.96
Cr(acac) <sub>3</sub>	1.43	0.02	-	-
<b>n(OH/sample)<sup>2</sup></b>	<b>2.04</b>	-	-	-

<sup>1</sup> chemical shift after reaction with TMDP. <sup>2</sup> number of OH-groups in mol per each mol sample.

### 3.1.2. Silicic acid ester-based CE

Silicic acid esters or silyl ethers, characterized by the Si-O-C linkage, find widespread application as protective groups in organic chemistry, particularly for alcohols.<sup>243-245</sup>

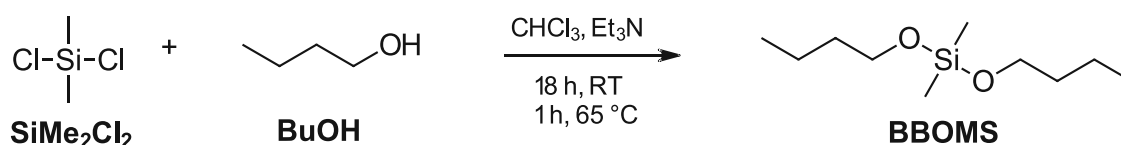
Additionally, bifunctional silicic acid esters can serve as linkers in polymer structures, typified by the general linkage O-Si(R)<sub>2</sub>-O, where R can represent any carbon chain.<sup>219</sup>

Furthermore, the degradation of these compounds results in the formation of non-toxic and non-inflammatory by-products, a contrast to e.g. ester-based molecules such as BHET. During degradation of esters, carboxylic acids are formed, which potentially lead to inflammation in the surrounding tissue.<sup>246</sup> Nevertheless, silicic acid esters exhibit a faster degradation under acidic conditions, with the degradation rate diminishing as the pH value increases.<sup>219</sup>

Since the degradability of silicic acid esters tends to be lower in the neutral range, only chain extenders based on dimethyl esters (O-Si(Me)<sub>2</sub>-O) were prepared in the following chapter, since the steric hindrance around the silicon atom is lowest in this case. Furthermore, due to the higher flexibility of the Si-O bond compared to the C-O bond,<sup>248</sup> different mechanical properties are expected compared to the reference polymers TPU-BHET, TPU-BHPC and Pellethane.

#### Model compound bis(butyloxy)dimethylsilane (BBOMS)

To find the best reaction conditions for silicic ester-based chain extenders, the model compound BBOMS was synthesized according to Javaherian *et al.*<sup>306</sup> with some adjustments (Scheme 12). Briefly, 1-butanol (BuOH, 2.1 eq.) and triethylamine (Et<sub>3</sub>N, 2.1 eq.) were cooled to 0°C with an ice bath. Afterwards dimethyldichlorosilane (SiMe<sub>2</sub>Cl<sub>2</sub>, 1 eq.) was added under argon atmosphere. The exact reaction conditions are explained in the experimental section. Et<sub>3</sub>NHCl salt was removed via filtration and the crude product was extracted with CHCl<sub>3</sub> and H<sub>2</sub>O, resulting in a clear liquid with a yield of 84.2 %. The successful synthesis was verified via <sup>1</sup>H-NMR spectroscopy (Appendix, 1. NMR). Especially, the peak at 0.07 ppm resulting from two methyl groups located at the silicon atom (Si(CH<sub>3</sub>)<sub>2</sub>) has to be highlighted, as the further discussion of the silicic acid ester-based CEs refers to this. As expected from the structure of BBOMS (Scheme 12), this peak shows a proton number of 6.

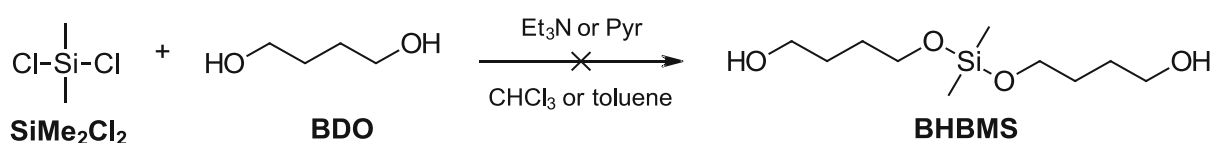


Scheme 12: Synthesis of model compound bis(butyloxy)dimethylsilane (BBOMS).

## Synthesis attempts of bis (2-hydroxybutoxy) dimethyl silane (BHBMS)

The preparation of bis (2-hydroxybutoxy) dimethyl silane (BHBMS) was carried out according to literature and the synthesis of BBOMS above.<sup>306</sup> Five synthesis attempts of BHBMS were carried out with different ratios of 1,4-butanediol (BDO) to freshly distilled dimethyldichlorosilane ( $\text{SiMe}_2\text{Cl}_2$ , 1.5 g) (2:1, 3:1, 4:1), different acid scavengers (triethylamine or pyridine), solvents ( $\text{CHCl}_3$  or toluene) and temperatures. All solvents were removed under vacuum and 5 mL  $\text{CHCl}_3$  was added before extraction (5 x 10 mL chloroform; 200 mL  $\text{H}_2\text{O}$ ). Finally, the reaction mixture was dried under vacuum (high vacuum, >0.1 mbar), resulting in a clear or slightly yellow liquid.

The general synthesis scheme is shown in Scheme 13 and an overview of the exact reaction conditions are given in Table 14.



Scheme 13: General synthesis scheme for bis (2-hydroxybutoxy) dimethyl silane (BHBMS).

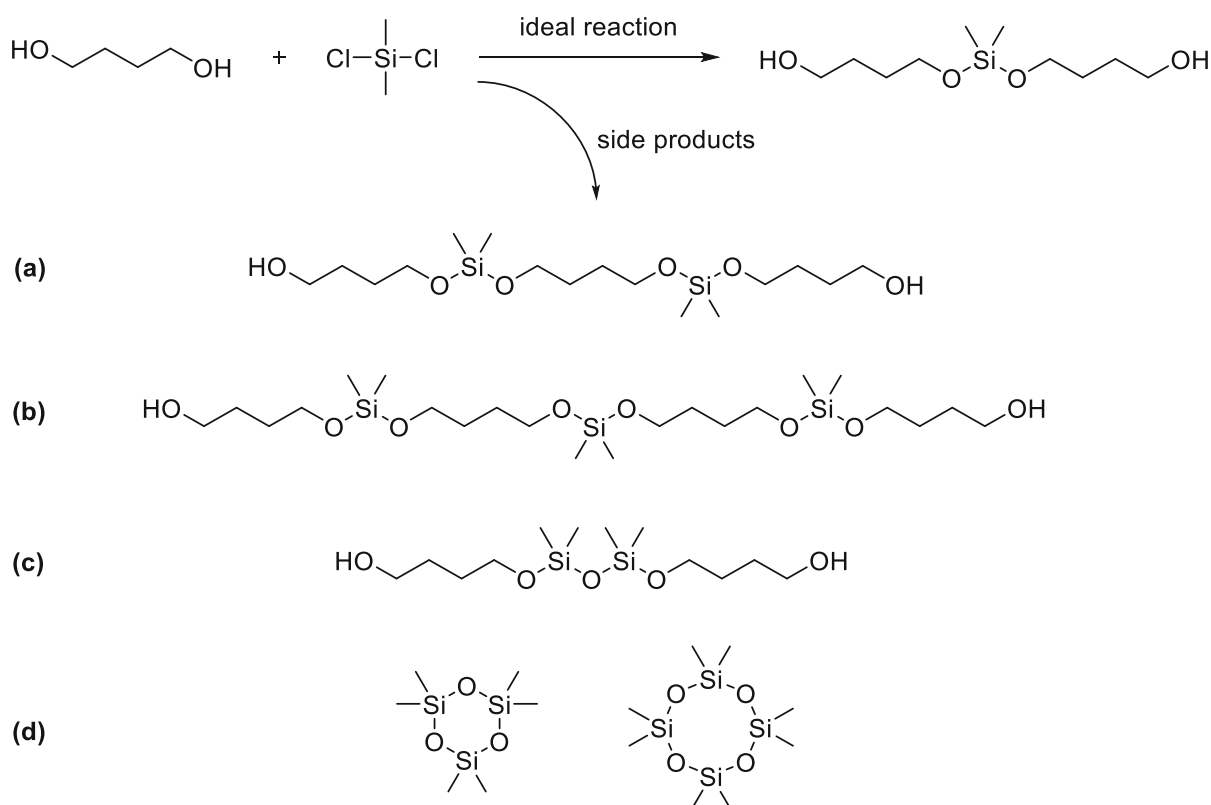
Table 14: Selected reaction conditions for BHBMS synthesis with different ratios of BHBMS to  $\text{SiMe}_2\text{Cl}_2$ , different acid scavengers, solvents, temperatures, raw amounts and determined protons for  $(\text{CH}_3)_2\text{Si}$  via  $^1\text{H-NMR}$  spectra.

ratio (BDO/ $\text{SiMe}_2\text{Cl}_2$ )	base	solvent	Ice bath	Reaction conditions		$m_{\text{total}}$ / mg	protons ( $\text{Me}_2\text{SiR}_2$ )
2 / 1	$\text{Et}_3\text{N}$	$\text{CHCl}_3$	+	5h (50°C)	16h (rt)	874	9
2 / 1	Pyr	$\text{CHCl}_3$	+	-	22h (rt)	929	14
3 / 1	$\text{Et}_3\text{N}$	toluene	+	5h (120°C)	19h (rt)	991	12
3 / 1	Pyr	$\text{CHCl}_3$	+	5h (50°C)	16h (rt)	1017	16
4 / 1	Pyr	$\text{CHCl}_3$	-	5h (60°C)	16h (rt)	872	12

Table 14 shows that the obtained amounts ( $m_{\text{total}}$ ) after filtration and drying of the individual synthesis experiments are relatively low compared to the amount used of  $\text{SiMe}_2\text{Cl}_2$  (1.5 g) and that the different reaction conditions have only a small influence on them (872-1017 mg). However, a large difference can be seen in the  $^1\text{H-NMR}$  spectra (Appendix, 1. NMR spectra). It was observed that the proton ratios are not correct in any of the five synthesis approaches. For a simple overview, all peaks have been referenced to the signal of  $\text{CH}_2\text{-O}$ . The deviation in the signal for the two methyl groups next to the silicon atom has to be highlighted and is clearly recognizable. According to the structure of BHBMS (Scheme 13), this signal should be 6 protons. However, the number of protons in the signal is significantly higher in all experiments (Table 14, Protons  $\text{Me}_2\text{SiR}_2$ ). Looking at this value, the first reaction approach with BDO/ $\text{SiMe}_2\text{Cl}_2$  (2:1), triethylamine as acid scavenger and  $\text{CHCl}_3$  as solvent shows the best result.

However, according to  $^1\text{H-NMR}$  measurements, side reactions also occurred here (9H instead of 6H for  $\text{Me}_2\text{Si}$ ). Possible by-products are shown in Scheme 14.

By formation of dimers, trimers, etc. (a, b), the  $\text{Me}_2\text{Si}$  signal would be increased, as the ratio of  $\text{BuOH}$  to  $\text{Me}_2\text{Si}$  in by-product (a), for example, is 3:2 instead of 2:1. For by-product (b) the ratio would be 4:3 et cetera. Another possibility would be the formation of (poly)dimethyl siloxane units (c, d). These would also increase the ratio of  $\text{BuOH}$  to  $\text{Me}_2\text{Si}$  in a reaction mixture compared to the target ratio of 2:1.



Scheme 14: Ideal reaction and a selection of possible side products of 1,4-butanediol and dimethyldichlorosilane.

Besides,  $^1\text{H-NMR}$  spectroscopy, also GC-MS measurements were performed for BHBMS reaction mixture. GC spectrum of the best approach of BHBMS ( $\text{BDO}:\text{Me}_2\text{Cl}_2\text{Si} = 2:1$ ,  $\text{Et}_3\text{N}$ ) is shown in Figure 45 left. Three peaks were detected and the associated MS spectra are presented in Figure 45 right. Unfortunately, none of the MS spectra are fitting to the fragment pattern of BHBMS, but showing some (poly)dimethylsilane-units as demonstrated above in Scheme 14 (c, d). The GC spectra of the other synthesis approaches show even more than three peaks and are therefore not discussed further in this chapter. As the amount of the most promising synthesis attempt was less than 1 g and GC-MS measurement did not verify presence of the actual product BHBMS, no further purification was tried and a commercially available silicic acid ester for TPU synthesis was used, namely bis(4-aminophenoxy) dimethylsilane (BAPDMS).

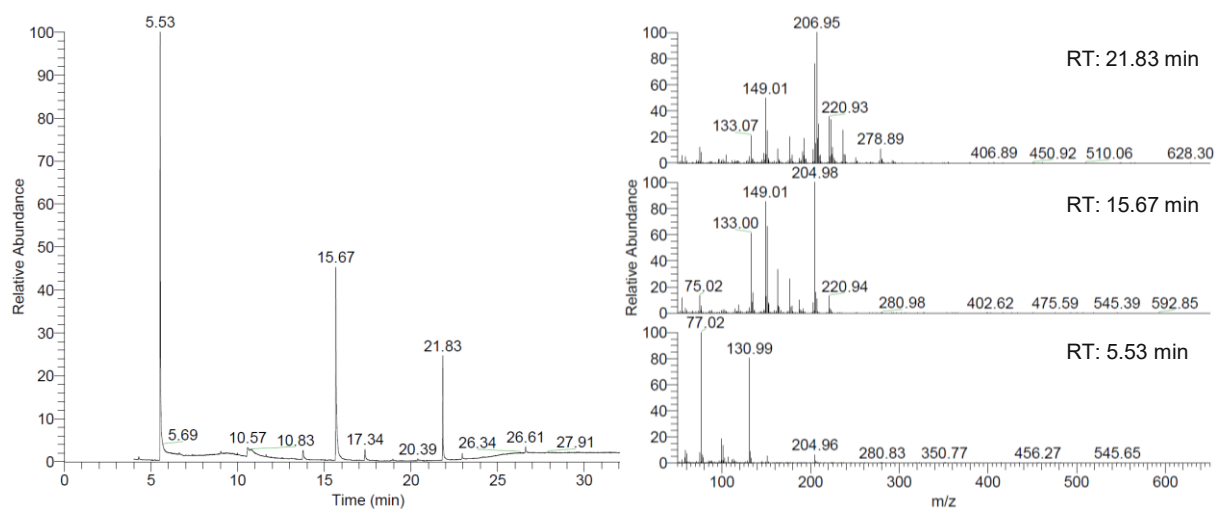


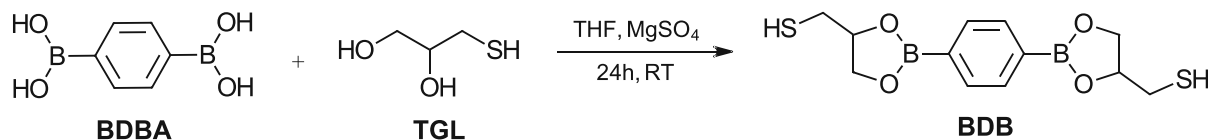
Figure 45: GC-MS spectra of synthesis attempt of BHBMS ( $BDO:Me_2Cl_2Si = 2:1$ ,  $Et_3N$ ) in DCM ( $1 \text{ mg mL}^{-1}$ ). Three peaks were detected in GC spectra (left) with the associated MS spectra (right).

### 3.1.3. Boronic acid ester-based CE

Beside thermoplastic polyurethanes (TPUs), and thermoplastic polyurea urethanes (TPUUs) we are also synthesized thermoplastic polythiourethanes (TPTUs). They also show very good mechanical and physical properties and are also biocompatible.<sup>307</sup> In contrast to polyurethanes, they show more ordered domains and higher flexibility due to the incorporated sulfur atom.<sup>308, 309</sup> Furthermore, during synthesis they show less side-reaction as reported for polyurethanes like the formation of allophanates and urethanes.<sup>310, 311</sup>

Additionally, we introduced a boronic acid ester-based chain extender into TPTUs. Boronic acids are mild organic Lewis acids with a trivalent boron atom, substituted with one alkyl and two hydroxyl residues.<sup>249-251</sup> Replacing the hydroxy groups with alkoxy or aryloxy groups is easy due to the lack of hydrogen donor capability, resulting in the formation of boronic acid esters (also called boronate esters or boronic esters).<sup>251-253</sup>

The synthesis of 2,2'-(1,4-phenylene)-bis[4-mercaptan-1,3,2-dioxaborolane] (BDB) was performed according to literature with some adjustments.<sup>222, 312</sup> The reaction scheme is shown in Scheme 15. 1-Thioglycerol (TGL) was distilled under reduced pressure (3 mbar) at 145 °C to avoid the formation of disulfides. Benzene-1,4-diboronic acid (BDDBA) was used without any purification for the synthesis. TGL and BDDBA were dissolved in THF and deionized water. After a clear solution was observed, MgSO<sub>4</sub> was added in portions within 1 h to remove water. After stirring for 24 h at room temperature the solution was filtrated to remove MgSO<sub>4</sub> and was dried under vacuum. For further purification the powder was dissolved in toluene. TGL was not soluble in toluene and could therefore be removed via precipitation. Finally, BDB was recrystallized from toluene at 70 °C with good yields of 82.6 %. The successful synthesis of BDB was confirmed via <sup>1</sup>H-NMR and <sup>13</sup>C-APT-NMR spectroscopy (Appendix, 1. NMR spectra). Furthermore, a narrow melting range of 109.3 – 111.2 °C affirmed a clean product, which enables further use of BDB for TPU synthesis.



Scheme 15: Synthesis of 2,2'-(1,4-phenylene)-bis[4-mercaptan-1,3,2-dioxaborolane] (BDB).

### 3.2. TPUs, TPUUs and TPTUs with one CE

The chain extenders BHBEP (bis(4-hydroxybutyl) ethyl phosphate), BAPDMS (bis(4-aminophenoxy) dimethylsilane) and BDB (2,2'-(1,4-phenylene)-bis[4-mercaptan-1,3,2-dioxaborolane]), which were prepared or purified in chapter 3.1. Synthesis and purification of CEs, are now used to synthesize TPUs, TPUUs and TPTUs. By using the diamine BAPDMS, urea groups are incorporated into the polymer in addition to the urethane groups.

In addition to thermoplastic polyurethanes (TPUs), and thermoplastic polyurea urethanes (TPUUs) we are also synthesized thermoplastic polythiourethanes (TPTUs) with the CE molecule BDB. In general, thiourethanes have excellent mechanical and physical properties as well as biocompatibility.<sup>307</sup> In contrast to polyurethanes, they have more ordered domains and higher flexibility, which is due to the presence of sulfur atoms.<sup>308, 309</sup> In addition, fewer side reactions occur during their synthesis compared to polyurethanes, such as the formation of allophanates and urethanes.<sup>310, 311</sup>

For comparison, another TPTU was synthesized based on 1,2-bis(2-mercaptoethoxy)-ethane (BMEE) as CE to investigate the influence of thiourethanes on the mechanical and degradation characteristics. The chemical structures of the CE molecules are shown in Figure 46.

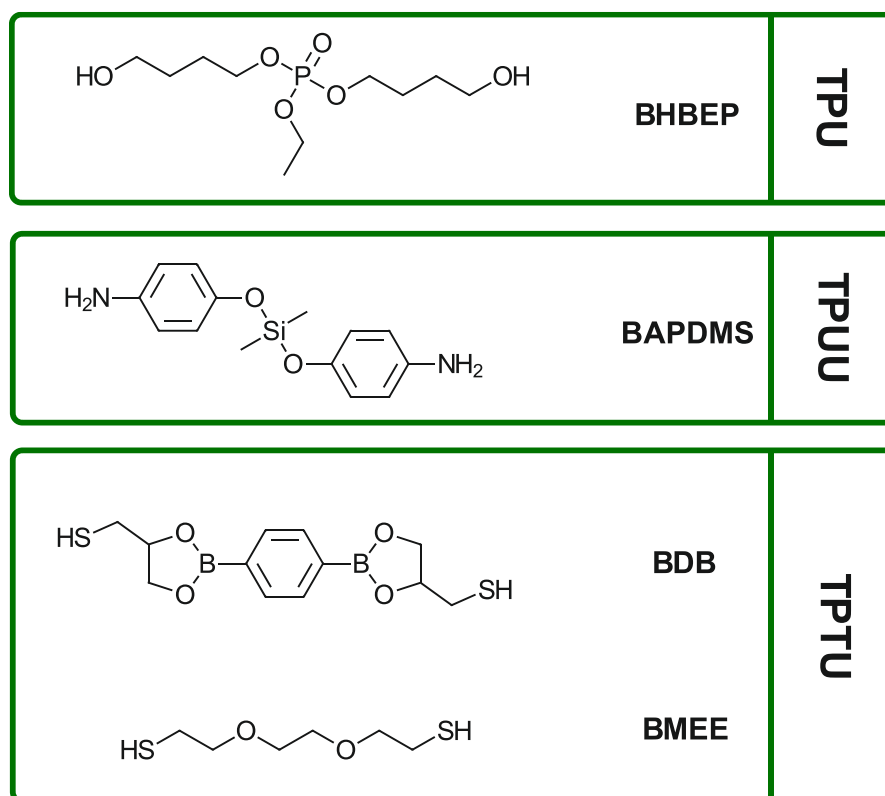


Figure 46: Chemical structures of chain extenders (CE) for thermoplastic polyurethanes (TPU), thermoplastic polyurea urethanes (TPUU) and thermoplastic polythiourethanes (TPTU). BHBEP (bis(4-hydroxybutyl) ethyl phosphate), BAPDMS (bis(4-aminophenoxy) dimethylsilane), BDB (2,2'-(1,4-phenylene)-bis[4-mercaptan-1,3,2-dioxaborolane]) and BMEE (1,2-bis(2-mercaptoethoxy)ethane).

### 3.2.1. Synthesis of TPUs, TPUUs and TPTUs with one CE

For the synthesis of silicic acid ester-based polymers, the chain extender bis(4-aminophenoxy)-dimethylsilane (BAPDMS) was selected because of its commercial availability. BAPDMS was purchased from ABCR in a given purity of 97 % and was therefore purified before the synthesis, according to Rafiemanzelat *et al.*,<sup>313</sup> via recrystallisation from diethyl ether.

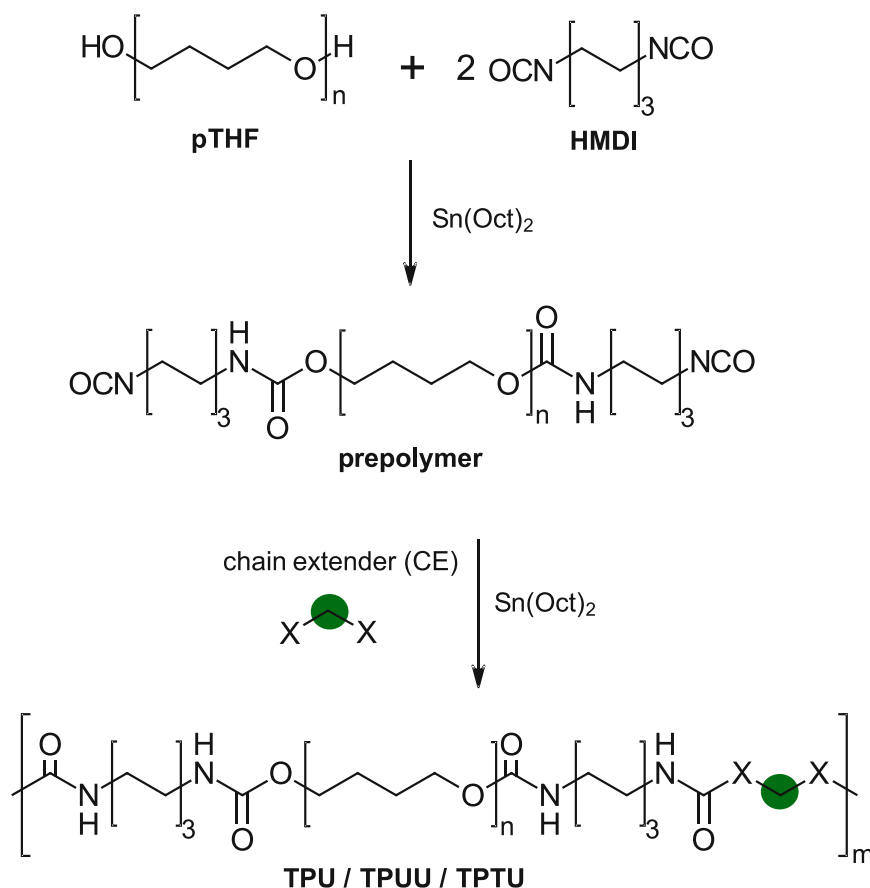
Analogous to the synthesis of reference polymers TPU-BHET and TPU-BHPC (chapter 1. Reference polymers) the synthesis of TPUU-BAPDMS was carried out (Scheme 16). However, due to the poor solubility of BAPDMS in dry DMF, larger amounts of solvent were required (25 mL instead of 5 mL for CE addition step). For purification TPUU-BAPDMS was precipitated in diethyl ether, resulting in a dark brown solid with good yields of 83.7 %.

The synthesis of TPTU-BDB was carried out analogous to the synthesis of TPU-BHET. The chain extender 2,2'-(1,4-phenylene)bis[4-thioethyl-1,3,2-dioxaborolane] (BDB) was dried under high vacuum (< 0.1 mbar) for 2 days at room temperature, respectively. As BDB shows a good solubility in DMF, the same amounts of solvent were used as for the synthesis of reference polymers. After complete reaction, the polymer was precipitated in diethyl ether and dried under vacuum at 40 °C, resulting in a white solid with good yield of 87.6 %. In Scheme 16 the reaction scheme of TPTU-BDB is shown.

In order to have a thiourethane-based polymer as a reference in addition to the reference TPUs, the chain extender 1,2-bis(2-mercaptoethoxy)ethane (BMEE) was used for the synthesis of TPTU-BMEE (Scheme 16). BMEE was distilled under vacuum (5 mbar) at 160 °C. The temperature should therefore not be further increased because of the possibility to form disulfides. The relatively poor yield of 82.4 % compared to other polymer syntheses can be explained by the extremely viscous reaction solution prior to precipitation. Transferring the solution to the dropping funnel would have required a large amount of DMF, which would have negatively affected the precipitability of the polymer.

In addition, bis(4-hydroxybutyl) ethyl phosphate (BHBEP) was used in a synthesis attempt to prepare the phosphate ester-based TPU-BHBEP. Unfortunately, none of the attempts resulted in a processable TPU. The “best” approach resulted in a non-solid but still viscous polymer that could not be further characterized in terms of mechanical properties and degradation behavior because it was not possible to prepare polymer films out of it.





Scheme 16: General synthesis of TPU / TPTU / TPUU by using diols, dithiols or diamines as chain extenders (CE), X=OH, NH<sub>2</sub> or SH. For TPUs, BHBEP (bis(4-hydroxybutyl) ethyl phosphate, not possible to synthesize) was used. For TPUUs, BAPDMS (bis(4-aminophenoxy) dimethylsilane) was chosen and for TPTUs, BDB (2,2'-(1,4-phenylene)-bis[4-mercaptan-1,3,2-dioxaborolane]) and BMEE (1,2-bis(2-mercaptoethoxy)ethane) were selected as chain extenders.

### 3.2.2. General characterization of polymers with one CE

To confirm the polymer component ratios of 1/2/1 between macrodiol (pTHF), diisocyanate (HMDI) and the chain extenders (CE) and to determine the hard-block content, <sup>1</sup>H-NMR spectroscopy of all synthesized polymers in DMSO-*d*<sub>6</sub> was measured. To gain a preliminary understanding of the polymers' macromolecular nature, molecular weights were determined by gel permeation chromatography (GPC). Furthermore, the strength of physical crosslinking was evaluated through ATR-IR spectroscopy.

After several unsuccessful attempts to synthesize bis(2-hydroxybutoxy) dimethyl silane (BHBMS), the commercially available chain extender BAPDMS was chosen because of its relatively easy purification by recrystallization with diethyl ether.<sup>313</sup>

BAPDMS shows a very interesting structure because of its two aromatic rings connected via a silicic acid ester. On the one hand, the aromatic structure should result in an increased rigidity and on the other hand the Si-O bond is known to be much more flexible compared to C-O bond.<sup>248</sup> Predicting the properties of the final polymer is therefore very difficult.

The chain extender 2,2'-(1,4-phenylene)-bis[4-mercaptan-1,3,2-dioxaborolane] (BDB) was selected on the one hand because of the characteristics of boronic acid esters which consists of a dynamic covalent B-O bond.<sup>249, 254, 255</sup> Furthermore, due to the nature of the synthesis of BDB it was easy to introduce thiourethane groups into the polymer by using 1-thioglycerol. The thiol group does not react with the hydroxy group of benzene-1,4-diboronic acid (BDBA) under the reaction conditions.<sup>222, 312</sup>

In addition, a reference TPTU was prepared using 1,2-bis(2-mercaptoethoxy)ethane (BMEE) as CE to evaluate the effect of thiourethanes on mechanical properties and degradation behavior (TPTU-BMEE). The chemical structures of the components of inorganic ester-based polymers and the reference materials TPU-BHET and TPU-BHPC are displayed in Figure 47.

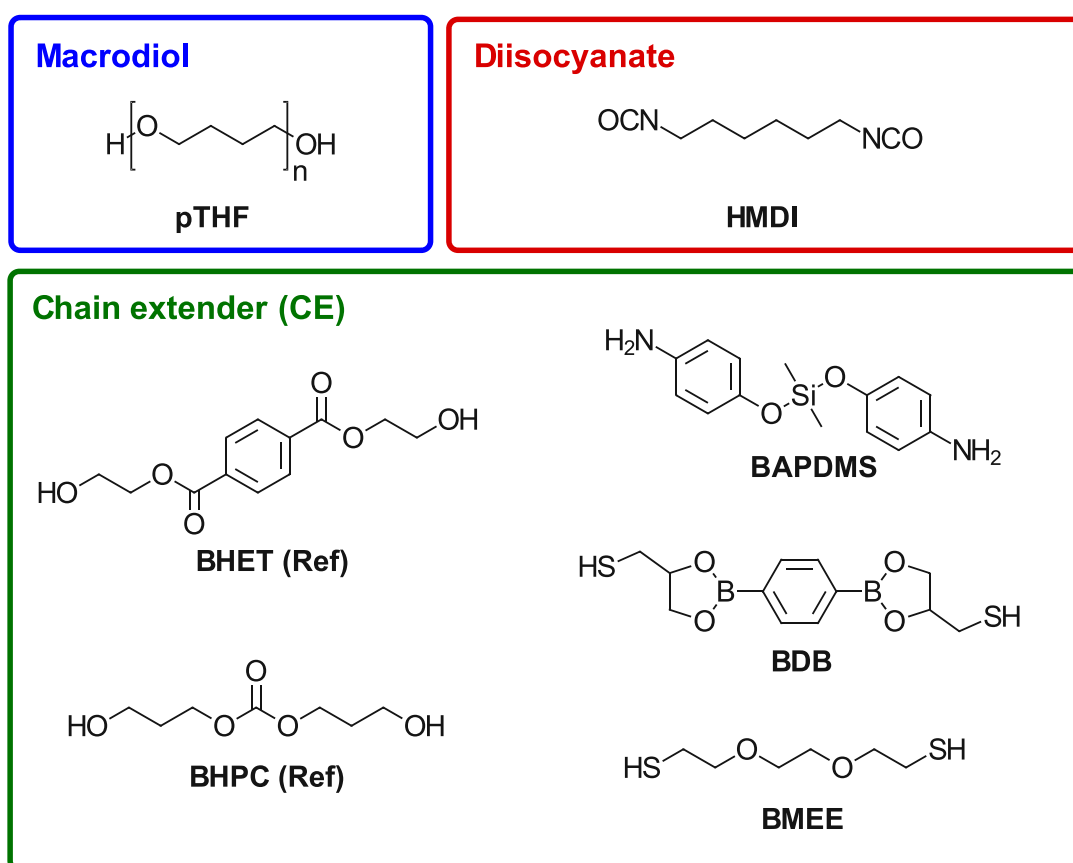


Figure 47: Structures of components for TPU, TPUU and TPTU synthesis: pTHF (polytetrahydrofuran) as macrodiol, HMDI (hexamethylenediisocyanate), BHET (bis(2-hydroxyethyl)terephthalate, reference), BHPC (bis(hydroxypropyl)carbonate, reference) and BAPDMS (bis(4-aminophenoxy) dimethylsilane), BDB (2,2'-(1,4-phenylene)-bis[4-mercaptan-1,3,2-dioxaborolane]) and BMEE (1,2-bis(2-mercaptoethoxy)ethane) as chain extenders.

## NMR and ATR-IR spectroscopy

The targeted ratio of pTHF/HMDI/CE (1/2/1) in TPUU-BAPDMS, TPTU-BDB and TPTU- BMEE was verified by  $^1\text{H-NMR}$  spectroscopy.  $^1\text{H-NMR}$  spectra of the prepared polymers are shown in the appendix section (1. NMR).

To investigate the nature of hydrogen bonding interactions via hard-block formation FTIR spectroscopy was performed.<sup>97, 291</sup> The most information on this can be obtained by taking a closer look at the amine region (N-H,  $3500\text{-}3100\text{ cm}^{-1}$ ) and the carbonyl region (C=O,  $1760\text{-}1650\text{ cm}^{-1}$ ). The shift and the shape of the absorption bands show us whether the urethane group is free or bound by H-bonds.<sup>291-294</sup> Furthermore, by comparing the spectra of different polymers, it is possible to estimate, which forms the strongest hydrogen bonds and how strongly sterically hindered the hard-blocks are. Since pTHF and HMDI were used as components for all polymers, the relative strength of the hydrogen bonds are only dependent on the selected chain extender.

The amine region (Figure 48 left) shows that the siloxane based TPUU-BAPDMS has the highest steric hindrance compared to the all other polymers due to the broadest absorption band. Furthermore, TPUU-BAPDMS shows a peak shift to higher wavenumbers indicating the weakest hydrogen bond interactions between the hard-blocks. The relatively low hydrogen bond interaction of the silicic acid ester-based TPUU could be explained by the possible steric hindrance by methyl groups of the oxygen atoms next to  $\text{SiMe}_2$ . Furthermore, less atoms are available for the formation of H-bonds for BAPDMS (2x O, 2x N) compared to BHET (6x O).

The boronic ester based TPTU-BDB on the other hand shows significantly lower steric demands compared to BHET, despite both having a similar aromatic structure. The peak of TPTU-BDB is even sharper than the band of Pellethane and the carbonate based TPU-BHPC. This difference may be attributed to the more flexible nature of the thiourethane moiety, which is a consequence of the sulfur atoms.<sup>308, 309</sup> Nonetheless, the thiourethane reference TPTU- BMEE displayed a broader N-H peak compared to the boronic ester based TPTU-BDB, although BMEE is a sterically low demanding, aliphatic chain extender.

Furthermore, NH absorption bands of TPTU-BDB and TPTU- BMEE showed a slight shift to higher wavenumbers compared to TPU-BHET and Pellethane, suggesting lower hydrogen bonding strength, which can be explained by the fact that hydrogen bonds involving  $\text{S}\cdots\text{H}$  interactions are weaker than those involving  $\text{O}\cdots\text{H}$ .<sup>314</sup>

Despite the amine region, the carbonyl region is shown between  $1760\text{-}1650\text{ cm}^{-1}$  (Figure 48 right). For the siloxane based TPUU-BAPDMS free carbonyls were identified at  $\sim 1720\text{ cm}^{-1}$  and a weak but broader absorption band at  $\sim 1665\text{ cm}^{-1}$ . According to Yilgor *et al.*<sup>97</sup> this peak results from unordered hydrogen bonds between urea groups. Ordered H-bonds would be located at  $\sim 1650\text{ cm}^{-1}$ , which are not present in the absorption spectrum.

At approximately  $1740\text{ cm}^{-1}$ , no absorption bands were observed in any of the polymers, beside the carbonate based TPU-BHPC, indicating the absence of free C=O groups without hydrogen bonds.<sup>97</sup> For boronic ester based TPTU-BDB and the thiourethane reference TPTU-BMEE, the peak intensity at around  $1720\text{ cm}^{-1}$  was lower than the peaks between  $1685\text{--}1695\text{ cm}^{-1}$ , which is a result of a higher content of ordered to disordered H-bonds.<sup>97</sup>

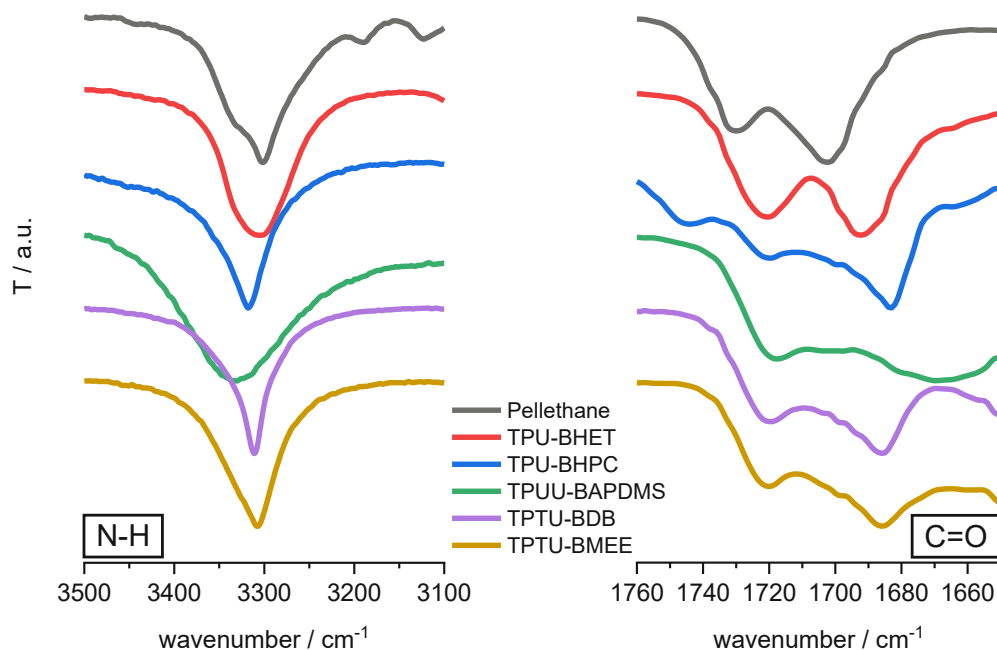


Figure 48: ATR-FTIR spectra of TPUU-BAPDMS, TPTU-BDB and TPTU-BMEE compared to Pellethane, TPU-BHET and TPU-BHPC. The amine region ( $3500\text{--}3100\text{ cm}^{-1}$ ) and the carbonyl region ( $1760\text{--}1650\text{ cm}^{-1}$ ) are shown, which are both characteristic for the H-bond interactions between hard-blocks in TPUs, TPUUs and TPTUs.

### Molecular weight and hard-block content

The number-average molar mass  $\overline{M}_n$  and the polydispersity were determined via GPC measurements, which are shown in Table 15. In contrast to the reference polymers, the siloxane based TPUU-BAPDMS (10.2 kDa) has a quite low molecular weight. A reason for that could be the increased amount of solvent which was necessary to dissolve BAPDMS and therefore a longer reaction time and larger amount of residual moisture in the solvent, which could lead to an incomplete reaction.

An even lower  $\overline{M}_n$  was determined for TPTU-BDB (6.4 kDa), which is surprising because the observed viscosity of the polymer solution after synthesis was comparable to them of the reference polymers TPU-BHET and TPU-BHPC. Furthermore, the  $\overline{M}_n$  of the repeating units of the polymers are between 1.5 and 1.65 kDa, which means a derived low degree of polymerization (DP) of about 4 for TPTU-BDB. Due to the low molecular weights of the siloxane based TPUU-BAPDMS and the boronic ester based TPTU-BDB, they are expected to have poor mechanical properties compared to the reference polymers. The thiourethane reference TPTU-BMEE on the other hand shows an even higher  $\overline{M}_n$  than the benchmark material Pellethane, which should lead to outstanding mechanical properties. Nevertheless, the

polydispersity of all polymers is within a narrow range between 1.6 to 2.1 and therefore as expected at about 2.

Beside GPC measurements, a further insight into the low  $\overline{M}_n$  of siloxane based TPUU-BAPDMS and boronic ester based TPTU-BDB gives the theoretical and calculated hard-block content ( $HB_{th}$  and  $HB_{cal}$ , Table 15). As a constant ratio of 1:2:1 (pTHF:HMDI:CE) was used for all polymers the theoretical hard-block content is located in a narrow range between 34.0 to 39.3 wt%. In contrast to that the hard-block content calculated via  $^1H$ -NMR spectroscopy (Appendix, 1. NMR spectra) deviates strongly for the silicic acid ester-based TPUU compared to the theoretical values and is nearly the half for TPUU-BAPDMS as expected. A reason for the low calculated HB content could be a poor incorporation of the CE into the polymer chain, which would also lead to a low molecular weight. A previous reaction of the isocyanates with water would also lead to a lower  $\overline{M}_n$  and subsequently prevent the incorporation of BAPDMS into the already reacted isocyanates. Surprisingly, boronic ester based TPTU-BDB shows only a slightly lower calculated hard-block content compared to the theoretical value, as for all other polymers, although the  $\overline{M}_n$  is the lowest for TPTU-BDB. The hard-block content for Pellethane could not be determined because of the unknown molecular weight of the macrodiol (pTHF) and the unknown ratio between macrodiol, diisocyanate and chain extender.

Table 15: Overview of synthesized polymers and commercially available Pellethane in terms of number-average molar mass  $\overline{M}_n$ , polydispersity (PDI) and hard-block content (theoretical and calculated).

polymer	$\overline{M}_n$ / kDa <sup>a</sup>	PDI <sup>b</sup>	$HB_{th}$ / wt% <sup>c</sup>	$HB_{cal}$ / wt% <sup>d</sup>
Pellethane	56.3	1.9	-	-
TPU-BHET	23.3	2.1	37.1	33.5
TPU-BHPC	17.3	1.7	34.0	31.3
TPUU-BAPDMS	10.2	1.6	37.9	19.9
TPTU-BDB	6.4	1.8	39.3	36.1
TPTU- BMEE	62.2	2.1	34.2	32.8

<sup>a</sup> Number-average molar mass. <sup>b</sup> polydispersity. <sup>c</sup> theoretical hard-block content ( $HB_{th}$ ). <sup>d</sup> calculated hard-block content from  $^1H$ -NMR ( $HB_{cal}$ ).

### 3.2.3. Mechanical and thermal properties of polymers with one CE

Evaluating the suitability of a thermoplastic polyurethane for use as a vascular graft requires a thorough examination of its mechanical properties, such as elongation at break, ultimate tensile strength, and elastic modulus. The goal is to closely match these mechanical properties to those of natural tissue to ensure optimal compatibility and performance when used in vascular grafts.

Tensile tests were measured of solution cast polymer films as described detailed in the Materials and Methods section. The glass transition temperature  $T_g$  was determined via

Dynamic Mechanical Thermal Analysis (DMTA) by the maximum of the loss modulus curve (Appendix, 3. DMTA spectra).

Table 16 shows the number-average molar mass  $\overline{M}_n$ , calculated hard-block content, mechanical properties and glass transition temperature. The mechanical properties are furthermore demonstrated graphically in Figure 49.

The thiourethane reference TPTU-BMEE shows even higher elongation and ultimate tensile strength but also higher elastic modulus. It is known from literature that thiourethanes tend to be more flexible compared to urethanes and have more ordered domains,<sup>308, 309</sup> which underlines the observed superior mechanical properties. Furthermore, BMEE is able to form strong hydrogen bonds due to the two containing oxygen atoms per each molecule. In contrast to that, boronic ester based TPTU-BDB performed less favorably, although it is also a thiourethane. Due to its bulkier structure compared to BMEE, BDB can perhaps form hydrogen bonds less easily. Although, the chain extender BHET, which was used for the internal reference material TPU-BHET, has also a similar bulky aromatic structure as boronic ester based BDB, but shows quite good mechanical properties. Therefore, it can be assumed that BHET can more easily form hydrogen-bond interactions compared to BDB. However, the mechanical properties of boronic ester based TPTU-BDB are much better than expected for such a low  $\overline{M}_n$  (6.4 kDa). Comparable molecular weights could be obtained for siloxane based TPUU-BAPDMS (10.2 kDa). In contrast to boronic ester based TPTU-BDB, with acceptable mechanical properties, these showed extremely poor mechanical characteristics.

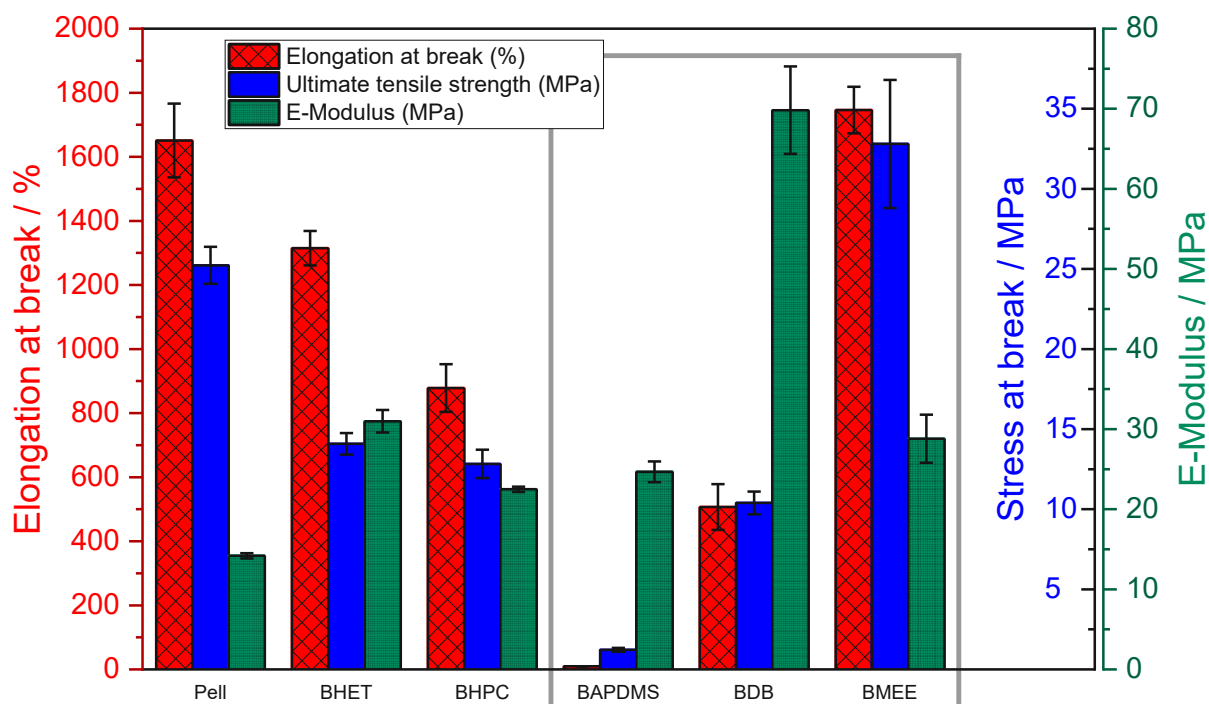


Figure 49: Elongation at break, ultimate tensile strength and elastic modulus of inorganic ester-based TPUUs and TPTUs in comparison with reference polymers TPU-BHET, TPU-BHPC and commercially available Pellethane.

For siloxane based TPUU-BAPDMS, only a single polymer film could be prepared for tensile testing, but it was not reproducible and therefore no  $T_g$  could be determined. The best obtained solution cast polymer film for tensile testing also showed some cracking before removal from the Teflon mold and was extremely brittle after removal (Figure 50). The color is derived from the natural dark brown color of BAPDMS. Siloxane based TPUU-BAPDMS shows extremely low elongation at break (10 %) and ultimate tensile strength (1.2 MPa) compared to the reference polymers TPU-BHET, TPU-BHPC and Pellethane (> 850 %; > 12.8 MPa). The siloxane based TPUU-BAPDMS also shows a very low calculated hard-block content compared to the reference polymers (Table 15, Table 16). This indicates that the siloxane based chain extender BAPDMS was probably not fully incorporated into the polymer chain. A stoichiometric imbalance due to impurities of BAPDMS can be excluded as it was successfully recrystallized from diethyl ether.<sup>313</sup>  $^1\text{H-NMR}$  and  $^{13}\text{C-APT-NMR}$  spectra after recrystallization of BAPDMS are shown in the appendix section (1. NMR). However, due to the increased amount of solvent required to dissolve BAPDMS (2.5 times more DMF was necessary), the reaction time in the second polymerization step may have been prolonged and more isocyanates could have reacted with the residual water in the solvent (dry DMF, < 20 ppm  $\text{H}_2\text{O}$ ). For the other TPU syntheses, 10 mL DMF was used for the CE addition, which would lead to a side reaction of approx. 0.1 % of the NCO groups at a residual moisture content of 20 ppm  $\text{H}_2\text{O}$ . In the case of BAPDMS, 25 mL DMF was used, resulting in the reaction of approx. 0.25 % of the NCO groups with water. These resulting amines cannot subsequently polymerize with the diamine-based BAPDMS and the proportion of hard-blocks (HMDI+CE) is lower than expected.

In addition to tensile tests, DMTA measurements were performed (Appendix, 3. DMTA spectra). The  $T_g$  for TPTU-BDB was  $-64\text{ }^\circ\text{C}$  and therefore lower compared to TPTU-BMEE ( $-56\text{ }^\circ\text{C}$ ) and TPU-BHPC ( $-57\text{ }^\circ\text{C}$ ). Both values are between the glass transition temperatures of Pellethane and TPU-BHET (Table 16).

Table 16: Comparison of number-average molar mass  $\overline{M}_n$ , calculated hard-block content, mechanical properties and glass transition temperature of inorganic ester-based TPUUs and TPTUs with reference polymers.

polymer (CE)	$\overline{M}_n$ / kDa <sup>a</sup>	HB <sub>cal</sub> / wt% <sup>b</sup>	$\epsilon_b$ / % <sup>c</sup>	TS / MPa <sup>d</sup>	E / MPa <sup>e</sup>	$T_g$ / °C <sup>f</sup>
Pellethane	56.3	-	1651 ± 115	25.2 ± 1.2	14.2 ± 0.3	-52
BHET	23.3	33.5	1315 ± 54	14.1 ± 0.7	31.0 ± 1.4	-71
BHPC	17.3	31.3	878 ± 75	12.8 ± 0.9	22.5 ± 0.3	-57
BAPDMS	10.2	19.9	10 ± 0	1.2 ± 0.1	24.7 ± 1.3	-
BDB	6.4	36.1	507 ± 72	10.4 ± 0.7	69.8 ± 5.5	-64
BMEE	62.2	32.8	1746 ± 73	32.8 ± 4.0	28.8 ± 3.0	-56

<sup>a</sup> Number-average molar mass. <sup>b</sup> calculated hard-block content from  $^1\text{H-NMR}$  (HB<sub>cal</sub>). <sup>c</sup> Elongation at break  $\epsilon_b$ .

<sup>d</sup> tensile strength TS. <sup>e</sup> elastic modulus E. <sup>f</sup> Glass transition temperature  $T_g$  obtained from the maxima of loss modulus curves.

As a result, siloxane based TPUU-BAPDMS showed mechanical properties that are too poor for further use. Boronic ester based TPTU-BDB, on the other hand, showed promising mechanical properties, but they were inferior to those of the reference materials. Excellent mechanical properties have been achieved with the thiourethane reference TPTU-BMEE, some of which are better than those of the Pellethane.

Nevertheless, all spectra confirm a  $T_g$  below 0 °C for all polymers (Table 16), which would make them suitable as vascular grafts at body temperature.

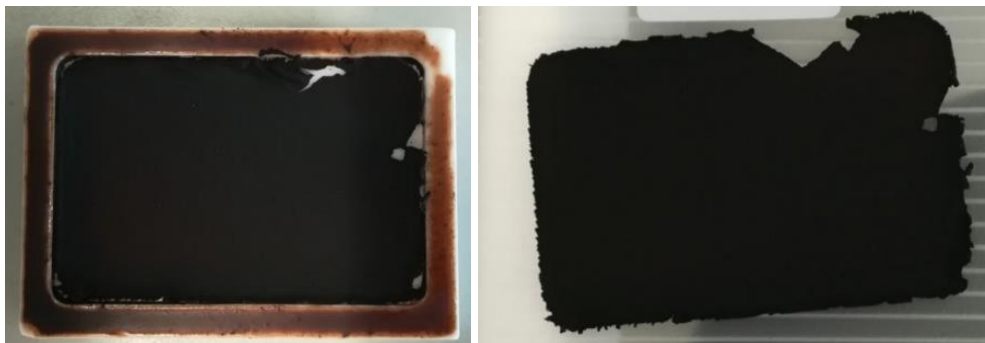


Figure 50: TPUU-BAPDMS in a Teflon-mold (left) and after removing from the mold (right), shows brittle behavior.

### 3.2.4. Degradation behavior of polymers with one CE

The degradation behavior of silicic acid ester-based TPUU-BAPDMS could not be investigated because the polymer films were not reproducible as already discussed above.

Degradation characteristics of TPTUs were investigated (boronic ester based TPTU-BDB and thiourethane reference TPTU-BMEE) and were compared with TPU-BHET and Pellethane. Degradation studies were performed in phosphate-buffered saline solution (PBS 4x, pH=7.4) at body temperature (37 °C) and at elevated temperature (90 °C) to accelerate the process of hydrolytic degradation. As expected the TPTU with BMEE as chain extender shows the lowest mass erosion at both temperatures after Pellethane (Figure 51) because no cleavable moieties are present in the molecule compared to BHET (ester) or BDB (B-O bond). After 70 days at 37 °C about 97.5% of the original mass is still left compared to about 93% at 90 °C. The carboxylic ester cleavable TPU-BHET shows a bit faster degradation in terms of mass erosion compared to the thiourethane reference TPTU-BMEE. The fastest degradation is observed for boronic ester based TPTU-BDB. Because TPTU-BMEE shows very slow degradation, it can be assumed that the degradation of TPTU-BDB is caused of the cleavable B-O bond of the boronic acid ester moiety and not by the thiourethane group.



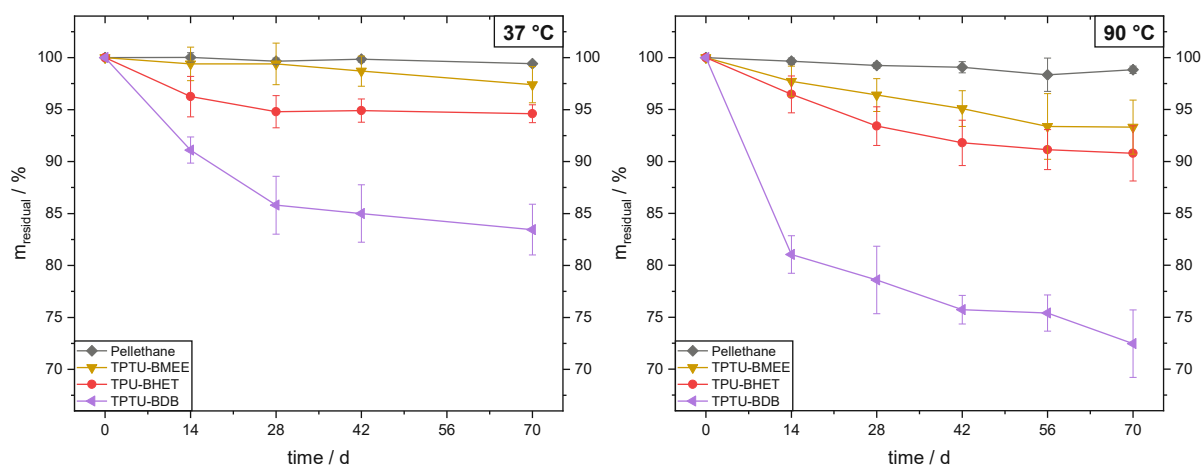


Figure 51: Residual mass  $m_{\text{residual}}$  in % of Pellethane, TPTU-BMEE, TPU-BHET and TPTU-BDB in PBS buffer solution (4x) at 37 °C (left) and at 90 °C (right).

Furthermore, to the mass erosion, Figure 52 shows molecular weight change during degradation process in PBS buffer solution at 37 °C and 90 °C. The number-average molar mass  $\overline{M}_n$  of the polymer before degradation acts as reference value (100 %). After each time period  $\overline{M}_n$  was determined via GPC in triplicates via conventional calibration method. Figure 52 left shows number-average molar mass changes at 37 °C over a time period of 70 days. The thiourethane reference TPTU-BMEE shows the smallest molecular weight decrease after Pellethane followed by carboxylic ester based TPU-BHET. In contrast to that for boronic ester based TPTU-BDB a constant increase of  $\overline{M}_n$  during 70 days is observed, resulting in even an absolute increase of molecular weight of ~16 % compared to the starting point.

Because Figure 51 showed a decrease of mass a possible explanation for this behavior could be a leaching out of small molecular weight species. Therefore, the  $\overline{M}_n$  would increase due to a higher content of higher molecular weight species.

Further insights especially in the degradation behavior of boronic ester based TPTU-BDB gives the GPC degradation study at 90 °C (Figure 52 right). For TPU-BHET as expected a faster decrease of  $\overline{M}_n$  is observed at 90 °C. The thiourethane reference TPTU-BMEE shows nearly the same results as TPU-BHET. Compared to these results boronic ester based TPTU-BDB shows an extremely high increase of molecular weight during the first 7 days of ~640 %. Due to this surprising result a  $\overline{M}_n$  determination via triple detection was carried out for TPTU-BDB resulting in an increase of 440 % after 7 days. For all other time points which were measured for thiourethane reference TPTU-BMEE and carboxylic ester based TPU-BHET no GPC measurements were possible for boronic ester based TPTU-BDB due to insoluble specimens in any investigated solvents (Hexafluoro-2-propanol, THF, DMF, DMSO, MeCN, MeOH, EtOH, acetone, dioxane,  $\text{CHCl}_3$ , DCM, water, ethyl acetate).

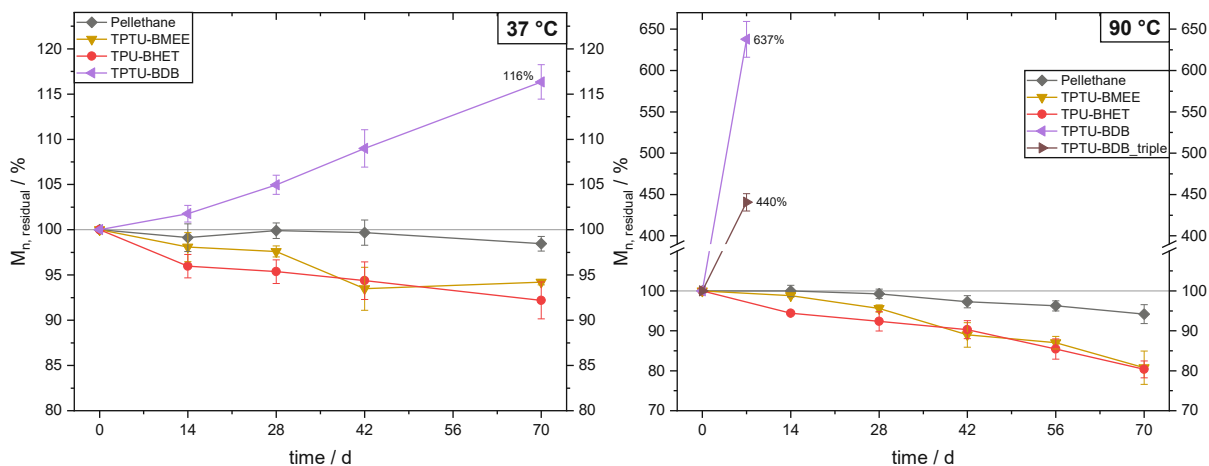


Figure 52: Development of number-average molar mass  $\overline{M}_n$ , residual in % of original  $\overline{M}_n$ , before degradation over a time period of 70 days of Pellethane, TPTU-BMEE, TPU-BHET and TPTU-BDB in PBS buffer solution (4x) at 37 °C (left) and 90 °C (right). TPTU-BDB (90 °C) was further measured via triple detection method.

### Degradation behavior at different pH values

In order to gain a deeper insight into the degradation behavior of boronic ester based TPTU-BDB, further degradation studies were performed in acidic and basic buffer solutions. Degradation studies of TPTU-BDB and TPU-BHET at 90 °C were performed at three different pH-values (Acetate buffer, pH=5; PBS buffer, pH=7.4 and carbonate-bicarbonate buffer, pH=10).

Beside the gravimetric study (Figure 53 left) also a GPC study (Figure 53 right) was done. In terms of mass erosion TPU-BHET degrades faster under basic conditions than under acidic conditions. Boronic ester based TPTU-BDB shows an even lower degradation rate at pH=5, compared to pH=7.4. The fastest degradation is observed under basic conditions. Furthermore, TPTU-BDB shows a very fast degradation within the first 7 days by a  $m_{residual}$  of 75-83 % depending on the pH value. Although TPU-BHET shows the highest degradation rate within the first 7 days but only mass loss of about 5-8 %. Between 14 and 70 days of degradation time, boronic ester based TPTU-BDB shows only a low degradation rate. Especially the high degradation rate of TPU-BDB within the first 7 days could be an indication of a fast “washing-out” of a polymer species or a polymer part which is further discussed by GPC measurements.

Figure 53 right shows the molecular weight change of BDB- and BHET-based TPUs. For TPU-BHET at pH=5 and 10 a nearly parallel decrease of  $M_n$  could be observed resulting in ~50-60% % of the original molecular weight after 70 days. Thereby, TPU-BHET degrades fast under basic conditions as already observed for mass erosion.

In contrast to that boronic ester based TPTU-BDB shows an increase in molecular weight compared to the reference before degradation. At pH=5 an increase of about 300 % of the original  $\overline{M}_n$  was observed after 70 days. The samples of the degradation study at pH=7.4 were not dissolvable anymore after 14 days, therefore only GPC-data after 7 days were collected with an  $\overline{M}_n$  increase of about 640 %. At pH=10, no GPC-measurement was possible for TPTU-BDB even after 7 days. Non-soluble, but swollen samples of TPTU-BDB are show in Figure 54.

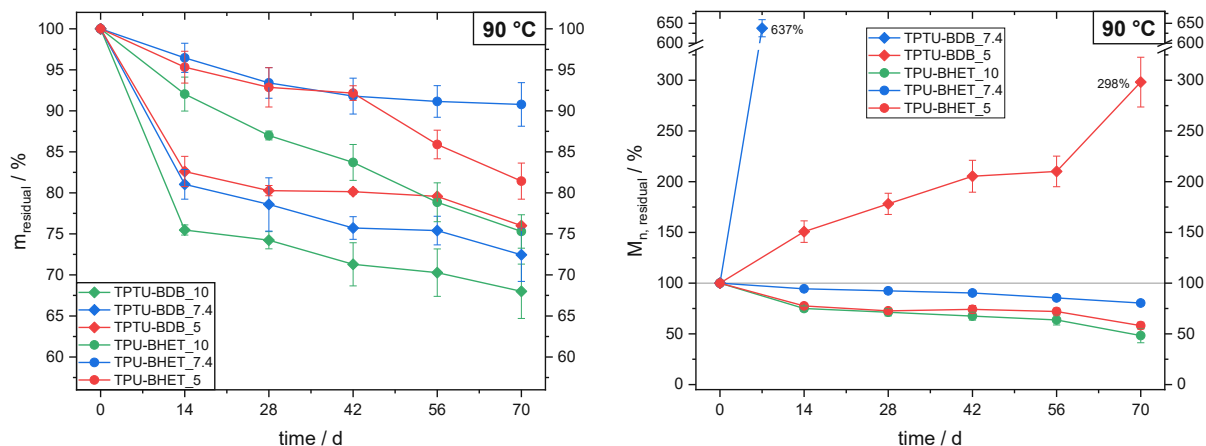


Figure 53: Residual mass  $m_{residual}$  in % (left) and development of molecular weight  $M_n$ , residual in % of original  $M_n$  before degradation (right) of TPU-BHET and TPTU-BDB after degradation in acetate buffer (pH=5), in PBS buffer solution (pH=7.4) and carbonate-bicarbonate buffer (pH=10) at 90 °C.



Figure 54: Non-soluble TPTU-BDB after degradation of 14d (left) and 21d (middle) in PBS and after 7d (right) at pH=10. Top row shows insoluble but swollen samples in hexafluoro-2-propanol. Bottom row shows degraded samples after drying.

## Degradation investigated via FTIR spectroscopy

Besides, mass erosion experiments and GPC-measurements, degradation behavior of boronic ester based TPTU-BDB and carboxylic ester based TPU-BHET was investigated via ATR-FTIR spectroscopy. Figure 55 shows FTIR spectra of TPTU-BDB and TPU-BHET before degradation and after a degradation time of 28 days at pH=5; 7.4 and 10. At  $\sim 3300\text{ cm}^{-1}$   $R_2\text{-NH-}$  and  $R\text{-OH}$  regions are shown. TPTU-BDB before degradation shows a sharper peak ( $R_2\text{-NH-}$ ) compared to the samples after degradation, which could be a result of the formation of OH groups because of an overlay of  $R_2\text{-NH-}$  and  $R\text{-OH}$  groups. In the region of  $\sim 850\text{ cm}^{-1}$  and  $\sim 660\text{ cm}^{-1}$  aromatic bands resulting from BDB could be found only for the spectrum of boronic ester based TPTU-BDB before degradation. This assumes a “washing-out” of benzene-1,4-diboronic acid during degradation. This is underlined by Romanos *et al.*,<sup>315</sup> where IR bands of borates were investigated, especially B-O at  $\sim 1320\text{ cm}^{-1}$  and B-C at  $\sim 1020\text{ cm}^{-1}$ . Both could only be identified in the spectrum of TPTU-BDB before degradation.

In contrast to the FTIR spectra of TPTU-BDB, the spectra of TPU-BHET (Figure 55 bottom) shows no significant changes in the above-mentioned regions. The aromatic bands at  $\sim 850\text{ cm}^{-1}$  and  $\sim 660\text{ cm}^{-1}$  are present at all different pH-values after 28 days of degradation time.

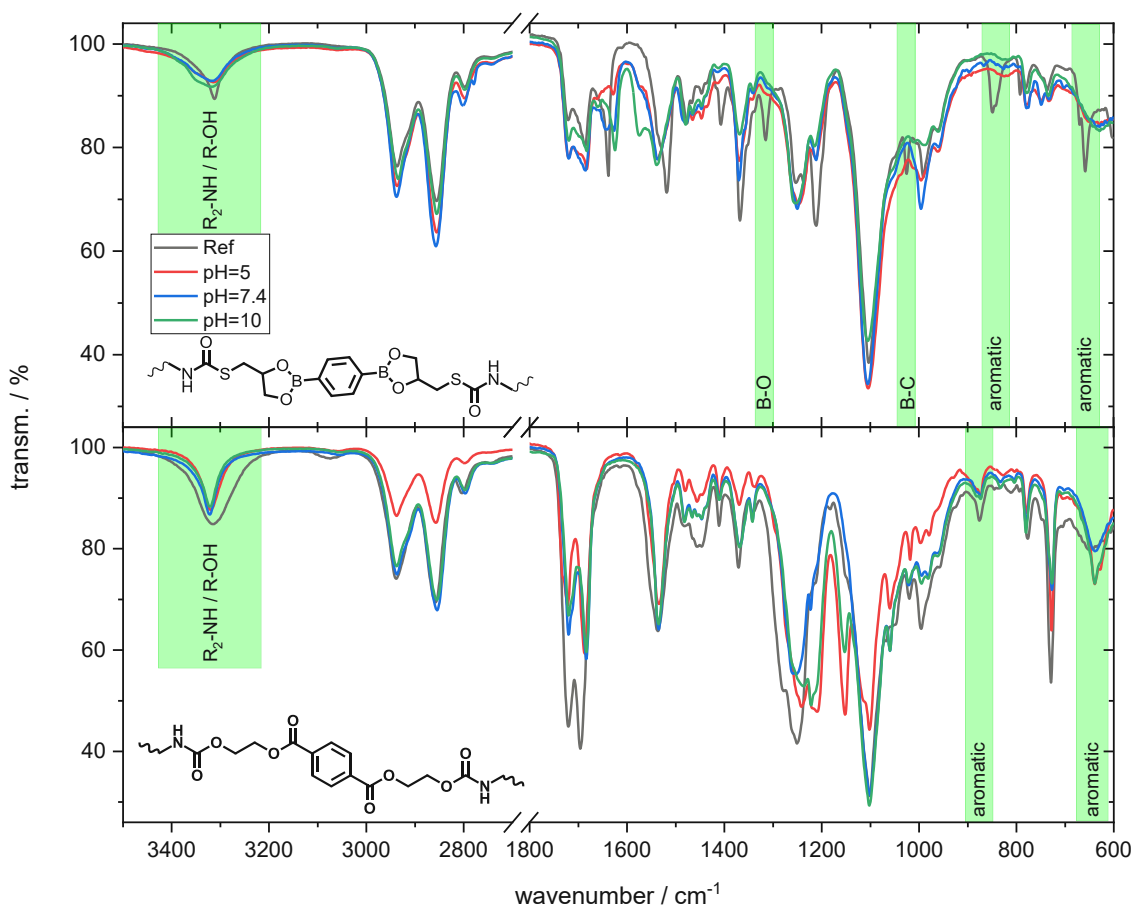
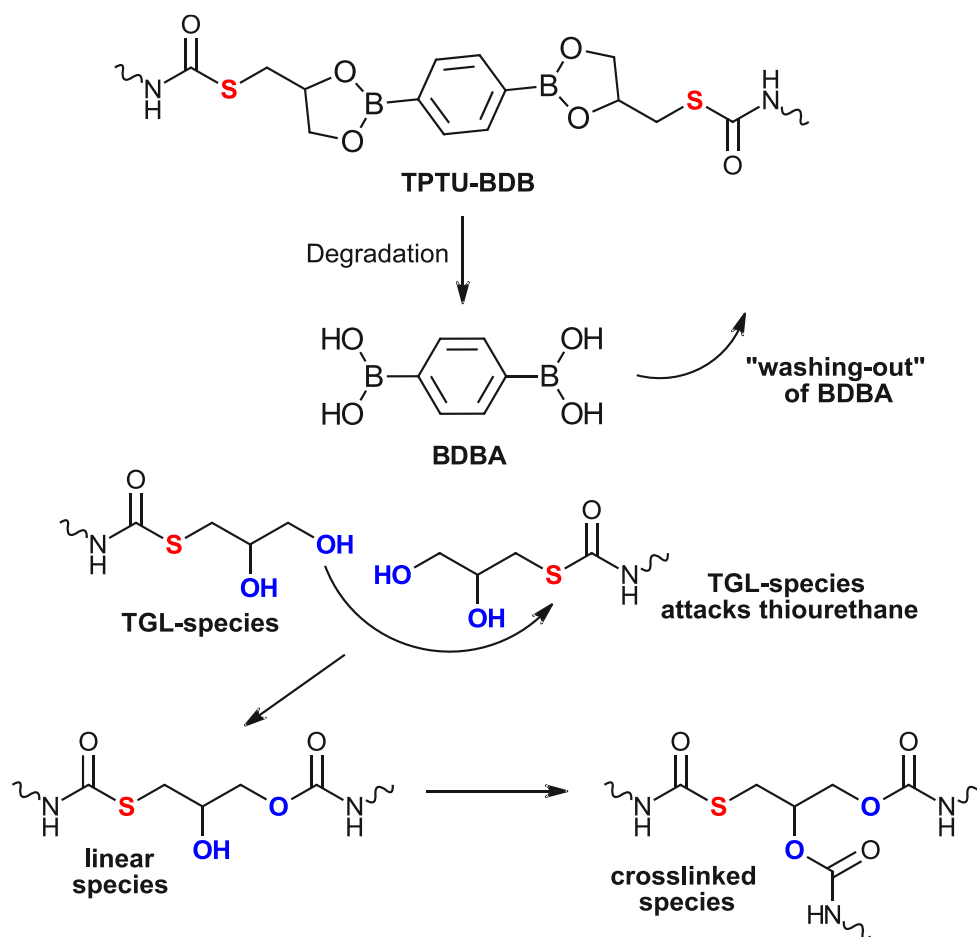


Figure 55: FTIR spectrum of TPTU-BDB (Ref-top), TPU-BHET (Ref-bottom) and both polymers after a degradation time of 28 days at different pH-values (pH=5, 7.4 and 10) between  $3500\text{--}2700\text{ cm}^{-1}$  and  $1800\text{--}600\text{ cm}^{-1}$ .

## Crosslinking of thiourethanes in presence of glycerol and BDBA

Based on the observed “washing out” of benzene-1,4-diboronic acid during degradation investigated via ATR-FTIR measurements, a possible explanation for the insoluble specimen and the extreme increase of the molecular weight of boronic ester based TPTU-BDB could be the way of degradation shown in Scheme 17.

To investigate possible side reactions of the thiourethane groups with hydroxy groups<sup>316</sup> in presence of benzene-1,4-diboronic acid (BDBA) during degradation of TPTU-BDB, the thiourethane based reference TPTU-BMEE was stored in PBS buffer solution at 90 °C for 7 days. Equimolar amounts (based on CE BMEE) of BDBA and 1,2,3-propanetriol (glycerol, Gly) were also added. Another sample was treated with a large excess of glycerol (600 eq. to CE) and BDBA (40 eq.). Glycerol was added to illustrate a reaction of thiourethanes with hydroxy groups. If a reaction will occur, the linear TPTU-BMEE would form a branched or crosslinked polymer and thus leading to an increase of molecular weight or to insoluble species with the tri-functional glycerol, which could then also happen with the TGL-species of boronic ester based TPTU-BDB (Scheme 17).



Scheme 17: Assumed degradation of TPTU-BDB by “washing-out” of BDBA and crosslinking via “intramolecular” reaction of hydroxy terminated TGL-species (thioglycerol-species) with thiourethane moieties.

Figure 56 shows the molecular weight  $\overline{M}_n$  change of the thiourethane reference TPTU-BMEE after a degradation time of 7 days at 90 °C with addition of benzene-1,4-diboronic acid (BDBA) and Glycerol (Gly) compared to boronic ester based TPTU-BDB.

It was clearly shown that there is no increase in molecular weight of TPTU-BMEE (95.2 %) treated with equimolar amounts of glycerol and BDBA compared to TPTU-BDB (637.8 %).

However, a significant increase in molecular weight of about 40% was observed in the TPTU-BMEE sample with excess glycerol and BDBA, which is still low compared to TPTU-BDB. In addition, an excess of 1-butanol (600 eq. to CE) was added to TPTU-BMEE.

This clearly showed that a reaction with alcohols was taking place as the solution turned brown and complete degradation of the polymer was observed (Figure 57).

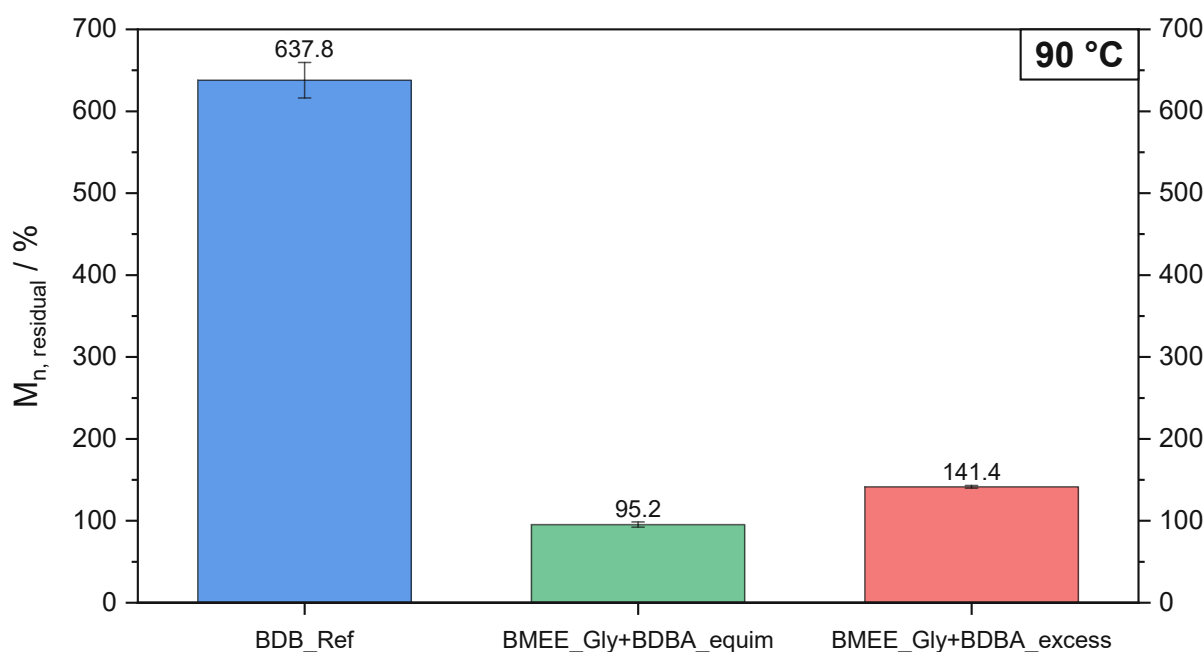


Figure 56: Development of number-average molar mass  $\overline{M}_n$ , residual in % of original  $\overline{M}_n$ , before degradation over a time period of 7 days of TPTU-BDB (BDB\_Ref) and TPTU-BMEE with equimolar amounts of Gly and BDBA (middle) and with an excess of Gly (600 eq.) and BDBA (40 eq.) compared to the chain extender (BMEE).



Figure 57: Degraded TPTU-BMEE samples with excess of 1-butanol (right), glycerol and BDB (middle) and without any additions after storing in PBS buffer solution (4x) at 90 °C for 7 days.

Thus, the increase in molecular weight of BDB-based polymers can be due to a reaction of hydroxy groups with the thiourethane moiety. A reason why this phenomenon was only observed with an excess of glycerol could be explained that glycerol was dissolved in the buffer solution and the thiourethane reference TPTU-BMEE was of course not dissolved and therefore only small amounts of glycerol are able to penetrate into the sample (no intermolecular reaction). By using a large excess, the amount of glycerol, which can penetrate into the polymer film is high enough to enable reactions with thiourethane groups. In contrast to that, hydroxy terminated TGL-species at TPTU-BDB are able to react in a “intramolecular” way as TGL is covalently bond to the polymer.

### 3.2.5. Model compounds of boronic acid esters

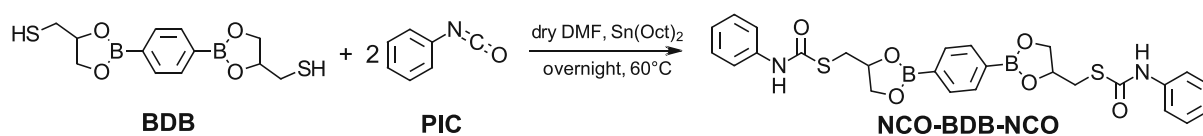
In order to get a further insight into the behavior of thiourethanes and boronic acid esters compared to carboxylic ester-based urethanes, model compounds based on BDB and BHET were prepared. Compared to the polymers, the degradation of these could be analyzed more easily by  $^1\text{H-NMR}$  spectroscopy. For this reason, an aromatic phenyl isocyanate (PIC) was used for these compounds instead of an aliphatic isocyanate, since the aromatic protons do not overlap with the aliphatic protons surrounding the thiourethane or urethane moieties. Besides,  $^1\text{H-NMR}$  spectroscopy, the thiourethane formation and temperature stability was investigated via FTIR spectroscopy.

#### Synthesis of NCO-BDB-NCO

For the synthesis of the model compound NCO-BDB-NCO, the aim was to reproduce the polymer synthesis of TPTU-BDB as close as possible and therefore it was not optimized for this compound.

Therefore, 2,2'-(1,4-phenylene)bis[4-thioethyl-1,3,2-dioxaborolane] (BDB) was dried for 2 days at reduced pressure ( $< 0.1$  mbar) and phenyl isocyanate (PIC) was distilled at 30 mbar at  $95^\circ\text{C}$  directly before synthesis. Briefly, a solution of PIC in dry DMF was added to BDB under argon atmosphere and the catalyst stannous octoate ( $\text{Sn}(\text{Oct})_2$ ) was added. The mixture was stirred overnight at  $60^\circ\text{C}$  (Scheme 18). The reaction solution was precipitated in diethyl ether and was filtered, resulting in a white solid with a yield of 58.7 %. The poor yield can be explained by the fact that the precipitation did not work optimally and product remained in solution. However, as mentioned above, the synthesis of the model compound should be as similar as possible to the synthesis of TPTU-BDB.

The successful formation of NCO-BDB-NCO was validated via  $^1\text{H-NMR}$  and  $^{13}\text{C-APT-NMR}$  spectroscopy as evidenced in the appendix section (Appendix, 1. NMR spectra). Additionally, a narrow melting range of  $210.4\text{-}214.5^\circ\text{C}$  confirmed a clean product.



Scheme 18: Synthesis of model compound NCO-BDB-NCO.



To prove the formation of thiourethanes, FTIR spectra of both educts (BDB, PIC) and the model compound NCO-BDB-NCO were measured. A comparison of these spectra is shown in Figure 58. Between 3200 and 3300  $\text{cm}^{-1}$  a secondary amine band could be identified for NCO-BDB-NCO which indicates the formation of thiourethanes. This band is not evident in the spectra of the educts. Also, a small band at about 2550  $\text{cm}^{-1}$  which results from a thiol moiety is only detected in the spectrum of BDB.

Furthermore, the isocyanate absorption band between 2150 and 2350  $\text{cm}^{-1}$  could be identified only in the spectrum of phenyl isocyanate (PIC) and is no longer identifiable in the spectrum of NCO-BDB-NCO.

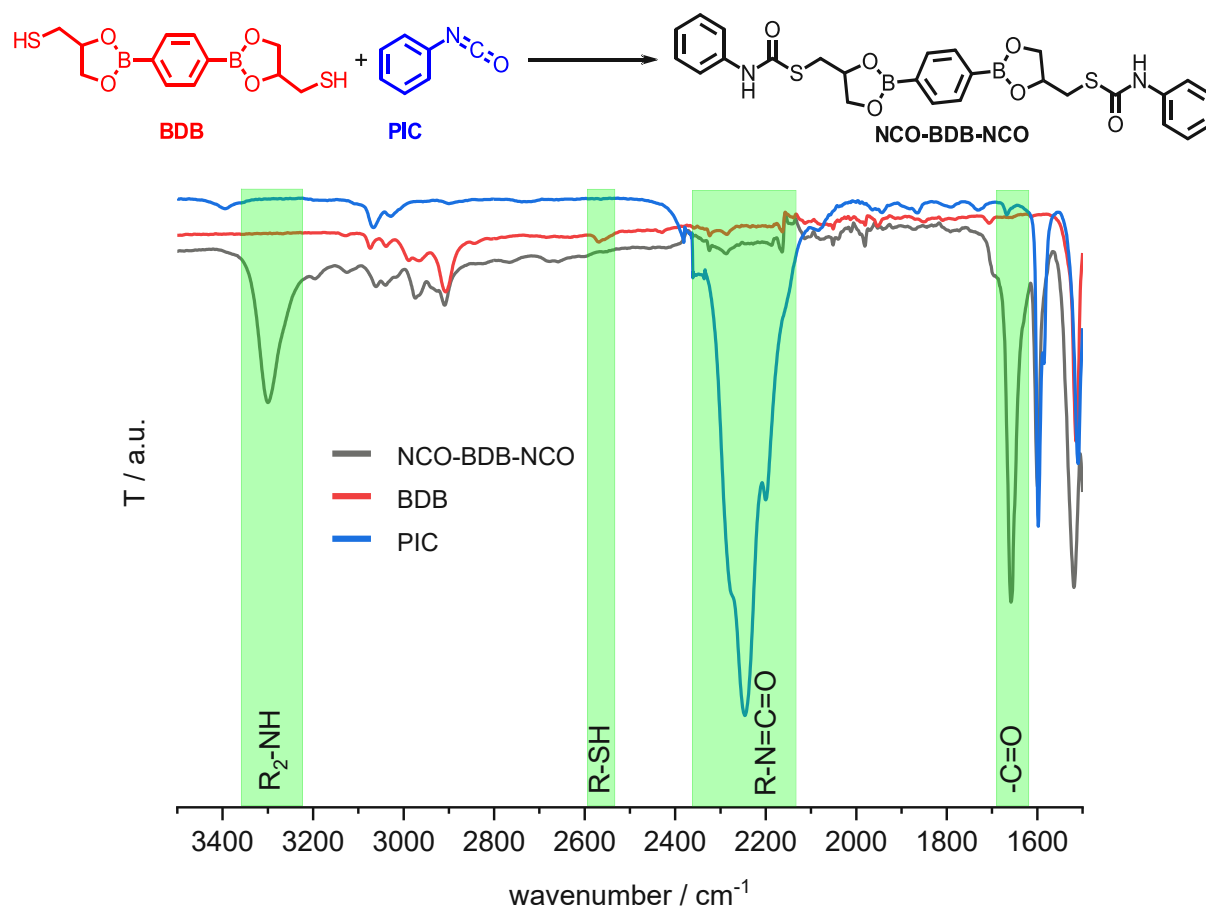
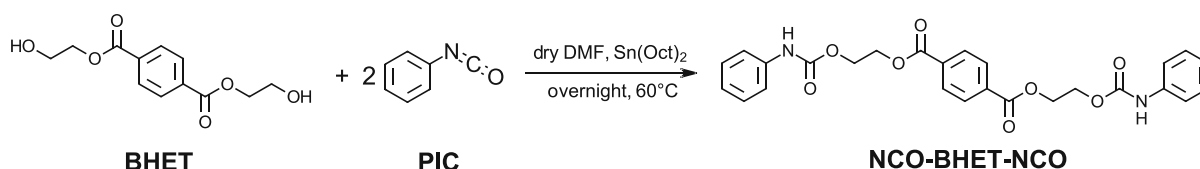


Figure 58: Comparison of FTIR spectra of model compound NCO-BDB-NCO and the educts 2,2'-(1,4 phenylene)-bis[4-thioethyl-1,3,2-dioxaborolane] (BDB) and phenyl isocyanate (PIC).

### Synthesis of NCO-BHET-NCO

According to BDB based model compound (NCO-BDB-NCO), the synthesis of NCO-BHET-NCO was performed (Scheme 19). The yield was only 61.4 %, because of the above discussed circumstances. Also, NCO-BHET-NCO was partially soluble in diethyl ether and therefore the yield after precipitation quite low compared to TPU-BHET synthesis. After drying the solid product shows a white coloring.

The purity of NCO-BHET-NCO was confirmed via <sup>1</sup>H-NMR and <sup>13</sup>C-APT-NMR spectroscopy (Appendix, 1. NMR spectra). Furthermore, a melting range of 183.4-191.2 °C was observed.



Scheme 19: Synthesis of model compound NCO-BHET-NCO.

## Degradation behavior of model compounds via $^1\text{H-NMR}$ spectroscopy

Figure 59 shows the comparison of  $^1\text{H-NMR}$  spectra of the model compounds NCO-BDB-NCO and NCO-BHET-NCO in  $\text{DMSO-}d_6$  and after 24 h after the addition of  $\text{D}_2\text{O}$ . As described in Cash *et al.*<sup>254</sup> boronic acid esters as BDB show a reversible formation of boronic acid in presence of water. After 24 h the peaks b, c, c' and d shifts about 1 ppm to lower values. The aromatic region shows no difference in both spectra. Furthermore, a peak at  $\sim 4$  ppm appears which could result from acidified  $\text{H}_3\text{O}^+$  or HO-B due to the formation of benzene-1,4-diboronic acid.  $\text{H}_2\text{O}$  in  $\text{DMSO-}d_6$  shows under neutral conditions a chemical shift of 3.33 ppm.<sup>317</sup> In contrast to NCO-BDB-NCO, the  $^1\text{H-NMR}$  spectra of NCO-BHET-NCO show no peak shifts after the addition of  $\text{D}_2\text{O}$  and storing for 24 h, with the exception of a peak at  $\sim 4$  ppm which was also observed in the spectrum of NCO-BDB-NCO. This peak could be resulting from an acidification of the solution due to the formation of carboxylic acids by degrading ester moieties. Furthermore, peak broadening is observed for all peaks after the addition of  $\text{D}_2\text{O}$ .

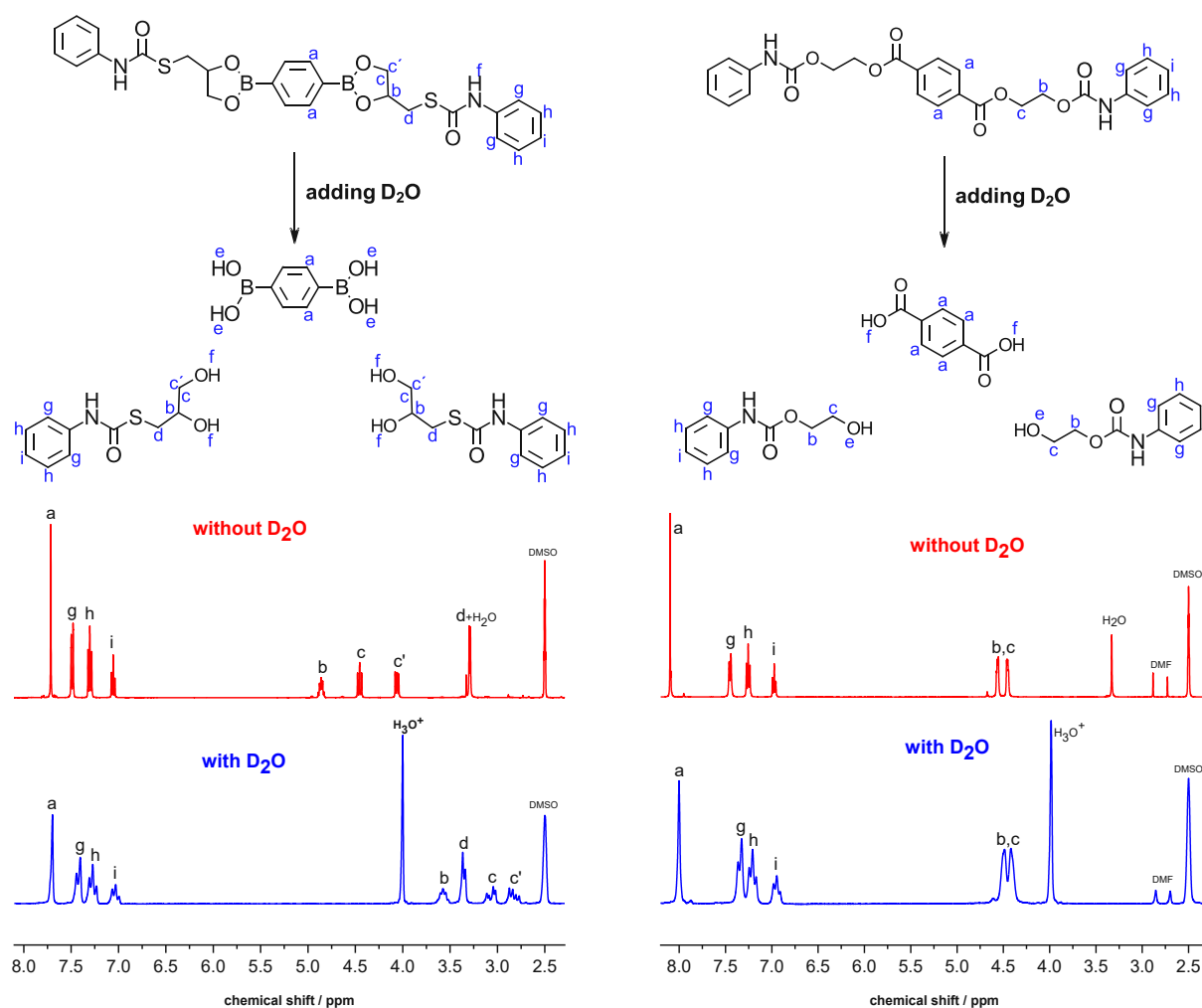


Figure 59: Comparison of expected degradation processes and  $^1\text{H-NMR}$  spectra of model compounds NCO-BDB-NCO (left) and NCO-BHET-NCO (right) in  $\text{DMSO-}d_6$  with and without  $\text{D}_2\text{O}$  after 24 h.

## Temperature stability test of thiourethanes and boronic acid esters via FTIR

The stability of the thiourethane bond and the B-O bonds in TPTU-BDB were investigated via FTIR measurements of the model compound NCO-BDB-NCO at different temperatures (Figure 60). Furthermore, the same study was carried out for NCO-BHET-NCO to give further insights in the temperature stability of urethanes and ester bonds in TPU-BHET (Figure 61).

In Figure 60 FTIR spectra of the model compound NCO-BDB-NCO at different temperatures are shown. Measurements were performed at 25, 40, 60, 80, 100, 120 °C and after cooling down from 120 °C to 25 °C (cooled to 25 °C). There is no significant change of the absorption bands for the secondary amine (~3300 cm<sup>-1</sup>), thiol (~2700 cm<sup>-1</sup>) and the carbonyl band (~1650 cm<sup>-1</sup>) at all measured temperatures. Only the region between 1800 and 2400 cm<sup>-1</sup> is changing. Therefore, the lowest transmission is observed at 120 °C but is nearly going back after cooling down to 25 °C to the original values for 25 °C.

The reason for this is that the same sample was always measured at different temperatures without remeasuring the background in between. Apparently, the background noise changes between ~1800 and 2400 cm<sup>-1</sup> when the temperature is increased, but this could be proven by a separate measurement (Figure 62). Hereby, the instrument was heated to 100 °C, a background measurement was performed and then the sample itself was measured at 100 °C. In this spectrum (100°C Baseline) no absorption band can be detected in the range between 1800 and 2400 cm<sup>-1</sup> in contrast to the spectrum without measuring a new background (100°C).

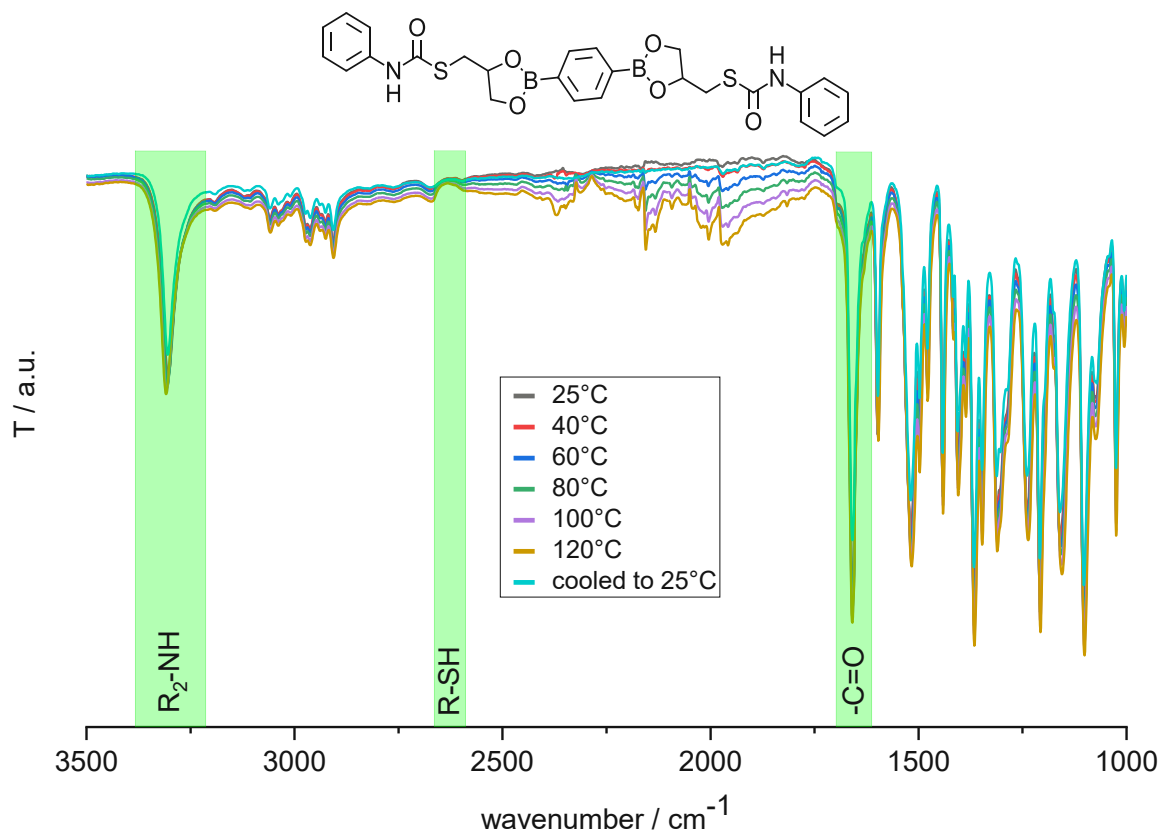


Figure 60: Comparison of FTIR spectra of model compound NCO-BDB-NCO at different temperatures.

The same temperature program as mentioned above was performed for NCO-BHET-NCO (Figure 61). No changes of the absorption bands of the secondary amine ( $\sim 3300\text{ cm}^{-1}$ , urethane,  $\text{R}_2\text{-NH}$ ), urethane,  $\text{R}_2\text{-NH}$ ), aromatic region ( $\sim 3100\text{ cm}^{-1}$ ,  $=\text{C-H}$ ), aliphatic region ( $\sim 2900\text{ cm}^{-1}$ ,  $-\text{C-H}$ ) and the carbonyl bands ( $\sim 1600\text{-}1750\text{ cm}^{-1}$ ,  $-\text{C=O}$ ) are observed at any temperature. As for NCO-BDB-NCO only the region between  $1800$  and  $2400\text{ cm}^{-1}$  is changing, as explained above.

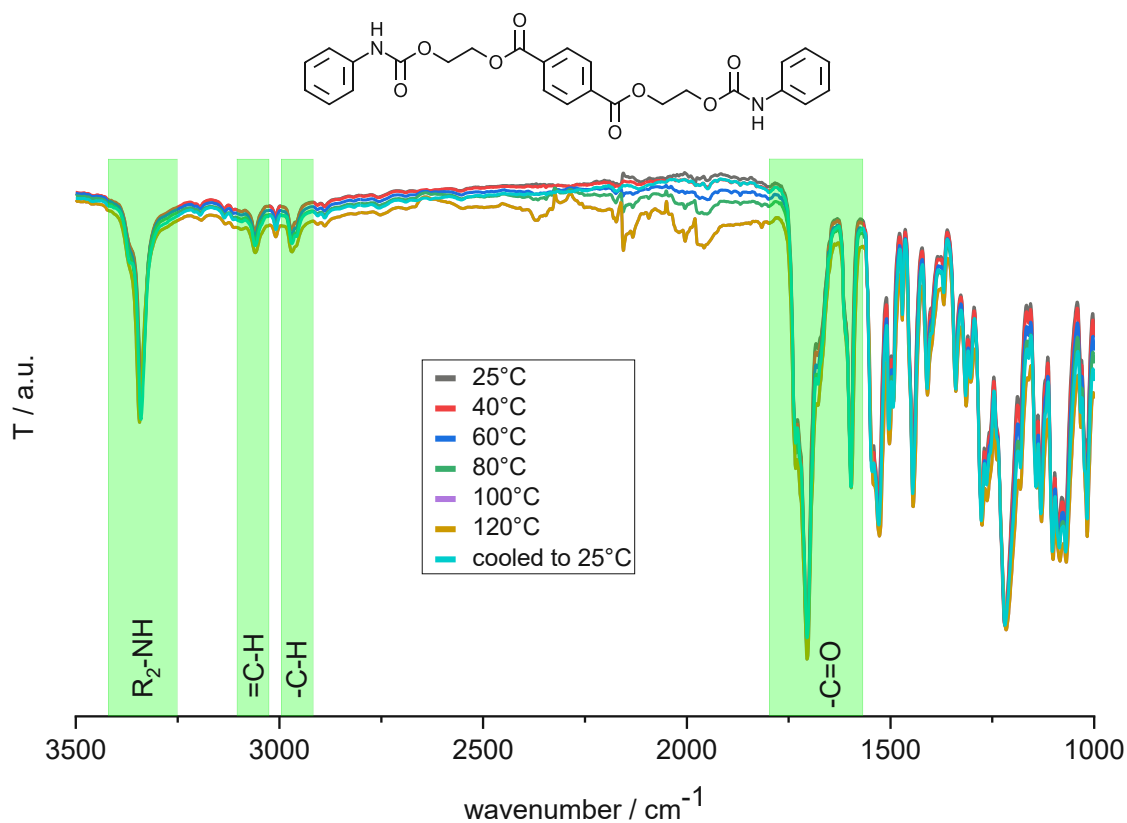


Figure 61: Comparison of FTIR spectra of model compound NCO-BHET-NCO at different temperatures.

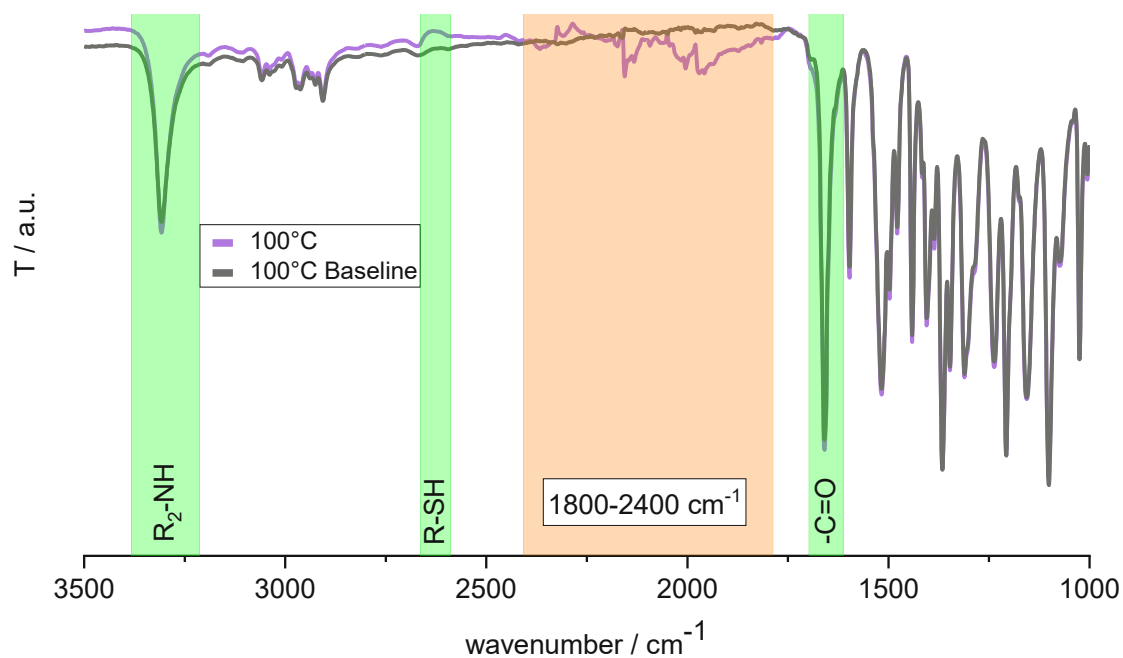


Figure 62: Change of background noise in FTIR between  $1800$  and  $2400\text{ cm}^{-1}$  at  $100\text{ }^\circ\text{C}$ .

Unfortunately, it was not possible to produce a TPU with the phosphate ester-based chain extender BHBEF. Despite several attempts, the polymer could only be produced once in a still soluble, non-crosslinked form. However, it could not be processed into a film and therefore no further tests such as tensile tests or degradation studies could be performed.

Reproducibility of siloxane based TPUU-BAPDMS was also not possible. Only one polymer film could be produced for mechanical tests, but this material showed very poor mechanical stability.

The boronic ester based TPTU-BDB was successfully produced. The degradability could be increased compared to carboxyl ester-based TPUs such as TPU-BHET and TPU-BHEF. Good results were obtained in the mechanical tests, but still inferior to the reference materials TPU-BHET and TPU-BHPC. The thiourethane reference material TPTU-BMEE has excellent mechanical properties, some of which exceed those of the benchmark material Pellethane. However, BMEE is not suitable as a degradable chain extender because degradation studies showed only a low degradation rate.

Compared to the reference polymers, boronic ester based TPTU-BDB shows a significantly higher degradation rate during mass erosion. However, an increase in molecular weight was observed at 37 °C. This increase was particularly evident at 90 °C, where it was approximately 600 % within 7 days. After this time, the samples were insoluble, which may indicate crosslinking. More detailed studies of boronic ester based TPTU-BDB showed a pH-dependent increase in molecular weight in different buffer solutions, which also increased with increasing pH. ATR-IR spectroscopy revealed a “washing-out” of benzene-1,4-diboronic acid (BDBA), as the characteristic B-O and B-C bands were no longer detectable after degradation. The OH-terminated thiourethanes formed by the “washing-out” of BDBA could lead to crosslinking by intramolecular reactions between free OH groups and the thiourethane group, as demonstrated by model reactions between thiourethane-based TPTU-BMEE by addition of glycerol.

Based on the results obtained in this chapter, the combination of carboxylic ester based BHET and another chain extender (BHBEF, BAPDMS or BDB) in different ratios to each other will be tested in the following to see what effect it has on the mechanical properties and the degradation behavior compared to the polymers with only one chain extender. Priority is given to the combination of BHET with BDB, as boronic ester based TPTU-BDB showed good degradation behavior, but the mechanical properties were worse than with TPU-BHET.

### 3.3. TPUs with two different CEs

As shown in chapter 3.2. TPUs, TPUUs and TPTUs with one CE, the phosphate based TPU-BHBEP could not be successfully prepared and the siloxane based TPUU-BAPDMS showed a very brittle behavior, which made the preparation of polymer films very difficult. Nevertheless, the boronic ester based TPTU-BDB showed very interesting properties, such as a significantly increased hydrolytic degradation rate compared to the reference materials. However, since the mechanical properties were inferior to the reference materials, TPUs, TPUUs, and TPTUs with a combination of two different chain extenders are prepared in this chapter. Since the carboxylic ester-based reference material TPU-BHET showed very good mechanical properties, the chain extenders BHBEP, BAPDMS and BDB were combined with BHET in different ratios. The aim is to increase the mechanical properties compared to phosphate based TPU-BHBEP, siloxane based TPUU-BAPDMS and boronic ester TPTU-BDB and at the same time to increase the degradation rate compared to the carboxylic ester based reference polymer TPU-BHET. Figure 63 shows the used chain extenders. BHET represents the base CE, which is mixed with varying proportions of BHBEP (bis(4-hydroxybutyl)ethyl phosphate), BAPDMS (bis(4-aminophenoxy)dimethylsilane) or BDB (2,2'-(1,4-phenylene)-bis[4-mercaptan-1,3,2-dioxaborolane]). As in the previous chapters, polytetrahydrofuran (pTHF) and hexamethylene diisocyanate (HMDI) are used as macrodiol and diisocyanate to make the change in properties dependent only on the chosen mixing ratio of the CEs. For ease of nomenclature, the distinction between TPU, TPUU, and TPTU is omitted in this chapter and the polymeric species with two CEs are generally labeled as TPUs.

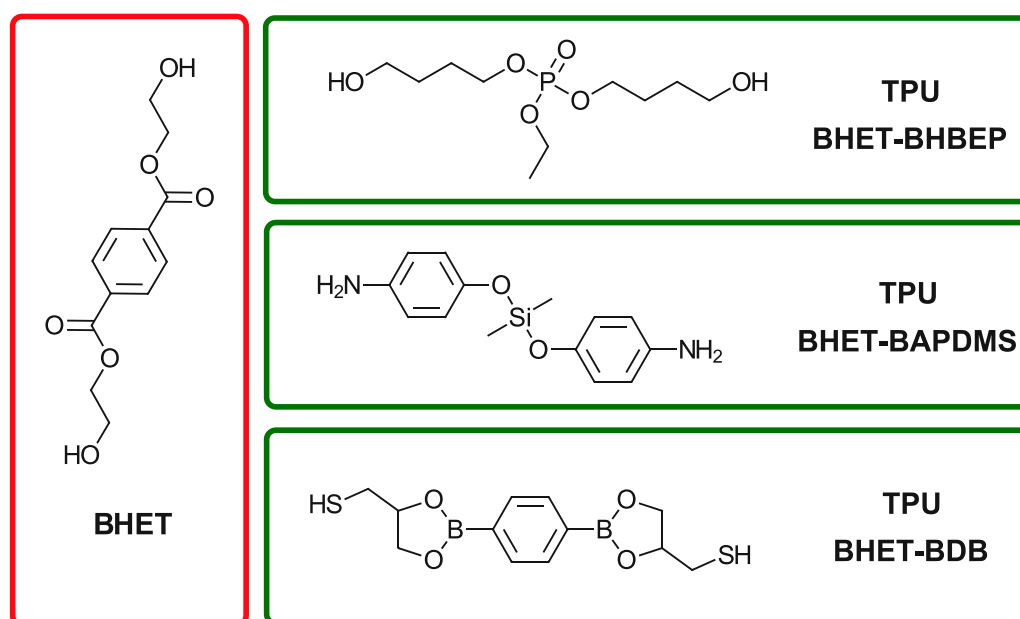


Figure 63: Chemical structures of chain extenders (CE) for thermoplastic polyurethanes (TPUs) with two different CEs. BHET (bis(hydroxyethylene)terephthalate) was used in combination BHBEP (bis(4-hydroxybutyl) ethyl phosphate) or BAPDMS (bis(4-aminophenoxy) dimethylsilane) or BDB (2,2'-(1,4-phenylene)-bis[4-mercaptan-1,3,2-dioxaborolane]) in different ratios.

### 3.3.1. Synthesis of TPUs with two different CEs

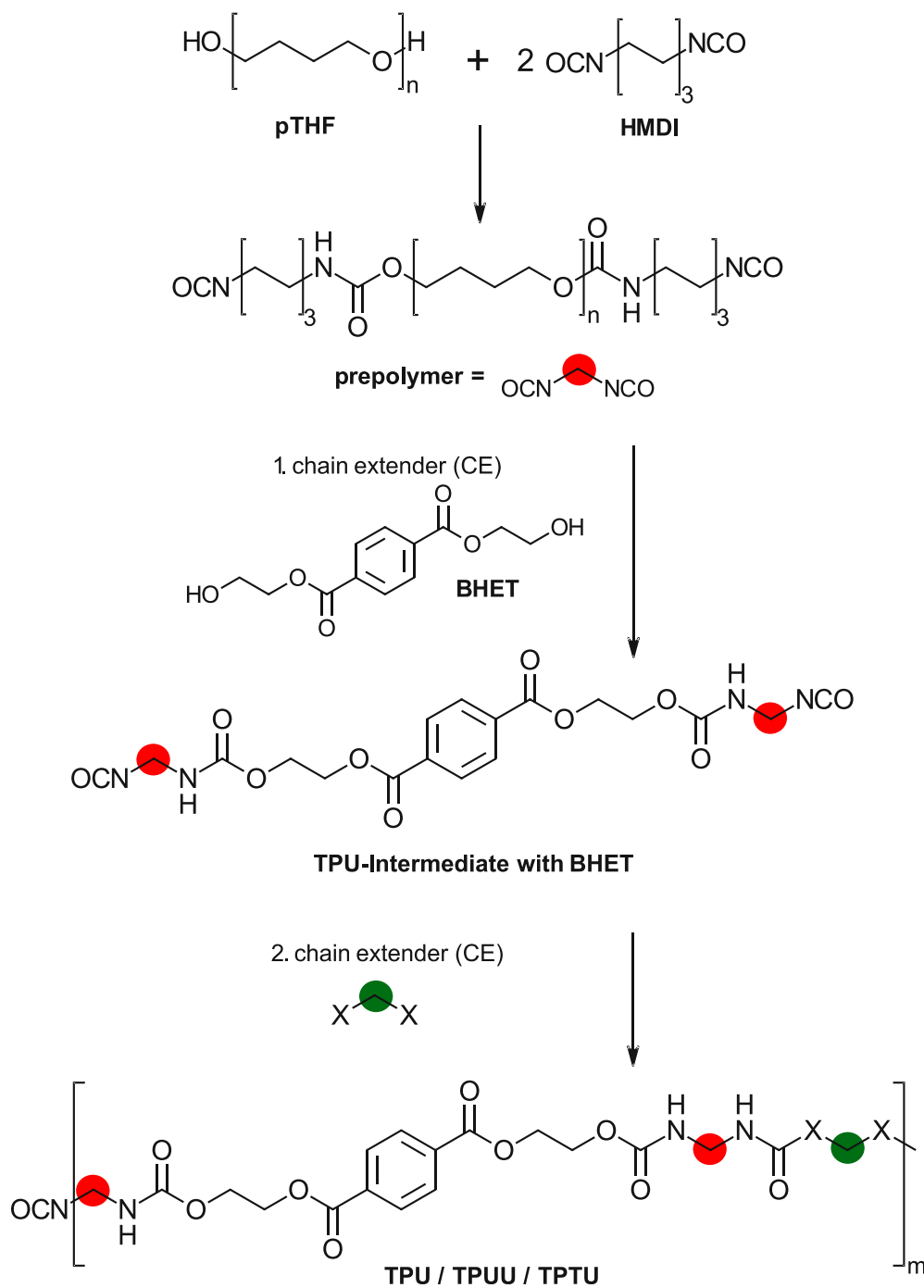
The synthesis of TPUs with two different chain extenders ratios was carried out until the formation of the prepolymer according to the previous described TPU synthesis. Afterwards, the first chain extender (BHET) was added and stirred for 3h to ensure a complete conversion of BHET (TPU-Intermediate). Then the second chain extender (BHBEP, BAPDMS or BDB) was added and stirred overnight (Scheme 20). BHET was always added as the first chain extender to enable a comparable synthesis process.

By using phosphate based BHBEP as second CE, TPU-BHET-BHBEP (75:25) was prepared. Before the polymer synthesis bis(4-hydroxybutyl) ethyl phosphate (BHBEP) was dried under reduced pressure under constant stirring at room temperature for two days (< 0.1 mbar). BHBEP shows a very good solubility as BHET in DMF and therefore, the same amounts of solvent could be used for the polymer synthesis. As a component ratio 1/2/0.75/0.25 (pTHF/HMDI/BHET/BHBEP) was used for the synthesis. For purification the polymer was precipitated in diethyl ether, as a coarser precipitate was formed compared to former used petroleum ether. Afterwards solvents were removed by drying at 50 °C and a white solid was obtained. The yield was lower compared to previous described polymers with 78.1 %, which could be explained by a still finer precipitate compared to other TPU synthesis.

Siloxane based TPU-BHET-BAPDMS (75:25) was synthesized with a ratio of BHET/BAPDMS (75/25) until the formation of the prepolymer according to the described reference polymer synthesis. For the addition of the second chain extender BAPDMS larger amounts of dry DMF were necessary to dissolve it (10 ml instead of 5 mL). Due to the lower additional solvent amounts compared to the synthesis of TPUU-BAPDMS it should not have a huge impact on the final polymer. Final purification was carried out by precipitation in diethyl ether, resulting in a brown solid with good yields of 84.8 %.

Boronic ester based TPU-BHET-BDB was synthesized in three different CE ratios (75:25, 50:50 and 25:75), because it was the most promising candidate as the previous chapter showed. The synthesis was performed as described above. Good yields between 86.2 – 93.4 % were obtained for TPU-BHET-BDB with all CE-ratios.





Scheme 20: Three-step synthesis of TPUs by using two different chain extenders (CE), X=OH, NH<sub>2</sub> or SH. As first chain extender BHET (bis(hydroxyethylene)terephthalate) was used, followed by the addition of BHBEP (bis(4-hydroxybutyl) ethyl phosphate), BAPDMS (bis(4-aminophenoxy) dimethylsilane) or BDB (2,2'-(1,4-phenylene)-bis[4-mercaptan-1,3,2-dioxaborolane]) as second CE in the third reaction step.

### 3.3.2. General characterization of polymers with two different CEs

<sup>1</sup>H-NMR spectroscopy in DMSO-*d*<sub>6</sub> was performed for all synthesized polymers to verify the proportions of TPU components, the ratios of chain extenders and the content of hard-blocks. Initial information on the macromolecular properties of the polymers was obtained by determining the molecular weight using gel permeation chromatography (GPC). In addition, the strength of the physical cross-linking was evaluated by ATR-FTIR spectroscopy.

For TPU-BHET-BHBEP (75:25), as second CE, bis(4-hydroxybutyl) ethyl phosphate (BHBEP) was chosen as a hydrolytic and enzymatic degradable chain extender.<sup>180, 238-240</sup> Furthermore, phosphates show a higher hydrolytic degradation rate compared to phosphites or phosphonates.<sup>237</sup> Another advantage of phosphates is their tunable degradability. For example, if the ethoxy side group is replaced with a longer alkyl group or an aryl group the rate of degradation can be reduced.<sup>237</sup>

As already described in detail in chapter 3.2. TPUs, TPUUs and TPTUs with one CE, the mechanical properties of siloxane based TPUU-BAPDMS did not prove to be particularly good. Nevertheless, BAPDMS exhibits an intriguing structure characterized by two aromatic rings linked by a siloxane unit. The aromatic structure is expected to increase stiffness, while the Si-O bond is known for its greater flexibility in contrast to the C-O bond.<sup>248</sup> Consequently, BAPDMS was incorporated into siloxane based TPU-BHET-BAPDMS (75:25) to benefit from these properties.

As boronic ester based TPTU-BDB shows the most promising results of all inorganic ester-based polymers in chapter 3.2. TPUs, TPUUs and TPTUs with one CE, TPU-BHET-BDB was prepared and characterized most detailed with three different CE ratios (75:25, 50:50 and 25:75).

In addition, carboxylic ester based TPU-BHET and carbonate based TPU-BHPC, established in our research group were used as reference polymers.<sup>133, 183, 283</sup> All polymers consist of polytetrahydrofuran (pTHF) as soft-block and hexamethylene diisocyanate (HMDI) to enable comparability of the materials depending on the combination of chain extenders. The chemical structures of the components for TPUs with two different CEs are shown in Figure 64.

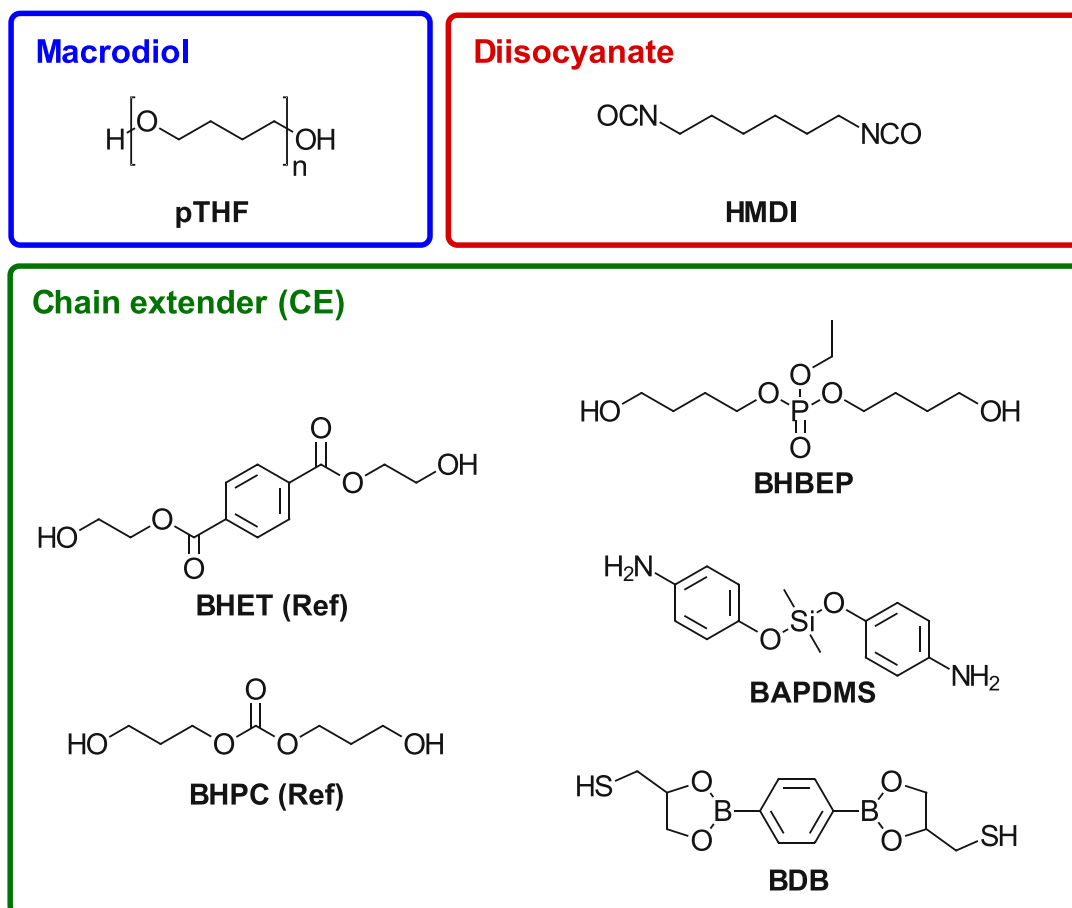


Figure 64: Structures of components for TPU synthesis with two CEs: pTHF (polytetrahydrofuran) as macrodiol, HMDI (hexamethylenediisocyanate), BHET (bis(2-hydroxyethyl)terephthalate, base and reference), BHPC (bis(hydroxypropyl)carbonate, reference) and BHBEP (bis(4-hydroxybutyl) ethyl phosphate), BAPDMS (bis(4-aminophenoxy) dimethylsilane) and BDB (2,2'-(1,4-phenylene)-bis[4-mercaptan-1,3,2-dioxaborolane]).

### NMR and ATR-IR spectroscopy

<sup>1</sup>H-NMR spectroscopy was used to confirm the ratio between pTHF, HMDI, BHET and second chain extenders. Furthermore, the hard-block content was determined via <sup>1</sup>H-NMR spectroscopy by comparing the integrals of CH<sub>2</sub> (pTHF) and the aromatic CH (BHET). All <sup>1</sup>H-NMR spectra are shown in the appendix section (1. NMR spectra).

Hydrogen-bonding characteristics by hard-block formation of phosphate based TPU-BHET-BHBEP (75:25) and siloxane based TPU-BHET-BAPDMS (75:25) were investigated via Fourier Transform Infrared Spectroscopy (FTIR).<sup>97, 291</sup> The reference polymers TPU-BHET, TPU-BHPC and Pellethane were chosen as reference spectra (Figure 65). For a clearer presentation boronic ester based TPU-BHET-BDB (75:25, 50:50, 25:75) is shown in a separate figure and is compared to TPU-BHET and TPTU-BDB (Figure 66). A closer look was taken at the amine region (N-H, 3500-3100 cm<sup>-1</sup>) and the carbonyl region (C=O, 1760-1650cm<sup>-1</sup>) which gives information about steric hindrance of the CE and about the degree of hydrogen bond interactions.<sup>291-294</sup>

In the amine region (Figure 65 left) the peak for phosphate based TPU-BHET-BHBEP (75:25) shows the same shift as carbonate based TPU-BHPC, but slightly broader which can be explained by the bulkier structure of BHET compared to BHPC. Nevertheless, it has to be highlighted that carboxylic ester based TPU-BHET shows a much broader peak compared to TPU-BHET-BHBEP (75:25) although the polymer consists only of 25 % phosphate based BHBEP and 75 % BHET. Furthermore, the amine peak shifts a bit to higher regions compared to TPU-BHET which describes weaker hydrogen bond interactions for TPU-BHET-BHBEP (75:25). The siloxane based TPU-BHET-BAPDMS (75:25) shows a comparable peak shape to TPU-BHET, which is not surprising due to the high BHET content. Nevertheless, a slight shift to higher wavelengths can be observed, which indicates weaker hydrogen bond interactions within the hard-blocks, comparable to those of TPU-BHPC. From FTIR spectra it can be assumed that the hydrogen bond interaction and therefore the physical crosslinking can be increased for TPU-BHET-BAPDMS compared to “pure” siloxane based TPUU-BAPDMS, as the peak for TPUU-BAPDMS shows the highest wavenumber.

Figure 66 left illustrates the broadening of the NH peak in boronic ester based TPU-BHET-BDB with increasing BHET content. A broader NH peak indicates higher steric hindrance of the urethane group and is a direct indicator of a more sterically demanding chain extender. It is noteworthy that boronic ester based BDB, although both have a similar aromatic structure, has significantly lower steric requirements compared to BHET. This difference can be attributed to the more flexible nature of the thiourethane moiety resulting from the presence of sulfur atoms.<sup>308, 309</sup> In addition, all NH absorption bands exhibited a nearly uniform shift, suggesting a comparable strength of hydrogen bonding. This observation is surprising, considering that hydrogen bonds with S···H interactions are generally weaker than those with O···H.<sup>314</sup>

The carbonyl region between 1760 and 1650  $\text{cm}^{-1}$  of phosphate based TPU-BHET-BHBEP (75:25) (Figure 65 right) is best comparable with the spectra of TPU-BHET. Both spectra show absorption bands at  $\sim 1720 \text{ cm}^{-1}$  and  $1690 \text{ cm}^{-1}$ , which result from disordered and ordered hydrogen bonds, respectively. Only the peak intensity of the disordered H-bonds is higher for TPU-BHET-BHBEP (75:25) compared to the peak of TPU-BHET and Pellethane, which is an indication of a lower amount of ordered H-bonds compared to disordered H-bonds.<sup>97</sup> Due to weaker hydrogen bond interaction in TPU-BHET-BHBEP (75:25) compared to the reference polymers, also poorer mechanical properties are expected, which are discussed later.

For siloxane based TPU-BHET-BAPDMS (75:25) no peak for H-bond interactions between urea bonds are observed but signals for the hydrogen bonded carbonyls by urethanes ( $1700\text{-}1680 \text{ cm}^{-1}$ ) and free C=O bands at  $1730\text{-}1720 \text{ cm}^{-1}$ . The peak shapes are comparable to those of TPU-BHET, although the free C=O is more intense for TPU-BHET-BAPDMS (75:25).

As observed for TPU-BHPC no absorption bands at  $\sim 1740\text{ cm}^{-1}$  are present for all other polymers, which shows us that there are no free carbonyls without hydrogen bonds.<sup>97</sup>

For boronic ester based TPU-BHET-BDB (Figure 66 right) at approximately  $1740\text{ cm}^{-1}$ , also no absorption bands were observed in any of the polymers, indicating the absence of free C=O groups without hydrogen bonds.<sup>97</sup> With the exception of TPTU-BHET-BDB (25:75), the peak intensity at around  $1720\text{ cm}^{-1}$  was lower than the peaks between  $1685\text{-}1695\text{ cm}^{-1}$ , which is a result of a higher content of ordered to disordered H-bonds.<sup>97</sup>

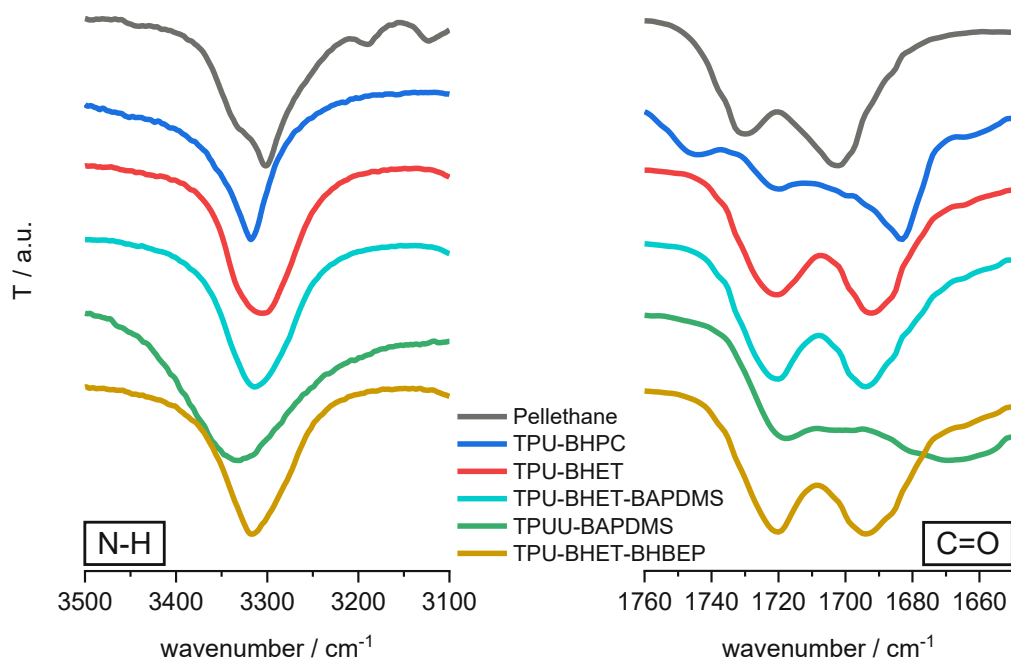


Figure 65: ATR-FTIR spectra of TPU-BHET-BHBEP (75:25), TPU-BHET-BAPDMS (75:25) compared to reference polymers Pellethane, TPU-BHPC and TPU-BHET and TPUU-BAPDMS. The amine region ( $3500\text{-}3100\text{ cm}^{-1}$ ) and the carbonyl region ( $1760\text{-}1650\text{ cm}^{-1}$ ) are shown.

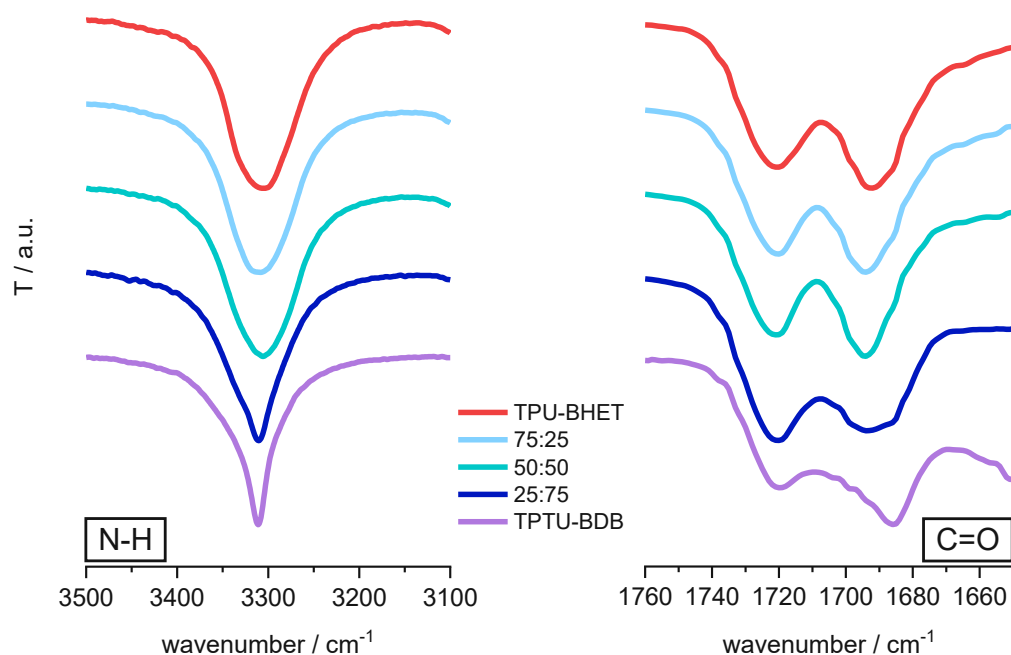


Figure 66: ATR-FTIR spectra of reference TPU-BHET, TPTU-BHET-BDB with different CE ratios (75:25, 50:50, 25:75) and TPTU-BDB. The amine region ( $3500\text{-}3100\text{ cm}^{-1}$ ) and the carbonyl region ( $1760\text{-}1650\text{ cm}^{-1}$ ) are shown.

## Molecular weight and hard-block content

Molecular weight and polydispersity were determined by GPC measurements in THF in a range between 9.2 and 13.7 kDa for TPUs with two different CEs and are thus lower than for the reference polymers TPU-BHET, TPU-BHPC and Pell (Table 17). TPU-BHET-BAPDMS (75:25) shows a comparable  $\overline{M}_n$  to siloxane based TPUU-BAPDMS and is also in the same range as phosphate ester based TPU-BHET-BHBEP (75:25) with values between 10.2 and 10.5 kDa. In addition, the polydispersity of these polymers is in a narrow range between 1.6 and 1.9, which promises uniform properties. However, the addition of a second chain extender to the phosphate and silicic acid ester-based TPUs did not significantly increase the molecular weight. For boronic acid ester-based TPUs, the addition of BHET as an additional CE leads to an increase in  $\overline{M}_n$ , so that the value for TPU-BHET-BDB (50:50, 13.7 kDa) is approximately double that of "pure" boronic ester based TPTU-BDB (6.4 kDa). The polydispersity for BDB-containing polymers is also in a narrow range between 1.8 and 2.0.

The theoretical and calculated hard-block content ( $HB_{th}$  and  $HB_{cal}$ , Table 17) provides further insight into the low  $\overline{M}_n$ , especially for phosphate and silicic acid ester-based TPUs. Since a constant ratio of 1:2:1 (pTHF:HMDI:CE) was used for all polymers, the theoretical hard-block content of TPUs with two CEs is in a narrow range between 37.3 and 38.7 wt%. In contrast, the hard-block content calculated by  $^1H$  NMR spectroscopy (Appendix, 1. NMR spectra) for TPU-BHET-BHBEP (75:25) and even more so for TPU-BHET-BAPDMS (75:25) deviates strongly from the theoretical values. One reason for the low calculated HB content could be a poor incorporation of BHBEP and BAPDMS into the polymer chain, which would also explain the low molecular weight. A prior reaction of the isocyanates with water would also result in a lower  $\overline{M}_n$  and subsequently prevent the incorporation of the CEs into the already reacted isocyanates. For TPUs containing BDB, the calculated hard-block contents are also lower than the theoretical values, but the deviations are small and amount to a maximum of 5.1 % for TPU-BHET-BDB (75:25).

Table 17: Overview of synthesized TPUs with two CE and reference polymers in terms of number-average molar mass  $\overline{M}_n$ , polydispersity (PDI) and hard-block content (theoretical and calculated).

polymer	$\overline{M}_n$ / kDa <sup>a</sup>	PDI <sup>b</sup>	$HB_{th}$ / wt% <sup>c</sup>	$HB_{cal}$ / wt% <sup>d</sup>
Pellethane	56.3	1.9	-	-
TPU-BHET	23.3	2.1	37.1	33.5
TPU-BHPC	17.3	1.7	34.0	31.3
TPU-BHET-BHBEP (75:25)	10.3	1.9	37.3	31.1
TPU-BHET-BAPDMS (75:25)	10.5	1.8	37.3	22.4
TPUU-BAPDMS	10.2	1.6	37.9	19.9
TPU-BHET-BDB (75:25)	11.9	1.8	37.7	32.4
TPU-BHET-BDB (50:50)	13.7	1.9	38.2	34.6
TPU-BHET-BDB (25:75)	9.2	2.0	38.7	35.7
TPTU-BDB	6.4	1.8	39.3	36.1

### 3.3.3. Mechanical and thermal properties of polymers with two different CEs

To evaluate the suitability of a thermoplastic polyurethane for use as a vascular graft, it is critical to analyze its mechanical properties, such as elongation at break, ultimate tensile strength, and elastic modulus. The goal is to closely match the mechanical properties of the final graft to those of natural tissue to ensure optimal compatibility and performance when used as a vascular graft.

The mechanical properties of TPUs with two CEs were evaluated by tensile testing of polymer films prepared by solution casting (ISO 527, Type 5B, bone-shaped). The glass transition temperature ( $T_g$ ) was determined using Dynamic Mechanical Thermal Analysis (DMTA) as shown in Appendix, 3. DMTA spectra. Detailed information on the solution casting and tensile testing methods is provided in the Materials and Methods section.

The number average molar mass  $\overline{M}_n$ , calculated hard-block content, mechanical properties, and  $T_g$  are shown in Table 18. For better illustration, the mechanical properties are also shown graphically in Figure 67 and Figure 68.

Table 18: Comparison of number-average molar mass  $\overline{M}_n$ , calculated hard-block content, mechanical properties and glass transition temperature of inorganic ester-based TPUs with two CEs with reference polymers.

polymer (CE)	$\overline{M}_n$ / kDa <sup>a</sup>	HB <sub>cal</sub> / wt% <sup>b</sup>	$\epsilon_b$ / % <sup>c</sup>	TS / MPa <sup>d</sup>	E / MPa <sup>e</sup>	$T_g$ / °C <sup>f</sup>
Pellethane	56.3	-	1651 ± 115	25.2 ± 1.2	14.2 ± 0.3	-52
BHET	23.3	33.5	1315 ± 54	14.1 ± 0.7	31.0 ± 1.4	-71
BHPC	17.3	31.3	878 ± 75	12.8 ± 0.9	22.5 ± 0.3	-57
BHET-BHBEP (75:25)	10.3	31.1	89 ± 6	3.1 ± 0.1	20.1 ± 1.4	-57
BHET-BAPDMS (75:25)	10.5	22.4	77 ± 9	3.6 ± 0.1	23.1 ± 1.2	-55
BAPDMS	10.2	19.9	10 ± 0	1.2 ± 0.1	24.7 ± 1.3	-
BHET-BDB (75:25)	11.9	32.4	199 ± 13	6.8 ± 0.2	47.8 ± 4.6	-65
BHET-BDB (50:50)	13.7	34.6	263 ± 9	6.1 ± 0.2	38.9 ± 2.8	-67
BHET-BDB (25:75)	9.2	35.7	186 ± 15	9.1 ± 1.0	56.6 ± 9.9	-66
BDB	6.4	36.1	507 ± 72	10.4 ± 0.7	69.8 ± 5.5	-64

<sup>a</sup> Number-average molar mass. <sup>b</sup> calculated hard-block content from <sup>1</sup>H-NMR (HB<sub>cal</sub>). <sup>c</sup> Elongation at break  $\epsilon_b$ .

<sup>d</sup> tensile strength TS. <sup>e</sup> elastic modulus E. <sup>f</sup> Glass transition temperature  $T_g$  obtained from the maxima of loss modulus curves.

As expected from the IR spectroscopy (Figure 65), molecular weight  $\overline{M}_n$  and calculated hard-block content, the phosphate based TPU-BHET-BHBEP (75:25) shows poorer mechanical properties compared to the reference polymers TPU-BHET, TPU-BHPC and Pellethane. It shows a combination of low elongation at break (~ 90 %) and low ultimate tensile strength (~ 3 MPa) with a relatively high elastic modulus (~ 20 MPa). Therefore, the material would not fulfill the requirements for a tissue engineered vascular graft. The glass transition temperature is similar to that of TPU-BHPC. The poor mechanical properties are probably due to a combination of an impurity in the chain extender BHBEP (resulting in low molecular weight and low calculated hard-block content, see 3.1.1. Phosphate ester-based CE), less favorable H-bond formation (FTIR, Figure 65), and a flexible aliphatic structure of BHBEP in contrast to

BHET. Nevertheless, it is still surprising that such a small amount of BHBEP (25% of CE) has such a large effect on the mechanical properties.

Similarly, the siloxane based TPU-BHET-BAPDMS (75:25) shows poor mechanical properties even though it was mainly BHET that was used as CE. Nevertheless, all three measured parameters could be improved compared to TPUU-BAPDMS as higher elongation at break, higher ultimate tensile strength and lower elastic modulus. Another interesting observation can be seen in the  $T_g$  values (Table 18). Although only a small amount of the silicic acid ester-based CE was used in TPU-BHET-BAPDMS (75:25), the  $T_g$  increases by 16 °C compared to the reference polymer TPU-BHET and shows a comparable glass transition temperature to TPU-BHPC or Pellethane. This means that the  $T_g$  is far below 37 °C and the material would be suitable for a vascular graft application from this point on.

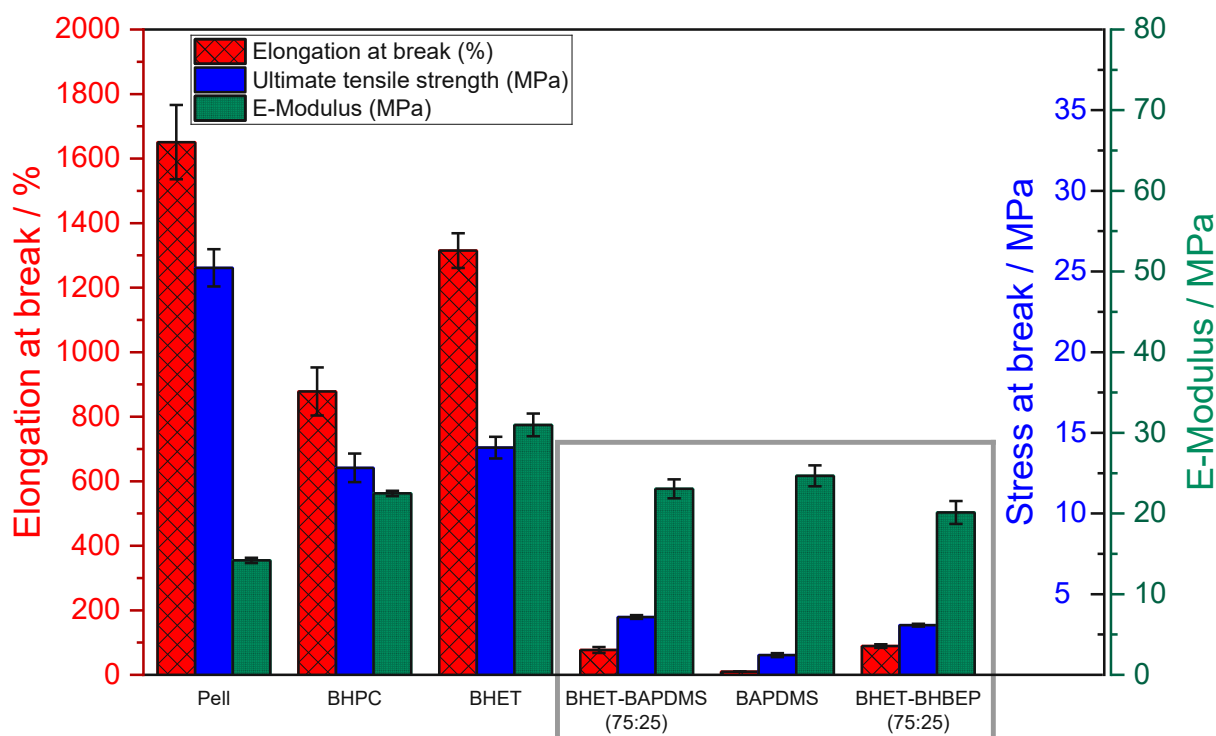


Figure 67: Elongation at break, ultimate tensile strength and elastic modulus of inorganic ester-based TPUs with two CEs in comparison with reference polymers.

For a better overview, boronic acid ester-based TPUs with two CEs are shown separately in Figure 68. TPU-BHET and TPTU-BDB are shown as references. Surprisingly, TPU-BHET-BDB (75:25, 50:50 and 25:75), which have a combination of BHET and BDB as chain extenders, show lower elongation at break, ultimate tensile strength and elastic modulus than TPTU-BDB and TPU-BHET, respectively. Although a reduction in elastic modulus and thus stiffness was required, the reduced elasticity and ultimate tensile strength are not desirable. Perhaps the structural differences between the two chain extenders could lead to less favorable hard-block formation, which could not be demonstrated by FTIR spectroscopy in



section 3.3.2. General characterization of polymers with two different CEs. In addition, the molecular weight has a direct influence on the mechanical properties. However, since TPU-BHET-BDB batches (9.2-13.7 kDa) show higher values compared to TPTU-BDB (6.4 kDa), an increased mechanical strength would be assumed from this point of view. All DMTA spectra confirm a  $T_g$  below 0 °C for all BDB containing TPUs (Table 18), which would make them suitable as vascular grafts at body temperature. The  $T_g$  for all TPU-BHET-BDB batches was in the narrow range between -67 and -65 °C and therefore in between TPTU-BDB and TPU-BHET.

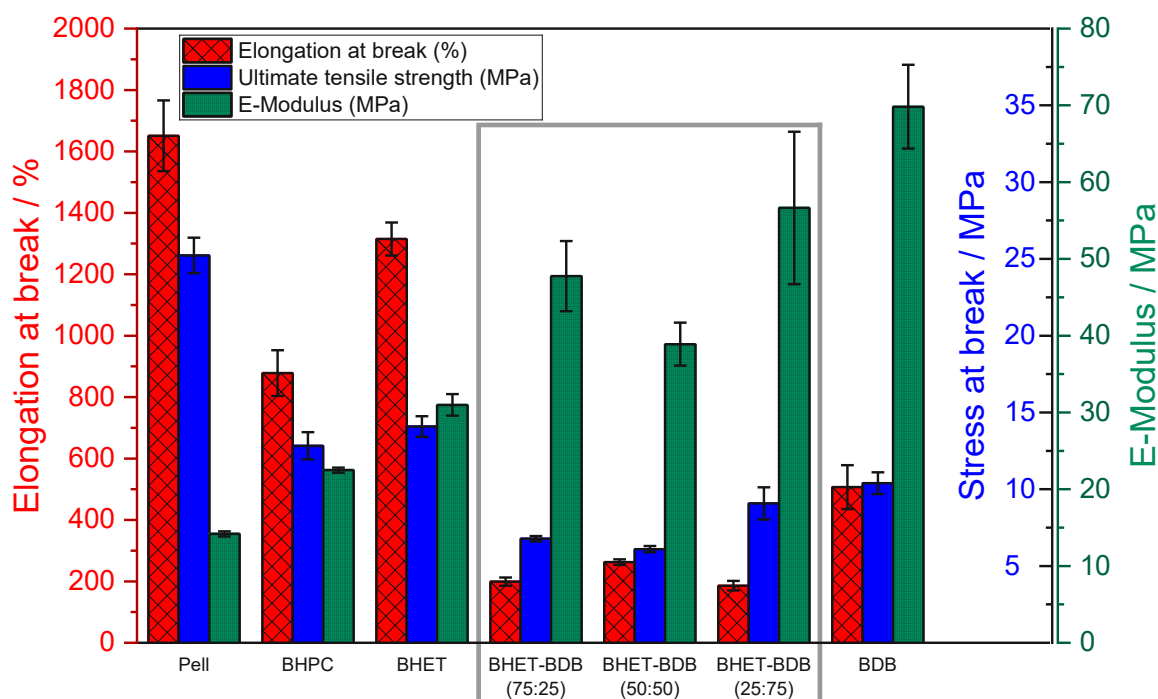


Figure 68: Elongation at break, ultimate tensile strength and elastic modulus of TPU-BHPC, TPU-BHET, TPTU-BHET-BDB and TPTU-BDB in comparison with commercially available Pellethane.

### 3.3.4. Degradation behavior of polymers with two different CEs

To investigate the degradation behavior of TPUs with two different CEs, circular specimens were punched out of solution cast polymer films with a diameter of 1 cm and a mass between 20 and 30 mg. The samples were weighted in dry state and then stored in separate vials with 20 mL of PBS buffer solution (pH=7.4, fourfold buffer capacity). The degradation studies were performed at 37 °C and 90 °C in triplicates for 70 days. A detailed description of the procedure is shown in the Materials and methods section.

TPU-BHET-BHBEP (75:25) as phosphate-based polymer shows both, hydrolytic and enzymatic degradability.<sup>180, 238-240</sup> This fact makes them promising materials in the field of tissue engineering.<sup>237</sup> The ethyl ester “side-group” of BHBEP was chosen to enable a faster degradation compared to higher molecular weight side-chains.<sup>237</sup> The hydrophilic ethoxy side chain enables an access of water, resulting in a hard-block degradable TPU. Figure 69 shows mass erosion and Figure 70 molecular weight change of TPU-BHET-BHBEP (75:25) at 37 °C and 90 °C compared to the reference polymers TPU-BHET and Pellethane. It can be observed that a replace of 25 % of BHET with BHBEP leads to an increased degradation rate in terms of mass erosion and molecular weight loss.

The degradation behavior of siloxane based TPU-BHET-BAPDMS (75:25) demonstrates, how even small amounts of the silicic acid ester-based chain extender affects the degradation rate. On the one hand, based on previous studies by Parrott *et al.*,<sup>219</sup> these polymers would be expected to degrade slower than ester-based polymers because the Si-O bond is relatively stable in a neutral environment, but an increased degradation rate with decreased pH. Therefore, a CE with dimethyl side groups was chosen to minimize steric hindrance at the silicon atom and increase hydrolytic degradability in a neutral environment.

Figure 69 shows the mass erosion of TPU-BHET-BAPDMS (75:25) at 37 °C and at 90 °C in PBS buffer solution (4x, pH=7.4) over a time period of 70 days. The degradation curve is very similar to that of TPU-BHET, but with a slightly higher degradation rate. TPU-BHET-BAPDMS (75:25) loses about 3 % more mass after 70 days compared to TPU-BHET at both measured temperatures. The change in molar mass over the degradation process also shows the same behavior as TPU-BHET (Figure 70). This was expected due to the low amount of BAPDMS as second CE. However, it can be clearly seen that a low amount of the silicic acid ester-based chain extender increases the rate of degradation in terms of mass erosion and molecular weight change. This leads to the conclusion that sterically less hindered silicic acid esters (e.g. Me<sub>2</sub>SiR<sub>2</sub>) as bis(4-aminophenoxy)dimethylsilane (BAPDMS) also degrade hydrolytically under a neutral environment.

Nevertheless, comparing phosphate based BHBEP and siloxane based BAPDMS based polymers, the phosphate ester degrades faster in terms of mass erosion at 90 °C and by molecular weight change at both temperatures. Only at 37 °C TPU-BHET-BAPDMS (75:25) shows a higher degradation rate compared to TPU-BHET-BHBEP (75:25).

Comparing the degradation curves of mass loss (Figure 69) and molecular weight change (Figure 70) can also be used to determine whether it is a case of surface or bulk erosion.<sup>213</sup> As mass and molecular weight decreased simultaneously, TPU-BHET-BHBEP (75:25) and TPU-BHET-BAPDMS (75:25) could be classified as bulk eroding materials.

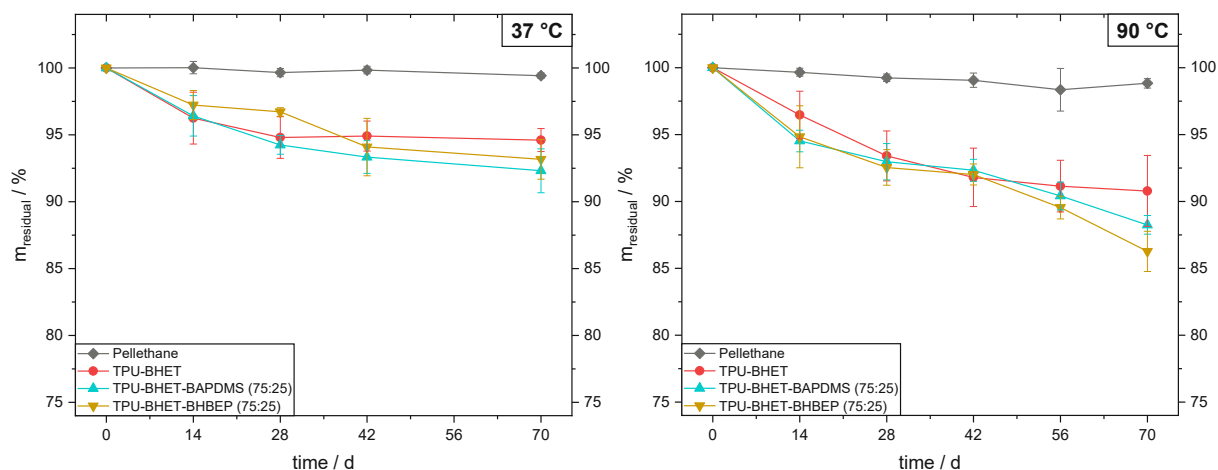


Figure 69: Residual mass  $m_{\text{residual}}$  in % of TPU-BHET, TPU-BHET-BAPDMS (75:25), TPU-BHET-BHBEP (75:25) and commercially available Pellethane in PBS buffer solution (4x) at 37 °C (left) and at 90 °C (right).

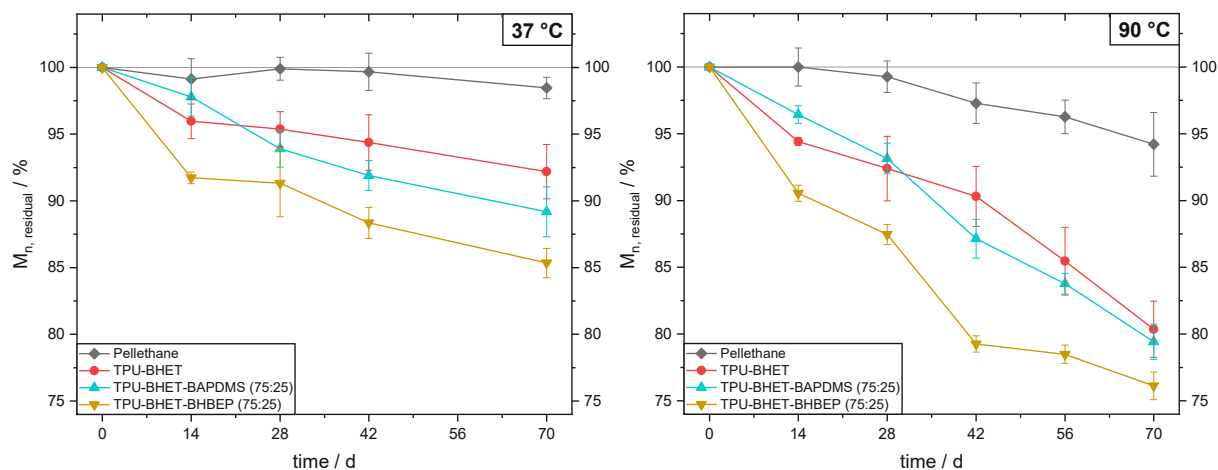


Figure 70: Development of number-average molar mass  $\overline{M}_n$ , residual in % of original  $\overline{M}_n$ , before degradation over a time period of 70 days of TPU-BHET-BAPDMS (75:25), TPU-BHET-BHBEP (75:25) and TPU-BHET, Pellethane as references in PBS buffer solution (4x) at 37 °C (left) and 90 °C (right).

The degradation behavior of boronic ester based TPU-BHET-BDB (75:25, 50:50, 25:75) were investigated and were compared with TPU-BHET, TPTU-BDB and Pellethane. Degradation studies were performed under the same conditions as described above. Figure 71 shows the mass erosion at 37 °C and 90 °C. Figure 72 presents the development of the  $\overline{M}_n$  change at both temperatures.

In terms of mass erosion, it can be observed that the degradation rate of TPU-BHET-BDB (75:25, 50:50, 25:75) increases gradually with increasing BDB content at both temperatures. This demonstrated that it is possible to fine-tune the degradation rate by combining two different chain extenders.

Furthermore, to the mass erosion, Figure 72 left presents the development of the  $\overline{M}_n$  change at 37 °C over a time period of 70 days. As already described in the previous chapter 3.2.4. Degradation behavior of polymers with one CE, TPTU-BDB shows a constant increase of  $\overline{M}_n$  during 70 days, resulting in an absolute increase of molecular weight of ~16 % compared to the starting point. The observed mass reduction as shown in Figure 71 is attributed to the release of low molecular weight units. Consequently,  $\overline{M}_n$  would increase due to an increased proportion of higher molecular weight species.

In contrast to boronic ester based TPTU-BDB, all mixed polymers TPU-BHET-BDB (75:25, 50:50, 25:75) showed a faster degradation compared to TPU-BHET and TPTU-BDB. An increase in molecular weight as observed for TPTU-BDB could not even be measured for TPU-BHET-BDB (25:75), even though a BHET:BDB ratio of 25:75 was used.

Further insights give the GPC degradation study at 90 °C (Figure 72 right). As for TPTU-BDB an  $\overline{M}_n$  increase for all TPU-BHET-BDB batches is also observed. By increasing BDB content as CE,  $\overline{M}_n$  increases stepwise. Furthermore, TPU-BHET-BDB (75:25 and 50:50) were not dissolvable anymore after 14 days in any investigated solvents (Hexafluoro-2-propanol, THF, DMF, DMSO, MeCN, MeOH, EtOH, acetone, dioxane, CHCl<sub>3</sub>, DCM, water, ethyl acetate).

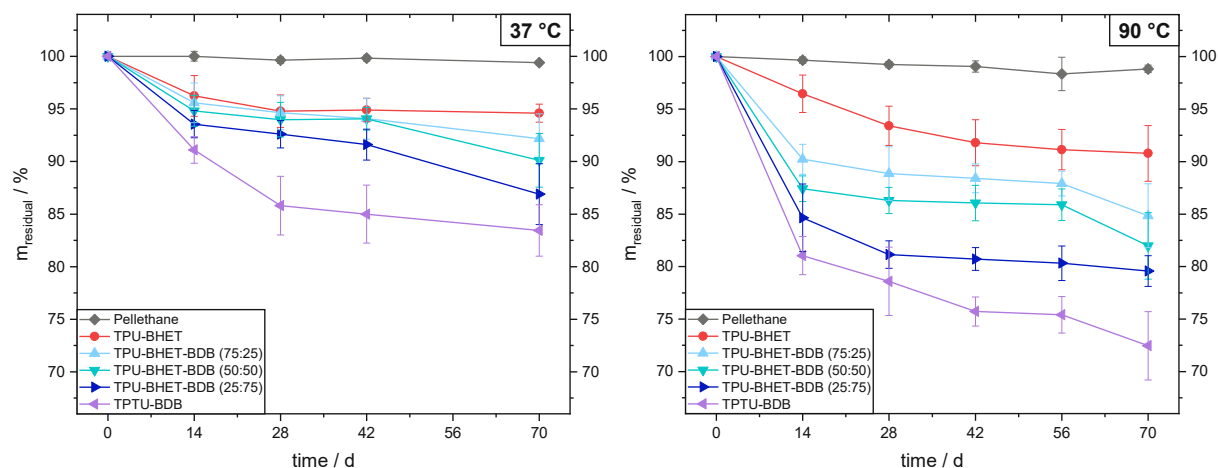


Figure 71: Residual mass  $m_{\text{residual}}$  in % of TPU-BHET, TPU-BHET-BDB batches, TPTU-BDB and commercially available Pellethane in PBS buffer solution (4x) at 37 °C (left) and at 90 °C (right).

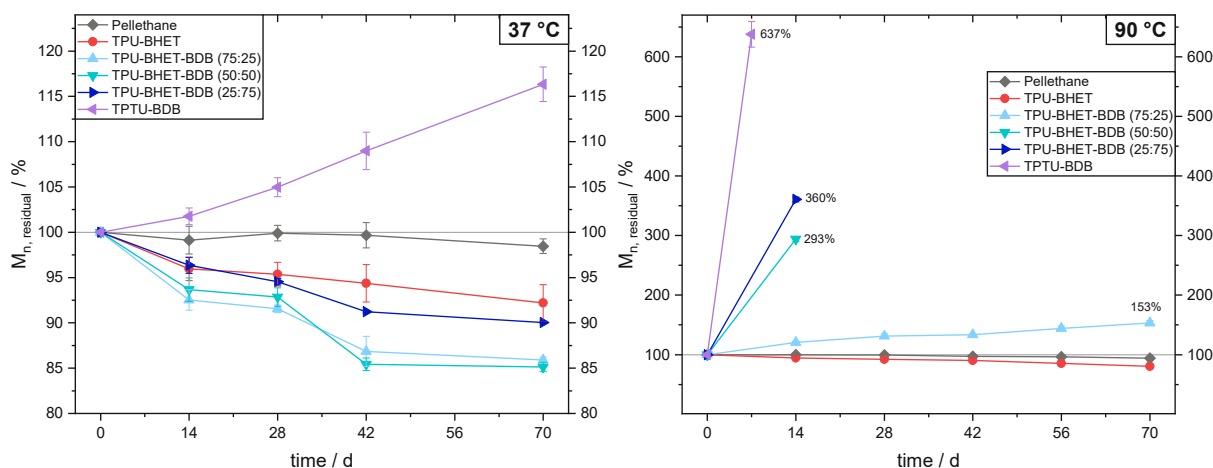


Figure 72: Development of number-average molar mass  $\overline{M}_n$ , residual in % of original  $\overline{M}_n$ , before degradation over a time period of 70 days of TPU-BHET, TPU-BHET-BDB batches, TPTU-BDB and Pellethane as reference in PBS buffer solution (4x) at 37 °C (left) and 90 °C (right).

The combination of two different chain extenders was chosen to improve the mechanical properties of the inorganic ester-based TPUs and at the same time achieve a higher degradation rate compared to the reference polymers.

By combining siloxane based BAPDMS with BHET, TPU-BHET-BAPDMS (75:25) was prepared. Compared to TPU-BAPDMS, the material shows better mechanical properties for all measured parameters, in particular an increased elongation at break and ultimate tensile strength and a reduced elastic modulus. However, these are still significantly worse than those of the reference polymers. As mentioned above, phosphate based TPU-BHBEP could not be reproducibly produced. But, by combining BHET and BHBEP, TPU-BHET-BAPDMS (75:25) could be synthesized. Nevertheless, the mechanical properties are similar to those of TPU-BHET-BAPDMS (75:25).

The degradation studies showed that phosphate based TPU-BHET-BHBEP (75:25) and siloxane based TPU-BHET-BAPDMS (72:25) have a very similar degradation rate for mass erosion, with a slightly higher rate for the BHBEP-based TPU. There is a clear difference in molecular weight reduction, with TPU-BHET-BHBEP (75:25) degrading faster.

For boronic ester based TPU-BHET-BDB, three different ratios of BHET and BDB were tested, namely 75:25, 50:50 and 25:75. Surprisingly, the TPU-BHET-BDB batches all show worse elongation at break and ultimate tensile strength than the "pure" polymers TPU-BHET and TPTU-BDB. However, they have a slightly better elastic modulus than TPTU-BDB. Thus, the combination of BHET and BDB did not improve the mechanical properties compared to TPTU-BDB. It could be that the formation of hard-blocks is worse due to the different structure of BHET and BDB and therefore the mechanical properties decreased.

However, the degradation studies of boronic ester based TPU-BHET-BDB clearly showed that the degradation rate can be fine-tuned by combining two different CEs. With a gradual increase in the BDB content, a gradual increase in the degradation rate in terms of mass erosion can be observed.

Moreover, at 37 °C, in contrast to TPTU-BDB, no increase in molecular weight can be observed for any of the TPU-BHET-BDB approaches. At 90 °C, however, a gradual increase can be observed. The higher the BDB content, the greater the increase in molecular weight. This shows that this phenomenon is not unique to TPTU-BDB.

## 4. Influence of disulfides in the CE

Introducing inorganic ester-based chain extenders (CE), namely 2,2'-(1,4-phenylene)bis[4-thioethyl-1,3,2-dioxaborolane] (BDB), the degradation rate of thermoplastic polyurethanes (TPUs) could be significantly increased compared to the use of carboxyl ester-based CEs, namely bis(hydroxyethylene)terephthalate (BHET) and bis(2-hydroxyethyl)furan-2,5-dicarboxylate (BHEF). However, it has been shown that a faster degradable chain extender has a negative effect on the mechanical properties of the polymer. In order to perform well in both areas, mechanical properties and degradation rate, a different approach is needed.

Since carboxylic acid esters, silicic acid esters, phosphates, and boronic acid esters are all hydrolytically degradable polymer concepts, another approach has been introduced, specifically reduction-responsive biodegradable polymers. These materials are characterized by the presence of disulfide bonds in the backbone and can be cleaved in a reductive environment by thiol-disulfide exchange.<sup>226, 262, 263</sup> This faster process compared to hydrolytic degradation distinguishes them from polymers such as aliphatic polyesters and polycarbonates.<sup>264, 265</sup>

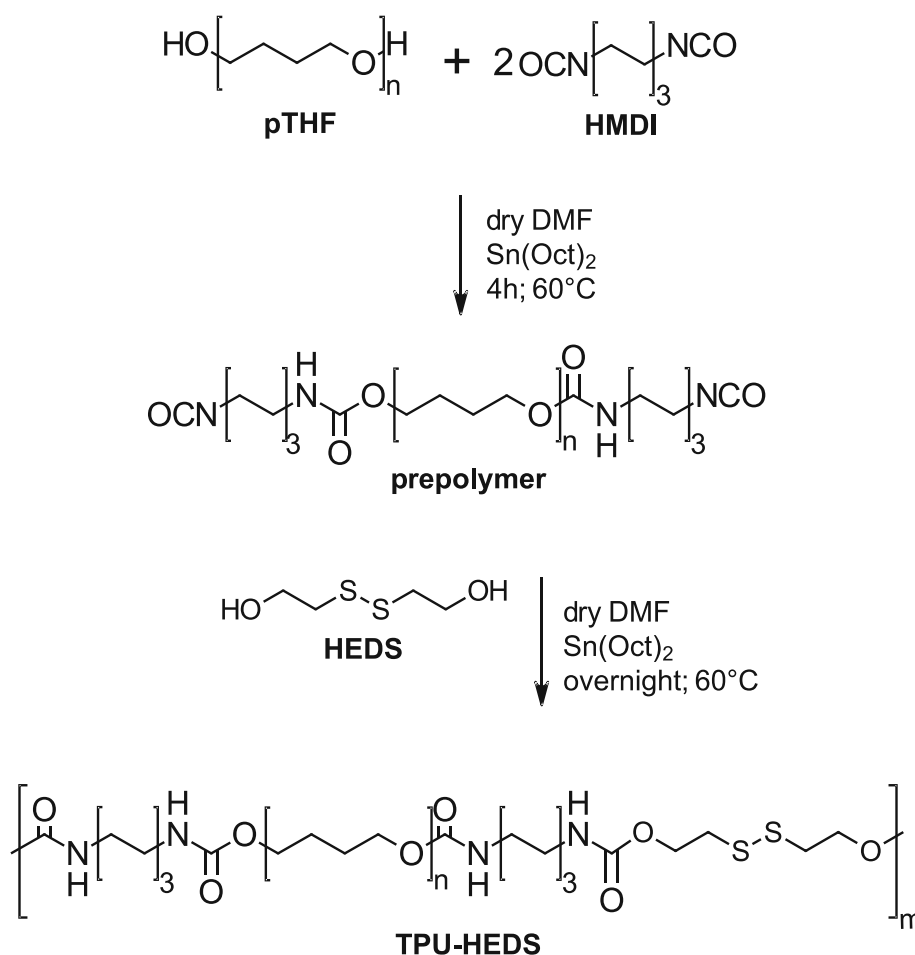
This concept may also be relevant to vascular grafts, as some enzymes such as protein disulfide isomerases,<sup>271</sup> thioredoxins<sup>272</sup> and glutaredoxin-1<sup>272</sup> are present in human plasma that can cleave disulfide bonds and therefore may be able to increase the rate of graft degradation. Based on this information, the disulfide-based chain extender 2-hydroxyethyl disulfide (HEDS) was selected as a reductive/enzymatic, non-acidic, cleavable building block, because of its commercial availability and its easy purification via distillation.<sup>280</sup>

Furthermore, by combining two chain extenders (BHET and BDB) in boronic ester based TPU-BHET-BDB, it was shown that it is possible to fine-tune the degradation rate by using different CE ratios. Therefore, this concept will be also applied to disulfide-based CEs by combining BHET with HEDS in different ratios to merge hydrolytically and reductively degradable TPUs.

## 4.1. Synthesis of TPU-HEDS

Analogous to the synthesis of reference polymers TPU-BHET and TPU-BHPC (chapter 1. Reference polymers), the synthesis of the disulfide based TPU-HEDS was carried out (Scheme 21).

Before the polymer synthesis HEDS has to be distilled under high vacuum (< 0.1 mbar) at maximum 150 °C. It is important that the temperature does not exceed 170 °C for a prolonged period of time, as already started disulfide bond breaking has been observed. As BHET and BHPC, HEDS shows a good solubility in dry DMF and therefore, the same amounts of solvent could be used for the polymer synthesis. Furthermore, the same ratio of 1/2/1 (pTHF/HMDI/HEDS) was used as this composition was already established in the reference polymers and to enable a better comparability. After synthesis the polymer was precipitated in petroleum ether. After drying at 50 °C, a white solid was obtained in good yields (93.8 %).



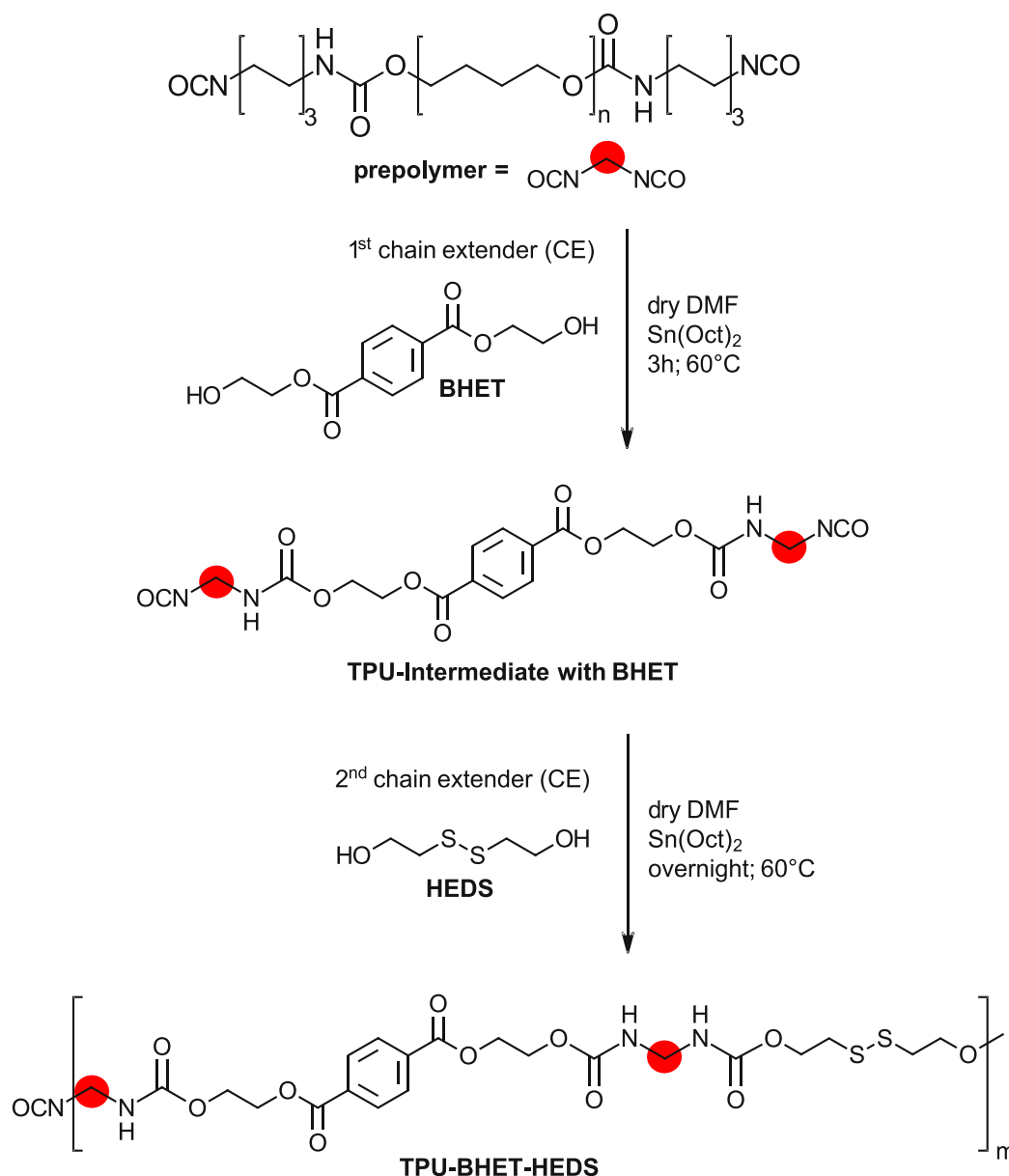
Scheme 21: Synthesis of TPU-HEDS via two-step polymerization. 1<sup>st</sup> step: prepolymer formation from polytetrahydrofuran (pTHF) and hexamethylene diisocyanate (HMDI), 2<sup>nd</sup> step: polyaddition reaction with the chain extender 2-hydroxyethyl disulfide (HEDS).



## 4.2. Synthesis of TPU-BHET-HEDS

In order to combine the concept of a reductively degradable chain extender with the already known hydrolytically degradable bis(hydroxyethylene) terephthalate (BHET), TPUs with different ratios of BHET and HEDS were produced.

The synthesis of TPU-BHET-HEDS with different chain extender ratios of BHET/HEDS (75/25, 50/50 and 25/75) was carried out until the formation of the prepolymer according to the previous described TPU synthesis. Afterwards, the first chain extender (BHET) was added and stirred for 3 h to ensure a complete conversion of BHET (TPU-Intermediate). Afterwards the second chain extender (HEDS) was added und stirred overnight (Scheme 22). BHET was always added as the first chain extender to enable a comparable synthesis process. TPU-BHET-HEDS for all ratios results in a white solid with yields between 83.8 to 92.6 %.



Scheme 22: Synthesis of TPU-BHET-HEDS with different chain extender ratios via three-step polymerization.

### 4.3. General characterization

To confirm the ratios of TPU components, the chain extender ratios in disulfide based TPU-BHET-HEDS and the hard-block content,  $^1\text{H-NMR}$  spectroscopy was performed for all synthesized polymers in  $\text{DMSO-}d_6$ . To get a first insight into the macromolecular nature of the polymers, molecular weights were determined via gel permeation chromatography (GPC). Furthermore, the strength of physical crosslinking was evaluated via ATR-IR spectroscopy. For TPU-HEDS, 2-hydroxyethyl disulfide (HEDS) was selected as disulfide-based chain extender because of its commercial availability and its easy purification via distillation. Furthermore, TPUs with mixed chain extender (BHET and HEDS) were synthesized to investigate the impact of different hard-blocks in a polymer on its mechanical properties and its degradation behavior. Especially, the combination of a rigid aromatic based diol (BHET) and a more flexible aliphatic diol (HEDS) has to be highlighted and could lead to a higher elongation at break and a lower ultimate tensile strength compared to TPU-BHET, and therefore resulting in mechanical properties, which should be closer to the benchmark material Pellethane. Finally, the incorporation of HEDS into the hard-block should lead to a reductive induced degradation. To mimic the presence of disulfide cleaving enzymes dithiothreitol (DTT)<sup>274</sup> and tris(2-carboxyethyl) phosphine (TCEP)<sup>275</sup> were used. The chemical structures of the components of TPU-BHET and TPU-HEDS are demonstrated in Figure 73.

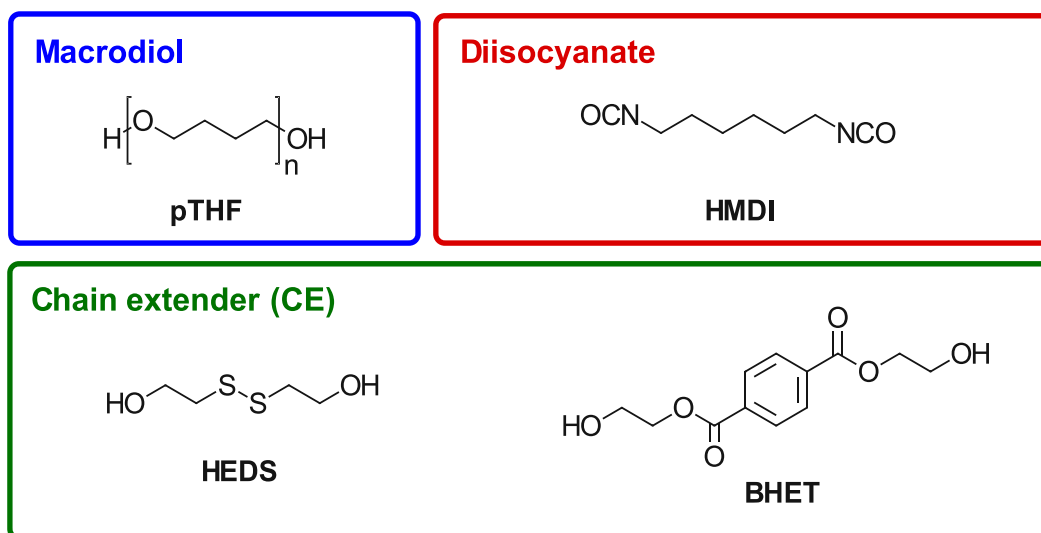


Figure 73: Structures of components for TPU-BHET, TPU-BHET-HEDS (different CE ratios) and TPU-HEDS: pTHF (polytetrahydrofuran) as macrodiol, HMDI (hexamethylenediisocyanate) as diisocyanate, BHET (bis(hydroxyethyl) terephthalate) and HEDS (2-hydroxyethyl disulfide) as chain extenders.

## NMR and ATR-IR spectroscopy

$^1\text{H-NMR}$  spectroscopy was used on the one hand to determine the ratio between pTHF, HMDI and HEDS and on the other hand to confirm the ratio between BHET and HEDS for TPU-BHET-HEDS (75:25, 50:50 and 25:75).

As already mentioned before under section 1.4. General characterization of reference materials, the hard-block content was also determined via  $^1\text{H-NMR}$  spectroscopy by comparing the integrals of  $\text{CH}_2$  (pTHF) and  $\text{CH}_2\text{-S}$  (HEDS). All spectra are shown in the appendix (1. NMR spectra).

The differences of hydrogen-bonding between hard segments for TPU-HEDS and TPU-BHET-HEDS with different chain extender ratios was investigated via Fourier Transform Infrared Spectroscopy (FTIR).<sup>97, 291</sup> As reference material only TPU-BHET was selected in order to make the figure clearer and therefore the graphical comparability easier (Figure 74).

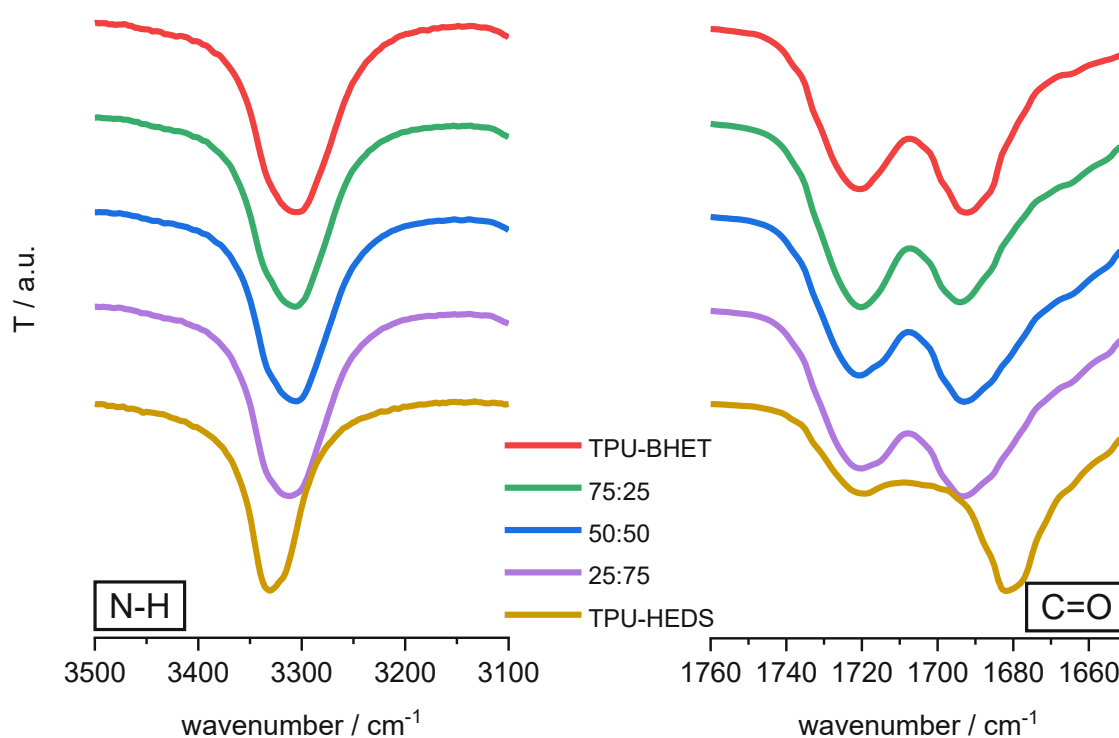


Figure 74: ATR-FTIR spectra of reference TPU-BHET, TPU-BHET-HEDS with different CE ratios (75:25, 50:50, 25:75) and TPU-HEDS. The amine region ( $3500\text{-}3100\text{ cm}^{-1}$ ) and the carbonyl region ( $1760\text{-}1650\text{ cm}^{-1}$ ) are shown, which are both characteristic for the hydrogen bond interactions and therefore for hard-block formation of TPUs.

The focus was set on the amine region ( $\text{N-H}$ ,  $3500\text{-}3100\text{ cm}^{-1}$ ) and the carbonyl region ( $\text{C=O}$ ,  $1760\text{-}1650\text{ cm}^{-1}$ ), which gives detailed information about ordered and disordered hydrogen bonds of urethanes in thermoplastic polyurethanes.<sup>291-294</sup> The amine region in Figure 74 (left) demonstrates a shift to higher wavenumbers from TPU-BHET to TPU-HEDS, which indicates a weakening of the hydrogen bonds with increasing content of HEDS as chain extender.

This can be explained on the one hand by generally weaker hydrogen bonds between S...H compared to O...H.<sup>314</sup> On the other hand, due to its structure, BHET (6xO), can also form more H-bonds compared to HEDS (2xO, 2xS) in absolute terms (chemical structures are shown in Figure 73). Furthermore, a peak narrowing from TPU-BHET to TPU-HEDS can be observed in the amine region, which can be explained by the less steric hindrance of linear aliphatic HEDS compared to the bulkier aromatic based BHET. It must be highlighted that the peak narrowing is most noticeable from TPU-BHET-HEDS (25:75) to TPU-HEDS, which shows that a small content of BHET (25% of CE) leads already to a peak broadening in FTIR spectra.

In the carbonyl region (Figure 74 right) no absorption bands at  $\sim 1740\text{ cm}^{-1}$  are observed for all polymers, which would show us the free C=O without hydrogen bonds.<sup>97</sup> At  $\sim 1720\text{ cm}^{-1}$  (disordered H-bonds) and at  $1680\text{-}1690\text{ cm}^{-1}$  (ordered H-bonds) absorption bands are observed for all polymers. Especially, the weak band at  $1720\text{ cm}^{-1}$  compared to the intense signal at  $1680\text{ cm}^{-1}$  has to be highlighted because it shows for TPU-HEDS a very high content of ordered hydrogen bonds compared to disordered H-bonds.<sup>97</sup>

### Molecular weight and hard-block content

For all HEDS containing TPUs a constant ratio of 1:2:1 (pTHF:HMDI:CE) was used for synthesis to ensure a comparability with the reference polymers. Therefore, the theoretical hard-block content is in the same range (36.1 - 32.9 %, Table 19) for all polymers. With increasing content of HEDS the hard-block content also decreases due to the lower molecular weight of HEDS compared to BHET. Compared to TPU-BHET, all TPUs containing HEDS show a higher deviation between  $HB_{th}$  and  $HB_{cal}$ . One possible explanation is a decreased isocyanate content of the prepolymer due to formation of amines in presence of residual moisture. As a result, reduced amounts of chain extender (HEDS) could be incorporated in the second synthesis step, as diols cannot react with amines, resulting in a lower hard-block content compared to complete conversion.

Table 19: Overview of synthesized polymers and commercially available Pellethane in terms of number-average molar mass  $\overline{M}_n$ , polydispersity (PDI) and hard-block content (theoretical and calculated).

polymer	$\overline{M}_n$ / kDa <sup>a</sup>	PDI <sup>b</sup>	$HB_{th}$ / wt% <sup>c</sup>	$HB_{cal}$ / wt% <sup>d</sup>
TPU-BHET	23.3	2.1	37.1	33.5
TPU-BHET-HEDS (75:25)	21.8	2.1	36.1	31.5
TPU-BHET-HEDS (50:50)	20.9	1.9	35.1	31.7
TPU-BHET-HEDS (25:75)	28.2	2.5	34.0	29.8
TPU-HEDS	29.4	2.0	32.9	27.3
Pellethane	56.3	1.9	-	-
TPU-BHPC	17.3	1.7	34.0	31.3

<sup>a</sup> Number-average molar mass. <sup>b</sup> polydispersity. <sup>c</sup> theoretical hard-block content ( $HB_{th}$ ). <sup>d</sup> calculated hard-block content from <sup>1</sup>H-NMR ( $HB_{cal}$ ).

Beside the hard-block content, the number-average molar mass  $\overline{M}_n$  and the polydispersity (PDI) was determined for HEDS containing TPUs via GPC, which are shown in Table 19. The molecular weight  $\overline{M}_n$  for TPU-BHET-HEDS (75:25 and 50:50) was slightly lower compared to the reference TPU-BHET, but higher than TPU-BHPC, with comparable PDIs. TPU-BHET-HEDS (25:75) and TPU-HEDS show higher molecular weight than TPU-BHET but still lower as Pellethane. From the molecular weight point of view, good mechanical properties for HEDS containing TPUs are expected,<sup>297</sup> although the hard-block content  $HB_{cal}$  is slightly lower than those of the reference polymers.

#### 4.4. Mechanical and thermal properties

The mechanical characteristics were assessed by tensile testing of solution cast polymer films (ISO 527, Type 5B, bone-shaped). The film thickness ranged from 20 to 40  $\mu\text{m}$ . The glass transition temperature ( $T_g$ ) was determined by DMTA (Appendix, 3. DMTA spectra). For a comprehensive account of the solution casting and tensile testing procedures, please refer to the Materials and Methods section.

As above mentioned, the molecular weight  $\overline{M}_n$  of the new synthesized polymers is a little lower or even higher compared to the reference TPU-BHET. The mechanical properties are shown in Table 20 and graphically in Figure 75. TPU-HEDS shows excellent mechanical properties. Especially, the combination of increasing elongation at break and ultimate tensile strength with decreasing elastic modulus compared to TPU-BHET must be emphasized as the material performs between TPU-BHET and the benchmark Pellethane in all three values.

Table 20: Comparison of number-average molar mass  $\overline{M}_n$ , calculated hard-block content, mechanical properties and glass transition temperature of HEDS based TPUs with reference polymers.

polymer (CE)	$\overline{M}_n$ / kDa <sup>a</sup>	$HB_{cal}$ / wt% <sup>b</sup>	$\epsilon_b$ / % <sup>c</sup>	TS / MPa <sup>d</sup>	E / MPa <sup>e</sup>	$T_g$ / °C <sup>f</sup>
BHET	23.3	33.5	1315 ± 54	14.1 ± 0.7	31.0 ± 1.4	-71
BHET-HEDS (75:25)	21.8	31.5	1096 ± 95	11.2 ± 0.9	24.3 ± 2.0	-61
BHET-HEDS (50:50)	20.9	31.7	1214 ± 46	11.0 ± 0.3	17.4 ± 0.4	-60
BHET-HEDS (25:75)	28.2	29.8	911 ± 93	8.5 ± 2.4	16.5 ± 1.1	-61
HEDS	29.4	27.3	1415 ± 45	14.7 ± 0.3	22.2 ± 0.2	-54
Pellethane	56.3	-	1651 ± 115	25.2 ± 1.2	14.2 ± 0.3	-52
BHPC	17.3	31.3	878 ± 75	12.8 ± 0.9	22.5 ± 0.3	-57

<sup>a</sup> Number-average molar mass. <sup>b</sup> calculated hard-block content from <sup>1</sup>H-NMR ( $HB_{cal}$ ). <sup>c</sup> Elongation at break  $\epsilon_b$ .

<sup>d</sup> tensile strength TS. <sup>e</sup> elastic modulus E. <sup>f</sup> Glass transition temperature  $T_g$  obtained from the maxima of loss modulus curves.

This is surprising since HEDS can form fewer H-bonds in the hard-block than BHET. This was already shown by FTIR of the amine region (Figure 74 left). However, the observation in the carbonyl region (Figure 74 right) could provide an explanation, since only a weak band for disordered H-bonds and a very defined absorption band for ordered H-bonds was observed.

On the other hand, an increased molecular weight  $\overline{M}_n$  compared to TPU-BHET may also be an explanation.

Compared to TPU-HEDS and TPU-BHET all polymers with a combination of BHET and HEDS as CE show lower elongation at break, ultimate tensile strength and elastic moduli. One reason could be the more complex synthesis, since an additional step was necessary to incorporate the second chain extender. This leads to increased sources of possible errors (water content, stoichiometric errors, etc.). However, the molecular weights  $\overline{M}_n$  of the mixed polymers are not significantly lower (Table 20). TPU-BHET-HEDS (25:75), for example, shows a higher molecular weight than the reference TPU-BHET.

Moreover, FTIR spectra of the carbonyl region (Figure 74 right) shows a comparatively high proportion of disordered H-bonds ( $1720\text{ cm}^{-1}$ ) compared to ordered H-bonds ( $1690\text{ cm}^{-1}$ ). It is possible that structurally different chain extenders (aliphatic HEDS, aromatic BHET) interfere with the formation of H-bonds and therefore lead to comparatively poorer mechanical properties than the polymers with only one chain extender.

In addition to tensile tests, DMTA measurements were conducted (Appendix, 3.DMTA spectra), which confirm a  $T_g$  below  $0\text{ }^\circ\text{C}$  for all HEDS based TPUs (Table 20) and show their applicability at body temperature. The  $T_g$  for all TPU-BHET-HEDS was at  $-60\text{ }^\circ\text{C}$  and therefore higher compared to TPU-BHET, but lower than Pellethane and TPU-BHPC. TPU-HEDS shows nearly the same  $T_g$  as Pellethane.

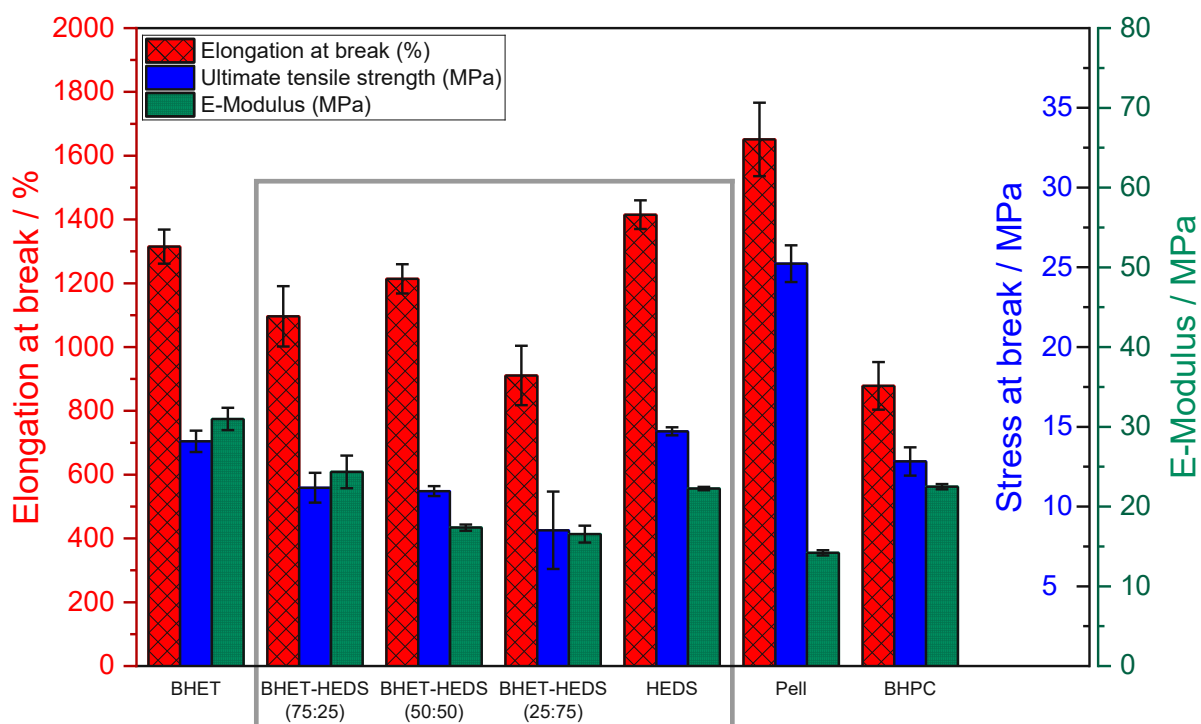


Figure 75: Elongation at break, ultimate tensile strength and elastic modulus of TPU-BHET, TPU-BHET-HEDS, TPU-HEDS and TPU-BHPC in comparison with commercially available Pellethane.

## 4.5. Degradation behavior

To investigate the degradation behavior of HEDS based TPUs, polymer films were prepared via solution casting and circular specimens were punched out with a diameter of 1 cm. These platelets show a mass between 20 and 30 mg. The samples were weighted in dry state and then stored in separate vials with 20 mL of PBS buffer solution (pH=7.4) with fourfold buffer capacity. The degradation studies were performed in triplicates at 37 °C and 90 °C for a period of 70 days. Afterwards the samples were washed with distilled water, to remove salts from the buffer solution and dried under reduced pressure (< 0.1 mbar) until constant weight was reached. Furthermore, GPC measurements were performed in triplicates of the degraded samples.

TPU-HEDS was synthesized, as a non-acidic degradable TPU in addition to TPU-BHPC and in contrast to TPU-BHET. As expected TPU-HEDS shows a lower degradation rate compared to TPU-BHET at 37 °C and at 90 °C in terms of mass erosion (Figure 76). This could be explained by the chemical structure of the chain extenders. HEDS contains a disulfide moiety, which is more stable against hydrolytic degradation compared to the ester based BHET. TPU-BHET-HEDS (75:25, 50:50, 25:75) show all a degradation rate between TPU-BHET and TPU-HEDS. Especially, at a degradation temperature of 37 °C (Figure 76 left), it could be demonstrated that the degradation rate (mass erosion) could be slowed down stepwise by exchanging a faster degradable CE (BHET) with a slower degradable CE (HEDS). Surprisingly, this behavior is not observed for the molecular weight. All three polymers with a mixture of both chain extenders show a faster decrease of  $\overline{M}_n$  compared to TPU-BHET and TPU-HEDS at 37 °C (Figure 77 left).

Comparing mass erosion (Figure 76) and molecular weight change (Figure 77) an already significant degradation within the first 14 days at both temperatures was observed. Therefore, the degradation behavior is rather an indication of bulk degradation than surface erosion because there is a constant decrease of both terms over the whole time period.

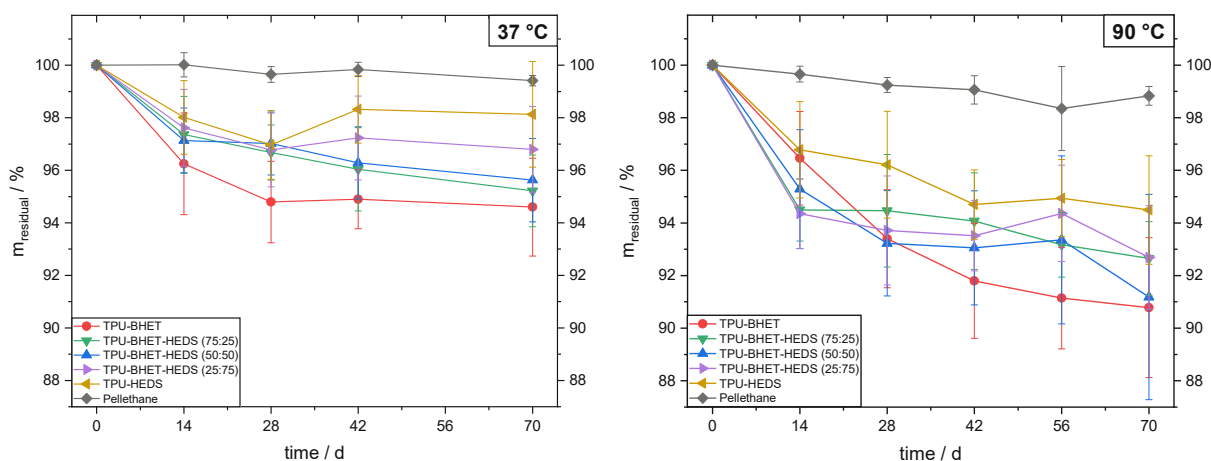


Figure 76: Residual mass  $m_{\text{residual}}$  in % of TPU-BHET, TPU-BHET-HEDS, TPU-HEDS and commercially available Pellethane in PBS buffer solution (4x) at 37 °C (left) and at 90 °C (right).

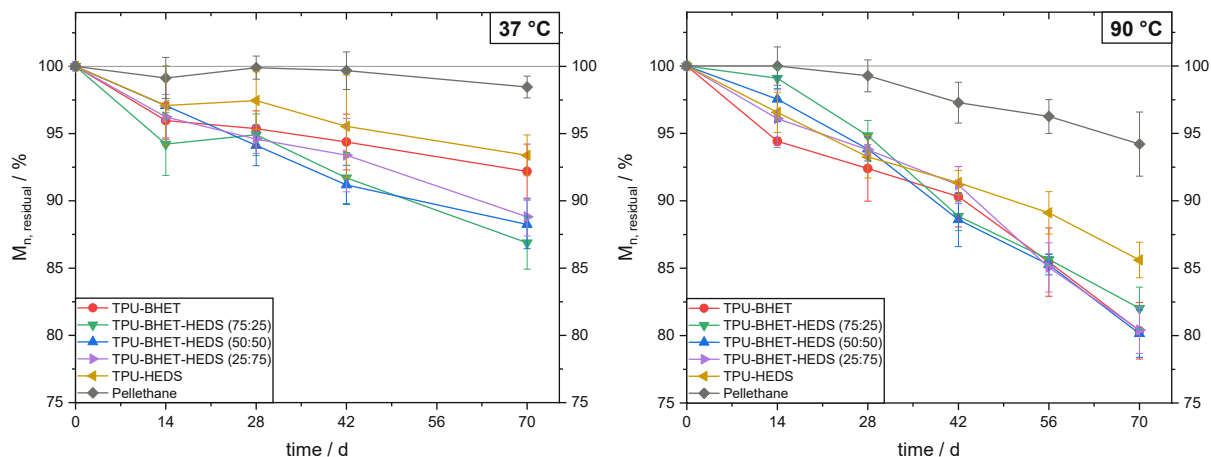


Figure 77: Development of number-average molar mass  $\overline{M}_n$ , residual in % of original  $\overline{M}_n$ , before degradation over a time period of 70 days of TPU-BHET, TPU-BHET-HEDS, TPU-HEDS and Pellethane as reference in PBS buffer solution (4x) at 37 °C (left) and 90 °C (right).

Besides, investigating the degradation behavior by mass erosion and  $\overline{M}_n$  decrease, the mechanical properties of TPU-BHET and TPU-HEDS after 7 days in PBS buffer solution at 90 °C was compared (Figure 78). As expected, TPU-HEDS shows less change in mechanical properties after 7 days of degradation compared to TPU-BHET. Surprisingly, the ongoing degradation has only a little effect on ultimate tensile strength and elastic moduli of both polymers, but a large effect on the elongation at break. For TPU-BHET the maximum elongation is reduced from ~900 % to ~500 % and for TPU-HEDS from ~1300 % to ~1000 %.

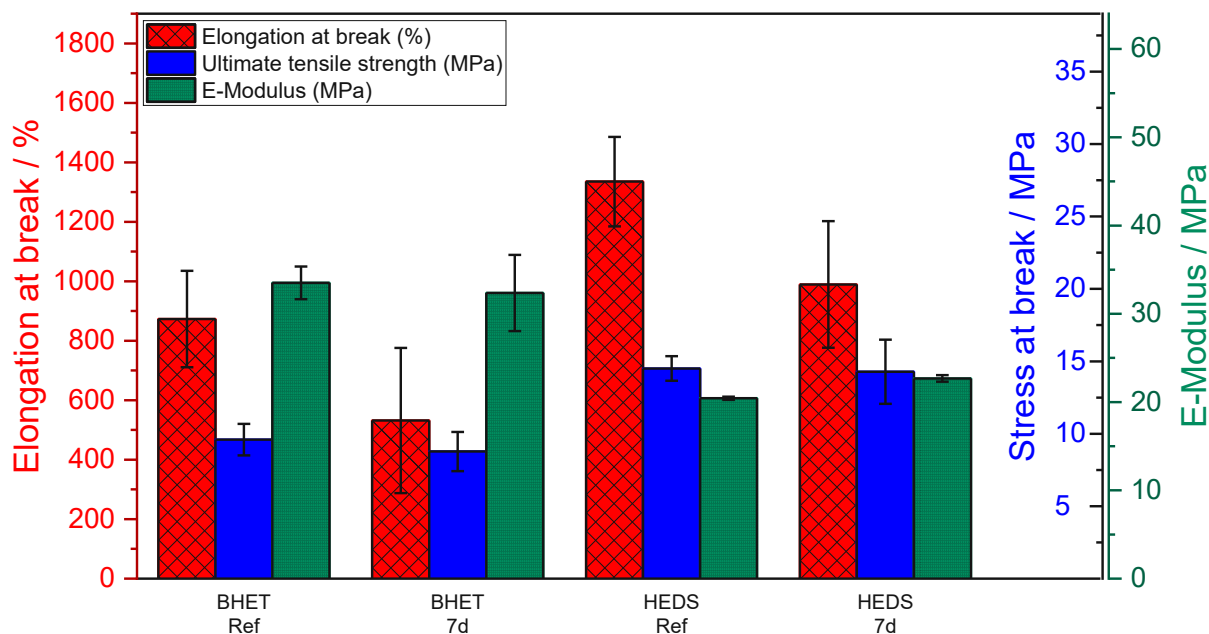


Figure 78: Comparison of mechanical properties of TPU-BHET and TPU-HEDS before and after degradation at 90 °C in PBS buffer solution (4x) within 7 days.



## Influence of DTT and TCEP to mimic reductive degradation

As already mentioned above 2-hydroxyethyl disulfide (HEDS) is an reductive non-acidic cleavable chain extender.<sup>280</sup> This is especially of interest for use as a vascular implant as there are enzymes in the human blood, which are able to cleave disulfide bonds.<sup>269, 270</sup>

To simulate an reductive/enzymatically active environment, additional degradation studies with dithiothreitol (DTT) and tris(2-carboxyethyl)phosphine (TCEP) were carried out in PBS buffer solution at 37 °C. DTT is a widely known reagent for reducing disulfides in proteins.<sup>273, 274</sup>

TCEP is an alternative reducing agent for disulfides that is also used frequently in biochemistry.<sup>275</sup> Compared to DTT it is more bulky and reduces e.g. cystines in folded proteins only slowly.<sup>276</sup> Chemical structures of both reducing agents are shown in Figure 79.

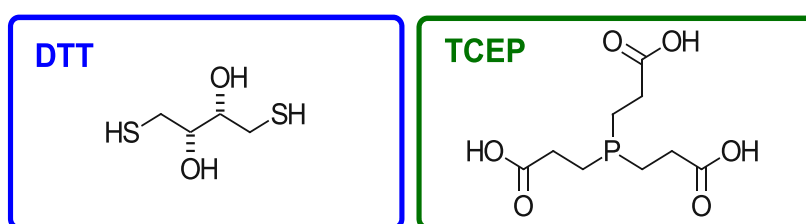


Figure 79: Chemical structures of Dithiothreitol (DTT, racemate) and tris(2-carboxyethyl)phosphine (TCEP).

Figure 80 shows mass erosion and the molecular weight decrease of TPU-BHET and TPU-HEDS under reductive conditions by adding DTT or TCEP as reducing agents for disulfides. As reference TPU-BHET and TPU-HEDS were not treated with DTT or TCEP.

It can be observed that the addition of DTT leads to a tremendous increase of degradation rate of TPU-HEDS but not for TPU-BHET. Furthermore, the molecular weight decreases already very fast within the first 14 days resulting in less than 10 % of the original molecular weight after 28 days. The mass erosion, on the other hand, occurs much slower.

By treating the materials with TCEP no significant change of the mass is observed but a molecular weight decrease is occurring between 14 and 28 days. Nevertheless, compared to DTT, this samples had still a  $\overline{M}_n$  of more than 70 % of the original  $\overline{M}_n$  after 70 days.

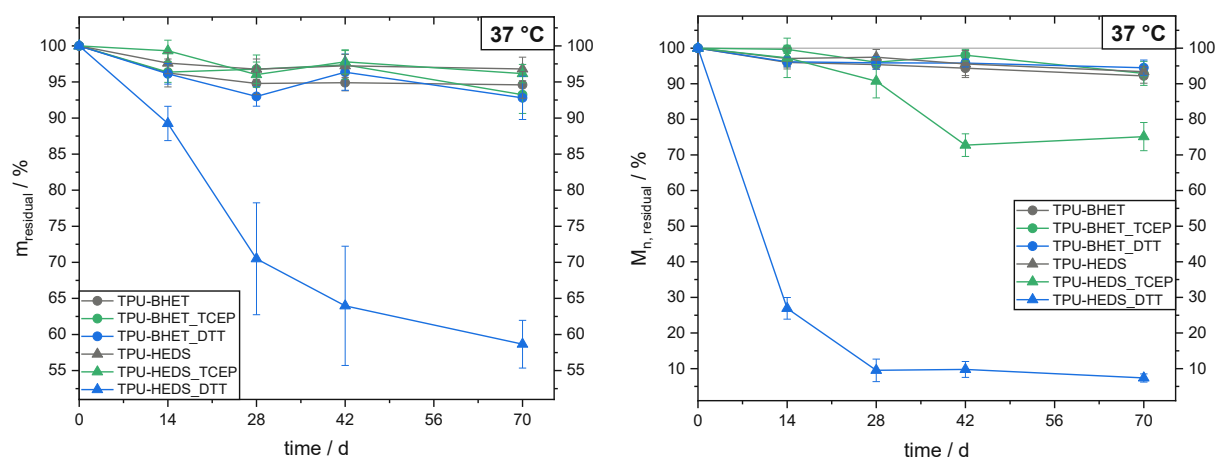


Figure 80: Mass erosion (left) and  $\overline{M}_n$ -change (right) of TPU-BHET and TPU-HEDS under reductive conditions.

A reason for the difference of the degradation speed between both reducing agents could be the more bulky structure of TCEP as it was described already by Cline *et al.*<sup>276</sup> Because TPU-HEDS is of course not in a dissolved state in the degradation media (PBS, pH=7.4), disulfides are protected from a reduction by TCEP due to hydrogen bonds between the hard-blocks. DTT, on the other hand, is a much smaller molecule and therefore can potentially penetrate the hard-blocks and is able to cleave the disulfide bonds. Nevertheless, it could be demonstrated that TPU-HEDS is suitable as a reductive degradable TPU.

By using the reductively degradable chain extender 2-hydroxyethyl disulfide (HEDS), the mechanical properties were improved in all three measured parameters compared to the reference polymer TPU-BHET. Increased elongation at break and ultimate tensile strength were achieved in combination with reduced stiffness. Thus, TPU-HEDS already shows similar mechanical properties to the benchmark material Pellethane.

Unfortunately, the mechanical properties could not be improved by combining BHET and HEDS in different ratios compared to the "pure" polymers TPU-BHET and TPU-HEDS.

In PBS buffer solution (pH=7.4) at 37 °C and 90 °C, TPU-HEDS shows a low degradation rate in terms of mass erosion compared to TPU-BHET, as the disulfide bond shows a lower hydrolytic degradation than the ester bond. In the case of TPU-BHET-HEDS, as in the previous chapter for the boronic ester based TPU-BHET-BDB, there is a gradual change in the degradation rate with a change in the ratio between BHET and HEDS. This would also allow fine-tuning of the degradation rate in terms of mass erosion for this material.

However, this gradual change in degradation rate cannot be observed for the molecular weight change at 37 °C. All TPU-BHET-HEDS approaches degrade faster than TPU-BHET and TPU-HEDS. At 90 °C they show a very similar degradation behavior to TPU-BHET. As with mass erosion, TPU-HEDS again shows the lowest degradation rate for molecular weight change at both temperatures.

To evaluate the reductive degradation of TPU-HEDS, dithiothreitol (DTT) or tris(2-carboxyethyl)phosphine (TCEP) was added to the polymer film. In the presence of DTT, TPU-HEDS showed a significantly increased degradation rate in terms of mass erosion and molecular weight reduction compared to TPU-BHET. However, the reduction of disulfide groups with TCEP was much slower than that with DTT. This may be due to the sterically more demanding structure of TCEP compared to DTT. Nevertheless, by using the chain extender HEDS, the mechanical properties could be significantly improved compared to TPU-BHET and at the same time a higher degradation rate could be achieved using the concept of reductive degradation.

## SUMMARY AND CONCLUSION

The aim of this work was to synthesize new thermoplastic polyurethanes (TPUs), polyurea urethanes (TPUUs) and polythiourethanes (TPTUs) and to characterize them primarily with respect to their mechanical properties and degradation behavior. The properties must meet the requirements for use as a vascular implant material. These include mechanical properties of the final graft that are as close as possible to those of a natural blood vessel and a degradation rate in a biological environment that allows the formation of new endogenous tissue.

Numerous studies have shown that TPUs are an excellent material for these applications due to their segmented structure of high-molecular-weight, flexible soft-blocks and low-molecular-weight, stiffer hard-blocks (Figure 81).<sup>111, 112</sup> The segmented structure also allows a variety of combinations of macrodiols, diisocyanates, and chain extenders (CEs) and therefore fine-tunable final properties.

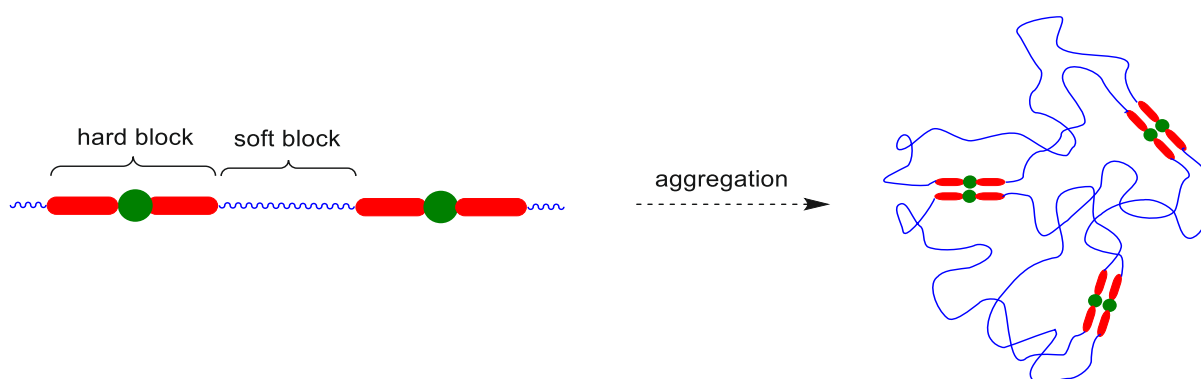


Figure 81: Aggregation of thermoplastic polyurethanes due to segmented structure via hard- and soft-blocks.

In the first chapter of this thesis, the hard-block degradable reference materials TPU-BHET and TPU-BHPC were synthesized, which are already known in this working group and proved to be promising due to their degradation behavior and mechanical properties.<sup>133, 152, 183, 283</sup>

For both polymers, the macrodiol polytetrahydrofuran (pTHF,  $\overline{M}_n=1000 \text{ g mol}^{-1}$ ) and the diisocyanate hexamethylene diisocyanate (HMDI) were used in order to obtain a comparable prepolymer structure and to make the resulting properties dependent only on the choice of the chain extender. The commercially available non-degradable Pellethane<sup>®</sup>-2363-80A was used as a benchmark material.<sup>288, 289</sup> The structures of the individual components are shown in Figure 82.

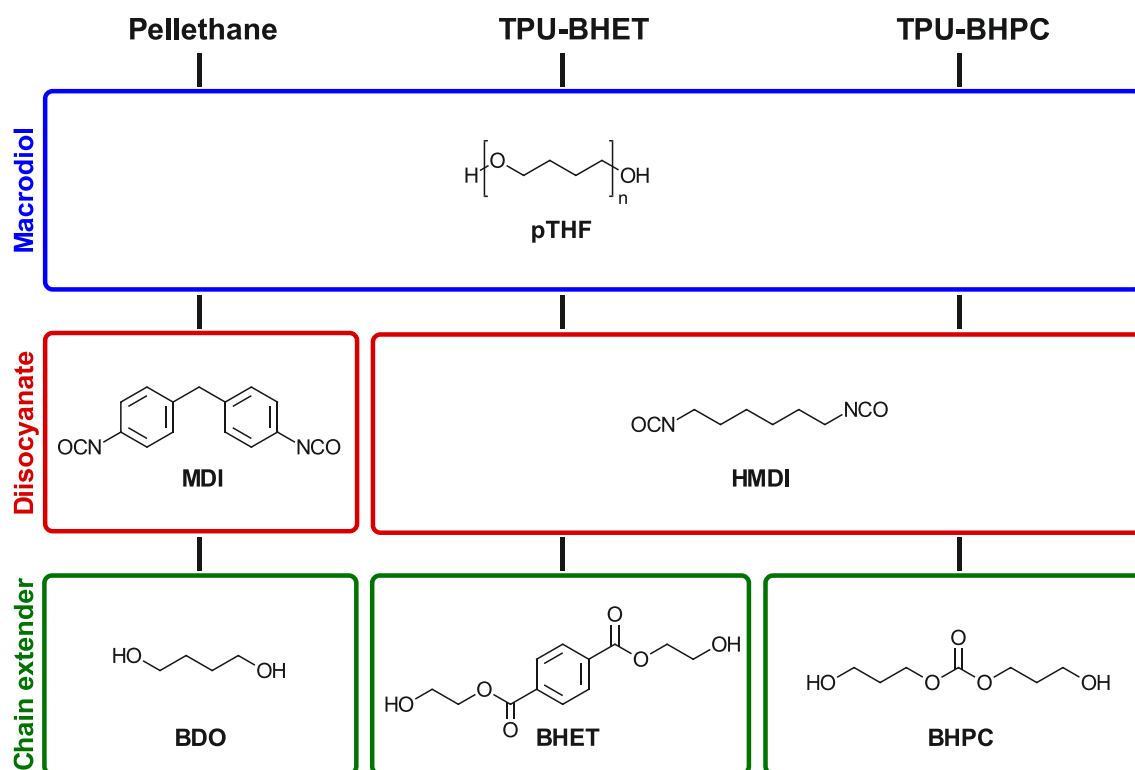


Figure 82: Composition of reference TPUs. The commercially available Pellethane consists of polytetrahydrofuran (pTHF), 4,4'-methylene diphenyl diisocyanate (MDI) and 1,4-butanediol (BDO) as chain extender. In contrast to that TPU-BHET and TPU-BHPC uses hexamethylene diisocyanate (HMDI) as diisocyanate and bis(hydroxyethylene)terephthalate (BHET) or bis(hydroxypropyl)carbonate (BHPC) as chain extenders.

The reference polymers TPU-BHET and TPU-BHPC were successfully prepared with their chain extenders bis(hydroxyethylene) terephthalate (BHET) and bis(hydroxypropyl) carbonate (BHPC). They show good mechanical properties compared to the benchmark material Pellethane and therefore serve as a comparison for all other materials produced in this work. However, the preferred combination of relatively high elongation at break, high ultimate tensile strength and low elastic modulus of Pellethane could not be achieved with these materials. The carboxylic ester-based hard-block degradable TPU-BHET also serves as a reference material for all degradation studies in this thesis.

In the second chapter, an attempt was made to improve the good mechanical properties of TPU-BHET, combined with a relatively slow degradation rate, by using another carboxylic ester-based chain extender, namely bis(2-hydroxyethyl)furan-2-5-dicarboxylate (BHEF, Figure 83), which is a furan-based analog of BHET. The use of BHEF instead of BHET is based on the recognition that polyethylene-2,5-furan dicarboxylate (PEF) has a number of remarkable physical, mechanical, and thermal properties, some of which are superior to those of polyethylene terephthalate (PET).<sup>228, 234</sup> Another notable advantage over BHET is that BHEF is produced from furan-2,5-dicarboxylic acid (FDCA), which is an important sustainably building block in chemistry.<sup>230, 233</sup>

In the scope of this work, the chain extender BHEF was prepared in sufficient purity to be used for the successful synthesis of TPU-BHEF. This material showed good processability for polymer film preparation and showed comparable elongation at break to TPU-BHPC and similar elastic modulus to TPU-BHET. In terms of ultimate tensile strength, it has the lowest measured value compared to the reference materials. An explanation for the poorer mechanical properties, especially compared to TPU-BHET, can be found in the formation of hydrogen bonds between the hard-blocks. This was estimated using ATR-FTIR spectroscopy measurements. It was found that TPU-BHEF, and thus the chain extender BHEF, is less able to form hydrogen bonds between the individual hard-blocks than BHET. This also has a negative effect on the mechanical properties. Another explanation, especially for the lower elongation of TPU-BHEF, could be the increased stiffness of BHEF compared to BHET, as described by Burgess *et al.*,<sup>234</sup> since the carbonyl substituents in BHEF allow less rotation. Another reason may be the lower molecular weight of TPU-BHEF compared to TPU-BHET. Nevertheless, an improvement in the degradation rate was achieved with TPU-BHEF both at 37 °C and at 90 °C in terms of mass erosion and molecular weight degradation, but only to a relatively small extent.

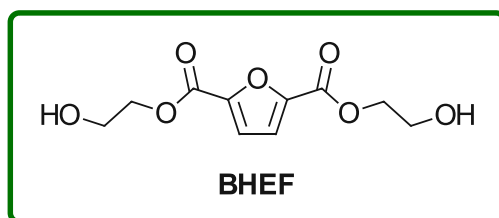


Figure 83: Structure of carboxylic ester based chain extender BHEF (bis(2-hydroxyethyl)furan-2,5-dicarboxylate).

To further increase the degradation rate, the concept of inorganic ester-based chain extenders was introduced in the third chapter. Specifically, CE molecules based on phosphate-, silicic acid-, and boronic acid esters were used because they have interesting degradation mechanisms and properties according to literature.<sup>181, 210, 219-223, 235, 236</sup>

Bis(4-hydroxybutyl)ethyl phosphate (BHBEP) and 2,2'-(1,4-phenylene)-bis[4-mercaptan-1,3,2-dioxaborolane] (BDB) were self-synthesized as chain extenders. Unfortunately, BHBEP could not be purified by column chromatography, but the determination of the hydroxyl number by <sup>31</sup>P-NMR confirmed a sufficiently high purity for a polymer synthesis experiment. Commercially available bis(4-aminophenoxy)dimethylsilane (BAPDMS) had to be purified for the polyaddition reaction. Due to the synthesis and availability of BDB and BAPDMS, there was no diol-based alternative, so the distinction between thermoplastic polyurethanes (TPUs, diol-CE), polyurea urethanes (TPUUs, diamine-CE) and polythiourethanes (TPTUs, dithiole-CE) was introduced in this chapter.

Due to the small number of TPTUs known in the literature to serve as a comparison, the chain extender 1,2-bis(2-mercaptoethoxy)ethane (BMEE) and therefore TPTU-BMEE was prepared as an additional reference material. The structures of the CEs are shown in Figure 84.

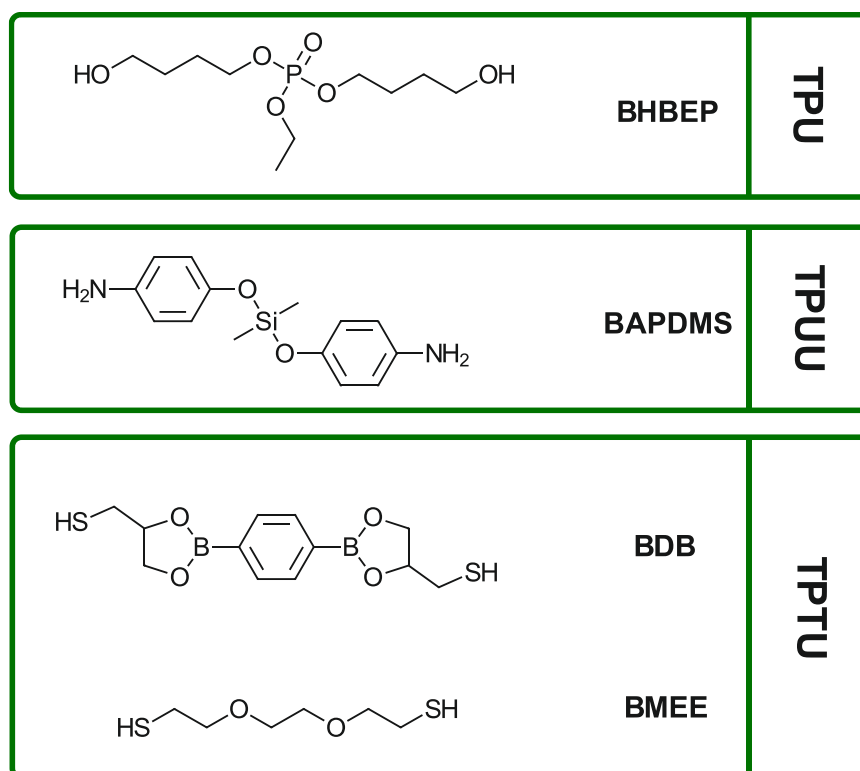


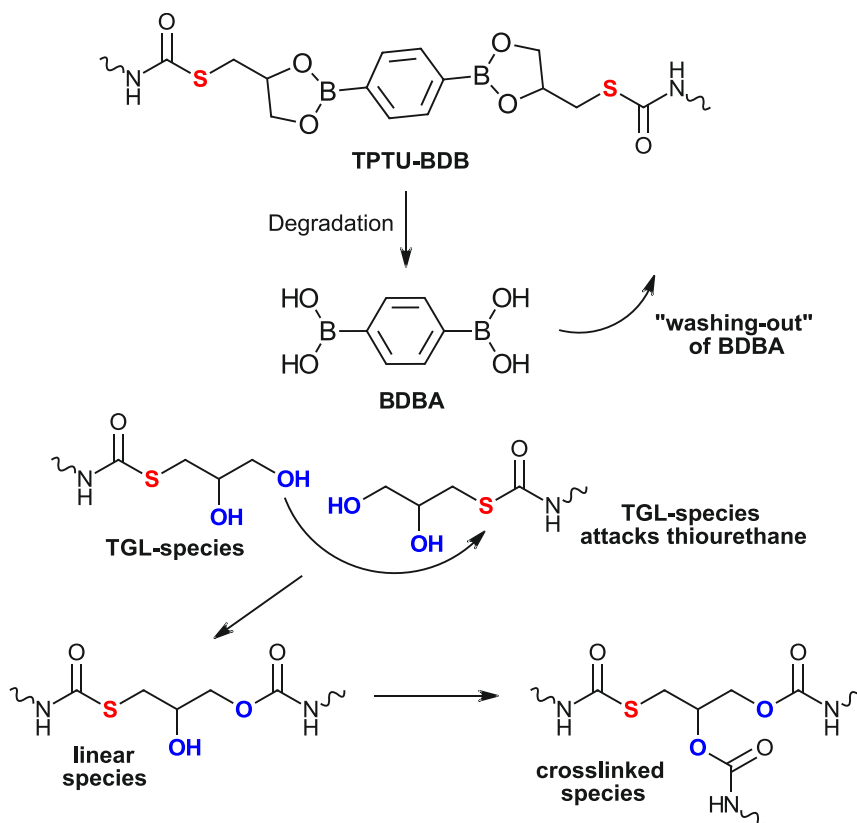
Figure 84: Structures of inorganic ester-based chain extenders (CE) for thermoplastic polyurethanes (TPU), thermoplastic polyurea urethanes (TPUU) and thermoplastic polythiourethanes (TPTU). BHBEP (bis(4-hydroxybutyl) ethyl phosphate), BAPDMS (bis(4-aminophenoxy) dimethylsilane), BDB (2,2'-(1,4-phenylene)-bis[4-mercaptan-1,3,2-dioxaborolane]) and BMEE (1,2-bis(2-mercaptoethoxy)ethane).

Unfortunately, the corresponding polymers TPU-BHBEP and TPUU-BAPDMS with phosphate based BHBEP and siloxane based BAPDMS could not be reproducibly synthesized. In the case of TPU-BHBEP, the polymer could not be processed into a polymer film and therefore no further investigations were carried out regarding mechanical properties and degradation behavior. In the case of TPUU-BAPDMS, this was only possible once for mechanical tests, but these showed far too poor properties for use as a vascular implant material.

In contrast to these two polymers, boronic ester based TPTU-BDB was successfully synthesized and showed good mechanical properties, although inferior to those of the reference materials. Particularly noteworthy is the very high elastic modulus and thus the highly increased stiffness compared to TPU-BHET and TPU-BHPC. The thiourethane-based reference polymer TPTU-BMEE, on the other hand, performed excellently and showed in some cases even better mechanical properties than the benchmark material Pellethane.

However, the boronic acid-based CE showed a significantly higher degradation rate during mass erosion compared to carboxylic ester based TPU-BHET. Specifically, after 70 days, only about 70 % of TPTU-BDB remains at 90 °C, while about 90 % of TPU-BHET remains. The thiourethane based reference TPTU-BMEE, on the other hand, showed a very low degradation rate between Pellethane and TPU-BHET due to the lack of cleavable groups in the CE.

When looking at the molecular weight during the degradation study, an increase in  $\overline{M}_w$  was observed for boronic ester based TPTU-BDB at 37 °C, which was even more noticeable at 90 °C, reaching approximately 600 % after only 7 days. The subsequent samples could no longer be dissolved, which could indicate cross-linking. A more detailed investigation using ATR-FTIR spectroscopy revealed a "washing-out" of benzene-1,4-diboronic acid (BDDBA) during the degradation study. The resulting OH-terminated polythiourethanes could lead to crosslinking by intramolecular reactions between free OH groups and the thiourethane group, as shown by model reactions between TPTU-BMEE with the addition of glycerol (Scheme 23). The degradation behavior of BDB was also investigated by <sup>1</sup>H-NMR spectroscopy using model compounds of BDB with phenyl isocyanate (NCO-BDB-NCO). A "washing-out" of benzene-1,4-diboronic acid (BDDBA) was detected by the peak shifts of 1-thioglycerol, which was also previously shown for the polymer TPTU-BDB by FTIR spectroscopy. In contrast, no "washing-out" of terephthalic acid was observed for the BHET-based model compound NCO-BHET-NCO.



Scheme 23: Predicted degradation of TPTU-BDB by "washing-out" of BDDBA and crosslinking via "intramolecular" reaction of hydroxy terminated polythiourethanes.

Since boronic ester based TPTU-BDB showed a good degradation rate, but performed worse than the reference materials in terms of mechanical properties, another concept was introduced. TPUs were synthesized with a combination of two different chain extenders. Specifically, boronic ester based BDB, phosphate based BHBEP and siloxane based BAPDMS were each combined with the already known BHET to improve the mechanical properties and still achieve a higher degradation rate than with TPU-BHET. It was also possible to produce reproducible TPUs containing BHBEP and BAPDMS as CE. However, these were only used in a small proportion of 25 % as CE in combination with 75 % BHET. The polymers TPU-BHET-BHBEP (75:25) and TPU-BHET-BAPDMS (75:25) were synthesized. Both polymers showed similar mechanical properties, but were still too poor for further application. However, the degradation rate could be increased compared to TPU-BHET by adding BHBEP or BAPDMS.

The combination of boronic ester based BDB and carboxylic ester based BHET was tested in three different ratios (75:25, 50:50 and 25:75). Surprisingly, the elongation at break and the ultimate tensile strength could not be improved by the addition of BHET compared to "pure" TPTU-BDB. Only the elastic modulus showed a slight improvement over TPTU-BDB. Thus, the combination of BHET and BDB did not improve the mechanical properties compared to TPTU-BDB. A possible explanation could be a poorer formation of hard-blocks due to the different structure of the CEs.

The degradability studies of the TPU-BHET-BDB approaches clearly showed that the degradation rate can be precisely controlled by the combination of two CEs. With increasing BDB content, a gradual increase in the degradation rate in terms of mass erosion was observed. Furthermore, no increase in molecular mass was observed in the TPU-BHET-BDB samples at 37 °C compared to TPTU-BDB. However, a gradual increase was observed at 90 °C. Thus, as the BDB content increased, the molecular weight also increased. This shows that this phenomenon is not exclusive to TPTU-BDB.

Summarizing the inorganic ester-based chain extenders, the use of the boronic acid-based BDB can significantly increase the degradation rate compared to the carboxylic acid ester based TPU-BHET and TPU-BHEF. However, the use of the faster degrading CE has a negative effect on mechanical performance.



In order to achieve sufficiently good properties in both areas, the degradation concept was completely changed in the last chapter. In contrast to the purely hydrolytically degradable carboxylic acid-, phosphate-, silicic acid- and boronic acid esters, a reductively degradable disulfide-based CE was introduced, namely 2-hydroxyethyl disulfides (HEDS, Figure 85). TPU-HEDS showed excellent mechanical properties and improvements were achieved in all three measured parameters compared to TPU-BHET. In particular, an increase in elongation at break and ultimate tensile strength combined with a reduction in stiffness was achieved, which is already very close to the benchmark material Pellethane. As already observed with TPU-BHET-BDB, the combination of BHET with HEDS did not improve the mechanical properties compared to TPUs with only one CE. This underlines the assumption that a combination of two different chain extenders could lead to poorer hard-block formation. Regarding the degradation rate, TPU-HEDS showed a lower hydrolytic degradation rate in a neutral medium (PBS, pH=7.4) than TPU-BHET, but a significantly increased degradation rate in a reductive environment could be demonstrated using dithiothreitol (DTT) and tris(2-carboxyethyl)phosphine (TCEP). For the TPU-BHET-HEDS approaches, it can be seen again that the degradation rate can be fine-tuned using different CE ratios.

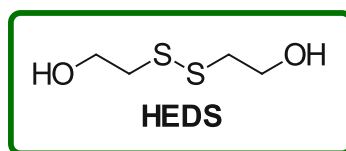


Figure 85: Structure of the disulfide-based chain extender HEDS (2-hydroxyethyl disulfide).

In conclusion, it can be said that BHEF can be used as a renewable CE alternative to BHET. TPU-BHEF shows good mechanical properties and a slightly higher degradation rate could be achieved compared to TPU-BHET.

Among the inorganic ester-based materials, only TPTU-BDB showed satisfying results. In particular, the significantly higher degradation rate compared to the reference materials makes it a promising replacement for carboxylic ester-based TPUs.

Unfortunately, the use of the phosphate- and silicic acid ester-based CEs (BHBEP and BAPDMS) did not show the good results required for use as a vascular graft material. Even in combination with BHET, these chain extenders could not significantly improve the mechanical properties.

The most promising results were obtained with the disulfide-based chain extender HEDS. TPU-HEDS produced with this chain extender exhibited extremely good mechanical properties, almost as good as those of the benchmark material Pellethane. Furthermore, the reductively cleavable disulfide bond in the CE allows a very high degradation rate of the material in neutral buffer medium (PBS) under reductive conditions.

An overview of the mechanical properties and degradation behavior of the reference materials and the best-performing representatives of the individual CE concepts are shown in Figure 86 and Figure 87.

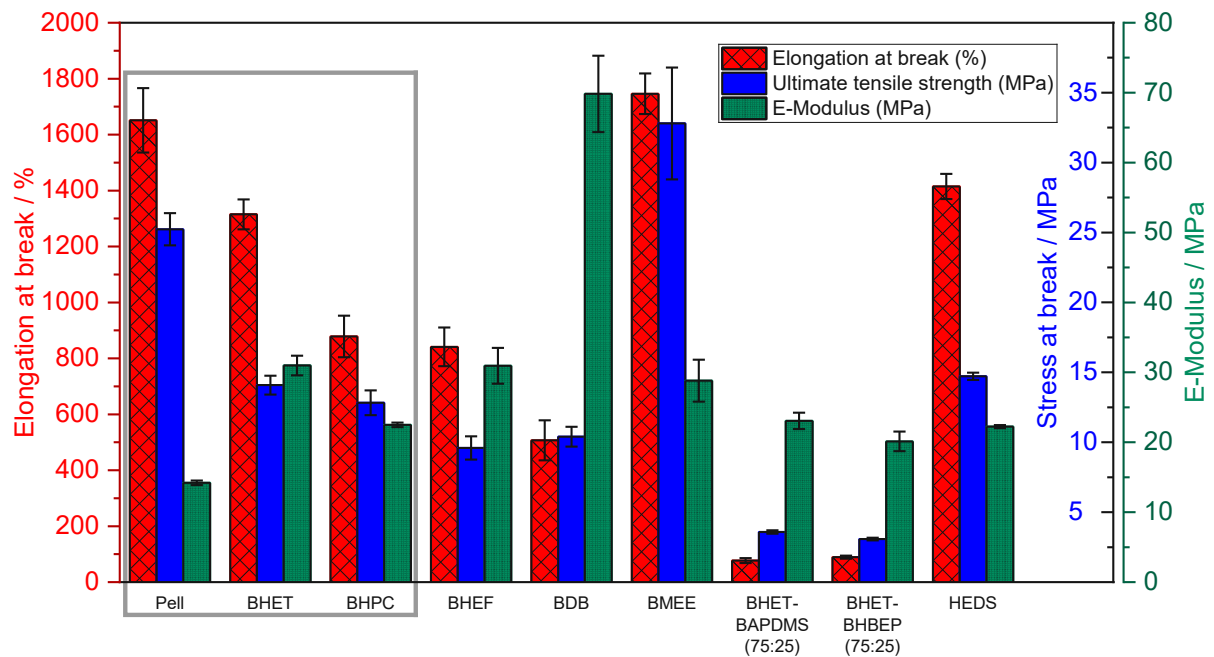


Figure 86: Best obtained mechanical properties of polymers by choice of the chain extender.

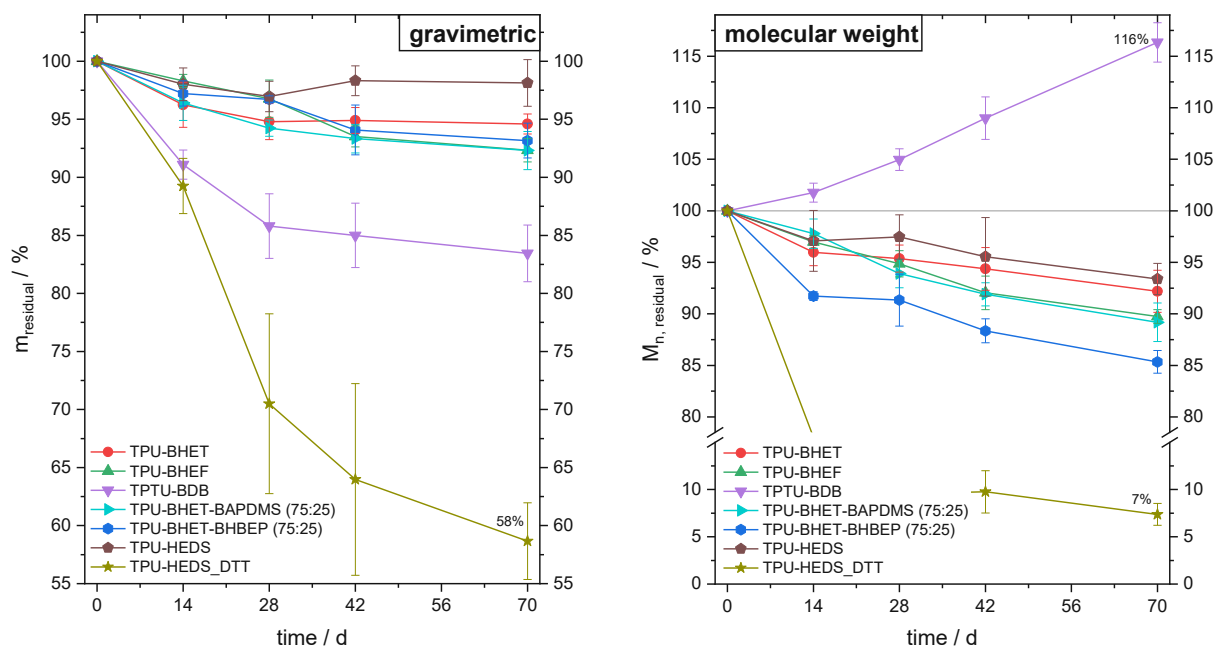
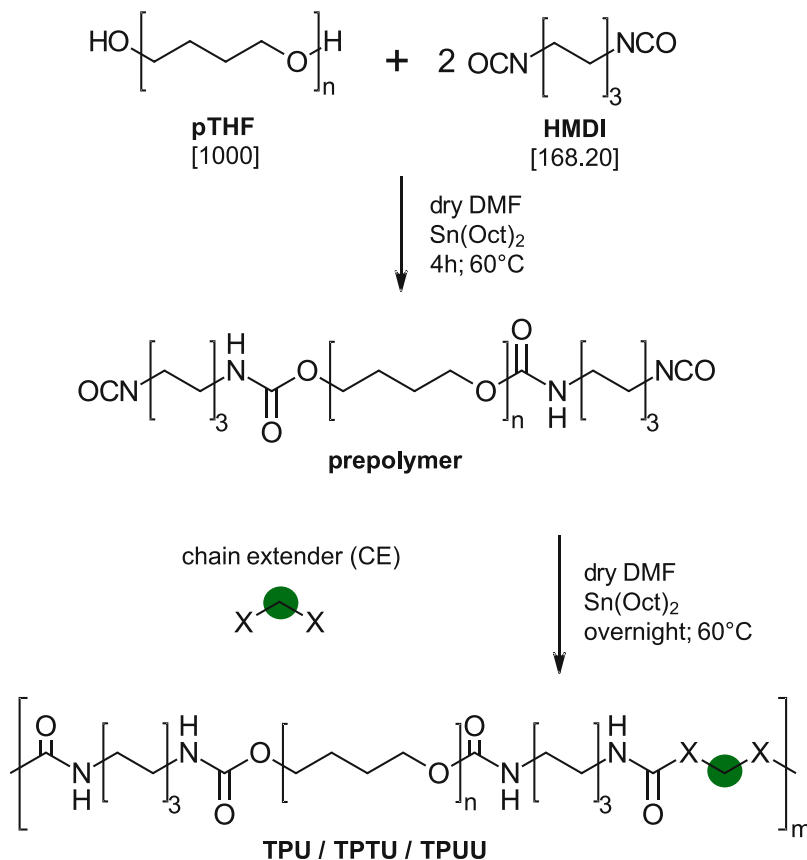


Figure 87: Mass erosion (left) and  $\overline{M}_n$ -change (right) of a selection of synthesized degradable polymers during this thesis. TPU-HEDS is furthermore shown under reductive conditions in presence of dithiothreitol (DTT). Pellethane and TPTU-BMEE are not included, because of their non-cleavable CE structure.

# EXPERIMENTAL PART

## 1. Reference polymers

### 1.1. General polymer procedure / Synthesis of TPU-BHET



Scheme 24: General synthesis of TPU / TPTU / TPUU by using diols, dithiols or diamines as chain extenders (CE), X=OH, NH<sub>2</sub> or SH.

Table 21: Used reactants in general synthesis of TPU, TPTU or TPUU.

reactant	equivalents	M / g mol <sup>-1</sup>	n / mmol	m / g	V / mL
pTHF	1	1.000*	5.0	5.000	-
HMDI	2	168.20	10.0	1.682	-
CE <sup>1</sup>	1	-	5.0	-	-
Sn(Oct) <sub>2</sub>	0.1	405.12	0.2	0.063	0.05
dry DMF	solvent	-	-	-	20.00

<sup>1</sup> CE: chain extender, \* exact M determined via hydroxy-number titration.  
For all polymer synthesis the use of dry and clean reactants and solvents must be ensured.

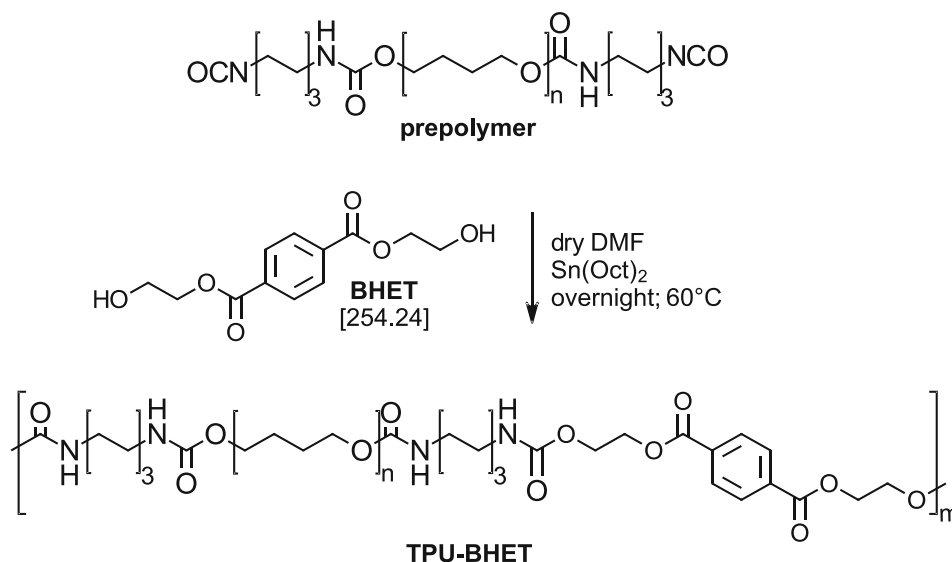
For all polymer synthesis the use of dry and clean reactants and solvents must be ensured. Furthermore, it is also necessary to determine the exact molecular weight of the macrodiol pTHF and the isocyanate content of the diisocyanate HMDI before synthesis. The necessary purification and characterization steps prior to TPU/TPTU and TPUU synthesis are explained in the next chapter 0. Synthesis of TPU-BHET.

The synthesis of TPUs, TPTUs and TPUU were performed as described previously.<sup>103</sup> (Scheme 24). The reaction was carried out with standard Schlenk-techniques.

Before the reaction, polytetrahydrofuran (pTHF) was dried under vacuum (< 0.1 mbar) at 90 °C for 24 h. A water content below 50 ppm was confirmed by Karl-Fischer titration for pTHF and dry DMF as well. Hexamethylenediisocyanate (HMDI) was freshly distilled at least two days before the reaction. Polytetrahydrofuran (pTHF, 5.0 g, 5 mmol, 1 eq.,  $M_n=1000$  g/mol) was weighed into a three-necked round bottom flask and was again dried for another 3 h at 60 °C. Hexamethylenediisocyanate (HMDI, 1.68 g, 10 mmol, 2 eq.) was diluted in dry DMF (5 mL) and added to pTHF at 60 °C under argon. The syringe and transfer vessel were rinsed with dry DMF (5 mL) in portions. Stannous octoate ( $\text{Sn}(\text{Oct})_2$ , 0.05 mL, 0.2 eq.) was added and the reaction mixture was stirred for 4 h at 60 °C, resulting in prepolymer formation.

Then the chain extender (CE, 5 mmol, 1 eq.) was dissolved in dry DMF (5 mL) and was added to the reaction mixture at 60 °C under argon atmosphere (yield and used CEs for each polymer are listed above, Table 21). The syringe and transfer vessel were rinsed with additional dry DMF (5 mL) in portions. Afterwards, the mixture was stirred overnight at the same reaction conditions. For purification, the polymer was precipitated in petroleum ether or diethyl ether (800 mL) and dried under vacuum at 50 °C.

## Synthesis of TPU-BHET



Scheme 25: Synthesis of TPU-BHET starting from the prepolymer.

Table 22: Used reactants in synthesis of TPU-BHET.

Reactant	Equivalents	M / g mol <sup>-1</sup>	n / mmol	m / g	V / mL
pTHF	1	1,000.00	5.0	5.000	-
HMDI	2	168.20	10.0	1.682	-
BHET	1	254.24	5.0	1.271	-
Sn(Oct) <sub>2</sub>	0.1	405.12	0.2	0.063	0.05
dry DMF	solvent	-	-	-	20.00

Before the TPU synthesis, the chain extender bis(hydroxyethylene)terephthalate (BHET) was recrystallized from deionized water. The synthesis of TPU-BHET until prepolymer formation was performed as described before in 1.1. General polymer procedure / Synthesis of TPU-BHET. The reaction scheme starting from the prepolymer is shown in Scheme 25 and the used reactants are listed in Table 22.

After prepolymer formation bis(hydroxyethylene)terephthalate (BHET, 1.27 g, 5 mmol, 1 eq.) was dissolved in dry DMF (5 mL) and was added to the reaction mixture at 60 °C under argon atmosphere. The syringe and transfer vessel were rinsed with additional dry DMF (5 mL) in portions. Afterwards, the mixture was stirred overnight at the same reaction conditions. For purification, the polymer was precipitated in petroleum ether (800 mL) and dried under vacuum at 50 °C, resulting in a white solid.

Yield: 7.2 g (90.6 %)

GPC:  $\overline{M}_w$  = 49.7 kDa,  $\overline{M}_n$  = 23.3, kDa, PDI = 2.1

<sup>1</sup>H-NMR (400 MHz, DMSO-*d*<sub>6</sub>, δ): 1.19 (8H, CH<sub>2</sub>); 1.34 (8H, CH<sub>2</sub>); 1.49 (34H, CH<sub>2</sub>); 2.92 (8H, CH<sub>2</sub>-NH); 3.39 (64H, CH<sub>2</sub>-O + xH<sub>2</sub>O); 4.30 (4H, CH<sub>2</sub>-O); 4.45 (4H, CH<sub>2</sub>-O); 6.98-7.19 (4H, NH); 8.07 (4H, CH<sup>Ar</sup>) ppm

FTIR (solid): 3314 cm<sup>-1</sup> (N-H, urethane); 2938 cm<sup>-1</sup> (C-H); 2858 cm<sup>-1</sup> (C-H); 1720 cm<sup>-1</sup> (C=O, ester); 1695 cm<sup>-1</sup> (C=O...H-N, urethane); 1536 cm<sup>-1</sup> (N-H, urethane + C-N, urethane); 1250 cm<sup>-1</sup> (C-O, ether); 1101 cm<sup>-1</sup> (C-C)

### Water content of reactants and solvents

Polytetrahydrofuran was dried at 90 °C and high vacuum (< 0.1 mbar) for at least 24 h. residual water content had to be below 50 ppm and was confirmed via Karl-Fischer titration. DMF was purchased in extra dry quality from Acros Organics and the water content was also determined before each polymer synthesis. Chain extenders were dried at room temperature and high vacuum (< 0.1 mbar) for at least 2 days. Liquids were injected directly into the Karl-Fischer titration device. Solids were dissolved in a defined amount of dry solvent before injection.

## Hydroxy value of polytetrahydrofuran (pTHF)

The determination of the molecular weight of the macrodiol polytetrahydrofuran (pTHF) was done via hydroxy end group titration according to DIN 53240-1. The acetylation reagent was prepared by mixing 70 mL freshly distilled pyridine and 30 mL freshly distilled acetic anhydride. For acetylation, about 1 g pTHF (0.1 mg accuracy) was mixed with 25 mL freshly distilled pyridine, 10 mL of acetylation reagent and was refluxed for 1 h. Then, the mixture was cooled until room temperature and 10 mL deionized water was added. Afterwards, the solution was heated until 100 °C for another 10 min. Finally, the solution was titrated potentiometric with 0.5 M methanolic KOH. The blank samples were treated the same as described, only without pTHF. Titrations for the macrodiol and blank samples were done in triplicates.

## Isocyanate-content of hexamethylene diisocyanate (HMDI)

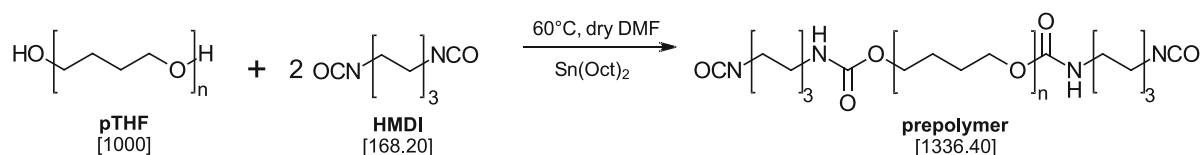
The isocyanate content of hexamethylene diisocyanate (HMDI) was determined according to DIN EN ISO 11909.

For dibutyl amine solution (2 M) dry toluene and freshly distilled dibutyl amine was used. For titration, about 2 g (0.1 mg accuracy) crude HMDI (before distillation) was weighted into a 500 mL Erlenmeyer flask and dissolved in 25 mL dry toluene. Then 20 mL dibutyl amine solution (2 M) was added and the mixture was stirred for 15 min. Finally, 150 mL ethanol was added and the solution was titrated potentiometric with 0.5 M hydrochloric acid. Blank samples were prepared in the same way as HMDI without adding isocyanate. Due to the low NCO-content of crude isocyanates, HMDI was distilled freshly before each polymer synthesis.

## Isocyanate-content of prepolymer

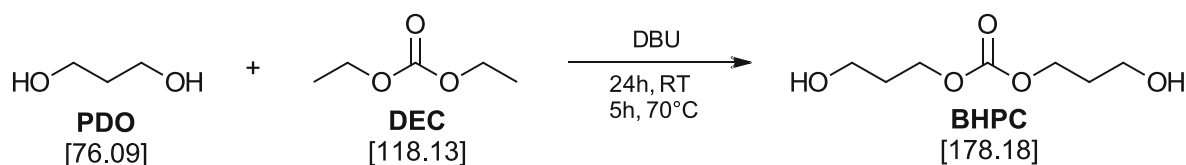
Before the reaction, pTHF was dried under vacuum (< 0.1 mbar) at 90 °C for 24 h. A water content below 50 ppm was confirmed by Karl-Fischer titration. Hexamethylenediamine (HMDI) was distilled freshly for the reaction. pTHF (5.0 g, 5 mmol, 1 eq.,  $M_w=1000$  g/mol) was weighed into a three-necked round bottom flask and was again dried for another 3 h. HMDI (1.68 g, 10 mmol, 2 eq.) was diluted in dry DMF (5 mL) and added to pTHF at 60 °C under argon. The syringe and transfer vessel are rinsed with dry DMF (5 mL). Stannous octoate ( $\text{Sn}(\text{Oct})_2$ , 0.05 mL, cat.) was added and the reaction mixture was stirred at 60 °C (Scheme 26).

After 1, 2, 3, 4, 5, 6, 7, 21 and 22 h samples of about 0.5 g were taken for isocyanate-content determination titration according to DIN EN ISO 11909, which is described before with some adjustments. For prepolymer titration 0.5 M dibutyl amine solution was used instead of 2 M.



Scheme 26: Synthesis of prepolymer for isocyanate content determination.

## 1.2. Synthesis of the CE bis(hydroxypropyl)carbonate (BHPC)



Scheme 27: Synthesis of bis(hydroxypropyl)carbonate (BHPC) via diethyl carbonate.

Table 23: Used reactants in synthesis of BHPC via diethyl carbonate.

Reactant	Equivalents	M / g mol <sup>-1</sup>	n / mmol	m / g	V / mL
PDO	3	76.09	195.6	14.88	14.2
DBU	0.1	152.24	6.7	1.02	1.0
DEC	1	118.13	65.2	7.70	7.9

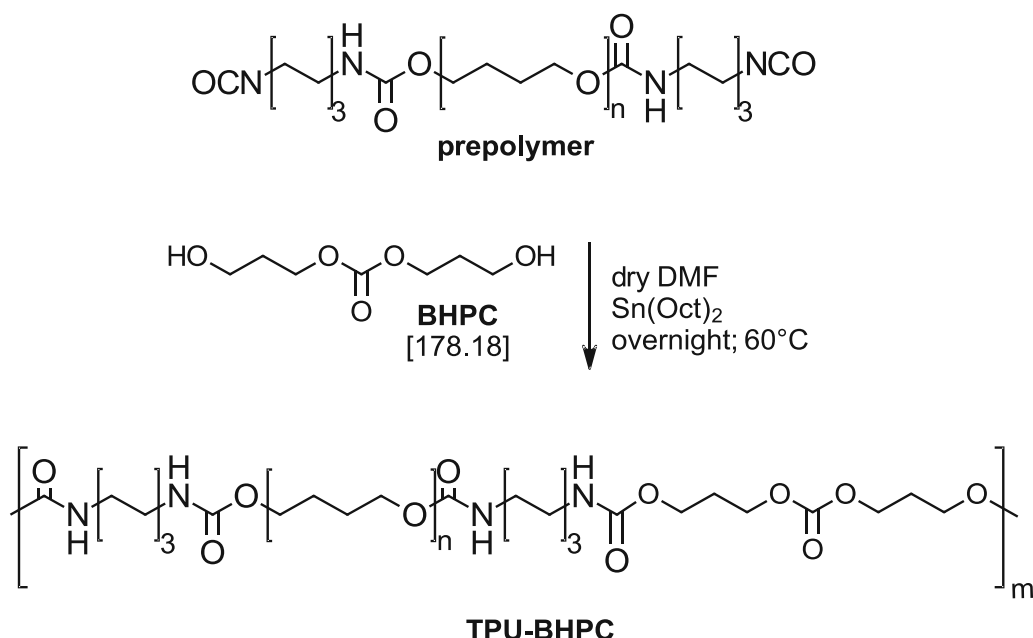
The synthesis was performed according to literature with some adjustments.<sup>152, 318</sup> The reaction scheme is shown in Scheme 27 and the used chemicals are listed in Table 23. 1,3-Propanediol and diethyl carbonate were distilled freshly before the synthesis. 1,3-Propanediol (PDO, 14.88 g, 14.17 mL, 195.55 mmol, 3 eq.) and 1,8-diazabicyclo[5.4.0]undec-7-en (DBU, 1 mL, 1.02 g, 0.1 eq.) has been filled in a three-necked round bottom flask under argon. Then diethyl carbonate (DEC, 7.70 g, 7.9 mL, 65.18 mmol, 1 eq.) was added dropwise very slowly. The reaction was stirred for 24 h at room temperature. Afterwards the temperature was increased until 70 °C for 5 h and ethanol was removed via distillation continuously under slightly reduced pressure (~400 mbar). Purification was done via column chromatography with ethyl acetate. The final product was detected via thin-layer chromatography, resulting in a clear liquid.

Yield: 3.36 g (18.84 mmol; 28.9 %)

TLC: R<sub>f</sub> = 0.45 (ethyl acetate)

<sup>1</sup>H-NMR (200 MHz, CDCl<sub>3</sub>, δ): 1.88 (4H, q, CH<sub>2</sub>); 2.61 (2H, br, OH); 3.68 (4H, t, CH<sub>2</sub>-OH); 4.25 (4H, t, CH<sub>2</sub>-O) ppm

### 1.3. Synthesis of TPU-BHPC



Scheme 28: Synthesis of TPU-BHPC via two-step polymerization.

Table 24: Used reactants in synthesis of TPU-BHPC.

Reactant	Equivalents	M / g mol <sup>-1</sup>	n / mmol	m / g	V / mL
pTHF	1	1,000.00	5.0	5.000	-
HMDI	2	168.20	10.0	1.682	-
BHPC	1	254.24	5.0	0.891	-
Sn(Oct) <sub>2</sub>	0.1	405.12	0.2	0.063	0.05
dry DMF	solvent	-	-	-	20.00

The synthesis of TPU-BHPC until prepolymer formation was performed as described before in 1.1. General polymer procedure / Synthesis of TPU-BHET. The reaction scheme starting from the prepolymer is shown in Scheme 28.

After prepolymer formation bis(hydroxypropyl)carbonate (BHPC, 0.89 g, 5 mmol, 1 eq.) was dissolved in dry DMF (5 mL) and was added to the reaction mixture at 60 °C under argon atmosphere. The syringe and transfer vessel were rinsed with additional dry DMF (5 mL) in portions. Afterwards, the mixture was stirred overnight at the same reaction conditions. For purification, the polymer was precipitated in petroleum ether (800 mL) and dried under vacuum at 50 °C, resulting in a white-transparent solid.



Yield: 6.9 g (91.9 %)

GPC:  $\overline{M}_w = 28.6$  kDa,  $\overline{M}_n = 17.3$ , kDa, PDI = 1.7

$^1\text{H-NMR}$  (200 MHz, DMSO-*d*<sub>6</sub>,  $\delta$ ): 1.22 (8H, CH<sub>2</sub>); 1.35 (8H, CH<sub>2</sub>); 1.50 (38H, CH<sub>2</sub>); 1.73-1.87 (4H, CH<sub>2</sub>); 2.92-2.95 (8H, CH<sub>2</sub>-NH); 3.32 (38H, CH<sub>2</sub>-O); 3.94 (4H, CH<sub>2</sub>-O); 4.12 (4H, CH<sub>2</sub>-O); 7.09 (4H, NH) ppm

FTIR (solid): 3317 cm<sup>-1</sup> (N-H, urethane); 2939 cm<sup>-1</sup> (C-H); 2860 cm<sup>-1</sup> (C-H); 1719 cm<sup>-1</sup> (C=O, ester); 1683 cm<sup>-1</sup> (C=O...H-N, urethane); 1536 cm<sup>-1</sup> (N-H, urethane + C-N, urethane); 1250 cm<sup>-1</sup> (C-O, ether); 1104 cm<sup>-1</sup> (C-C)

## 1.4. General characterization of reference materials

### Hard-block content of polymers

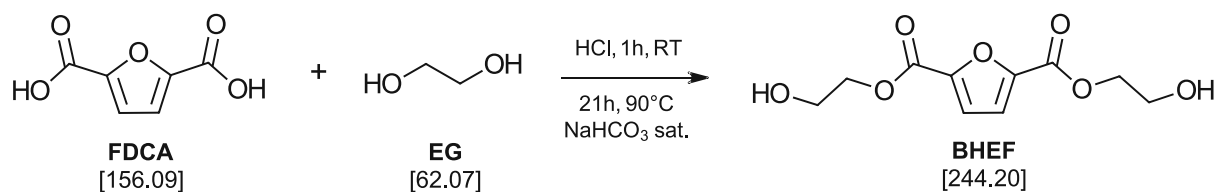
The theoretical hard-block content, is given as wt% of hexamethylene diisocyanates (HMDI) and the chain extender (CE) compared to the total weight of the polymer (Eqn.7) for a given ratio of 1:2:1 (MD:DI:CE). The calculated hard-block content can be determined from the  $^1\text{H-NMR}$  spectra of the final polymers (Appendix, 1. NMR spectra), by further comparing the integrals of CH<sub>2</sub> (polytetrahydrofuran) and the integral of representative protons of the chain extender molecule.

$$\frac{M(CE) + 2 * M(DI)}{M(CE) + 2 * M(DI) + M(MD) * f(NMR)} = \%HB_{th/cal} \quad \text{Eqn.7}$$

M	molar mass of CE, DI and MD, g mol <sup>-1</sup>
CE	chain extender
DI	diisocyanate (HMDI)
MD	macrodiol (pTHF)
f(NMR)	$^1\text{H-NMR}$ factor (ratio between pTHF and CE, <u>for %HB<sub>th</sub>=1</u> )
%HB	Hard-block content, in wt%

## 2. Further carboxylic ester-based CE

### 2.1. Synthesis of BHEF



Scheme 29: Synthesis of bis(2-hydroxyethyl)furan-2-5-dicarboxylate (BHEF).

Table 25: Used reactants in synthesis of BHEF.

Reactant	Equivalents	M / g mol <sup>-1</sup>	n / mmol	m / g	V / mL
FDCA	1	156.09	6.4	1.00	-
EG	20	62.07	128.1	7.95	7.1
HCl	2.5	36.46	16.3	0.60	0.5
NaHCO <sub>3</sub> sat.	-	-	-	-	5.0

The synthesis was performed according to literature with some adjustments.<sup>227, 228</sup> The synthesis scheme is shown in Scheme 29 and the used chemicals are listed in Table 25. Furan-2,5-dicarboxylic acid (FDCA, 1.00 g, 6.4 mmol, 1 eq.) and ethylene glycol (EG, 7.95 g, 128.13 mmol, 7.1 mL, 20 eq.) were placed in a round-bottom flask equipped with a condenser. At room temperature concentrated hydrochloric acid (HCl, 0.6 g, 16.3 mmol, 0.5 mL, 2.5 eq.) was added slowly. Then the reaction solution was stirred for 15 min at room temperature. Then the reaction temperature was slowly increased until 90 °C within an hour and was stirred for 21 h. After cooling to room temperature, a saturated sodium bicarbonate solution (NaHCO<sub>3</sub>, 5 mL) was added dropwise until the reaction solution was neutralized. Afterwards the excess of EG was removed under vacuum at 50 °C (< 0.1 mbar). Then the raw product was dissolved in acetone and was filtered to remove impurities (e.g. NaHCO<sub>3</sub>). The raw product was again dried under vacuum resulting in a slightly yellow powder. The final purification was done via column chromatography with acetone. The final product was detected via thin-layer chromatography, resulting in a white powder.

Yield: 0.87 g (3.56 mmol; 55.6 %)

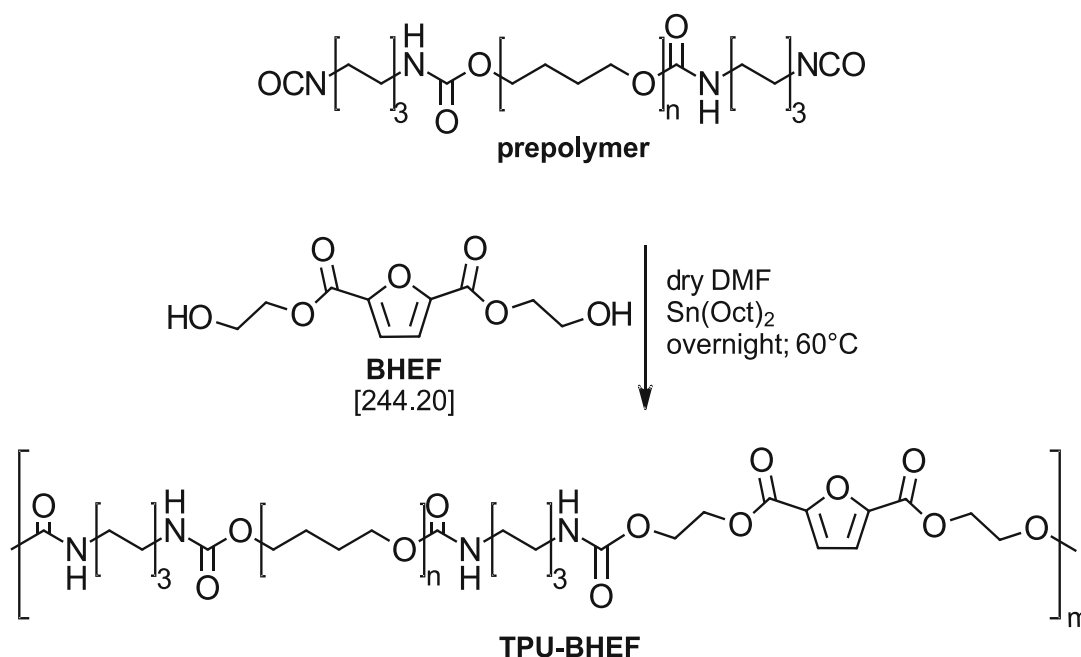
Mp: 86.1 – 87.4 °C [Lit: 91 °C]<sup>227</sup>

TLC: R<sub>f</sub> = 0.85 (acetone)

<sup>1</sup>H-NMR (400 MHz, DMSO-*d*<sub>6</sub>, δ): 3.68 (4H, q, CH<sub>2</sub>); 4.31 (4H, t, CH<sub>2</sub>-O); 4.94 (2H, t, OH); 7.44 (2H, s, CH<sup>Ar</sup>) ppm

<sup>13</sup>C-NMR (APT, 101 MHz, DMSO-*d*<sub>6</sub>, δ): 58.85 (CH<sub>2</sub>); 66.98 (CH<sub>2</sub>-OH); 119.17 (CH<sup>Ar</sup>); 146.22 (C<sup>q</sup>); 157.55 (C=O) ppm

## 2.2. Synthesis of TPU-BHEF



Scheme 30: Synthesis of TPTU-BHEF via two-step polymerization.

Table 26: Used reactants in synthesis of TPU-BHEF.

Reactant	Equivalents	M / g mol <sup>-1</sup>	n / mmol	m / g	V / mL
pTHF	1	1,000.00	1.8	1.813	-
HMDI	2	168.20	3.6	0.610	-
BHEF	1	244.20	1.8	0.443	-
$\text{Sn}(\text{Oct})_2$	0.1	405.12	0.06	0.025	0.02
dry DMF	solvent	-	-	-	8.00

The synthesis of TPU-BHEF until prepolymer formation was performed as described before in 1.1. General polymer procedure / Synthesis of TPU-BHET. The reaction scheme starting from the prepolymer is shown in Scheme 30 and the used reactants are listed in Table 26.

After prepolymer formation bis(2-hydroxyethyl)furan-2,5-dicarboxylate (BHEF, 0.443 g, 1.8 mmol, 1 eq.) was dissolved in dry DMF (2 mL) and was added to the reaction mixture at 60 °C under argon atmosphere. The syringe and transfer vessel were rinsed with additional dry DMF (2 mL) in portions. Afterwards, the mixture was stirred overnight at the same reaction conditions. For purification, the polymer was precipitated in diethyl ether (500 mL) and dried under vacuum at 50 °C, resulting in a white solid.

Yield: 2.1 g (74.7 %)

GPC:  $\overline{M}_w$  = 30.1 kDa,  $\overline{M}_n$  = 17.8, kDa, PDI = 1.7

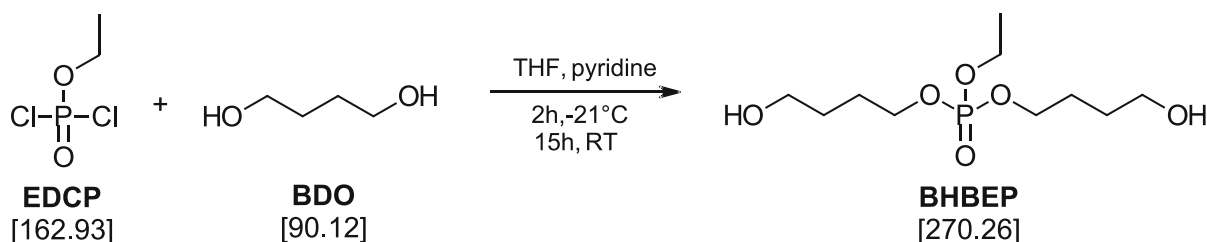
$^1\text{H-NMR}$  (400 MHz,  $\text{DMSO-}d_6$ ,  $\delta$ ): 1.20 (8H,  $\text{CH}_2$ ); 1.34 (8H,  $\text{CH}_2$ ); 1.50 (55H,  $\text{CH}_2$ ); 2.93 (8H,  $\text{CH}_2\text{-NH}$ ); 3.32 (65H,  $\text{CH}_2\text{-O} + x\text{H}_2\text{O}$ ); 4.25-4.30 (4H,  $\text{CH}_2\text{-O}$ ); 4.45 (4H,  $\text{CH}_2\text{-O}$ ); 7.00-7.24 (4H, NH); 7.40-7.44 (4H, CH) ppm

FTIR (solid):  $3314\text{ cm}^{-1}$  (N-H, urethane);  $2935\text{ cm}^{-1}$  (C-H);  $2855\text{ cm}^{-1}$  (C-H);  $1721\text{ cm}^{-1}$  (C=O, ester);  $1682\text{ cm}^{-1}$  (C=O $\cdots$ H-N, urethane);  $1537\text{ cm}^{-1}$  (N-H, urethane + C-N, urethane);  $1455\text{ cm}^{-1}$  (C=C);  $1262\text{ cm}^{-1}$  (C-O, ether);  $1104\text{ cm}^{-1}$  (C-C)

### 3. Inorganic ester-based CEs

#### 3.1. Synthesis and purification of CEs

##### 3.1.1. Phosphate ester-based CE



Scheme 31: Synthesis of bis(4-hydroxybutyl) ethyl phosphate (BHBEP).

Table 27: Used reactants in synthesis of BHBEP.

Reactant	Equivalents	M / g mol <sup>-1</sup>	n / mmol	m / g	V / mL
EDCP	1	162.93	24.0	3.91	2.9
BDO	2.5	90.12	60.0	5.41	5.3
dry pyridine	2.5	79.10	60.0	4.75	4.8
dry THF	solvent	-	-	-	40

The synthesis was adjusted according to literature (Scheme 31, Table 27).<sup>302</sup> All used chemicals were distilled freshly and dried with molecular sieve (3Å). The whole reaction was carried out under argon atmosphere. Dry THF (20 mL) was filled in a flame-dried three-necked round bottom flask, equipped with two dropping funnels and an argon-valve. One dropping funnel was charged with 1,4-butanediol (BDO, 5.41 g, 60.0 mmol, 2.5 eq.), dry pyridine (4.75 g, 60.0 mmol, 2.5 eq.) and dry THF (20 mL). The other dropping funnel was charged with ethyl dichlorophosphate (EDCP, 3.91 g, 24.0 mmol, 1 eq.) and dry THF (20 mL). The reaction flask was cooled to -21 °C. Both mixtures were added with approximately the same speed over a period of about 30 min. After complete addition the mixture was stirred for about 2 h at -21 °C and then overnight at room temperature. To remove pyridinium hydrochloride the reaction solution was stored at -35 °C for about 2 h and was filtrated to remove precipitate. Finally, all solvents were removed under vacuum, resulting in a slightly yellow liquid.

Yield: 6.02 g (22.3 mmol; 92.9 %)

HPLC: 97.1 % (H<sub>2</sub>O:MeCN=70:30)

<sup>1</sup>H-NMR (400 MHz, CDCl<sub>3</sub>, δ): 1.26 (3H, t, CH<sub>3</sub>); 1.55 (4H, m, CH<sub>2</sub>), 1.69-1.83 (4H, m, CH<sub>2</sub>), 3.54 (4H, br, CH<sub>2</sub>-OH); 4.08 (6H, m, CH<sub>2</sub>-O), 4.42 (2H, br, OH) ppm

<sup>13</sup>C-NMR (101 MHz, CDCl<sub>3</sub>, δ): 16.05 (CH<sub>3</sub>); 29.23 (CH<sub>2</sub>); 29.81 (CH<sub>2</sub>); 62.25 (CH<sub>2</sub>-OH); 64.13 (CH<sub>2</sub>-O), 67.43 (a, CH<sub>2</sub>-O) ppm

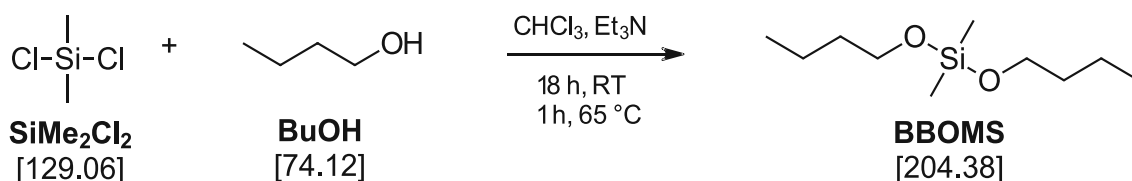
<sup>31</sup>P-NMR (600 MHz, CDCl<sub>3</sub>, δ): 3.15 (product) ppm

### Hydroxy number of BHBEP via $^{31}\text{P}$ -NMR

The determination of the hydroxy-group content was performed according to literature.<sup>262, 303</sup> As internal standard a solution of cyclohexanol (CycOH, 40.58 mg, 40.52 mmol) and chromium(III) acetylacetonate ( $\text{Cr}(\text{acac})_3$ , 5.00 mg, 1.43 mmol) in dry pyridine was prepared. Then a specific amount of sample (max. 200 mmol OH-group equivalents) was dissolved in dry pyridine (100  $\mu\text{L}$ ),  $\text{CDCl}_3$  (100  $\mu\text{L}$ ) and internal standard solution (100  $\mu\text{L}$ ). Separately, 2-chloro-4,4,5,5-tetramethyl-1,3,2-dioxaphospholane (TMDP, 100  $\mu\text{L}$ , 114.9 mg, 630 mmol) was dissolved in  $\text{CDCl}_3$  (400  $\mu\text{L}$ ). Finally, both solutions were mixed together for a few minutes and  $^{31}\text{P}$ -NMR spectrum was measured.

### 3.1.2. Silicic acid ester-based CE

#### Synthesis of model compound bis(butyloxy)dimethylsilane (BBOMS)



Scheme 32: Synthesis of model compound bis(butyloxy)dimethylsilane (BBOMS).

Table 28: Used reactants in synthesis of BBOMS.

Reactant	Equivalents	M / g mol <sup>-1</sup>	n / mmol	m / g	V / mL
BuOH	2.1	74.12	24.41	1.81	2.2
SiMe <sub>2</sub> Cl <sub>2</sub>	1	129.06	11.62	1.50	1.4
CHCl <sub>3</sub>	solvent	-	-	-	15.0
Et <sub>3</sub> N	2.2	101.19	25.57	2.59	3.6

The synthesis was adjusted according to literature (Scheme 32, Table 28).<sup>306</sup> 1-Butanol (BuOH) and triethylamine (Et<sub>3</sub>N) were distilled before the reaction, Et<sub>3</sub>N was additionally dried with 4 Å molecular sieve. 1-Butanol (BuOH, 1.81 g, 2.2 mL, 24.41 mmol, 2.1 eq.), Et<sub>3</sub>N (2.59 g, 3.6 mL, 25.57 mmol, 2.2 eq.) and dry CHCl<sub>3</sub> (15 mL) were filled in a three-necked round bottom flask under argon atmosphere. The mixture was cooled down until 0°C. Then dimethyldichlorosilane (SiMe<sub>2</sub>Cl<sub>2</sub>, 1.5 g, 1.4 mL, 11.62 mmol, 1 eq.) was added dropwise and very slowly to the mixture. The reaction mixture was cooled for another 30 min and was then stirred overnight at room temperature. At the next day reaction mixture was heated up until 65°C for 1 h and was stirred afterwards at room temperature overnight. For purification the solution was filtered to remove Et<sub>3</sub>NHCl salt and the product was extracted (4 x 15 mL CHCl<sub>3</sub>; 100 mL H<sub>2</sub>O). Finally, the product was dried under vacuum (> 0.1 mbar), resulting in a clear liquid.

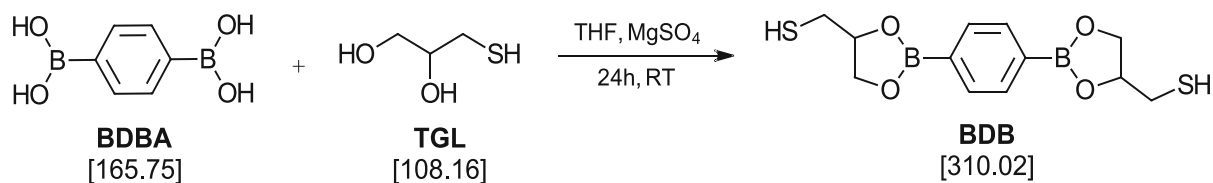
Yield: 2.0 g (9.79 mmol; 84.2 %)

<sup>1</sup>H-NMR (200 MHz, CDCl<sub>3</sub>, δ): 0.07 (6H, s, CH<sub>3</sub>-Si); 0.88 (6H, t, CH<sub>3</sub>), 1.34 (4H, m, CH<sub>2</sub>), 1.50 (4H, m, CH<sub>2</sub>); 3.63 (4H, t, CH<sub>2</sub>-O) ppm

#### Purification of bis(4-aminophenoxy) dimethylsilane (BAPDMS)

Before the polymer synthesis, the chain extender bis(4-aminophenoxy) dimethylsilane (BAPDMS) was recrystallized from diethyl ether.<sup>313</sup>

### 3.1.3. Boronic acid ester-based CE



Scheme 33: Synthesis of 2,2'-(1,4-phenylene)-bis[4-mercaptan-1,3,2-dioxaborolane] (BDB).

Table 29: Used reactants in synthesis of BDB.

Reactant	Equivalents	M / g mol <sup>-1</sup>	n / mmol	m / g	V / mL
BDBA	1	165.75	36.2	6.00	-
TGL	2.05	108.16	74.2	8.03	-
MgSO <sub>4</sub>	2.3	120.37	83.1	10.00	-
water	0.30	18.00	10.86	0.20	0.20
THF	solvent	-	-	-	160.00

The synthesis was performed according to literature with some adjustments.<sup>222, 312</sup> The synthesis scheme is shown in Scheme 33 and the used chemicals are listed in Table 29. 1-Thioglycerol was distilled freshly directly before synthesis. Benzene-1,4-diboronic acid (BDBA, 6.00 g, 36.2 mmol, 1 eq.) and 1-thioglycerol (TGL, 8.03 g, 74.2 mmol, 2.05 eq.) were dissolved in THF (160 mL) and deionized water (0.2 mL, 10.86 mmol, 0.3 eq.). After complete dissolution of all components, magnesium sulfate (10.00 g, 83.1 mmol, 2.3 eq.) is added slowly over a period of about 1 h. The reaction mixture is then stirred for 24 h at room temperature. Afterwards, the solution was filtrated to remove magnesium sulfate and dried under vacuum resulting in a slightly yellow powder. For further purification the powder was dissolved in toluene (200 mL). Precipitated 1-thioglycerol was removed and the dissolved product was recrystallized from toluene at 70 °C.

Yield: 9.27 g (29.9 mmol; 82.6 %);

Mp: 109.3 – 111.2 °C [Lit: unknown]

GC-MS (DCM): 97.7%

<sup>1</sup>H-NMR (400 MHz, DMSO-*d*<sub>6</sub>, δ): 2.39 (2H, t, SH); 2.80 (4H, dd, CH<sub>2</sub>); 4.12 (2H, dd, CH<sub>2</sub>-O); 4.42 (2H, dd, CH<sub>2</sub>-O), 4.75 (2H, m, CH-O); 7.74 (4H, s, CH<sup>Ar</sup>) ppm

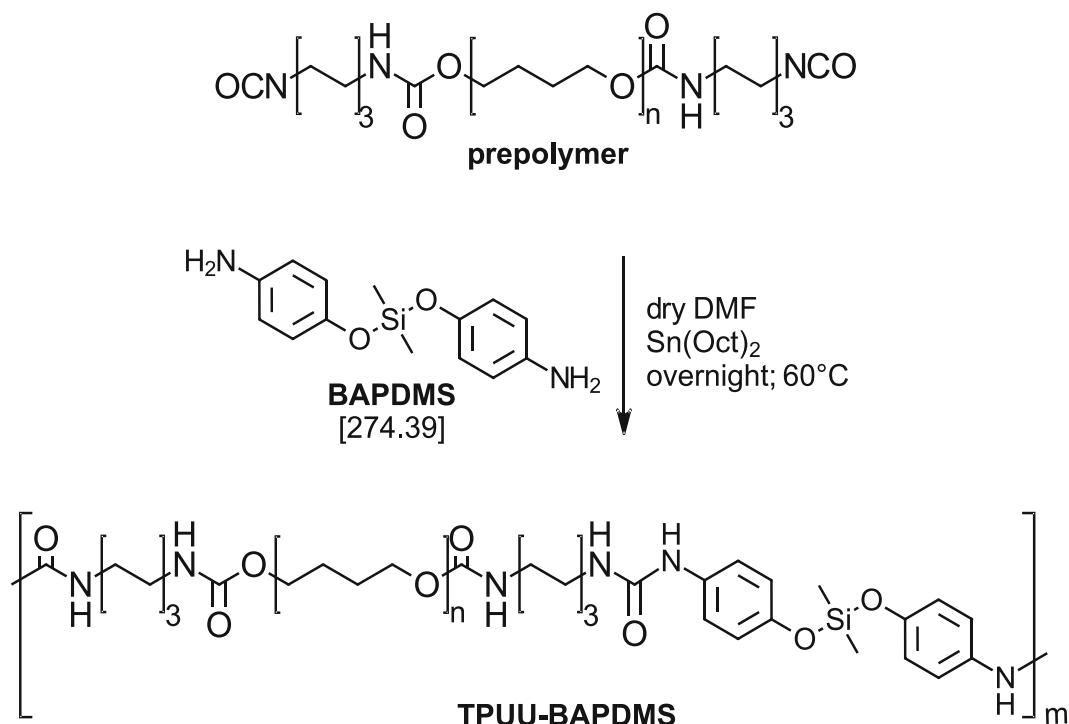
<sup>13</sup>C-NMR (APT, 101 MHz, DMSO-*d*<sub>6</sub>, δ): 28.71 (-CH<sub>2</sub>-SH); 69.25 (CH<sub>2</sub>-O); 77.12 (CH-O); 133.84 (CH<sup>Ar</sup> / C<sup>Ar</sup>)



## 3.2. TPUs, TPUUs and TPTUs with one CE

### 3.2.1. Synthesis of TPUs, TPUUs and TPTUs with one CE

#### Synthesis of TPUU-BAPDMS



Scheme 34: Synthesis of TPUU-BAPDMS via two-step polymerization.

Table 30: Used reactants in synthesis of TPUU-BAPDMS.

Reactant	Equivalents	M / g mol <sup>-1</sup>	n / mmol	m / g	V / mL
pTHF	1	1,000.00	5.0	5.000	-
HMDI	2	168.20	10.0	1.682	-
BAPDMS	1	274.39	5.0	1.372	-
Sn(Oct) <sub>2</sub>	0.1	405.12	0.2	0.063	0.05
dry DMF	solvent	-	-	-	40.00

Before the polymer synthesis, the chain extender bis(4-aminophenoxy) dimethylsilane (BAPDMS) was recrystallized from diethyl ether.<sup>313</sup> <sup>1</sup>H-NMR and <sup>13</sup>C-APT-NMR spectra after recrystallization are shown in the appendix section (1. NMR). The synthesis of TPUU-BAPDMS until prepolymer formation was performed as described before in 1.1. General polymer procedure / Synthesis of TPU-BHET. The reaction scheme starting from the prepolymer is shown in Scheme 34 and the reactants are listed in Table 30.

After prepolymer formation bis(4-aminophenoxy) dimethylsilane (BAPDMS, 1.37 g, 5 mmol, 1 eq.) was dissolved in dry DMF (25 mL) and was added to the reaction mixture at 50 °C under argon atmosphere. The syringe and transfer vessel were rinsed with additional dry DMF (5 mL) in portions. Afterwards, the mixture was stirred overnight at the same reaction conditions. For purification, the polymer was precipitated in diethyl ether (800 mL) and dried under vacuum at 40 °C, resulting in a brown solid.

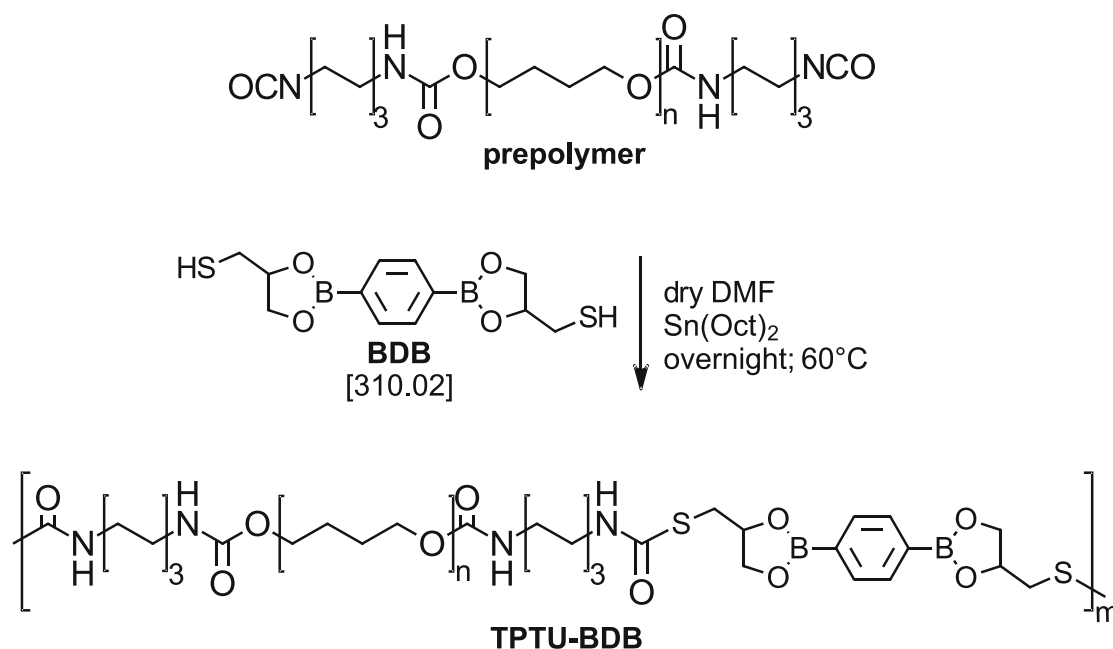
Yield: 6.7 g (83.7 %)

GPC:  $\overline{M}_w$  = 19.4 kDa,  $\overline{M}_n$  = 10.5, kDa, PDI = 1.8

$^1\text{H-NMR}$  (400 MHz, DMSO-*d*6,  $\delta$ ): -0.07-0.06 (6H, CH<sub>3</sub>-Si); 1.25 (8H, CH<sub>2</sub>); 1.35 (8H, CH<sub>2</sub>); 1.50 (78H, CH<sub>2</sub>); 2.95-3.04 (8H, CH<sub>2</sub>-NH); 3.33 (71H, CH<sub>2</sub>-O + xH<sub>2</sub>O); 5.92 (2H, NH); 6.59-6.63 (4H, CH<sup>Ar</sup>); 7.00 (2H, NH); 7.10-7.15 (4H, CH<sup>Ar</sup>)

FTIR (solid): 3330 cm<sup>-1</sup> (N-H, urethane); 2935 cm<sup>-1</sup> (C-H); 2854 cm<sup>-1</sup> (C-H); 1717 cm<sup>-1</sup> (C=O, ester); 1669 cm<sup>-1</sup> (C=O...H-N, urethane); 1545 cm<sup>-1</sup> (N-H, urethane + C-N, urethane); 1366 cm<sup>-1</sup> (C-N); 1234 cm<sup>-1</sup> (C-O, ether); 1104 cm<sup>-1</sup> (C-C); 934 cm<sup>-1</sup> (Si-O); 832 cm<sup>-1</sup> (=C-H<sup>Ar</sup>); 848 cm<sup>-1</sup> (=C-H<sup>Ar</sup>); 804 cm<sup>-1</sup> (=C-H<sup>Ar</sup>)

### Synthesis of TPTU-BDB



Scheme 35: Synthesis of TPTU-BDB via two-step polymerization.

Table 31: Used reactants in synthesis of TPTU-BDB.

Reactant	Equivalents	M / g mol <sup>-1</sup>	n / mmol	m / g	V / mL
pTHF	1	1,000.00	5.0	5.000	-
HMDI	2	168.20	10.0	1.682	-
BDB	1	310.02	5.0	1.550	-
Sn(Oct) <sub>2</sub>	0.1	405.12	0.2	0.063	0.05
dry DMF	solvent	-	-	-	20.00

The synthesis of TPTU-BDB until prepolymer formation was performed as described before in 1.1. General polymer procedure / Synthesis of TPU-BHET. The reaction scheme starting from the prepolymer is shown in Scheme 35 and the used chemicals are listed in Table 31.

After prepolymer formation 2,2'-(1,4-phenylene)bis[4-thioethyl-1,3,2-dioxaborolane] (BDB, 1.55 g, 5 mmol, 1 eq.) was dissolved in dry DMF (5 mL) and was added to the reaction mixture at 60 °C under argon atmosphere. The syringe and transfer vessel were rinsed with additional dry DMF (5 mL) in portions. Afterwards, the mixture was stirred overnight at the same reaction conditions. For purification, the polymer was precipitated in diethyl ether (800 mL) and dried under vacuum at 40 °C, resulting in a white solid.

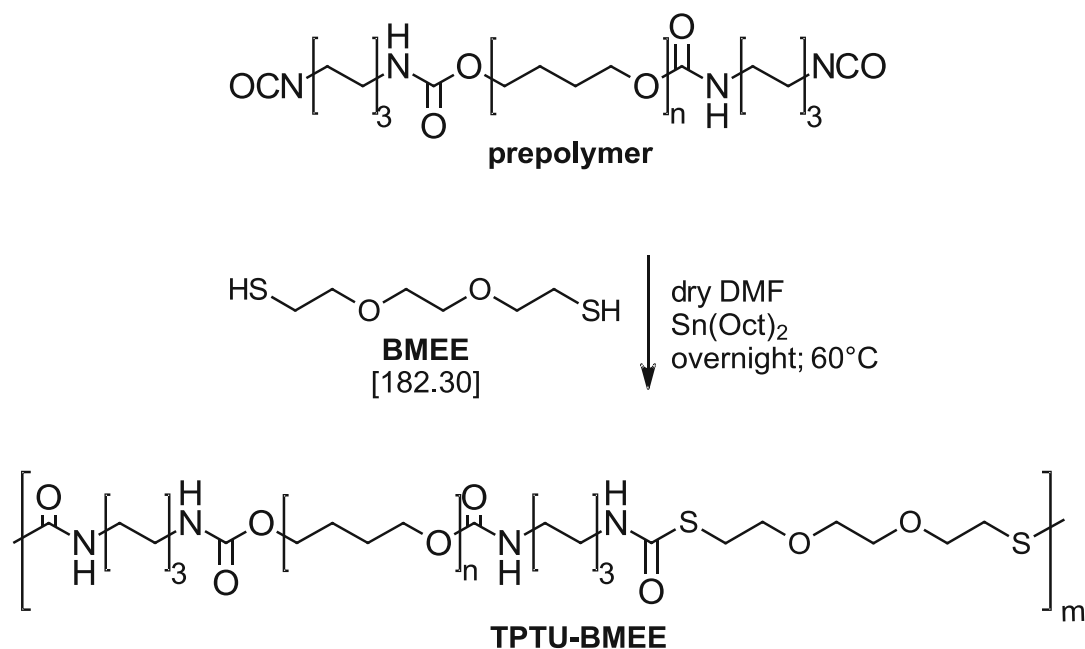
Yield: 7.2 g (87.6 %)

GPC:  $\overline{M}_w$  = 11.6 kDa,  $\overline{M}_n$  = 6.4 kDa, PDI = 1.8

<sup>1</sup>H-NMR (400 MHz, DMSO-*d*<sub>6</sub>, δ): 1.21 (8H, CH<sub>2</sub>); 1.36 (8H, CH<sub>2</sub>); 1.50 (33H, CH<sub>2</sub>); 2.94 (8H, CH<sub>2</sub>-NH); 3.07-3.18 (8H, CH<sub>2</sub>); 3.33 (50H, CH<sub>2</sub>-O + xH<sub>2</sub>O); 4.39 (2H, CH); 7.00 (4H, NH); 7.73-7.78 (4H, CH<sup>Ar</sup>) ppm

FTIR (solid): 3311 cm<sup>-1</sup> (N-H, urethane); 2935 cm<sup>-1</sup> (C-H); 2855 cm<sup>-1</sup> (C-H); 1720 cm<sup>-1</sup> (C=O, ester); 1685 cm<sup>-1</sup> (C=O...H-N, urethane); 1518 cm<sup>-1</sup> (N-H, urethane + C-N, urethane); 1314 cm<sup>-1</sup> (B-O); 1211 cm<sup>-1</sup> (C-O, ether); 1103 cm<sup>-1</sup> (C-C); 1025 cm<sup>-1</sup> (B-C); 990 cm<sup>-1</sup> (B-C); 848 cm<sup>-1</sup> (=C-H<sup>Ar</sup>); 792 cm<sup>-1</sup> (C-S); 780 cm<sup>-1</sup> (C-S); 658 cm<sup>-1</sup> (C-S)

## Synthesis of TPTU-BMEE



Scheme 36: Synthesis of TPTU-BMEE via two-step polymerization as thiourethane reference polymer.

Table 32: Used reactants in synthesis of reference TPTU-BMEE.

Reactant	Equivalents	M / g mol <sup>-1</sup>	n / mmol	m / g	V / mL
pTHF	1	1,000.00	5.0	5.000	-
HMDI	2	168.20	10.0	1.682	-
BMEE	1	182.30	5.0	0.912	-
Sn(Oct) <sub>2</sub>	0.1	405.12	0.2	0.063	0.05
dry DMF	solvent	-	-	-	20.00

Before the TPU synthesis, the chain extender 1,2-bis(2-mercaptoethoxy)ethane (BMEE) was distilled under vacuum (5 mbar) at 160 °C. The synthesis of TPTU-BMEE until prepolymer formation was performed as described before in 1.1. General polymer procedure / Synthesis of TPU-BHET. The reaction scheme starting from the prepolymer is shown in Scheme 36 and the reactants are listed in Table 32.

After prepolymer formation 1,2-bis(2-mercaptoethoxy)ethane (BMEE, 0.91 g, 5 mmol, 1 eq.) was dissolved in dry DMF (5 mL) and was added to the reaction mixture at 60 °C under argon atmosphere. The syringe and transfer vessel were rinsed with additional dry DMF (5 mL) in portions. Afterwards, the mixture was stirred overnight at the same reaction conditions. For purification, the polymer was precipitated in diethyl ether (800 mL) and dried under vacuum at 40 °C, resulting in a white solid.

Yield: 6.3 g (82.4 %)

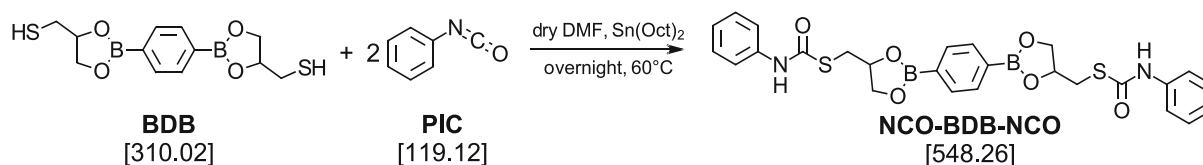
GPC:  $\overline{M}_w$  = 128.5 kDa,  $\overline{M}_n$  = 62.2, kDa, PDI = 2.1

$^1\text{H-NMR}$  (400 MHz,  $\text{DMSO-}d_6$ ,  $\delta$ ): 1.22 (8H,  $\text{CH}_2$ ); 1.38 (8H,  $\text{CH}_2$ ); 1.50 (33H,  $\text{CH}_2$ ); 2.93 (8H,  $\text{CH}_2\text{-NH}$ ); 3.06 (4H,  $\text{CH}_2\text{-SH}$ ); 3.33 (30H,  $\text{CH}_2\text{-O} + x\text{H}_2\text{O}$ ); 3.45-3.49 (8H,  $\text{CH}_2\text{-O}$ ); 7.00 (4H, NH) ppm

FTIR (solid):  $3307\text{ cm}^{-1}$  (N-H, urethane);  $2935\text{ cm}^{-1}$  (C-H);  $2853\text{ cm}^{-1}$  (C-H);  $1720\text{ cm}^{-1}$  (C=O, ester);  $1685\text{ cm}^{-1}$  (C=O...H-N, urethane);  $1641\text{ cm}^{-1}$  (N-H);  $1523\text{ cm}^{-1}$  (N-H, urethane + C-N, urethane);  $1367\text{ cm}^{-1}$  (C-N);  $1251\text{ cm}^{-1}$  (C-O, ether);  $1209\text{ cm}^{-1}$  (C-O-C);  $1104\text{ cm}^{-1}$  (C-C);  $848\text{ cm}^{-1}$  (=C-H<sup>Ar</sup>);  $779\text{ cm}^{-1}$  (C-S);  $734\text{ cm}^{-1}$  (C-S);  $618\text{ cm}^{-1}$  (C-S)

### 3.2.5. Model compounds of boronic acid esters

#### Synthesis of NCO-BDB-NCO



Scheme 37: Synthesis of model compound NCO-BDB-NCO.

Table 33: Used reactants in synthesis of model compound NCO-BDB-NCO.

Reactant	Equivalents	M / g mol <sup>-1</sup>	n / mmol	m / g	V / mL
BDB	1	310.02	4.0	1.24	-
PIC	2.1	119.12	8.4	1.00	-
Sn(Oct) <sub>2</sub>	0.1	405.12	0.2	0.06	0.05
dry DMF	solvent	-	-	-	10

2,2'-(1,4-Phenylene)bis[4-thioethyl-1,3,2-dioxaborolane] (BDB, 1.24 g, 4 mmol, 1 eq.) was dried in a three-necked round-bottom flask (< 0.1 mbar). Then freshly distilled phenyl isocyanate (PIC, 1.0 g, 8.4 mmol, 2.1 eq.) was diluted with dry DMF (10 mL) and was added to BDB under argon atmosphere. The syringe and transfer vessel were rinsed with dry DMF (5 mL). Stannous octoate (Sn(Oct)<sub>2</sub>, 0.05 mL) was added and the reaction mixture was stirred overnight at 60 °C under argon atmosphere. The reaction solution was precipitated in diethyl ether and was filtered, resulting in a white solid. Finally, the product was dried under reduced pressure at 40 °C. The reaction scheme is shown in Scheme 37 and the used chemicals are listed in Table 33.

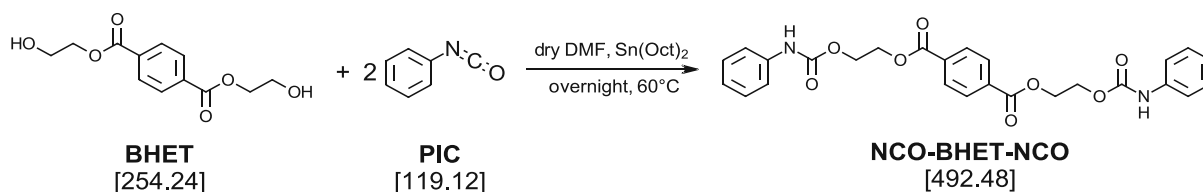
Yield: 1.31 g (2.34 mmol; 58.7 %)

Mp: 210.4 – 214.5 °C [Lit: unknown]

<sup>1</sup>H-NMR (400 MHz, DMSO-d<sub>6</sub>, δ): 3.29 (4H, d, CH<sub>2</sub>), 4.06 (2H, t, CH<sub>2</sub>-O); 4.45 (2H, t, CH<sub>2</sub>-O), 4.86 (2H, m, CH-O); 7.06 (2H, t, CH<sup>Ar</sup>); 7.30 (4H, t, CH<sup>Ar</sup>); 7.48 (4H, d, CH<sup>Ar</sup>); 7.72 (4H, s, CH<sup>Ar</sup>); 10.39 (2H, s, NH) ppm

<sup>13</sup>C-NMR (APT, 101 MHz, DMSO-d<sub>6</sub>, δ): 33.84 (CH<sub>2</sub>-S); 69.46 (CH<sub>2</sub>-O); 75.75(CH-O); 119.03 (CH<sup>Ar</sup>); 123.52 (CH<sup>Ar</sup>); 128.89 (CH<sup>Ar</sup>); 133.44(C<sup>Ar</sup>-B); 133.83 (CH<sup>Ar</sup>); 138.78 (C<sup>Ar</sup>-NH); 163.89 (C=O) ppm

## Synthesis of NCO-BHET-NCO



Scheme 38: Synthesis of model compound NCO-BHET-NCO.

Table 34: Used reactants in synthesis of model compound NCO-BHET-NCO.

Reactant	Equivalents	M / g mol <sup>-1</sup>	n / mmol	m / g	V / mL
BHET	1	254.24	4.7	1.19	-
PIC	2.1	119.12	9.9	1.17	-
Sn(Oct) <sub>2</sub>	0.1	405.12	0.2	0.06	0.05
dry DMF	solvent	-	-	-	10

Bis(2-hydroxyethyl)terephthalate (BHET, 1.19 g, 4.7 mmol, 1 eq.) was dried in a three-necked round-bottom flask (< 0.1 mbar). Then freshly distilled phenyl isocyanate (PIC, 1.17 g, 9.9 mmol, 2.1 eq.) was diluted with dry DMF (10 mL) and was added to BHET under argon atmosphere. The syringe and transfer vessel are rinsed with dry DMF (5 mL). Stannous octoate (Sn(Oct)<sub>2</sub>, 0.05 mL) was added and the reaction mixture was stirred overnight at 60 °C under argon atmosphere. The reaction solution was precipitated first in diethyl ether and was filtered, resulting in a white solid. Finally, the product was dried under reduced pressure at 40 °C. The reaction scheme is shown in Scheme 38 and the used reactants are listed in Table 34.

Yield: 1.45 g (2.95 mmol; 61.4 %)

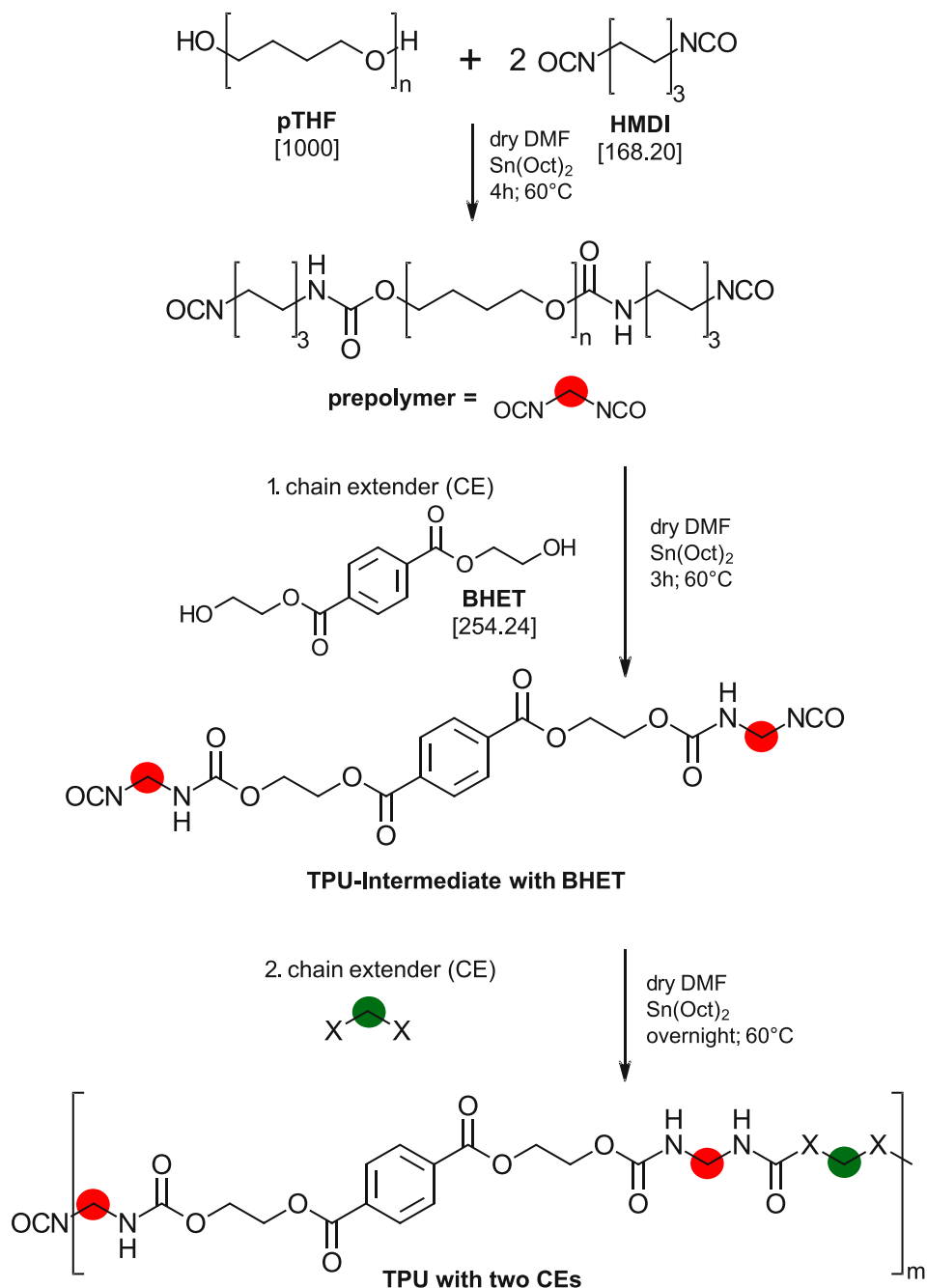
Mp: 183.4 – 191.2 °C [Lit: unknown]

<sup>1</sup>H-NMR (400 MHz, DMSO-d<sub>6</sub>, δ): 4.45 (4H, t, CH<sub>2</sub>-O), 4.55 (4H, t, CH<sub>2</sub>-O), 6.97 (2H, t, CH<sup>Ar</sup>); 7.26 (4H, t, CH<sup>Ar</sup>); 7.44 (4H, d, CH<sup>Ar</sup>); 8.10 (4H, s, CH<sup>Ar</sup>); 9.75 (2H, s, NH) ppm

<sup>13</sup>C-NMR (APT, 101 MHz, DMSO-d<sub>6</sub>, δ): 62.15 (CH<sub>2</sub>-O); 63.77 (CH<sub>2</sub>-O); 118.23 (CH<sup>Ar</sup>); 122.48 (CH<sup>Ar</sup>); 128.72 (CH<sup>Ar</sup>); 129.58 (CH<sup>Ar</sup>); 133.51 (C<sup>Ar</sup>); 138.95 (C<sup>Ar</sup>-NH); 153.29 (C=O); 164.90 (C=O) ppm

### 3.3. TPUs with two different CEs

#### 3.3.1. Synthesis of TPUs with two different CEs



Scheme 39: Three-step synthesis of TPU by using two different chain extenders (CE), X=OH, NH<sub>2</sub> or SH.

Table 35: Used reactants in general synthesis of TPU, TPTU or TPUU with two different chain extenders.

Reactant	Equivalents	M / g mol <sup>-1</sup>	n / mmol	m / g	V / mL
pTHF	1	1,000.00	5.0	5.000	-
HMDI	2	168.20	10.0	1.682	-
BHET (1.CE)	1-x	254.24	5.0 - x	-	-
2.CE	x	-	x	-	-
Sn(Oct) <sub>2</sub>	0.1	405.12	0.2	0.063	0.05
dry DMF	solvent	-	-	-	20.00

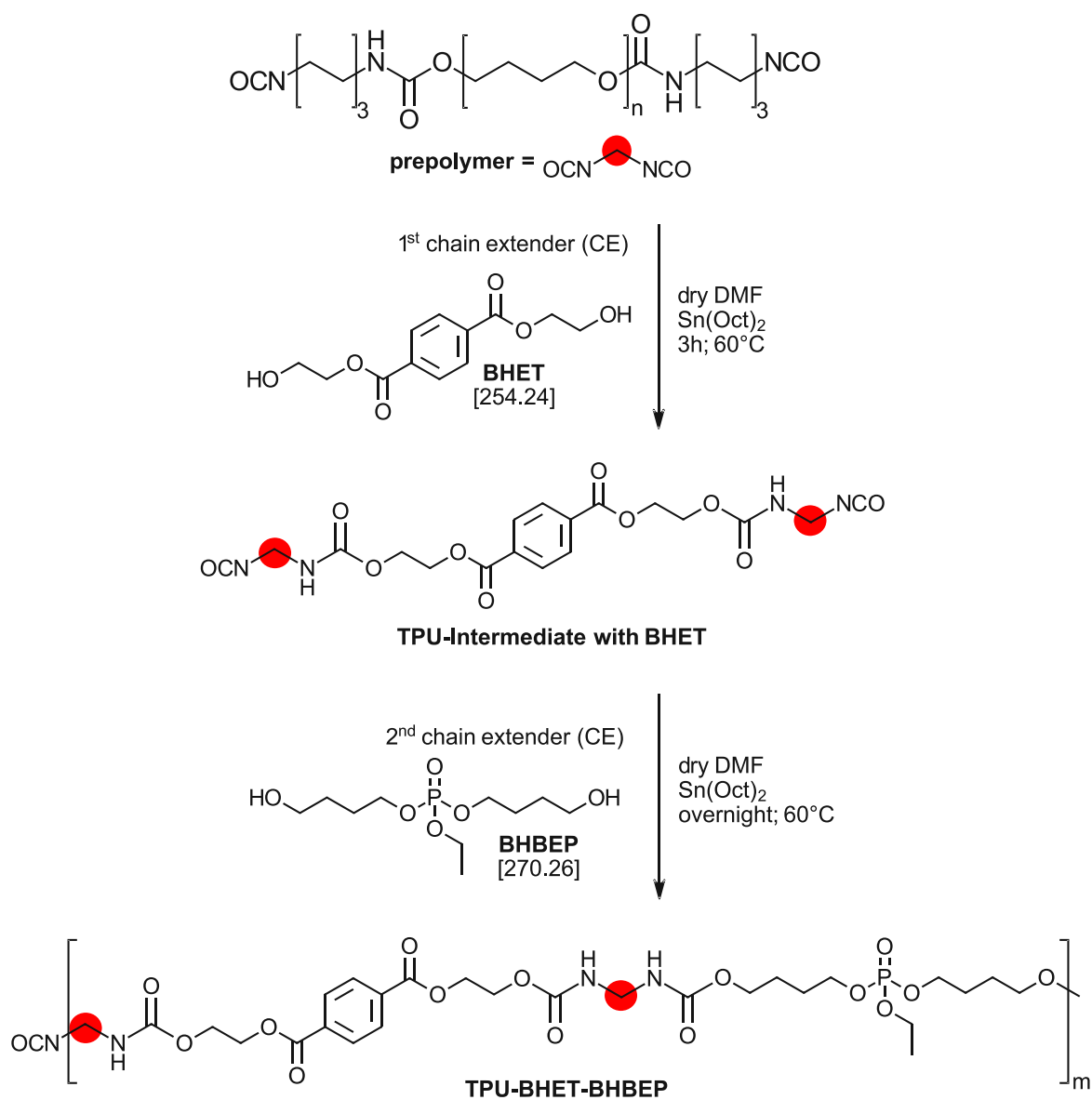


The synthesis of TPUs with two different chain extenders was performed as previously described with some adjustments.<sup>103</sup> The synthesis scheme is shown in Scheme 39 and the used chemicals are listed in Table 35. The reaction was carried out with standard Schlenk-techniques. Before the reaction, polytetrahydrofuran (pTHF) was dried under vacuum (< 0.1 mbar) at 90 °C for 24 h. A water content below 50 ppm was confirmed by Karl-Fischer titration for pTHF and dry DMF as well.

Hexamethylenediisocyanate (HMDI) was freshly distilled for the reaction. Polytetrahydrofuran (pTHF, 5.0 g, 5 mmol, 1 eq.,  $M_n=1000$  g/mol) was weighed into a three-necked round bottom flask and was again dried for another 3 h. Hexamethylenediisocyanate (HMDI, 1.68 g, 10 mmol, 2 eq.) was diluted in dry DMF (5 mL) and added to pTHF at 60 °C under argon. The syringe and transfer vessel were rinsed with dry DMF (5 mL) in portions. Stannous octoate ( $\text{Sn}(\text{Oct})_2$ , 0.05 mL, 0.2 eq.) was added and the reaction mixture was stirred for 4 h at 60 °C, resulting in the prepolymer formation.

Then the first chain extender bis(hydroxyethylene)terephthalate (BHET, 1.CE, 1-x eq.) was dissolved in dry DMF (2.5 mL) and was added to the reaction mixture at 60 °C under argon atmosphere. The syringe and transfer vessel were rinsed with additional dry DMF (5 mL) in portions. Afterwards, the mixture was stirred for 3 h at the same reaction conditions. Then the second chain extender (2.CE, x eq.) was dissolved in dry DMF (2.5 mL) and was added to the TPU-Intermediate mixture under argon atmosphere. The syringe and transfer vessel were rinsed again with additional dry DMF (5 mL) in portions. For purification, the polymer was precipitated in petroleum ether or diethyl ether (800 mL) and dried under vacuum at 50 °C.

## Synthesis of TPU-BHET-BHBEP (75:25)



Scheme 40: Synthesis of TPU-BHET-BHBEP with a chain extender ratio of 75:25 (BHET:BHBEP).

Table 36: Used reactants in synthesis of TPU-BHET-BHBEP.

Reactant	Equivalents	M / g mol <sup>-1</sup>	n / mmol	m / g	V / mL
pTHF	1	1,000.00	5.0	5.000	-
HMDI	2	168.20	10.0	1.682	-
BHET	0.75	254.24	3.75	0.953	-
BHBEP	0.25	270.26	1.25	0.338	-
$\text{Sn}(\text{Oct})_2$	0.1	405.12	0.2	0.063	0.05
dry DMF	solvent	-	-	-	20.00

Before the synthesis of TPU-BHET-BHBEP, the chain extender bis(hydroxyethylene) terephthalate (BHET) was recrystallized from deionized water and bis(4-hydroxybutyl) ethyl phosphate (BHBEP) was dried under vacuum (< 0.1 mbar). The synthesis of TPU-BHET-BHBEP until prepolymer formation was performed as described before in 3.3.1. Synthesis of TPUs with two different CEs. The reaction scheme starting from the prepolymer is shown in Scheme 40 and the reactants are listed in Table 36.

After prepolymer formation the first chain extender bis(hydroxyethylene)terephthalate (BHET, 0.95 g, 3.75 mmol, 0.75 eq.) was dissolved in dry DMF (2.5 mL) and was added to the reaction mixture at 60 °C under argon atmosphere. The syringe and transfer vessel were rinsed with additional dry DMF (5 mL) in portions. Afterwards, the mixture was stirred for 3 h at the same reaction conditions. Then the second chain extender bis(4-hydroxybutyl) ethyl phosphate (BHBEP, 0.34 g, 1.25 mmol, 0.25 eq.) was dissolved in dry DMF (2.5 mL) and was added to the TPU-Intermediate mixture under argon atmosphere. The syringe and transfer vessel were rinsed again with additional dry DMF (5 mL) in portions. For purification, the polymer was precipitated in diethyl ether (1000 mL) and dried under vacuum at 50 °C, resulting in a slightly yellow solid.

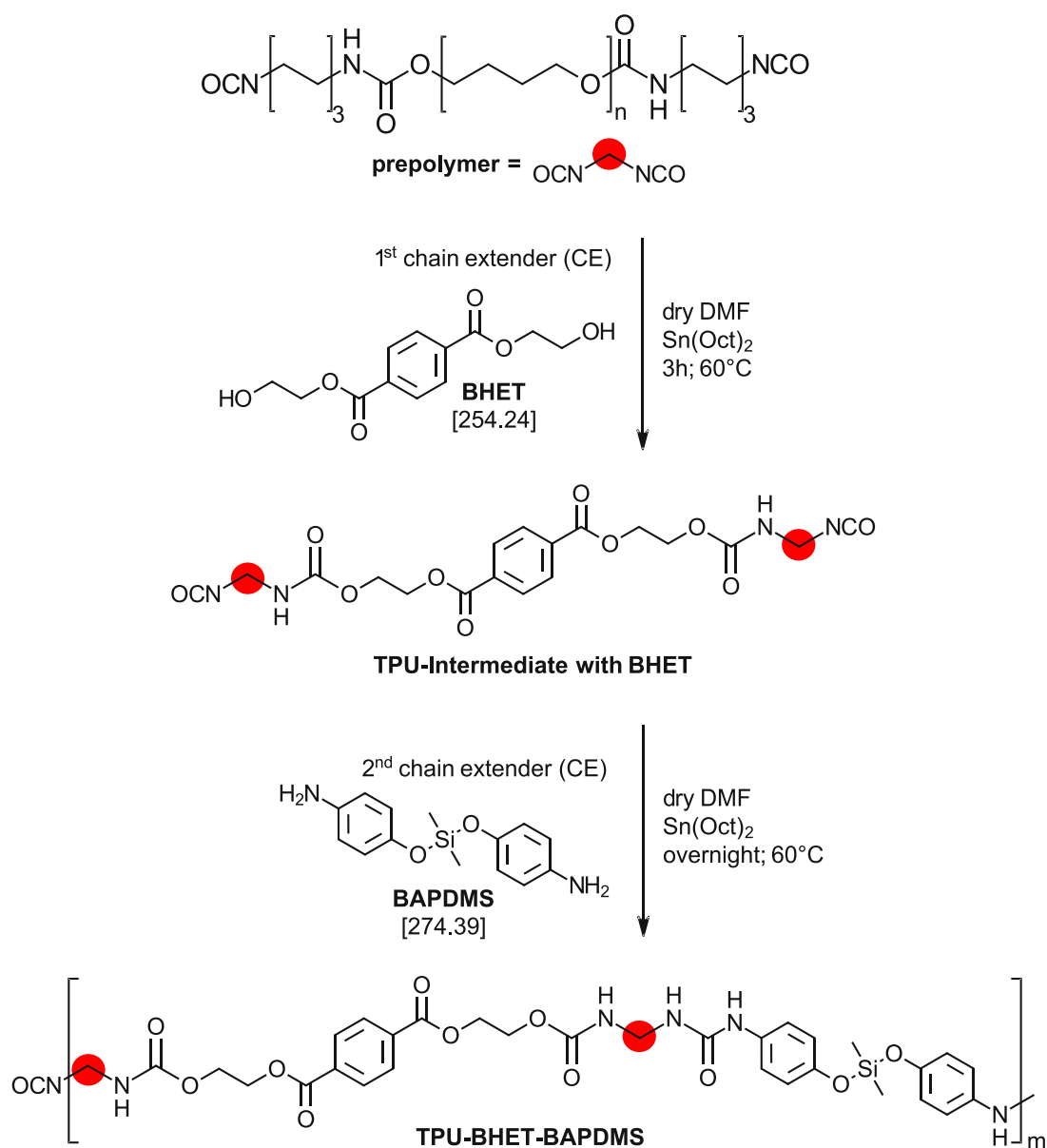
Yield: 6.2 g (78.1 %)

GPC:  $\overline{M}_w$  = 19.2 kDa,  $\overline{M}_n$  = 10.3, kDa, PDI = 1.9

<sup>1</sup>H-NMR (400 MHz, DMSO-*d*<sub>6</sub>, δ): 1.21 (8H, CH<sub>2</sub>); 1.24 (1H, CH<sub>2</sub>); 1.35 (8H, CH<sub>2</sub>); 1.50 (42H, CH<sub>2</sub>); 1.80 (1H, CH<sub>2</sub>); 2.94 (8H, CH<sub>2</sub>-NH); 3.32 (64H, CH<sub>2</sub>-O); 3.68 (1H, CH<sub>2</sub>-O); 4.04 (1.5H, CH<sub>2</sub>-O-P); 4.29 (3H, CH<sub>2</sub>-O); 4.44 (3H, CH<sub>2</sub>-O); 6.99-7.19 (4H, NH); 8.07 (3H, CH<sup>Ar</sup>) ppm

FTIR (solid): 3316 cm<sup>-1</sup> (N-H, urethane); 2935 cm<sup>-1</sup> (C-H); 2855 cm<sup>-1</sup> (C-H); 1720 cm<sup>-1</sup> (C=O, ester); 1693 cm<sup>-1</sup> (C=O...H-N, urethane); 1536 cm<sup>-1</sup> (N-H, urethane + C-N, urethane); 1370 cm<sup>-1</sup> (C-N); 1256 cm<sup>-1</sup> (C-O, ether); 1100 cm<sup>-1</sup> (C-C); 1021 cm<sup>-1</sup> (P-O); 981 cm<sup>-1</sup> (P-O); 874 cm<sup>-1</sup> (=C-H<sup>Ar</sup>); 808 cm<sup>-1</sup> (=C-H<sup>Ar</sup>); 778 cm<sup>-1</sup> (=C-H<sup>Ar</sup>)

## Synthesis of TPU-BHET-BAPDMS (75:25)



Scheme 41: Synthesis of TPU-BHET-BAPDMS with a chain extender ratio of 75:25 (BHET:BAPDMS).

Table 37: Used reactants in synthesis of TPU-BHET-BAPDMS (75:25).

Reactant	Equivalents	M / g mol <sup>-1</sup>	n / mmol	m / g	V / mL
pTHF	1	1,000.00	5.0	5.000	-
HMDI	2	168.20	10.0	1.682	-
BHET	0.75	254.24	3.75	0.953	-
BAPDMS	0.25	274.39	1.25	0.343	-
$\text{Sn}(\text{Oct})_2$	0.1	405.12	0.2	0.063	0.05
dry DMF	solvent	-	-	-	27.50

Before the synthesis of TPU-BHET-BAPDMS (75:25), the chain extender bis(hydroxyethylene) terephthalate (BHET) was recrystallized from deionized water and bis(4-aminophenoxy) dimethylsilane (BAPDMS) was recrystallized from diethyl ether.<sup>313</sup> The synthesis of TPUU-BHET-BAPDMS until prepolymer formation was performed as described before in 3.3.1. Synthesis of TPUs with two different CEs. The reaction scheme starting from the prepolymer is shown in Scheme 41 and the used chemicals are listed in Table 37.

After prepolymer formation the first chain extender bis(hydroxyethylene)terephthalate (BHET, 0.95 g, 3.75 mmol, 0.75 eq.) was dissolved in dry DMF (2.5 mL) and was added to the reaction mixture at 60 °C under argon atmosphere. The syringe and transfer vessel were rinsed with additional dry DMF (5 mL) in portions. Afterwards, the mixture was stirred for 3 h at the same reaction conditions. Then the reaction temperature was reduced to 50 °C and the second chain extender bis(4-aminophenoxy) dimethylsilane (BAPDMS, 0.34 g, 5 mmol, 0.25 eq.) was dissolved in dry DMF (10 mL) and was added to the TPU-Intermediate mixture under argon atmosphere. The syringe and transfer vessel were rinsed again with additional dry DMF (5 mL) in portions. Then the reaction solution was stirred overnight at 60 °C. For purification, the polymer was precipitated in diethyl ether (1000 mL) and dried under vacuum at 40 °C, resulting in a brown solid.

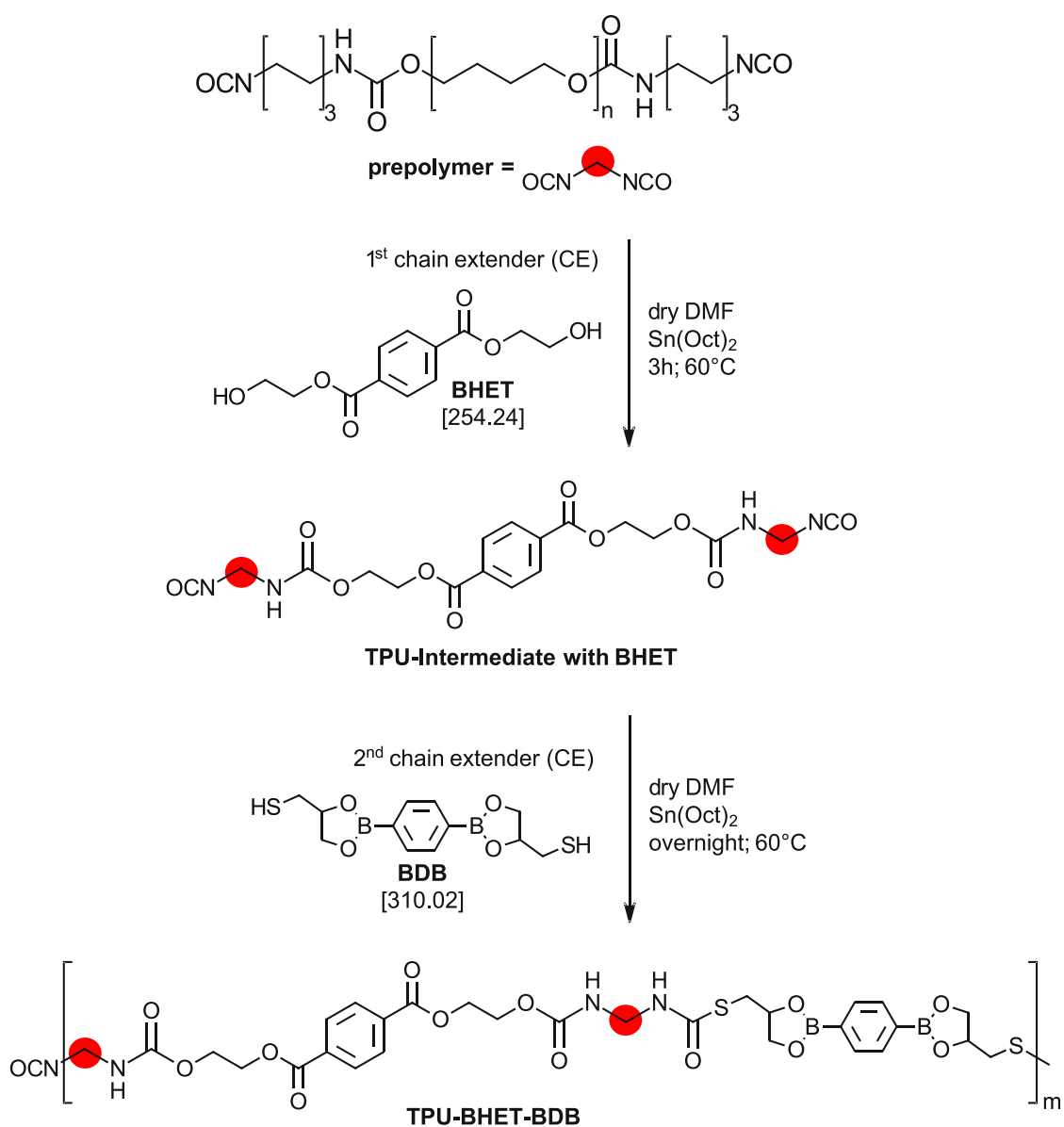
Yield: 6.4 g (84.8 %)

GPC:  $\overline{M}_w$  = 16.4 kDa,  $\overline{M}_n$  = 10.2, kDa, PDI = 1.6

<sup>1</sup>H-NMR (400 MHz, DMSO-*d*<sub>6</sub>, δ): -0.00-0.06 (6H, CH<sub>3</sub>-Si); 1.19 (8H, CH<sub>2</sub>); 1.34 (8H, CH<sub>2</sub>); 1.49 (60H, CH<sub>2</sub>); 2.92 (8H, CH<sub>2</sub>-NH); 3.33 (68H, CH<sub>2</sub>-O + xH<sub>2</sub>O); 4.29 (3H, CH<sub>2</sub>-O); 4.45 (3H, CH<sub>2</sub>-O); 6.60-6.62 (1H, CH<sup>Ar</sup>); 6.99 (2H, NH); 7.11-7.13 (1H, CH<sup>Ar</sup>); 7.19 (2H, NH); 7.99-8.07 (3H, CH<sup>Ar</sup>) ppm

FTIR (solid): 3319 cm<sup>-1</sup> (N-H, urethane); 2937 cm<sup>-1</sup> (C-H); 2856 cm<sup>-1</sup> (C-H); 1721 cm<sup>-1</sup> (C=O, ester); 1694 cm<sup>-1</sup> (C=O...H-N, urethane); 1536 cm<sup>-1</sup> (N-H, urethane + C-N, urethane); 1370 cm<sup>-1</sup> (C-N); 1342 cm<sup>-1</sup> (N-H), 1251 cm<sup>-1</sup> (C-O, ether); 1101 cm<sup>-1</sup> (C-C); 1020 cm<sup>-1</sup> (Si-O); 996 cm<sup>-1</sup> (Si-O); 874 cm<sup>-1</sup> (=C-H<sup>Ar</sup>); 804 cm<sup>-1</sup> (=C-H<sup>Ar</sup>); 778 cm<sup>-1</sup> (=C-H<sup>Ar</sup>)

## Synthesis of TPU-BHET-BDB (75:25, 50:50, 25:75)



Scheme 42: Synthesis of TPU-BHET-BDB with different chain extender ratios via three-step polymerization.

Table 38: Used reactants in synthesis of TPTU-BHET-BDB with different chain extender ratios.

Reactant	Equivalents	M / g mol <sup>-1</sup>	n / mmol	m / g	V / mL
pTHF	1	1,000.00	5.0	5.000	-
HMDI	2	168.20	10.0	1.682	-
BHET	0.75 / 0.50 / 0.25	254.24	3.75 / 2.50 / 1.25	-	-
BDB	0.25 / 0.50 / 0.75	310.02	1.25 / 2.50 / 3.75	-	-
$\text{Sn}(\text{Oct})_2$	0.1	405.12	0.2	0.063	0.05
dry DMF	solvent	-	-	-	20.00

Before the synthesis of TPTU-BHET-BDB, the chain extender bis(hydroxyethylene)terephthalate (BHET) was recrystallized from deionized water. The synthesis of TPU-BHET-BDB until prepolymer formation was performed as described before in 3.3.1. Synthesis of TPUs with two different CEs. The reaction scheme starting from the prepolymer is shown in Scheme 42 and the reactants are listed in Table 38.

After prepolymer formation the first chain extender bis(hydroxyethylene)terephthalate (BHET, exact amounts for each polymer see table below) was dissolved in dry DMF (2.5 mL) and was added to the reaction mixture at 60 °C under argon atmosphere. The syringe and transfer vessel were rinsed with additional dry DMF (5 mL) in portions. Afterwards, the mixture was stirred for 3 h at the same reaction conditions. Then the reaction temperature was reduced to 60 °C and the second chain extender 2,2'-(1,4-phenylene)bis[4-thioethyl-1,3,2-dioxaborolane] (BDB, exact amounts for each polymer see table below) was dissolved in dry DMF (2.5 mL) and was added to the TPU-Intermediate mixture under argon atmosphere. The syringe and transfer vessel were rinsed again with additional dry DMF (5 mL) in portions. Then the mixture was stirred overnight at 60 °C. For purification, the polymer was precipitated in diethyl ether (800 mL) and dried under vacuum at 40 °C, resulting in a white solid.

Table 39: Different chain extender ratios of BHET and BDB for TPTU-BHET-BDB synthesis.

polymer-code	eq. (BHET/BDB) total 1 eq.	m (BHET/BDB) / g	n (BHET/BDB) / mmol
TPU-BHET-BDB (75:25)	0.75 / 0.25	0.953 / 0.388	3.75 / 1.25
TPU-BHET-BDB (50:50)	0.50 / 0.50	0.636 / 0.775	2.50 / 2.50
TPU-BHET-BDB (25:75)	0.25 / 0.75	0.318 / 1.163	1.25 / 3.75

#### TPU-BHET-BDB (75:25):

Yield: 7.0 g (93.4 %)

GPC:  $\overline{M}_w$  = 21.2 kDa,  $\overline{M}_n$  = 11.9, kDa, PDI = 1.8

<sup>1</sup>H-NMR (400 MHz, DMSO-*d*<sub>6</sub>, δ): 1.21 (8H, CH<sub>2</sub>); 1.34 (8H, CH<sub>2</sub>); 1.50 (39H, CH<sub>2</sub>); 2.93 (8H, CH<sub>2</sub>-NH); 3.07-3.16 (2H, CH<sub>2</sub>); 3.32 (42H, CH<sub>2</sub>-O); 4.29 (3H, CH<sub>2</sub>-O); 4.38 (0.5H, CH); 4.45 (3H, CH<sub>2</sub>-O); 6.99-7.19 (4H, NH); 7.63-7.73 (4H, CH<sup>Ar</sup>); 8.08 (3H, CH<sup>Ar</sup>) ppm

FTIR (solid): 3308 cm<sup>-1</sup> (N-H, urethane); 2934 cm<sup>-1</sup> (C-H); 2855 cm<sup>-1</sup> (C-H); 1720 cm<sup>-1</sup> (C=O, ester); 1694 cm<sup>-1</sup> (C=O...H-N, urethane); 1535 cm<sup>-1</sup> (N-H, urethane + C-N, urethane); 1369 cm<sup>-1</sup> (B-O); 1257 cm<sup>-1</sup> (C-O, ether); 1100 cm<sup>-1</sup> (C-C); 1025 cm<sup>-1</sup> (B-C); 990 cm<sup>-1</sup> (B-C); 875 cm<sup>-1</sup> (=C-H<sup>Ar</sup>); 775 cm<sup>-1</sup> (C-S); 727 cm<sup>-1</sup> (C-S); 658 cm<sup>-1</sup> (C-S)

### TPU-BHET-BDB (50:50):

Yield: 6.6 g (90.1 %)

GPC:  $\overline{M}_w$  = 25.9 kDa,  $\overline{M}_n$  = 13.7, kDa, PDI = 1.9

$^1\text{H-NMR}$  (400 MHz, DMSO-*d*<sub>6</sub>,  $\delta$ ): 1.21 (8H, CH<sub>2</sub>); 1.35 (8H, CH<sub>2</sub>); 1.50 (39H, CH<sub>2</sub>); 2.94 (8H, CH<sub>2</sub>-NH); 3.07-3.17 (4H, CH<sub>2</sub>); 3.32 (57H, CH<sub>2</sub>-O + xH<sub>2</sub>O); 4.29 (2H, CH<sub>2</sub>-O); 4.38 (1H, CH); 4.45 (2H, CH<sub>2</sub>-O); 7.00-7.20 (4H, NH); 7.63-7.80 (2H, CH<sup>Ar</sup>); 8.08 (2H, CH<sup>Ar</sup>) ppm

FTIR (solid): 3305 cm<sup>-1</sup> (N-H, urethane); 2933 cm<sup>-1</sup> (C-H); 2854 cm<sup>-1</sup> (C-H); 1720 cm<sup>-1</sup> (C=O, ester); 1694 cm<sup>-1</sup> (C=O...H-N, urethane); 1536 cm<sup>-1</sup> (N-H, urethane + C-N, urethane); 1368 cm<sup>-1</sup> (B-O); 1258 cm<sup>-1</sup> (C-O, ether); 1099 cm<sup>-1</sup> (C-C); 1021 cm<sup>-1</sup> (B-C); 980 cm<sup>-1</sup> (B-C); 875 cm<sup>-1</sup> (=C-H<sup>Ar</sup>); 775 cm<sup>-1</sup> (C-S); 727 cm<sup>-1</sup> (C-S); 658 cm<sup>-1</sup> (C-S)

### TPU-BHET-BDB (25:75):

Yield: 6.6 g (86.2 %)

GPC:  $\overline{M}_w$  = 18.3 kDa,  $\overline{M}_n$  = 9.2, kDa, PDI = 2.0

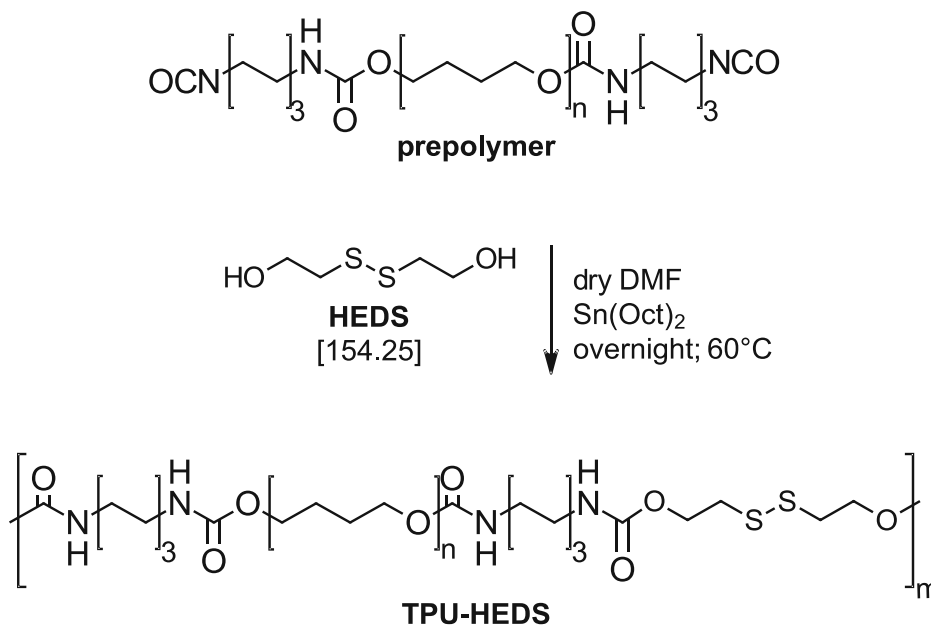
$^1\text{H-NMR}$  (400 MHz, DMSO-*d*<sub>6</sub>,  $\delta$ ): 1.21 (8H, CH<sub>2</sub>); 1.35 (8H, CH<sub>2</sub>); 1.50 (33H, CH<sub>2</sub>); 2.92 (8H, CH<sub>2</sub>-NH); 3.06-3.17 (6H, CH<sub>2</sub>); 3.32 (31H, CH<sub>2</sub>-O); 4.29 (1H, CH<sub>2</sub>-O); 4.37 (1.5H, CH); 4.45 (1H, CH<sub>2</sub>-O); 6.99-7.19 (4H, NH); 7.63-7.78 (3H, CH<sup>Ar</sup>); 8.08 (1H, CH<sup>Ar</sup>) ppm

FTIR (solid): 3310 cm<sup>-1</sup> (N-H, urethane); 2935 cm<sup>-1</sup> (C-H); 2855 cm<sup>-1</sup> (C-H); 1720 cm<sup>-1</sup> (C=O, ester); 1693 cm<sup>-1</sup> (C=O...H-N, urethane); 1532 cm<sup>-1</sup> (N-H, urethane + C-N, urethane); 1368 cm<sup>-1</sup> (B-O); 1252 cm<sup>-1</sup> (C-O, ether); 1100 cm<sup>-1</sup> (C-C); 1024 cm<sup>-1</sup> (B-C); 990 cm<sup>-1</sup> (B-C); 849 cm<sup>-1</sup> (=C-H<sup>Ar</sup>); 778 cm<sup>-1</sup> (C-S); 728 cm<sup>-1</sup> (C-S); 658 cm<sup>-1</sup> (C-S)



## 4. Influence of disulfides in the CE

### 4.1. Synthesis of TPU-HEDS



Scheme 43: Synthesis of TPU-HEDS via two-step polymerization.

Table 40: Used reactants in synthesis of TPU-HEDS.

Reactant	Equivalents	M / g mol <sup>-1</sup>	n / mmol	m / g	V / mL
pTHF	1	1,000.00	5.0	5.000	-
HMDI	2	168.20	10.0	1.682	-
HEDS	1	154.25	5.0	0.771	-
Sn(Oct) <sub>2</sub>	0.1	405.12	0.2	0.063	0.05
dry DMF	solvent	-	-	-	20.00

Before the TPU synthesis, the chain extender 2-hydroxyethyl disulfide (HEDS) was distilled under vacuum (< 0.1 mbar) at 150 °C. The synthesis of TPU-HEDS until prepolymer formation was performed as described in 1.1. General polymer procedure / Synthesis of TPU-BHET. The reaction scheme starting from the prepolymer is shown in Scheme 43 and the used chemicals are listed in Table 40.

After prepolymer formation 2-hydroxyethyl disulfide (HEDS, 0.77 g, 5 mmol, 1 eq.) was dissolved in dry DMF (5 mL) and was added to the reaction mixture at 60 °C under argon atmosphere. The syringe and transfer vessel were rinsed with additional dry DMF (5 mL) in portions. Afterwards, the mixture was stirred overnight at the same reaction conditions. For purification, the polymer was precipitated in petroleum ether (800 mL) and dried under vacuum at 50 °C, resulting in a white solid.

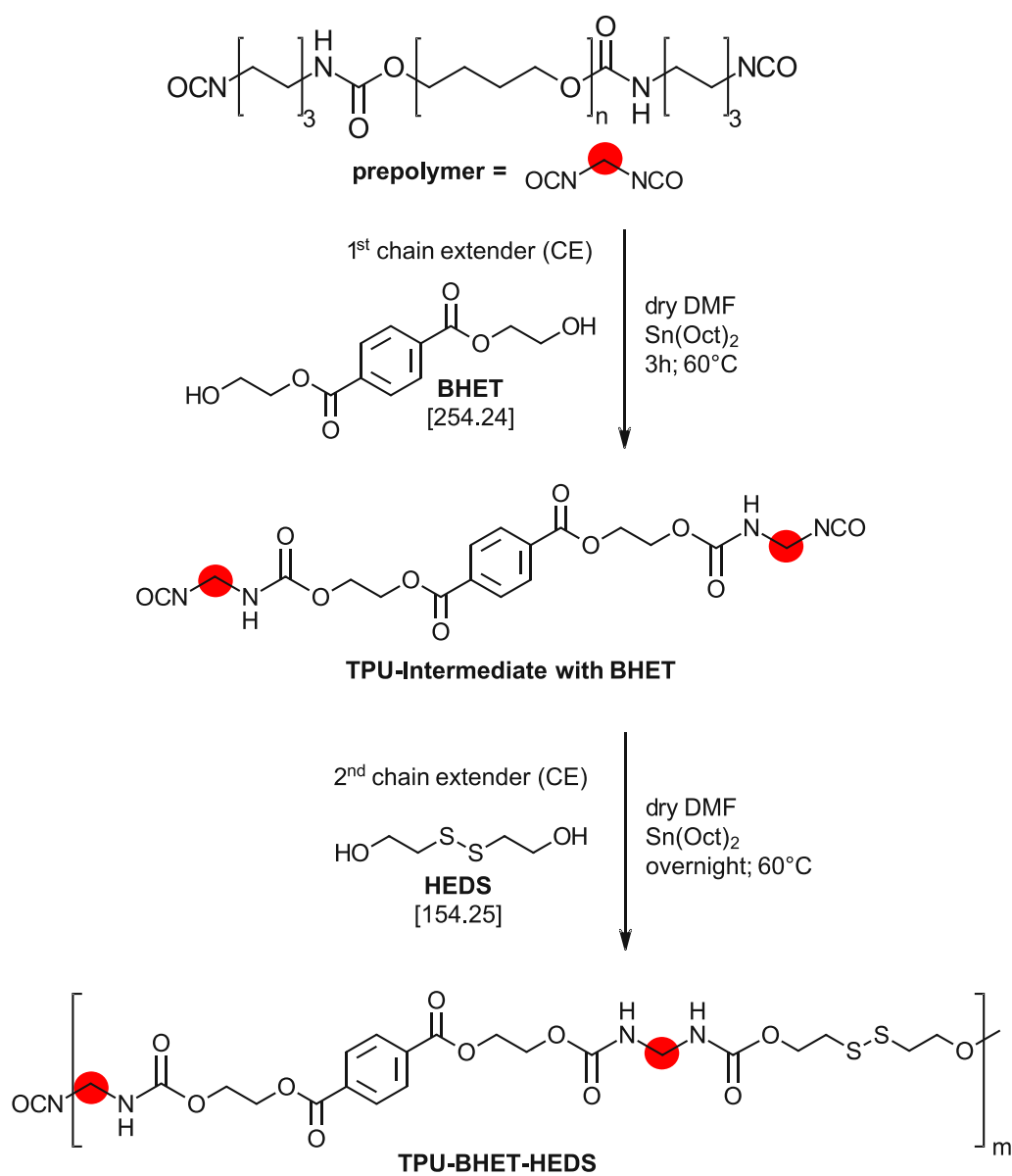
Yield: 7.0 g (93.8 %)

GPC:  $\overline{M}_w$  = 59.9 kDa,  $\overline{M}_n$  = 29.4, kDa, PDI = 2.0

$^1\text{H-NMR}$  (400 MHz,  $\text{DMSO-}d_6$ ,  $\delta$ ): 1.22 (8H,  $\text{CH}_2$ ); 1.36 (8H,  $\text{CH}_2$ ); 1.50 (42H,  $\text{CH}_2$ ); 2.93 (8H,  $\text{CH}_2\text{-NH}$ ); 3.49 (43H,  $\text{CH}_2\text{-O}$ ); 3.91 (4H,  $\text{CH}_2\text{-O}$ ); 4.15 (4H,  $\text{CH}_2\text{-S}$ ); 6.99-7.15 (4H, NH) ppm

FTIR (solid):  $3330\text{ cm}^{-1}$  (N-H, urethane);  $2936\text{ cm}^{-1}$  (C-H);  $2855\text{ cm}^{-1}$  (C-H);  $1719\text{ cm}^{-1}$  (C=O, ester);  $1681\text{ cm}^{-1}$  (C=O $\cdots$ H-N, urethane);  $1532\text{ cm}^{-1}$  (N-H, urethane + C-N, urethane);  $1262\text{ cm}^{-1}$  (C-O, ether);  $1104\text{ cm}^{-1}$  (C-C);  $779\text{ cm}^{-1}$  (C-S);  $733\text{ cm}^{-1}$  (C-S)

## 4.2. Synthesis of TPU-BHET-HEDS



Scheme 44: Synthesis of TPU-BHET-HEDS with different chain extender ratios, starting from prepolymer formation.

Table 41: Used reactants in synthesis of TPU-BHET-HEDS with different chain extender ratios.

Reactant	Equivalents	M / g mol <sup>-1</sup>	n / mmol	m / g	V / mL
pTHF	1	1,000.00	5.0	5.000	-
HMDI	2	168.20	10.0	1.682	-
BHET	0.75 / 0.50 / 0.25	254.24	3.75 / 2.50 / 1.25	-	-
HEDS	0.25 / 0.50 / 0.75	154.25	1.25 / 2.50 / 3.75	-	-
$\text{Sn}(\text{Oct})_2$	0.1	405.12	0.2	0.063	0.05
dry DMF	solvent	-	-	-	20.00

Before the synthesis of TPU-BHET-HEDS, the chain extender bis(hydroxyethylene) terephthalate (BHET) was recrystallized from deionized water and 2-hydroxyethyl disulfide (HEDS) was distilled under vacuum (< 0.1 mbar) at maximum 150 °C. The synthesis of TPU-BHET-HEDS until prepolymer formation was performed as described before in 3.3.1. Synthesis of TPUs with two different CEs. The reaction scheme starting from the prepolymer is shown in Scheme 44 And the reactants are listed in Table 41.

After prepolymer formation the first chain extender bis(hydroxyethylene)terephthalate (BHET, exact amounts for each polymer see table below) was dissolved in dry DMF (2.5 mL) and was added to the reaction mixture at 60 °C under argon atmosphere. The syringe and transfer vessel were rinsed with additional dry DMF (5 mL) in portions. Afterwards, the mixture was stirred for 3 h at the same reaction conditions. Then the second chain extender 2-hydroxyethyl disulfide (HEDS, exact amounts for each polymer see table below) was dissolved in dry DMF (2.5 mL) and was added to the TPU-Intermediate mixture under argon atmosphere. The syringe and transfer vessel were rinsed again with additional dry DMF (5 mL) in portions. For purification, the polymer was precipitated in petroleum ether (800 mL) and dried under vacuum at 50 °C, resulting in a white solid.

Table 42: Different chain extender ratios of BHET and HEDS for TPU-BHET-HEDS synthesis.

polymer-code	eq. (BHET/HEDS) total 1 eq.	m (BHET/HEDS) / g	n (BHET/HEDS) / mmol
TPU-BHET-HEDS (75:25)	0.75 / 0.25	0.953 / 0.193	3.75 / 1.25
TPU-BHET-HEDS (50:50)	0.50 / 0.50	0.636 / 0.386	2.50 / 2.50
TPU-BHET-HEDS (25:75)	0.25 / 0.75	0.318 / 0.578	1.25 / 3.75

#### TPU-BHET-HEDS (75:25):

Yield: 6.9 g (92.6 %)

GPC:  $\overline{M}_w$  = 44.9 kDa,  $\overline{M}_n$  = 21.8, kDa, PDI = 2.1

<sup>1</sup>H-NMR (400 MHz, DMSO-*d*<sub>6</sub>, δ): 1.20 (8H, CH<sub>2</sub>); 1.34 (8H, CH<sub>2</sub>); 1.50 (38H, CH<sub>2</sub>); 2.92 (8H, CH<sub>2</sub>-NH); 3.32 (34H, CH<sub>2</sub>-O); 3.62 (1H, CH<sub>2</sub>-O); 4.15 (1H, CH<sub>2</sub>-S); 4.29 (3H, CH<sub>2</sub>-O); 4.45 (3H, CH<sub>2</sub>-O); 6.98-7.19 (4H, NH); 8.07 (3H, CH<sup>Ar</sup>) ppm

FTIR (solid): 3306 cm<sup>-1</sup> (N-H, urethane); 2934 cm<sup>-1</sup> (C-H); 2855 cm<sup>-1</sup> (C-H); 1720 cm<sup>-1</sup> (C=O, ester); 1694 cm<sup>-1</sup> (C=O...H-N, urethane); 1536 cm<sup>-1</sup> (N-H, urethane + C-N, urethane); 1255 cm<sup>-1</sup> (C-O, ether); 1099 cm<sup>-1</sup> (C-C); 875 cm<sup>-1</sup> (=C-H<sup>Ar</sup>); 774 cm<sup>-1</sup> (C-S); 727 cm<sup>-1</sup> (C-S)

### TPU-BHET-HEDS (50:50):

Yield: 6.5 g (90.0 %)

GPC:  $\overline{M}_w = 40.4$  kDa,  $\overline{M}_n = 20.9$  kDa, PDI = 1.9

$^1\text{H-NMR}$  (400 MHz, DMSO-*d*6,  $\delta$ ): 1.21 (8H, CH<sub>2</sub>); 1.35 (8H, CH<sub>2</sub>); 1.50 (35H, CH<sub>2</sub>); 2.93 (8H, CH<sub>2</sub>-NH); 3.32 (35H, CH<sub>2</sub>-O); 3.62 (2H, CH<sub>2</sub>-O); 4.15 (2H, CH<sub>2</sub>-S); 4.29 (2H, CH<sub>2</sub>-O); 4.45 (2H, CH<sub>2</sub>-O); 6.99-7.17 (4H, NH); 8.08 (2H, CH<sup>Ar</sup>) ppm

FTIR (solid): 3309 cm<sup>-1</sup> (N-H, urethane); 2934 cm<sup>-1</sup> (C-H); 2856 cm<sup>-1</sup> (C-H); 1720 cm<sup>-1</sup> (C=O, ester); 1692 cm<sup>-1</sup> (C=O...H-N, urethane); 1536 cm<sup>-1</sup> (N-H, urethane + C-N, urethane); 1252 cm<sup>-1</sup> (C-O, ether); 1099 cm<sup>-1</sup> (C-C); 876 cm<sup>-1</sup> (=C-H<sup>Ar</sup>); 774 cm<sup>-1</sup> (C-S); 726 cm<sup>-1</sup> (C-S)

### TPU-BHET-HEDS (25:75):

Yield: 6.0 g (83.8 %)

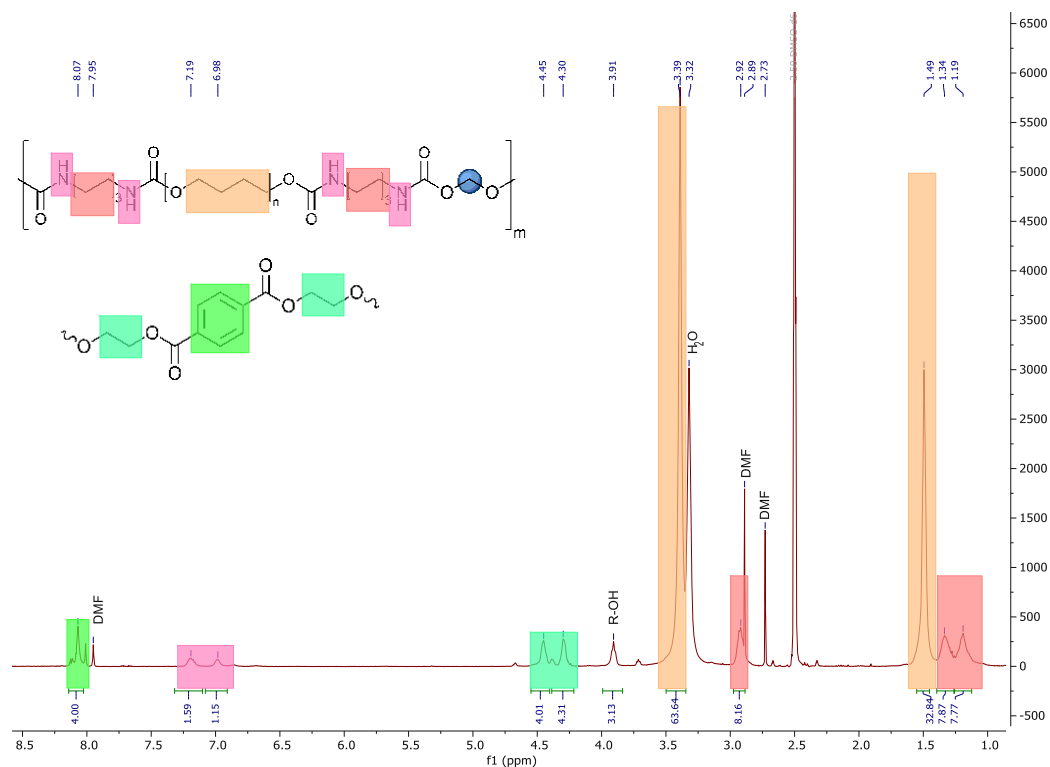
GPC:  $\overline{M}_w = 69.9$  kDa,  $\overline{M}_n = 28.2$  kDa, PDI = 2.5

$^1\text{H-NMR}$  (400 MHz, DMSO-*d*6,  $\delta$ ): 1.22 (8H, CH<sub>2</sub>); 1.36 (8H, CH<sub>2</sub>); 1.50 (40H, CH<sub>2</sub>); 2.93 (8H, CH<sub>2</sub>-NH); 3.33 (38H, CH<sub>2</sub>-O); 3.62 (3H, CH<sub>2</sub>-O); 4.15 (3H, CH<sub>2</sub>-S); 4.29 (1H, CH<sub>2</sub>-O); 4.45 (1H, CH<sub>2</sub>-O); 7.00-7.15 (4H, NH); 8.08 (1H, CH<sup>Ar</sup>) ppm

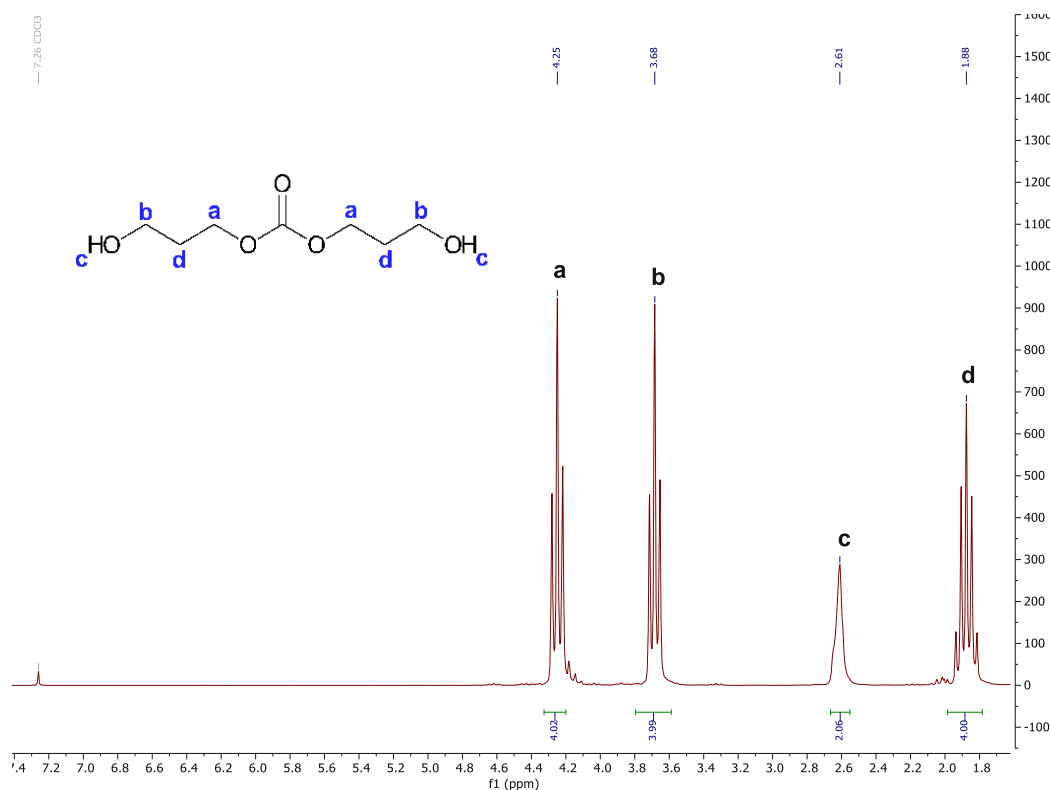
FTIR (solid): 3312 cm<sup>-1</sup> (N-H, urethane); 2935 cm<sup>-1</sup> (C-H); 2856 cm<sup>-1</sup> (C-H); 1720 cm<sup>-1</sup> (C=O, ester); 1693 cm<sup>-1</sup> (C=O...H-N, urethane); 1536 cm<sup>-1</sup> (N-H, urethane + C-N, urethane); 1252 cm<sup>-1</sup> (C-O, ether); 1100 cm<sup>-1</sup> (C-C); 876 cm<sup>-1</sup> (=C-H<sup>Ar</sup>); 774 cm<sup>-1</sup> (C-S); 727 cm<sup>-1</sup> (C-S)

# APPENDIX

## 1. NMR spectra

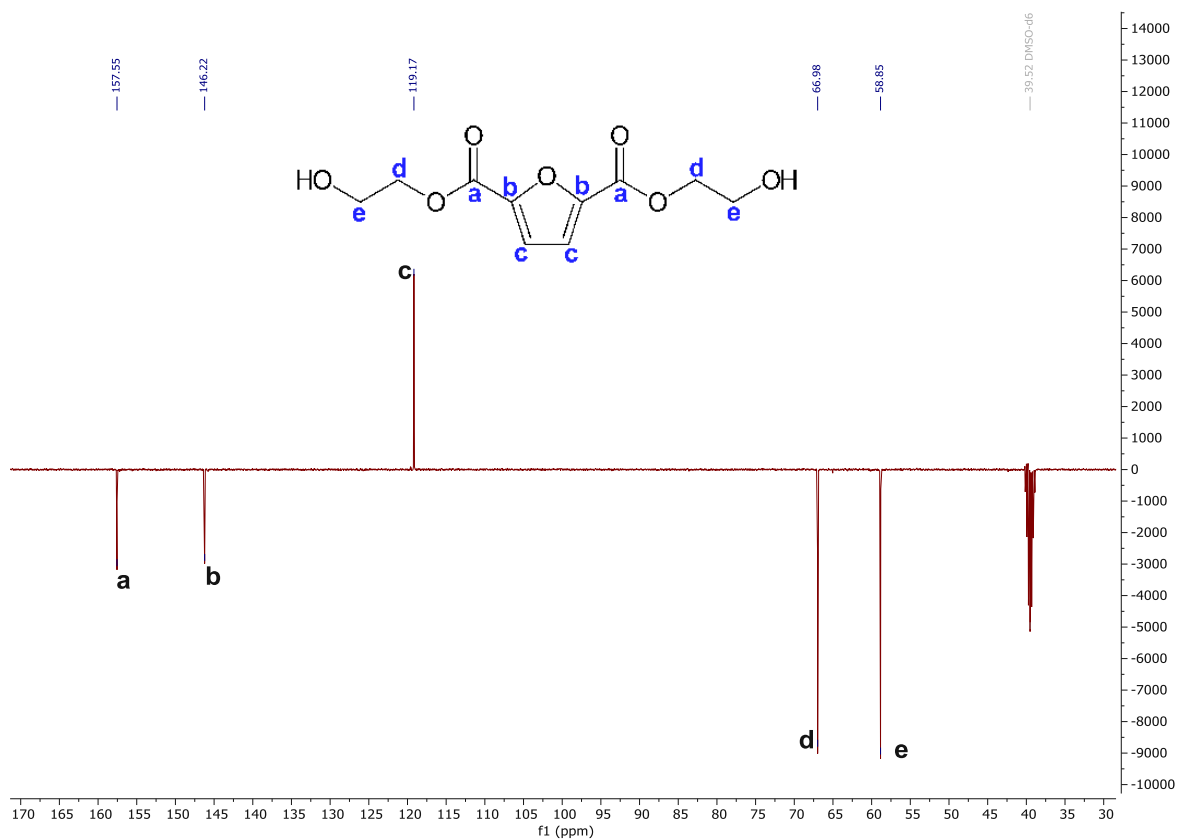


Appendix 1: <sup>1</sup>H-NMR spectrum of TPU-BHET in DMSO-d<sub>6</sub>.

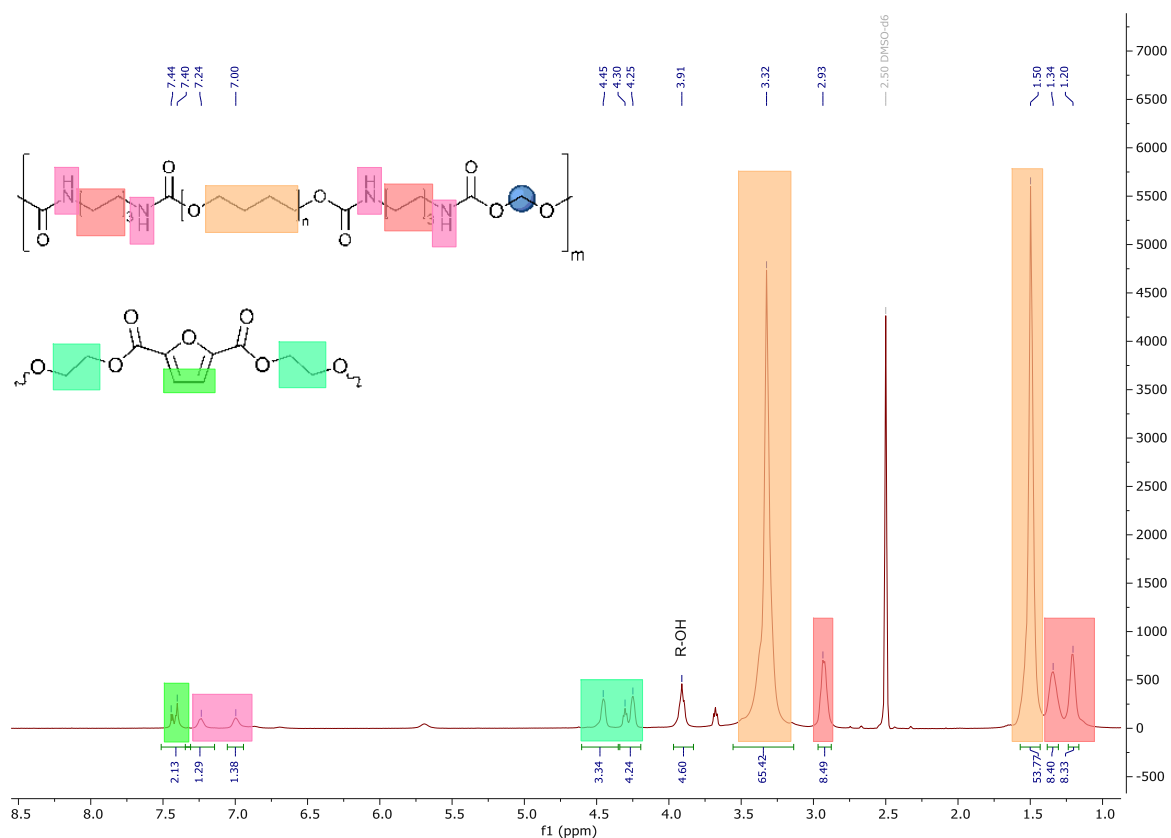


Appendix 2: <sup>1</sup>H-NMR spectrum of bis(hydroxypropyl)carbonate (BHPC) via diethyl carbonate in CDCl<sub>3</sub>.



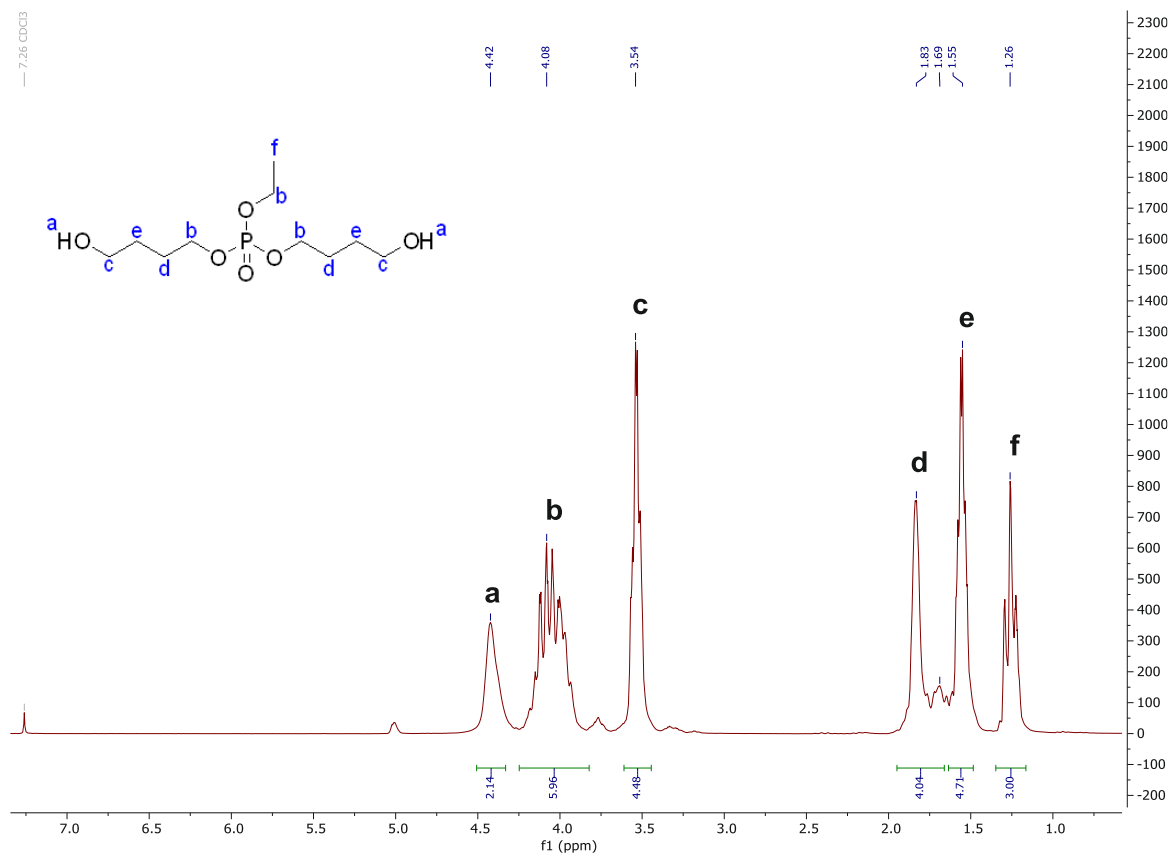


Appendix 5:  $^{13}\text{C}$ -APT-NMR spectrum of bis(2-hydroxyethyl)furan-2,5-dicarboxylate (BHEF) in DMSO- $d_6$ .

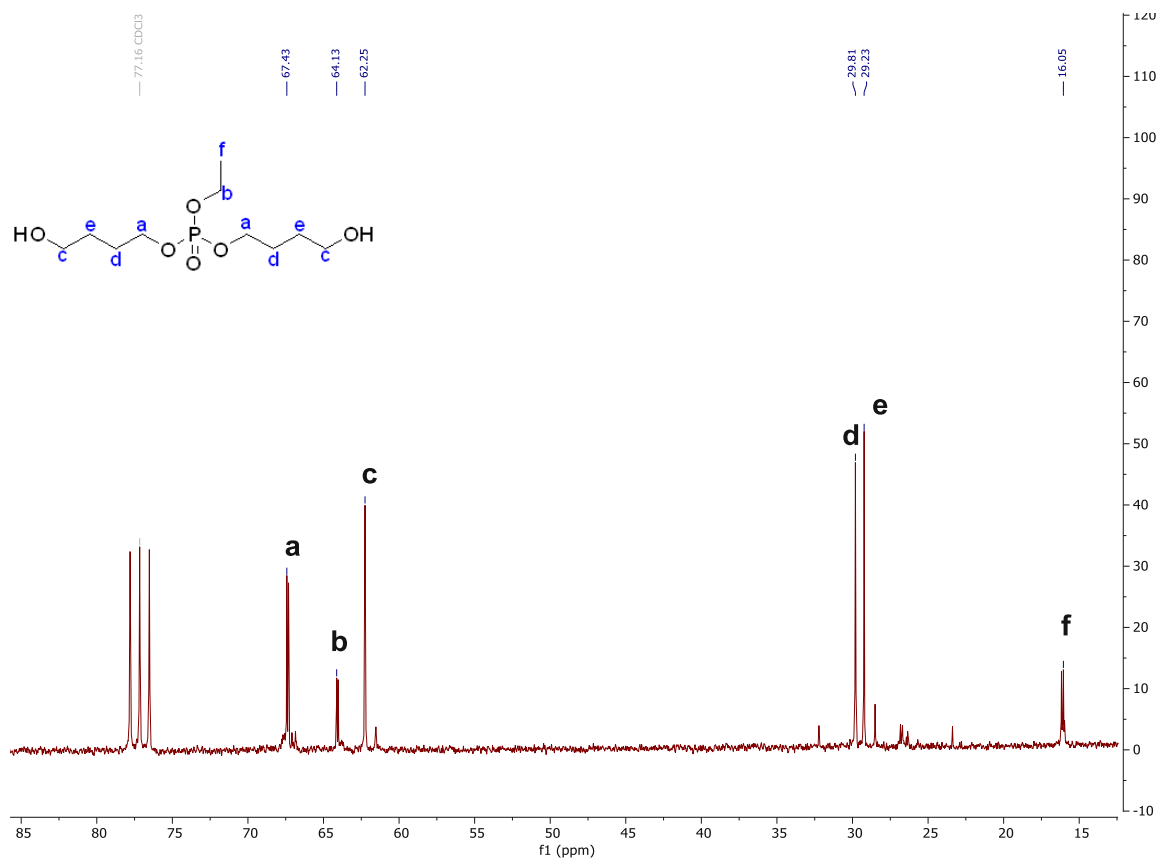


Appendix 6:  $^1\text{H}$ -NMR spectrum of TPU-BHEF in DMSO- $d_6$ .

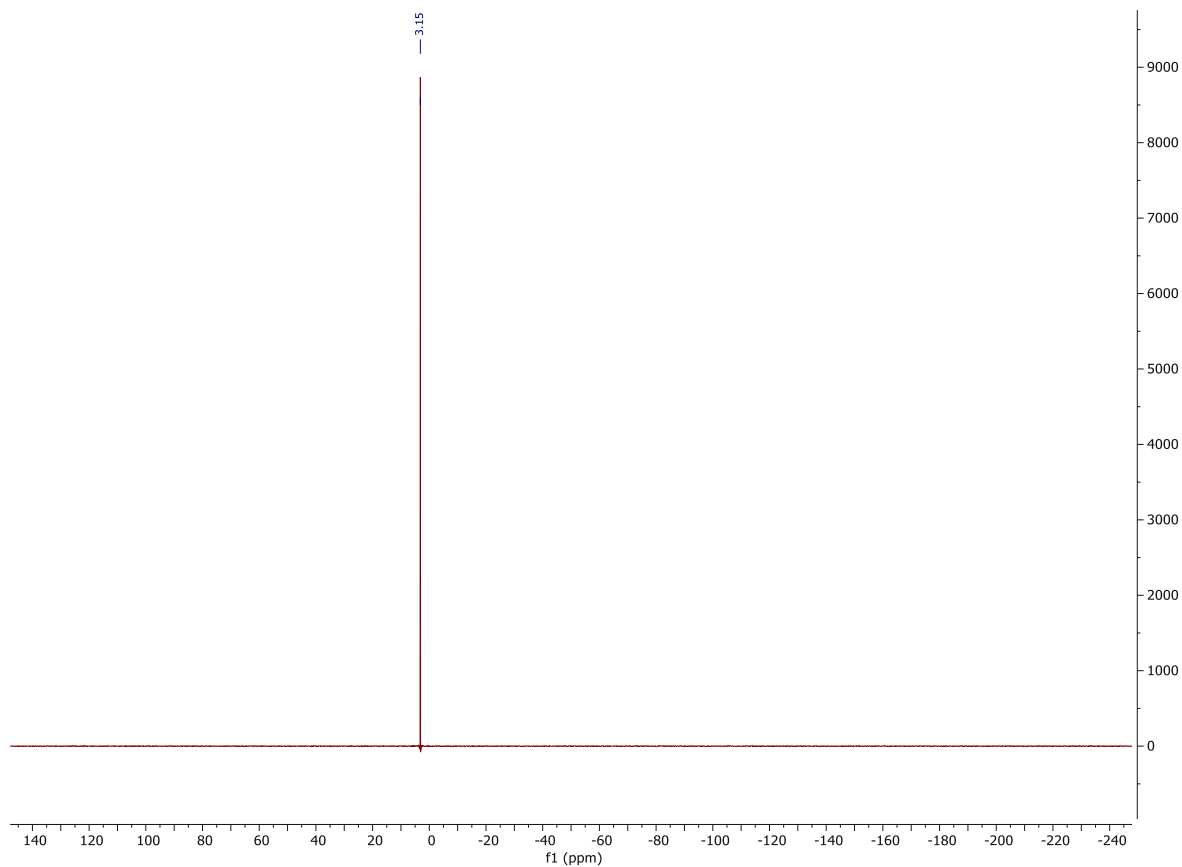




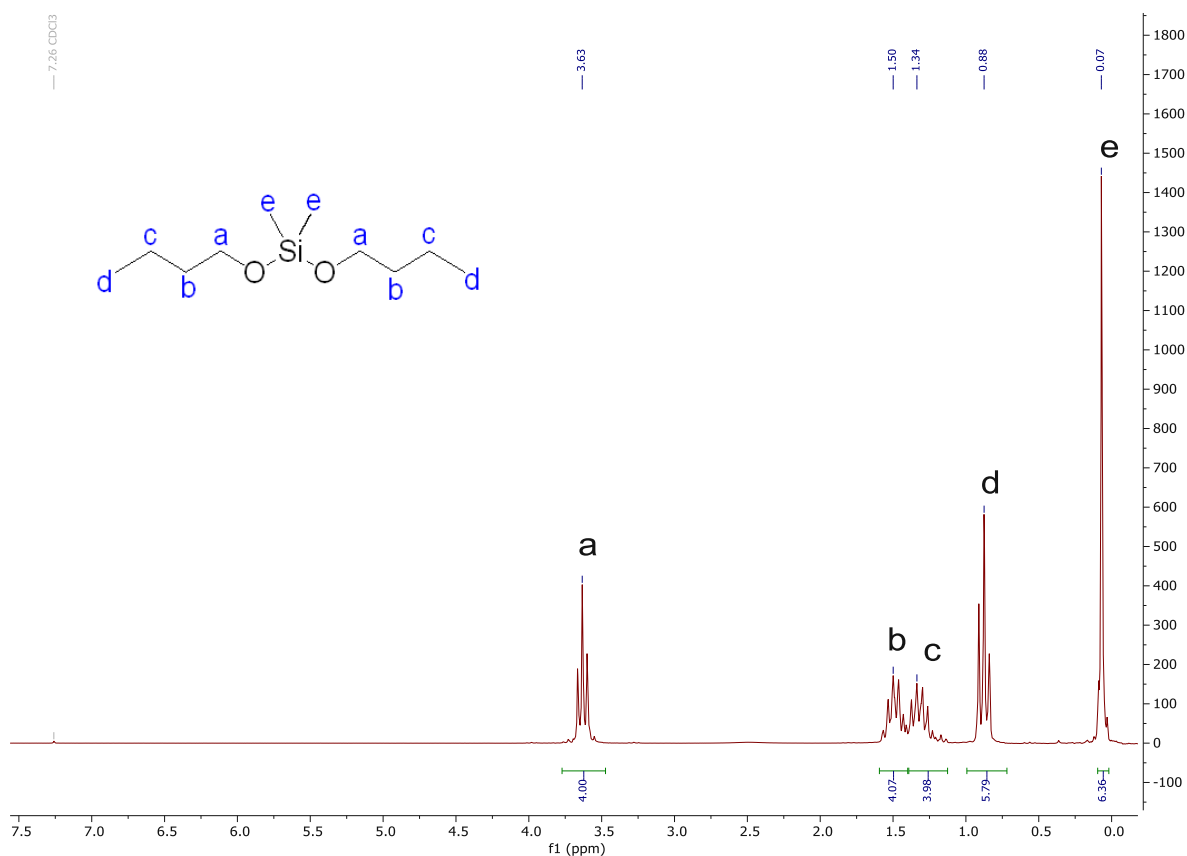
Appendix 7: <sup>1</sup>H-NMR spectrum of bis(4-hydroxybutyl) ethyl phosphate (BHBEP) in CDCl<sub>3</sub>.



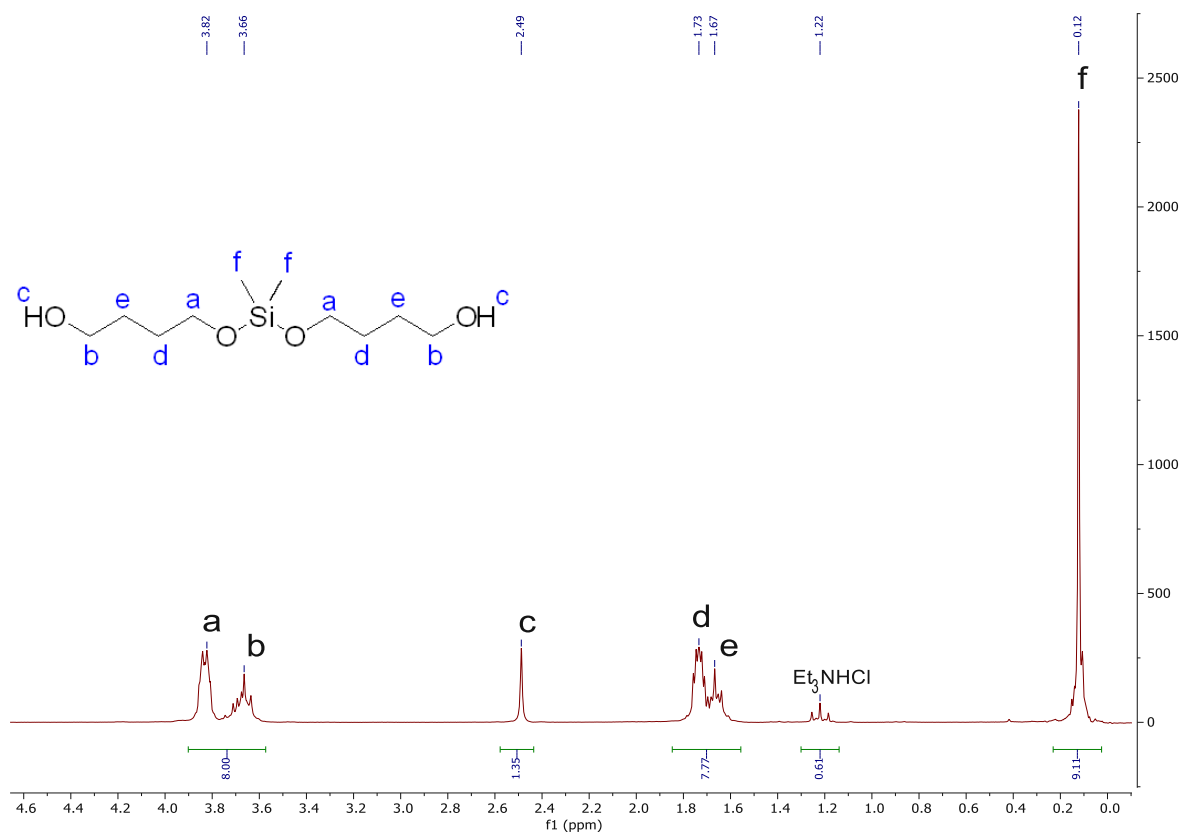
Appendix 8: <sup>13</sup>C-NMR spectrum of bis(4-hydroxybutyl) ethyl phosphate (BHBEP) in CDCl<sub>3</sub>.



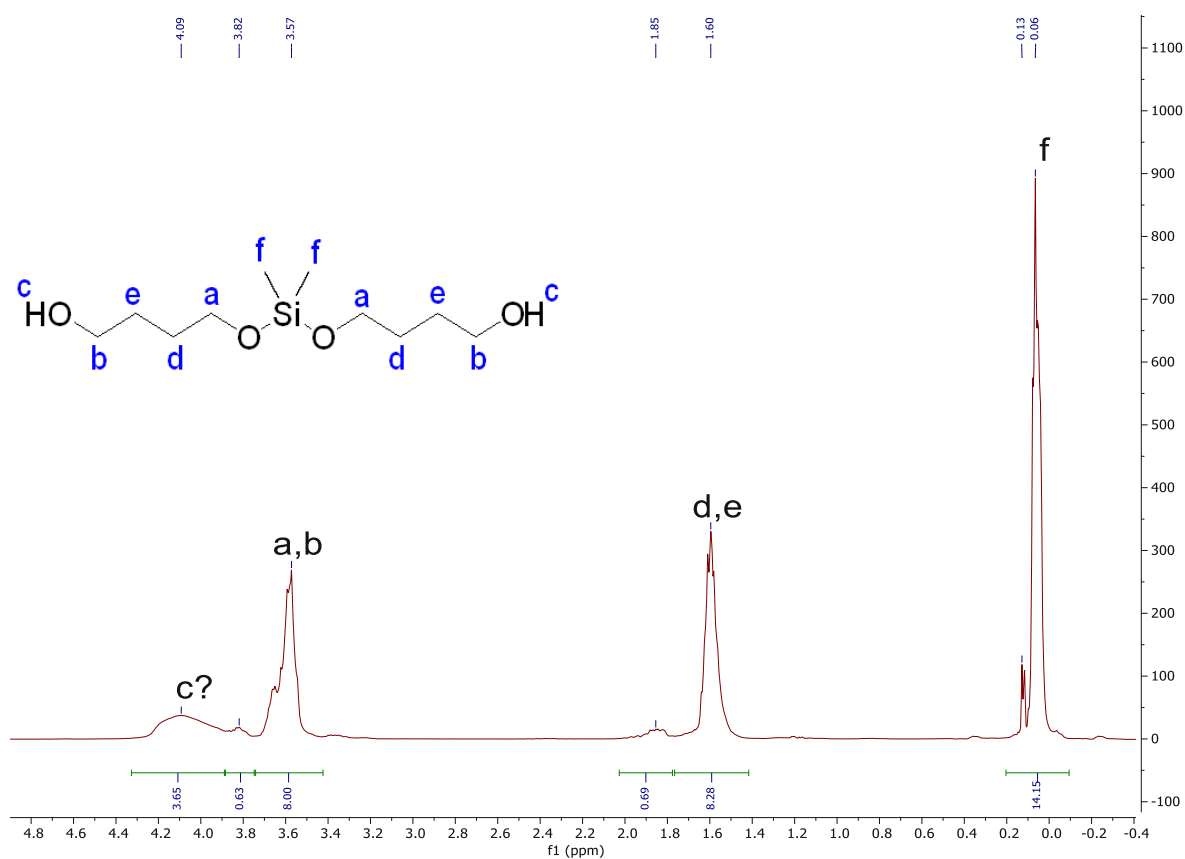
Appendix 9:  $^{31}\text{P}$ -NMR spectrum of bis(4-hydroxybutyl) ethyl phosphate (BHBEP) in  $\text{CDCl}_3$ .



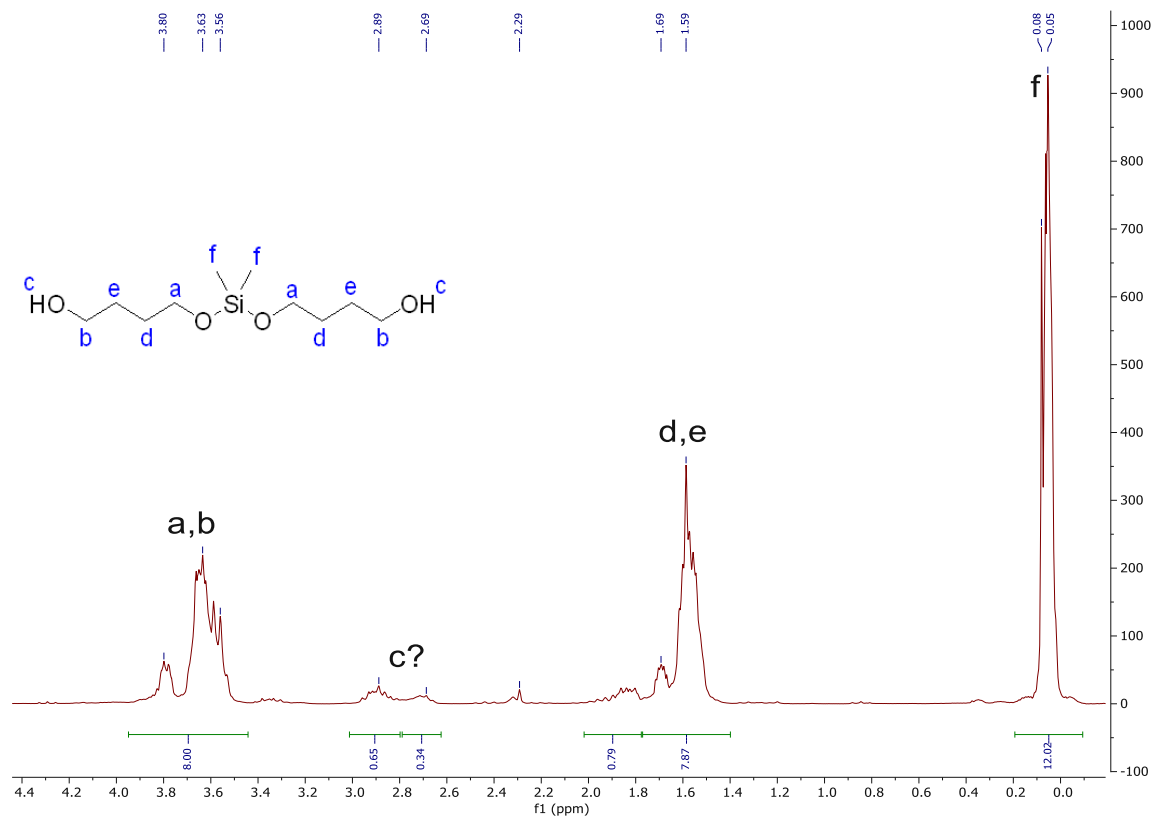
Appendix 10:  $^1\text{H}$ -NMR spectrum model compound bis(butyloxy)dimethylsilane (BBOMS) in  $\text{CDCl}_3$ .



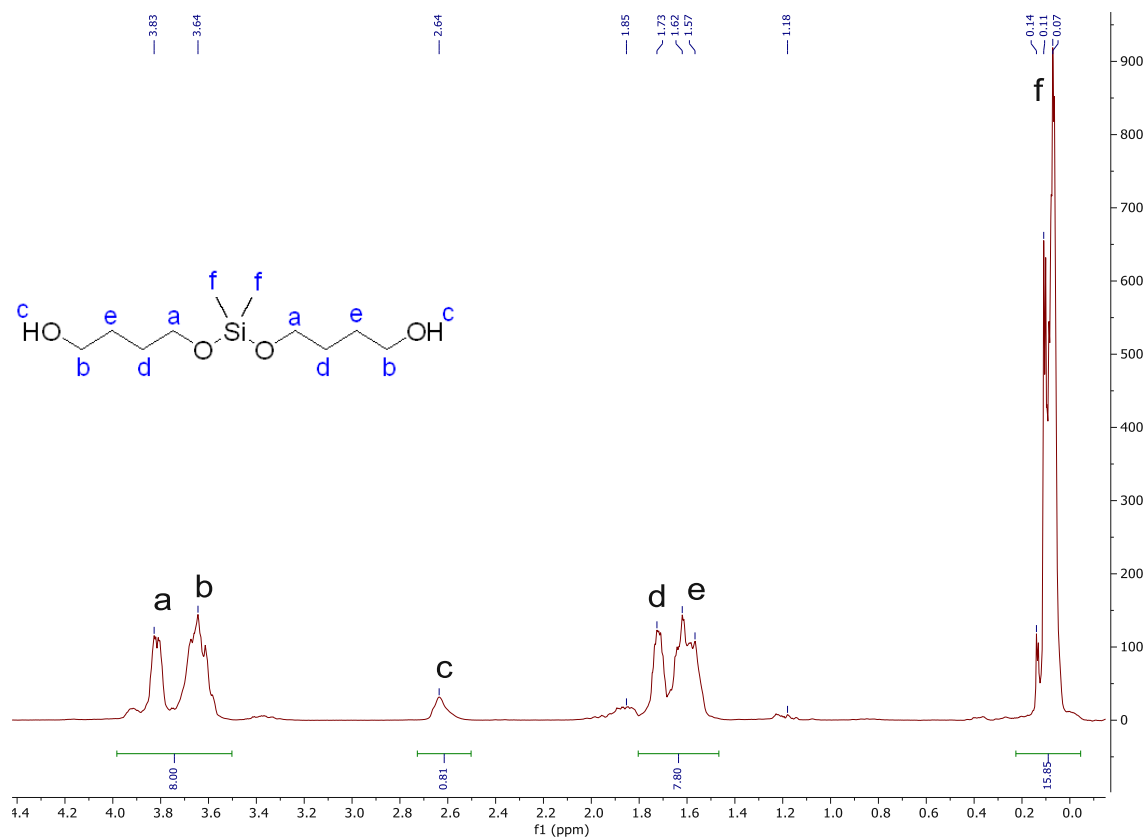
Appendix 11: <sup>1</sup>H-NMR spectrum of BHBMS (BDO : Me<sub>2</sub>Cl<sub>2</sub>Si = 2:1, Et<sub>3</sub>N, CHCl<sub>3</sub>) in CDCl<sub>3</sub>.



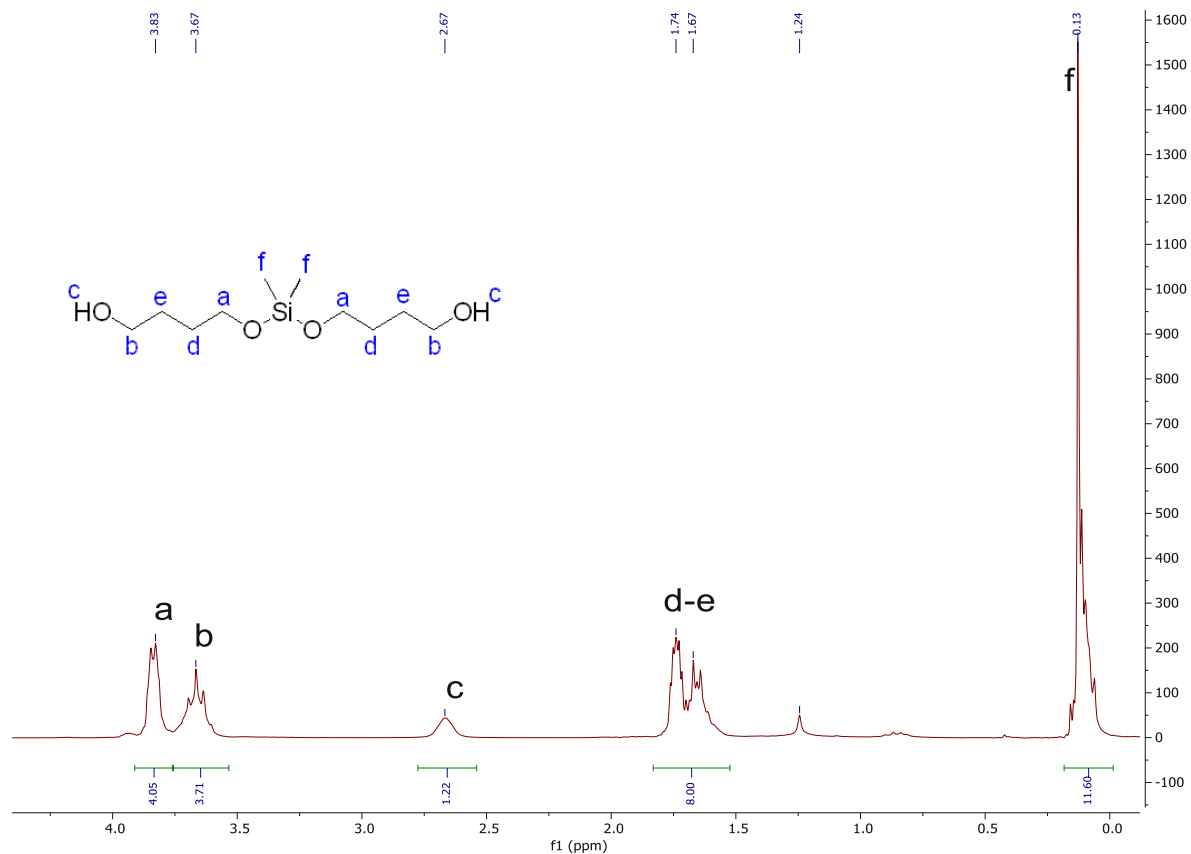
Appendix 12: <sup>1</sup>H-NMR spectrum of BHBMS (BDO : Me<sub>2</sub>Cl<sub>2</sub>Si = 2:1, pyridine, CHCl<sub>3</sub>) in CDCl<sub>3</sub>.



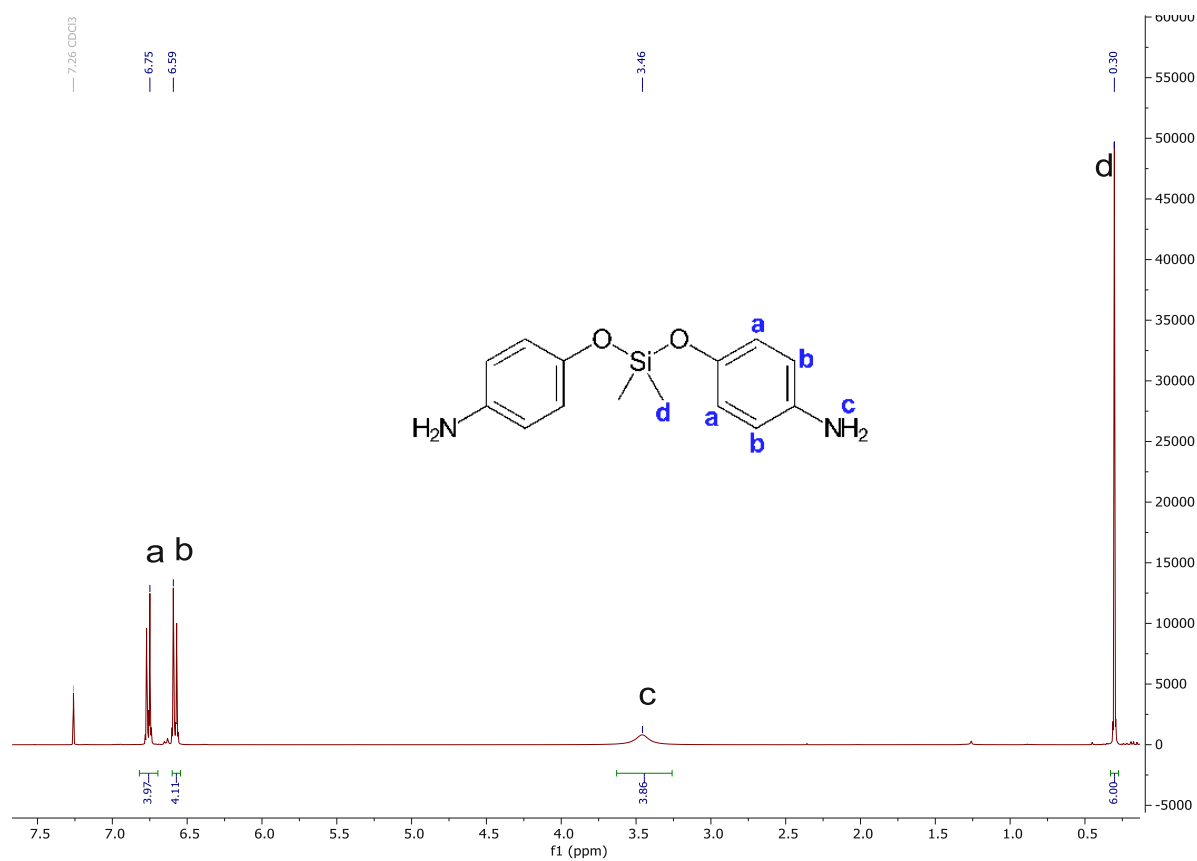
Appendix 13:  $^1\text{H-NMR}$  spectrum of BHBMS (BDO :  $\text{Me}_2\text{Cl}_2\text{Si}$  = 3:1,  $\text{Et}_3\text{N}$ , toluene) in  $\text{CDCl}_3$ .



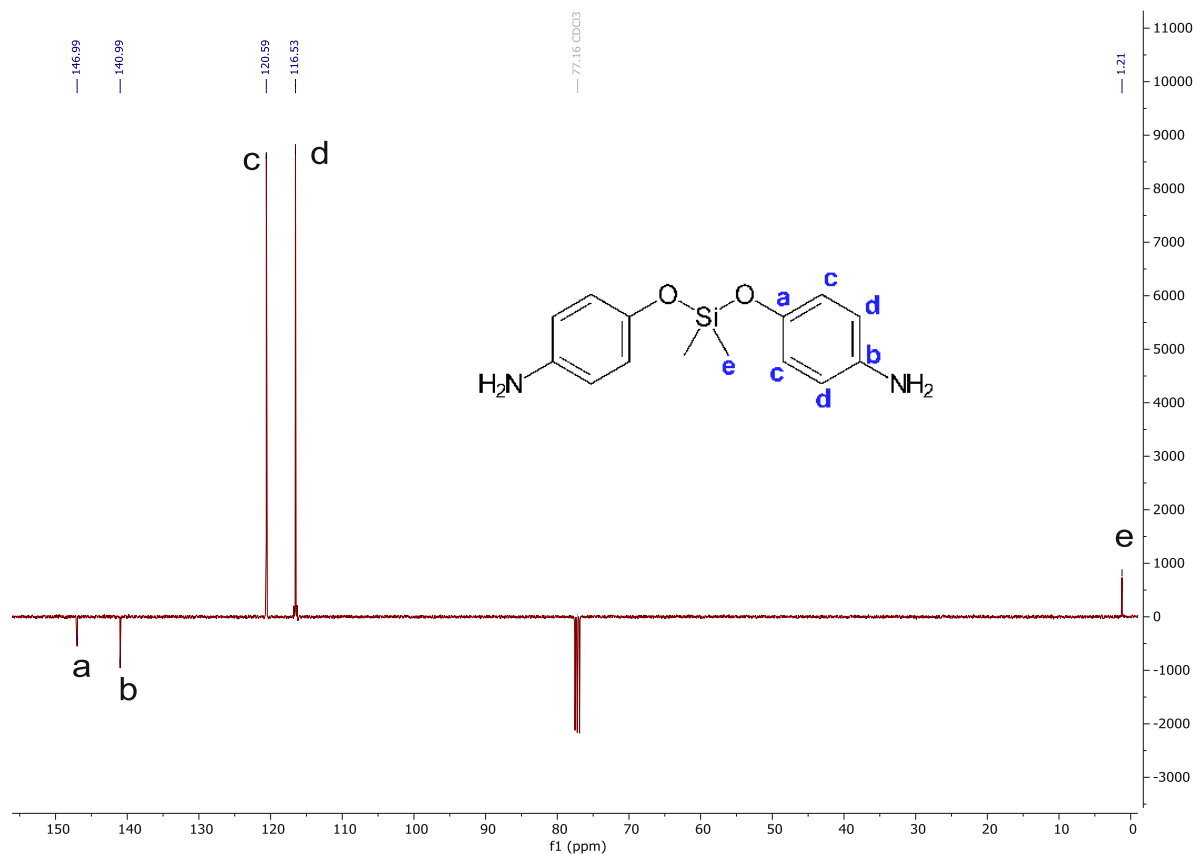
Appendix 14:  $^1\text{H-NMR}$  spectrum of BHBMS (BDO :  $\text{Me}_2\text{Cl}_2\text{Si}$  = 3:1, pyridine,  $\text{CHCl}_3$ ) in  $\text{CDCl}_3$ .



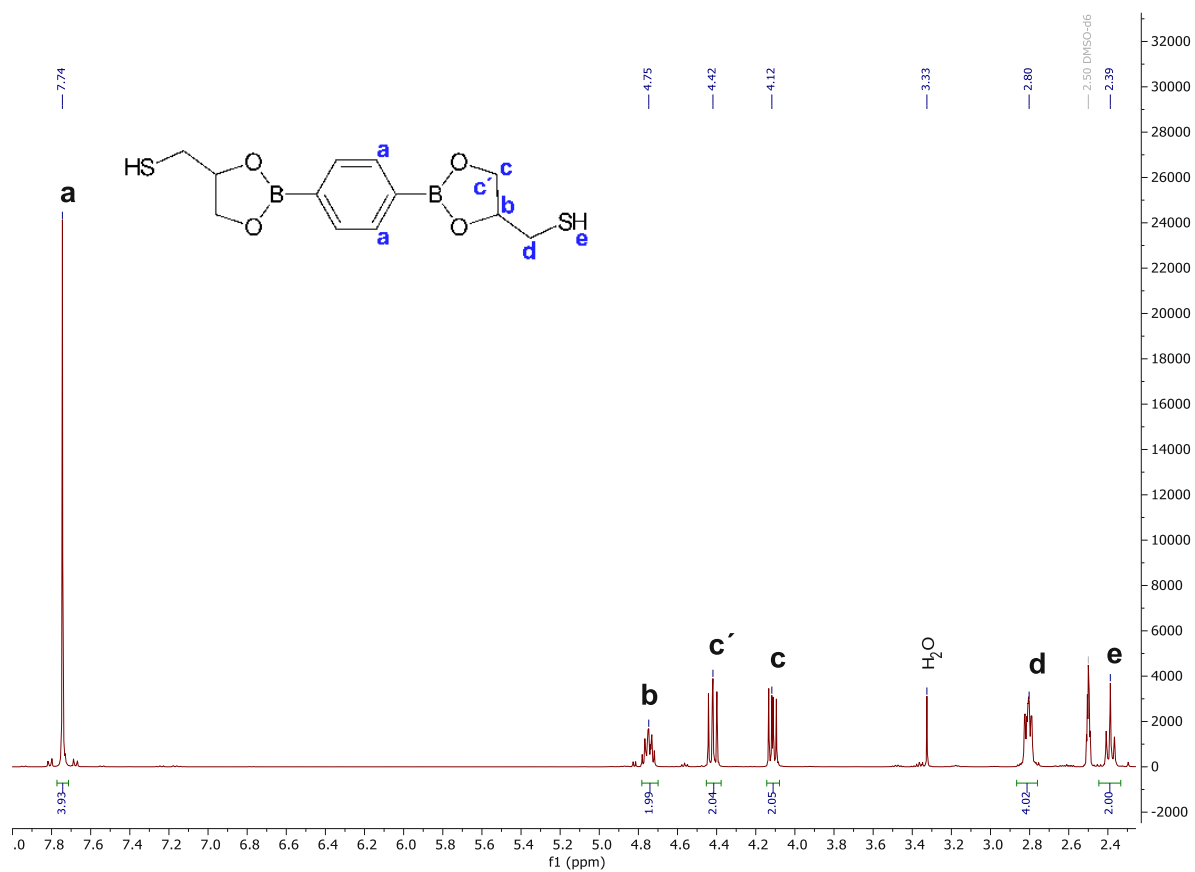
Appendix 15: <sup>1</sup>H-NMR spectrum of BHBMS (BDO : Me<sub>2</sub>Cl<sub>2</sub>Si = 4:1, pyridine, CHCl<sub>3</sub>) in CDCl<sub>3</sub>.



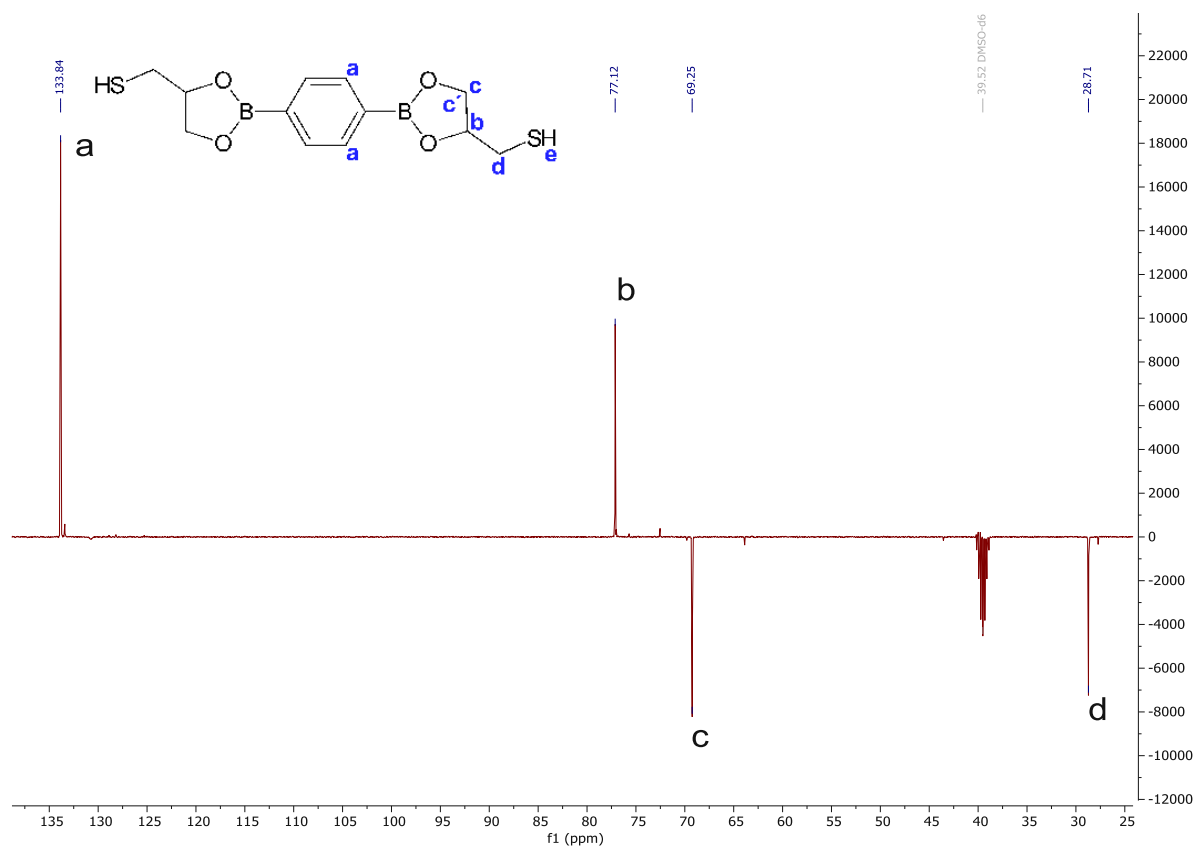
Appendix 16: <sup>1</sup>H-NMR spectrum of BAPDMS in CDCl<sub>3</sub> after recrystallization from diethyl ether.



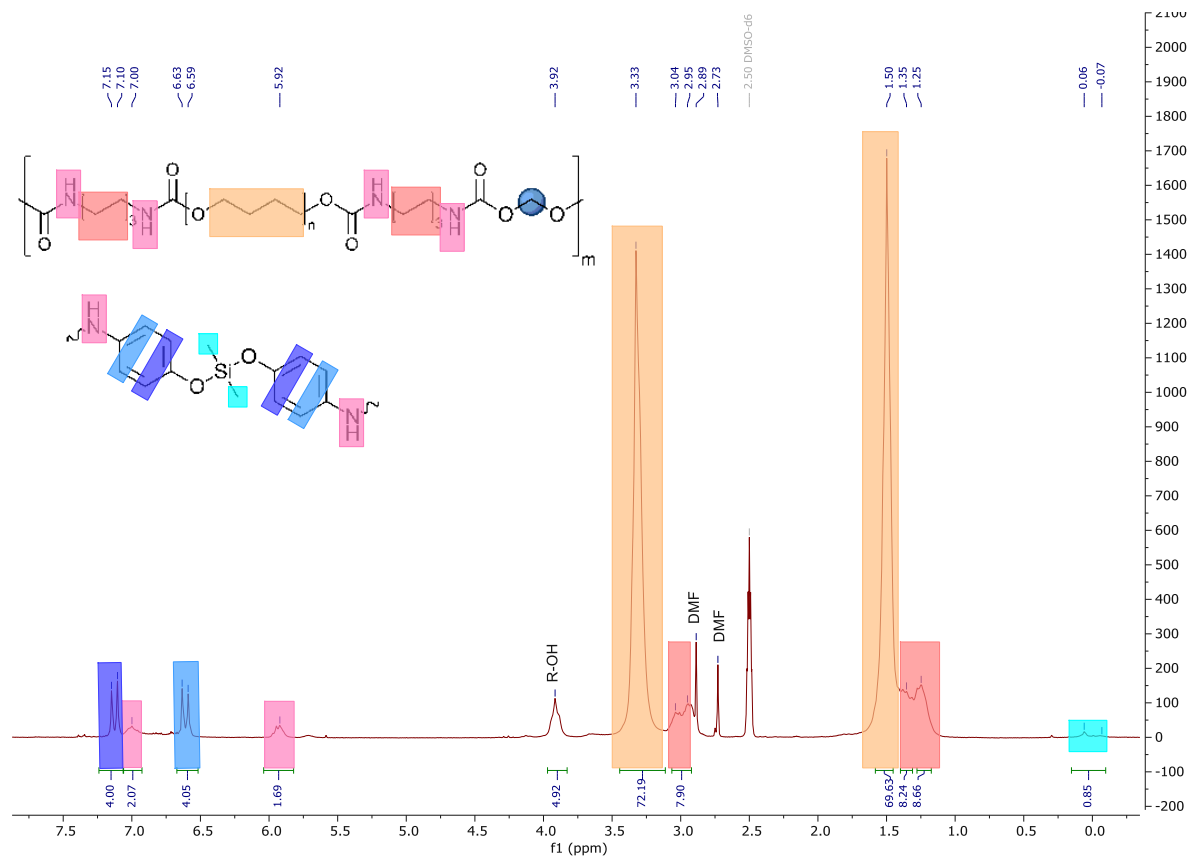
Appendix 17: <sup>13</sup>C-APT-NMR spectrum of BAPDMS in CDCl<sub>3</sub> after recrystallization from diethyl ether.



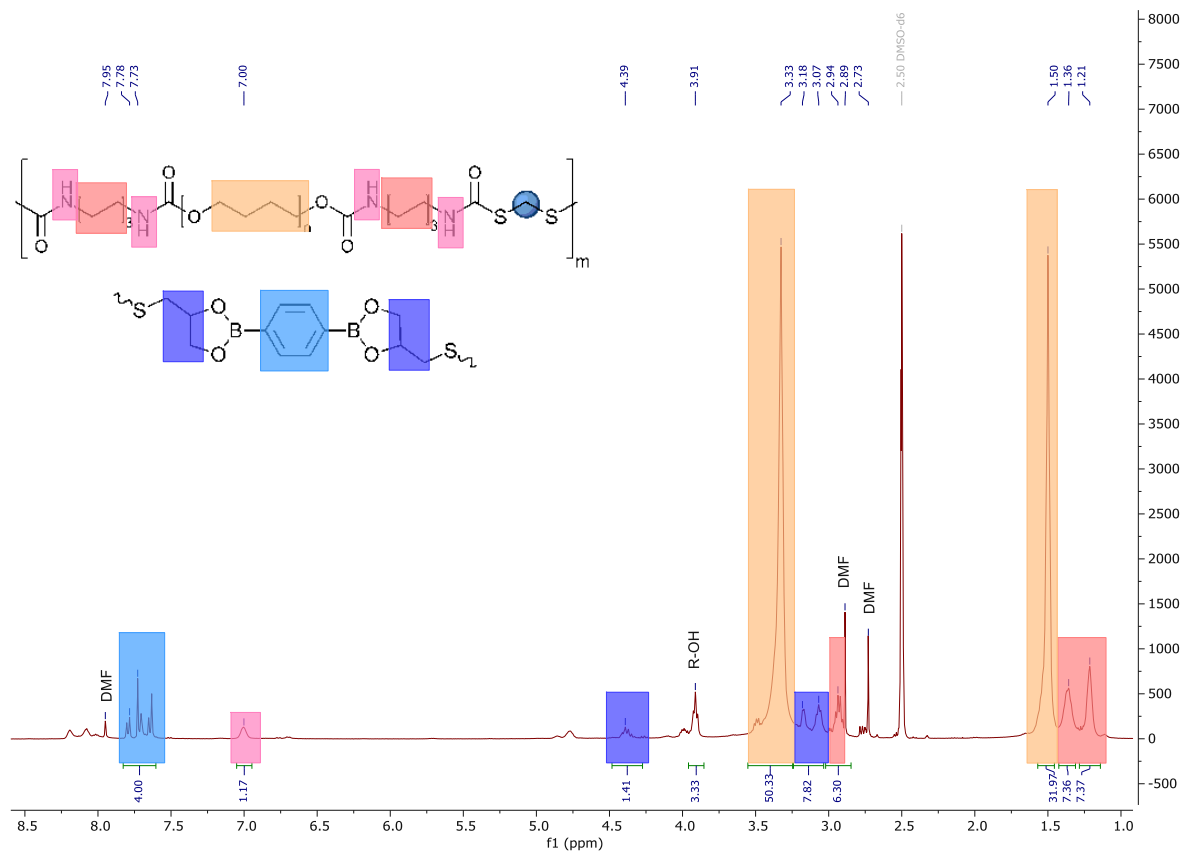
Appendix 18: <sup>1</sup>H-NMR spectrum of 2,2'-(1,4-phenylene)-bis[4-mercaptan-1,3,2-dioxaborolane] (BDB) in DMSO-d<sub>6</sub>.



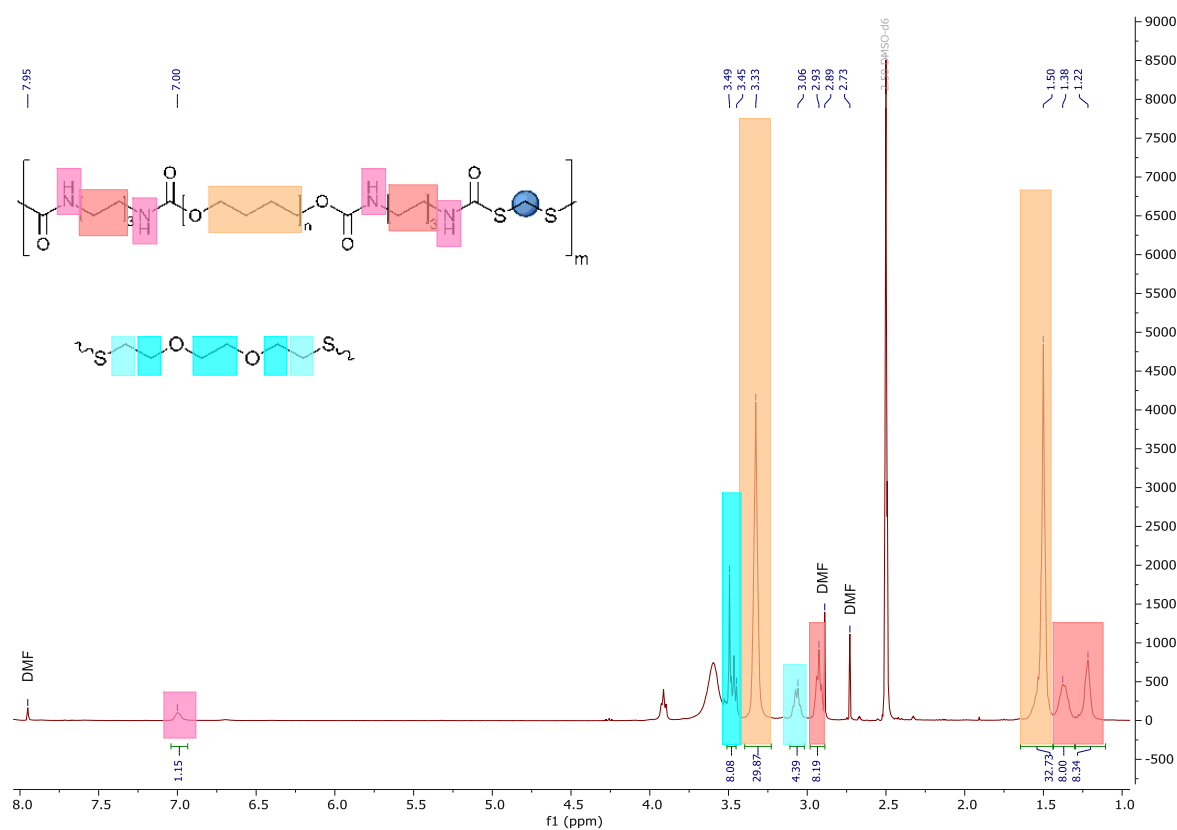
Appendix 19:  $^{13}\text{C}$ -APT-NMR spectrum of 2,2'-(1,4-phenylene)-bis[4-mercaptan-1,3,2-dioxaborolane] (BDB) in DMSO- $d_6$ .



Appendix 20:  $^1\text{H}$ -NMR spectrum of TPUU-BAPDMS in DMSO- $d_6$ .

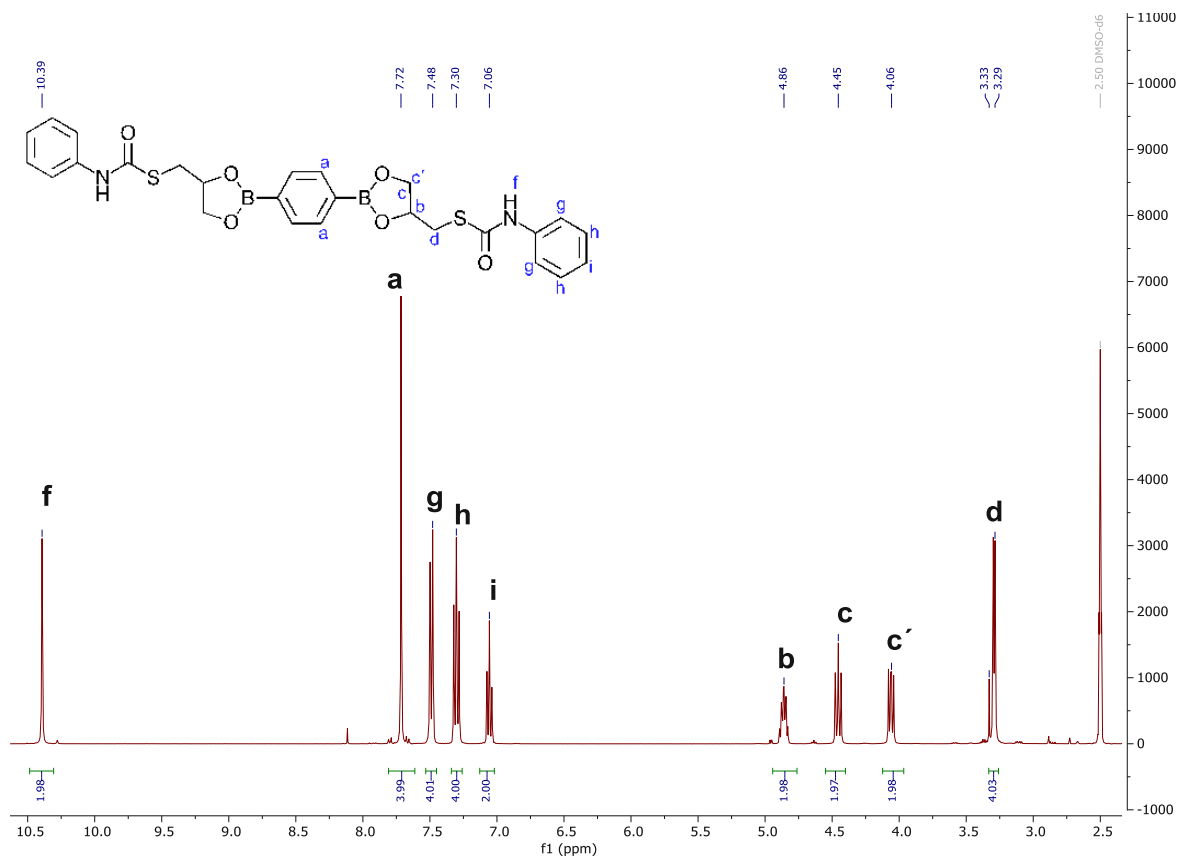


Appendix 21:  $^1\text{H-NMR}$  spectrum of TPTU-BDB in DMSO-d<sub>6</sub>.

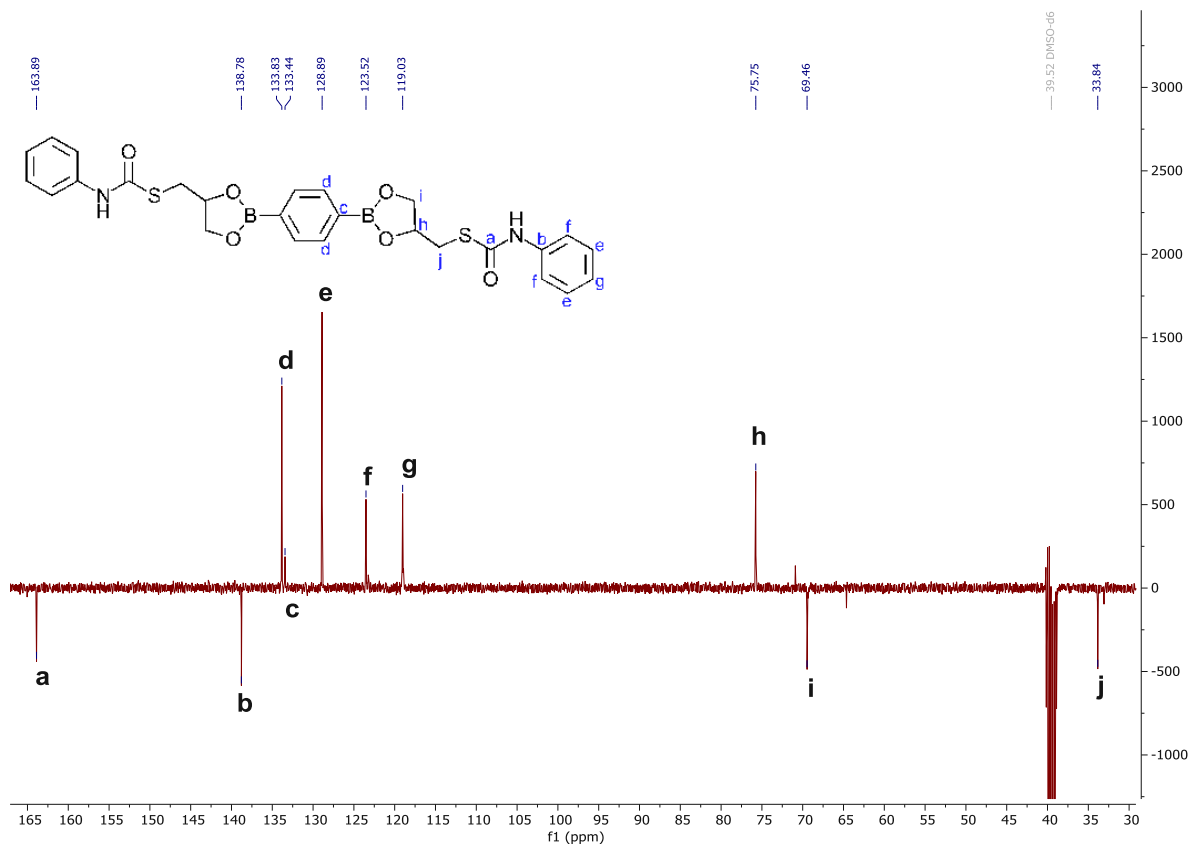


Appendix 22:  $^1\text{H-NMR}$  spectrum of TPTU-BMEE in DMSO-d<sub>6</sub>.

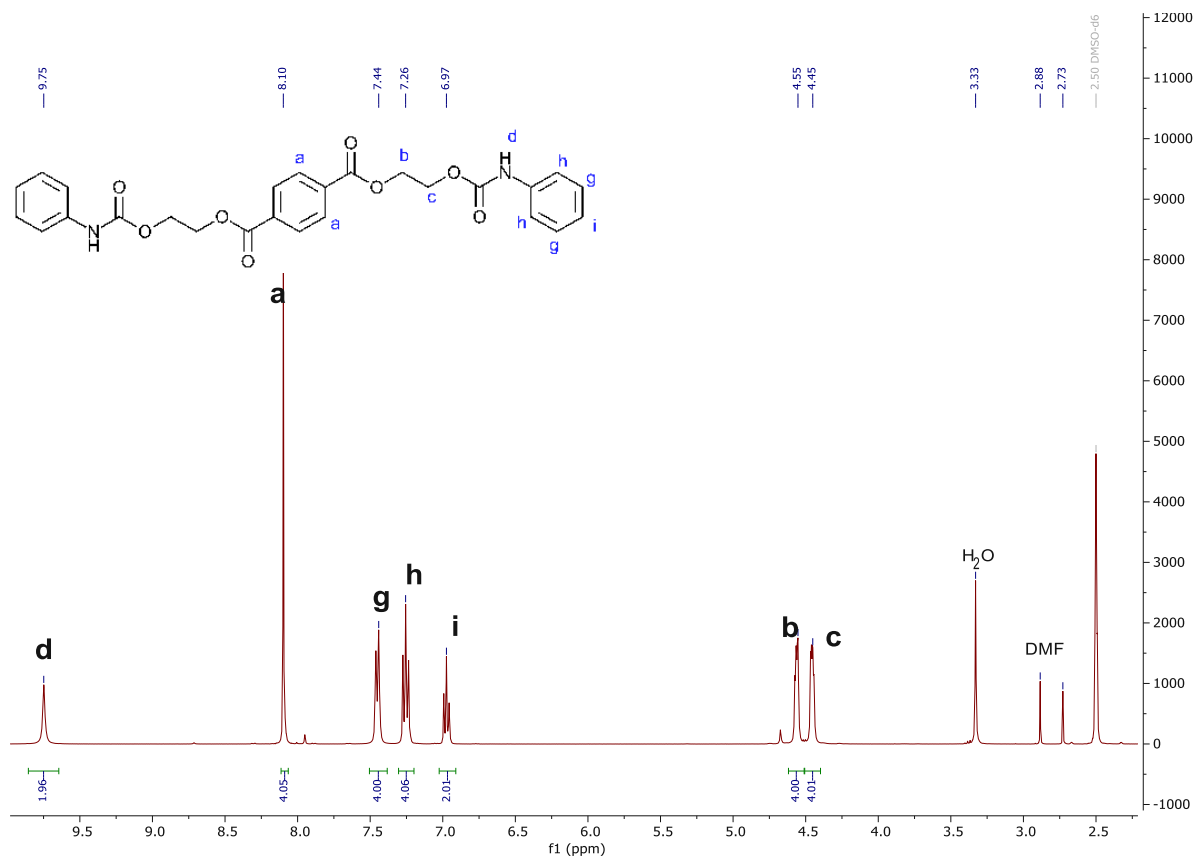




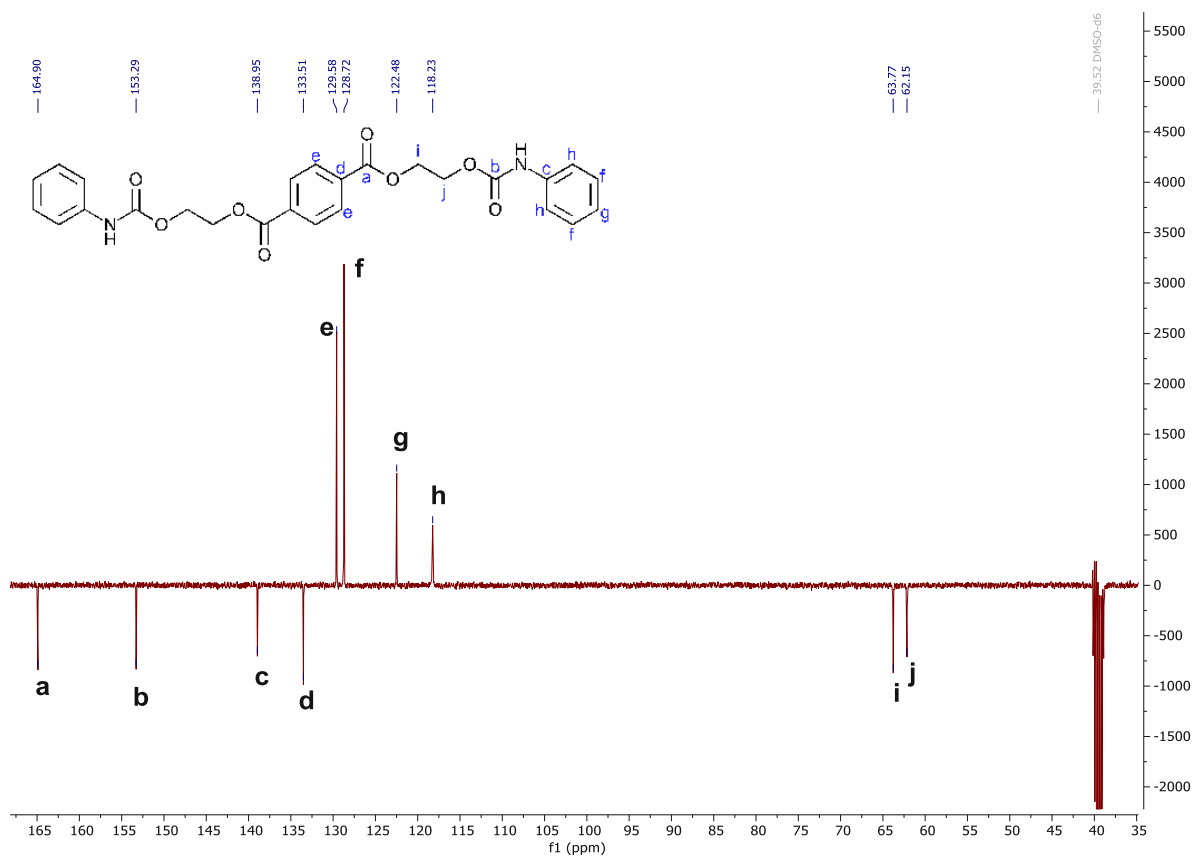
Appendix 23:  $^1\text{H-NMR}$  spectrum of model compound NCO-BDB-NCO in DMSO- $d_6$ .



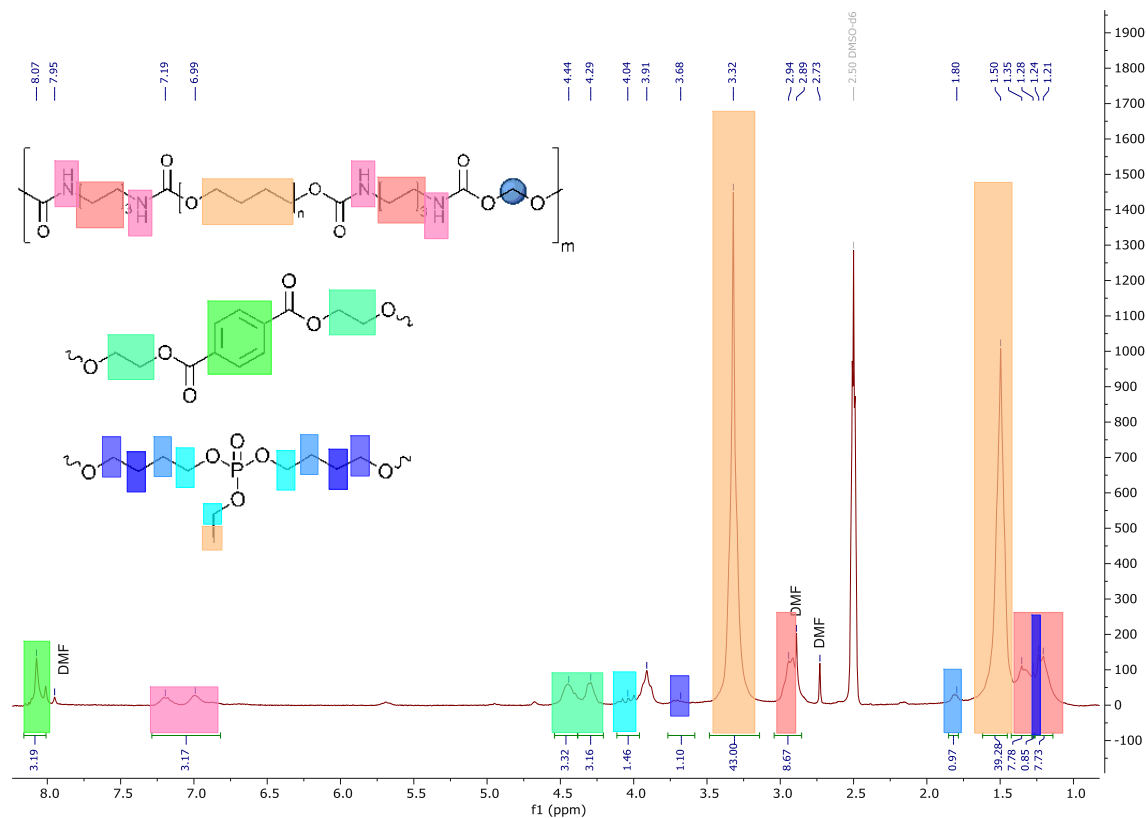
Appendix 24:  $^{13}\text{C-APT-NMR}$  spectrum of model compound NCO-BDB-NCO in DMSO- $d_6$ .



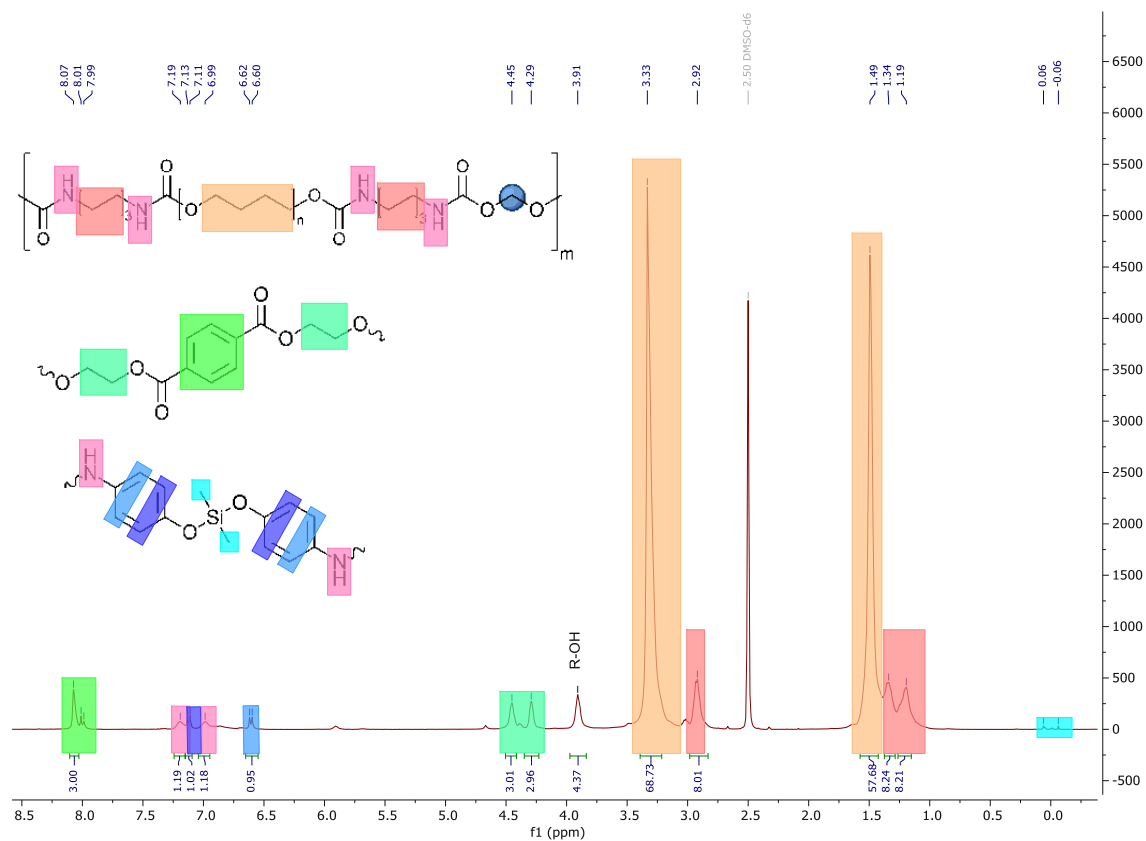
Appendix 25:  $^1\text{H-NMR}$  spectrum of model compound NCO-BHET-NCO in DMSO-d<sub>6</sub>.



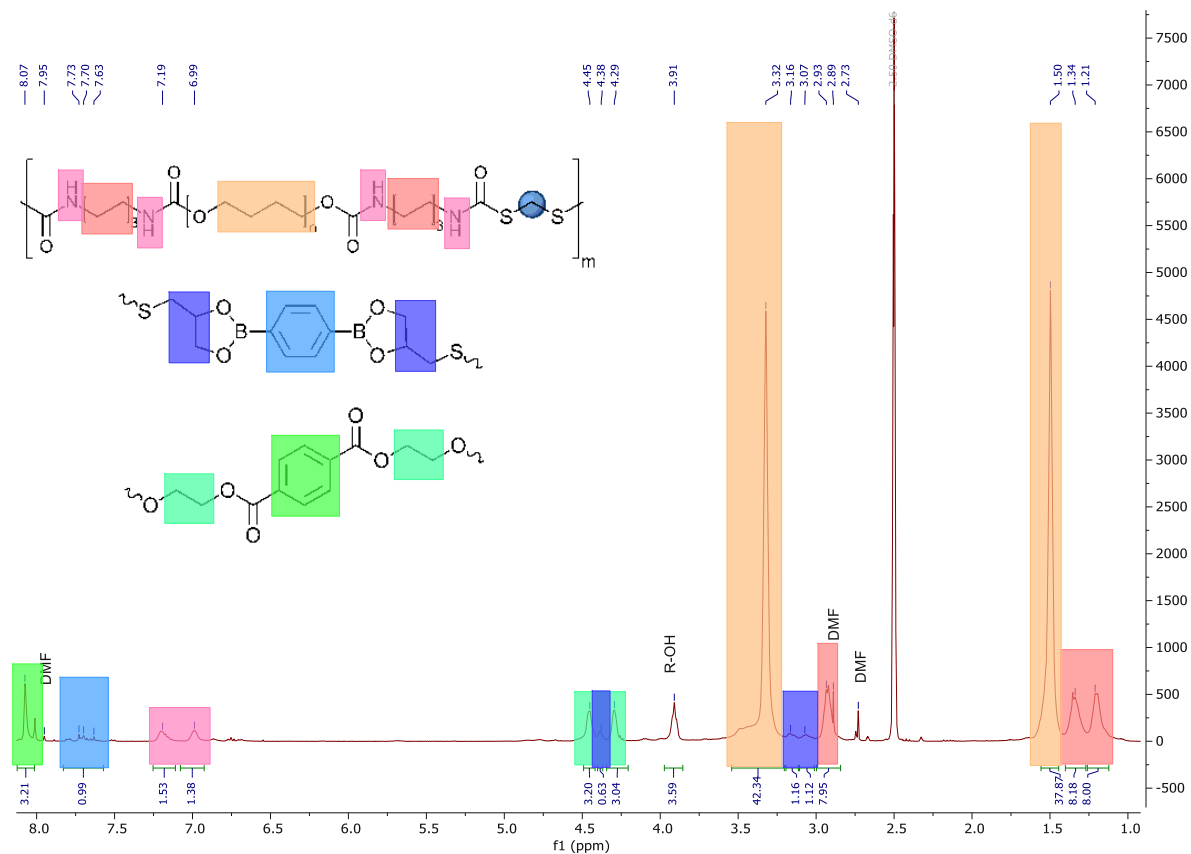
Appendix 26:  $^{13}\text{C-APT-NMR}$  spectrum of model compound NCO-BHET-NCO in DMSO-d<sub>6</sub>.



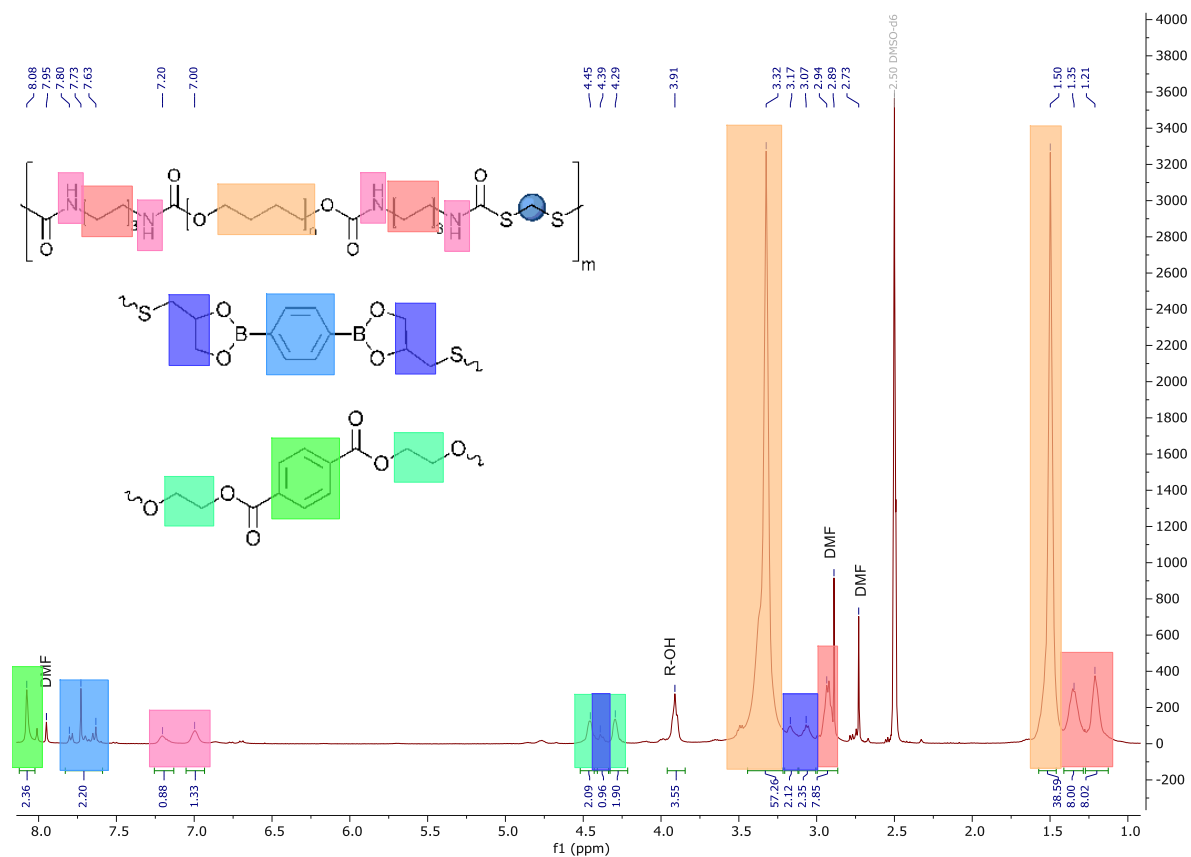
Appendix 27:  $^1\text{H-NMR}$  spectrum of TPU-BHET-BHBEP (75:25) in DMSO- $d_6$ .



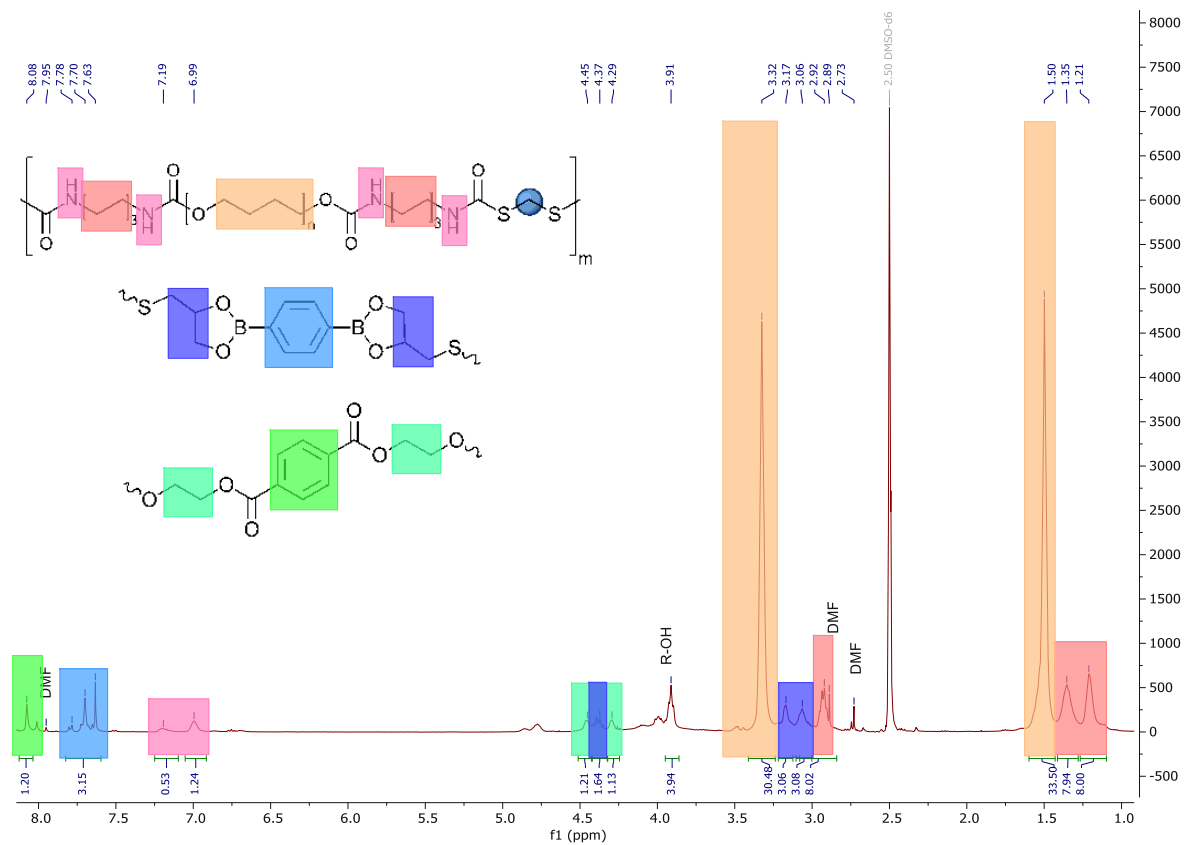
Appendix 28:  $^1\text{H-NMR}$  spectrum of TPU-BHET-BAPDMS (75:25) in DMSO- $d_6$ .



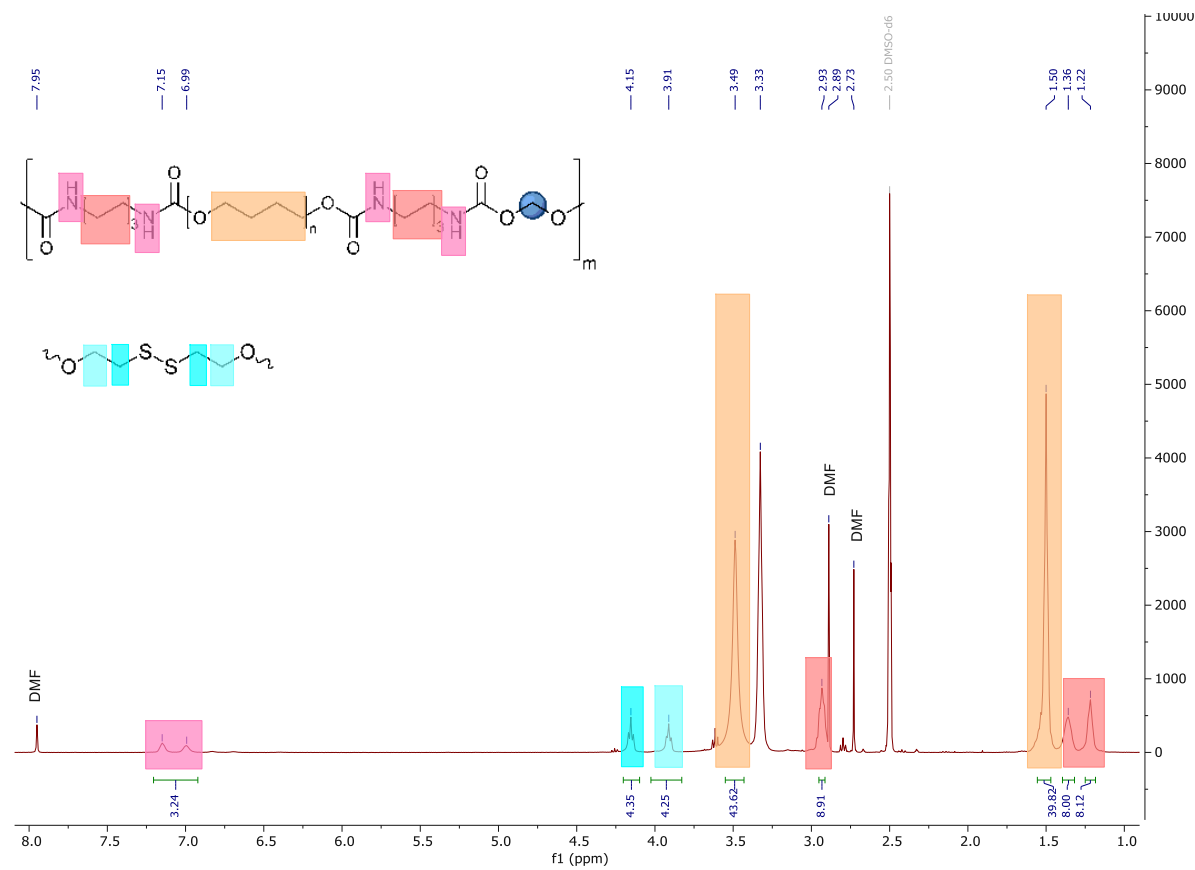
Appendix 29:  $^1\text{H-NMR}$  spectrum of TPU-BHET-BDB (75:25) in DMSO-d<sub>6</sub>.



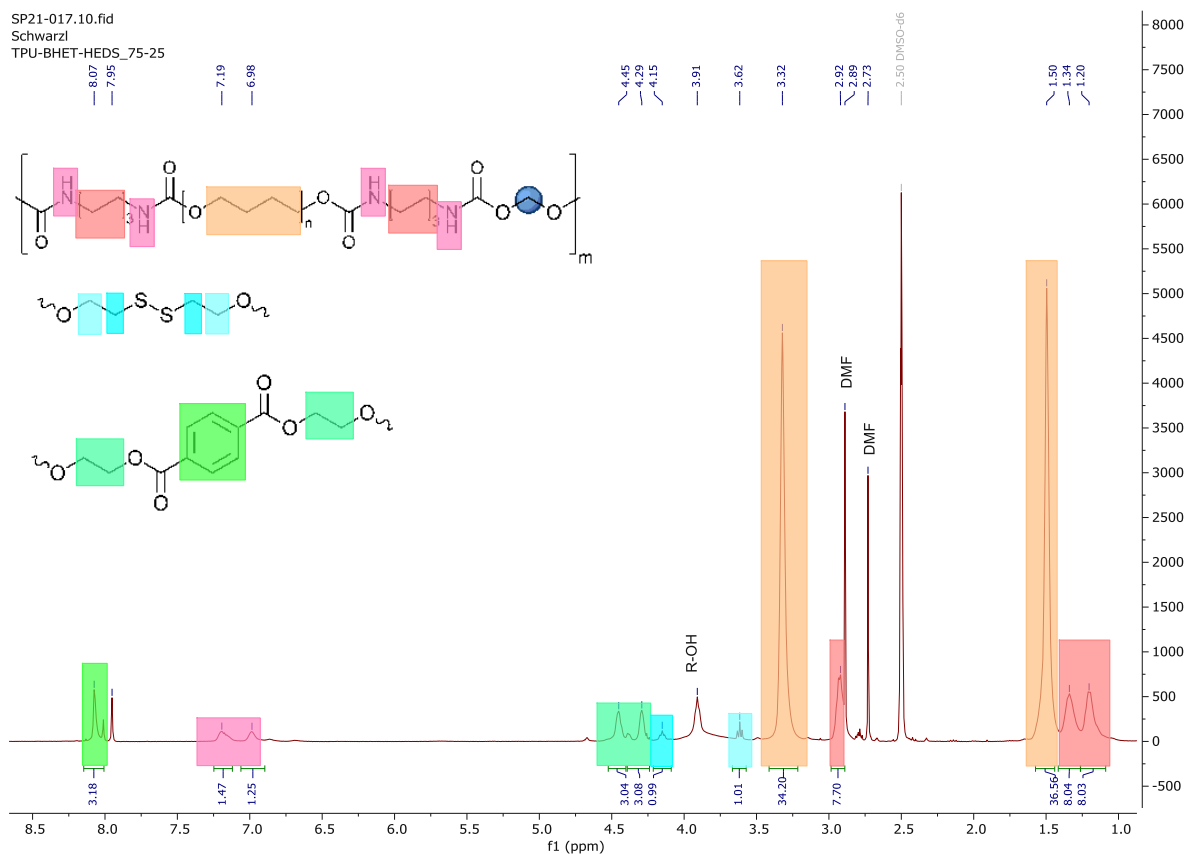
Appendix 30:  $^1\text{H-NMR}$  spectrum of TPU-BHET-BDB (50:50) in DMSO-d<sub>6</sub>.



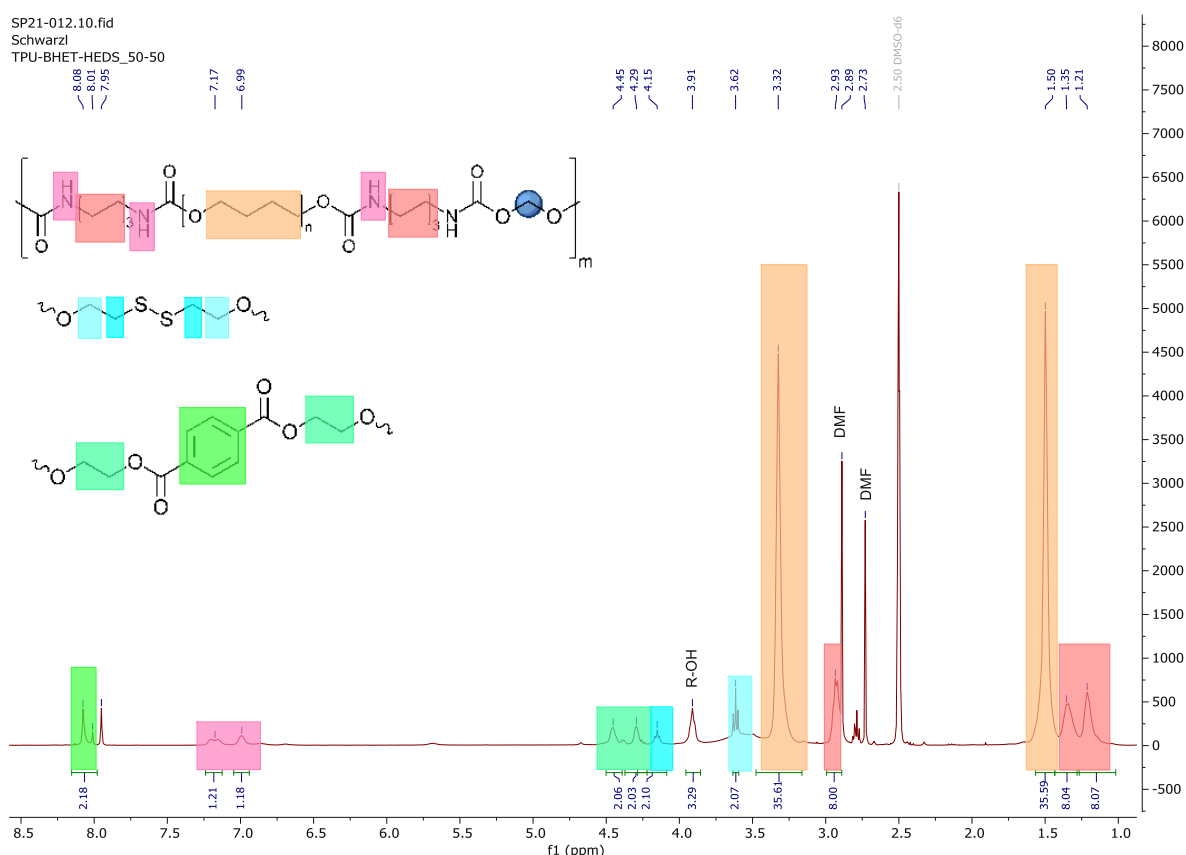
Appendix 31: <sup>1</sup>H-NMR spectrum of TPU-BHET-BDB (25:75) in DMSO-d<sub>6</sub>.



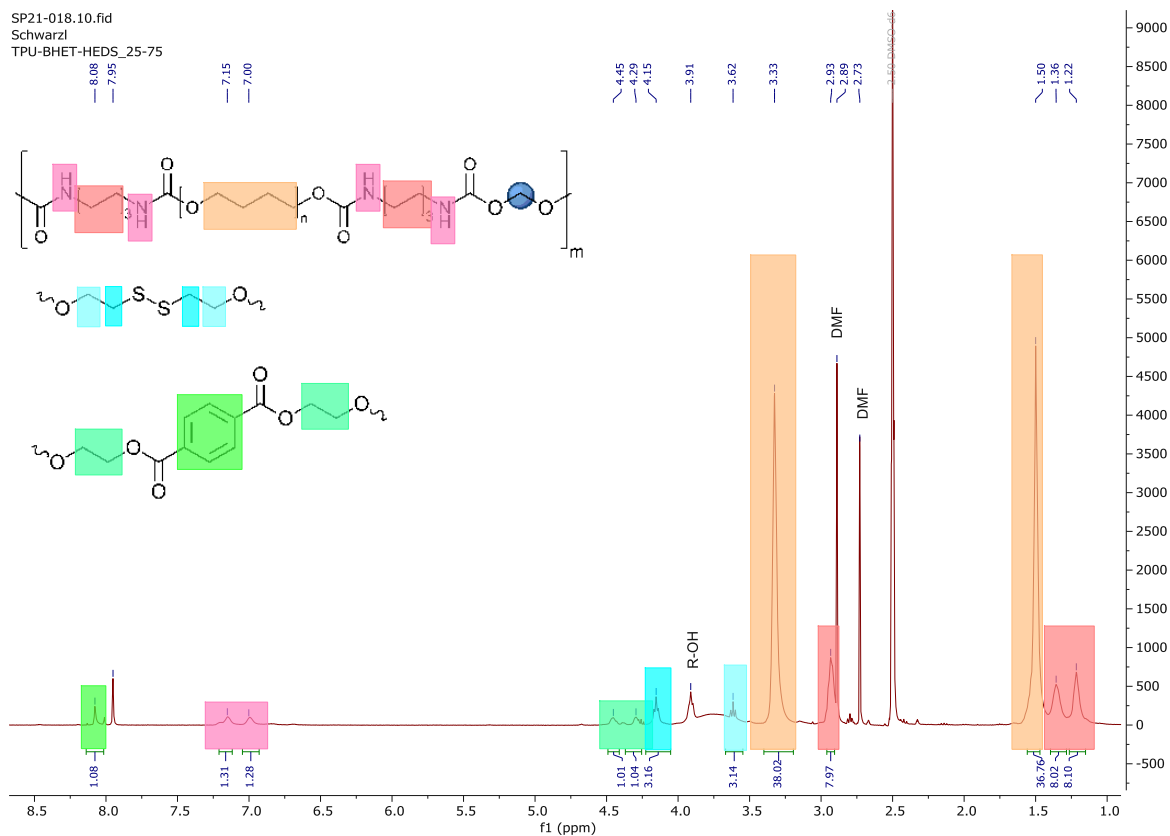
Appendix 32: <sup>1</sup>H-NMR spectrum of TPU-HEDS in DMSO-d<sub>6</sub>.



Appendix 33:  $^1\text{H-NMR}$  spectrum of TPU-BHET-HEDS (75:25) in DMSO-d6.

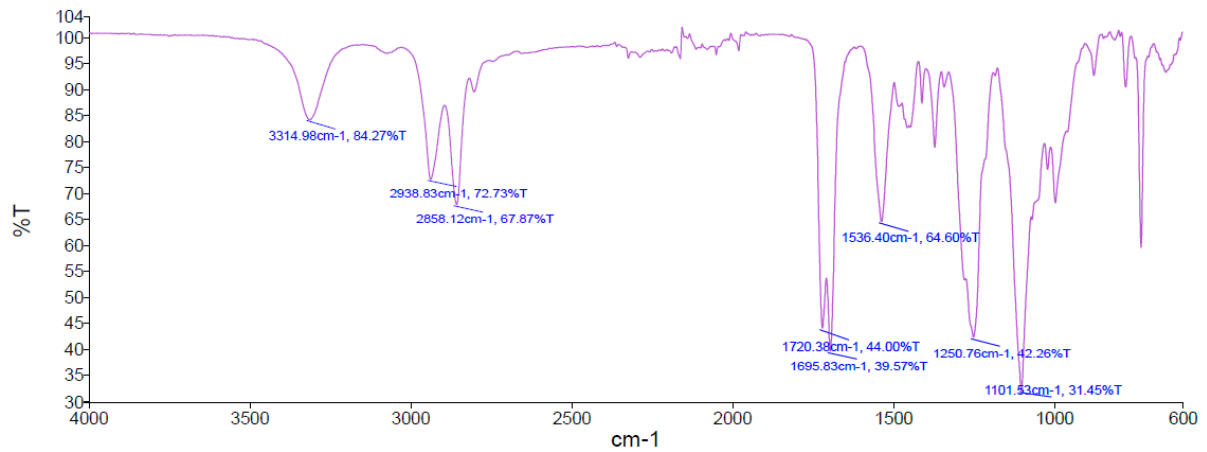


Appendix 34:  $^1\text{H-NMR}$  spectrum of TPU-BHET-HEDS (50:50) in DMSO-d6.

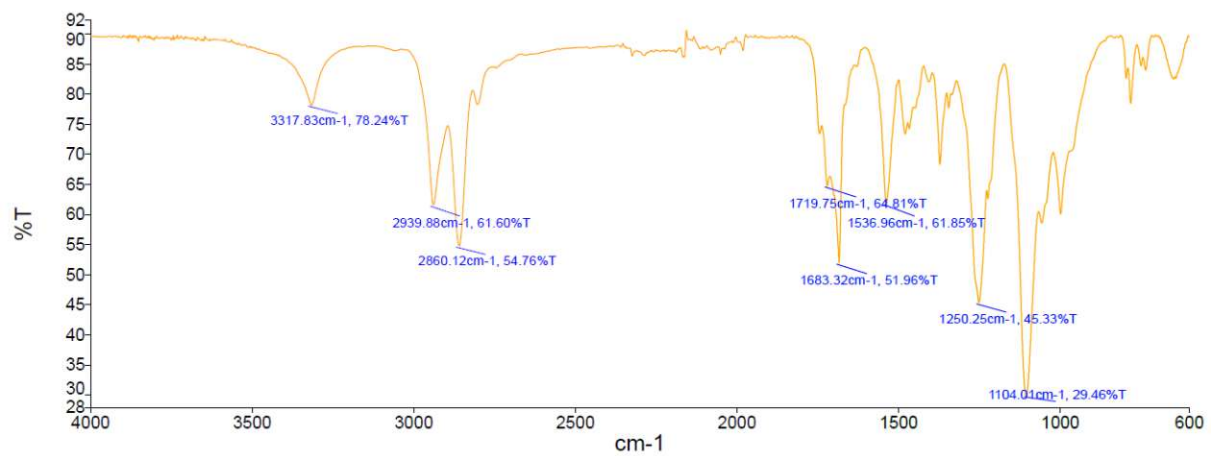


Appendix 35:  $^1\text{H-NMR}$  spectrum of TPU-BHET-HEDS (25:75) in DMSO- $d_6$ .

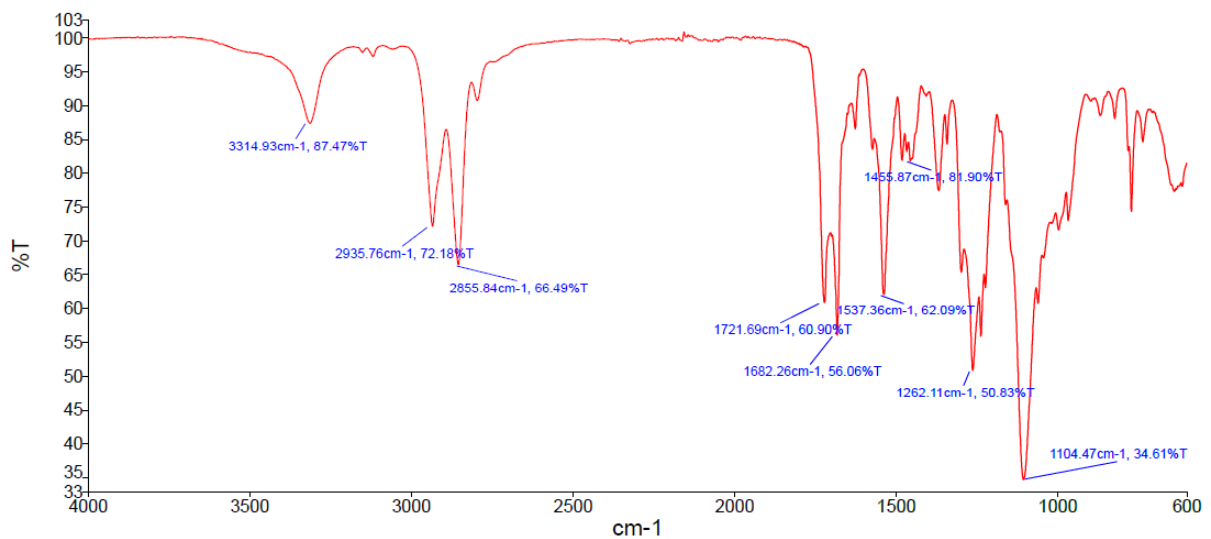
## 2. ATR-FTIR spectra



Appendix 36: FTIR spectrum of TPU-BHET.

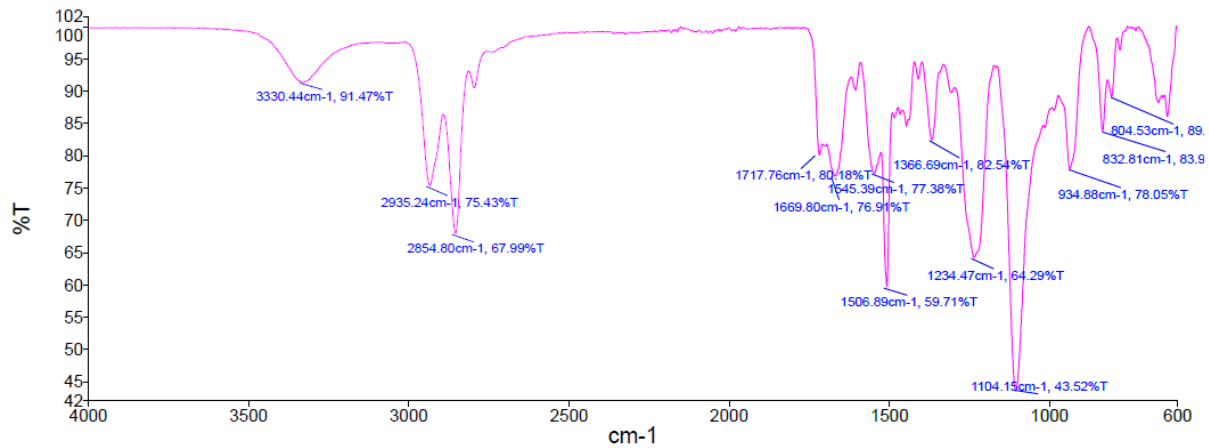


Appendix 37: FTIR spectrum of TPU-BHPC.

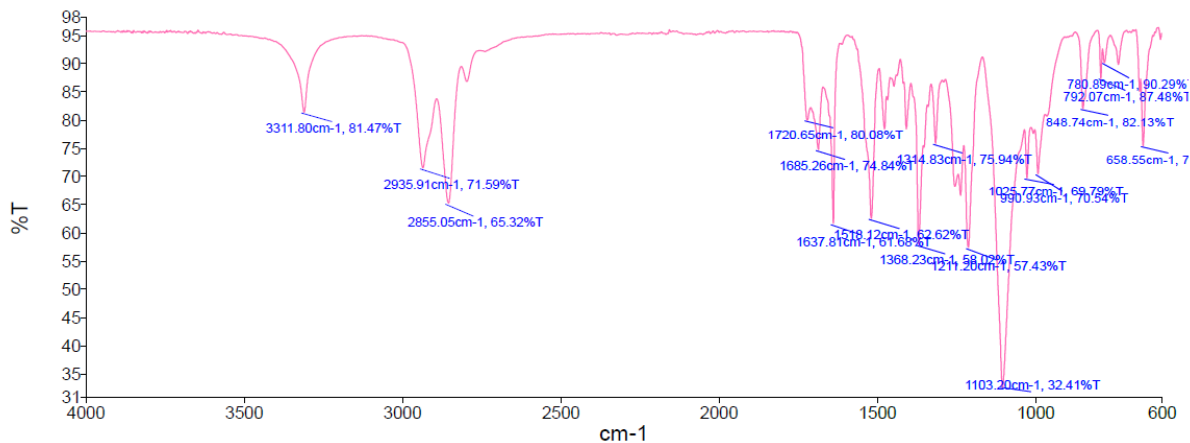


Appendix 38: FTIR spectrum of TPU-BHEF.

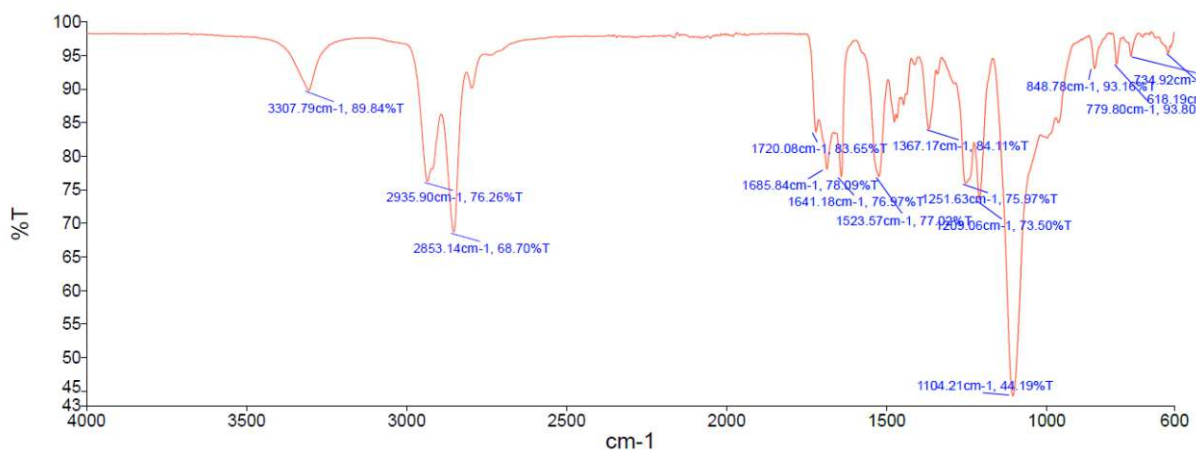




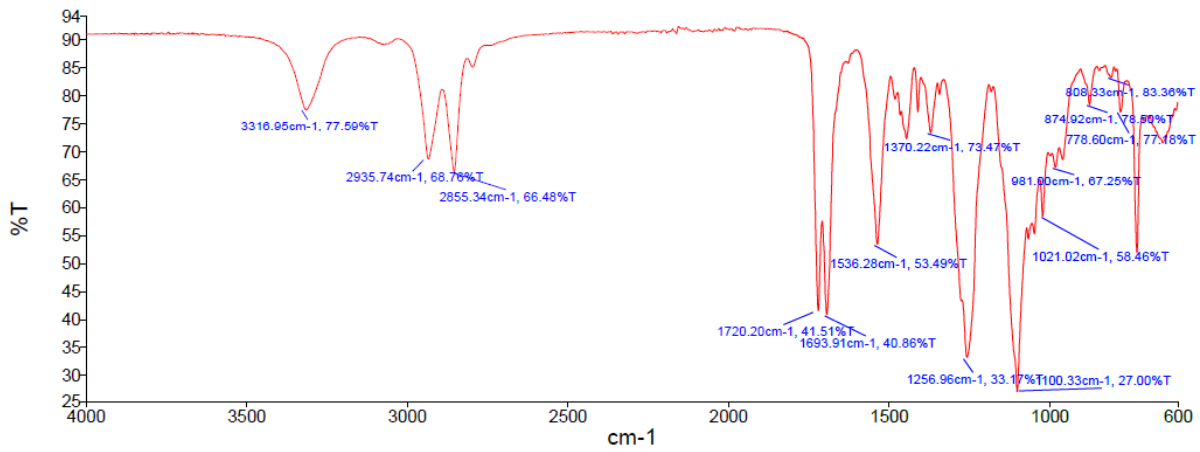
Appendix 39: FTIR spectrum of TPUU-BAPDMS.



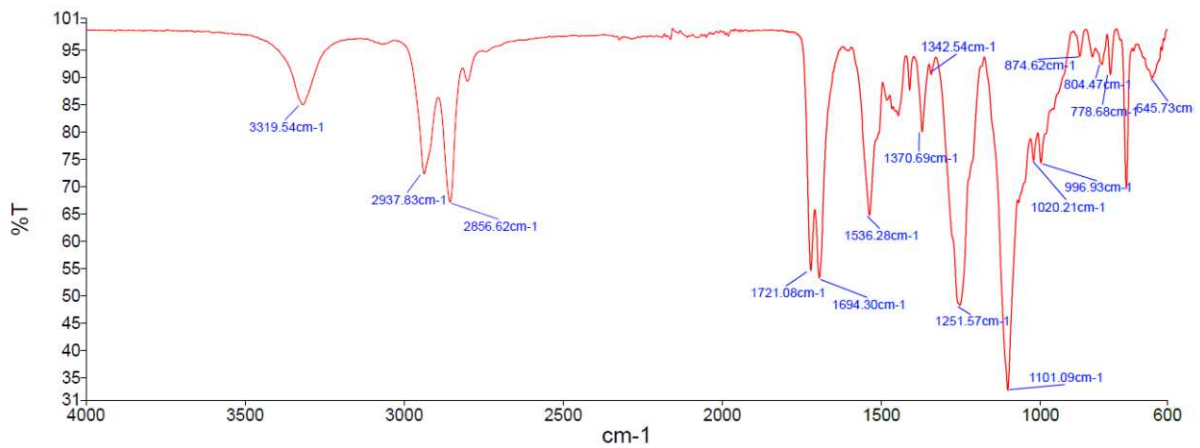
Appendix 40: FTIR spectrum of TPTU-BDB.



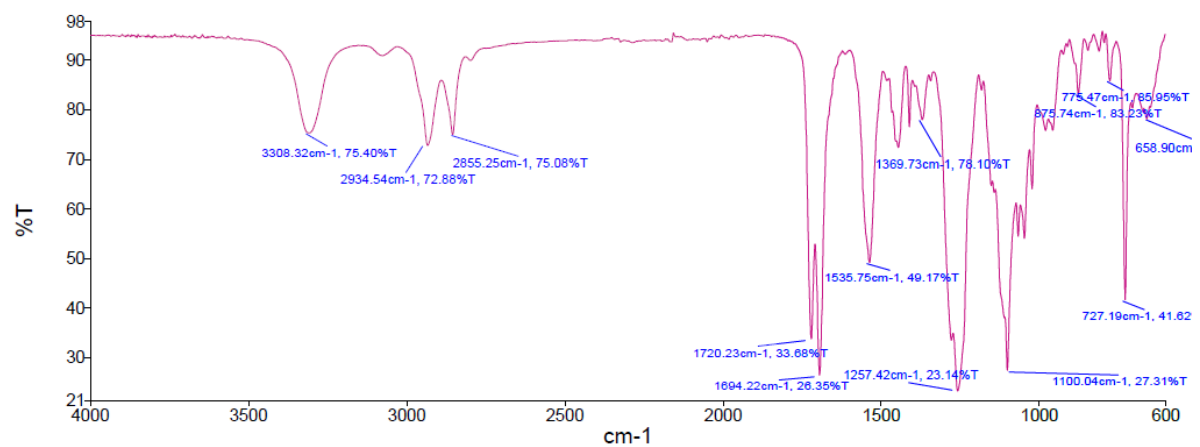
Appendix 41: FTIR spectrum of TPTU-BMEE.



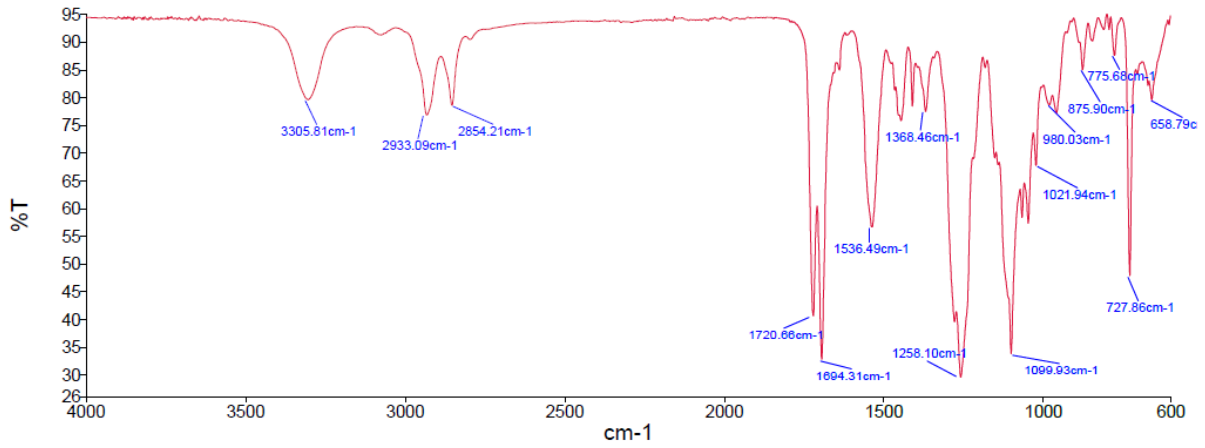
Appendix 42: FTIR spectrum of TPU-BHET-BHBEP (75:25).



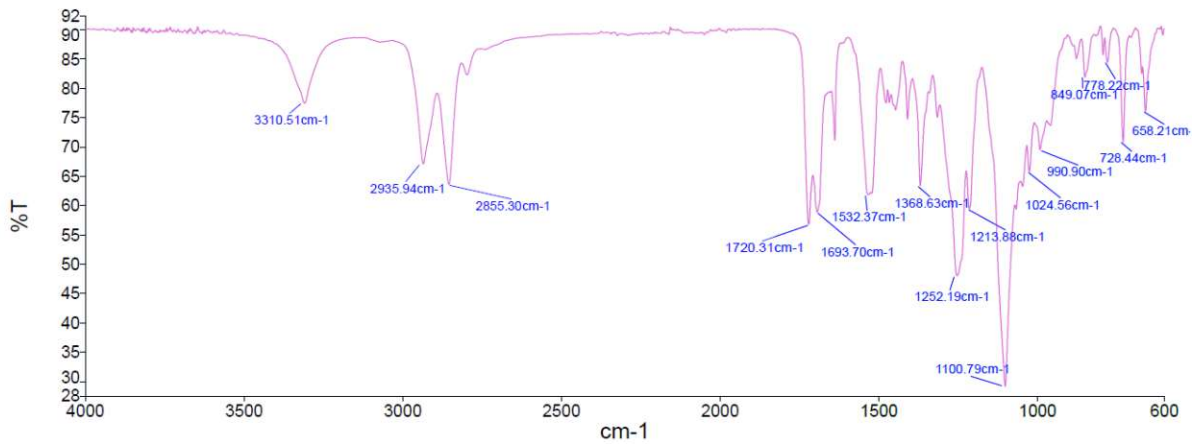
Appendix 43: FTIR spectrum of TPU-BHET-BAPDMS (75:25).



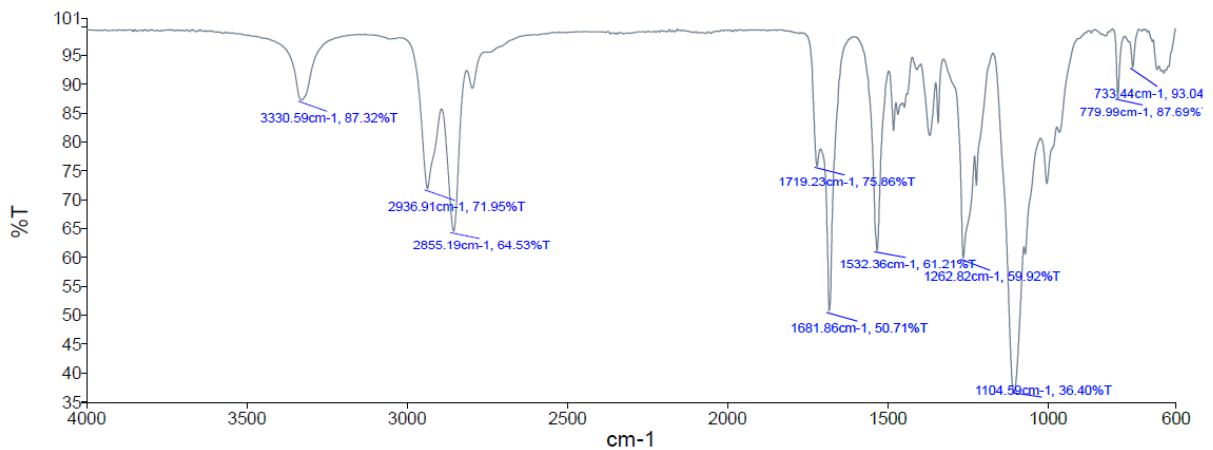
Appendix 44: FTIR spectrum of TPU-BHET-BDB (75:25).



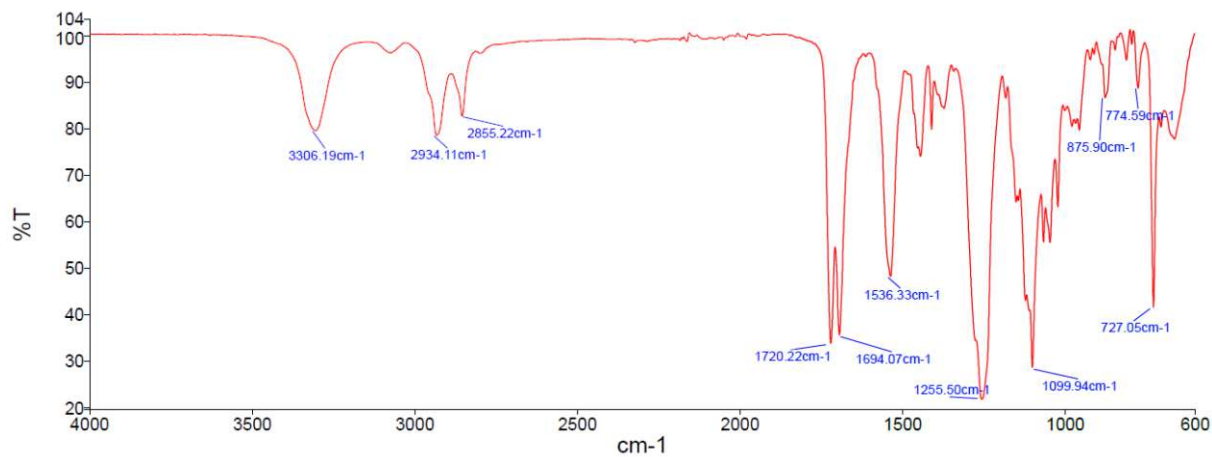
Appendix 45: FTIR spectrum of TPU-BHET-BDB (50:50).



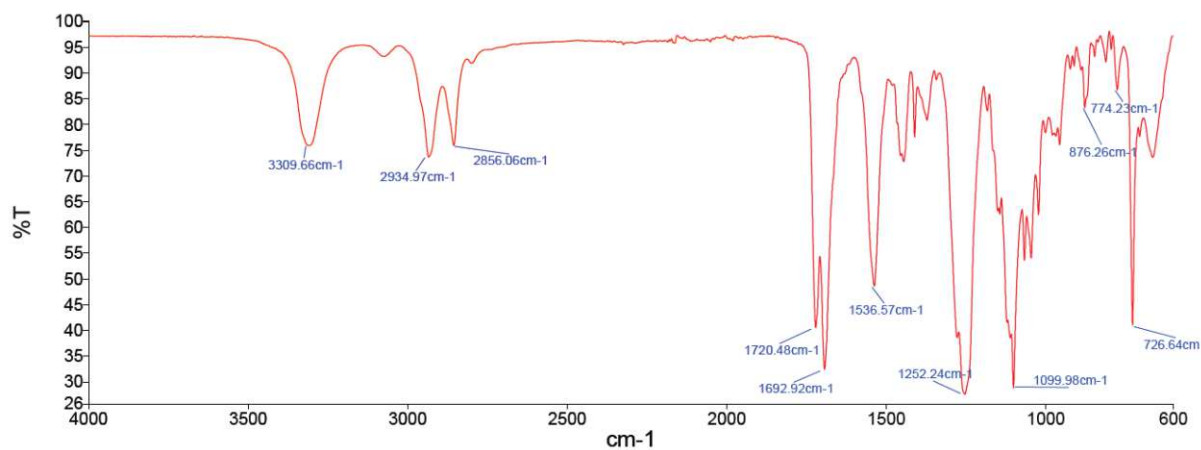
Appendix 46: FTIR spectrum of TPU-BHET-BDB (25:75).



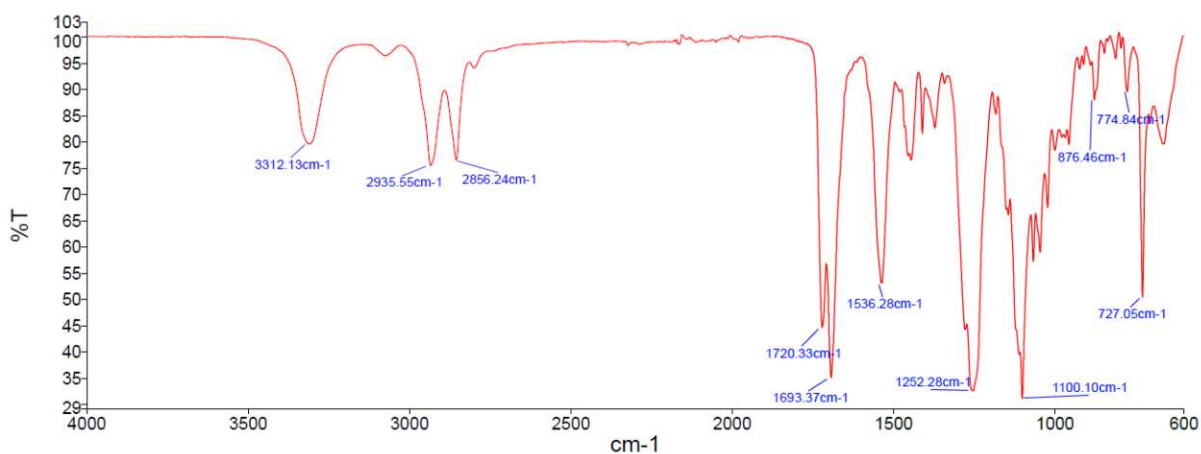
Appendix 47: FTIR spectrum of TPU-HEDS.



Appendix 48: FTIR spectrum of TPU-BHET-HEDS (75:25).

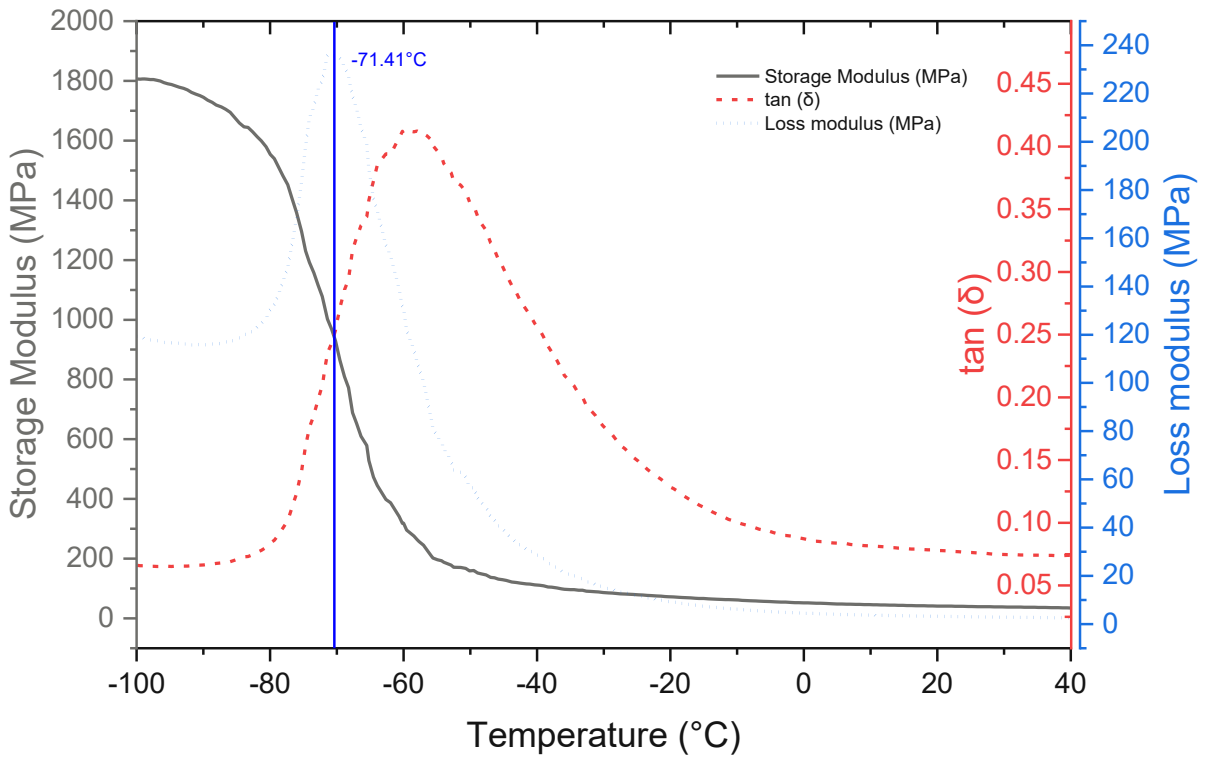


Appendix 49: FTIR spectrum of TPU-BHET-HEDS (50:50).

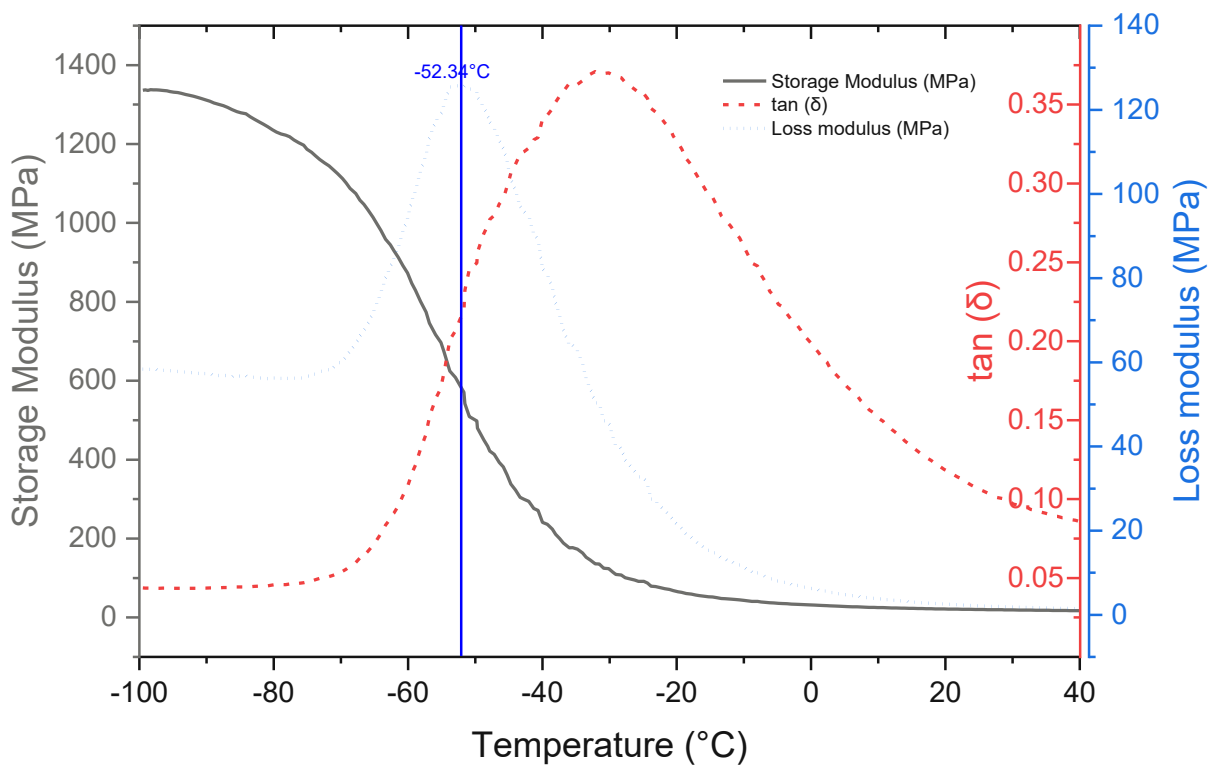


Appendix 50: FTIR spectrum of TPU-BHET-HEDS (25:75).

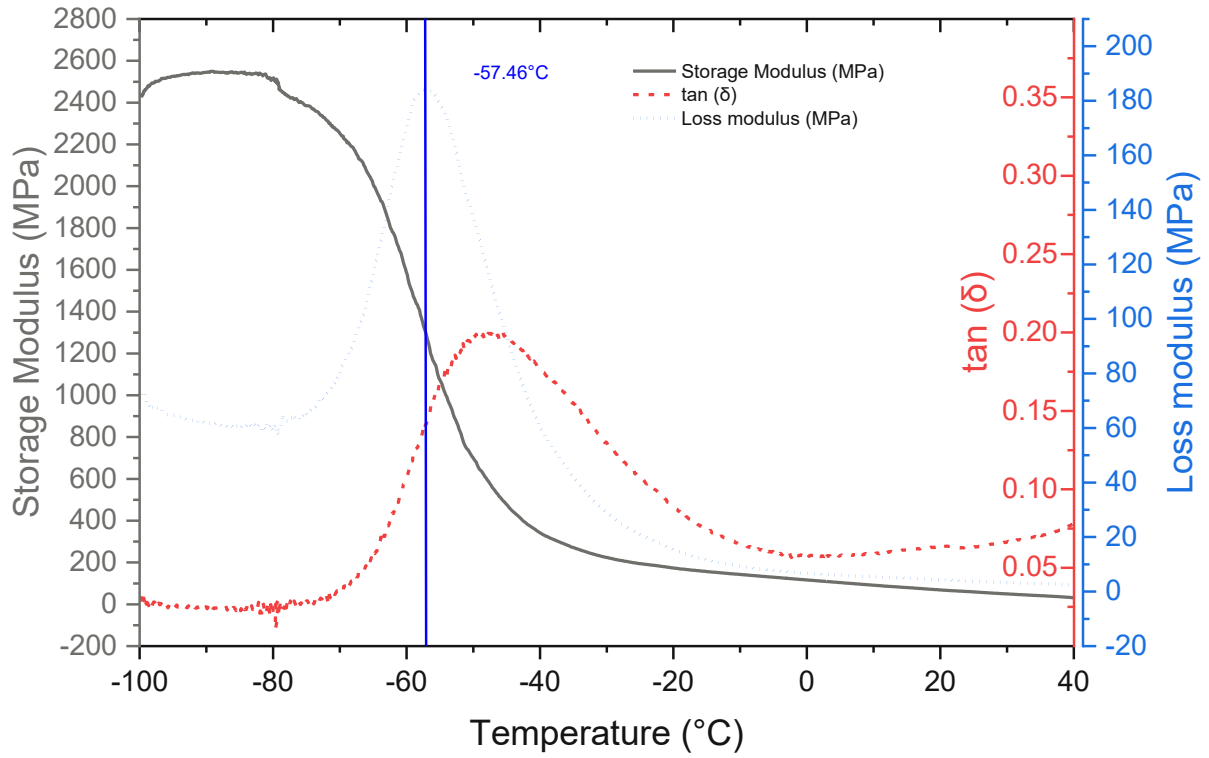
### 3. DMTA spectra



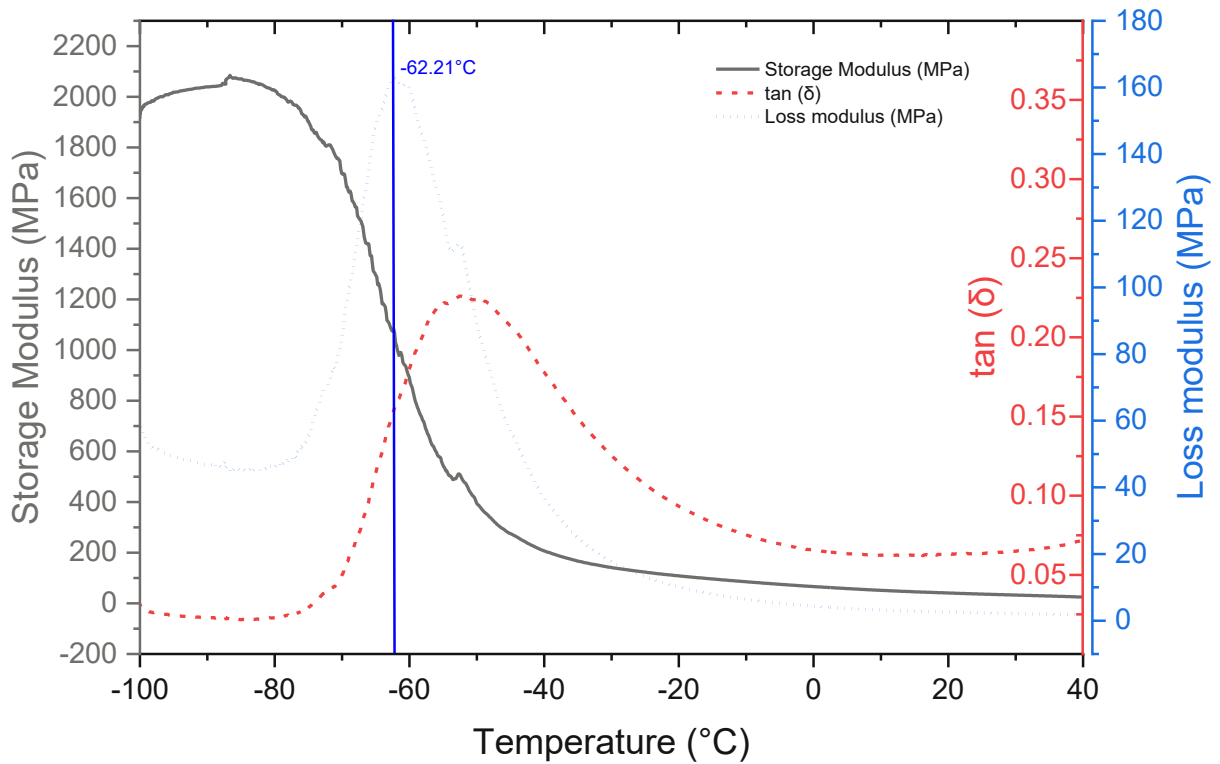
Appendix 51: DMTA of TPU-BHET.



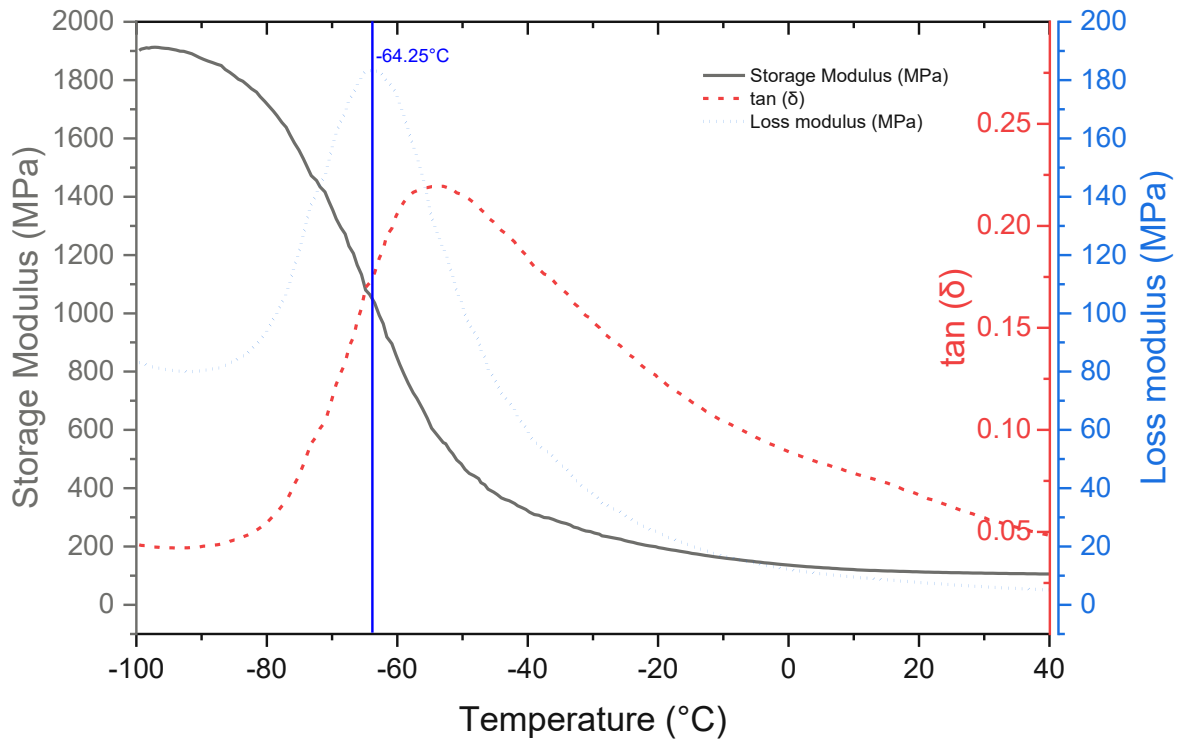
Appendix 52: DMTA of Pellethane.



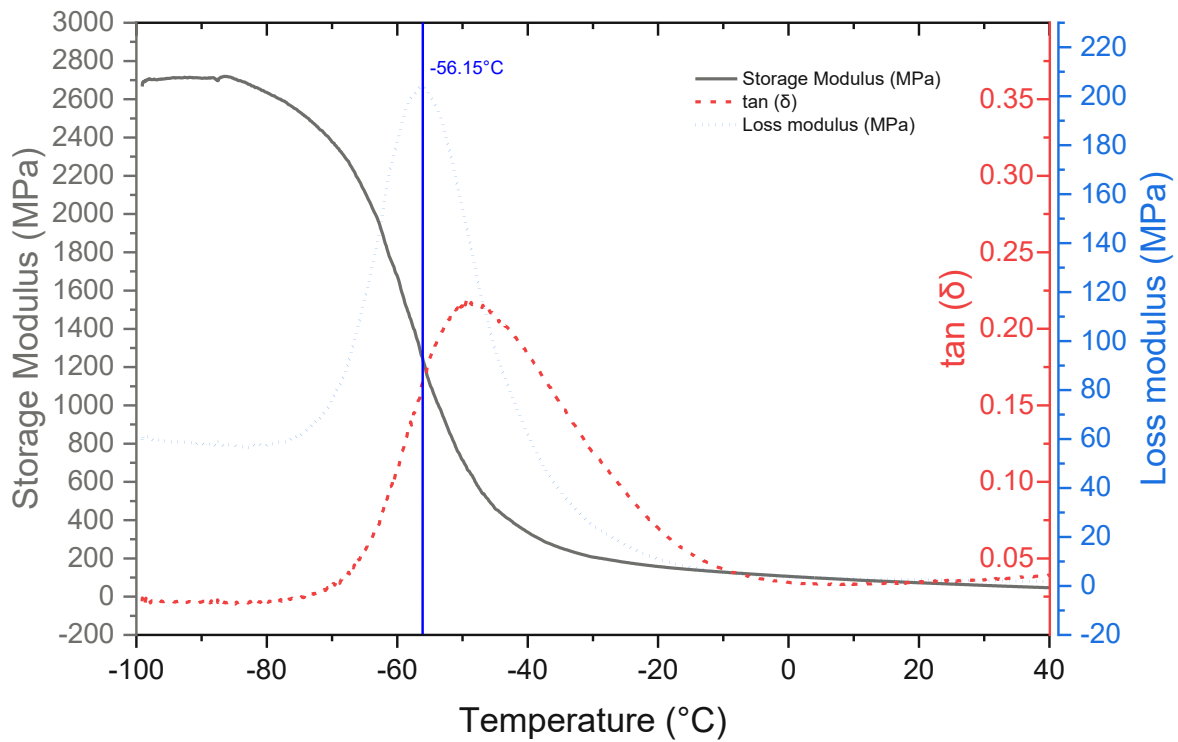
Appendix 53: DMTA of TPU-BHPC.



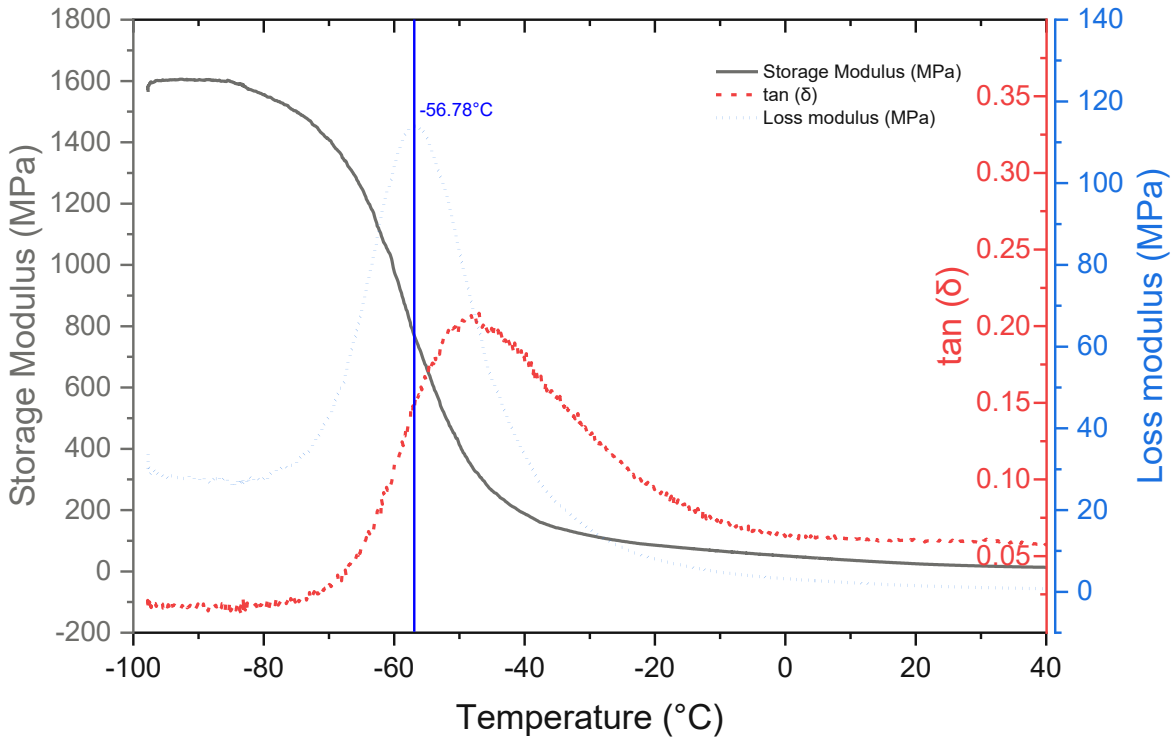
Appendix 54: DMTA of TPU-BHEF.



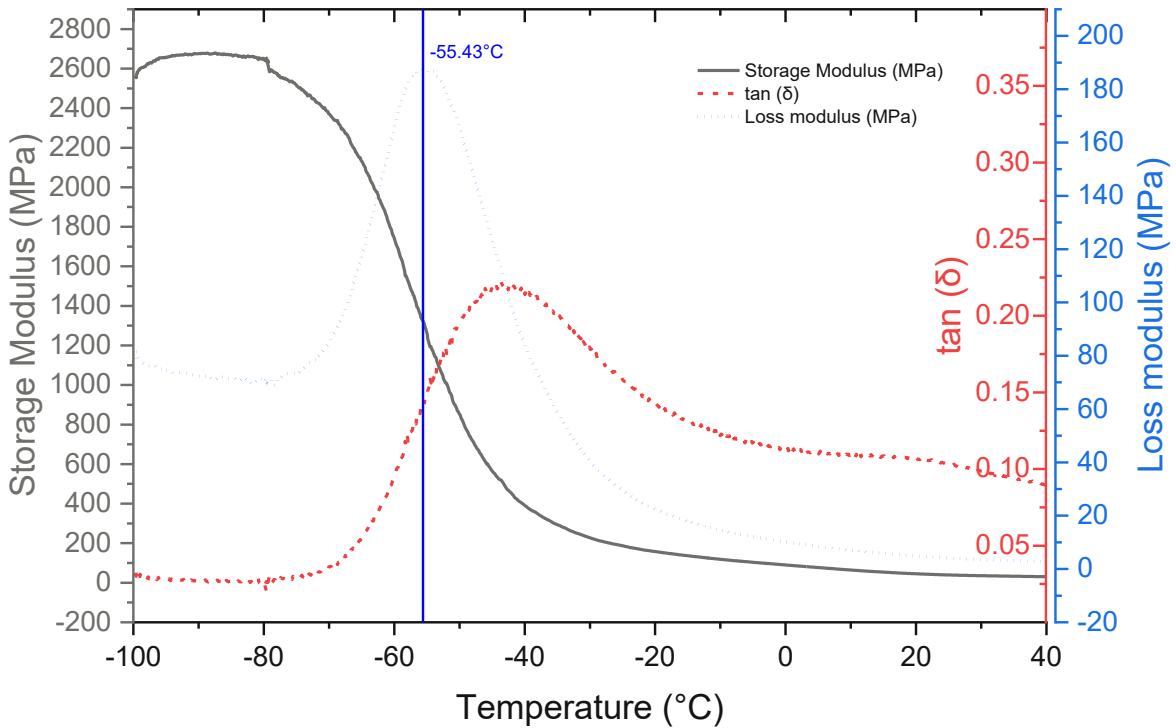
Appendix 55: DMTA of TPTU-BDB.



Appendix 56: DMTA of TPTU-BMEE.

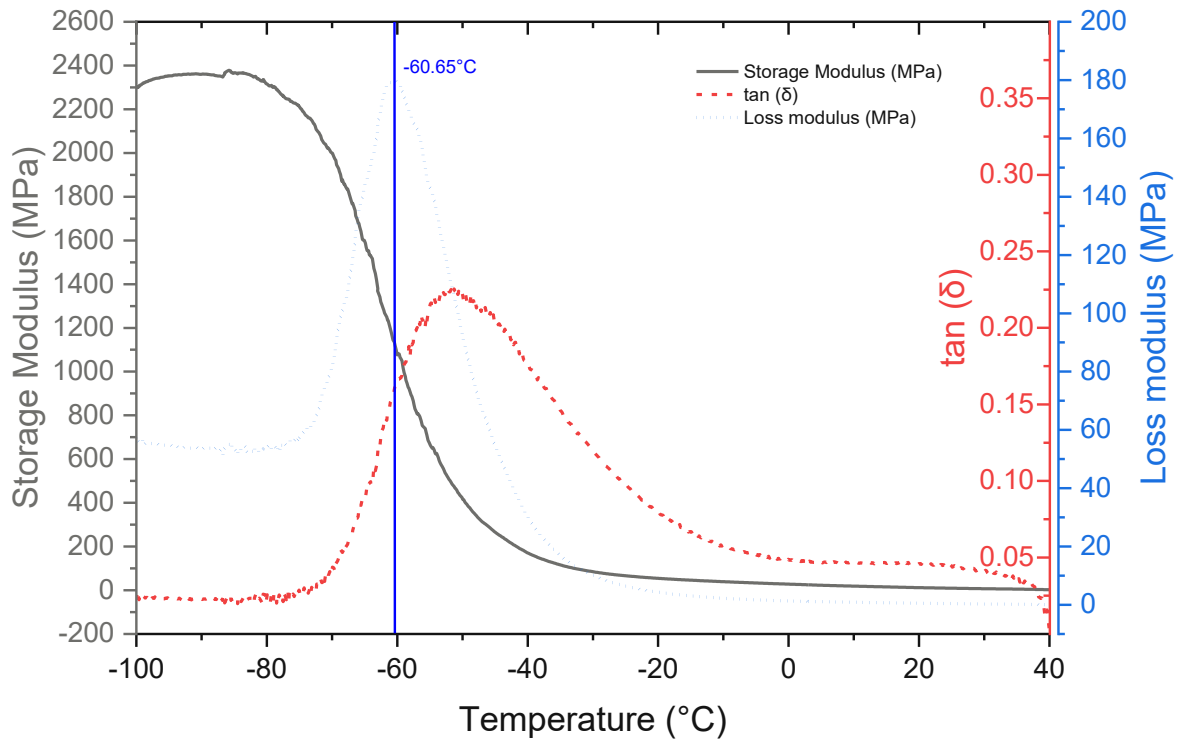


Appendix 57: DMTA of TPU-BHET-BHBEP (75:25).

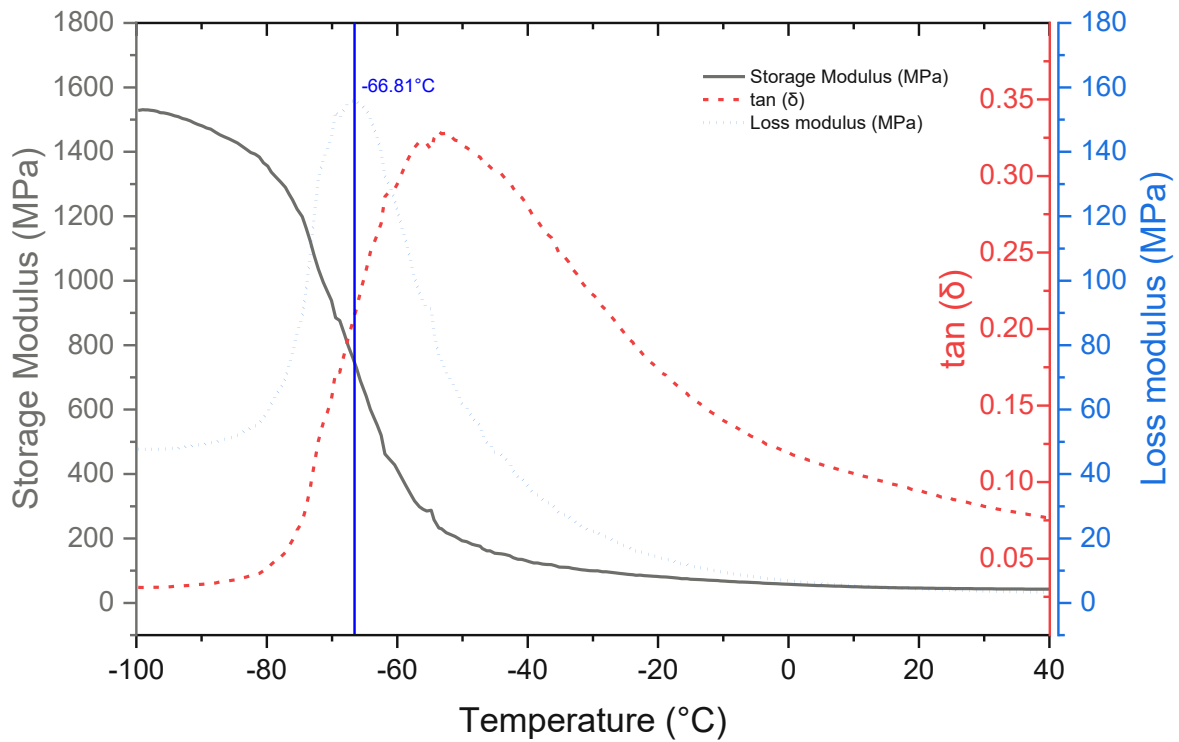


Appendix 58: DMTA of TPU-BHET-BAPDMS (75:25).

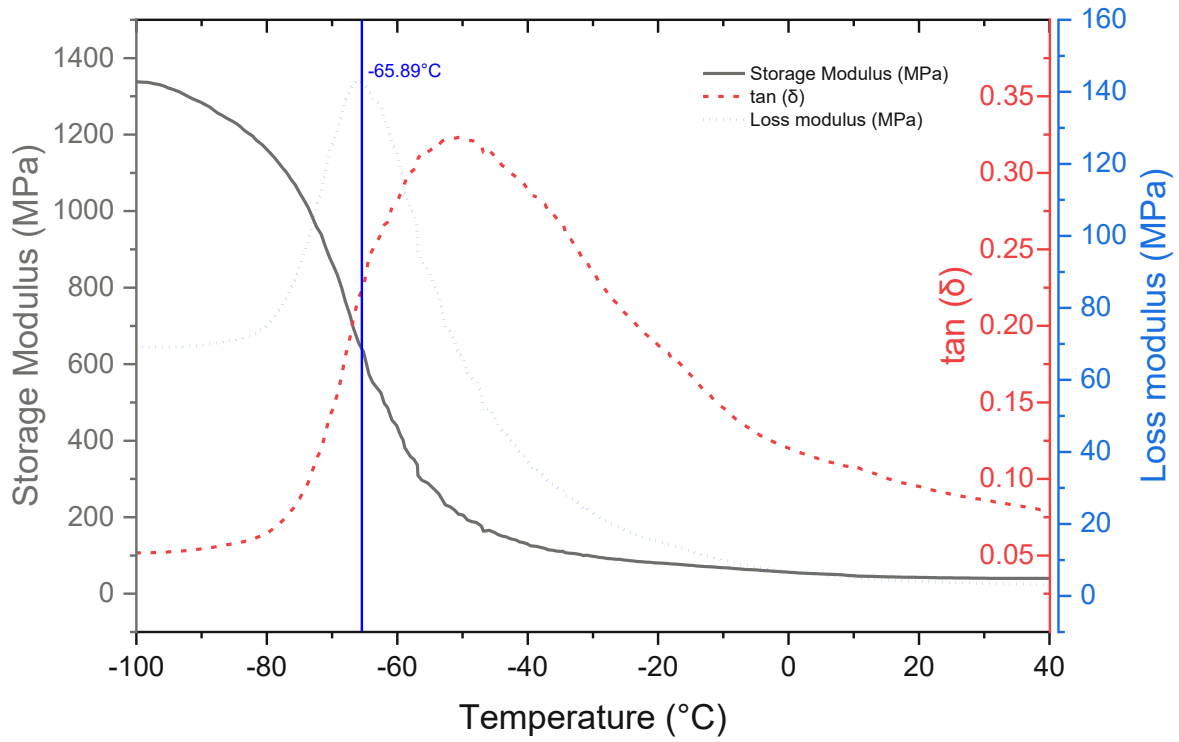




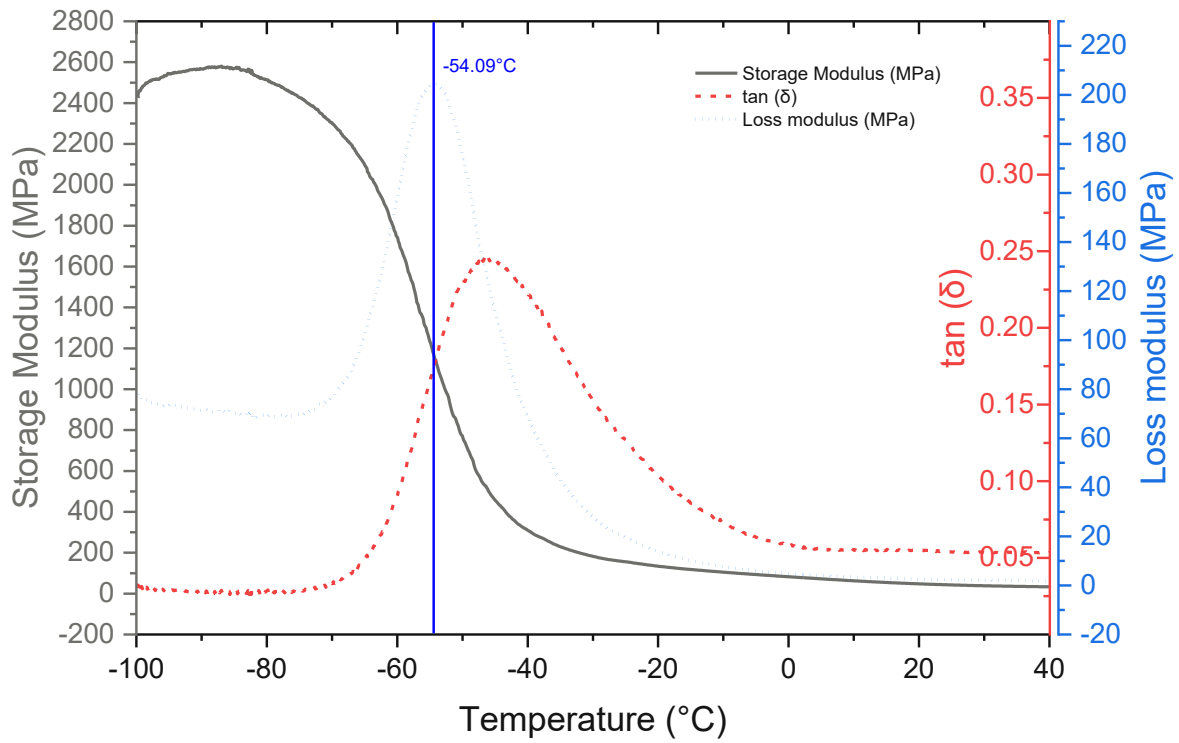
Appendix 59: DMTA of TPU-BHET-BDB (75:25).



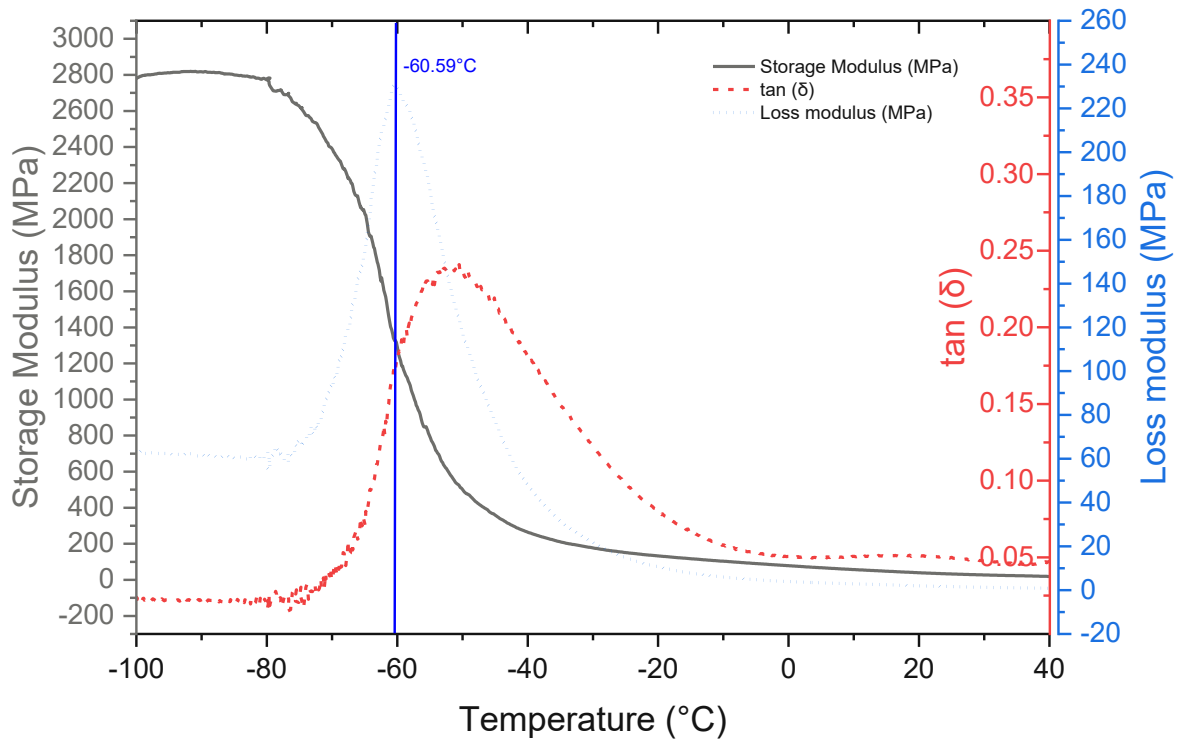
Appendix 60: DMTA of TPU-BHET-BDB (50:50).



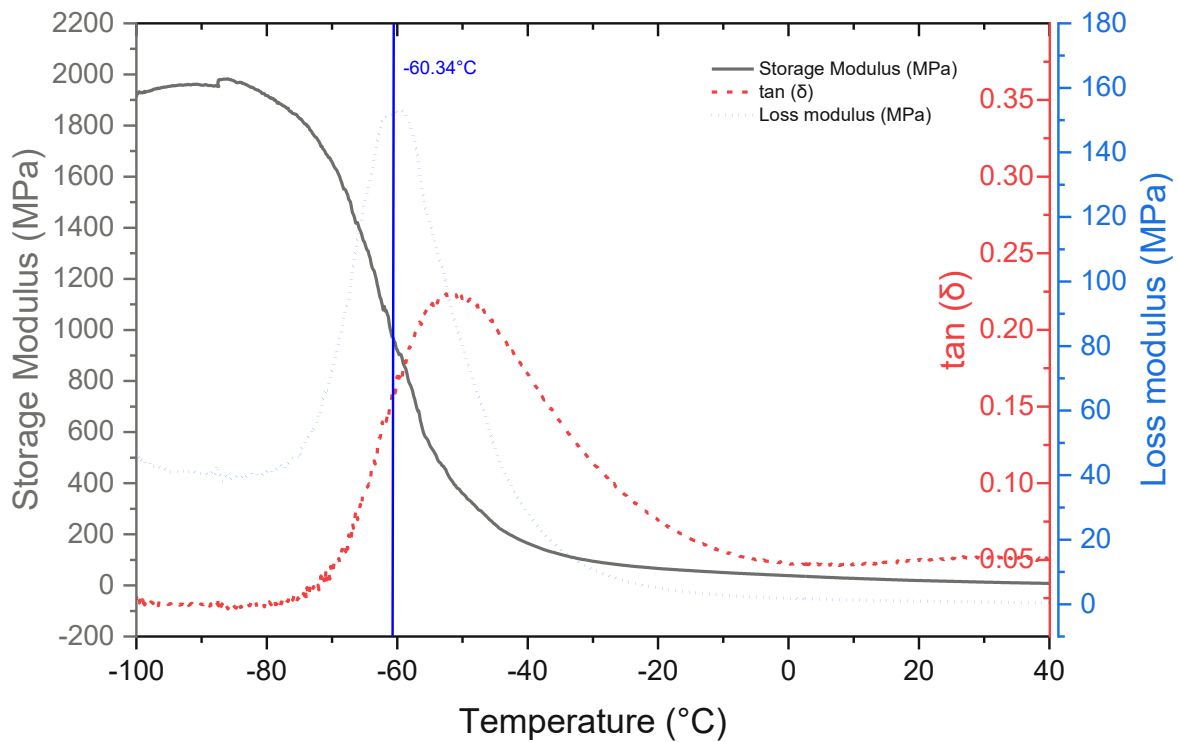
Appendix 61: DMTA of TPU-BHET-BDB (25:75).



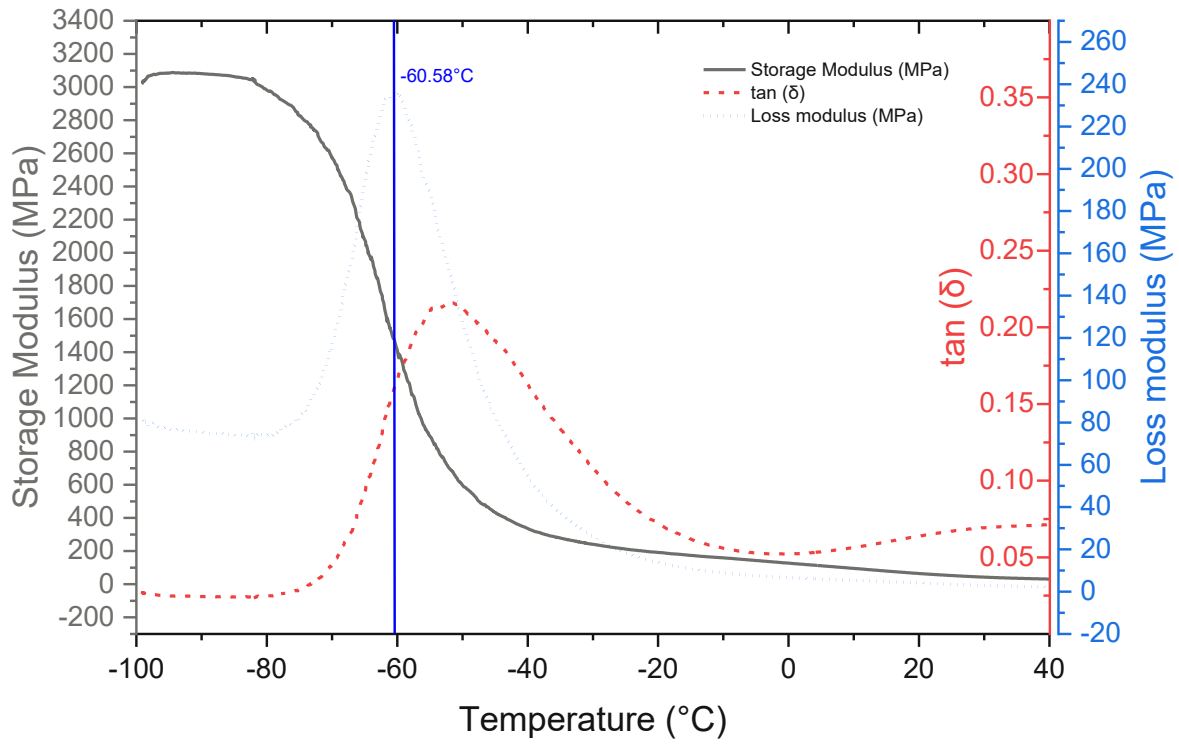
Appendix 62: DMTA of TPU-HEDES.



Appendix 63: DMTA of TPU-BHET-HEDS (75:25).

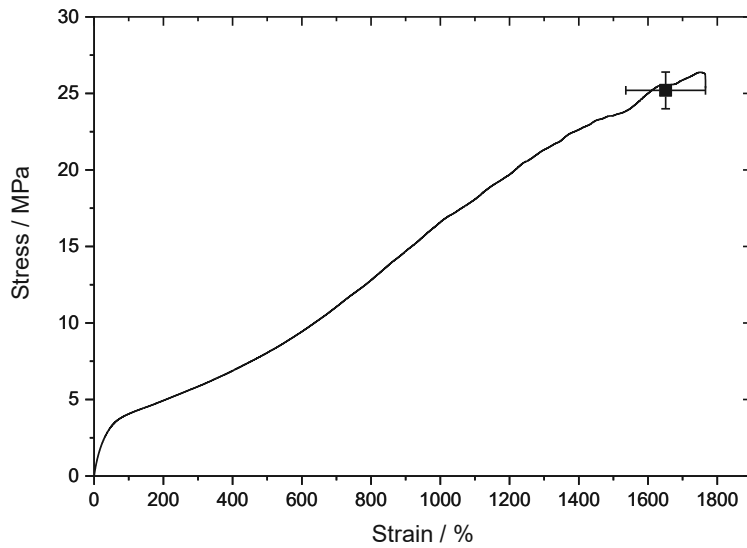


Appendix 64: DMTA of TPU-BHET-HEDS (50:50).

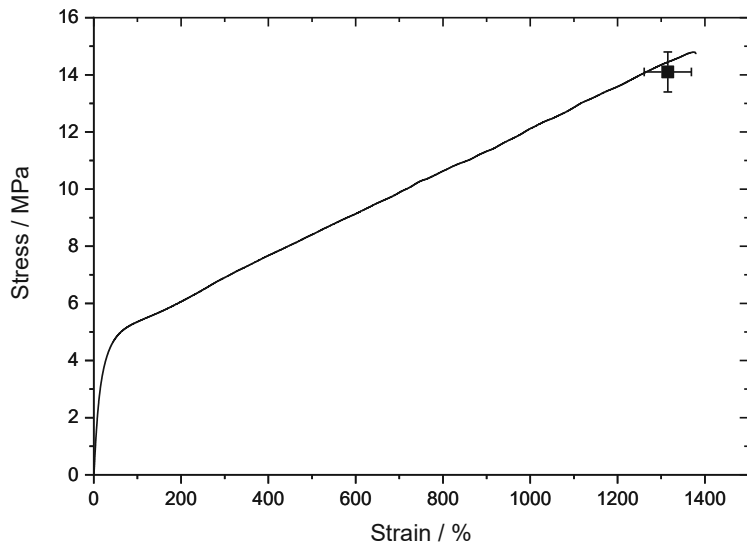


Appendix 65: DMTA of TPU-BHET-HEDS (25:75).

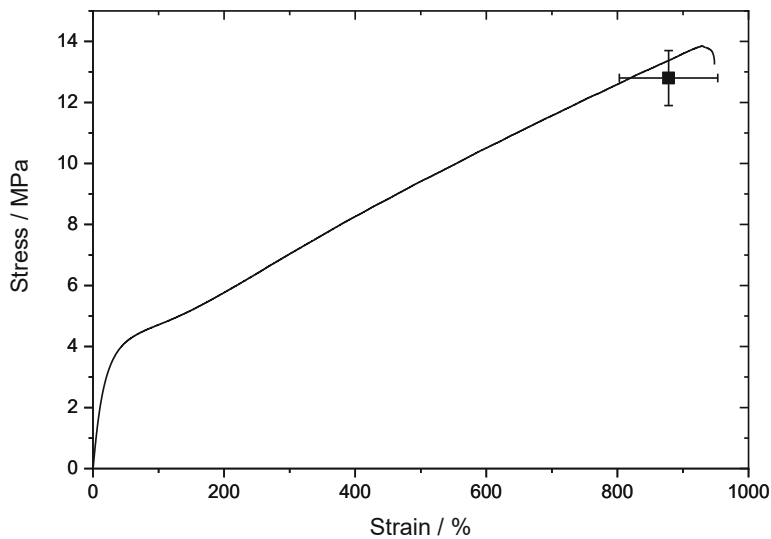
## 4. Tensile testing



Appendix 66: Representative Stress-Strain curve of benchmark material Pellethane.



Appendix 67: Representative Stress-Strain curve of reference material TPU-BHET.



Appendix 68: Representative Stress-Strain curve of reference material TPU-BHPC.

## MATERIALS AND METHODS

Reagents and solvents were purchased in a quality suitable for synthesis and, if necessary, purified according to standard organic procedures<sup>319</sup>. Non-synthesized chemicals were purchased from their respective suppliers and used as received unless otherwise mentioned (Table 43). Absolute tetrahydrofuran (THF), methanol (MeOH), toluene, methylene chloride (CH<sub>2</sub>Cl<sub>2</sub>) and dioxane were purchased from Donau Chemie and dried using a PureSolvSystem (Amesbury, USA).

Table 43: Commercially available reagents and solvents, including supplier, purification method and CAS number.

reagent or solvent	supplier, purification	CAS-Nr.
1,1,1,3,3,3-Hexafluoro-2-propanol (HFIP)	Fluorochem	920-66-1
1,2-Bis(2-mercaptoethoxy)ethane (BMEE)	TCI	14970-87-7
1,4-Butanediol	Fluka	110-63-4
1,8-Diazabicyclo[5.4.0]undec-7-ene (DBU)	ABCR	6674-22-2
1-3-Propanediol	AcrosOrganics	504-63-2
1-Thioglycerol	Sigma-Aldrich	96-27-5
2,6-Di- <i>tert</i> -butyl-4-methylphenol (BHT)	Sigma-Aldrich	128-37-0
2-chloro-4,4,5,5-tetramethyl-1,3,2-dioxaphospholane (TMDP)	Sigma-Aldrich	14812-59-0
2-Hydroxyethyl disulfide (HEDS)	ABCR, distilled	1892-29-1
Acetic anhydride	Fluka, distilled	108-24-7
Acetone-d <sub>6</sub>	Eurisotop	666-52-4
Acetonitrile-d <sub>3</sub> (MeCN-d <sub>3</sub> )	Eurisotop	2206-26-0
Benzene-1,4-diboronic acid	ABCR	4612-26-4
Bis(4-aminophenoxy)dimethylsilane (BAPDMS)	ABCR, recryst.	1223-16-1
Bis(hydroxyethylene)terephthalate (BHET)	Sigma-Aldrich, recryst.	959-26-2
Chloroform-d (CDCl <sub>3</sub> )	Eurisotop	865-49-6
Chromium(III)acetylacetonate (Cr(acac) <sub>3</sub> )	Fluka	21679-31-2
Cyclohexanol	Sigma-Aldrich	108-93-0
Deuterium oxide (D <sub>2</sub> O)	Eurisotop	7789-20-0
Diethyl carbonate	Fluka	105-58-8
Dimethyl carbonate	Fluka	616-38-6
Dimethyl sulfoxide-d <sub>6</sub> (DMSO-d <sub>6</sub> )	Eurisotop	2206-27-1
Dimethylformamide (DMF dry), ExtraDry, AcroSeal	AcrosOrganics	68-12-2
Ethyl acetate	VWR	141-78-6
Ethyl dichlorophosphate	TCI	1498-51-7
Ethylene glycol	Sigma-Aldrich	107-21-1
Furan-2-5-dicarboxylic acid (FDCA)	BLD Pharmatech	3238-40-2
Hexamethylene diisocyanate (HMDI)	Fluka	822-06-0
Hydrochloric acid (HCl)	VWR	7647-01-0
Magnesium sulfate (MgSO <sub>4</sub> )	Roth	7487-88-9
N,N-Dibutylamine	TCI, distilled	111-92-2
Pellethane 2363-80A	Lubrizol	-
Phenyl isocyanate	Fluka	103-71-9

Polytetrahydrofuran (pTHF), Mw=1000 g mol <sup>-1</sup>	Sigma Aldrich	25190-06-1
Pyridine	ABCR, distilled	110-86-1
Sodium bicarbonate (NaHCO <sub>3</sub> )	Donau Chemie	144-55-8
Sulfuric acid (H <sub>2</sub> SO <sub>4</sub> )	Fluka	7664-93-9
Tin(II) 2-ethylhexanoate	Sigma-Aldrich	301-10-0
Triethylamine (Et <sub>3</sub> N)	Roth	121-44-8

**<sup>1</sup>H-NMR, <sup>13</sup>C-NMR and <sup>31</sup>P-NMR-spectra** were recorded on a Bruker Advance DRX-400 FT-NMR spectrometer at 400 MHz for <sup>1</sup>H-NMR spectra and at 101 MHz for <sup>13</sup>C-NMR spectra. <sup>31</sup>P-NMR spectra for hydroxy-content measurements were performed on a Bruker Advance spectrometer with 600 MHz. Signals were referenced to the used NMR-solvent, purchased from Eurisotop. <sup>1</sup>H: CDCl<sub>3</sub>: 7.26 ppm, D<sub>2</sub>O: 4.79 ppm, DMSO-d<sub>6</sub>: 2.50 ppm, CD<sub>2</sub>Cl<sub>2</sub>: 5.32 ppm, CD<sub>3</sub>CN: 1.94 ppm; <sup>13</sup>C: CDCl<sub>3</sub>: 77.16 ppm, DMSO-d<sub>6</sub>: 39.52 ppm, CD<sub>2</sub>Cl<sub>2</sub>: 53.84 ppm, CD<sub>3</sub>CN: 1.32 ppm. The chemical shifts are reported in ppm and fine structures are given as: s = singlet, d = doublet, t = triplet, q = quartet, dd = doublet of doublet, m = multiplet. Resulting spectra were analyzed via the software MestReNova v12.0.4-22023 by Mestrelab Research S.L.

**Melting points** were determined by an Optimelt MPA100 automated melting point apparatus (Stanford Research System) with a heating rate of 1 °C min<sup>-1</sup>.

**Column chromatography** was performed with silica gel 60-F254 from Merck and was carried out on a Büchi MPLC Flash System (pump module C-605, control unit C-620, UV-Photometer C-635, fraction collector C-660).

**Thin layer chromatography (TLC)** was done on aluminum foils, coated with silica 60-F254 from Merck. Spot detection was done with potassium permanganate (KMnO<sub>4</sub>).

**Karl Fischer titrations** were conducted on an Envirotech CA-21 moisture meter containing Aquamicon™-anode solution AX Karl Fischer Reagent (methanol, propylene carbonate, 2,2'-iminodiethanol, sulfodioxide, iodine) and Aquamicon™-cathode solution CXU Karl Fischer Reagent (methanol, ethane-1,2-diol, choline chloride) both from Mitsubishi Chemical Corporation. The measurements were performed in triplicates. Sample weights were determined with mg accuracy. Liquid samples could be injected directly into the system, while solid samples were dissolved in a well-defined amount of dry solvent in combination with a blank titration of the solvent itself. The titration instrument displayed the amount of residual water in ppm.

**Potentiometric titrations** were performed on a Metrohm system consisting of the dosage unit 736 GP Titrino. For isocyanate titrations a 2 M aqueous HCl solution was used. Hydroxy-number determination was performed with a 0.5 M methanolic KOH solution.

**Gel permeation chromatography (GPC)** was performed on a Malvern Viscotek GPCmax VE2001 TDA system equipped with a Viscotek SEC-MALS 9 light scattering detector, a Viscotek TDA 305-021 RI+Visc detector, and a UV Detector Module 2550 for TDA 305 and a three-column system (PSS SDC columns with particle sizes 100 Å, 1,000 Å and 100,000 Å). As eluent dry THF (stabilized with 250 ppm butylated hydroxytoluene (BHT) to hinder radical formation) was used. Samples were prepared in concentrations between 2-3 mg mL<sup>-1</sup> THF-solution spiked with 0.5 mg mL<sup>-1</sup> BHT as flow-rate marker and were syringe-filtered (200 nm, PTFE). For TPUs additionally 10 vol% of Hexafluoro-2-propanol was added for complete dissolving of the sample. For all measurements, a flow rate of 0.8 ml min<sup>-1</sup> and isothermal conditions at 35 °C were used and a run-time of 70 min. Standard calibration was done with polystyrene standards between 480 and 44kDa. In case of triple detection, the dn/dc value was determined by injecting samples at five different injection volumes between 80 and 120 µl and analyzing the slope of the signals. For triple detection calibration method, a narrow PS-standard (*M<sub>w</sub>* = 105 kDa) and a broad PS standard (*M<sub>w</sub>* = 245 kDa), both supplied by Malvern, were used. Data evaluation was done via OmniSEC 5.12 by Malvern.

**High performance liquid chromatography (HPLC)** was performed on a HP Series 1100 Chemstation HPLC system equipped with a diode array and a Waters Xterra MS C18 reversed-phase column. Samples were prepared as 1-2 mg mL<sup>-1</sup> solutions with HPLC-grade solvents. Usually with a water/acetonitrile mixture (70:30).

**Solution Casting** was used for preparing polymer films for mechanical testing and degradation experiments. For each film 0.5 g of polymer was dissolved in 5 mL Hexafluoro-2-propanol at 45 °C. Polymer solutions were filled in a PTFE mold (60 x 40 x 2 mm) and dried first at ambient conditions for 2 days and finally under reduced pressure at room temperature until constant mass. Subsequently the samples were stored in a desiccator equipped with drying agent to ensure dry environment.

**Tensile testing** was carried out on a Zwick Z050 universal testing machine with a strain rate of 50 mm min<sup>-1</sup> and 100 N load cell. Mechanical testing specimens were punched of the solution cast polymer films (ISO 527, Type 5B, bone-shaped). Each sample was tested at least in quadruplicates with a sample thickness between 20 and 40 µm.

**ATR-FTIR** measurements were performed on a PerkinElmer Spectrum 65 FT-IR Spectrometer equipped with a Specac Heated GoldenGate Controller between 4000 and 600 cm<sup>-1</sup> and 16 scans at 25 °C. Measurements at elevated temperatures were conducted with a Eurotherm 2216E temperature controller. The software PerkinElmer Spectrum (Version 10.03.07) was used for data evaluation.



**Dynamic Mechanical Thermal Analysis (DMTA)** was used to determine the glass transition temperature ( $T_g$ ) of solution cast polymer films. DMTA was performed on an Anton Paar 2980 DMA V1.7B instrument with a frequency of 1Hz and an amplitude of 1% between -100 °C and 50 °C by Stefan Zellhofer. Thickness of the samples was between 20 – 40.

**Gas chromatography-mass spectrometry (GC-MS)** were conducted on a Thermo Scientific Trace GC Ultra equipped with an ITQ 1100 MS and a AS 3000 auto-sampler to identify the purity of reagents and final products.

**Degradation studies** were performed with circular specimens, which were punched out of solution cast polymer films with a diameter of 1 cm, a thickness of 40 – 60  $\mu\text{m}$  and a mass between 20 and 30 mg. Degradation studies were performed in PBS buffer solution (pH=7.4) at a constant temperature (37 °C or 90 °C), in acetate buffer solution (pH=5) and in carbonate-bicarbonate buffer solution (pH=10). Afterwards, buffer solution was decanted off and the samples were washed with deionized water. Absorbed salts were removed by immersing the samples in distilled water for 3 h and subsequent drying in vacuo until constant mass was reached. All measurements were performed in triplicates.

**Research tools:** Literature searches were performed using SciFinder<sup>n</sup> by CAS, Google Scholar and Reaxys. Writing was done using Microsoft<sup>®</sup> Word 2019 MSO. Textediting and paraphrasing were done with the help of deepl.com and ChatGPT 3.5. Citations were added using EndNote X9.1 software. Diagrams were plotted using Origin 2019b. Chemical drawings marked as Schemes were created using ChemDoodle<sup>®</sup> V 10.3.0 software from iChemLabs<sup>TM</sup>. Illustrations identified as figures were created using Microsoft<sup>®</sup> PowerPoint<sup>®</sup> 2019 MSO.

# ABBREVIATIONS

Abbreviation	Meaning
BAPDMS	Bis(4-aminophenoxy)dimethylsilane
BDB	2,2'-(1,4-phenylene)-bis[4-mercaptan-1,3,2-dioxaborolane]
BDO	1,4-Butanediol
BHBEP	Bis(4-hydroxybutyl) ethyl phosphate
BHEF	Bis(2-hydroxyethyl)furan-2,5-dicarboxylate
BHET	Bis(hydroxyethylene)terephthalate
BHPC	Bis(3-hydroxypropyl) carbonate
BHT	Butylated hydroxytoluene
BMEE	1,2-Bis(2-mercaptoethoxy)ethane
CABG	Coronary Artery Bypass Graft
CE	chain extender
CHCl <sub>3</sub>	Chloroform
Cr(acac) <sub>3</sub>	Chromium(III)acetylacetonate
CycOH	Cyclohexanol
DBU	1,8-Diazabicyclo[5.4.0]undec-7-ene
DEC	Diethyl carbonate
DMC	Dimethyl carbonate
DMF	Dimethylformamide
DMSO	Dimethyl sulfoxide
DMTA	Dynamic Mechanical Thermal Analysis
DTI	Direct Thrombin Inhibitors
ECM	Extracellular Matrix
EDGE	Ethylene Glycol Glycidyl Ether
EG	Ethylene glycol
Et <sub>3</sub> N	Triethylamine
EtOAc	Ethyl acetate
FDCA	Furan-2-5-dicarboxylic acid
FTIR	Fourier-Transform Infrared Spectroscopy
GAGs	Glycosaminoglycans
GC-MS	Gas-Chromatography Mass-Spectrometry
GPC	Gel Permeation Chromatography
HA	Hyaluronic acid
HCl	Hydrochloric acid
HEDS	2-Hydroxyethyl disulfide
HFiP	1,1,1,3,3,3-Hexafluoro-2-propanol
HMDI	Hexamethylene diisocyanate
HPLC	High-Performance Liquid Chromatography
Int	Integral
KFT	Karl-Fischer titration
LMWH	Low Molecular Weight Heparin
Mp	Melting point
NCO	Isocyanate
NMR	nuclear magnetic resonance

OHZ	Hydroxy-number / Hydroxy-value
PCL	Poly( $\epsilon$ -caprolactone)
PDO	1-3-Propanediol
Pell / Pellethane	Pellethane 2363-80A
PET	Poly(ethylene therephtalate)
PGA	Poly(glycolic acid)
PHAs	Polyhydroxyalkanoates
PLA	Poly(lactic acid)
PTA	Percutaneous Transluminal Angioplasty
PTCA	Percutaneous Transluminal Coronary Angioplasty
PTFE	Polytetrafluoroethylene
pTHF	Polytetrahydrofuran
PU	Polyurethane
RT	Room Temperature (25 °C)
Sn(Oct) <sub>2</sub>	Tin(II) 2-ethylhexanoate
TE	Tissue Engineering
THF	Tetrahydrofuran
TLC	Thin Layer Chromatography
TMDP	2-chloro-4,4,5,5-tetramethyl-1,3,2-dioxaphospholane
TPTU	Thermoplastic poly(thio)urethane
TPU	Thermoplastic polyurethane
TPUU	Thermoplastic polyurea urethane
UFH	Unfractionated Heparin
VTE	Vascular Tissue Engineering

## REFERENCES

---

1. Stefanovska, A., Physics of the human cardiovascular system. *Contemporary Physics* **1999**, *40* (1), 31-55.
2. Steenhoven, v., A.A., Velocity profiles in large arteries. *The physics of heart and circulation* **1993**, 295-320.
3. Fung, Y. C., *Biomechanics-Circulation*. Springer: New York, 1997; Vol. 2, p 572.
4. CourseHero; Blood Vessel Structure and Function. <https://www.coursehero.com/study-guides/boundless-ap/blood-vessel-structure-and-function/> (accessed 2023, May 04).
5. pslides; Artery and Vein Diagram. <https://pslides.com/templates/artery-and-vein-diagram-for-powerpoint/> (accessed 2023, May 02).
6. Schmidt, R. T., Herhard; Lang, Florian, *Physiologie des Menschen*. Springer: Berlin, 2013; Vol. 28.
7. Staubesand, J. S., Erwin; , *Neuere Aspekte der Sklerosierungstherapie: Varizen, Ösophagusvarizen, Varikozelen, Organzysten*. Springer: Berlin, 2013.
8. Armstrong, M. Top Global Causes of Death. <https://www.statista.com/chart/20522/most-common-causes-of-death-global/> (accessed 2023, May 05).
9. Choi, D.; Hwang, K.-C.; Lee, K.-Y.; Kim, Y.-H., Ischemic heart diseases: Current treatments and future. *Journal of Controlled Release* **2009**, *140* (3), 194-202.
10. Gaede, P.-M., *GEO Themenlexikon Band 9: Medizin und Gesundheit - Diagnose, Heilkunst, Arzneien*. Wissenmedia: 2006; Vol. 1.
11. Michaels Andrew, D.; Chatterjee, K., Angioplasty Versus Bypass Surgery for Coronary Artery Disease. *Circulation* **2002**, *106* (23), e187-e190.
12. Gaede, P.-M., *GEO Themenlexikon Band 10: Medizin und Gesundheit - Diagnose, Heilkunst, Arzneien*. Wissenmedia: 2007; Vol. 1.
13. Yang, Y.-m.; Moussa, I., Percutaneous coronary intervention and drug-eluting stents. *CMAJ* **2005**, *172* (3), 323-325.
14. MedWorldIndia; Angioplasty, Stenting, Interventional Cardiology Treatments for Blocked Heart Blood Vessels. <http://roboticheartsurgeryinindia.blogspot.com/2014/01/angioplasty-stenting-interventional.html> (accessed 2023, April 22).
15. Van Belle, E.; Abolmaali, K.; Bauters, C.; McFadden, E. P.; Lablanche, J.-M.; Bertrand, M. E., Restenosis, late vessel occlusion and left ventricular function six months after balloon angioplasty in diabetic patients. *Journal of the American College of Cardiology* **1999**, *34* (2), 476-485.
16. CardiovascularInterventions, P. A. Coronary Artery Bypass Graft Surgery (CABG). <https://orlandocvi.com/procedure/coronary-artery-bypass-graft-surgery/> (accessed 2023, March 27).
17. Gaede, P.-M., *GEO Themenlexikon Band 11: Medizin und Gesundheit - Diagnose, Heilkunst, Arzneien*. Wissenmedia: 2007; Vol. 1.
18. Hirsh, J., Low-Molecular-Weight Heparin. *Circulation* **1998**, *98* (15), 1575-1582.
19. Anderson, J. L.; Adams, C. D.; Antman, E. M.; Bridges, C. R.; Califf, R. M.; Casey, D. E., Jr.; Chavey, W. E., 2nd; Fesmire, F. M.; Hochman, J. S.; Levin, T. N.; Lincoff, A. M.; Peterson, E. D.; Theroux, P.; Wenger, N. K.; Wright, R. S., ACC/AHA 2007 guidelines for the management of patients with unstable angina/non ST-elevation myocardial infarction. *Circulation* **2007**, *116* (7), e148-304.
20. Gori, A.; Lodigiani, G.; Colombaroli, S. G.; Bergamaschi, G.; Vitali, A., Cell Penetrating Peptides: Classification, Mechanisms, Methods of Study, and Applications. *ChemMedChem* **2023**, *18* (17), e202300236.
21. van den Berg, A.; Dowdy, S. F., Protein transduction domain delivery of therapeutic macromolecules. *Current Opinion in Biotechnology* **2011**, *22* (6), 888-893.
22. Formiga, F. R.; Tamayo, E.; Simón-Yarza, T.; Pelacho, B.; Prósper, F.; Blanco-Prieto, M. J., Angiogenic therapy for cardiac repair based on protein delivery systems. *Heart Failure Reviews* **2012**, *17* (3), 449-473.

23. Khan, S.; Villalobos, M. A.; Choron, R. L.; Chang, S.; Brown, S. A.; Carpenter, J. P.; Tulenko, T. N.; Zhang, P., Fibroblast growth factor and vascular endothelial growth factor play a critical role in endotheliogenesis from human adipose-derived stem cells. *J Vasc Surg* **2017**, *65* (5), 1483-1492.
24. Pugh, C. W.; Ratcliffe, P. J., Regulation of angiogenesis by hypoxia: role of the HIF system. *Nature medicine* **2003**, *9* (6), 677-84.
25. Hu, C.; Yang, J.; Qi, Z.; Wu, H.; Wang, B.; Zou, F.; Mei, H.; Liu, J.; Wang, W.; Liu, Q., Heat shock proteins: Biological functions, pathological roles, and therapeutic opportunities. *MedComm* **2022**, *3* (3), e161.
26. Söti, C.; Nagy, E.; Giricz, Z.; Vigh, L.; Csermely, P.; Ferdinandy, P., Heat shock proteins as emerging therapeutic targets. *British journal of pharmacology* **2005**, *146* (6), 769-80.
27. Ferdinandy, P., Myocardial ischaemia/reperfusion injury and preconditioning: effects of hypercholesterolaemia/hyperlipidaemia. *British journal of pharmacology* **2003**, *138* (2), 283-285.
28. Kaji, E. H.; Leiden, J. M., Gene and Stem Cell Therapies. *JAMA* **2001**, *285* (5), 545-550.
29. Ginn, S. L.; Amaya, A. K.; Alexander, I. E.; Edelstein, M.; Abedi, M. R., Gene therapy clinical trials worldwide to 2017: An update. *The journal of gene medicine* **2018**, *20* (5), e3015.
30. Beeres, S. L.; Atsma, D. E.; van Ramshorst, J.; Schalij, M. J.; Bax, J. J., Cell therapy for ischaemic heart disease. *Heart (British Cardiac Society)* **2008**, *94* (9), 1214-26.
31. Blum, A.; Balkan, W.; Hare, J. M., Advances in cell-based therapy for peripheral vascular disease. *Atherosclerosis* **2012**, *223* (2), 269-277.
32. Williams, A. R.; Hare, J. M., Mesenchymal stem cells: biology, pathophysiology, translational findings, and therapeutic implications for cardiac disease. *Circulation research* **2011**, *109* (8), 923-40.
33. Williams, A. R.; Trachtenberg, B.; Velazquez, D. L.; McNiece, I.; Altman, P.; Rouy, D.; Mendizabal, A. M.; Pattany, P. M.; Lopera, G. A.; Fishman, J.; Zambrano, J. P.; Heldman, A. W.; Hare, J. M., Intramyocardial stem cell injection in patients with ischemic cardiomyopathy: functional recovery and reverse remodeling. *Circulation research* **2011**, *108* (7), 792-6.
34. Atala, A., Engineering tissues, organs and cells. *J Tissue Eng Regen Med* **2007**, *1*, 83-96.
35. Chen, F.; Yoo, J. J.; Atala, A., Acellular collagen matrix as a possible "off the shelf" biomaterial for urethral repair. *Urology* **1999**, *54* (3), 407-410.
36. Dahms; Piechota; Dahiya; Lue; Tanagho, Composition and biomechanical properties of the bladder acellular matrix graft: comparative analysis in rat, pig and human. *British Journal of Urology* **1998**, *82* (3), 411-419.
37. Yoo, J. J.; Meng, J.; Oberpenning, F.; Atala, A., Bladder augmentation using allogenic bladder submucosa seeded with cells. *Urology* **1998**, *51* (2), 221-225.
38. Noh, S.; Myung, N.; Park, M.; Kim, S.; Zhang, S.-U.; Kang, H.-W., 3D Bioprinting for Tissue Engineering. In *Clinical Regenerative Medicine in Urology*, Kim, B. W., Ed. Springer Singapore: Singapore, 2018; pp 105-123.
39. Couet, F.; Rajan, N.; Mantovani, D., Macromolecular Biomaterials for Scaffold-Based Vascular Tissue Engineering. *Macromolecular Bioscience* **2007**, *7* (5), 701-718.
40. Nerem, R. M.; Seliktar, D., Vascular tissue engineering. *Annual review of biomedical engineering* **2001**, *3*, 225-43.
41. Conte, M., The ideal small arterial substitute: a search for the Holy Grail? *FASEB journal : official publication of the Federation of American Societies for Experimental Biology* **1998**, *12*, 43-5.
42. Campbell, J. H.; Walker, P.; Chue, W.-L.; Daly, C.; Cong, H.-L.; Xiang, L.; Campbell, G. R., Body cavities as bioreactors to grow arteries. *International Congress Series* **2004**, *1262*, 118-121.
43. Shepherd, B.; Jay, S.; Saltzman, W.; Tellides, G.; Pober, J., Human Aortic Smooth Muscle Cells Promote Arteriole Formation by Coengrafted Endothelial Cells. *Tissue engineering. Part A* **2008**, *15*, 165-73.
44. L'Heureux, N.; Paquet, S.; Labbe, R.; Germain, L.; Auger, F. A., A completely biological tissue-engineered human blood vessel. *FASEB journal : official publication of the Federation of American Societies for Experimental Biology* **1998**, *12* (1), 47-56.
45. Bilodeau, K.; Mantovani, D., Bioreactors for Tissue Engineering: Focus on Mechanical Constraints. A Comparative Review. *Tissue engineering* **2006**, *12* (8), 2367-2383.

46. Chandy, T., Biocompatibility of materials and its relevance to drug delivery and tissue engineering. In *Biointegration of Medical Implant Materials (Second Edition)*, Sharma, C. P., Ed. Woodhead Publishing: 2020; pp 297-331.
47. Roeder, R.; Wolfe, J.; Lianakis, N.; Hinson, T.; Geddes, L. A.; Obermiller, J., Compliance, elastic modulus, and burst pressure of small-intestine submucosa (SIS), small-diameter vascular grafts. *Journal of Biomedical Materials Research* **1999**, *47* (1), 65-70.
48. Caves, J. M.; Kumar, V. A.; Xu, W.; Naik, N.; Allen, M. G.; Chaikof, E. L., Microcrimped collagen fiber-elastin composites. *Adv Mater* **2010**, *22* (18), 2041-2044.
49. Hutmacher, D. W., Scaffold design and fabrication technologies for engineering tissues--state of the art and future perspectives. *Journal of biomaterials science. Polymer edition* **2001**, *12* (1), 107-24.
50. Roh, J. D.; Sawh-Martinez, R.; Brennan, M. P.; Jay, S. M.; Devine, L.; Rao, D. A.; Yi, T.; Mirensky, T. L.; Nalbandian, A.; Udelsman, B.; Hibino, N.; Shinoka, T.; Saltzman, W. M.; Snyder, E.; Kyriakides, T. R.; Pober, J. S.; Breuer, C. K., Tissue-engineered vascular grafts transform into mature blood vessels via an inflammation-mediated process of vascular remodeling. *Proc Natl Acad Sci U S A* **2010**, *107* (10), 4669-4674.
51. Berglund, J. D.; Mohseni, M. M.; Nerem, R. M.; Sambanis, A., A biological hybrid model for collagen-based tissue engineered vascular constructs. *Biomaterials* **2003**, *24* (7), 1241-1254.
52. Weinberg, C. B.; Bell, E., A blood vessel model constructed from collagen and cultured vascular cells. *Science (New York, N.Y.)* **1986**, *231* (4736), 397-400.
53. Chupa, J. M.; Foster, A. M.; Sumner, S. R.; Madhally, S. V.; Matthew, H. W. T., Vascular cell responses to polysaccharide materials:: in vitro and in vivo evaluations. *Biomaterials* **2000**, *21* (22), 2315-2322.
54. Pieper, J. S.; Hafmans, T.; Veerkamp, J. H.; van Kuppevelt, T. H., Development of tailor-made collagen-glycosaminoglycan matrices: EDC/NHS crosslinking, and ultrastructural aspects. *Biomaterials* **2000**, *21* (6), 581-593.
55. Charulatha, V.; Rajaram, A., Influence of different crosslinking treatments on the physical properties of collagen membranes. *Biomaterials* **2003**, *24* (5), 759-767.
56. Gosline, J.; Lillie, M.; Carrington, E.; Guerette, P.; Ortlepp, C.; Savage, K., Elastic proteins: biological roles and mechanical properties. *Philos Trans R Soc Lond B Biol Sci* **2002**, *357* (1418), 121-132.
57. Leach, J. B.; Wolinsky, J. B.; Stone, P. J.; Wong, J. Y., Crosslinked  $\alpha$ -elastin biomaterials: towards a processable elastin mimetic scaffold. *Acta Biomaterialia* **2005**, *1* (2), 155-164.
58. McClure, M. J.; Sell, S. A.; Simpson, D. G.; Walpoth, B. H.; Bowlin, G. L., A three-layered electrospun matrix to mimic native arterial architecture using polycaprolactone, elastin, and collagen: a preliminary study. *Acta Biomater* **2010**, *6* (7), 2422-33.
59. Ye, Q.; Zünd, G.; Benedikt, P.; Jockenhoevel, S.; Hoerstrup, S. P.; Sakyama, S.; Hubbell, J. A.; Turina, M., Fibrin gel as a three dimensional matrix in cardiovascular tissue engineering. *European Journal of Cardio-Thoracic Surgery* **2000**, *17* (5), 587-591.
60. Jockenhoevel, S.; Zund, G.; Hoerstrup, S. P.; Chalabi, K.; Sachweh, J. S.; Demircan, L.; Messmer, B. J.; Turina, M., Fibrin gel – advantages of a new scaffold in cardiovascular tissue engineering. *European Journal of Cardio-Thoracic Surgery* **2001**, *19* (4), 424-430.
61. Cummings, C. L.; Gawlitta, D.; Nerem, R. M.; Stegemann, J. P., Properties of engineered vascular constructs made from collagen, fibrin, and collagen-fibrin mixtures. *Biomaterials* **2004**, *25* (17), 3699-706.
62. Huang, Y.; Onyeri, S.; Siewe, M.; Moshfeghian, A.; Madhally, S. V., In vitro characterization of chitosan-gelatin scaffolds for tissue engineering. *Biomaterials* **2005**, *26* (36), 7616-7627.
63. Drury, J. L.; Mooney, D. J., Hydrogels for tissue engineering: scaffold design variables and applications. *Biomaterials* **2003**, *24* (24), 4337-4351.
64. Zhang, M.; Li, X. H.; Gong, Y. D.; Zhao, N. M.; Zhang, X. F., Properties and biocompatibility of chitosan films modified by blending with PEG. *Biomaterials* **2002**, *23* (13), 2641-2648.
65. Mao, J.; Zhao, L.; Yin, Y.; Yao, F., Structure and properties of bilayer chitosan-gelatin scaffolds. *Biomaterials* **2003**, *24*, 1067-74.

66. Sarasam, A.; Madihally, S. V., Characterization of chitosan–polycaprolactone blends for tissue engineering applications. *Biomaterials* **2005**, *26* (27), 5500-5508.
67. Laurent, T. C.; Laurent, U. B.; Fraser, J. R., The structure and function of hyaluronan: An overview. *Immunology and cell biology* **1996**, *74* (2), A1-7.
68. Fraser, J. R.; Laurent, T. C.; Laurent, U. B., Hyaluronan: its nature, distribution, functions and turnover. *Journal of internal medicine* **1997**, *242* (1), 27-33.
69. Yamada, T.; Kawasaki, T., Microbial synthesis of hyaluronan and chitin: New approaches. *Journal of Bioscience and Bioengineering* **2005**, *99* (6), 521-528.
70. O'Regan, M.; Martini, I.; Crescenzi, F.; De Luca, C.; Lansing, M., Molecular mechanisms and genetics of hyaluronan biosynthesis. *International Journal of Biological Macromolecules* **1994**, *16* (6), 283-286.
71. Grigolo, B.; Roseti, L.; Fiorini, M.; Fini, M.; Giavaresi, G.; Nicoli Aldini, N.; Giardino, R.; Facchini, A., Transplantation of chondrocytes seeded on a hyaluronan derivative (Hyaff®-11) into cartilage defects in rabbits. *Biomaterials* **2001**, *22* (17), 2417-2424.
72. Yoo, H. S.; Lee, E. A.; Yoon, J. J.; Park, T. G., Hyaluronic acid modified biodegradable scaffolds for cartilage tissue engineering. *Biomaterials* **2005**, *26* (14), 1925-1933.
73. Chang, C.-H.; Liu, H.-C.; Lin, C.-C.; Chou, C.-H.; Lin, F.-H., Gelatin–chondroitin–hyaluronan tri-copolymer scaffold for cartilage tissue engineering. *Biomaterials* **2003**, *24* (26), 4853-4858.
74. Pavicic, T.; Gauglitz, G. G.; Lersch, P.; Schwach-Abdellaoui, K.; Malle, B.; Korting, H. C.; Farwick, M., Efficacy of cream-based novel formulations of hyaluronic acid of different molecular weights in anti-wrinkle treatment. *Journal of drugs in dermatology : JDD* **2011**, *10* (9), 990-1000.
75. Hubbell, J. A., Biomaterials in Tissue Engineering. *Bio/Technology* **1995**, *13* (6), 565-576.
76. Xue, L.; Greisler, H., Biomaterial in the development and future of vascular grafts. *Journal of vascular surgery : official publication, the Society for Vascular Surgery [and] International Society for Cardiovascular Surgery, North American Chapter* **2003**, *37*, 472-80.
77. Reed, A. M.; Gilding, D. K., Biodegradable polymers for use in surgery — poly(ethylene oxide)/poly(ethylene terephthalate) (PEO/PET) copolymers: 2. In vitro degradation. *Polymer* **1981**, *22* (4), 499-504.
78. Gautier, E.; Fuertes, P.; Cassagnau, P.; Pascault, J.-P.; Fleury, E., Synthesis and rheology of biodegradable poly(glycolic acid) prepared by melt ring-opening polymerization of glycolide. *Journal of Polymer Science Part A: Polymer Chemistry* **2009**, *47* (5), 1440-1449.
79. Middleton, J. C.; Tipton, A. J., Synthetic biodegradable polymers as orthopedic devices. *Biomaterials* **2000**, *21* (23), 2335-2346.
80. Iwasaki, K.; Kojima, K.; Kodama, S.; Paz, A. C.; Chambers, M.; Umezumi, M.; Vacanti, C., Bioengineered Three-Layered Robust and Elastic Artery Using Hemodynamically-Equivalent Pulsatile Bioreactor. *Circulation* **2008**, *118*, S52-7.
81. Mooney, D. J.; Organ, G.; Vacanti, J. P.; Langer, R., Design and fabrication of biodegradable polymer devices to engineer tubular tissues. *Cell transplantation* **1994**, *3* (2), 203-10.
82. Chu, C. F. L.; Lu, A.; Liszkowski, M.; Sipehia, R., Enhanced growth of animal and human endothelial cells on biodegradable polymers. *Biochimica et Biophysica Acta (BBA) - General Subjects* **1999**, *1472* (3), 479-485.
83. Burkersroda, F.; Schedl, L.; Göpferich, A., Why degradable polymers undergo surface erosion or bulk erosion. *Biomaterials* **2002**, *23*, 4221-31.
84. Chen, G.-Q.; Wu, Q., The application of polyhydroxyalkanoates as tissue engineering materials. *Biomaterials* **2005**, *26* (33), 6565-6578.
85. Akhtar, S., Physicomechanical properties of bacterial P(HB - HV) polyesters and their uses in drug delivery. **1990**.
86. Shum-Tim, D.; Stock, U.; Hrkach, J.; Shinoka, T.; Lien, J.; Moses, M. A.; Stamp, A.; Taylor, G.; Moran, A. M.; Landis, W.; Langer, R.; Vacanti, J. P.; Mayer, J. E., Tissue engineering of autologous aorta using a new biodegradable polymer. *The Annals of Thoracic Surgery* **1999**, *68* (6), 2298-2304.
87. Yang, K.-K.; Wang, X.-L.; Wang, Y.-Z., POLY(p-DIOXANONE) AND ITS COPOLYMERS. *Journal of Macromolecular Science, Part C* **2002**, *42* (3), 373-398.

88. Greisler, H. P.; Ellinger, J.; Schwarcz, T. H.; Golan, J.; Raymond, R. M.; Kim, D. U., Arterial regeneration over polydioxanone prostheses in the rabbit. *Archives of surgery (Chicago, Ill. : 1960)* **1987**, 122 (6), 715-21.
89. Sell, S. A.; McClure, M. J.; Barnes, C. P.; Knapp, D. C.; Walpoth, B. H.; Simpson, D. G.; Bowlin, G. L., Electrospun polydioxanone–elastin blends: potential for bioresorbable vascular grafts. *Biomedical Materials* **2006**, 1 (2), 72-80.
90. Janik, H.; Sienkiewicz, M.; Kucinska-Lipka, J., Handbook of Thermoset Plastics (Third Edition) In *Handbook of Thermoset Plastics (Third Edition)*, Dodiuk, H.; Goodman, S. H., Eds. William Andrew Publishing: Boston, 2014; pp 253-295.
91. de Souza, F. M.; Kahol, P. K.; Gupta, R. K., Introduction to Polyurethane Chemistry. In *Polyurethane Chemistry: Renewable Polyols and Isocyanates*, American Chemical Society: 2021; Vol. 1380, pp 1-24.
92. Remya, V. R.; Patil, D.; Abitha, V.; Rane, A.; Mishra, R., Biobased materials for polyurethane dispersions. *Chemistry International* **2015**, 2, 158-167.
93. Zieleniewska, M.; Auguścik, M.; Prociak, A.; Rojek, P.; Ryszkowska, J., Polyurethane-urea substrates from rapeseed oil-based polyol for bone tissue cultures intended for application in tissue engineering. *Polymer Degradation and Stability* **2014**, 108, 241-249.
94. Jenkins, A. D.; Kratochvíl, P.; Stepto, R. F. T.; Suter, U. W., Glossary of basic terms in polymer science (IUPAC Recommendations 1996). *Pure and Applied Chemistry* **1996**, 68 (12), 2287-2311.
95. Carothers, W. H., Polymers and polyfunctionality. *Transactions of the Faraday Society* **1936**, 32 (0), 39-49.
96. Fache, M.; Viola, A.; Auvergne, R.; Boutevin, B.; Caillol, S., Biobased epoxy thermosets from vanillin-derived oligomers. *European Polymer Journal* **2015**, 68, 526-535.
97. Yilgor, I.; Yilgor, E., Structure-Morphology-Property Behavior of Segmented Thermoplastic Polyurethanes and Polyureas Prepared without Chain Extenders. *Polymer Reviews* **2007**, 47 (4), 487-510.
98. Yilgör, I.; Yilgör, E.; Wilkes, G. L., Critical parameters in designing segmented polyurethanes and their effect on morphology and properties: A comprehensive review. *Polymer* **2015**, 58, A1-A36.
99. Dodge, J., Polyurethanes and Polyureas. In *Synthetic Methods in Step-Growth Polymers*, 2003; pp 197-263.
100. Li, X.-y.; Li, Q.-f.; Zhao, Y.-h.; Kang, M.-q.; Wang, J.-w., Utilization of carbon dioxide in polyurethane. *Journal of Fuel Chemistry and Technology* **2022**, 50 (2), 195-209.
101. Prisacariu, C., *Polyurethane Elastomers: From Morphology to Mechanical Aspects*. Springer Vienna: 2011.
102. Versteegen, R. M.; Sijbesma, R. P.; Meijer, E. W., Synthesis and Characterization of Segmented Copoly(ether urea)s with Uniform Hard Segments. *Macromolecules* **2005**, 38 (8), 3176-3184.
103. Seidler, K.; Ehrmann, K.; Steinbauer, P.; Rohatschek, A.; Andriotis, O. G.; Dworak, C.; Koch, T.; Bergmeister, H.; Grasl, C.; Schima, H.; J. Thurner, P.; Liska, R.; Baudis, S., A structural reconsideration: Linear aliphatic or alicyclic hard segments for biodegradable thermoplastic polyurethanes? *Journal of Polymer Science Part A: Polymer Chemistry* **2018**, 56 (19), 2214-2224.
104. González-Campos, J. B.; Luna-Bárceñas, G.; Zárate-Triviño, D. G.; Mendoza-Galván, A.; Prokhorov, E.; Villaseñor-Ortega, F.; Sanchez, I. C., Polymer States and Properties. In *Handbook of Polymer Synthesis, Characterization, and Processing*, 2013; pp 15-39.
105. Nair, L. S.; Laurencin, C. T., Biodegradable polymers as biomaterials. *Progress in Polymer Science* **2007**, 32 (8), 762-798.
106. Cozzens, D.; Wei, X.; Faust, R., Electrospinning of biostable polyisobutylene-based thermoplastic polyurethanes. *Journal of Polymer Science Part B: Polymer Physics* **2013**, 51 (6), 452-459.
107. Santerre, J. P.; Woodhouse, K.; Laroche, G.; Labow, R. S., Understanding the biodegradation of polyurethanes: From classical implants to tissue engineering materials. *Biomaterials* **2005**, 26 (35), 7457-7470.



108. Khatoon, H.; Ahmad, S., Polyurethane: A Versatile Scaffold for Biomedical Applications. *Significances of Bioengineering & Biosciences* **2018**, *2*, 1-3.
109. Joseph, J. V.; Patel, R.; Wenham, A. M.; Smith, J. R., Biomedical applications of polyurethane materials and coatings. *Transactions of the IMF* **2018**, *96*, 121 - 129.
110. Hulbert, S. F.; Bowman, L. S., Porous Polymeric Orthopedic Implants. In *Polymers in Medicine and Surgery*, Kronenthal, R. L.; Oser, Z.; Martin, E., Eds. Springer US: Boston, MA, 1975; pp 161-166.
111. Ercolani, E.; Del Gaudio, C.; Bianco, A., Vascular tissue engineering of small-diameter blood vessels: reviewing the electrospinning approach. *Journal of Tissue Engineering and Regenerative Medicine* **2015**, *9* (8), 861-888.
112. Grasl, C.; Bergmeister, H.; Stoiber, M.; Schima, H.; Weigel, G., Electrospun polyurethane vascular grafts: in vitro mechanical behavior and endothelial adhesion molecule expression. *Journal of biomedical materials research. Part A* **2010**, *93* (2), 716-23.
113. Soletti, L.; Nieponice, A.; Hong, Y.; Ye, S.-H.; Stankus, J. J.; Wagner, W. R.; Vorp, D. A., In vivo performance of a phospholipid-coated bioerodable elastomeric graft for small-diameter vascular applications. *Journal of Biomedical Materials Research Part A* **2011**, *96A* (2), 436-448.
114. Hong, Y.; Ye, S.-H.; Pelinescu, A. L.; Wagner, W. R., Synthesis, Characterization, and Paclitaxel Release from a Biodegradable, Elastomeric, Poly(ester urethane)urea Bearing Phosphorylcholine Groups for Reduced Thrombogenicity. *Biomacromolecules* **2012**, *13* (11), 3686-3694.
115. Hong, Y.; Ye, S.-H.; Nieponice, A.; Soletti, L.; Vorp, D. A.; Wagner, W. R., A small diameter, fibrous vascular conduit generated from a poly(ester urethane)urea and phospholipid polymer blend. *Biomaterials* **2009**, *30* (13), 2457-2467.
116. Ding, X.; Chin, W.; Lee, C. N.; Hedrick, J. L.; Yang, Y. Y., Peptide-Functionalized Polyurethane Coatings Prepared via Grafting-To Strategy to Selectively Promote Endothelialization. *Advanced Healthcare Materials* **2018**, *7* (5).
117. Davoudi, P.; Assadpour, S.; Derakhshan, M. A.; Ai, J.; Solouk, A.; Ghanbari, H., Biomimetic modification of polyurethane-based nanofibrous vascular grafts: A promising approach towards stable endothelial lining. *Materials Science and Engineering: C* **2017**, *80*, 213-221.
118. Taite, L. J.; Yang, P.; Jun, H.-W.; West, J. L., Nitric oxide-releasing polyurethane-PEG copolymer containing the YIGSR peptide promotes endothelialization with decreased platelet adhesion. *Journal of Biomedical Materials Research Part B: Applied Biomaterials* **2008**, *84B* (1), 108-116.
119. Jun, H.-W.; Taite, L. J.; West, J. L., Nitric Oxide-Producing Polyurethanes. *Biomacromolecules* **2005**, *6* (2), 838-844.
120. Del Gaudio, C.; Ercolani, E.; Galloni, P.; Santilli, F.; Baiguera, S.; Polizzi, L.; Bianco, A., Aspirin-loaded electrospun poly( $\epsilon$ -caprolactone) tubular scaffolds: potential small-diameter vascular grafts for thrombosis prevention. *Journal of Materials Science: Materials in Medicine* **2013**, *24* (2), 523-532.
121. Punnakitikashem, P.; Truong, D.; Menon, J. U.; Nguyen, K. T.; Hong, Y., Electrospun biodegradable elastic polyurethane scaffolds with dipyridamole release for small diameter vascular grafts. *Acta Biomaterialia* **2014**, *10* (11), 4618-4628.
122. Xu, C.; Hong, Y., Rational design of biodegradable thermoplastic polyurethanes for tissue repair. *Bioactive Materials* **2022**, *15*, 250-271.
123. Blit, P. H.; Battiston, K. G.; Yang, M.; Paul Santerre, J.; Woodhouse, K. A., Electrospun elastin-like polypeptide enriched polyurethanes and their interactions with vascular smooth muscle cells. *Acta Biomaterialia* **2012**, *8* (7), 2493-2503.
124. Boffito, M.; Di Meglio, F.; Mozetic, P.; Giannitelli, S. M.; Carmagnola, I.; Castaldo, C.; Nurzynska, D.; Sacco, A. M.; Miraglia, R.; Montagnani, S.; Vitale, N.; Brancaccio, M.; Tarone, G.; Basoli, F.; Rainer, A.; Trombetta, M.; Ciardelli, G.; Chiono, V., Surface functionalization of polyurethane scaffolds mimicking the myocardial microenvironment to support cardiac primitive cells. *PLOS ONE* **2018**, *13* (7), e0199896.
125. Wong, C. S.; Liu, X.; Xu, Z.; Lin, T.; Wang, X., Elastin and collagen enhances electrospun aligned polyurethane as scaffolds for vascular graft. *Journal of Materials Science: Materials in Medicine* **2013**, *24* (8), 1865-1874.

126. D'Amore, A.; Yoshizumi, T.; Luketich, S. K.; Wolf, M. T.; Gu, X.; Cammarata, M.; Hoff, R.; Badylak, S. F.; Wagner, W. R., Bi-layered polyurethane – Extracellular matrix cardiac patch improves ischemic ventricular wall remodeling in a rat model. *Biomaterials* **2016**, *107*, 1-14.
127. Lisi, A.; Briganti, E.; Ledda, M.; Losi, P.; Grimaldi, S.; Marchese, R.; Soldani, G., A Combined Synthetic-Fibrin Scaffold Supports Growth and Cardiomyogenic Commitment of Human Placental Derived Stem Cells. *PLOS ONE* **2012**, *7* (4), e34284.
128. Chen, R.; Qiu, L.; Ke, Q.; He, C.; Mo, X., Electrospinning Thermoplastic Polyurethane-Contained Collagen Nanofibers for Tissue-Engineering Applications. *Journal of Biomaterials Science, Polymer Edition* **2009**, *20* (11), 1513-1536.
129. Ehrmann, K. Development of Thermoplastic Elastomers for Cardiovascular Tissue Regeneration. Dissertation, TU Wien, Vienna, 2020.
130. Touchet, T. J.; Cosgriff-Hernandez, E. M., 1 - Hierarchal structure–property relationships of segmented polyurethanes. In *Advances in Polyurethane Biomaterials*, Cooper, S. L.; Guan, J., Eds. Woodhead Publishing: 2016; pp 3-22.
131. Panwiryarat, W.; Tanrattanakul, V.; Pilard, J.-F.; Pasetto, P.; Khaokong, C., Effect of the diisocyanate structure and the molecular weight of diols on bio-based polyurethanes. *Journal of Applied Polymer Science* **2013**, *130* (1), 453-462.
132. Zhang, C.; Zhang, N.; Wen, X., Improving the elasticity and cytophilicity of biodegradable polyurethane by changing chain extender. *Journal of Biomedical Materials Research Part B: Applied Biomaterials* **2006**, *79B* (2), 335-344.
133. Baudis, S.; Ligon, S. C.; Seidler, K.; Weigel, G.; Grasl, C.; Bergmeister, H.; Schima, H.; Liska, R., Hard-block degradable thermoplastic urethane-elastomers for electrospun vascular prostheses. *Journal of Polymer Science Part A: Polymer Chemistry* **2012**, *50* (7), 1272-1280.
134. Ratner, B. D.; Hoffman, A. S.; Schoen, F. J.; Lemons, J. E., *Biomaterials science: an introduction to materials in medicine*. Elsevier: 2004.
135. Ma, Z.; Hong, Y.; Nelson, D. M.; Pichamuthu, J. E.; Leeson, C. E.; Wagner, W. R., Biodegradable Polyurethane Ureas with Variable Polyester or Polycarbonate Soft Segments: Effects of Crystallinity, Molecular Weight, and Composition on Mechanical Properties. *Biomacromolecules* **2011**, *12* (9), 3265-3274.
136. Guan, J.; Sacks, M. S.; Beckman, E. J.; Wagner, W. R., Synthesis, characterization, and cytocompatibility of elastomeric, biodegradable poly(ester-urethane)ureas based on poly(caprolactone) and putrescine. *Journal of Biomedical Materials Research* **2002**, *61* (3), 493-503.
137. Martina, M.; Hutmacher, D. W., Biodegradable polymers applied in tissue engineering research: a review. *Polymer International* **2007**, *56* (2), 145-157.
138. Hettrich, W.; Becker, R., New isocyanates from amino acids. *Polymer* **1997**, *38* (10), 2437-2445.
139. Sobczak, M., Biodegradable Polyurethane Elastomers for Biomedical Applications – Synthesis Methods and Properties. *Polymer-Plastics Technology and Engineering* **2015**, *54* (2), 155-172.
140. Xu, C.; Huang, Y.; Wu, J.; Tang, L.; Hong, Y., Triggerable Degradation of Polyurethanes for Tissue Engineering Applications. *ACS Applied Materials & Interfaces* **2015**, *7* (36), 20377-20388.
141. De Groot, J. H.; De Vrijer, R.; Wildeboer, B. S.; Spaans, C. S.; Pennings, A. J., New biomedical polyurethane ureas with high tear strengths. *Polymer Bulletin* **1997**, *38* (2), 211-218.
142. Gunatillake, P. A.; Adhikari, R., Biodegradable polyurethanes: Design, synthesis, properties and potential applications. In *Biodegradable Polymers: Processing, Degradation and Applications*, 2011; pp 431-470.
143. Chan-Chan, L.; Vargas-Coronado, R.; Cervantes-Uc, J.; Cauich-Rodríguez, J.; Rath, R.; Phelps, E.; García, A.; del Barrio, J. S. R.; Parra, J.; Merhi, Y.; Tabrizian, M., Platelet adhesion and human umbilical vein endothelial cell cytocompatibility of biodegradable segmented polyurethanes prepared with 4,4'-methylene bis(cyclohexyl isocyanate), poly(caprolactone) diol and butanediol or dithioerythritol as chain extenders. *Journal of Biomaterials Applications* **2013**, *28* (2), 270-277.
144. Barikani, M.; Honarkar, H.; Barikani, M., Synthesis and characterization of polyurethane elastomers based on chitosan and poly( $\epsilon$ -caprolactone). *Journal of Applied Polymer Science* **2009**, *112* (5), 3157-3165.

145. Takahara, A.; Hadano, M.; Yamaguchi, T.; Otsuka, H.; Kidoaki, S.; Matsuda, T., Characterization of Novel Biodegradable Segmented Polyurethanes Prepared from Amino-Acid Based Diisocyanate. *Macromolecular Symposia* **2005**, *224* (1), 207-218.
146. Hassan, M. K.; Mauritz, K. A.; Storey, R. F.; Wiggins, J. S., Biodegradable aliphatic thermoplastic polyurethane based on poly( $\epsilon$ -caprolactone) and L-lysine diisocyanate. *Journal of Polymer Science Part A: Polymer Chemistry* **2006**, *44* (9), 2990-3000.
147. Zhang, J.-Y.; Beckman, E. J.; Hu, J.; Yang, G.-G.; Agarwal, S.; Hollinger, J. O., Synthesis, Biodegradability, and Biocompatibility of Lysine Diisocyanate–Glucose Polymers. *Tissue engineering* **2002**, *8* (5), 771-785.
148. van Minnen, B.; Stegenga, B.; van Leeuwen, M. B.; van Kooten, T. G.; Bos, R. R., A long-term in vitro biocompatibility study of a biodegradable polyurethane and its degradation products. *Journal of biomedical materials research. Part A* **2006**, *76* (2), 377-85.
149. Soletti, L.; Hong, Y.; Guan, J.; Stankus, J. J.; El-Kurdi, M. S.; Wagner, W. R.; Vorp, D. A., A bilayered elastomeric scaffold for tissue engineering of small diameter vascular grafts. *Acta Biomater* **2010**, *6* (1), 110-22.
150. Courtney, T.; Sacks, M. S.; Stankus, J.; Guan, J.; Wagner, W. R., Design and analysis of tissue engineering scaffolds that mimic soft tissue mechanical anisotropy. *Biomaterials* **2006**, *27* (19), 3631-8.
151. Guan, J.; Sacks, M. S.; Beckman, E. J.; Wagner, W. R., Biodegradable poly(ether ester urethane)urea elastomers based on poly(ether ester) triblock copolymers and putrescine: synthesis, characterization and cytocompatibility. *Biomaterials* **2004**, *25* (1), 85-96.
152. Ehrmann, K.; Potzmann, P.; Dworak, C.; Bergmeister, H.; Eilenberg, M.; Grasl, C.; Koch, T.; Schima, H.; Liska, R.; Baudis, S., Hard Block Degradable Polycarbonate Urethanes: Promising Biomaterials for Electrospun Vascular Prostheses. *Biomacromolecules* **2020**, *21* (2), 376-387.
153. Cohn, D.; Hotovely-Salomon, A., Biodegradable multiblock PEO/PLA thermoplastic elastomers: molecular design and properties. *Polymer* **2005**, *46* (7), 2068-2075.
154. Gorna, K.; Polowinski, S.; Gogolewski, S., Synthesis and characterization of biodegradable poly( $\epsilon$ -caprolactone urethane)s. I. Effect of the polyol molecular weight, catalyst, and chain extender on the molecular and physical characteristics. *Journal of Polymer Science Part A: Polymer Chemistry* **2002**, *40* (1), 156-170.
155. Tatai, L.; Moore, T. G.; Adhikari, R.; Malherbe, F.; Jayasekara, R.; Griffiths, I.; Gunatillake, P. A., Thermoplastic biodegradable polyurethanes: the effect of chain extender structure on properties and in-vitro degradation. *Biomaterials* **2007**, *28* (36), 5407-17.
156. Guo, Q.; Knight, P. T.; Mather, P. T., Tailored drug release from biodegradable stent coatings based on hybrid polyurethanes. *Journal of Controlled Release* **2009**, *137* (3), 224-233.
157. Marcos-Fernández, A.; Abraham, G. A.; Valentín, J. L.; Román, J. S., Synthesis and characterization of biodegradable non-toxic poly(ester-urethane-urea)s based on poly( $\epsilon$ -caprolactone) and amino acid derivatives. *Polymer* **2006**, *47* (3), 785-798.
158. Skarja, G. A.; Woodhouse, K. A., In vitro degradation and erosion of degradable, segmented polyurethanes containing an amino acid-based chain extender. *Journal of biomaterials science. Polymer edition* **2001**, *12* (8), 851-73.
159. Bil, M.; Ryszkowska, J.; Kurzydłowski, K. J., Effect of polyurethane composition and the fabrication process on scaffold properties. *Journal of Materials Science* **2009**, *44*, 1469-1476.
160. Woźniak, P.; Bil, M.; Ryszkowska, J.; Wychowański, P.; Wróbel, E.; Ratajska, A.; Hoser, G.; Przybylski, J.; Kurzydłowski, K. J.; Lewandowska-Szumieł, M., Candidate bone-tissue-engineered product based on human-bone-derived cells and polyurethane scaffold. *Acta Biomaterialia* **2010**, *6* (7), 2484-2493.
161. da Silva, G. R.; da Silva-Cunha, A.; Behar-Cohen, F.; Ayres, E.; Oréfice, R. L., Biodegradation of polyurethanes and nanocomposites to non-cytotoxic degradation products. *Polymer Degradation and Stability* **2010**, *95* (4), 491-499.
162. Tsai, M.-C.; Hung, K.-C.; Hung, S.-C.; Hsu, S.-h., Evaluation of biodegradable elastic scaffolds made of anionic polyurethane for cartilage tissue engineering. *Colloids and Surfaces B: Biointerfaces* **2015**, *125*, 34-44.

163. Chen, T. K.; Shieh, T. S.; Chui, J. Y., Studies on the First DSC Endotherm of Polyurethane Hard Segment Based on 4,4'-Diphenylmethane Diisocyanate and 1,4-Butanediol. *Macromolecules* **1998**, *31* (4), 1312-1320.
164. Speckhard, T. A.; Hwang, K. K. S.; Cooper, S. L.; Chang, V. S. C.; Kennedy, J. P., Properties of polyisobutylene polyurethane block copolymers: 3. Hard segments based on 4,4'-dicyclohexylmethane diisocyanate (H12MDI) and butane diol. *Polymer* **1985**, *26* (1), 70-78.
165. Król, P., Synthesis methods, chemical structures and phase structures of linear polyurethanes. Properties and applications of linear polyurethanes in polyurethane elastomers, copolymers and ionomers. *Progress in Materials Science* **2007**, *52* (6), 915-1015.
166. Klinedinst, D. B.; Yilgör, I.; Yilgör, E.; Zhang, M.; Wilkes, G. L., The effect of varying soft and hard segment length on the structure–property relationships of segmented polyurethanes based on a linear symmetric diisocyanate, 1,4-butanediol and PTMO soft segments. *Polymer* **2012**, *53* (23), 5358-5366.
167. Hirt, T. D.; Neuenschwander, P.; Suter, U. W., Synthesis of degradable, biocompatible, and tough block-copolyesterurethanes. *Macromolecular Chemistry and Physics* **1996**, *197* (12), 4253-4268.
168. Guelcher, S. A.; Gallagher, K. M.; Didier, J. E.; Klinedinst, D. B.; Doctor, J. S.; Goldstein, A. S.; Wilkes, G. L.; Beckman, E. J.; Hollinger, J. O., Synthesis of biocompatible segmented polyurethanes from aliphatic diisocyanates and diurea diol chain extenders. *Acta Biomaterialia* **2005**, *1* (4), 471-484.
169. Stankus, J. J.; Soletti, L.; Fujimoto, K.; Hong, Y.; Vorp, D. A.; Wagner, W. R., Fabrication of cell microintegrated blood vessel constructs through electrohydrodynamic atomization. *Biomaterials* **2007**, *28* (17), 2738-2746.
170. Wang, C.; Wang, H.; Zou, F.; Chen, S.; Wang, Y., Development of Polyhydroxyalkanoate-Based Polyurethane with Water-Thermal Response Shape-Memory Behavior as New 3D Elastomers Scaffolds. *Polymers* **2019**, *11* (6), 1030.
171. Asensio, M.; Costa, V.; Nohales, A.; Bianchi, O.; Gómez, A. C. M., Tunable Structure and Properties of Segmented Thermoplastic Polyurethanes as a Function of Flexible Segment. *Polymers (Basel)* **2019**, *11* (12).
172. Zhang, C.; Wen, X.; Vyavahare, N. R.; Boland, T., Synthesis and characterization of biodegradable elastomeric polyurethane scaffolds fabricated by the inkjet technique. *Biomaterials* **2008**, *29* (28), 3781-3791.
173. Jing, X.; Mi, H.-Y.; Salick, M. R.; Cordie, T. M.; Peng, X.-F.; Turng, L.-S., Electrospinning thermoplastic polyurethane/graphene oxide scaffolds for small diameter vascular graft applications. *Materials Science and Engineering: C* **2015**, *49*, 40-50.
174. Hong, Y.; Guan, J.; Fujimoto, K. L.; Hashizume, R.; Pelinescu, A. L.; Wagner, W. R., Tailoring the degradation kinetics of poly(ester carbonate urethane)urea thermoplastic elastomers for tissue engineering scaffolds. *Biomaterials* **2010**, *31* (15), 4249-4258.
175. Tatai, L.; Moore, T. G.; Adhikari, R.; Malherbe, F.; Jayasekara, R.; Griffiths, I.; Gunatillake, P. A., Thermoplastic biodegradable polyurethanes: The effect of chain extender structure on properties and in-vitro degradation. *Biomaterials* **2007**, *28* (36), 5407-5417.
176. Gissselfält, K.; Edberg, B.; Flodin, P., Synthesis and properties of degradable poly(urethane urea)s to be used for ligament reconstructions. *Biomacromolecules* **2002**, *3* (5), 951-8.
177. Garrett, J. T.; Xu, R.; Cho, J.; Runt, J., Phase separation of diamine chain-extended poly(urethane) copolymers: FTIR spectroscopy and phase transitions. *Polymer* **2003**, *44* (9), 2711-2719.
178. Skarja, G. A.; Woodhouse, K. A., Structure-property relationships of degradable polyurethane elastomers containing an amino acid-based chain extender. *Journal of Applied Polymer Science* **2000**, *75* (12), 1522-1534.
179. Maafi, E. M.; Malek, F.; Tighzert, L., Synthesis and characterization of new polyurethane based on polycaprolactone. *Journal of Applied Polymer Science* **2010**, *115* (6), 3651-3658.
180. Dahiyat, B. I.; Hostin, E.; Posadas, E. M.; Leong, K. W., Synthesis and characterization of putrescine-based poly(phosphoester-urethanes). *Journal of Biomaterials Science, Polymer Edition* **1993**, *4* (5), 529-543.
181. Dahiyat, B. I.; Posadas, E. M.; Hirose, S.; Hostin, E.; Leong, K. W., Degradable biomaterials with elastomeric characteristics and drug-carrier function. *Reactive Polymers* **1995**, *25* (2), 101-109.

182. de Paz, M. V.; Zamora, F.; Begines, B.; Ferris, C.; Galbis, J. A., Glutathione-Mediated Biodegradable Polyurethanes Derived from l-Arabinitol. *Biomacromolecules* **2010**, *11* (1), 269-276.
183. Potzmann, P. New building blocks for thermoplastic polyurethane elastomers for vascular tissue engineering. Master Thesis, TU Wien, Vienna, 2011.
184. Ochiai, B.; Amemiya, H.; Yamazaki, H.; Endo, T., Synthesis and properties of poly(carbonate-urethane) consisting of alternating carbonate and urethane moieties. *Journal of Polymer Science Part A: Polymer Chemistry* **2006**, *44* (9), 2802-2808.
185. Guan, J.; Wagner, W. R., Synthesis, characterization and cytocompatibility of polyurethaneurea elastomers with designed elastase sensitivity. *Biomacromolecules* **2005**, *6* (5), 2833-2842.
186. Magnin, A.; Pollet, E.; Phalip, V.; Avérous, L., Evaluation of biological degradation of polyurethanes. *Biotechnology Advances* **2020**, *39*, 107457.
187. Beldi, M.; Medimagh, R.; Chatti, S.; Marque, S.; Prim, D.; Loupy, A.; Delolme, F., Characterization of cyclic and non-cyclic poly-(ether-urethane)s bio-based sugar diols by a combination of MALDI-TOF and NMR. *European Polymer Journal* **2007**, *43* (8), 3415-3433.
188. Woodruff, M. A.; Hutmacher, D. W., The return of a forgotten polymer—Polycaprolactone in the 21st century. *Progress in Polymer Science* **2010**, *35* (10), 1217-1256.
189. Heijkants, R. G. J. C.; Calck, R. V. v.; van Tienen, T. G.; de Groot, J. H.; Buma, P.; Pennings, A. J.; Veth, R. P. H.; Schouten, A. J., Uncatalyzed synthesis, thermal and mechanical properties of polyurethanes based on poly( $\epsilon$ -caprolactone) and 1,4-butane diisocyanate with uniform hard segment. *Biomaterials* **2005**, *26* (20), 4219-4228.
190. Bagdi, K.; Molnár, K.; Kállay, M.; Schön, P.; Vancsó, J. G.; Pukánszky, B., Quantitative estimation of the strength of specific interactions in polyurethane elastomers, and their effect on structure and properties. *European Polymer Journal* **2012**, *48* (11), 1854-1865.
191. Ruan, C.; Hu, N.; Ma, Y.; Li, Y.; Liu, J.; Zhang, X.; Pan, H., The interfacial pH of acidic degradable polymeric biomaterials and its effects on osteoblast behavior. *Scientific Reports* **2017**, *7* (1), 6794.
192. Hakkarainen, M.; Höglund, A.; Odelius, K.; Albertsson, A. C., Tuning the release rate of acidic degradation products through macromolecular design of caprolactone-based copolymers. *J Am Chem Soc* **2007**, *129* (19), 6308-12.
193. Artham, T.; Doble, M., Biodegradation of aliphatic and aromatic polycarbonates. *Macromol Biosci* **2008**, *8* (1), 14-24.
194. Gleadall, A.; Pan, J.; Kruff, M.-A.; Kellomäki, M., Degradation mechanisms of bioresorbable polyesters. Part 1. Effects of random scission, end scission and autocatalysis. *Acta Biomaterialia* **2014**, *10* (5), 2223-2232.
195. Mazurek-Budzyńska, M.; Behl, M.; Razzaq, M. Y.; Nöchel, U.; Rokicki, G.; Lendlein, A., Hydrolytic stability of aliphatic poly(carbonate-urea-urethane)s: Influence of hydrocarbon chain length in soft segment. *Polymer Degradation and Stability* **2019**, *161*, 283-297.
196. Jansen, J.; Koopmans, S. A.; Los, L. I.; van der Worp, R. J.; Podt, J. G.; Hooymans, J. M. M.; Feijen, J.; Grijpma, D. W., Intraocular degradation behavior of crosslinked and linear poly(trimethylene carbonate) and poly(D,L-lactic acid). *Biomaterials* **2011**, *32* (22), 4994-5002.
197. Zhu, R.; Wang, Y.; Zhang, Z.; Ma, D.; Wang, X., Synthesis of polycarbonate urethane elastomers and effects of the chemical structures on their thermal, mechanical and biocompatibility properties. *Heliyon* **2016**, *2* (6), e00125.
198. Anju, S.; Prajitha, N.; Sukanya, V. S.; Mohanan, P. V., Complicity of degradable polymers in health-care applications. *Materials Today Chemistry* **2020**, *16*, 100236.
199. Mahajan, N.; Gupta, P., New insights into the microbial degradation of polyurethanes. *RSC Advances* **2015**, *5* (52), 41839-41854.
200. Wang, F.; Li, Z.; Lannutti, J. L.; Wagner, W. R.; Guan, J., Synthesis, characterization and surface modification of low moduli poly(ether carbonate urethane)ureas for soft tissue engineering. *Acta Biomaterialia* **2009**, *5* (8), 2901-2912.
201. Xu, C.; Huang, Y.; Tang, L.; Hong, Y., Low-Initial-Modulus Biodegradable Polyurethane Elastomers for Soft Tissue Regeneration. *ACS Applied Materials & Interfaces* **2017**, *9* (3), 2169-2180.

202. Christenson, E. M.; Patel, S.; Anderson, J. M.; Hiltner, A., Enzymatic degradation of poly(ether urethane) and poly(carbonate urethane) by cholesterol esterase. *Biomaterials* **2006**, *27* (21), 3920-3926.
203. Xie, F.; Zhang, T.; Bryant, P.; Kurusingal, V.; Colwell, J. M.; Laycock, B., Degradation and stabilization of polyurethane elastomers. *Progress in Polymer Science* **2019**, *90*, 211-268.
204. Trinca, R. B.; Felisberti, M. I., Effect of diisocyanates and chain extenders on the physicochemical properties and morphology of multicomponent segmented polyurethanes based on poly(L-lactide), poly(ethylene glycol) and poly(trimethylene carbonate). *Polymer International* **2015**, *64* (10), 1326-1335.
205. Mirhosseini, M. M.; Haddadi-Asl, V.; Jouibari, I. S., How the soft segment arrangement influences the microphase separation kinetics and mechanical properties of polyurethane block polymers. *Materials Research Express* **2019**, *6* (8), 085311.
206. Kim, H. D.; Huh, J. H.; Kim, E. Y.; Park, C. C., Comparison of properties of thermoplastic polyurethane elastomers with two different soft segments. *Journal of Applied Polymer Science* **1998**, *69* (7), 1349-1355.
207. Macdougall, L.; Culver, H.; Lin, C.-C.; Bowman, C.; Anseth, K., 1.3.2F - Degradable and Resorbable Polymers. In *Biomaterials Science (Fourth Edition)*, Wagner, W. R.; Sakiyama-Elbert, S. E.; Zhang, G.; Yaszemski, M. J., Eds. Academic Press: 2020; pp 167-190.
208. Piskin, E., Biodegradable polymers as biomaterials. *Journal of Biomaterials Science, Polymer Edition* **1995**, *6* (9), 775-795.
209. Shalaby, S. W.; Burg, K. J. L. In *Absorbable and Biodegradable Polymers*, 2003.
210. Treiser, M.; Abramson, S.; Langer, R.; Kohn, J., Chapter I.2.6 - Degradable and Resorbable Biomaterials. In *Biomaterials Science (Third Edition)*, Ratner, B. D.; Hoffman, A. S.; Schoen, F. J.; Lemons, J. E., Eds. Academic Press: 2013; pp 179-195.
211. Göpferich, A., Mechanisms of polymer degradation and erosion. *Biomaterials* **1996**, *17* (2), 103-114.
212. Williams, D., Zhang, X., I - Introduction. In *Definitions of Biomaterials for the Twenty-First Century*, Williams, D.; Zhang, X., Eds. Elsevier: 2019; pp 1-14.
213. Burkeroth, F. v.; Schedl, L.; Göpferich, A., Why degradable polymers undergo surface erosion or bulk erosion. *Biomaterials* **2002**, *23* (21), 4221-4231.
214. Tamada, J. A.; Langer, R., Erosion kinetics of hydrolytically degradable polymers. *Proceedings of the National Academy of Sciences* **1993**, *90* (2), 552-556.
215. Woodard, L. N.; Grunlan, M. A., Hydrolytic Degradation and Erosion of Polyester Biomaterials. *ACS Macro Letters* **2018**, *7* (8), 976-982.
216. Tabata, Y.; Gutta, S.; Langer, R., Controlled Delivery Systems for Proteins Using Polyanhydride Microspheres. *Pharmaceutical Research* **1993**, *10* (4), 487-496.
217. Wei, B.; Tao, Y.; Wang, X.; Tang, R.; Wang, J.; Wang, R.; Qiu, L., Surface-Eroding Poly(ortho ester amides) for Highly Efficient Oral Chemotherapy. *ACS Applied Materials & Interfaces* **2015**, *7* (19), 10436-10445.
218. He, W.; Benson, R., 8 - Polymeric Biomaterials. In *Applied Plastics Engineering Handbook (Second Edition)*, Kutz, M., Ed. William Andrew Publishing: 2017; pp 145-164.
219. Parrott, M. C.; Luft, J. C.; Byrne, J. D.; Fain, J. H.; Napier, M. E.; DeSimone, J. M., Tunable Bifunctional Silyl Ether Cross-Linkers for the Design of Acid-Sensitive Biomaterials. *Journal of the American Chemical Society* **2010**, *132* (50), 17928-17932.
220. Wang, Y.; Fan, S.; Xiao, D.; Xie, F.; Li, W.; Zhong, W.; Zhou, X., Novel Silyl Ether-Based Acid-Cleavable Antibody-MMAE Conjugates with Appropriate Stability and Efficacy. *Cancers* **2019**, *11* (7), 957.
221. Shieh, P.; Nguyen, H. V.; Johnson, J. A., Tailored silyl ether monomers enable backbone-degradable polynorbornene-based linear, bottlebrush and star copolymers through ROMP. *Nature chemistry* **2019**, *11* (12), 1124-1132.
222. Chen, Y.; Tang, Z.; Zhang, X.; Liu, Y.; Wu, S.; Guo, B., Covalently Cross-Linked Elastomers with Self-Healing and Malleable Abilities Enabled by Boronic Ester Bonds. *ACS Applied Materials & Interfaces* **2018**, *10* (28), 24224-24231.

223. Sinawehl, L.; Wolff, R.; Koch, T.; Stampfl, J.; Liska, R.; Baudis, S., Photopolymers Based on Boronic Esters for the Enhanced Degradation of 3D-Printed Scaffolds. *ACS Applied Polymer Materials* **2023**, *5* (7), 5758-5771.
224. Wang, J.; Zheng, Z.; Chen, L.; Tu, X.; Wang, X., Glutathione-responsive biodegradable poly(urea-urethane)s containing L-cystine-based chain extender. *Journal of biomaterials science. Polymer edition* **2013**, *24* (7), 831-48.
225. Lu, H.; Sun, P.; Zheng, Z.; Yao, X.; Wang, X.; Chang, F.-C., Reduction-sensitive rapid degradable poly(urethane-urea)s based on cystine. *Polymer Degradation and Stability* **2012**, *97* (4), 661-669.
226. Meng, F.; Hennink, W. E.; Zhong, Z., Reduction-sensitive polymers and bioconjugates for biomedical applications. *Biomaterials* **2009**, *30* (12), 2180-98.
227. Gomes, M.; Gandini, A.; Silvestre, A. J. D.; Reis, B., Synthesis and characterization of poly(2,5-furan dicarboxylate)s based on a variety of diols. *Journal of Polymer Science Part A: Polymer Chemistry* **2011**, *49* (17), 3759-3768.
228. Kim, M.; Su, Y.; Aoshima, T.; Fukuoka, A.; Hensen, E. J. M.; Nakajima, K., Effective Strategy for High-Yield Furan Dicarboxylate Production for Biobased Polyester Applications. *ACS Catalysis* **2019**, *9* (5), 4277-4285.
229. Gandini, A., The irruption of polymers from renewable resources on the scene of macromolecular science and technology. *Green Chemistry* **2011**, *13* (5), 1061-1083.
230. Bozell, J. J.; Petersen, G. R., Technology development for the production of biobased products from biorefinery carbohydrates—the US Department of Energy’s “Top 10” revisited. *Green Chemistry* **2010**, *12* (4), 539-554.
231. Gandini, A., Furans as offspring of sugars and polysaccharides and progenitors of a family of remarkable polymers: a review of recent progress. *Polymer Chemistry* **2010**, *1* (3), 245-251.
232. Moreau, C.; Belgacem, M. N.; Gandini, A., Recent Catalytic Advances in the Chemistry of Substituted Furans from Carbohydrates and in the Ensuing Polymers. *Topics in Catalysis* **2004**, *27* (1), 11-30.
233. Sajid, M.; Zhao, X.; Liu, D., Production of 2,5-furandicarboxylic acid (FDCA) from 5-hydroxymethylfurfural (HMF): recent progress focusing on the chemical-catalytic routes. *Green Chemistry* **2018**, *20* (24), 5427-5453.
234. Burgess, S. K.; Leisen, J. E.; Kraftschik, B. E.; Mubarak, C. R.; Kriegel, R. M.; Koros, W. J., Chain Mobility, Thermal, and Mechanical Properties of Poly(ethylene furanoate) Compared to Poly(ethylene terephthalate). *Macromolecules* **2014**, *47* (4), 1383-1391.
235. Watson, B. M.; Kasper, F. K.; Mikos, A. G., Phosphorous-containing polymers for regenerative medicine. *Biomedical Materials* **2014**, *9* (2), 025014.
236. Becker, G.; Ackermann, L.-M.; Schechtel, E.; Klapper, M.; Tremel, W.; Wurm, F. R., Joining Two Natural Motifs: Catechol-Containing Poly(phosphoester)s. *Biomacromolecules* **2017**, *18* (3), 767-777.
237. Bauer, K. N.; Tee, H. T.; Velencoso, M. M.; Wurm, F. R., Main-chain poly(phosphoester)s: History, syntheses, degradation, bio- and flame-retardant applications. *Progress in Polymer Science* **2017**, *73*, 61-122.
238. Wachiralarpphaithoon, C.; Iwasaki, Y.; Akiyoshi, K., Enzyme-degradable phosphorylcholine porous hydrogels cross-linked with polyphosphoesters for cell matrices. *Biomaterials* **2007**, *28* (6), 984-93.
239. Huang, S.-W.; Zhuo, R.-X., Recent Advances in Polyphosphoester and Polyphosphoramidate-Based Biomaterials. *Phosphorus, Sulfur, and Silicon and the Related Elements* **2008**, *183* (2-3), 340-348.
240. Wang, D.-A.; Williams, C. G.; Yang, F.; Cher, N.; Lee, H.; Elisseff, J. H., Bioresponsive Phosphoester Hydrogels for Bone Tissue Engineering. *Tissue engineering* **2005**, *11* (1-2), 201-213.
241. Polloni, A. E.; Chiaradia, V.; do Amaral, R. J. F. C.; Kearney, C.; Gorey, B.; de Oliveira, D.; de Oliveira, J. V.; de Araújo, P. H. H.; Sayer, C.; Heise, A., Polyesters with main and side chain phosphoesters as structural motives for biocompatible electrospun fibres. *Polymer Chemistry* **2020**, *11* (12), 2157-2165.

242. Sample, C. S.; Lee, S.-H.; Bates, M. W.; Ren, J. M.; Lawrence, J.; Lensch, V.; Gerbec, J. A.; Bates, C. M.; Li, S.; Hawker, C. J., Metal-Free Synthesis of Poly(silyl ether)s under Ambient Conditions. *Macromolecules* **2019**, *52* (5), 1993-1999.
243. Greene, T. W.; Wuts, P. G. M., The Role of Protective Groups in Organic Synthesis. In *Protective Groups in Organic Synthesis*, 1999.
244. Trost, B. M.; Caldwell, C. G., The di-*t*-butylsilylene protecting group for diols. *Tetrahedron Letters* **1981**, *22* (50), 4999-5002.
245. Kumagai, D.; Miyazaki, M.; Nishimura, S.-I., Cyclic di-*t*-butylsilylenediyl ether group as a convenient protective group for the glycoconjugate synthesis. *Tetrahedron Letters* **2001**, *42* (10), 1953-1956.
246. Li, C.; Guo, C.; Fitzpatrick, V.; Ibrahim, A.; Zwierstra, M. J.; Hanna, P.; Lechtig, A.; Nazarian, A.; Lin, S. J.; Kaplan, D. L., Design of biodegradable, implantable devices towards clinical translation. *Nature Reviews Materials* **2020**, *5* (1), 61-81.
247. Bunton, C. M.; Bassampour, Z. M.; Boothby, J. M.; Smith, A. N.; Rose, J. V.; Nguyen, D. M.; Ware, T. H.; Csaky, K. G.; Lippert, A. R.; Tsarevsky, N. V.; Son, D. Y., Degradable Silyl Ether-Containing Networks from Trifunctional Thiols and Acrylates. *Macromolecules* **2020**, *53* (22), 9890-9900.
248. Weinhold, F.; West, R., The Nature of the Silicon-Oxygen Bond. *Organometallics* **2011**, *30* (21), 5815-5824.
249. Cheng, F.; Jäkle, F., Boron-containing polymers as versatile building blocks for functional nanostructured materials. *Polymer Chemistry* **2011**, *2* (10), 2122-2132.
250. Entwistle, C. D.; Marder, T. B., Boron chemistry lights the way: optical properties of molecular and polymeric systems. *Angewandte Chemie (International ed. in English)* **2002**, *41* (16), 2927-31.
251. Hall, D. G., Structure, Properties, and Preparation of Boronic Acid Derivatives. In *Boronic Acids*, 2011; pp 1-133.
252. Springsteen, G.; Wang, B., A detailed examination of boronic acid-diol complexation. *Tetrahedron* **2002**, *58* (26), 5291-5300.
253. Brooks, W. L.; Sumerlin, B. S., Synthesis and Applications of Boronic Acid-Containing Polymers: From Materials to Medicine. *Chemical reviews* **2016**, *116* (3), 1375-97.
254. Cash, J. J.; Kubo, T.; Bapat, A. P.; Sumerlin, B. S., Room-Temperature Self-Healing Polymers Based on Dynamic-Covalent Boronic Esters. *Macromolecules* **2015**, *48* (7), 2098-2106.
255. Niu, W.; O'Sullivan, C.; Rambo, B. M.; Smith, M. D.; Lavigne, J. J., Self-repairing polymers: poly(dioxaborolane)s containing trigonal planar boron. *Chemical Communications* **2005**, (34), 4342-4344.
256. Martínez-Aguirre, M. A.; Villamil-Ramos, R.; Guerrero-Alvarez, J. A.; Yatsimirsky, A. K., Substituent Effects and pH Profiles for Stability Constants of Arylboronic Acid Diol Esters. *The Journal of organic chemistry* **2013**, *78* (10), 4674-4684.
257. Li, L.; Chen, X.; Torkelson, J. M., Reprocessable Polymer Networks via Thiourethane Dynamic Chemistry: Recovery of Cross-link Density after Recycling and Proof-of-Principle Solvolysis Leading to Monomer Recovery. *Macromolecules* **2019**, *52* (21), 8207-8216.
258. Deng, C. C.; Brooks, W. L. A.; Abboud, K. A.; Sumerlin, B. S., Boronic Acid-Based Hydrogels Undergo Self-Healing at Neutral and Acidic pH. *ACS Macro Letters* **2015**, *4* (2), 220-224.
259. Saed, M. O.; Gablier, A.; Terentejv, E. M., Liquid Crystalline Vitrimers with Full or Partial Boronic-Ester Bond Exchange. *Advanced Functional Materials* **2020**, *30* (3), 1906458.
260. Shi, W.; Hass, B.; Kuss, M. A.; Zhang, H.; Ryu, S.; Zhang, D.; Li, T.; Li, Y.-I.; Duan, B., Fabrication of versatile dynamic hyaluronic acid-based hydrogels. *Carbohydrate Polymers* **2020**, *233*, 115803.
261. Wang, Y.; Yu, H.; Yang, H.; Hao, X.; Tang, Q.; Zhang, X., An Injectable Interpenetrating Polymer Network Hydrogel with Tunable Mechanical Properties and Self-Healing Abilities. *Macromolecular Chemistry and Physics* **2017**, *218*, 1700348.
262. Meng, X.; Crestini, C.; Ben, H.; Hao, N.; pu, Y.; Ragauskas, A.; Argyropoulos, D., Determination of hydroxyl groups in biorefinery resources via quantitative <sup>31</sup>P NMR spectroscopy. *Nature Protocols* **2019**, *14*.



263. Raina, S.; Missiakas, D., Making and breaking disulfide bonds. *Annual review of microbiology* **1997**, *51*, 179-202.
264. Ikada, Y.; Tsuji, H., Biodegradable polyesters for medical and ecological applications. *Macromolecular Rapid Communications* **2000**, *21* (3), 117-132.
265. Saltzman, W. M.; Fung, L. K., Polymeric implants for cancer chemotherapy. *Advanced drug delivery reviews* **1997**, *26* (2-3), 209-230.
266. Townsend, D. M.; Tew, K. D.; Tapiero, H., The importance of glutathione in human disease. *Biomedicine & pharmacotherapy = Biomedecine & pharmacotherapie* **2003**, *57* (3-4), 145-55.
267. Arnér, E. S. J.; Holmgren, A., Physiological functions of thioredoxin and thioredoxin reductase. *European Journal of Biochemistry* **2000**, *267* (20), 6102-6109.
268. Wu, G.; Lupton, J. R.; Turner, N. D.; Fang, Y.-Z.; Yang, S., Glutathione Metabolism and Its Implications for Health. *The Journal of Nutrition* **2004**, *134* (3), 489-492.
269. Butera, D.; Cook, K. M.; Chiu, J.; Wong, J. W. H.; Hogg, P. J., Control of blood proteins by functional disulfide bonds. *Blood* **2014**, *123* (13), 2000-2007.
270. Farrah, T.; Deutsch, E. W.; Omenn, G. S.; Campbell, D. S.; Sun, Z.; Bletz, J. A.; Mallick, P.; Katz, J. E.; Malmström, J.; Ossola, R., A high-confidence human plasma proteome reference set with estimated concentrations in PeptideAtlas. *Molecular & cellular proteomics* **2011**, *10* (9).
271. Kozlov, G.; Määttänen, P.; Thomas, D. Y.; Gehring, K., A structural overview of the PDI family of proteins. *The FEBS Journal* **2010**, *277* (19), 3924-3936.
272. Holmgren, A., Thioredoxin and glutaredoxin systems. *Journal of Biological Chemistry* **1989**, *264* (24), 13963-13966.
273. Cleland, W. W., Dithiothreitol, a New Protective Reagent for SH Groups\*. *Biochemistry* **1964**, *3* (4), 480-482.
274. Lukesh, J. C., III; Palte, M. J.; Raines, R. T., A Potent, Versatile Disulfide-Reducing Agent from Aspartic Acid. *Journal of the American Chemical Society* **2012**, *134* (9), 4057-4059.
275. Rüegg, U. T.; Rudinger, J., Reductive cleavage of cystine disulfides with tributylphosphine. In *Methods in Enzymology*, Academic Press: 1977; Vol. 47, pp 111-116.
276. Cline, D. J.; Redding, S. E.; Brohawn, S. G.; Psathas, J. N.; Schneider, J. P.; Thorpe, C., New Water-Soluble Phosphines as Reductants of Peptide and Protein Disulfide Bonds: Reactivity and Membrane Permeability. *Biochemistry* **2004**, *43* (48), 15195-15203.
277. Zhang, L.; Chen, L.; Rowan, S. J., Trapping Dynamic Disulfide Bonds in the Hard Segments of Thermoplastic Polyurethane Elastomers. *Macromolecular Chemistry and Physics* **2017**, *218* (1), 1600320.
278. Wang, J.; Sun, P.; Zheng, Z.; Wang, F.; Wang, X., Glutathione-responsive biodegradable polyurethanes based on dithiodiundecanol. *Polymer Degradation and Stability* **2012**, *97* (11), 2294-2300.
279. Wang, J.; Zheng, Z.; Chen, L.; Tu, X.; Wang, X., Glutathione-responsive biodegradable poly(urea-urethane)s containing L-cystine-based chain extender. *Journal of Biomaterials Science, Polymer Edition* **2013**, *24* (7), 831-848.
280. Fang, D.; Pi, M.; Pan, Z.; Song, N.; He, X.; Li, J.; Luo, F.; Tan, H.; Li, Z., Stable, Bioresponsive, and Macrophage-Evading Polyurethane Micelles Containing an Anionic Tripeptide Chain Extender. *ACS Omega* **2019**, *4* (15), 16551-16563.
281. Begines, B.; Zamora, F.; de Paz, M. V.; Hakkou, K.; Galbis, J. A., Polyurethanes derived from carbohydrates and cystine-based monomers. *Journal of Applied Polymer Science* **2015**, *132* (3).
282. Ferris, C.; Violante de Paz, M.; Aguilar-de-Leyva, Á.; Caraballo, I.; Galbis, J. A., Reduction-sensitive functionalized copolyurethanes for biomedical applications. *Polymer Chemistry* **2014**, *5* (7), 2370-2381.
283. Baudis, S. Development and Processing of Materials for Vascular Tissue Regeneration. Dissertation, TU Wien, Vienna, 2010.
284. Pêgo, A. P.; Grijpma, D. W.; Feijen, J., Enhanced mechanical properties of 1,3-trimethylene carbonate polymers and networks. *Polymer* **2003**, *44* (21), 6495-6504.

285. van Leeuwen, A. C.; Huddleston Slater, J. J. R.; Gielkens, P. F. M.; de Jong, J. R.; Grijpma, D. W.; Bos, R. R. M., Guided bone regeneration in rat mandibular defects using resorbable poly(trimethylene carbonate) barrier membranes. *Acta Biomaterialia* **2012**, *8* (4), 1422-1429.
286. Hanaor, D. A. H.; Chironi, I.; Karatchevtseva, I.; Triani, G.; Sorrell, C. C., Single and mixed phase TiO<sub>2</sub> powders prepared by excess hydrolysis of titanium alkoxide. *Advances in Applied Ceramics* **2012**, *111* (3), 149-158.
287. Lohmeijer, B. G. G.; Pratt, R. C.; Leibfarth, F.; Logan, J. W.; Long, D. A.; Dove, A. P.; Nederberg, F.; Choi, J.; Wade, C.; Waymouth, R. M.; Hedrick, J. L., Guanidine and Amidine Organocatalysts for Ring-Opening Polymerization of Cyclic Esters. *Macromolecules* **2006**, *39* (25), 8574-8583.
288. Bergmeister, H.; Grasl, C.; Walter, I.; Plasenzotti, R.; Stoiber, M.; Schreiber, C.; Losert, U.; Weigel, G.; Schima, H., Electrospun small-diameter polyurethane vascular grafts: ingrowth and differentiation of vascular-specific host cells. *Artificial organs* **2012**, *36* (1), 54-61.
289. Bergmeister, H.; Schreiber, C.; Grasl, C.; Walter, I.; Plasenzotti, R.; Stoiber, M.; Bernhard, D.; Schima, H., Healing characteristics of electrospun polyurethane grafts with various porosities. *Acta Biomater* **2013**, *9* (4), 6032-40.
290. Mrad, O.; Saunier, J.; Aymes Chodur, C.; Rosilio, V.; Agnely, F.; Aubert, P.; Vigneron, J.; Etcheberry, A.; Yagoubi, N., A comparison of plasma and electron beam-sterilization of PU catheters. *Radiation Physics and Chemistry* **2010**, *79* (1), 93-103.
291. Coleman, M. M.; Lee, K. H.; Skrovanek, D. J.; Painter, P. C., Hydrogen bonding in polymers. 4. Infrared temperature studies of a simple polyurethane. *Macromolecules* **1986**, *19* (8), 2149-2157.
292. Yilgor, I.; Yilgor, E.; Guler, I. G.; Ward, T. C.; Wilkes, G. L., FTIR investigation of the influence of diisocyanate symmetry on the morphology development in model segmented polyurethanes. *Polymer* **2006**, *47* (11), 4105-4114.
293. Hernandez, R.; Weksler, J.; Padsalgikar, A.; Choi, T.; Angelo, E.; Lin, J. S.; Xu, L.-C.; Siedlecki, C. A.; Runt, J., A Comparison of Phase Organization of Model Segmented Polyurethanes with Different Intersegment Compatibilities. *Macromolecules* **2008**, *41* (24), 9767-9776.
294. Papadimitrakopoulos, F.; Sawa, E.; MacKnight, W. J., Investigation of a monotropic liquid crystal polyurethane based on biphenol, 2,6-tolylene diisocyanate, and a six methylene containing flexible spacer. 2. IR spectroscopic phase characterization. *Macromolecules* **1992**, *25* (18), 4682-4691.
295. Okuyama, K.-i.; Sugiyama, J.-i.; Nagahata, R.; Asai, M.; Ueda, M.; Takeuchi, K., An environmentally benign process for aromatic polycarbonate synthesis by efficient oxidative carbonylation catalyzed by Pd-carbene complexes. *Green Chemistry* **2003**, *5* (5), 563-566.
296. Zhao, Y.; Zhu, Y.; Sui, G.; Chen, F.; Zhang, Q.; Fu, Q., The effect of hard block content on the orientation and mechanical properties of olefin block copolymer films as obtained via melt stretching. *RSC Advances* **2015**, *5* (100), 82535-82543.
297. Szycher, M., Structure–Property Relations in Polyurethanes. In *Szycher's Handbook of Polyurethanes*, CRC Press: 2012.
298. Nobbmann, U. Polydispersity – what does it mean for DLS and chromatography? <https://www.materials-talks.com/polydispersity-what-does-it-mean-for-dls-and-chromatography/> (accessed 09.10.2023).
299. Danaei, M.; Dehghankhold, M.; Ataei, S.; Hasanzadeh Davarani, F.; Javanmard, R.; Dokhani, A.; Khorasani, S.; Mozafari, M. R., Impact of Particle Size and Polydispersity Index on the Clinical Applications of Lipidic Nanocarrier Systems. *Pharmaceutics* **2018**, *10* (2).
300. Rogošić, M.; Mencer, H. J.; Gomzi, Z., Polydispersity index and molecular weight distributions of polymers. *European Polymer Journal* **1996**, *32* (11), 1337-1344.
301. Bergmeister, H.; Seyidova, N.; Schreiber, C.; Strobl, M.; Grasl, C.; Walter, I.; Messner, B.; Baudis, S.; Fröhlich, S.; Marchetti-Deschmann, M.; Griesser, M.; di Franco, M.; Krssak, M.; Liska, R.; Schima, H., Biodegradable, thermoplastic polyurethane grafts for small diameter vascular replacements. *Acta Biomaterialia* **2015**, *11*, 104-113.
302. Wolf, T.; Steinbach, T.; Wurm, F. R., A Library of Well-Defined and Water-Soluble Poly(alkyl phosphonate)s with Adjustable Hydrolysis. *Macromolecules* **2015**, *48* (12), 3853-3863.

303. Hatzakis, E.; Dais, P., Determination of Water Content in Olive Oil by  $^{31}\text{P}$  NMR Spectroscopy. *Journal of Agricultural and Food Chemistry* **2008**, *56* (6), 1866-1872.
304. Akim, L. G.; Argyropoulos, D. S.; Jouanin, L.; Leplé, J.-C.; Pilate, G.; Pollet, B.; Lapierre, C., Quantitative  $^{31}\text{P}$  NMR Spectroscopy of Lignins from Transgenic Poplars. **2001**, *55* (4), 386-390.
305. Granata, A.; Argyropoulos, D. S., 2-chloro-4,4,5,5-tetramethyl-1,3,2-dioxaphospholane, a reagent for the accurate determination of the uncondensed and condensed phenolic moieties in lignins. *Journal of agricultural and food chemistry* **1995**, *43* (6), 1538-1544.
306. Javaherian Naghash, H.; Hossein Sheikhabaei, M., Synthesis of a novel silicone based copolymeric surfactant and application in emulsion polymerization. *Journal of Polymer Engineering* **2013**, *33*.
307. Eglin, D.; Griffon, S.; Alini, M., Thiol-Containing Degradable Poly(thiourethane-urethane)s for Tissue Engineering. *Journal of Biomaterials Science, Polymer Edition* **2010**, *21* (4), 477-491.
308. Strzelec, K.; Bączek, N.; Ostrowska, S.; Wąsikowska, K.; Szyrkowska, M. I.; Grams, J., Synthesis and characterization of novel polythiourethane hardeners for epoxy resins. *Comptes Rendus Chimie* **2012**, *15* (11), 1065-1071.
309. Li, Q.; Zhou, H.; Wicks, D. A.; Hoyle, C. E.; Magers, D. H.; McAlexander, H. R., Comparison of Small Molecule and Polymeric Urethanes, Thiourethanes, and Dithiourethanes: Hydrogen Bonding and Thermal, Physical, and Mechanical Properties. *Macromolecules* **2009**, *42* (6), 1824-1833.
310. Lowe, A. B.; Bowman, C. N., *Thiol-x chemistries in polymer and materials science*. Royal Society of Chemistry: 2013; Vol. 6.
311. Gamardella, F.; Ramis, X.; De la Flor, S.; Serra, À., Preparation of poly(thiourethane) thermosets by controlled thiol-isocyanate click reaction using a latent organocatalyst. *Reactive and Functional Polymers* **2019**, *134*, 174-182.
312. Breuillac, A.; Kassalias, A.; Nicolaÿ, R., Polybutadiene Vitrimers Based on Dioxaborolane Chemistry and Dual Networks with Static and Dynamic Cross-links. *Macromolecules* **2019**, *52* (18), 7102-7113.
313. Rafiemanzelat, F.; Khoshfetrat, S. M.; Kolahdoozan, M., Fast and eco-friendly synthesis of novel soluble thermally stable poly(amide-imide)s modified with siloxane linkage with reduced dielectric constant under microwave irradiation in TBAB, TBPB and MeBulmCl via isocyanate method. *Journal of Applied Polymer Science* **2013**, *127* (4), 2371-2379.
314. Williams, M. A.; Ladbury, J. E., Hydrogen Bonds in Protein-Ligand Complexes. In *Protein-Ligand Interactions*, 2003; pp 137-161.
315. Romanos, J.; Beckner, M.; Stalla, D.; Tekeei, A.; Suppes, G.; Jalisatgi, S.; Lee, M.; Hawthorne, F.; Robertson, J. D.; Firlej, L.; Kuchta, B.; Wexler, C.; Yu, P.; Pfeifer, P., Infrared study of boron-carbon chemical bonds in boron-doped activated carbon. *Carbon* **2013**, *54*, 208-214.
316. Wen, Z.; Han, X.; Fairbanks, B. D.; Yang, K.; Bowman, C. N., Development of thiourethanes as robust, reprocessable networks. *Polymer* **2020**, *202*, 122715.
317. Babij, N. R.; McCusker, E. O.; Whiteker, G. T.; Canturk, B.; Choy, N.; Creemer, L. C.; Amicis, C. V. D.; Hewlett, N. M.; Johnson, P. L.; Knobelsdorf, J. A.; Li, F.; Lorsbach, B. A.; Nugent, B. M.; Ryan, S. J.; Smith, M. R.; Yang, Q., NMR Chemical Shifts of Trace Impurities: Industrially Preferred Solvents Used in Process and Green Chemistry. *Organic Process Research & Development* **2016**, *20* (3), 661-667.
318. Mutlu, H.; Ruiz, J.; Solleder, S. C.; Meier, M. A. R., TBD catalysis with dimethyl carbonate: a fruitful and sustainable alliance. *Green Chemistry* **2012**, *14* (6), 1728-1735.
319. Mayr, H., Unverzichtbar im Praktikum: Arbeitsmethoden in der Organischen Chemie. *Nachrichten aus der Chemie* **2006**, *54* (12), 1239-1239.